



NATIONAL AND KAPODISTRIAN  
UNIVERSITY OF ATHENS

SCHOOL OF SCIENCE  
FACULTY OF BIOLOGY

A STUDY OF MEMBRANE PROTEIN TRAFFICKING  
ENDOCYTOSIS AND DEGRADATION  
THROUGH THE DEVELOPMENT OF NEW GENETIC  
AND BIOCHEMICAL TOOLS

---

Ph.D. THESIS

**OLGA MARTZOUKOU**  
BIOLOGIST

ATHENS 2018

**Cover image:** Microscopic morphology of *Aspergillus nidulans* hyphae in a strain repressed for *ap1<sup>σ</sup>* expression, stained with calcofluor white and visualized with 'fire' LUT. Wider and shorter hyphae, with increased numbers of side branches and septal rings are observed. Notice also the differences in calcofluor deposition at the hyphal head, tip and the subapical segment. © Olga Martzoukou



ΕΛΛΗΝΙΚΗ ΔΗΜΟΚΡΑΤΙΑ

**Εθνικόν και Καποδιστριακόν  
Πανεπιστήμιον Αθηνών**

**Σχολή Θετικών Επιστημών  
Τμήμα Βιολογίας  
Τομέας Βοτανικής**

**Μελέτη της κυτταρικής διακίνησης, ενδοκύτωσης και αποδόμησης  
μεμβρανικών πρωτεϊνών μέσω της ανάπτυξης νέων γενετικών και  
βιοχημικών προσεγγίσεων**

ΔΙΔΑΚΤΟΡΙΚΗ ΔΙΑΤΡΙΒΗ

**Όλγα Μαρτζούκου  
Βιολόγος**

**Αθήνα, 2018**

«Η έγκριση διδακτορικής διατριβής από το Τμήμα Βιολογίας της Σχολής Θετικών Επιστημών του ΕΚΠΑ δεν υποδηλώνει αποδοχή των απόψεων του συγγραφέα (Ν. 5343/1932, άρθρο 202)»  
«Το κείμενο της Διδακτορικής Διατριβής δεν αποτελεί προϊόν λογοκλοπής»

### **Τριμελής Συμβουλευτική Επιτροπή**

Γ. Διαλλινάς, Καθηγητής Πανεπιστημίου Αθηνών (Επιβλέπων)

Σ. Ευθυμιόπουλος, Καθηγητής Πανεπιστημίου Αθηνών

Ι.Π. Τρουγκάκος, Αναπληρωτής Καθηγητής Πανεπιστημίου Αθηνών

### **Επταμελής Εξεταστική Επιτροπή**

Γ. Διαλλινάς, Καθηγητής Πανεπιστημίου Αθηνών (Επιβλέπων)

Σ. Ευθυμιόπουλος, Καθηγητής Πανεπιστημίου Αθηνών

Ι.Π. Τρουγκάκος, Αναπληρωτής Καθηγητής Πανεπιστημίου Αθηνών

Χ. Δελιδάκης, Καθηγητής Πανεπιστημίου Κρήτης

Κ. Χαραλαμπίδης, Αναπληρωτής Καθηγητής Πανεπιστημίου Αθηνών

Δ.Ι. Στραβοπόδης, Επίκουρος Καθηγητής Πανεπιστημίου Αθηνών

N. Takeshita, Επίκουρος Καθηγητής University of Tsukuba

Η υλοποίηση της διδακτορικής διατριβής συγχρηματοδοτήθηκε από το Fondation Santé και από το ΙΚΥ μέσω της πράξης «ΠΡΟΓΡΑΜΜΑ ΧΟΡΗΓΗΣΗΣ ΥΠΟΤΡΟΦΙΩΝ ΓΙΑ ΜΕΤΑΠΤΥΧΙΑΚΕΣ ΣΠΟΥΔΕΣ ΔΕΥΤΕΡΟΥ ΚΥΚΛΟΥ ΣΠΟΥΔΩΝ» του Επιχειρησιακού Προγράμματος «Ανάπτυξη Ανθρώπινου Δυναμικού, Εκπαίδευση και Διά Βίου Μάθηση», του ΕΣΠΑ 2014 - 2020 με τη συγχρηματοδότηση του Ευρωπαϊκού Κοινωνικού Ταμείου.



HELLENIC REPUBLIC

**National and Kapodistrian  
University of Athens**

School of Science  
**Faculty of Biology**  
**Department of Botany**

**A study of membrane protein trafficking, endocytosis and  
degradation through the development of new genetic and  
biochemical tools**

Ph.D. THESIS

**Olga Martzoukou**  
**Biologist**

**Athens, 2018**

### **Advisory committee**

G. Diallynas, Professor University of Athens (Supervisor)

S. Efthimiopoulos, Professor University of Athens

I.P. Trougkos, Associate Professor University of Athens

### **Examining committee**

G. Diallynas, Professor University of Athens (Supervisor)

S. Efthimiopoulos, Professor University of Athens

I.P. Trougkos, Associate Professor University of Athens

C. Delidakis, Professor University of Crete

K. Haralampidis, Associate Professor University of Athens

D.J. Stravopodis, Assistant Professor University of Athens

N. Takeshita, Assistant Professor University of Tsukuba

This research has been co-funded by a research grant from Fondation Santé and through the Action “Doctorate Scholarships Programs by the State Scholarships Foundation” by IKY and the European Social Fund (ESF), in the framework of the Operational Program “Education and Life Long Learning” within the NSRF 2014-2020 of the ESF.

Οι διαμεμβρανικές πρωτεΐνες στα ευκαρυωτικά κύτταρα ενσωματώνονται στη μεμβράνη του Ενδοπλασματικού Δικτύου (ΕΔ) συµμεταφραστικά. Προκειµένου να εξέλθουν από το ΕΔ µε κυστίδια τύπου COPII, απαιτείται µία σειρά ελέγχων που αφορά τόσο παράγοντες που εντοπίζονται στο πρωτεϊνικό μόριο, όπως για παράδειγµα η παρουσία συντηρηµένων µοτίβων εξόδου από το ΕΔ, όσο και η αλληλεπίδραση µε ρυθµιστικές πρωτεΐνες που διασφαλίζουν τη σωστή αναδίπλωση του µορίου. Μετά την έξοδο από το ΕΔ, οι πρωτεΐνες διακινούνται µέσω του Golgi δικτύου, πακετάρονται σε κυστίδια, µεταφέρονται στον τελικό τους υποκυτταρικό προορισµό (πλασµατική µεµβράνη και µεµβράνες οργανιδίων) και ενσωματώνονται στην κατάλληλη µεµβράνη. Επίσης, πολικά ευκαρυωτικά κύτταρα, όπως οι νευρώνες, τα µυϊκά ή οι παθογόνοι νηµατοειδείς µύκητες (πχ. *Aspergillus*) διαθέτουν µηχανισµούς που διαφοροποιούν την στόχευση και τοπολογία κάθε πρωτεΐνης σε διακριτά σηµεία της πλασµατικής µεµβράνης.

Η εύρυθµη κυτταρική λειτουργία βασίζεται επίσης στη συνεχή µετακίνηση µορίων µεταξύ των διάφορων υποκυτταρικών οργανιδίων. Σε αρκετά βήµατα αυτής της ενδοκυτταρικής κυκλοφορίας, συµµετέχουν ειδικά µεταφορικά 'καλυµµένα' κυστίδια τα οποία µεταφέρονται κατά µήκος των µικροσωληνίσκων σε µια διαδικασία βάδισης που διεξάγεται από σχετιζόµενες κινητήριες πρωτεΐνες (κινεσίνη, δυνείνη). Τα πρωτεϊνικά σύµπλοκα προσαρµογής (Adaptor Proteins, APs) φαίνεται να κατέχουν εξέχοντα ρόλο για τη δηµιουργία κυστιδίων µε κάλυµµα κλαθρίνης, στους περισσότερους ευκαρυωτικούς οργανισµούς, ενώ τα τρία µυκητιακά AP σύµπλοκα εµφανίζουν υψηλή οµολογία µε τα αντίστοιχα των υπόλοιπων ευκαρυωτών (AP-1, AP-2, AP-3). Κατέχουν βασικό ρόλο στην επιλογή, διακίνηση, ενδοκύτωση και ανακύκλωση διαµεµβρανικών φορτίων, ενώ τόσο η παρουσία λειτουργικών υποµονάδων αυτών, όσο και της ίδιας της κλαθρίνης έχει αναδειχθεί ως απαραίτητη για την οµοίωση και επιβίωση των κυττάρων. Ωστόσο, υπό το φως ανακαλύψεων των τελευταίων 10 ετών υπάρχει εξαιρετικά έντονο επιστηµονικό ενδιαφέρον, που αφορά στην ύπαρξη και ανεξαρτητών της κλαθρίνης, µονοπατιών διακίνησης πρωτεϊνών.

Από τις πιο σηµαντικές διαµεµβρανικές πρωτεΐνες είναι οι µεταφορείς υδατοδιαλυτών ουσιών και οι πρωτεΐνες που εµφανίζουν πολική εναπόθεση και συµµετέχουν σε διαδικασίες απαραίτητες για τη φυσιολογική ανάπτυξη του οργανισµού. Στη διατριβή αυτή µελετάται η σηµασία του διµερισµού πριν την έξοδο από το ΕΔ και διερευνάται η συµµετοχή των AP συµπλόκων στη στόχευση των διαµεµβρανικών πρωτεϊνών στην πλασµατική µεµβράνη, αλλά και στην ακόµη πιο ταχεία αποµάκρυνσή τους από αυτήν µέσω της διαδικασίας της ενδοκύτωσης, καθώς και ο ρόλος της κλαθρίνης σε αυτές τις διαδικασίες, µέσω της ανάπτυξης νέων γενετικών και βιοχηµικών προσεγγίσεων. Ο νηµατοειδής µύκητας *Aspergillus nidulans*, έχει αναδειχθεί ως



μοναδικό σύστημα μελετών όπου εφαρμόζονται συνδυαστικές προσεγγίσεις γενετικής και μικροσκοπίας επιφθορισμού. Ο εκτενώς μελετημένος μεταφορέας ουρικού οξέος-ξανθίνης, UarA, χρησιμοποιήθηκε ως το βασικό μόριο για τη διερεύνηση βασικών ερωτημάτων που σχετίζονται με τους μηχανισμούς που διέπουν την ενδοκυτταρική διακίνηση των μεταφορέων και το ρόλο του διμερισμού στην έξοδο από το ΕΔ, ενώ συγκεκριμένες πρωτεΐνες που εμφανίζουν πολική κατανομή στην κορυφαία περιοχή της πλασματικής μεμβράνης χρησιμοποιήθηκαν ως μόρια για τη μελέτη των γενικών μονοπατιών διακίνησης στα οποία εμπλέκονται τα AP σύμπλοκα.

Συγκεκριμένα, διερευνούμε το ρόλο του AP-1 συμπλόκου στη διακίνηση φορτίων και δείχνουμε ότι είναι απαραίτητο για την αύξηση, λόγω της συμμετοχής του στη μετακίνηση κυστιδίων μέσω μικροσωληνίσκων, προς την κορυφαία περιοχή της αναπτυσσόμενης υφής. Ακόμη, ταυτοποιούμε μοτίβα δέσμευσης της κλαθρίνης στην καρβοξυτελική περιοχή της β1 υπομονάδας και παρέχουμε αποδείξεις για την εμπλοκή του AP-1 τόσο στην ορθόδρομη μεταφορά εκκριτικών κυστιδίων που περιέχουν το RabE, όσο και στην ανάδρομη, εξαρτώμενη από τα RabA/RabB, ανακύκλωση ενδοσωμάτων. Επίσης δείχνουμε πως το AP-1 είναι σημαντικό για την οργάνωση των μικροσωληνίσκων και των σεπτινών, ερμηνεύοντας έτσι την αναγκαιότητα του για τα κύτταρα που αντιμετωπίζουν την πρόκληση της εξαρτώμενης από τον κυτταροσκελετό, πολικής αύξησης.

Μελετάμε επίσης τον ρόλο του AP-2 συμπλόκου, ο οποίος φαίνεται πως είναι ανεξάρτητος τοπολογικά και λειτουργικά από αυτόν της κλαθρίνης και σχετίζεται με τη διατήρηση της πολικής αύξησης στον *A. nidulans*. Παρέχουμε ακόμη κυτταρικές και γενετικές αποδείξεις πως το AP-2 αλληλεπιδρά με τους παράγοντες ενδοκύτωσης SlaB/End4 και SagA/End3 καθώς και τις λιπιδικές φλιππάσες, DnfA και DnfB, στην περιοχή συνεχούς ενδοκύτωσης των αναπτυσσόμενων υφών. Ο ρόλος του AP-2 στη διατήρηση της φυσιολογικής λιπιδικής σύστασης της κορυφαίας μεμβράνης και του κυτταρικού τοιχώματος, ενισχύεται από την αλληλεπίδρασή του με ένζυμα/πρωτεΐνες απαραίτητα για τη βιοσύνθεση σφιγγολιπιδίων, για το σχηματισμό λιπιδικών περιοχών πλούσιων σε στερόλη και για τη φυσιολογική εναπόθεση χιτίνης. Τα ευρήματά μας αποδεικνύουν, για πρώτη φορά, την ύπαρξη ενός μονοπατιού ενδοκυτταρικής μεταφοράς των πιο εξελιγμένων μυκήτων που λειτουργεί βασιζόμενο αποκλειστικά στην ύπαρξη του AP-2 συμπλόκου, χωρίς τη συμβολή κλαθρίνης.

Το σύνολο της διατριβής αυτής συνεισφέρει σημαντικά στην πρόωθηση της γνώσης που αφορά στην κατανόηση της λειτουργίας των ευκαρυωτικών κυττάρων τα οποία εμφανίζουν πολική αύξηση, με πιθανές προεκτάσεις και σε πολικά κύτταρα ανώτερων θηλαστικών, όπως οι νευρώνες. Ακόμη, δεδομένης της υψίστης σημασίας της μεμβρανικής διακίνησης στην εύρυθμη λειτουργία των κυττάρων, ανοίγονται νέοι δρόμοι στη εύρεση στοχευμένων προσεγγίσεων αντιμετώπισης παθολογικών μυκήτων.

In eukaryotic cells, transmembrane proteins are co-translationally inserted in the lipid bilayer of the Endoplasmic Reticulum (ER). In order for these proteins to exit the ER packaged in COPII vesicles, both ER-exit motifs and interacting regulatory proteins that ensure proper cargo folding, are required. Following ER-exit, transmembrane proteins are trafficked through the Golgi network, packaged in vesicles and targeted to their final subcellular destination (plasma membrane, endosomal, mitochondrial, vacuolar etc) where they are integrated in the correct lipid bilayer. Additionally, polar cells such as neurons, muscle cells or filamentous fungi (e.g. *Aspergillus*) utilize cellular mechanisms that control the targeting and topology of each protein to distinct areas of the plasma membrane.

The homeostasis of cellular function depends, largely, on the continuous movement of molecules between the subcellular compartments. Several steps of this intracellular protein trafficking implicate specific coated-vesicle formation and transport on microtubules (MTs), which function as tracks in a process propelled by their associated motor proteins (kinesin, dynein). Adaptor protein complexes (APs) are important for the formation of clathrin-coated vesicles for most eukaryotes, whereas all three fungal AP complexes are universally conserved (AP-1, AP-2 and AP-3). They play key roles in the selection, traffic, endocytosis and recycling of membrane cargoes, whilst the presence of functional adaptors and clathrin is indispensable for the homeostasis and survival of eukaryotic cells. Interestingly however, in light of the discoveries of the past 10 years, the existence of specialized clathrin-independent trafficking pathways has also been proposed.

Transporters and apically localized cargoes, are two of the most important categories of transmembrane proteins, that participate in processes necessary for normal development. In this thesis, we study protein dimerization prior to ER-exit and investigate the role of AP complexes in transmembrane protein trafficking to the plasma membrane, but also in their rapid removal via endocytosis, as well as the role of clathrin in these processes, through the development of new genetic and biochemical tools. The filamentous fungus *Aspergillus nidulans* has emerged as unique, genetically tractable, system to study protein trafficking via its amenability to *in vivo* epifluorescence and multidimensional microscopy. The extensively studied uric acid/xanthine symporter, UapA, is used as a model cargo for studying the mechanisms of intracellular trafficking of fungal transporters, and for investigating the role of dimer formation in ER-exit. Additionally, selected apical markers are used to investigate the general trafficking pathways in which AP complexes are implicated.

More specifically, we elucidate the role of AP-1 in cargo trafficking and show that it is essential for growth due to its involvement in microtubule-based movement of vesicles towards the apex of growing hyphae. Furthermore, we identify clathrin-binding motifs in the C-terminal region of

the  $\beta 1$  subunit, and we provide evidence that AP-1 is involved in both anterograde sorting of RabE<sup>Rab11</sup>-labeled secretory vesicles and RabA/B<sup>Rab5</sup>-dependent endosome recycling. Additionally, AP-1 is shown to be critical for microtubule and septin organization, further rationalizing its essentiality in cells that face the challenge of cytoskeleton-dependent polarized cargo traffic.

We also show that AP-2 has a clathrin-independent essential role in polarity maintenance and growth of *A. nidulans*, which was in line with experiments showing that AP-2 does not co-localize with clathrin. We provide genetic and cellular evidence that AP-2 interacts with endocytic markers SlaB/End4 and SagA/End3 and, most importantly, the lipid flippases DnfA and DnfB, specifically in the sub-apical collar region of growing hyphae. The role of AP-2 in the maintenance of proper apical membrane lipid and cell wall composition is further supported by its functional interaction with proteins/enzymes necessary for sphingolipid biosynthesis, apical sterol-rich membrane domains formation and chitin deposition. Our findings suggest, for the first time, that the AP-2 complex of higher fungal groups, including the most threatening fungal pathogens, has acquired, in the course of evolution, a specialized clathrin-independent function necessary for fungal polar growth.

Through this work, we gain insight on the mechanisms underlying the polarized mode of life of eukaryotic cells, with potential applications to mammalian polarized cells, such as neurons. Furthermore, given the utmost importance of membrane trafficking in cell survival, new pathways are emerging in finding targeted approaches to pathogenic fungi.

**Keywords:** fungi; traffic; exocytosis; endocytosis; AP-1; AP-2; clathrin; polar growth; oligomerization; transporters; cell biology; microtubules

## ACKNOWLEDGEMENTS

First and foremost I would like to express my sincere gratitude to my advisor Professor George Diallinas, who has been a tremendous mentor for me. I appreciate his guidance, motivation, and immense knowledge that made my Ph.D. experience productive and allowed me to grow as a scientist. I am also thankful for the example he has provided as a successful professor and a restless scientist, whose enthusiasm for research was deeply inspiring and motivational. Thank you for these remarkable four years, I learned a lot from you, not only about scientific research but also about culture, history, art, evolution and life.

Besides my advisor, I would like to thank the rest of my Advisory thesis committee: Professor Spiros Efthimiopoulos and Associate Professor Ioannis Trougakos, for their support, insightful comments and encouragement during all these years. A very special gratitude goes to Prof. Efthimiopoulos, for trusting me and providing access to the facilities used for all my microscopy experiments.

My sincere thanks also goes to the members of the Examining committee, Professor C. Delidakis, Associate Professor K. Haralampidis, Assistant Professor D.J. Stravopodis and Assistant Professor N. Takeshita, for serving as my committee members.

I would also like to thank Associate Professor D. Hatzinikolaou for his precious help with affinity chromatography and gel filtration techniques, as well as for his kindness, calming presence and daily interaction.

I am grateful to Associate Professor S. Christoforidis for the impeccable hospitality in his laboratory at IMBB-Forth in the city of Ioannina and his help with TIRF microscopy experiments, despite the difficult circumstances at the time of my visit.

It is also a great honor to have met Professor Claudio Scazzocchio. He is an exceptional man, professor and scientist and I feel extremely lucky to have exchanged ideas on my research projects, with him.

I would also like to thank Dr. Sotiris Amillis, for our excellent collaboration during these four years. I am deeply grateful for his constant willingness to help in every way possible, his immense aid with molecular cloning, his numerous contributions to our research projects, as well as for the endless insightful discussions, continuous support, patience, encouragement and his friendship.

I thank my fellow labmates for all the time we spent working together in the laboratory, the discussions, team spirit, and their optimism. I wish them all the best in what lies ahead. A special thanks goes to Georgia Papadaki for her kindness, generosity, genuine interest and her friendship. The joy and enthusiasm she has for biology and research is refreshing and contagious.

I also am thankful to the Fondation Santé and the National Scholarships Foundation. Without their financial support, it would not have been possible to conduct this research, especially under the difficult economic conditions in Greece.

Completing this work would have been all the more difficult, were it not for the support and love of my family and friends. I am grateful to my parents and brother for their advice and encouragement. I would also like to thank Tassos, Katerina, Elpida and Solon for supporting me through everything, and encouraging me throughout this experience.

## CONTENTS

Περίληψη .....	vi
Abstract .....	viii
Acknowledgements .....	x
Contents .....	xii
Abbreviations .....	xiv
1. INTRODUCTION .....	1
1.1 <i>Aspergillus nidulans</i> as a model eukaryote .....	1
1.1.1 Classification .....	1
1.1.2 Life cycle of <i>A. nidulans</i> .....	3
1.1.3 Growth and development .....	6
1.1.4 Establishment of <i>A. nidulans</i> as a model system .....	7
1.2 Organization of the fungal cell wall .....	11
1.2.1 A unique feature: The cell wall .....	11
1.2.2 The fungal plasma membrane .....	13
1.2.4 Fungal nucleobase transporters .....	17
1.3 Intracellular compartments and protein traffic .....	19
1.3.1 General aspects of vesicular transport .....	19
1.3.2 Molecular mechanisms of vesicular transport .....	22
1.3.3 From the ER to Golgi: Protein synthesis, targeting and transport .....	29
1.3.4 The Golgi apparatus .....	31
1.3.5 Transport to the cell cortex: Exocytosis .....	36
1.3.6 Remodeling the plasma membrane: Endocytosis .....	39
1.3.7 Post-endocytic trafficking .....	44
1.3.8 Endocytic recycling in polar cell growth .....	47
1.3.9 Degradation Pathway .....	49
1.3.10 The cytoskeleton: General aspects and its role in fungal protein trafficking .....	52
1.3.11 Motor proteins .....	58
1.4 Aims of this study .....	60
2. MATERIALS AND METHODS .....	62
2.1 Strains, culture media, growth and storage conditions .....	62
2.1.1 Strains used in this study .....	62
2.1.2 Culture media .....	66
2.1.3 Growth and Storage conditions .....	67
2.2 Genetic crosses and progeny analysis .....	68
2.3 Epifluorescence microscopy .....	68

2.4 Nucleic acid manipulations and plasmid constructions .....	69
2.5 Transformation of <i>Aspergillus nidulans</i> .....	71
2.6 Preparation and transformation of <i>Escherichia coli</i> .....	72
2.7 Protein extraction and purification .....	73
2.8 SDS-page and Western Blot.....	75
3.RESULTS .....	76
3.1 Purine transporter di-/oligomerization is critical for ER-exit .....	76
3.2 The AP complexes are dispensable for transporter trafficking .....	80
3.3 Vesicular trafficking of apical cargoes requires the AP-1 .....	86
3.4 The AP-2 complex has a specialized clathrin-independent role .....	96
4.DISCUSSION AND FUTURE RESEARCH .....	101
5.REFERENCES .....	108
6.APPENDIX .....	143
6.1 <i>Curriculum vitae</i> .....	143
6.2 List of oligonucleotides used in this study .....	146
6.3 Reprints of original publications .....	150

## ABBREVIATIONS

ABP	Actin-Binding Proteins
ADHI	Alcohol Dehydrogenase I
ADP	Adenosine Diphosphate
AP	Adaptor Protein complex
ARTs	Arrestin-Related Trafficking adaptors
Arf	ADP-Ribosylation Factor
ATP	Adenosine-Triphosphate
bp	Base pairs
BFA	Brefeldin A
BiFC	Bifluorescence Complementation assay
BMP	Bis(Monoacylglycero)Phosphate
Br	Branching
BSA	Bovine Serum Albumin
°C	Celsius degrees
CAR	Contractile Actomyosin Ring
CCV	Clathrin-Coated Vesicle
CGN	cis- Golgi Network
ChAPs	Chs5-Arf1-binding Proteins
ChS	Chitin Synthase
CIE	Clathrin-Independent Endocytosis
CM	Complete Media
CMAC	7-amino-4-chloromethyl coumarin
CME	Clathrin-Mediated Endocytosis
CoIP	Coimmunoprecipitation
COPI	Coat Protein Complex I
COPII	Coat Protein Complex II
CORVET	Class C Core Vacuole/Endosome Tethering Complex
CSC	Cargo Selection Complex
CSD	Chitin Synthase Domain
ΔACZ	uapAΔ uapCΔ azgAΔ
Da	Dalton
DDM	Dodecyl-β-D-maltoside
DUB	De-Ubiquitinating enzyme
EE	Early Endosome
EDTA	Ethylenediaminetetraacetic Acid
EGC	Early-Golgi Cisternae
ER	Endoplasmic Reticulum
ERAD	ER-Associated Degradation
ERES	ER Exit Site
ERGIC	ER-Golgi Intermediate Compartment
ESCRT	Endosomal Sorting Complex Required for Transport
EtBr	Ethidium Bromide
EtOH	Ethanol
F	Filamentous
GAE	Gamma-Adaptin Ear
GAP	GTPase-Activating Proteins
GARP	Golgi-Associated Retrograde Protein complex



GDP	Guanosine Diphosphate
GEF	Guanine Nucleotide Exchange Factor
GFP	Green Fluorescent Protein
GGA	Golgi-localized, Gamma adaptin-ear containing, Arf-binding proteins
GPI	Glycosyl Phosphatidylinositol
GTP	Guanosine 5'-Triphosphate
h	Hour
H <sub>2</sub> O <sub>dist</sub>	Distilled water
HOPS	Homotypic Fusion and Vacuole Protein Sorting
HRP	Horse Radish Peroxidase
I	Isotropic growth
K <sub>m</sub>	Michaelis-Menten constant
Lat B	Latrunculin B
LB	Luria-Bertani
LDL	Low Density Lipoprotein
LE	Late Endosome
LGC	Late-Golgi Cisternae
min	Minute
MCC	Membrane Compartment of Can1
MHC	Major Histocompatibility Complex
MM	Minimal media
MMD	Myosin Motor-like Domain
mRFP	Monomeric Red Fluorescent Protein
MT	Microtubules
MTOC	Microtubule Organizing Center
MVB	Multivesicular Body
NAT	Nucleobase–Ascorbate Transporters
NCS1	Nucleobase Cation Symporter family 1
NCS2	Nucleobase Cation Symporter family 2
NSF	N-ethylmaleimide-sensitive fusion protein)
paba	p-aminobenzoic acid
panto	D-pantothenic acid
PC	Phosphatidylcholine
PCR	Polymerase Chain Reaction
PE	Polarity Establishment
PEt	Phosphatidylethanolamine
PG	Phosphatidylglycerol
PI	Phosphatidylinositol
PIC	Protease inhibitors cocktail
PM	Plasma Membrane
PMa	Polarity Maintenance
PRT	Purine-Related Transporter family
PS	Phosphatidylserine
pyro	Pyridoxine
ribo	Riboflavin
ROI	Region Of Interest
rpm	Rounds per minute
RT	Room Temperature
sec	Second

S	Septation
SAT	Septal Actomyosin Tangle
SDS	Sodium Dodecyl Sulfate
SDS-PAGE	Sodium Dodecyl Sulfate Polyacrylamide Gel Electrophoresis
SHD1	Sla1 Homology Domain 1
SM	Sucrose Media
SNAP	Soluble NSF Attachment Protein
SNARE	Soluble NSF Attachment Protein Receptor
SNX	Sorting Nexin BAR subcomplex
SPB	Spindle Pole Bodies
SPK	Spitzenkörper
SRD	Sterol-Rich Domains
SR	SRP Receptor
SRP	Signal Recognition Particle
SV	Secretory Vesicle
ts	Thermosensitive
T <sub>m</sub>	Melting temperature
TCA	Trichloroacetic Acid
TGN	trans-Golgi Network
TIRF	Total Internal Reflection Fluorescence microscopy
TMR	Transmembrane Receptor
TMS	Transmembrane Segment
TRAPP	Transport Protein Particles
UA	Uric Acid
Ub	Ubiquitin
UPR	Unfolded Protein Response
Ura	Uracil
UV	Ultraviolet
VFT	VPS-Fifty-Three
wt	Wild type
X	Xanthine
YAC	Yeast Artificial Chromosome
YFP	Yellow Fluorescent Protein

# CHAPTER 1

## INTRODUCTION

### 1.1 *Aspergillus nidulans* AS A MODEL EUKARYOTE

#### 1.1.1 Classification

*Aspergillus nidulans* is a homothallic filamentous fungus commonly isolated from soil, that belongs to the genus *Aspergilli*, under the phylum of Ascomycota (asco-: ασκός= sac). This is the largest phylum of the Fungi Kingdom, counting more than 64000 species, including a variety of fungi ranging from unicellular yeasts to truffles and the commonly known black and green moulds (Kirk et al., 2008). The defining morphological characteristic of Ascomycota, and thus *Aspergilli*, is the saclike structure named “ascus” which typically carries eight ascospores, formed as a product of one meiosis followed by mitotic division. The term ‘Homothallic’ describes the ability of a single organism, to reproduce sexually which means that there are no mating types.

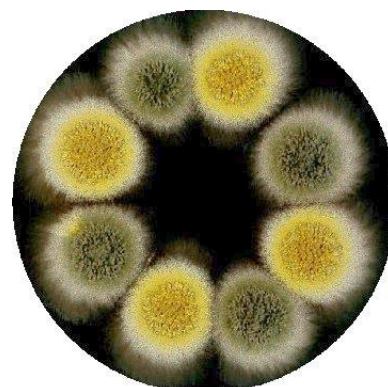


**Figure 1.1** Color mutants of *Aspergillus nidulans* grown in a petri dish (courtesy of R. Fischer, <http://www.fgsc.net/>).

The phylum Ascomycota is divided in three subphyla, based on phylogenetic analyses that took into account molecular sequence data. The subphylum Pezizomycotina (Ascomycotina) contains *A. nidulans* as well as most of the ascomycetes that form ascocarps, while the other two subphyla are the yeast-containing Saccharomycotina, with *Saccharomyces cerevisiae* being one of the most well-studied members and the basal group Taphrinomycotina (Kirk et al., 2008; Lutzoni et al., 2004).

The genus *Aspergilli* was described for the first time in 1729, by the priest and botanist Pietro Antonio Micheli, in his *Nova plantarum genera*. It received its name after *Aspergillum*, an instrument used by the Roman Catholic clergy to sprinkle holy water over the heads of the faithful. The morphology of the conidiophore, the structure that bears asexual spores, is the most important taxonomic character.

Several species of the genus *Aspergilli* are of medical and commercial importance. *A. oryzae* has been used in the East Asian cuisines for more than 2000 years for the production of local specialties, such as soyu (soy sauce), miso (fermented soybean paste) and sake (rice wine). However,

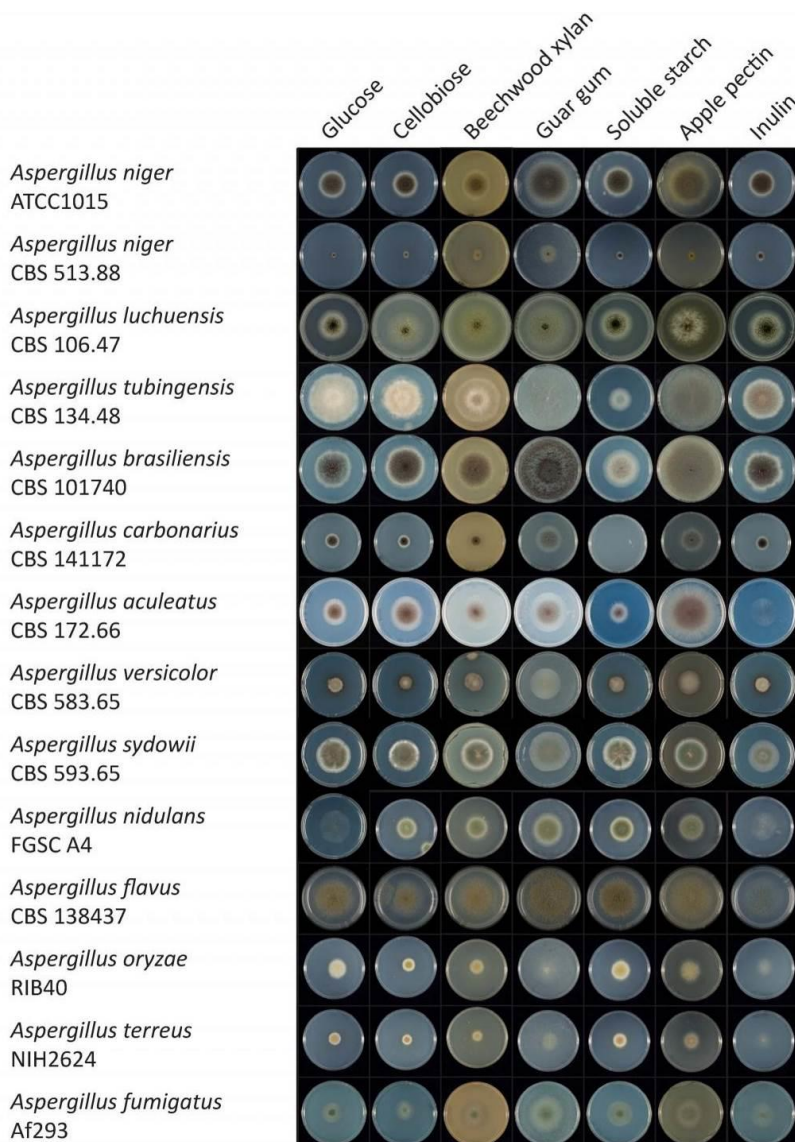


**Figure 1.2** Comparative growth of aspergilli in different culture media (Courtesy of Ad Wiebenga & Ronald de Vries, Westerdijk Fungal Biodiversity Institute, Utrecht, The Netherlands).

some *Aspergillus* species function as opportunistic pathogens, causing a group of diseases to animals, collectively known as Aspergilloses (*A. fumigatus*, *A. flavus*, *A. lentulus*). *A. flavus* produces aflatoxin B1, one of the most toxic and carcinogenic compounds ever known and is a pan-kingdom pathogen, causing serious disease in plants, insects and vertebrates (C. Scazzocchio, 2009). Fungi are more closely related to metazoans than to plants, while the modern classification of Ascomycota places *A. nidulans* in the subphylum Pezizomycotina, class Eurotiomycetes, order Eurotiales, family Aspergillaceae (Houbraken et al., 2014; Kirk et al., 2008).

The filamentous fungus *A. nidulans*, as well as many other fungal species, was initially named based on its asexual stage (anamorph) and then 'connected' to a sexual stage (teleomorph) with a different genus name. Cleistothecia are the fruiting bodies of the sexual reproductive stage of *Pezizomycotina* and contain the meiotic ascospores borne within asci. The cleistothecium producing mould had been observed before and given its own name: *Emericella*. Since 1905, the Botanical Code has allowed dual nomenclature for the same organism, depending on whether the name describes its asexual or sexual stage. When the sexual phase of an organism is discovered, this name takes precedence. According to these rules, *Aspergillus nidulans*, should be called *Emericella nidulans*, indexed as such within GenBank. However, it is most commonly referred to as *Aspergillus* (Houbraken et al., 2014).

### 1.1.2 Life cycle of *A. nidulans*

*A. nidulans* has a complex life cycle, which can be divided into three reproductive sub-cycles, the asexual, the sexual and the parasexual.

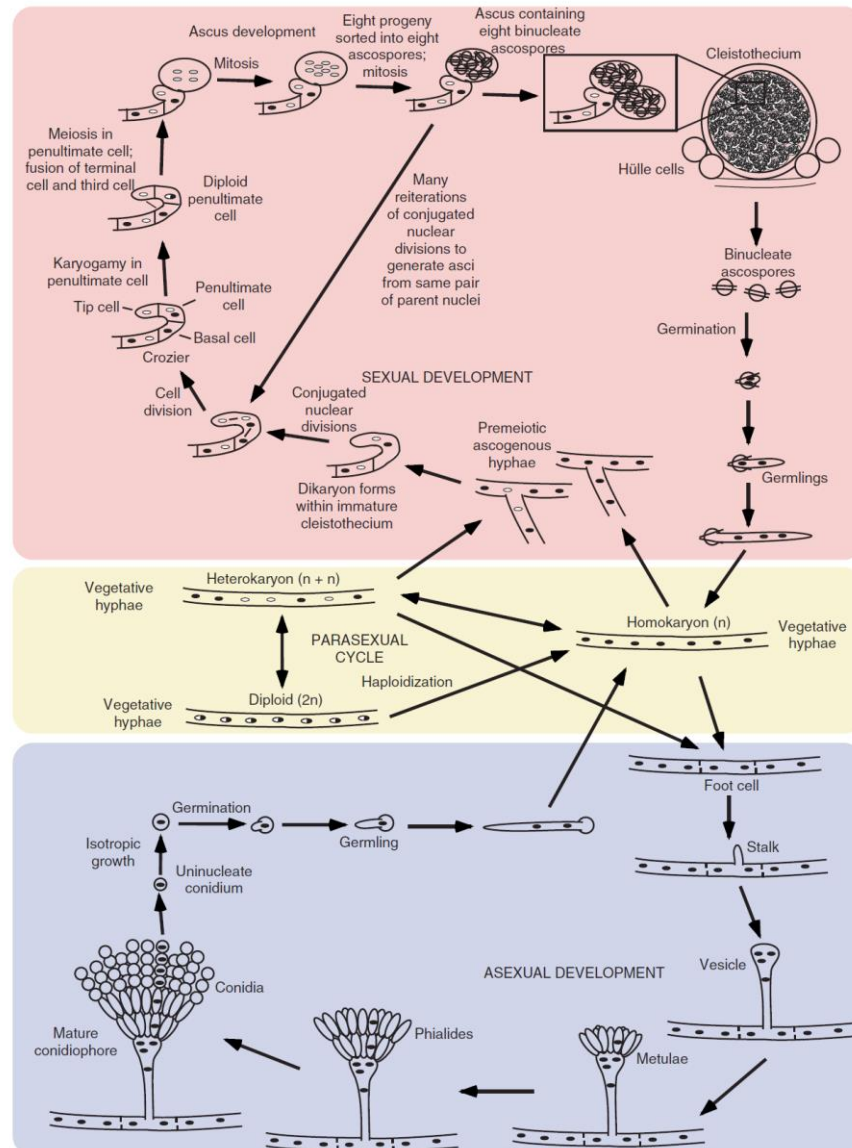


**Figure 1.3** Life cycles of *A. nidulans* (Todd et al., 2007).

The germination of dormant spores can be considered the initiating point for all three cycles. However, these spores can be either the product of a mitosis occurring during the asexual cycle, namely conidiospores, or meiotically derived during the sexual life cycle, termed ascospores. These resting spores are activated in response to proper environmental stimuli and become competent for isotropic growth, followed by polar extension and nuclear division in a process called germination.

### 1.1.2.1 Asexual reproduction

*A. nidulans* produces asexual spores for rapid distribution in the environment, but only after cells have gone through a minimum period of vegetative growth and are exposed to an air interface (Axelrod et al., 1973).

In the asexual reproductive cycle, the germination of uninucleate conidiospores leads to the formation of haploid vegetative filamentous hyphae that branch to give rise to conidiophores, on which more conidia are produced. Approximately 16 h after germination, hyphal differentiation can be macroscopically observed, followed by conidiation which becomes readily apparent 8 h later due to conidial pigmentation (Champe and Simon, 1992; Wu and Miller, 1997). This process begins with the differentiation of a thick-walled footcell, which forms an apically elongating conidiophore stalk. When apical extension ceases, expansion of the tip results in the development of the conidiophore vesicle, which gives rise to a layer of 60 primary sterigmata, called metulae. Metular budding in turn, results in the formation of an apical layer of about 120 secondary flask-shaped sterigmata, named phialides. Long chains of up to a hundred uninucleate conidiospores are produced via repeated asymmetric division of each phialide, reaching a total number of 10000 spores per conidiophores (Todd et al., 2007).

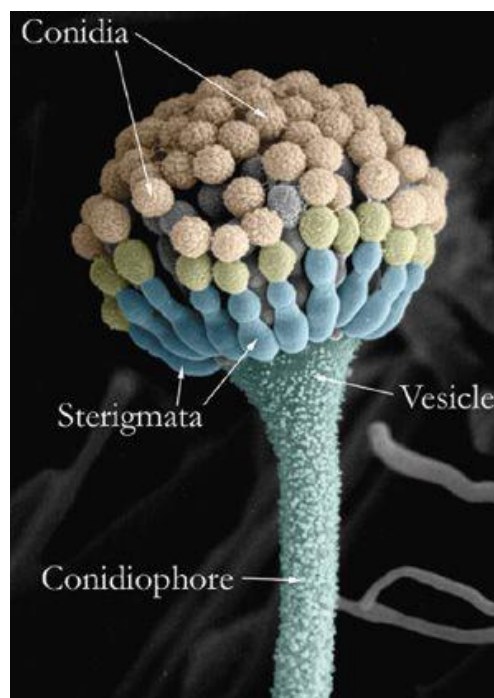


**Figure 1.4** Scanning electron micrograph of an *A. nidulans* conidiophore and attached conidia, after pseudo coloring (DeWitt, 1999).

### 1.1.2.2 Sexual reproduction

Termination of asexual reproduction and initiation of sexual sporulation begins in the center of the colony with the formation of multicellular reproductive structures, termed cleistothecia. Sexual ascospores produced therein are generally recruited for long-term survival of the fungus in soil. Various conditions such as nutrient supply or environmental stress play key roles in the initiation of sexual reproduction. This developmental process occurs inside premature cleistothecia and starts with simultaneous mitotic division of the two nuclei at the tip cell of an ascogenous hypha, in a structure called the “crozier”. Septa formation, along with the nuclear divisions, lead to the creation of a uninucleate tip cell, a binucleate penultimate cell and a uninucleate basal cell.

Enlargement of the penultimate cell and eventually, fusion of the two haploid nuclei (karyogamy) gives rise to a transient diploid zygote which undergoes meiotic and mitotic divisions to yield eight haploid binucleate ascospores, contained within an ascus. The terminal and basal cells fuse to generate a binucleate cell, which eventually forms a second ascus by repeating the process (Todd et al., 2007). The ascospore-containing asci, are dispersed in cleistothecia (cleistos: κλειστός= closed and -thekion: -θήκιον= small case) which are surrounded by thick-walled nurse cells, termed "Hülle cells" (Bruggeman et al., 2003; Swart et al., 2001). Each cleistothecium container, when mature, can contain more than 10,000 binucleate ascospores that are the meiotic progeny of one ascogenous hypha. Germination of the ascospores leads to reinitiation of the vegetative growth and continuation of the lifecycle.

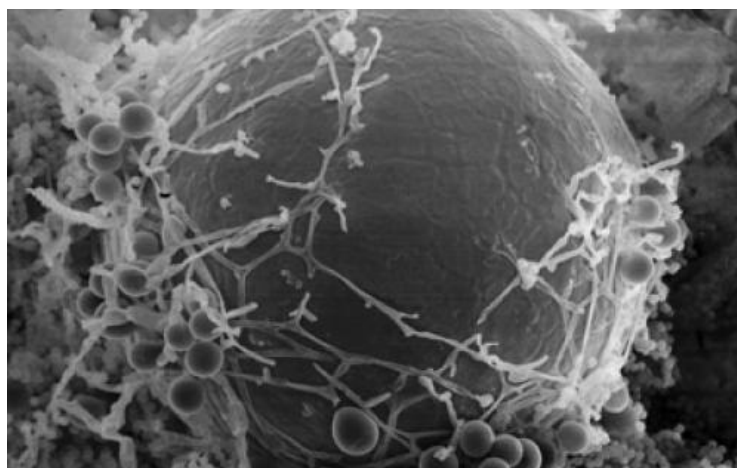


**Figure 1.5** Image of a cleistothecium container of sexual spores from *A. nidulans*, as seen by scanning electron microscopy. Notice the spherical Hülle cells on the periphery of the cleistothecium (<https://www.aspergillus.org.uk/>, courtesy of R. Fischer).

### 1.1.2.3 Parasexual reproduction

Along with the sexual cycle, *A. nidulans* also has a 'parasexual cycle'. When two different strains contribute to the creation of a mycelium through anastomoses of radially extending hyphal branches, a heterokaryon (hetero-: ἕτερος= different and -karyon: κάρυον= nucleus) is formed. The subsequent sharing of cytoplasmic material allows for mixing of the genetically distinct haploid nuclei, and fusion with a probability of  $10^{-6}$  to form relatively stable heterozygous diploid nuclei. These vegetative nuclei can give rise to a mycelium that divides mitotically via the asexual reproduction cycle. Diploid mycelia and haploid mycelia have the same architecture, but the latter contain half the number of nuclei. Spontaneous production of diploid recombinants by mitotic

crossing-over along with repeated loss of chromosomes, can lead to the generation of haploid recombinants with novel allelic combinations. Parts of the heterokaryotic mycelium are differentiated into ascogenous hyphae and undergo the sexual reproduction cycle, producing three types of cleistothecia: With either one hybrid nucleus, or one of the two parental nuclei. Classical genetics procedures are facilitated by the fact that one cleistothecium derives from only one fertilization event (Scazzocchio, 2009; Schoustra et al., 2007; Todd et al., 2007).

### 1.1.3 Growth and development

Multicellular eukaryotes face the challenge of localizing selected proteins to specific areas of their plasma membranes (PM). The subsequent morphological and functional asymmetric organization of the PM is a basic feature of cell polarity, which is fundamental for several physiological and developmental processes in a variety of organisms. Filamentous fungi provide the most prominent example of polarized cell growth, although animal embryogenesis, neuronal migration and neurite growth, cell migration, ion transport across epithelial cells, pollen tube growth and root hair development in specialized plant cells and bud emergence in *S. cerevisiae*, are also a few examples (Barnes and Polleux, 2009; Drubin and Nelson, 1996; Irazoqui and Lew, 2004; Kost et al., 1999; Rasband, 2010; Ridley et al., 2003; Tahirovic and Bradke, 2009). It is clear that germ tube emergence in filamentous fungi shares specific key features with budding in yeast (e.g. Proteins Cdc42, septins, Bni1 formin, Rho1 and Rho3), but in the former it is persistent and synchronous over an extended area, while in the latter it is sporadic and topologically limited (Momany, 2005, 2002). The growth mode of filamentous fungi is, therefore, significantly different from that of unicellular yeasts, as a switch from isotropic expansion to polar growth is necessary. Mutations in filamentous fungi polarity maintenance lead to a split tip, a phenotype never observed in yeast cells.

Fungal asexual spores (conidia) which contain a single nucleus arrested in G1 phase (Bergen and Morris, 1983) can remain in a dormant stage for years. When the spores of filamentous fungi break dormancy a consecutive order of events is initiated, leading to polar hyphal growth and mycelium formation. This series of ordered morphological events that occur during conidial germination can be separated in four stages. First, a commitment step: spore dormancy is broken due to environmental triggers such as the presence of water and air, inorganic salts, amino acids or fermentable sugars (Osherov and May, 2001). In the second phase of germination, a brief period of isotropic growth (I) results in the formation of a spherical spore with a twofold increased diameter, because of water uptake. Next, along with the first mitotic division, cell polarity is established (PE) at a marked site of the spore surface and the new germ tube is formed (Harris et al., 1999; Momany et al., 1999).



Finally, the morphogenetic machinery is redirected to the site of polarization and the axis of polarity is maintained (PMa). In filamentous fungi new material is added exclusively to the apical region (tip), resulting in an elongating germling that grows in a polar fashion. In budding yeast however, materials are dispersed and the bud grows isotropically (d'Enfert and Fontaine, 1997; Harris, 2006; Harris and Momany, 2004; Momany, 2002). After the tubular cell reaches a predetermined size, a nuclear division triggers synthesis of the first septum (S) at the base of the germ tube (Harris et al., 1994; Wolkow et al., 1996). Up to eight nuclei can be present in the same cell before

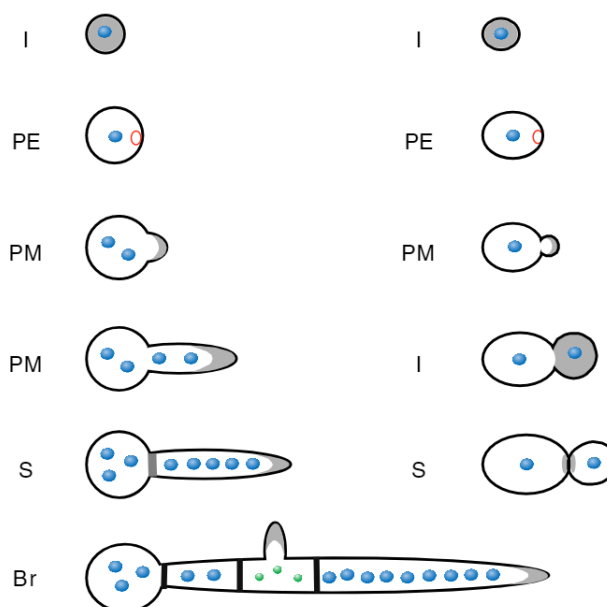


**Figure 1.6** Morphogenesis in filamentous fungi (left) and budding yeast (right). Gray areas depict isotropic growth; blue dots, interphase nuclei; green dots, mitotic nuclei; red circles, apical markers (Momany, 2002).

the appearance of the first septum. Each round of mitosis is followed by septation at regular distances along the hypha, resulting in multicellular hyphae. The nuclei in the apical compartment undergo synchronous mitosis, while those in the subapical compartments are arrested in interphase unless a branch forms. In filamentous fungi the number of nuclei per cell can vary, indicating that nuclear division may be uncoupled from polarized growth depending on environmental conditions (Wendland, 2001). In *A. nidulans*, the emergence of a second germ tube from the conidium occurs in a predictable position, most often at 180° to the first (Harris et al., 1999; Momany et al., 1999). Subapical branching (Br) establishes additional axes of polarity and leads to the formation of a network of interconnected cells, known as mycelium. The fungal mycelium can be observed macroscopically, as an amorphous collection of equivalent vegetative cells that form a radially symmetric colony expanding indefinitely at a constant rate of about 0.5mm h<sup>-1</sup> at 37°C (Lee and Adams, 1994).

#### 1.1.4 Establishment of *A. nidulans* as a model system

*A. nidulans* has emerged as a model microbial eukaryotic system for molecular biology and reverse genetics in the recent years, after being an important research tool for studying cell biology for over 70 years. It was about 1946 in Glasgow, when Guido Pontecorvo selected *A. nidulans*, as the

ideal genetic organism to raise the 'resolving power of genetic analysis'. Genetic crossing techniques and transformation protocols were developed in 1953 and 1983 respectively, while in 2005 it was one of the first organisms to have its genome sequenced in a collaboration between Monsanto and the Broad Institute (Galagan et al., 2005). It is 30 million base pairs in size and predicted to contain around 9,500 protein-coding genes on eight well-marked chromosomes with many color, auxotrophic and drug resistance markers. Its genes can be cloned, altered, disrupted, expressed under the control of regulatable promoters or deleted at will, in an integrative fashion at their normal locus or any other location in the genome (Morris and Enos, 1992), as isolated protoplasts can be efficiently and stably transformed. Uninucleate conidiospores are a useful tool in the direct screening of transformants, by plating on appropriate media. Any two strains of the homothallic fungus can be mated and although *A. nidulans* is normally haploid, it can be induced to grow as heterokaryon or as a stable vegetative diploid, useful for complementation analysis of mutations or detectable growth delay phenotypes under a variety of nutritional conditions. It can also serve as a host strain for the heterologous expression of genes isolated from other organisms, including even higher eukaryotes (Argyrou et al., 2001; Goudela et al., 2008). Moreover, *A. nidulans* grows rapidly on inexpensive solid or liquid media and produces conidia or ascospores that can be properly stored for long periods, at low temperatures. Colony morphology on solid media can reveal the genetic background of each inoculated strain, based on its distinct phenotype (shape, colour, sporulation) and thus provide vital information on the essentiality of genes studied. *A. nidulans* is closely related to a large number of other *Aspergillus* species of commercial and medical importance, such as *A. niger*, *A. oryzae*, *A. flavus*, and *A. fumigatus*, which have only asexual cycle (anamorph) but are exploited experimentally using methods and technologies developed for *A. nidulans* (Scazzocchio, 2006). The filamentous fungus has many beneficial traits to display, even when compared to the more extensively studied, *S. cerevisiae*. Notwithstanding the fact it has almost twice the number of genes of budding yeast, it lacks genetic redundancy, as it has not undergone genome duplication and therefore, gene insertion or deletion can be performed by a single transformation step with no need for further crossing or progeny analysis. Additionally, the orthologues of human and *A. nidulans* show a higher level of similarity than that between human and *S. cerevisiae*. The ease of sample preparation and the large size of extending hyphae facilitate *in vivo* studies with widefield, TIRF, confocal and superresolution fluorescent microscopic imaging. The organelles are more dispersed than in the unicellular yeasts and chimeric protein molecules of interest, tagged with fluorescent epitopes can be easily constructed with molecular cloning and generation of stable transformants.

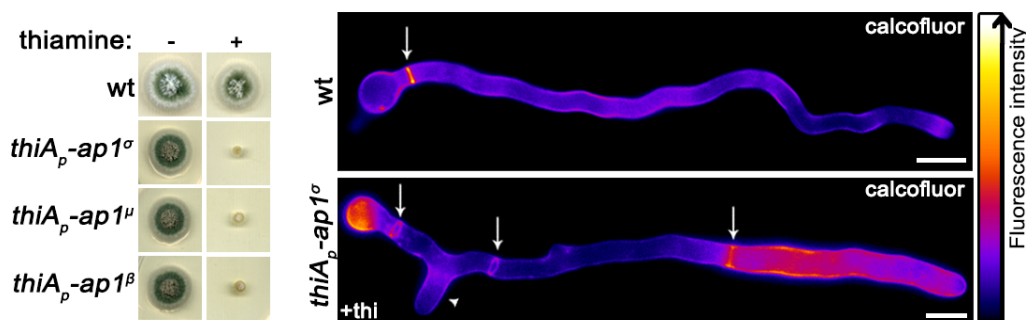


**Figure 1.7** Examples of growth tests (left panel) and microscopic observation of *A.nidulans* hyphae (right panel). Notice the reduced colony diameter, as a result of the use of a regulatable *thiA<sub>p</sub>* promoter for an essential gene. In the epifluorescence microscopy image, cell wall is stained with calcofluor and a ‘Fire’ Lookup Table is applied. For more details see Results (Martzoukou et al., 2018).

Last but not least, what absolutely distinguishes *A. nidulans* is the hyphal polar growth by apical extension, a process highly demanding in specialized molecular mechanisms for rapid protein trafficking and recycling, resembling the ones found in the polar cells of higher eukaryotes, such as neurons. The biological properties of *A. nidulans*, with its amenability to *in vivo* multidimensional microscopy and tractable genetic tools, make it ideally suited for basic biological research (Alexopoulos et al., 1996).

### 1.1.5 Fungal catabolic pathways

Nutrient utilization pathways increase the metabolic versatility of filamentous fungi, enabling them to utilize a surprisingly diverse array of complex compounds as alternative sources of nutrients, although fungi do not commonly encounter many of these. Expression upon demand of the appropriate catabolic pathways can be critical for survival under limited nutrient supply, but constitutive gene expression would lead to unnecessary loss of cellular resources. *A. nidulans* has the ability of utilizing a wide range of substances as carbon and/or nitrogen sources under the control of complex regulatory systems and thus, was used as a model system in the early 60s for the identification of the genes involved in secondary nitrogen catabolic pathways and the elucidation of the mechanisms underlying their genetic expression. For example, nitrate, nitrite, ammonium and most amino acids can be used as nitrogen sources but not all nitrogen sources are used in the same preference. Specific primary nitrogenous compounds such as ammonia, glutamine, glutamate and asparagine, are preferentially used, whereas secondary nitrogen sources are utilized in a highly regulated manner and only when the primary are unavailable (Caddick et al., 2006; Marzluf, 1997).

Purines, but not pyrimidines, can also be utilized as nitrogen sources in most microorganisms, including *Aspergilli* (de Koning and Diallinas, 2000). Characterization of the first eukaryotic transcription factors (UaY, NirA, CreA, AreA), revealed that genes for certain fungal

metabolic pathways share regulatory mechanisms of expression (Keller and Hohnt, 1997; Scazzocchio et al., 1982). Activation of the catabolic pathways in the presence of a substrate or an intermediate of the corresponding pathway is controlled at the level of transcription, but also requires a de-repression signal, occurring in the absence of a primary source (Marzluf, 1997).

AreA is a global transcription factor acting positively in synergy with the specific regulators such as NirA or UaY (Arst and Cove, 1973; Ravagnani et al., 1997; Scazzocchio et al., 1982). In *A. nidulans*, the complete purine utilization pathway has been described (Gournas et al., 2011) and it is highly conserved in most filamentous fungi, bacteria and plants, whereas most yeasts have degenerate variations of the purine degradation pathway (Pantazopoulou and Diallynas, 2007). Ammonium and glutamine are excellent nitrogen sources and their presence in the medium results in the repression of nitrogen secondary catabolic pathways (Caddick, 2004; C. Scazzocchio, 2009). Moreover, in the ethanol catabolism pathway, the alcohol dehydrogenase (ADHI) encoded by *alcA*, is induced by the presence of ethanol and repressed by the presence of CreA. CreA acts as a genuine repressor in the presence of favored carbon sources, competing with the binding of the pathway-specific factors (Lockington et al., 1987; C. Scazzocchio, 2009). Proline utilization is controlled in a similar manner, via PrnA-mediated positive regulation of pathway-specific gene expression (Cazelle et al., 1998). The genes involved in proline utilization are repressed efficiently only in the simultaneous presence of both repressing nitrogen and carbon sources, such as ammonium ions/glutamine that repress AreA and glucose that induces CreA, respectively (Gonzalez et al., 1997). However, when a carbon and a nitrogen primary source are absent, proline can serve as both sources (Arst and Cove, 1973; Scazzocchio, 1992). This multilevel regulation ensures that nutrient utilization pathways can respond to the demands of general cellular metabolism and the presence of specific pathway inducers.

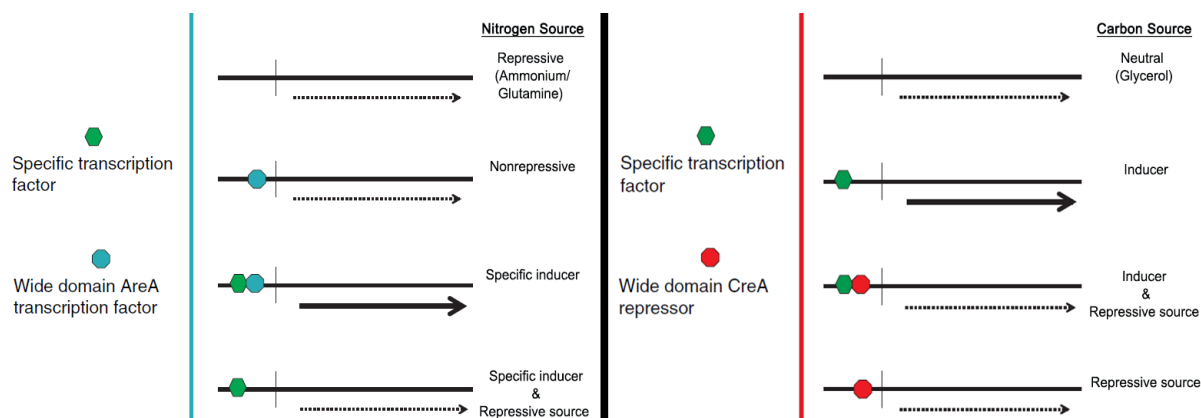


**Figure 1.8** General schemes for the transcriptional regulation of genes involved in the utilization of nitrogen sources (left panel) and carbon sources (right panel). The transcription factors AreA and CreA mediate nitrogen catabolite repression (NCR) and carbon metabolite repression (CMR), respectively. AreA is an activator, negated by the presence of ammonium/glutamine, whereas CreA is a repressor, activated by a repressive carbon source such as glucose (Adapted from Scazzocchio, 2009).

## 1.2 ORGANIZATION OF THE FUNGAL CELL WALL

### 1.2.1 A unique feature: The cell wall

The PM of fungi is covered by a thick cell wall, a complex and dynamic structure. Cell walls are essential for fungal viability and morphogenesis, while their unique biochemistry and absence of most of their conserved components in mammalian cells, make them excellent targets for antifungal agents (Gow, 2016; Latgé, 2007). Almost all fungal walls are designed in a similar way, with a unique structure that determines the cell shape and makes extremely difficult the lysis of the cell, without causing significant damage to the organelles. This problem was solved with the discovery of cell wall degrading enzymes produced in the gut juice of the snail *Helix pomatia* and later on by *Trichoderma spp.* The cell wall also serves as the site of several enzymes involved in nutrient exchange and component redistribution, such as carbohydrates. From a chemical viewpoint, fungal cell walls and plant cell walls are completely different. Although cellulose can be detected in some fungal walls, these organisms (Oomycete and Myxogastria) are not considered “True Fungi” due to their important biochemical differences. Thus, the chemical composition of the cell wall is closely correlated with the taxonomic classification of fungi.

The fungal cell wall is composed of 80-90% polysaccharides, which form a robust scaffold to which a variety of glycoproteins and other components are added, such as melanin pigments and waxes (Kendrick, 1992). The main cell wall component in Dikarya is chitin, a homopolymer of  $\beta$ -(1,4)-N-Acetylglucosamine, which self-associates to form microfibrils. It is generated by the integral cytoplasmic membrane synthases that translocate the polymeric product through the PM (Bowman and Free, 2006). Because chitin synthesis primarily occurs at the sites of active growth (tip, septa) it is regulated both temporally and spatially. Fungal chitin synthases are membrane-attached proteins with several transmembrane regions and can be divided into seven classes and three divisions (Fukuda et al., 2009; Lenardon et al., 2010). Class I, II, and III chitin synthases (ChS) belong to division I and class IV, V, and VI belong to division II. Notably, Class III, V and VI families are restricted to filamentous fungi, suggesting that they may play unique roles in polarized growth (Bowen et al., 1992; Specht et al., 1996; Takeshita et al., 2015).

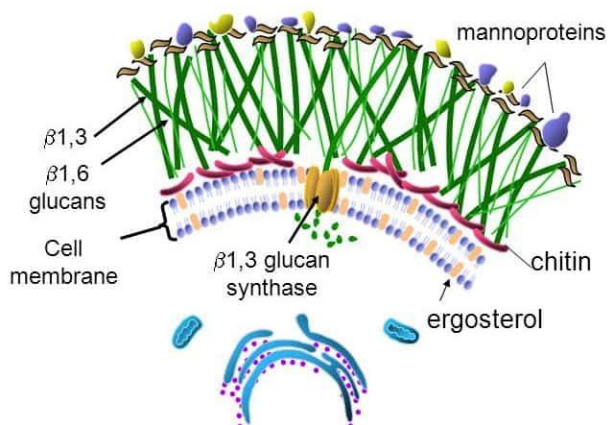


**Figure 1.9** Components and organization of the fungal cell wall (Merck & Co, 2001).

The six ChS genes isolated from *A. nidulans* are: *chsA*, *chsB*, *chsC*, *chsD*, *csmA* and *csmB*; these gene products belong to classes II, III, I, IV, V, and VI, respectively and play common roles in chitin biosynthesis: ChsA is involved with ChsC in septum formation and conidiation. Disruption of the *csmA* gene (class V) of *A. nidulans* results in chitin deficient cells that lyse in conventional medium. Disruption of the *chsD* gene (class IV) leads to a chitin deficiency during vegetative growth that is equal to that of *csmA* disruptants but the cells are not prone to lysis. CsmA and CsmB consist of a C-terminal chitin synthase domain (CSD) and an N-terminal myosin motor-like domain (MMD).

ChsB does not substantially contribute to the rigidity of the cell wall, but is necessary for normal branched growth and conidiation (Borgia et al., 1996; Bowen et al., 1992; Fujiwara et al., 1997; Fukuda et al., 2009; Motoyama et al., 1997, 1994; Specht et al., 1996; Takeshita et al., 2015).

Glucose polymers, mostly  $\beta(1,3)$  and  $\beta(1,6)$  glucans, are also synthesized by transmembrane glucan synthase enzymes and provide rigidity to the cell wall. This polymer is absent in mammals yet necessary for viability in yeast, which led to the development of effective antifungal drugs targeting its synthesis (Kartsonis et al., 2003). Moreover, structural glycosylated proteins (mannoproteins or mannans), are important cell wall components. Genomic as well as drug studies have shown that inhibition of cell wall synthases can lead to phenotypic changes, such as altered morphology or even fungal death (Banks et al., 2005; Latgé, 2007).

The unique mechanical and biological properties of the fungal walls are determined not only by their chemical composition but also by the ordered structure of the cell wall components. Microfibrillar components, such as  $\beta$ -glucan and chitin are mostly located on the inner surface of the cell wall, embedded in an amorphous matrix of polysaccharide and protein-polysaccharide. The porosity of cell wall serves as an important regulator of nutrient uptake and excretion, setting the size limit for enzyme release to around 20 kDa. During vegetative growth, the apical walls are transformed to less porous lateral walls, which causes a reduced excretion rate of exoenzymes

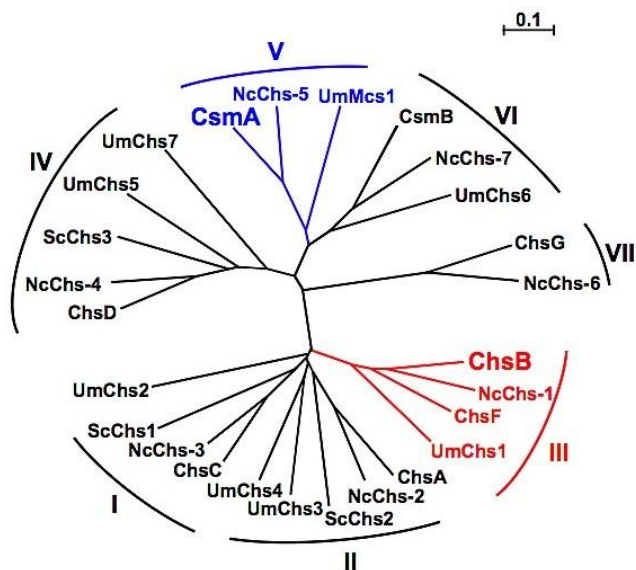


**Figure 1.10** Phylogenetic tree of the fungal chitin synthases. Class III and V synthases are shown in red and blue, respectively. Nc: *N. crassa*; Sc: *S. cerevisiae*; Um: *U. maydis* (Takeshita et al., 2015).

(Chang and Trevithick, 1974). The high rate of apical extension (1  $\mu\text{m}/\text{min}$ ) requires rapid cell wall formation, whereas cell wall damage leads to the activation of sophisticated mechanisms for wall repair, to avoid catastrophic breaching of the integrity of the surface. Understanding how the hyphal tip cell regulates intracellular traffic to address these challenges is important, and as apical growth requires localization of cell-wall-modifying enzymes to tip cells, the class III chitin synthase ChsB has emerged as a novel membrane cargo for the study of traffic mechanisms and vesicular transport (Hernández-González et al., 2018; Zhou et al., 2018).

### 1.2.2 The fungal plasma membrane

All cells share a universal feature: They are enclosed in a selective barrier, the Plasma Membrane (PM). This allows the cell to maintain its integrity, to concentrate the nutrients it gathers and retain the products it synthesizes, while excreting waste materials. At the subcellular level, functionally and chemically distinct lipid membranes also enclose the different organelles of the eukaryotic cell (ER, Golgi apparatus, mitochondria, nucleus etc). However, all biological membranes share a common general structure, of a very thin continuous lipid bilayer with embedded protein molecules, held together via noncovalent interactions. Most water-soluble molecules cannot permeate the lipid barrier, a process facilitated by membrane proteins that span the lipid bilayer.

#### 1.2.2.1 Lipid composition

The overall architecture of the fungal cell membrane is similar to that of the general eukaryotic cell membrane. Amphipathic lipids constitute about 50% of the mass of most membranes, with the most abundant category being the phospholipids. Biological membranes of fungi are enriched with a variety of lipids belonging to the class glycerophospholipids, sphingolipids (glycosphingolipids and sphingomyelin) and sterols. Glycerophospholipids have a backbone of glycerol-3-phosphate containing two fatty acyl chains along with various substituents like ethanolamine, serine and choline, while sphingolipids are composed of ceramide, which is N-acetylated phytosphingosine.

Biosynthesis of sphingolipids is required for cell cycle progression and the establishment and maintenance of cell polarity via control of the actin cytoskeleton in *A. nidulans*, while the complete pathway was studied and reported in the pathogenic *A. fumigatus* (Alcazar-Fuoli and Mellado, 2013; Cheng et al., 2001). Phospholipids like phosphatidic acid, phosphatidylcholine (PC), phosphatidylethanolamine (PEt), phosphatidylserine (PS), phosphatidylglycerol (PG), phosphatidylinositol (PI), cardiolipin and sphingomyelins (Sphingophospholipids: Inositol phosphate

ceramide, mannosyl-inositolphosphate-ceramide and mannosyl-diinositolphosphate-ceramide), are reported as cell membrane components in *S. cerevisiae* (van der Rest et al., 1995).

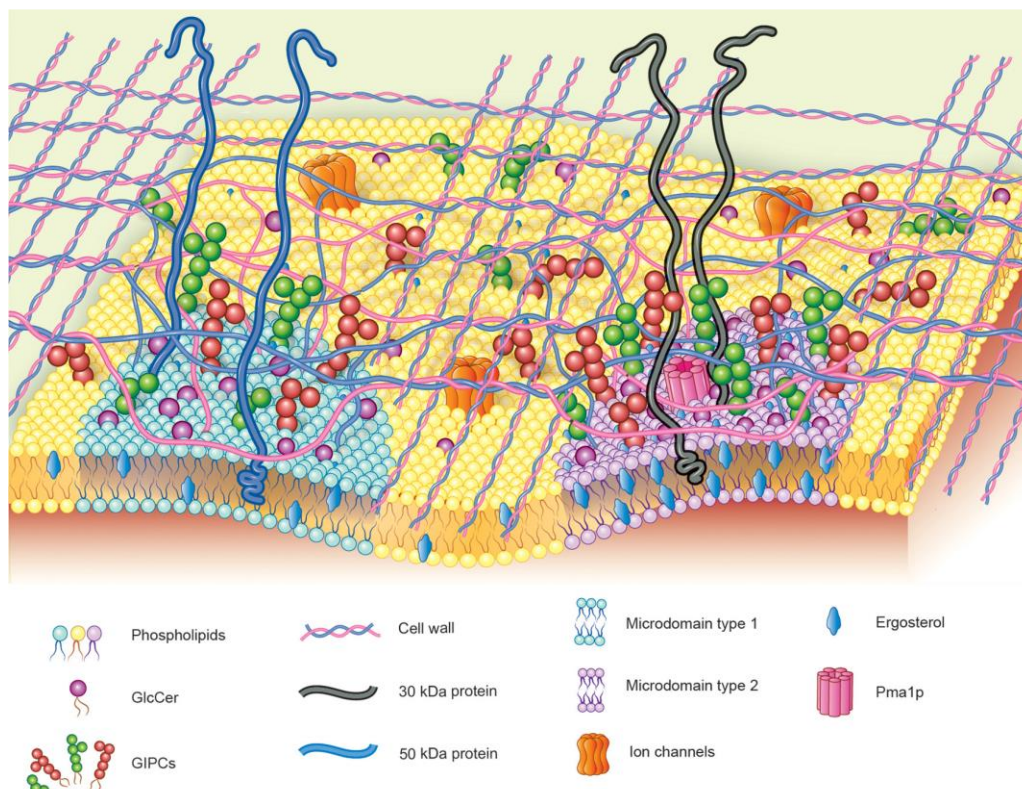


**Figure 1.11** Scheme of the fungal plasma membrane structure. Two types of microdomains are depicted, with and without ergosterol (Guimarães et al., 2014).

Sterols, also known as steroid alcohols are amphipathic lipids featuring rigid and compact ring structures. Cholesterol is the main animal sterol, but the fungal cell membrane typically contains ergosterol as the main component (Dupont et al., 2012). The most common method to study the effects of sphingolipid or ergosterol depletion in trafficking is to express the protein of interest in mutant strains altered in the relevant biosynthetic pathways. However, most of these mutants are lethal in *A. nidulans*. The viable temperature sensitive mutation *basA1<sup>ts</sup>* is an exception, where a block in sphingolipid biosynthesis occurs only at the non-permissive temperature (42 °C; Li et al., 2007). Alternative ways of sphingolipid or ergosterol depletion are based on specific drugs that target these molecules or their biosynthetic pathway, such as azoles and myriocin that block ergosterol and sphingolipid biosynthesis, respectively. Ergosterol presence affects the membrane fluidity of the fungi, thus the aforementioned drugs disintegrate the membrane and act as fungicides (Sant et al., 2016).



### 1.2.2.2 Microdomains of the Plasma Membrane

Plasma membrane microdomains, such as lipid rafts and caveolae have been reported in mammalian cells, however thus far there are no genes associated with the later in filamentous fungi. Lipid rafts are membrane microenvironments enriched in saturated phospholipids, sphingolipids, and sterol (Simons and Ikonen, 1997), thought to play important roles in various dynamic processes such as protein sorting, cell polarity, signal transduction and regulation of the activity of membrane proteins. In the plasma membranes of fungi, sterol-rich domains (SRDs) that are much larger than lipid rafts can be readily detected upon staining with filipin III, a fluorescent sterol-binding dye. Apical SRDs are observed at sites of polarized morphogenesis in *A. nidulans* and are regulated in a developmental manner. Their formation might be a result of lipid raft clustering, in which MesA and FloA, the microdomain scaffolding protein flotillin, are most likely involved (Alvarez et al., 2007; Pearson et al., 2004; Takeshita et al., 2012). Other known fungal membrane microdomains are MCC/eisosomes (MCC: Membrane compartment of Can1), static sites with punctate distribution across the PM implicated in nutrient-regulated protection from endocytosis (Gournas et al., 2018).

### 1.2.2.3 Assymetry of the lipid bilayer

Individual lipid molecules (e.g. phospholipids) are able to move inside the lipid bilayer in three possible ways. The first type of movement is rotational, meaning that the phospholipid rotates on its axis, which enables interactions with its immediate neighbors. The second type is lateral movement, where the phospholipid moves around in one leaflet, providing the membrane with a fluid structure (Luckey, 2008). Finally, it is possible for phospholipids to undergo transverse movement, moving between both leaflets of the bilayer in a “flip-flop” manner (Gurtovenko and Vattulainen, 2007). The lipid compositions of the inner and outer monolayers are strikingly different in many membranes, reflecting the different functions of the two faces of the lipid bilayer. Transverse movement is what allows the lipid asymmetry to be maintained through the catalyzed, ATP-dependent movement of phospholipids by lipid translocator proteins. Floppases move PC and sphingomyelin from the inner to the outer leaflet, while flippases predominantly transport in the opposite direction the negatively charged PS and to a lesser extent PEt, in order to maintain the charge gradient between the two monolayers. Enrichment of negatively charged PS at the cytosolic leaflet induces membrane curvature and promotes association with adaptor proteins, thus facilitating protein sorting and vesicle budding. Two well-studied lipid flippases of *A. nidulans* are the Type4 P-Type ATPases, DnfA and DnfB, which localize to sites of growth and endocytosis in the fungus (Schultzhaus et al., 2015, 2017; Schultzhaus and Shaw, 2016).

### 1.2.2.4 Membrane proteins

Protein molecules that span the lipid bilayer perform most of the specific functions of the membrane, such as transporting specific molecules across it, serving as links between the PM and the cytoskeleton or catalyzing enzymatic reactions. Embedded in the lipid bilayer are integral membrane proteins (transmembrane or monotopic), while peripheral membrane proteins are only temporarily associated with the surface of the bilayer or with other integral proteins. They are able to perform only rotational and lateral movement, but there is no transverse movement of proteins between the leaflets. Integral membrane proteins are tightly embedded in the lipid bilayer, whereas peripheral membrane proteins associate with their required leaflet.

The energy requirements to move either type of membrane protein across the bilayer would be excessive. Many different membrane proteins are necessary for proper cell function, a fact reflected in two numbers. Firstly, they represent about a third of the proteins found in living organisms (Engel and Gaub, 2008) and secondly, in a typical plasma membrane, proteins account for about 50% (w/w) of its mass (Luckey, 2008). Membrane proteins perform several essential cellular functions, regulated via a variety of membrane protein interactions. Major families of proteins found in the plasma membrane include membrane transport proteins, proteins involved in signal transduction, cell wall and cytoskeleton synthesis (Douglas and Konopka, 2016).

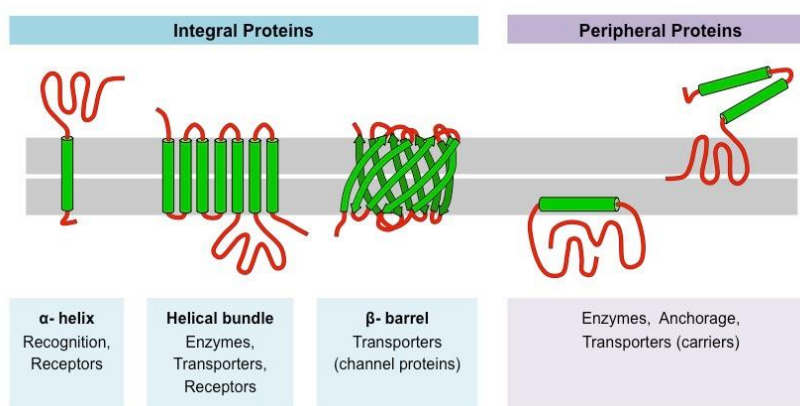


**Figure 1.12** Types of membrane proteins based on their structure (Raj and Mahalekshmi, 2018).

Transport membrane proteins such as pumps, channels/pores and transporters facilitate the transport of small ions and water-soluble molecules across cell membranes. Their biological importance is reflected by the observation that all known genomes include at least 5-20% genes coding for such proteins (<http://www.membranetransport.org/>). The importance of transport membrane proteins is also revealed from the fact that more than 60 human genetic diseases are caused by the malfunctioning of transporters and channels ([http://www.tcdb.org/disease\\_explore.php](http://www.tcdb.org/disease_explore.php)). Transmembrane receptors recognize and respond to

chemical signals and initiate specific cellular responses, typically through associated proteins. Membrane proteins are targeted by about 60% of approved drugs, because of their central role in almost every physiological process (Salom and Palczewski, 2011; Yildirim et al., 2007).

#### 1.2.4 Fungal nucleobase transporters

The fungal nucleobase-specific transporters are secondary active transporters that can be sorted into three evolutionary distinct protein families, based on cloning and genome sequencing (de Koning and Diallinas, 2000; Hyde et al., 2001). All of these families are catalysing the symport of purines with protons, but show a huge diversity of amino acid sequences, 3D structures and substrates. The first and most important family is the nucleobase-ascorbate transporter family (Nucleobase Ascorbate Transporters, NAT/Nucleobase Cation Symporters 2, NCS2) with homologues in archaea, Gram-negative and Gram-positive bacteria, diatoms, fungi, plants and animals. Members of NAT/NCS2 in *A. nidulans* catalyze the symport of uric acid and xanthine with protons (Argyrou et al., 2001; Diallinas et al., 1995; Karatza and Frillingos, 2005; Pantazopoulou and Diallinas, 2007).

Another recently studied family is the nucleobase cation symporter family 1 (NCS1), also known as the purine-related transporter family (PRT). Restricted to prokaryotes, fungi and plants and including transporters for purines, cytosine, uridine, allantoin, pyridoxine or thiamine (Kryptou et al., 2015, 2012; Papadaki et al., 2017; Sioupouli et al., 2017). Last but not least, the AzgA-like family with homologues in bacteria, archaea, fungi and plants that symport hypoxanthine–adenine–guanine and protons.

In general, secondary active transporters are integral membrane proteins with 4-14 transmembrane  $\alpha$ -helices, connected with intracellular and extracellular loops. Some transporters form dimers (e.g. bacterial  $\text{Na}^+$ /Leu symporter LeuT; Yamashita *et al.*, 2005), although there are examples of monomers (e.g. bacterial  $\text{H}^+$ /lactose symporter LacY; Abramson et al., 2003) or trimers (e.g. bacterial  $\text{Na}^+$ /aspartate symporter GltPh; Yernool et al., 2004). Crystallization of a few transporters has been achieved, in the presence of native or artificial substrates bound in the center of each monomer. As far as function is concerned, transport is described by Michaelis-Menten kinetics, similar to enzymatic reactions. Transporters are “saturable”, meaning that at high substrate concentrations all of the transporter molecules have their binding sites occupied and the rate of transport reaches a maximum ( $V_{\max}$ ). Each transporter protein binds specific substrates and has a different affinity constant ( $K_m$ ) for each of those substrates that is equal to the concentration of the solute when the transport velocity is half its maximum value.

### 1.2.4.1 The NAT/NCS2 family

The NAT/NCS2 family consists of over one hundred currently sequenced proteins, recognized by the conserved NAT signature motif, [Q/E/P]-N-X-G-X-X-X-T-[R/K/G] (Koukaki et al., 2005). Members of the family are usually 414-650 amino acids long and typically contain 14  $\alpha$ -helical transmembrane segments (TMSs) and cytoplasmic N- and C-termini. Most functionally characterized NATs recognize oxidized purines such as uric acid and xanthine, or uracil (only in bacteria), while all known bacterial, fungal and plant members are high-affinity H<sup>+</sup> symporters. However, SVCTs, two closely related mammalian members of the family, cotransport L-ascorbic acid (Vitamin C) and Na<sup>+</sup> (Diallinas and Gournas, 2008; Kourkoulou et al., 2018; Liang et al., 2001).

*A. nidulans* has two NAT members, namely UapA and UapC, both extensively characterized in terms of regulation of expression and structure–function relationships. UapC is a 580 amino acid long, very similar paralogue of UapA (62% identity), with a high affinity for xanthine and a moderate affinity for uric acid (Diallinas et al., 1995; Ravagnani et al., 1997; Valdez-Taubas et al., 2000, 2004). UapA on the other hand, is a high affinity (7-8  $\mu$ M), high capacity proton symporter, specific for the uptake of uric acid and xanthine, with a collection of more than two hundred mutants available and a recently revealed crystal structure at a resolution of 3.7 Å (Alguel et al., 2016). Kinetic studies combined with classical or reverse genetic approaches, had already pointed to specific amino acid residues that are involved in purine specificity, binding and transport, before solving the crystal structure. A few years before that, the first crystal structure of another member of the NAT family,

the uracil/H<sup>+</sup> symporter UraA from *Escherichia coli*, was also published (Lu et al., 2011). Based on its crystal structure, UapA has cytoplasmic N- and C-termini and contains 14 TMSs spatially arranged into a 7+7 fold, divided into a core domain (TMS 1–4 and 8–11) and a gate domain (TMS 5–7 and 12–14). Both UraA and UapA form dimers and most likely function by an elevator mechanism (Alguel et al., 2016; Yu et al., 2017), whereas recent experimental evidence reveals the importance of lipid binding for the stabilization of UapA in its dimeric form (Pyle et al., 2018). Eukaryotic NATs are highly regulated at the

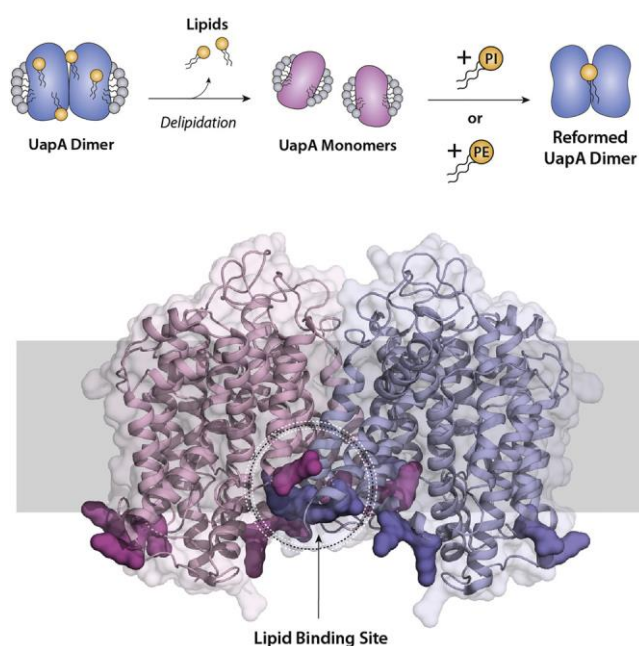


**Figure 1.13** Scheme highlighting the role of structural lipids in UapA dimer formation (Pyle et al., 2018).

transcriptional and post-translational level, in response to physiological and developmental signals. In fungi, post-translational control is mainly achieved by constant endocytosis and ammonium or substrate-elicited endocytosis, via ubiquitination and vacuolar targeting for degradation (Diallinas and Gournas, 2008; Gournas et al., 2010)

## 1.3 INTRACELLULAR COMPARTMENTS AND PROTEIN TRAFFIC

### 1.3.1 General aspects of vesicular transport

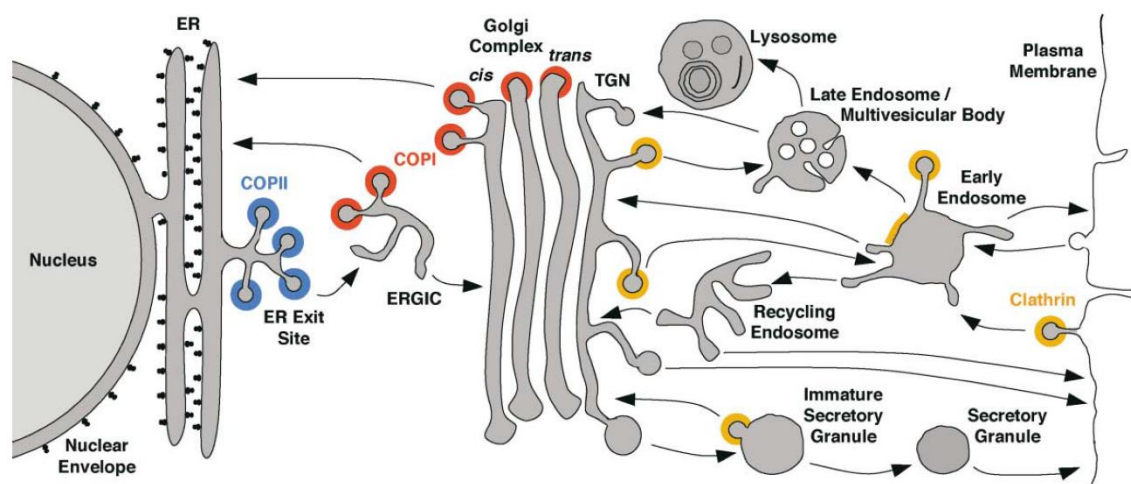


**Figure 1.14** Overview of intracellular trafficking pathways (Bonifacino and Glick, 2004).

Cellular function is based on the continuous trafficking of molecules between various subcellular compartments. In eukaryotic cells, the membrane proteins must be transported to their proper and specific destinations without disturbing the integrity of intracellular compartments. The presence and abundance of proteins on the plasma membrane (PM) is regulated by secretion of proteins (exocytosis, or anterograde trafficking), internalization and subsequent recycling or degradation of proteins (endocytosis or retrograde trafficking), and movement from one location on the PM to another (transcytosis).

The secretory pathway leads outward from the Endoplasmic Reticulum (ER) to the Golgi apparatus and cell surface, with a quality control route leading to lysosomes/vacuoles (Barlowe and Helenius, 2016). The long sub-cellular journey of exocytosis, is dynamically controlled in response to multiple and overlapping developmental and physiological signals, rather than being a default process (Coutinho et al., 2004; Dunne et al., 2002; Farhan et al., 2008; Forster et al., 2006; Schotman et al., 2009). Such signals not only promote or arrest exocytosis of a protein towards its target

membrane, but can also promote its rapid endocytosis from the plasma membrane, towards the cell interior, which can lead to degradation in the vacuole or recycling back to the cell surface. However, retrieval routes do exist, maintaining the backflow of selected components. Intracellular trafficking of membrane cargoes is performed with selected transport vesicles that have a specific protein and lipid composition.

During this process, small spherical transport vesicles or bigger randomly shaped organellar fragments carry proteins between the different compartments along highly organized, directional routes. Cargo proteins can be either soluble, derived from the lumen of a donor compartment as vesicles bud from its membrane, or transmembrane, stably embedded in the lipid bilayer. Transport is followed by vesicle fusion with the target compartment, while the original orientation of both proteins and lipids is preserved. Lipid composition is dynamically controlled in response to various signals. A dedicated system of kinases and phosphatases produce and hydrolyse specific phosphoinositides, including PtdIns(4,5)P on plasma membranes, PtdIns3P on early endosomes, PtdIns(3,5)P on late endosomes and PtdIns4P on the trans-Golgi network (Blumental-Perry et al., 2006; Feigenson, 2006). These lipids identify membranes of endocytic vesicles and allow them to recruit cytosolic proteins, involved in vesicular trafficking (van Meer et al., 2008). Early endosomal membranes resemble the PM, but when maturing to late endosomes, a decrease in sterols and phosphatidylserine (PS) is prominent, along with a significant rise in bis(monoacylglycero)phosphate (BMP) (Kobayashi et al., 2002). Fungal plasma membranes are enriched in sphingolipids and ergosterol, whereas enrichment of sphingolipids and sterols along the secretory pathway predicts their preferential incorporation into anterograde vesicles (Proszynski et al., 2005).

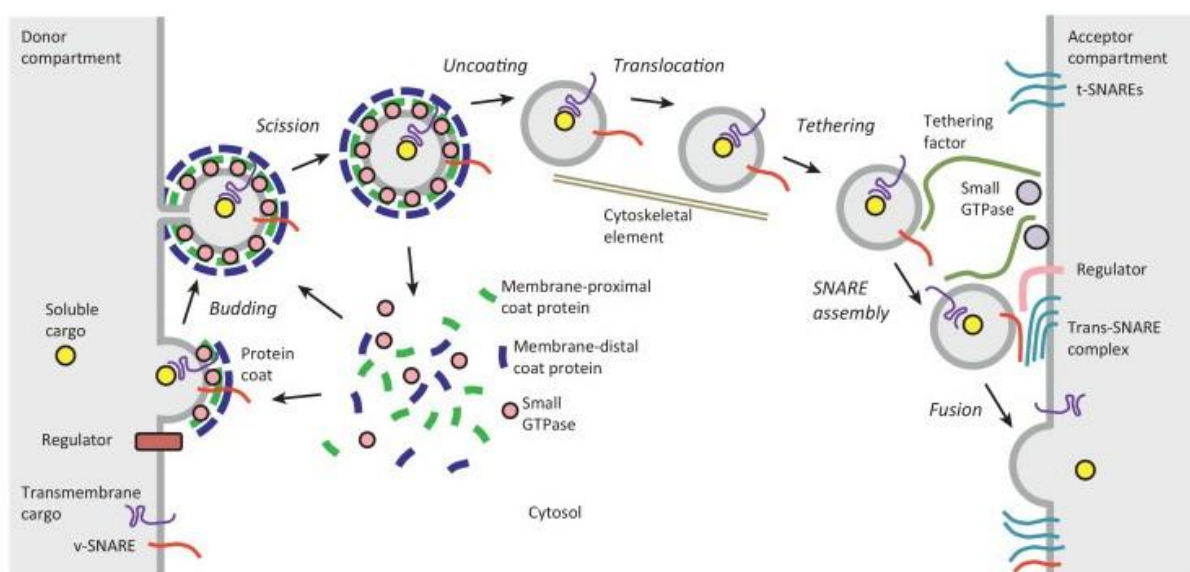


**Figure 1.15** Steps of vesicle budding and fusion (Bonifacino, 2014).

These emerge from their sites of formation, bud by scission and are subsequently targeted to a specific “acceptor” compartment, where they dock at and fuse with the target membrane. The final fusion of a transport vesicle involves many distinct steps, which are coordinated with the mediation of groups of accessory proteins, the majority of which are located in the cytoplasm at the periphery of the transport vesicle. These include coat proteins, as well as a number of adaptor complexes that appear to be involved in the binding of vesicles to the target-organelle (Bonifacino, 2014; Bonifacino and Glick, 2004).

The coat proteins are recruited onto the donor membrane, where they select the vesicle cargo and at the same time assemble into a scaffold for vesicle budding. In these processes, both cis-acting elements on the cargo proteins and trans-acting factors need to be orchestrated in a sequential manner to achieve proper trafficking. Therefore, selection and transport of the protein cargo to and from the plasma membrane also depends largely on specific organelle targeting signals within the proteins themselves, as each newly synthesized organelle protein must find its way to its final target organelle (Barlowe, 2003; Giraudo and Maccioni, 2003). The sorting of a protein begins with protein synthesis on a cytoplasmic ribosome and ends when the final destination is reached. When sorting signals that determine the trafficking and eventual location of proteins are contained in their amino acid sequence, polypeptides are guided from the cytosol into the nucleus, the ER, mitochondria, peroxisomes or other subcellular destinations. At each intermediate compartment, a decision is made as to whether the protein is to be retained there, or moved further.

An integral component of cellular trafficking, the cytoskeleton, plays a pivotal role in protein transport as the vesicles and endosomes move on microtubules or actin filaments. Movement from the emerging site of the vesicles to their final destination is called anterograde transport, while the opposite direction is called retrograde transport. In animals and filamentous fungi, but not in yeasts, microtubules (MTs) function as tracks in the subcellular transport of membrane-bound vesicles, and this process is propelled by their associated motor proteins (kinesin, dynein). The two pathways are interrelated in each intracellular trafficking step, while the importance of retrograde transport is significant in the recycling of various proteins and lipids (Riquelme et al., 2018; Xiang and Plamann, 2003).

In *A. nidulans* and other filamentous fungi, vesicular recycling seems to play a key role in establishing and maintaining the polar growth of elongating hyphae. New material is added via exocytosis exclusively to a specific membrane site, the apex, resulting in an extending tubular cell, the hypha. At the tip of growing hyphae, a position occupied by the so-called Spitzenkörper (SPK), there is a dense collection of vesicles, actin and microtubules (Riquelme and Sánchez-León, 2014; Steinberg et al., 2017; Taheri-Talesh et al., 2008). SPK is thought to organize vesicles bound for

fusion with the membrane at the hyphal tip and provide the membrane for tip growth. Hyphal tip cells characteristically gather their endocytic patches in a slightly subapical “collar” region. Because exocytosis predominates in the apex, a recycling pathway coupling subapical endocytosis with apex-directed exocytosis, polarizes cargoes. Thus, endocytosis is fundamental not only for the turnover of proteins, but also for the dynamic processes that recycle these proteins back to the PM (Tokarev et al., 2009).

Biochemical and genetic analyses have contributed in the elucidation of the molecular mechanisms involved in vesicular cargo transport, a process during which, vesicles that originate from a donor compartment dock at and fuse with a different acceptor compartment. Protein coats and Adaptor Proteins mediate the selection of cargoes and the formation of vesicles, while their targeting to the proper destination and fusion depend on specialized proteins, including Rabs and SNAREs. Precision in the control of these processes makes efficient cargo transfer possible, while preserving the identity of organelles (Bonifacino and Glick, 2004).

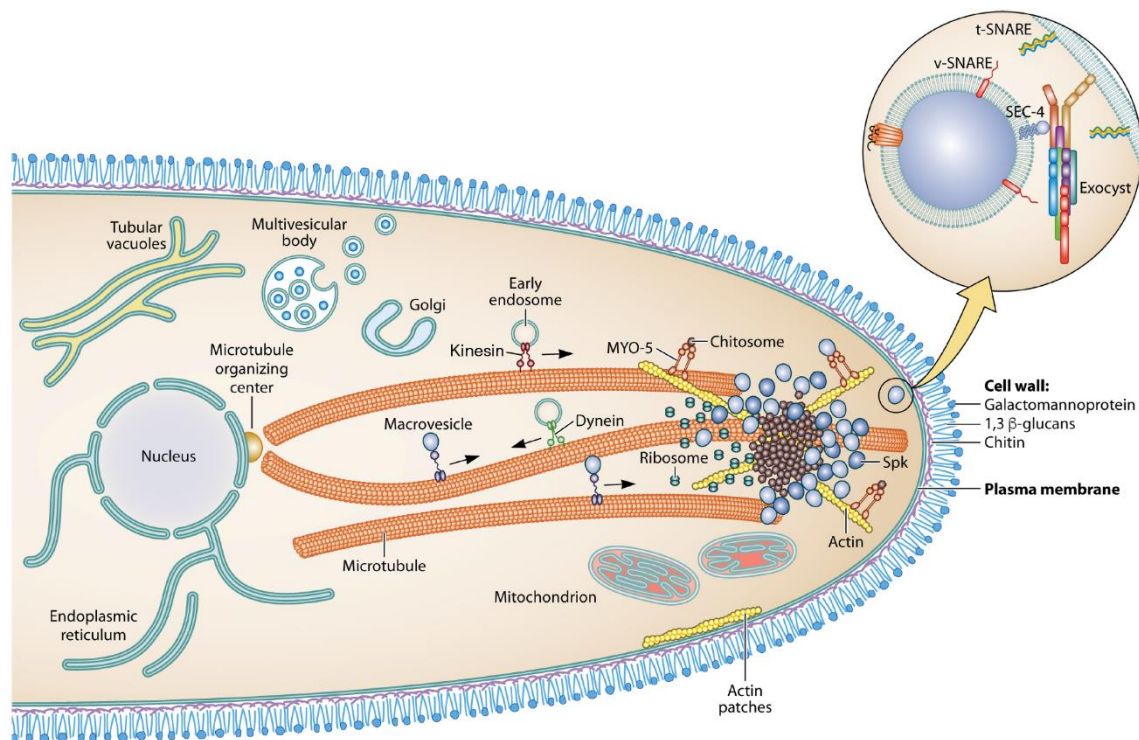


**Figure 1.16** Scheme of a fungal hyphal tip. Different vesicle populations accumulate at the Spitzenkörper (Spk). The main organelles of the secretory pathway and the microtubule and actin cytoskeletons, along with motor proteins, are displayed. The circle (top right) shows a macrovesicle carrying  $\beta$ -1,3-glucan synthase and the protein complexes required for vesicle fusion with the plasma membrane (Adapted from Riquelme, 2018).

### 1.3.2 Molecular mechanisms of vesicular transport

#### 1.3.2.1 Vesicle coats



The segregation of proteins into separate membrane domains is accomplished by assembling a special protein layer on the cytoplasmic face of the membrane, the coat. Most transport vesicles are formed from these specialized, coated regions, budding off as vesicles with a distinctive set of proteins covering their cytoplasmic surface. Coat discard precedes vesicle fusion with a target membrane, so that the two cytosolic sides of the membranes can interact directly and fuse. The coat performs two main functions, concentrating specific cargo proteins in a specialized patch and molding the forming vesicle. In this way, it selects the appropriate molecules for transport and encloses them inside the right carrier. Coat protein assembly, results in the formation of a curved cage-like lattice that shapes the vesicle by bending the membrane patch. This explains why vesicular carriers with the same type of coat often have a relatively uniform size and shape. The three distinct types of coated vesicles participate in different trafficking routes and are classified based on their surface proteins into Clathrin-coated, COPI-coated, and COPII-coated (Faini et al., 2013).

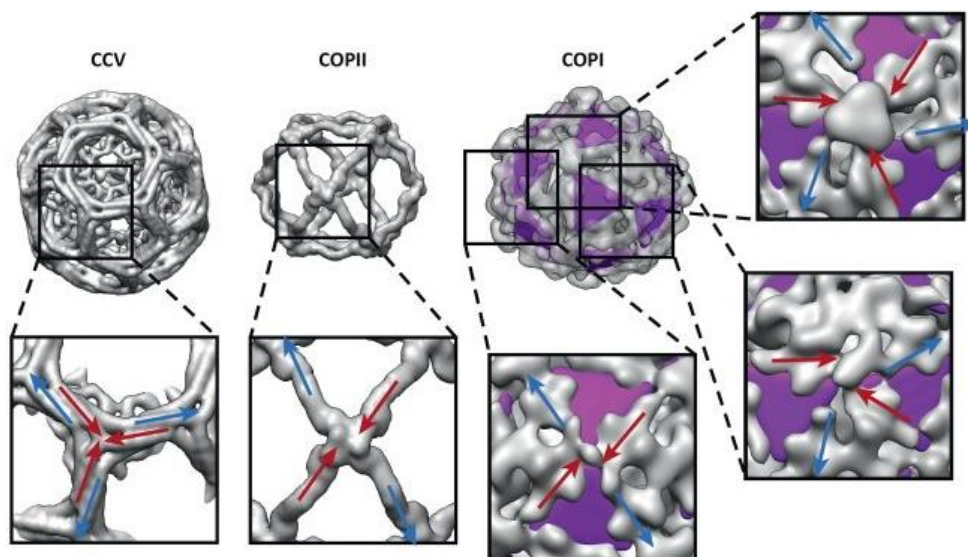


**Figure 1.17** Structural overview of the three main coats participating in intracellular transport pathways: clathrin, COPII, and COPI (Faini et al., 2013).

Clathrin-coated vesicles mediate transport from the Golgi and from the plasma membrane, whereas coatomers (COPI, COPII) mediate ER to Golgi transport, as well as intra-Golgi and the reverse Golgi to ER transport of dilysine-tagged proteins. COPII-coated vesicles bud from the ER and COPI-coated vesicles bud from the Golgi apparatus (Barlowe et al., 1994; Lee et al., 2004). They are hetero-oligomers composed of at least an alpha, beta, beta', gamma, delta, epsilon and zeta subunits that reversibly associate with Golgi vesicles to mediate protein transport and for budding from Golgi membranes (Gomez-Navarro and Miller, 2016; Stenbeck et al., 1993). For several coats, small GTP-binding proteins such as members of the ADP-ribosylation factor (Arf) family, as well as phosphoinositides, function as docking sites to initiate coat assembly for adaptor proteins. In turn,

the adaptors bind to scaffolding coat proteins, to accessory proteins that regulate coat function and to sorting signals in cargo transmembrane proteins that mediate their concentration in the coated membrane domains (Bonifacino, 2004; Bonifacino and Traub, 2003; Kirchhausen, 2000; Slepnev and De Camilli, 2000). The major component of clathrin coated vesicles (CCVs), is clathrin itself. CCVs emerge and appear to move in two directions, from the plasma membrane to the early endosomes and from the trans-Golgi network (TGN) to the endosomes. Native non-assembled clathrin exists as a three-legged structure called a triskelion. Each triskelion is composed of three clathrin heavy chains interacting at their C-termini. Each of the ~190kDa heavy chains has a ~25kDa light chain tightly bound to it. Heavy chains are involved in the formation of a clathrin “cage-like” structure and the three light ones in its stabilization (Kirchhausen, 2000; Robinson, 2015). Clathrin was recently visualized for the first time in *A. nidulans* and localized to three distinct subcellular sites: late Golgi cisternae (trans-Golgi equivalents of filamentous fungi), the endocytic collar (region of concentrated endocytosis just behind the hyphal apex) and in fast, long-range moving small puncta in nearly all hyphal compartments (Schultzhaus et al., 2017a).

### **1.3.2.2 Adaptors**

In addition to clathrin, the heterotetrameric Adaptor Proteins (APs) contribute to coat assembly by linking clathrin to the membrane, selecting the vesicle cargo and recruiting accessory proteins that regulate vesicle formation. Another major type of clathrin adaptor complexes are the monomeric GGA adaptors (Golgi-localized, Gamma adaptin-ear containing, Arf-binding proteins) (Bonifacino, 2004; Bonifacino and Lippincott-Schwartz, 2003; Robinson and Bonifacino, 2001).

AP complexes and especially AP-1 and AP-2, are the most important type of adaptors for the formation of clathrin-coated vesicles in most eukaryotes. They play key roles in the selection, traffic, endocytosis and recycling of membrane cargoes, whilst the presence of additional functional adaptors and clathrin is indispensable for the homeostasis and survival of all eukaryotic cells. AP-1 in several organisms but mostly in mammals, mediates the anterograde and/or retrograde transport between the TGN and endosomes, while AP-2 is involved in trafficking from the PM to the interior of the cell. A third AP complex, AP-3, has been implicated in direct transport between the Golgi and vacuoles thus bypassing the endosomes, while at least some of its functions are independent of clathrin (Dell’Angelica et al., 1998; Peden et al., 2004). The AP-4 and AP-5 complexes may be able to function independently of clathrin, and their roles in sorting pathways are rather specialized or minor (e.g. fungi do not have AP-4 or AP-5) (Hirst et al., 2011; Robinson and Bonifacino, 2001). Interestingly however, in light of the discoveries of the past 10 years, the existence of specialized clathrin-independent trafficking pathways has also been proposed, but their role remains somehow

controversial (Epp et al., 2013; Howes et al., 2010; Mayor and Pagano, 2007; Sandvig et al., 2011). All AP complexes are heterotetramers and consist of two large subunits (adaptins), the  $\beta$  subunit and the more divergent  $\gamma$ ,  $\alpha$ ,  $\delta$  or  $\epsilon$  subunit (100-140kDa), a medium ( $\mu$ ) subunit (~50kDa), and a small ( $\sigma$ ) subunit (~ 20kDa). The carboxy-terminal domains of the two large subunits project as 'ears' or 'appendage' domains, connected by flexible 'hinges' to the 'core' of the complex which consists of the medium and small subunits and the amino-terminal domains of the two large subunits. Yeast two-hybrid experiments have shown that the  $\gamma/\alpha/\delta/\epsilon$  subunits interact with the  $\sigma$  subunits, the  $\beta$  subunits interact with the  $\mu$  subunits and that the two large subunits interact with each other. Repression of expression of any AP subunit, has been reported to inactivate the function of the full complex (Guo et al., 2014).

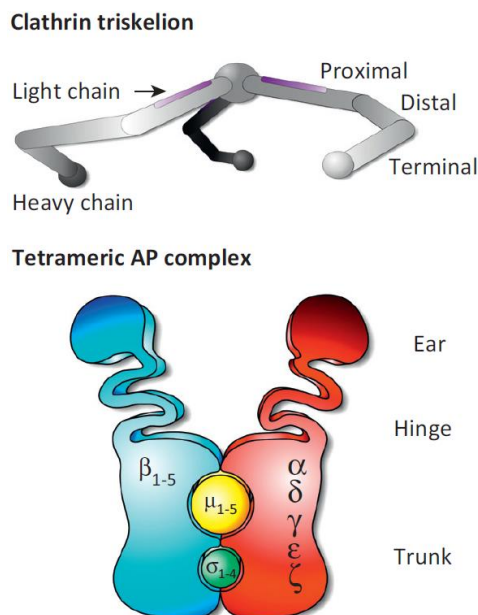


**Figure 1.18** A typical triskelion and a tetrameric AP complex (Robinson and Pimpl, 2014).

The  $\beta$  subunits are particularly important for clathrin recognition and binding, while clathrin-binding consensus sequences (L[L,I][D,E,N][L,F][D,E]) have been identified in the hinge domains of both  $\beta 1$  and  $\beta 2$  (clathrin box). The  $\mu$  and  $\beta$  subunits have been implicated in cargo selection. The  $\sigma$  subunit is necessary for the stabilization of the complex. The  $\alpha$  and  $\beta$  ear domains, recruit accessory proteins onto the membrane, where they participate in events such as vesicle scission and vesicle uncoating. The core domains also bind sorting signals that are contained in the cytosolic tails of cargo transmembrane proteins. AP-1 complex is linked to the TGN and endosomal membranes, and in most cases its role is indissolubly associated with clathrin. However, there is still some question about the directionality and/or the identity of the acceptor compartment, that is, whether AP-1 is involved in TGN-to-endosome traffic, endosome-to-TGN traffic, or both (Robinson, 2015).

The GGA clathrin adaptors belong to a family of abundantly expressed, Arf-dependent proteins responsible for the sorting of mannose-6-phosphate receptors between the TGN and endosomes. Their structure is that of a four-domain monomer with functions similar to those of the AP subunits: an N-terminal VHS (Vps27p/Hrs/Stam) domain, a GAT (GGA and TOM) domain, a hinge region, and a C-terminal GAE (gamma-adaptin ear) domain. The GAE domain is homologous to the C-terminal domain of the  $\gamma 1$ - and  $\gamma 2$ -adaptin subunit isoforms of AP-1, being responsible for the recruitment of accessory proteins that regulate clathrin-mediated endocytosis. Mammalian cells have three essential GGAs (GGA1, GGA2, GGA3) and yeast has two genes (Gga1 and Gga2). Double

knockout of Gga1 and Gga2 affects trafficking from TGN to the vacuole, while the single deletions have no detectable effect (Bonifacino, 2004; Guo et al., 2014).

Arf (ADP-ribosylation factor) proteins are a group of small GTP-binding proteins of the Ras superfamily that have important roles in the regulation of membrane traffic and the actin cytoskeleton, several of which are localized at the trans-Golgi network. Three classes of Arf proteins have been described in human, consisting of Arf1 and Arf3 (class I), Arf4 and Arf5 (class II), and Arf6 (class III). Class I Arfs, participate in the formation of intracellular transport vesicles and the selection of cargo, by recruiting to membranes various coat proteins such as the GGAs, AP-1, AP-3, AP-4, COPI and by activating lipid-modifying enzymes (Guo et al., 2014). Based on *in silico* analysis, it is predicted that *A. nidulans* encodes for six Arf family proteins. ArfA participates in hyphal growth through the secretory system, while ArfB shares similarity with ARF6 of *Homo sapiens* and Arf3p of *Saccharomyces cerevisiae* and functions in endocytosis, playing important roles in polarity establishment and maintenance during hyphal growth (Lee and Shaw, 2008a, 2008b). However, AP-complexes and GGAs have not been studied in filamentous fungi, while little is known about the role of Arfs in hyphal growth.

The activity of Arfs is regulated by specific guanine nucleotide exchange factors (GEFs) and GTPase-activating proteins (GAPs), that convert Arfs to their GTP-bound (active) and GDP-bound (inactive) forms and direct their specific activation and inactivation, respectively, at different cellular sites. Golgi Arf-GEFs belong to two subfamilies conserved across eukaryotes: GBF/Gea and BIG/Sec7. *A. nidulans* possesses only one homologue of the early Golgi Gea subfamily, *geaA*, and one of the late Golgi Sec7 subfamily, *hypB* (Arst et al., 2014).

### **1.3.2.3 Rabs**

The specialization of transport and fusion of transport vesicles and endosomes seems to be achieved by special regulatory mechanisms of trafficking, involving family members of SNAREs and Rabs. Vesicles are likely to encounter many potential target membranes before reaching their final destination, therefore, specificity is ensured with the recognition between surface markers on the vesicle and complementary receptors on the target membrane. Rab proteins play a key role in the specificity of vesicular transport, by ensuring the direction of the vesicle to specific spots on the target membrane. Like Arfs, they are also monomeric GTPases, associated with one or more membrane-enclosed organelles of the secretory or endocytic pathways. Rabs function as molecular markers on both vesicular and target membranes, regulating the assembly of other protein complexes such as Rab effectors. RAB GTPases and their GAP and GEF regulators, are major determinants of protein and lipid composition of membranous compartments (Behnia and Munro, 2005). Additional regulators can be motor proteins that propel vesicles along the cytoskeleton,

tethering proteins that link two membranes located more than 200 nm apart, or SNAREs that mediate membrane fusion. The same Rabs can associate with multiple effectors in a cooperative manner, which results in the formation of specialized membrane patches. The mammalian Rab5 for example, upon activation by Rab5-GEF, binds to endosomal membranes and participates in the binding of incoming CCVs. Rab7 has been localized to late endosomes and shown to be important in the late endocytic pathway, as it can replace Rab5 during transport from early to late endosomes, committing the cargo for degradation. Additionally, Rab11 and Rab4 mediate Golgi exit of secretory vesicles that traffic through the TGN to the PM, or recycling of vesicles derived from the endosome, respectively. In *A. nidulans*, two paralogues and several orthologues of human Rabs have been identified and/or characterized, such as RabA<sup>Rab5</sup>, RabB<sup>Rab5</sup>, RabC<sup>Rab6</sup>, RabD<sup>Rab8</sup>, RabE<sup>Rab11</sup>, RabF<sup>Rab4</sup>, RabO<sup>Rab1</sup>, RabS<sup>Rab7</sup>, RabT<sup>Rab2</sup>. Their functions in *A. nidulans* are summarized below (Table 1.1).

<i>A. nidulans</i>	Yeast homolog	Mammalian homolog	Localization	Function
RabA	Vps21	Rab5	Early endosomes	EE trafficking
RabB	Vps21	Rab5	Early endosomes	EE trafficking
RabC	Ypt6	Rab6	Early Golgi Late Golgi SPK	intra- Golgi (retrograde traffic) Endosome-to-Golgi (retrograde traffic) Secretion
RabD	Sec4	Rab8	SPK	<i>unknown</i>
RabE	Ypt31	Rab11	post Golgi Secretory vesicles SPK	exocytosis (anterograde traffic)
RabF	Ypt32	Rab4	<i>unknown</i>	<i>unknown</i>
RabO	Ypt1	Rab1	Early Golgi Late Golgi SPK	Autophagosome biogenesis ER-to-Golgi (anterograde traffic)
RabS	Ypt7	Rab7	Late endosomes Vacuoles	vacuolar biogenesis
RabT	Ypt31	Rab2	<i>unknown</i>	<i>unknown</i>

**Table 1.1** *S. cerevisiae* and mammalian homologs, subcellular localization and function of all Rab GTPases present in the genome of *A. nidulans* (Abenza et al., 2009, 2010, 2012; Pantazopoulou et al., 2014; Pantazopoulou and Peñalva, 2011; Pinar et al., 2013a; 2013b).

In *S. cerevisiae* and *A. nidulans*, anterograde Golgi traffic is governed by Rab1 and Rab11 homologues. Rab1 homologues (Ypt1 and RabO, respectively) (Jedd et al., 1995; Pinar et al., 2013a) mediate biogenesis of Golgi cisternae and anterograde traffic across them, while Rab11 homologues (Ypt31/Ypt32 and RabE, respectively) mediate the budding of exocytic carriers and control their transport to the PM (Jedd et al., 1997; Pantazopoulou et al., 2014).

### 1.3.2.4 SNAREs

Members of the SNARE family of membrane proteins are among the cargoes transported in vesicles (Kuehn et al., 1998; Ramakrishnan et al., 2012; Rein et al., 2002), also serving as catalysts of membrane fusion (Söllner et al., 1993). Thus, SNARE proteins have a double role, in both vesicle formation and fusion. Each transport step in the cell uses a specific set of SNAREs, and thus their packaging into vesicles is one important way to convey vesicle identity and ensure fusion at the correct target membrane (Rothman et al., 2000). The formation of SNARE bundles on vesicular and target membranes, provides the energy to fuse the appropriate membranes. However, additional components are also necessary to guarantee that vesicles will find their right target membrane (Brandhorst et al., 2006). These ‘tethering factors’ participate in the necessary membrane contact prior to membrane fusion (Cao et al., 1998; Whyte and Munro, 2002), through their association with specific membrane proteins or phospholipids.

All SNARE proteins have a highly conserved core structure, forming tetrameric complementary complexes that consist mostly of three SNAREs on the target membrane (t-SNAREs) and one SNARE on the vesicle membrane (v-SNARE). In *A. nidulans*, the mammalian synaptobrevin homologue, SynA, is a v-SNARE protein and SsoA is its complementary t-SNARE, both mediating fusion at the level of the PM (Taheri-Talesh et al., 2008). TlgB is also a t-SNARE, labeling the late Golgi compartment and mediating endosomal traffic in the retrograde pathway (Abeliovich et al., 1998; Amessou et al.,

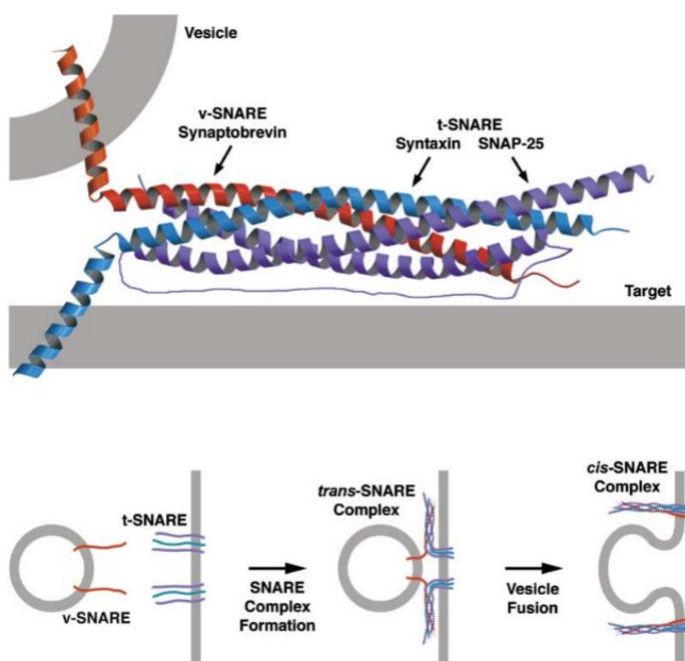


**Figure 1.19** Scheme of the structure and function of SNAREs. Syntaxin and SNAP-25 are t-SNARE subunits (Bonifacino and Glick, 2004).

2007; López-Berges et al., 2016). SedV is another t-SNARE, located at the early Golgi (Pantazopoulou and Peñalva, 2011). Compared to SNAREs, the tethering factors are a much more heterogeneous group of proteins. Tethering complexes interact with SNAREs and/or GTPases to regulate the specificity of vesicle fusion, but can also interact with coat complexes (Angers and Merz, 2011; Trahey and Hay, 2010). For normal vesicular transport to occur, vesicles must incorporate the appropriate complement of SNARE and Rab proteins in their membrane.

### 1.3.3 From the ER to Golgi: Protein synthesis, targeting and transport

The ER has a central role in lipid and transmembrane protein biosynthesis, for most of the cellular organelles including the ER itself, Golgi, vacuoles, endosomes and secretory vesicles. ER produces the bulk of the structural phospholipids and ergosterol in fungi, while the Golgi specializes in sphingolipid biosynthesis. Phosphoinositides participate in signalling and recognition, defining organelle identity and recruiting both soluble and membrane proteins to specific membranes, whereas sphingolipids may have an important role in the sorting of membrane proteins and lipids between the ER, the plasma membrane and endosomes or vacuoles, through lipid rafts (van Meer et al., 2008).

Secreted as well as soluble proteins destined for the lumen of the ER, Golgi and vacuoles, are first imported to the ER from the cytosol, while polytopic membrane proteins such as transporters, are co-translationally integrated in the ER membrane. This mechanistic step seems to be driven by the energy of polypeptide synthesis in the ribosome and several sequence-independent, amphipathicity-dependent, cis-acting elements on the protein itself. Transmembrane proteins possessing signal sequences are recognized at the ribosome by the signal recognition particle (SRP) while they are still undergoing synthesis. mRNA molecules encoding endomembrane resident proteins might alternatively be localized to the rough ER via interactions between an ER-localized mRNA binding protein (mRNA-BP) and sequence motifs in the mRNA. In both cases, this elicits their delivery to the ER protein translocation channel (Sec61), through interaction with the SRP receptor (SR $\alpha$  and SR $\beta$  subunits) where they start to fold and are subsequently released laterally into the ER membrane (Fewell and Brodsky, 2000; Gilmore and Mandon, 2012). Although the basic mechanism

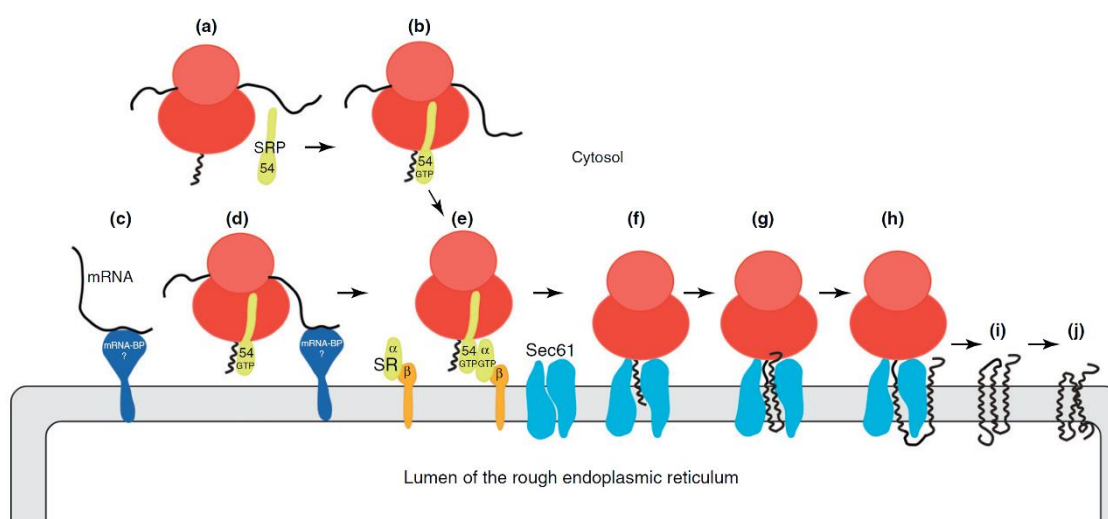


**Figure 1.20** Schematic representation of the co-translational translocation of a polytopic transmembrane protein. SR:SRP receptor; SRP: Signal recognition particle, the 54 kDa subunit contains the binding site for SR (Gilmore and Mandon, 2012).

of this ribosome-translocon targeting has been extensively studied in respect to ER translocation of small bacterial proteins, less is known on how polytopic transmembrane proteins acquire their final topology through this process.

What seems to be apparent is that co-translational integration of membrane proteins into ER is a high-fidelity mechanistic process controlled by intrinsic molecular elements of the ribosome, the translated sequence and the translocase complex (Nyathi et al., 2013). Importantly, this process is highly sensitive to proper protein folding (Quality Control), occurring during the translocation of the translated polypeptide. Once a membrane protein is properly folded within the ER membrane, which constitutes an important check-point, it then follows a vesicular trafficking pathway initially towards the Golgi, and subsequently towards the endosomal pathway, the vacuole or the plasma membrane. Protein misfolding by errors, stress or mutations often leads to translation arrest and protein turnover. Misfolded membrane proteins are targeted for ER-associated degradation (ERAD), which efficiently retro-translocates them from the ER into the cytosol for degradation via the ubiquitin-proteasome system (Ruggiano et al., 2014; Smith et al., 2011). Membrane and soluble ER chaperones are involved in every aspect of ER quality control. To achieve homeostasis, a balance in ER protein folding load with sufficient ER protein folding machinery, is necessary. For that, cells have evolved the unfolded protein response (UPR) as a cytoprotective mechanism to cope with an increase of unfolded proteins and the ER stress caused by them. The UPR orchestrates an increase in the folding capacity of the ER by promoting the up-regulation of transcriptional factors, involved in lipid synthesis, ERAD and protein folding. A parallel decrease in folding load is also triggered, through selective mRNA degradation and translational repression (Travers et al., 2000).

Central to the process of membrane protein exit from the ER is the concentrative packaging of protein cargoes in budding COPII vesicles. It is known that exiting of membrane proteins from the ER can be facilitated by signal sequences, such as the di-acidic motifs DXD and DXE, the di-hydrophobic motifs FF, YY, LL and FY and the tyrosine-based sorting motif YXX $\Phi$  (Barlowe, 2003). However, there are many examples of proteins that do not possess any known export signal. Although the basic mechanism of COPII action is relatively well characterized, the biophysical details of how the COPII vesicles bud remain to be fully understood. In particular, how this process is modified to meet the dynamic needs of the cell remains unclear. The COPII protein coat is formed on the ER membrane in a series of subsequent steps, that start with the recruitment of the GTPase Sar1, which binds the heterodimeric Sec23/24, which in turn interacts with the membrane. Sec24 serves as the principle cargo-binding adaptor. Following prebudding complex formation, heterodimers of Sec13/31 are recruited via interaction between Sec23 and Sec31. Sec13/31 drives membrane curvature, aided by the oligomerization of Sec23–Sec24 (Lee and Miller, 2007; Sato and



Nakano, 2007). After vesicle formation, downstream events lead to uncoating of transport vesicles and recycling of the COPII coat components.

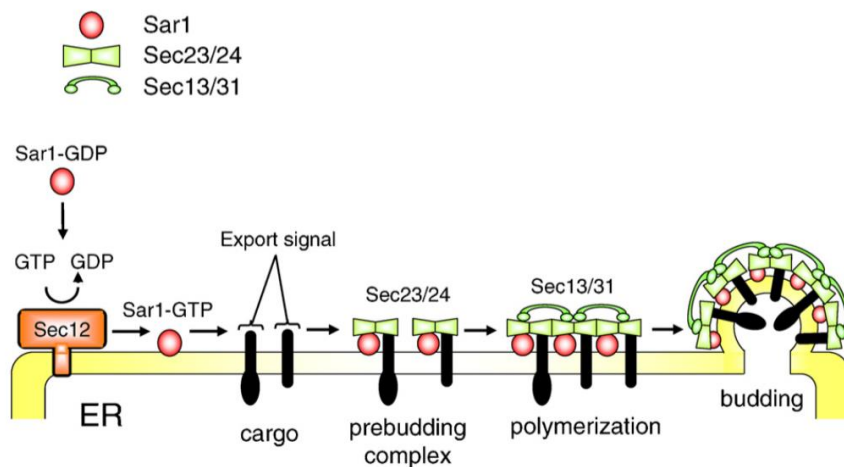


**Figure 1.21** COPII vesicle assembly and selective packaging of cargo proteins on the ER membrane (Sato and Nakano, 2007).

Traffic from ER to Golgi is bidirectional to ensure that proteins required for the formation of vesicles are recycled. After their ER-exit, COPII vesicles move cargo proteins to the ER-Golgi Intermediate Compartment (ERGIC), a network of membranes that constitutes the gateway to the Golgi complex (Ito et al., 2012; Szul and Sztul, 2011). Whether the ERGIC is a stationary compartment or a transient structure formed by the fusion of ER-derived vesicles which works as a carrier itself, remains elusive. ER to ERGIC transport is microtubule-dependent and thus, anterograde and retrograde transport between these compartments is dramatically reduced in the presence of inhibitors of microtubule polymerization (Tomás et al., 2010). In *S. cerevisiae* however, a “hug-and-kiss” mechanism was described for the transport of cargo from the ER-exit sites (ERES) to cis-Golgi, which ensures efficient and targeted transport. Specifically, the cis-Golgi approaches and contacts the ERES, the COPII coat collapses, the cis-Golgi captures cargo and leaves the ERES (Kurokawa et al., 2014). The removal of COPI and COPII coat has recently been attributed to auxilin, which can act as a chaperone and/or uncoating factor in the early secretory pathway (Ding et al., 2016).

#### 1.3.4 The Golgi apparatus

In most eukaryotes, the Golgi apparatus consists of several flattened, stacked, membrane compartments, called “cisternae”. Each Golgi stack has an entry face (*cis*) and an exit face (*trans*), both closely associated with special tubular and cisternal compartments, the *cis* Golgi network (CGN) and the *trans* Golgi network (TGN), respectively. The CGN is a collection of fused vesicles that

receives cargo from the ER, whereas the TGN segregates, packages and sends cargoes onward to post-Golgi organelles such as vacuoles, secretory vesicles or the PM. The lumen of the *trans* cisternae of the Golgi apparatus, is thought to be continuous with the TGN. In *A. nidulans* and most ascomycetes, the Golgi apparatus does not form stacks, but is instead organized in “Golgi equivalents”. These are a network of tubules, rings and fenestrated cisternae, remaining intact during mitosis. The fungal Golgi is not vectorially organized in the direction of secretion, thus for fungal cisternae, we use the terms “early” and “late” instead of *cis* and *trans*, as the Golgi network lacks *cis*-to-*trans* spatial organization. Both early and late Golgi elements are intermingled, predominate near the tip and are less abundant in more basal regions (Breakspear et al., 2007; Pantazopoulou and Peñalva, 2009).

The Golgi apparatus receives lipids and proteins from the ER, transports them to the trans-Golgi network (TGN) and dispatches them via small carriers to various subcellular destinations, usually covalently modifying them *en route*. Two widely accepted models of how cargoes are transported through the Golgi apparatus exist: the vesicular transport model and the cisternal maturation model. According to the vesicular transport model, the Golgi apparatus consists of relatively static cisternae, while the cargoes in transit utilize coated transport vesicles for an anterograde flow, in a *cis*-to-*trans* direction. A retrograde vesicular flow restores the original positioning of ER and Golgi-resident enzymes, maintaining a static structure. In the alternative cisternal maturation model, each Golgi cisterna progressively matures as it migrates through the Golgi stack. New ER-derived vesicles continually fuse to become a CGN, which then moves outward and matures into a *cis* cisterna, and so on. Cargo proteins are transported without exiting the cisternae, while the retrograde flow that retrieves the resident proteins in each step, is still COPI vesicle-mediated (Ito et al., 2012; Simon, 2008). This model is supported by microscopic observations in *A. nidulans*, demonstrating that a block in ER exit using the thermosensitive mutant *sarA<sup>sarr1</sup>* at the restrictive temperature, results in re-localization of the early Golgi markers (SedV, RerA) to the ER (Hernández-González et al., 2015). The cisternal maturation model is further supported by the acute trans-Golgi disorganization due to impairment of traffic between the ER and early Golgi (Pinar et al., 2013a), as well as the fact that late Golgi cisternae (LGC) mature into post-Golgi exocytic carriers (Pantazopoulou et al., 2014). Moreover, maturation of early into LGC (Losev et al., 2006; Matsuura-Tokita et al., 2006) and progression of LGC into clathrin-coated carriers (Daboussi et al., 2012) has been documented in *S. cerevisiae*. However, we cannot exclude the possibility that a combination of the two mechanisms is at play, as the two models are not mutually exclusive. A third mechanism could explain the functional segregation of the Golgi stack, based on the spatial sorting of lipids. In this model, the uniformly structured Golgi apparatus consists of a

membranous processing domain and a membranous export domain, thus separating the enzymatic modification of cargoes from their sorting into vesicles (Patterson et al., 2008; Simon, 2008).

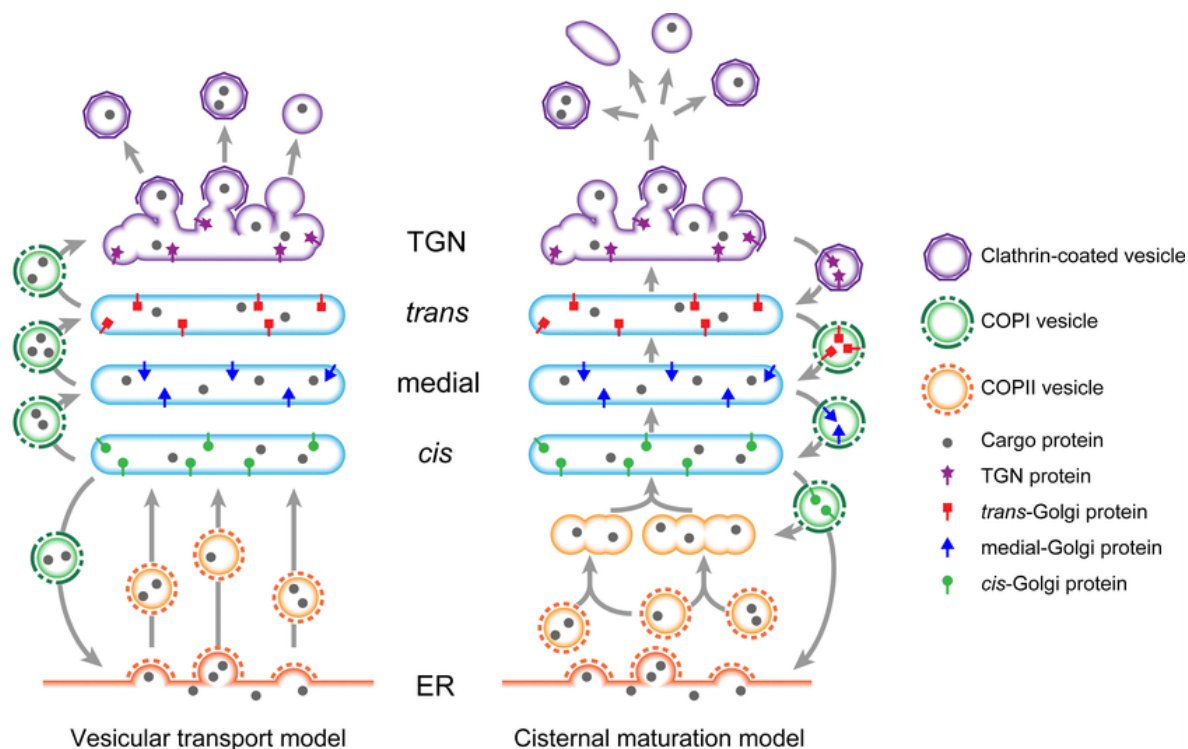


**Figure 1.22** Two major models for intra-Golgi trafficking. ER: Endoplasmic reticulum; TGN: Trans-Golgi network, the equivalent of fungal late-Golgi (Ito et al., 2014).

The trans-Golgi network (TGN) is a major sorting station, where cargoes such as membrane proteins are organized and enclosed into distinct transport vesicles, targeted to various downstream destinations (Guo et al., 2014). Clathrin-coated buds are described only at the TGN, whereas forming buds identified in other cisternae, do not contain clathrin (Ladinsky et al., 2002; Mogelsvang et al., 2004). The key proteins involved in cargo sorting at the TGN are adaptors such as the aforementioned APs and GGAs or Epsins and the Exomer. The epsin-related proteins belong to a class of monomeric adaptors that mediate traffic between the TGN and endosomes. Mammals have one functioning homologue, epsinR, and yeast has two, Ent3p and Ent5p. Double deletion in yeast causes trafficking defects in the TGN to endosome route, and in MVB sorting (Duncan et al., 2003; Friant et al., 2003). Fungal exomer on the other hand, directly traffics a chitin synthase III (Chs3p) and a fusion protein (Fus1p), from the TGN to the PM and has no known homologues in metazoans. In yeast, it is heterotetrameric and consists of two copies of Chs5 and two copies of ChAPs (Chs5-Arf1-binding proteins) (Sanchatjate and Schekman, 2006; Trautwein et al., 2006). Both the putative epsin-like protein of *A. nidulans*, and the exomer complex, remain uncharacterized.

Phospholipids also contribute to the sorting of cargoes, being recognized as binding sites for several cargo adaptors, including AP-1, GGAs and epsinR (Guo et al., 2010; Mills et al., 2003; Wang et al., 2007). Phosphatidylinositol 4-Phosphate (PI4P) is enriched predominantly at the TGN and phosphatidylserine (PS) at the luminal leaflet of the ER and Golgi, before being translocated by the aforementioned lipid flippases (Sebastian et al., 2012). PI4P-binding PH domain of human oxysterol binding protein ( $\text{PH}^{\text{OSBP}}$ ) is a soluble protein, efficiently recruited to the late Golgi and used widely as marker for studies in *A. nidulans* (Behnia and Munro, 2005; Levine and Munro, 2002; Pantazopoulou and Peñalva, 2009). The fungal Golgi Arf-GEF  $\text{HypB}^{\text{Sec7}}$ , homologue of the late Golgi BIG/Sec7p is another prototypical marker, displaying polarized distribution similar to that of  $\text{PH}^{\text{OSBP}}$ . It plays a role in the generation of carriers from the late Golgi bound to the endosomal system (Arst et al., 2014; Pantazopoulou and Peñalva, 2011). Early and late-Golgi cisternae (EGC and LGC, respectively) are transient, do not overlap and can be resolved by conventional microscopy, as early Golgi membranes are visualized with tagged versions of GrhA and SedV. LGC have an average lifetime of approximately 2 minutes (Pantazopoulou et al., 2014) and are excluded from a subapical region of the hypha, where exocytic carriers are accumulated, by a few microns gap (Pantazopoulou and Peñalva, 2009). Brefeldin A (BFA) has predictably two targets at the *A. nidulans* Golgi: the two Golgi Arf1 GEFs, that is GeaA, homologue of the early Golgi GBF1/Gea1p and  $\text{HypB}^{\text{Sec7}}$ . The Golgi organization is dramatically disrupted by BFA in fewer than 5 minutes, leading to arrest of apical extension, tip swelling and spatially distinct aggregate formation for early and trans-Golgi equivalents (Brefeldin bodies). Contrastingly, the ER components sec63 (translocon complex) and sec23 (COPII) during this incubation period are BFA-insensitive, indicating an acute characteristic behavior of the Golgi in response to the addition of BFA (Markina-Iñarrairaegui et al., 2013; Pantazopoulou and Peñalva, 2009; Yang et al., 2008).

Prolonged incubation times with BFA (>5-10 min, <30-45min), lead to SedV redirection to the ER, while the late Golgi remains ER-independent (Pantazopoulou,

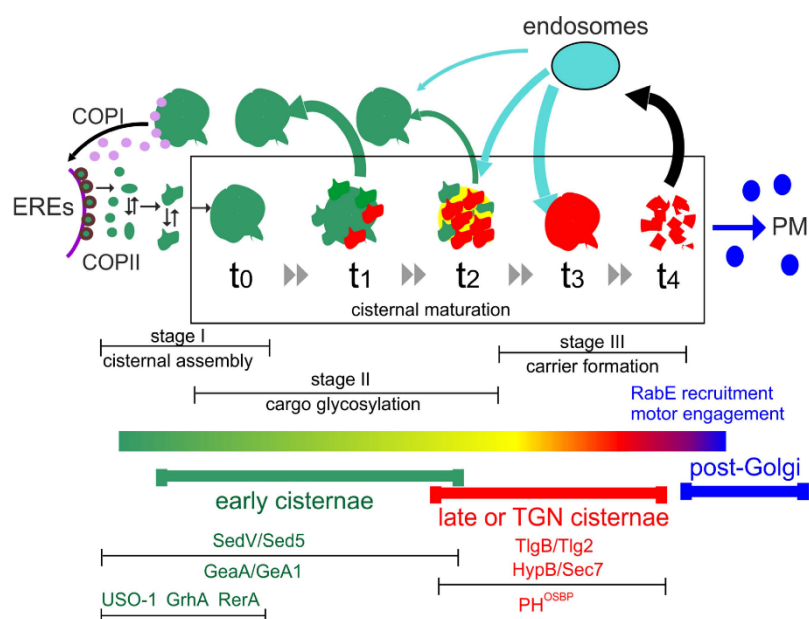


**Figure 1.23** Schematic representation of the cisternal maturation process in the Golgi of *A. nidulans*. The different functional stages and participating proteins are indicated (Steinberg et al., 2017).

2016; Pantazopoulou and Peñalva, 2011). Additionally, a block in Golgi assembly by thermosensitive mutants of the early-Golgi regulators, RabO and SedV, results in mis-localization of early Golgi markers to a cytoplasmic haze (Pinar et al., 2013a).

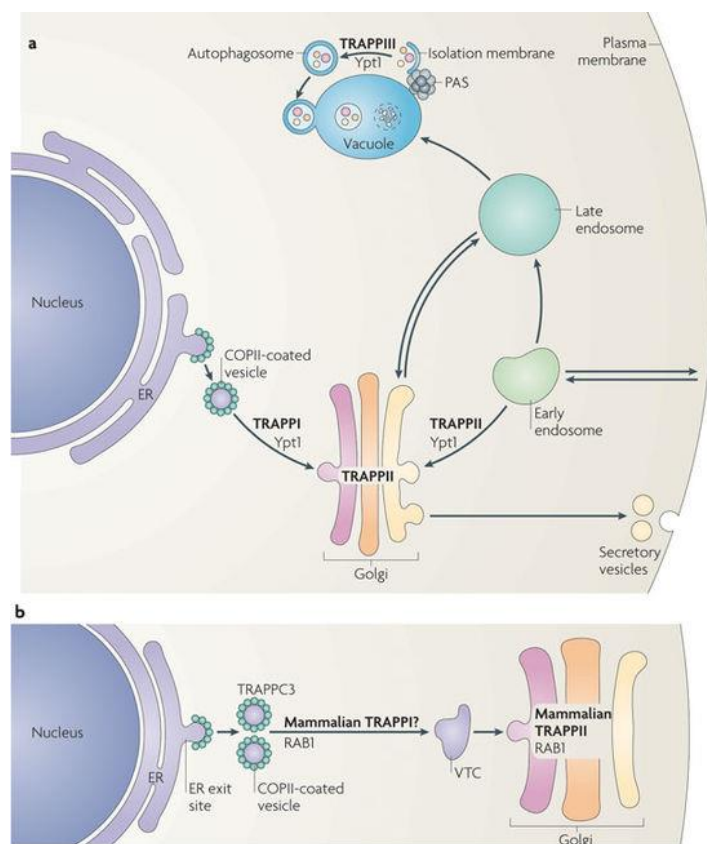


**Figure 1.24** An overview of the functions of TRAPP complexes in (a) fungal and (b) mammalian trafficking pathways (Barrowman et al., 2010).

Traffic through the Golgi apparatus is directed by the aforementioned small GTPases of the Arf and Rab families, and their effectors (GEFs and GAPs). In *A. nidulans*, Golgi-localized RabO and post-Golgi RabE are activated by the oligomeric complex Transport Protein Particles (TRAPPs) that function as GEFs and thus mediate nucleotide exchange on the RAB GTPases. Although three TRAPP complexes have been identified in fungi, only one stable complex, involved in Golgi traffic, has been characterized in mammals so far.

Fungal TRAPP II is composed of TRAPP I plus three additional subunits, HypA<sup>Trs120</sup>, HypC<sup>Trs130</sup> and Trs65 (Liang et al., 2007; Morozova et al., 2006; Shi et al., 2004). In *A. nidulans*, RabO is regulated by TRAPP I, whereas a specific association of TRAPP II with RabE<sup>RAB11</sup> has been detected *in vivo* as TRAPP II marks, and possibly determines, the Golgi-to-post-Golgi transition (Pinar et al., 2015). In yeast however, it is still unclear whether TRAPP II mediates nucleotide exchange on RAB1/Ypt1/RabO, RAB11/Ypt31/RabE, or both, as reports indicate that TRAPP II mediates nucleotide exchange on Ypt1, but not on Ypt31/Ypt32. It is postulated that TRAPP II tethers COPI-coated vesicles during intra-Golgi and early endosome to late Golgi traffic, through the activation of Ypt1 specifically in the late Golgi (Barrowman et al., 2010; Cai et al., 2008). Moreover, a third version, TRAPP III, specifically regulates the Ypt1 role in autophagy (Lynch-Day et al., 2010; Pinar et al., 2015).

### 1.3.5 Transport to the cell cortex: Exocytosis

In unpolarized cells, transport vesicles leaving the TGN normally reach the PM in a steady stream of uncoated vesicles, through the *constitutive secretory pathway*. However, a second more tightly controlled, *regulated secretory pathway* also operates in most secretory or polarized cells. Proteins are concentrated and stored until a stimulus triggers the fusion of the vesicles with the PM and cargo release, in a process known as “exocytosis” (Alberts et al., 2002, chap. 13). In polarized hyphae of filamentous fungi, a regulated secretory pathway has been partially characterized and involves the GTPase RabE. When RabE is recruited to LGCs, these acquire a post-Golgi identity and engage motor proteins, before dissipating into exocytic carriers bound for delivery to the apex, where they accumulate before fusing with the PM (Pantazopoulou et al., 2014).

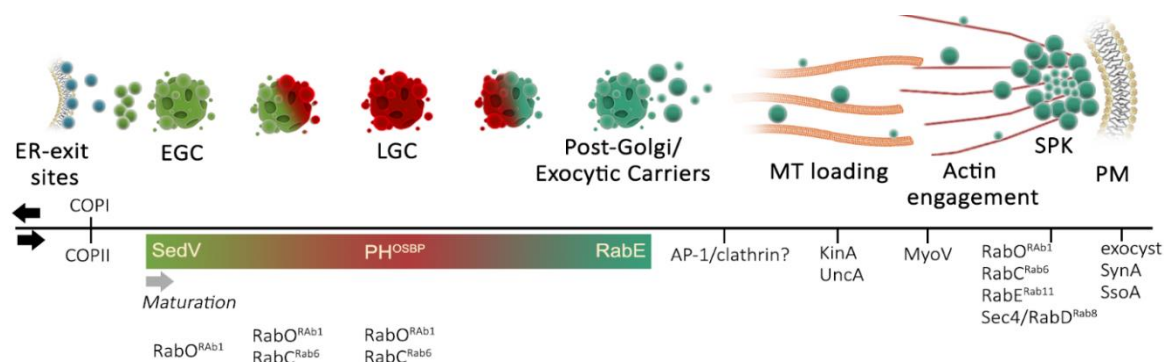


**Figure 1.25** A simplified schematic overview of the exocytic process in *A. nidulans* (@Olga Martzoukou).

In mammalian cells, coat assembly at the TGN is initiated by the recruitment of Arf1 to the membrane, which in turn binds to adaptor proteins (Gillingham and Munro, 2007). The membrane of the secretory vesicles that leave the TGN is only loosely wrapped around the clusters of secretory cargoes. Morphologically, these immature vesicles resemble LGC that have budded off. During maturation they can fuse with one another and their contents become concentrated, probably due to the continuous retrieval of membrane and the progressive acidification of the vesicle lumen, resulting from the increasing concentration of ATP-driven V-type H<sup>+</sup> pumps in the vesicle membrane. Once loaded, the secretory vesicle must travel to reach the site of secretion, especially in polarized cells such as neurons or filamentous hyphae. As will be discussed in detail later, microtubules guide vesicles to the cell surface with the help of motor proteins that propel the vesicles. In fungi, the Spitzenkörper (SPK) which literally means ‘apical body’, functions as an intermediate station after vesicle transport and before vesicle docking and fusion with the membrane at the apex. It is an apical organelle composed of vesicles, actin and ribosomes which is believed to function as a vesicle supply center, providing new material to the PM (Gierz and Bartnicki-Garcia, 2001; Harris et al., 2005; Riquelme and Sánchez-León, 2014). The SPK receives exocytic vesicles of different sizes and different lipid compositions (Hohmann-Marriott et al., 2006; Verdín et al., 2009) from the late-Golgi

(Schultzhaus et al., 2015) and spatio-temporally regulates their delivery to and fusion with the PM. Multiple proteins participate in the formation of the SPK, such as Rho and Rab GTPases, v- and t-SNAREs as well as polarisome and exocyst complexes. Vesicles of the SPK are organized into two strata and can also be divided into two populations based on their size, with the large so-called macrovesicles in the outer layer (70 to 90 nm in diameter) and the smaller microvesicles in the SPK core (30 to 40 nm in diameter) (Howard, 1981; Riquelme and Sánchez-León, 2014; Verdín et al., 2009).

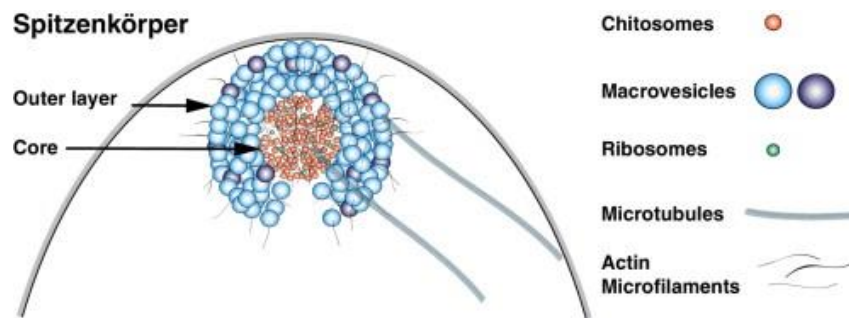


**Figure 1.26** Schematic representation of the two subpopulations of vesicles of the SPK in filamentous fungi such as *N.crassa* and *A.nidulans* (Riquelme and Sánchez-León, 2014).

In *N. crassa* these different exocytic vesicles are known to have different cargoes, with the 1,3 b-glucansynthase Gs1 located in the macrovesicles and the chitin synthase Chs1 present in the microvesicles/chitosomes (Verdín et al., 2009). While some CHSs in *A. nidulans* have been localized at the SPK (Takeshita et al., 2015), it remains to be elucidated whether they are distributed at the core or the outer SPK layer. However, the spatial distribution of the lipid flippases DnfA and DnfB in the two SPK layers was recently observed microscopically (Schultzhaus et al., 2015). Elusive actin microfilaments nucleate in the SPK core from the *A. nidulans* formin, SepA, a key part of the multiprotein polarisome complex that forms at the sites of active growth (Harris et al., 2005; Sharpless and Harris, 2002; Virag and Harris, 2006). It is unclear whether the polarisome is a component of the SPK, however this hypothesis is supported by the idea that SPK represents a microfilament-organizing center. Actin cable nucleation paves the way for the short, myosin V-dependent anterograde trafficking of vesicles and cargoes between the subapex and the apical region (Schultzhaus et al., 2016; Sharpless and Harris, 2002; Taheri-Talesh et al., 2012, 2008). Formins are a family of multidomain scaffold proteins that function as nucleators of actin filaments involved in actin-dependent morphogenetic events such as septum formation and polarized growth (Berepiki et al., 2011).

Secretory vesicles that accumulate at the SPK wait at the membrane until a signal triggers secretion, and they then fuse. The signal is often a chemical messenger, such as a hormone, or a

neurotransmitter, which often generates pulsed  $\text{Ca}^{2+}$  influxes (Takeshita et al., 2017; Wollman and Meyer, 2012). The SNARE proteins may be partly paired, but other proteins likely keep the SNAREs from completing the fusion reaction, until the  $\text{Ca}^{2+}$  influx releases this brake (De Haro et al., 2003; Schneggenburger and Neher, 2005).

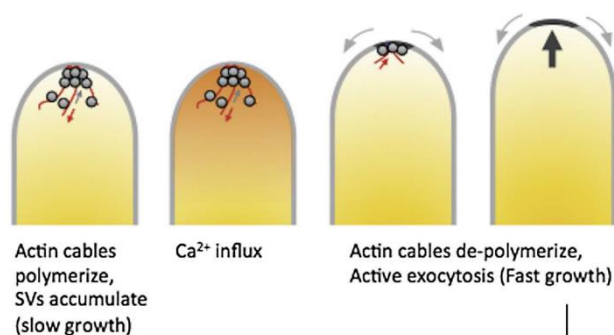


**Figure 1.27** Oscillatory hyphal growth in *A. nidulans* (Takeshita, 2018).

The exocyst is a conserved octameric protein complex (Sec3, Sec5, Sec6, Sec8, Sec10, Sec15, Exo70 and Exo84) that is implicated in the tethering of secretory vesicles to sites of exocytosis of the plasma membrane along with associated Sec1/Munc18 proteins (Carr et al., 1999; Guo et al., 1999a, 1999b; Novick et al., 1981; TerBush et al., 1996), prior to SNARE-mediated fusion (Wu and Guo, 2015). It was first characterized in *S. cerevisiae* (Novick et al., 1980; TerBush et al., 1996; TerBush and Novick, 1995), whereas the mammalian exocyst complex was first purified from rat brain, and was found in all the tissues examined (Hsu et al., 1998, 1996). Strains with a non-functional exocyst accumulate SVs in the cytoplasm and exhibit severely affected polarized growth, highlighting the importance of this complex in exocytosis and membrane expansion (Guo et al., 1999a). In *A. nidulans*, only SecC<sup>Sec3</sup> has been identified and shown to localize consistently to a small region of the PM at the apex, immediately anterior to the Spitzenkörper (Taheri-Talesh et al., 2008), whereas in *A. oryzae* the subcellular distribution of the exocyst was monitored at cortical caps of hyphal tips and at septa, through identification of a Sec3 orthologue (Hayakawa et al., 2011). In *Ashbya gossypii* the exocyst components Exo70p, Sec3p, and Sec5p were reported at either an apical cap, or the Spitzenkörper, depending on the rate of growth (slow or fast, respectively) (Kohli et al., 2008). Contrastingly, the exocyst of *C. albicans* forms a stable apical cap even upon cytoskeleton disruption (Jones and Sudbery, 2010). The first interaction to be described between the exocyst and Rab GTPases was that of Sec15 and Sec4 in yeast (RabD in *A. nidulans*) (Guo et al., 1999b). This interaction is specific for Sec4, because other Rab proteins such the ER-localized Ypt1 or the endosomal Ypt5, do not interact with Sec15. Sec4 in its active form, might promote exocyst recruitment to secretory vesicles and complex assembly (Guo et al., 1999b; Luo et al., 2014). Except for the interaction between Rab and Sec15, a second component of the exocyst, Sec10, binds to GTP-Arf6, a step crucial for the recycling of cargoes to the PM (Prigent et al., 2003). Sec15 was also shown to interact with the type-V myosin Myo2, which binds to both Sec4 and Ypt32 (homologue of human Rab11 or *A. nidulans* RabE), suggesting that Rab proteins control the exocyst function for



vesicle transport along the cytoskeleton (Lipatova et al., 2008; Zhang et al., 2011). The mammalian Sec15 interacts directly with Rab11, which is involved in the formation of vesicles from the TGN or recycling endosomes for subsequent delivery to the PM (Zhang et al., 2004). Upon fusion of a secretory vesicle with the PM, the membrane proteins and the lipids of these vesicles provide new material for the PM, while the soluble contents are removed from the cell by exocytosis. Even though the surface area of the PM is expected to be increased, this happens only transiently, because active endocytosis removes membrane components in a rate almost as fast as that of exocytosis. During secretory vesicle formation, a retrograde retrieval process that returns Golgi components to the apparatus is mediated by clathrin-coated vesicles that originate from the surface of immature secretory vesicles. Clathrin coats are often formed on budding secretory vesicles that have not yet pinched off from the Golgi apparatus.

In polarized *S. Pombe* hyphae, a special mechanism was shown to underlie the spatial confinement of exocytosis, as lateral ER-PM contacts restrict the available exocytic sites to the growing cell tips (Ng et al., 2018). This ER-PM association has also been observed in yeast, plants, neurons and muscle cells (Henkart et al., 1976; Sparkes et al., 2009; West et al., 2011; Wu et al., 2017). Moreover, lipid rafts, cholesterol and sphingolipids of the PM, were shown to play essential roles in the regulated exocytosis pathway of mammalian cells. The association of SNAREs with lipid rafts indicates a direct role in the concentration of cargoes at specific sites of the PM, whereas cholesterol depletion results in inhibition of exocytosis (Salaün et al., 2004).

Two examples of thoroughly studied polarized mammalian cells are epithelial and nerve cells. Distinct domains in their plasma membrane constitute targets for different types of vesicles, which raises the question whether organized delivery from the Golgi apparatus maintains the differences between distinct surface domains. A typical epithelial cell has an apical domain and a basolateral domain, separated by a ring of junctions. This prevents diffusion of proteins and lipids between the two domains, maintaining their different composition. Neuron on the other hand is compartmentalized into two molecularly and functionally distinct plasma membrane domains: the axon and the dendrites, specialized for sending and receiving signals, respectively (Barnes and Polleux, 2009; Lasiacka and Winckler, 2011). As far as protein targeting is concerned, the dendritic plasma membrane resembles the basolateral membrane of an epithelial cell, whereas the axonal membrane resembles the apical epithelial membrane.

### 1.3.6 Remodeling the plasma membrane: Endocytosis

The routes that lead inward from the cell surface start with the process of endocytosis (pinocytosis). All eukaryotic cells continually form small, cargo-loaded endocytic vesicles from the

PM for processing and degradation in the vacuole or recycling back to the cell surface through the endosomal system, either directly or via passage through the Golgi and the exocytic pathway (Seaman, 2008). The existence of clathrin-dependent and independent endocytosis mechanisms has been discussed in filamentous fungi, however, a deep characterization of the mechanisms that mediate endocytosis in hyphae requires further investigation.

The endocytic part of the cycle often begins at specialized regions on the inner surface of the plasma membrane that can contain clathrin, the AP-2 adaptor protein complex and accessory proteins (Ehrlich et al., 2004). Clathrin-mediated cargo endocytosis (CME) is involved in numerous biological processes, such as neural signaling, virus uptake or generation of cellular polarization. A complex machinery participates in the formation of CCVs, comprised of more than 50 different proteins that mark the endocytic positions, recruit cargo molecules and adaptors and promote membrane invagination and vesicle scission (Berro and Pollard, 2014; Boettner et al., 2011; Doherty and McMahon, 2009; Taylor et al., 2011; Weinberg and Drubin, 2012) and is largely conserved between mammals and yeast, whereas neurons mimic some mechanisms, present in filamentous fungi (Conibear, 2010; Egan et al., 2012a; Etxebeste and Espeso, 2016; Merrifield and Kaksonen, 2014). Actin is involved in endocytic internalization in both fungal and animal cells (Munn, 2001) but for the latter this role is non-obligatory (Engqvist-Goldstein and Drubin, 2003; Geli and Riezman, 1998; Qualmann et al., 2000).

Punctate cortical structures identified in fungi such as budding yeast and *A. nidulans*, have been suggested to function in endocytosis (Araujo-Bazán et al., 2008; Engqvist-Goldstein and Drubin, 2003; Geli and Riezman, 1998; Munn, 2001). Among the proteins found in these transient and highly motile cortical actin patches (Carlsson et al., 2002; Doyle and Botstein, 1996; Smith et al., 2001; Waddle et al., 1996), are the Arp2/3 complex and Abp1p/AbpA that are involved in actin nucleation and AP-2, clathrin, Sla2/Hip1R/SlaB, Ent1, Ent2, Las17/N-WASP, Sla1, Pan1/Eps15, End3/SagA, that mediate the inward movement (Baggett et al., 2003; Goode et al., 2015; Hoshi et al., 2016; Idrissi et al., 2008; Kaksonen et al., 2003; Skruzny et al., 2015; Sun et al., 2015; Youn et al., 2010).

Coat internalization is blocked by mutants of actin cytoskeletal proteins and by the actin inhibitor latrunculin B (Lat B) (Kaksonen et al., 2003; Martin et al., 2005; Sampson and Heath, 2005). In *A. nidulans*, the gene products of *sagA*, *slaB*, *arfB*, *fimA*, *myoA*, *wspA* have been reported to function in endocytosis (Araujo-Bazán et al., 2008; Hervás-Aguilar and Peñalva, 2010; Hoshi et al., 2016; Karachaliou et al., 2013; Lee et al., 2008; Upadhyay and Shaw, 2008; Yamashita and May, 1998).

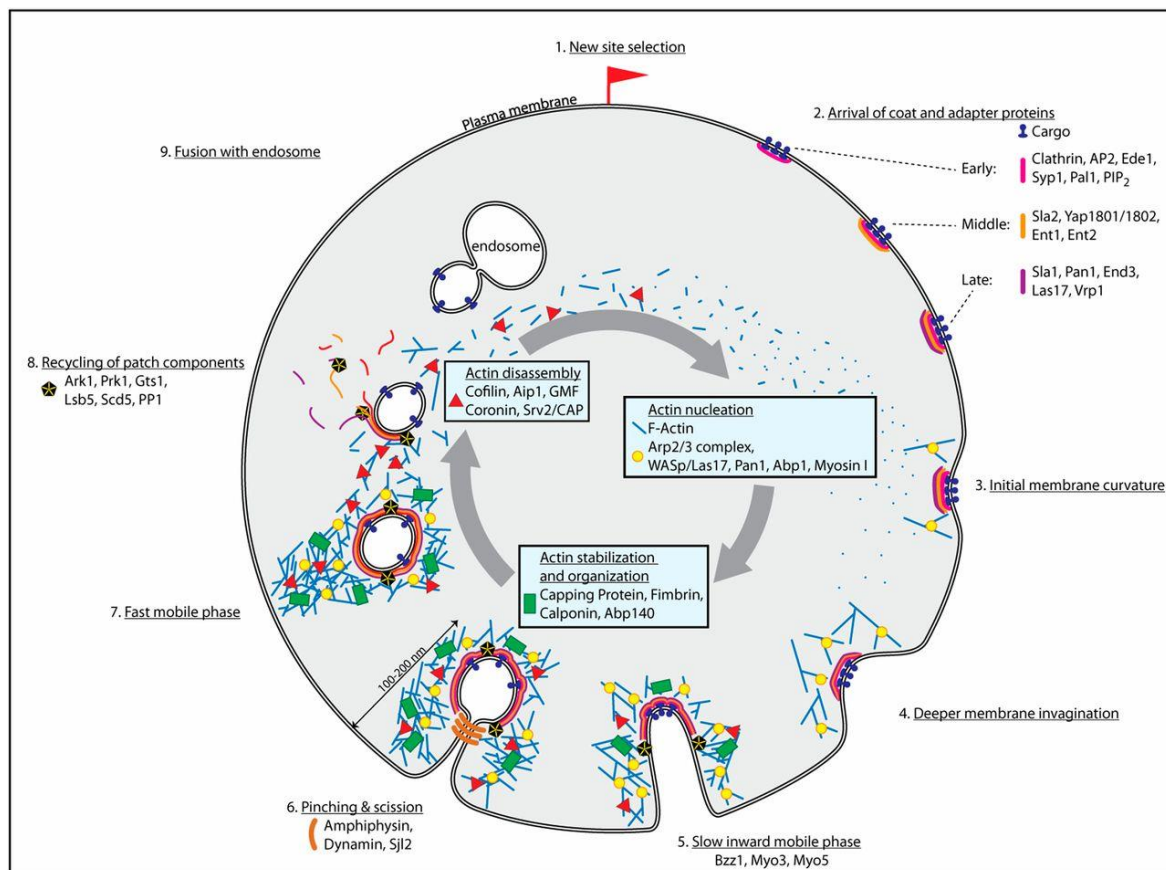


**Figure 1.28** Stages of clathrin-mediated endocytosis in *S. cerevisiae*, with the involvement of actin cytoskeleton and actin-associated proteins (Goode et al., 2015).

The AP-2 adaptor protein complex has been reported to mediate clathrin-dependent endocytosis in most eukaryotes, with the exception of mammals and yeast where an AP-2 independent role of clathrin was revealed (Brach et al., 2014; Conner and Schmid, 2003; Motley et al., 2003; Sorkin, 2004; Traub, 2009). AP-2 initiates the formation of the clathrin lattice at specific sites of the cytoplasmic membrane, selects the cargo for bud, bringing the two non-cytosolic leaflets into close proximity, in a process called pinching-off. The PI(4,5)P<sub>2</sub>-binding domain of dynamin tethers the protein to the membrane, whereas the GTPase domain regulates the rate of vesicle scission, along with amphiphysins (*A. nidulans* possesses two homologues, AmpA and AmpB) that recruit dynamin to the membrane in mammals, or stabilize the invaginating bud through their F-BAR domains in yeast (McMahon et al., 1997; Meinecke et al., 2013). Alternatively, in the filamentous fungus *A. nidulans*, the unconventional Myosin, MyoA, interacts with AbpA at endocytic sites (Matsuo et al., 2013; Yamashita et al., 2000). AmpA co-localizes with AbpA in endocytic patches showing marked predominance at the tips (Araujo-Bazán et al., 2008). Removal of the clathrin coat from the surface of the vesicle is necessary for efficient intracellular transport, fusion with the target membrane and delivery of the cargo. The released vesicle rapidly loses its clathrin coat in an ATP-

dependent process with the aid of auxilin, which in turn activates the Hsc70 uncoating chaperone (Brodsky et al., 2001; Loerke et al., 2009; Ungewickell et al., 1995; Xing et al., 2010).

Clathrin-mediated endocytosis is the best-characterized internalization pathway in eukaryotes, but it is now clear that a cell can have several pathways that do not use a clathrin coat, collectively referred to as clathrin-independent endocytosis (CIE). During this process, several proteins have been shown to play important roles such as RhoA, Rac, Cdc42, Arf6, or caveolae (Mayor and Pagano, 2007; Sandvig et al., 2011). In *S. cerevisiae*, a clathrin- and Arp2/3p-independent route for the uptake of FM4-64 has been discovered (Prosser et al., 2011). Surprisingly, the pathway depended on the actin nucleation, formin, Bni1p and the GTPase Rho1p, which are generally associated with exocytosis. The only formin in *A. nidulans* and the ortholog in *N. crassa*, SepA and Bni-1, respectively, are located at the Spitzenkörper and the apical region of the hypha and possibly participate in the production of actin filaments along which vesicles traffic to the apex (Lichius et al., 2012; Sharpless and Harris, 2002; Takeshita et al., 2008), while *A. nidulans* RhoA plays roles in polar growth, branching and cell wall construction (Guest et al., 2004).

In filamentous fungi the spatial regulation of endocytosis appears to be cargo-centric, as it can take place either predominately in specific sites of the elongating hypha, or uniformly across the plasma membrane, depending on the endocytosed cargo. For example, rapidly recycled apical proteins seem to undergo endocytosis mainly utilizing the endocytic machinery of a subapical endocytic region of the hyphal tip, commonly known as dynein loading zone or endocytic collar or endocytic ring (Abenza et al., 2009; Taheri-Talesh et al., 2008). On the other hand, transporters belonging to several different families are loaded into endosomes that are formed in seemingly random areas of the PM across the hypha (Diallinas, 2008; Gournas et al., 2010; Karachaliou et al., 2013). However, both endocytic modules share essential components of the endocytic machinery. Various proteins purportedly involved in endocytosis have been detected at the subapical endocytic collar and throughout the hypha at cortical foci, marked also by accumulated actin patches (Araujo-Bazán et al., 2008; Epp et al., 2013; Schultzhaus and Shaw, 2015; Taheri-Talesh et al., 2008; Upadhyay and Shaw, 2008).

Common components of endocytic pathways involve adaptors that recognize cytoplasmic sorting signals in cargo proteins and link the cargo with the coat proteins. Two types of sorting signals exist in general: covalently attached ubiquitin molecules and short peptide motifs. Each different adaptor is matched with each transmembrane protein, through the recognition of different sorting signals on the cargo, at the cell surface (Reider and Wendland, 2011). Ubiquitin (Ub) is a protein of 76 amino acids that can be covalently linked to cargoes prior to their internalization, via an enzymatic cascade of three components: E1 (Ub-activating), E2 (Ub-conjugating), and E3 (Ub-

ligase) (Varshavsky, 2012). The key enzyme that conjugates Ub to endocytic cargo proteins is the E3 ligase Rsp5 (Springael et al., 1999), influenced by protein kinases such as Npr1 (De Craene et al., 2001; Kaouass et al., 1998; MacGurn et al., 2011; Merhi and Andre, 2012).  $\alpha$ -Arrestins, a family consisting of 13 known members in *S. cerevisiae*, with six related proteins in human (Patwari and Lee, 2012), bridge Rsp5 and cargo substrates, especially transporters (Hatakeyama et al., 2010; Lin et al., 2008; Nikko et al., 2008; Nikko and Pelham, 2009; O'Donnell et al., 2010). The Ub ligase can bind to the [L/P]PxY motifs of the  $\alpha$ -arrestins through three WW domains, while many cargo proteins are able to functionally interact with multiple  $\alpha$ -arrestins (Lin et al., 2008; Nikko and Pelham, 2009). In *A. nidulans*, the arrestin-like protein, ArtA, is essential for the Hula<sup>Rsp5</sup>-dependent ubiquitination and endocytosis of a purine transporter of the NAT/NCS2 family, UapA, and two more transporters specific for the uptake of nitrogenous compounds, PrnB (L-proline) and AzgA (purines) (Karachaliou et al., 2013). In a similar manner in budding yeast, Rsp5 along with the arrestin-related trafficking adaptor (ART) protein Rod1, is involved in the endocytosis of Jen1, a monocarboxylate transporter (Becuwe and Léon, 2014). Moreover, the two epsin proteins in *S. cerevisiae*, Ent1, Ent2, and Sla1, participate in cargo endocytosis through their function as Ub-binding adaptor proteins (Dores et al., 2010; Stamenova et al., 2007). Importantly, binding of the yeast Sla1 and the mammalian CIN85 to E3 Ub ligases is necessary for the internalization of certain receptors (Szymkiewicz et al., 2002).

Peptide-based sorting motifs were first reported in studies of familial hypercholesterolemia, in which the Tyr-x-x-hydrophobic signal in the cytosolic tail of the LDL (low density lipoprotein) receptor directs internalization of LDL particles (Anderson et al., 1977). Up to now, numerous other sorting motifs have been identified in many animal cargo proteins, at several organelles throughout the exocytic and endocytic pathway. In yeast, the NPF(x)1,2D endocytic

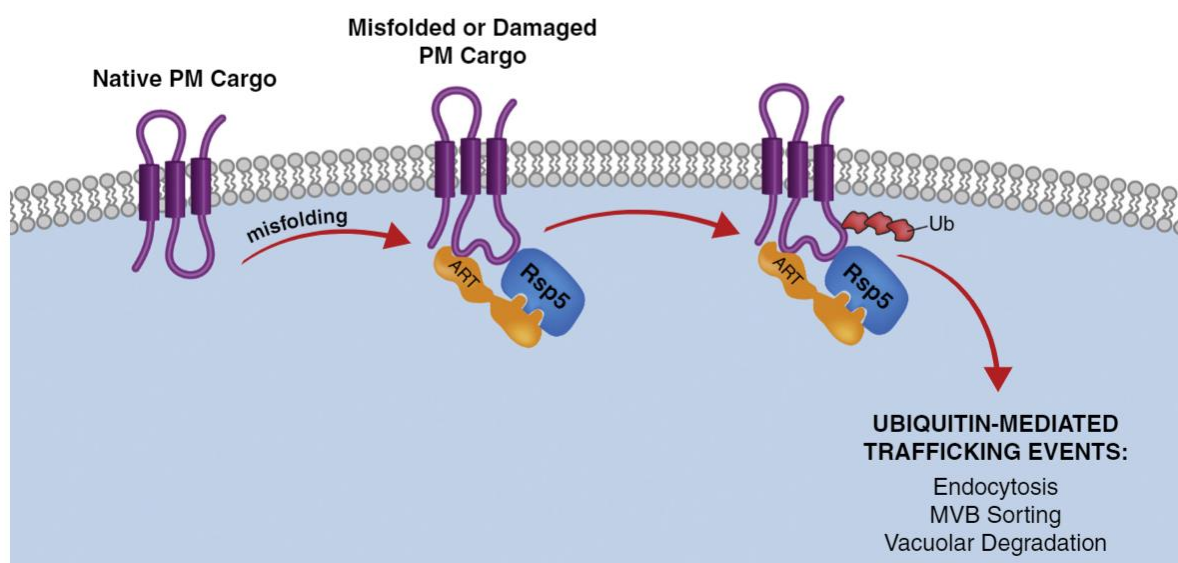


**Figure 1.29** Model of ART- and Rsp5-mediated endocytosis from the PM in yeast (MacGurn, 2014).

sorting motif which binds the adaptor protein Sla1, via its SH3-like SHD1 (Sla1 homology domain 1) (Howard et al., 2002; Mahadev et al., 2007; Paoluzi et al., 1998). Transmembrane cargoes that contain the NPF(x)<sub>1,2D</sub> motif include the cell-wall stress sensor Wsc1, the mating pheromone receptors Ste2 and Ste3, and the phospholipid flippases Dnf1 and Drs2 (Howard et al., 2002; Liu et al., 2007; Piao et al., 2007). In *A. nidulans*, the PM flippase DnfA<sup>Dnf1</sup> is also endocytosed through an NPFxD motif and recycled through the late Golgi (Schultzhaus et al., 2015).

Endocytic internalization is followed by sorting in Early endosomes (EEs), key components of the endocytic pathway playing roles in long-distance transport and supporting functions such as cytokinesis and cell migration in animal cells (Mendoza et al., 2014; Miserey-Lenkei and Colombo, 2016). EEs bind the small GTPase Rab5, homologue of RabA and RabB in *A. nidulans*, which controls biogenesis, membrane fusion and microtubule-dependent motility in animals (Abenza et al., 2009; Nielsen et al., 1999; Zeigerer et al., 2012; Zerial and McBride, 2001). In *S. cerevisiae* microtubule-based, long-range, transport does not exist possibly due its small size and spherical shape. Moreover, even though fungal endocytosis was described first in yeasts (Fernandez et al., 1990; Rath et al., 1993) and endocytic recycling supports their polar growth and survival (Valdez-Taubas and Pelham, 2003; Weinberg and Drubin, 2012), recent data suggest that *S. cerevisiae* seems to lack a distinct endomembrane system (Kasey et al., 2018). Contrastingly, in filamentous fungi, not only endocytosis supports hyphal growth, but also RabA and RabB-labeled EEs are transported bidirectionally (retrograde and anterograde) along microtubule tracks, at average speeds of 2 to 7  $\mu\text{m s}^{-1}$  and are labeled with the lipophilic fluorescent dye, FM4-64, shortly after internalization (Abenza et al., 2009; Peñalva, 2005; Steinberg, 2007; Zhou et al., 2018). RabA endosomal membranes do not overlap with vacuoles and colocalize with RabB on early endosomes and on relatively immotile, larger, late endosomes (Abenza et al., 2010). Hyphae reap the benefit of the anterograde movement of EEs, which assume the role of vehicles for the on-the-move translation and asymmetric distribution of mRNAs (Haag et al., 2015; Jansen et al., 2014). Furthermore, an EE-mediated transport of peroxisomes, lipid droplets and ER that was revealed recently points to the role of motile EEs in the distribution of specific organelles within hyphae (Guimaraes et al., 2015; Salogiannis and Reck-Peterson, 2017).

### 1.3.7 Post-endocytic trafficking

Most of the endocytosed material is incorporated into endosomes and depending on their ubiquitination state they can in turn follow two different pathways: Recycling back to the plasma membrane or traffic to the vacuole through the endocytic pathway, for degradation. Recycling occurs either indirectly via passage through the late Golgi and re-incorporation into secretory vesicles, or via a “quick recycling route” that sends EEs directly back to the PM in a Rab4-dependent

manner, in mammals (Grant and Donaldson, 2009; van der Sluijs et al., 1992). This direct recycling pathway has not been rigorously shown in *A. nidulans*, however a role of EEs in recycling for filamentous fungi is supported by the fact that they possess a homologue of the small GTPase Rab4, namely RabF (Fuchs et al., 2006). Moreover, an important breakthrough was the observation that the lipophilic dye FM4-64 which serves as an endocytosis marker, rapidly stains vesicles within the Spitzenkörper (Fischer-Parton et al., 2000; Harris et al., 2005), providing evidence for the interconnection of endocytic and secretory pathways. Early endosomes initially carry Rab5/RabB/Vps21 and the tethering complex CORVET. Non-recycled cargoes undergo targeting to the degradation pathway accompanied by maturation of EEs into late endosomes (LEs), with the release of Rab5 and the binding of Rab7/RabS/Ypt7 as shown in mammals (Rink et al., 2005), *A. nidulans* (Abenza et al., 2012), and *Ustilago maydis* (Higuchi et al., 2014) (For details see 1.3.9). The major signal determining the fate of endocytosed cargoes is ubiquitin, which not only acts as a signal for cargo endocytosis from the PM, but also can become critical later on the endocytic pathway (MacGurn et al., 2012).

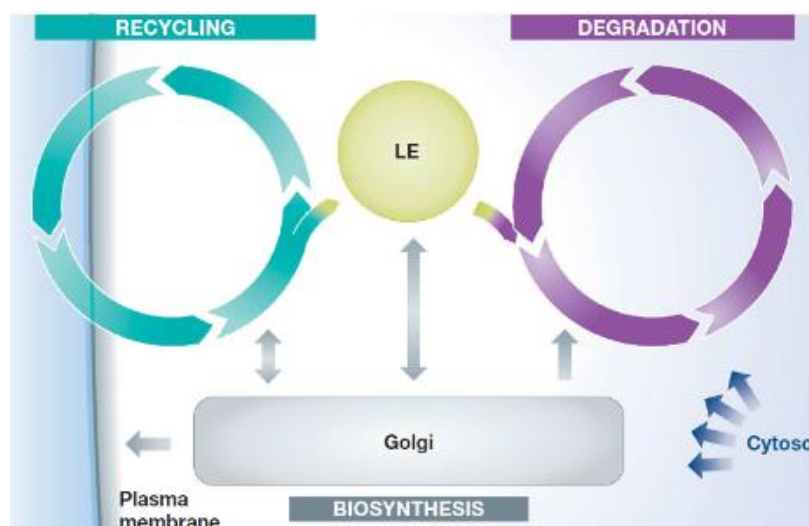


**Figure 1.30** Subcellular trafficking pathways of internalized proteins (Huotari and Helenius, 2011).

Endosomes function as a general sorting hub in the endocytic pathway of eukaryotic cells, as each of the membrane cargoes is subsequently destined to the proper target-organelle according to their respective sorting information. This major sorting station, termed recently as the “sorting Together with the Sorting Nexin BAR subcomplex (SNX; Vps5 and Vps17), the retromer mediates vesicle budding and cargo selection from the late endosome to the TGN. Transmembrane proteins are sent for recycling through the Golgi by formation of retromer-positive membrane tubules and the concomitant displacement of Rab7, which then becomes available for late endosome fusion (Burd and Cullen, 2014; Purushothaman et al., 2017; Seaman, 2012).

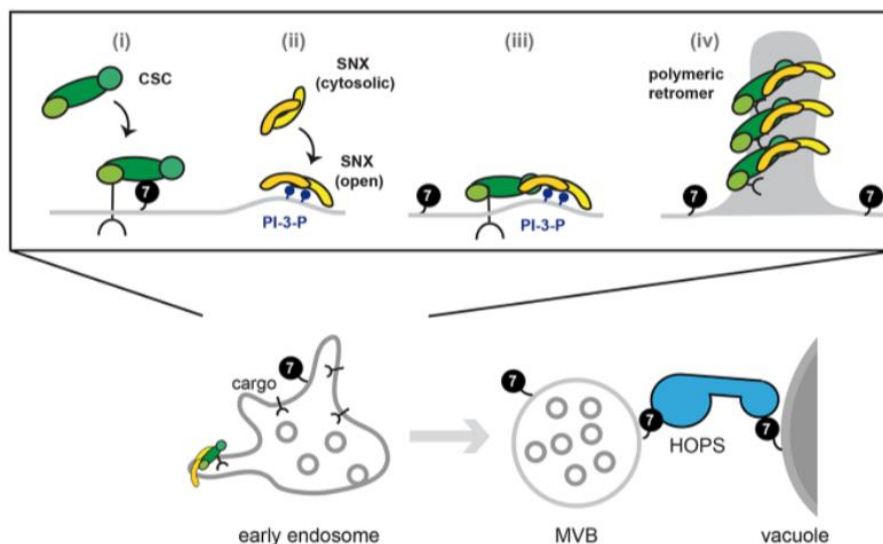


**Figure 1.31** Binding of the SNX subcomplex to CSC leads to retromer polymerization, and release of Ypt7 thus separating a retromer-positive tubule and a Ypt7-positive membrane. (Purushothaman et al., 2017).

The interplay between complexes such as the retromer and the WASH complex, highlight the importance of actin- and microtubule- based movement, as well as the central role of retromer, in endosomal protein sorting (Seaman, 2012). Among the identified retromer cargoes are membrane proteins such as receptors (Arighi et al., 2004; Fjorback et al., 2012; Nielsen et al., 2007; Seaman, 2004), transporters (Tabuchi et al., 2010), transport proteins (Eaton, 2008), enzymes (Arcones et al., 2016) and an apical protein required for cell polarity in epithelial cells (Pocha et al., 2011). Membrane recruitment of the retromer complex in budding yeast is achieved by bivalent recognition of the PI3K-effector SNX3 and the Rab7 GTPase, by the VPS35 retromer subunit (Harrison et al., 2014). An alternative endosomal recycling mechanism in *S. cerevisiae* depends on clathrin-coated vesicles (CCVs) and three different sets of adaptors, the AP-1 complex, GGAs and the epsin-like proteins Ent3/5, which recruit clathrin to the intracellular reservoir at the TGN/EE boundary, facilitating the loading of different cargoes and preventing vacuolar degradation (Arcones et al., 2016; Robinson, 2015).

The heterotetrameric Golgi-associated retrograde protein (GARP) tethering complex is required for fusion of retrograde transport vesicles from both the early and late endosomes to the trans-Golgi network (TGN) in a wide range of eukaryotes, including budding yeast and human. Comprised of the Vps51, Vps52, Vps53 and Vps54 subunits, GARP mediates the retrieval of recycling transmembrane proteins such as the vacuolar protein sorting receptor Vps10 and the v-SNARE Snc1, to the TGN (Bonifacino and Hierro, 2011; Morishita et al., 2007). Moreover, GARP-dependent endosome-to-TGN retrograde transport appears to be extremely important for the maintenance of post-Golgi anterograde transport of recycling transmembrane cargoes in HEK293 cells and in *A.*



*nidulans*, highlighting the necessity of dynein-mediated basipetal transport for proper recycling of selected cargoes (Hernández-González et al., 2018; Hirata et al., 2015). Vps52 is an effector of RabC<sup>RAB6</sup>/Ypt6, a Rab GTPase also involved in retrograde traffic from the endosomes to the Golgi, operating at the cytosolic surface of the late Golgi (Pantazopoulou and Peñalva, 2011; Siniosoglou and Pelham, 2001) along with the late Golgi t-SNARE syntaxin 16 and its fungal homologue TlgB<sup>Tlg2</sup> (Amessou et al., 2007; Lewis et al., 2000; Siniosoglou et al., 2000). *A. nidulans* TlgB is a Qa syntaxin that forms SNARE

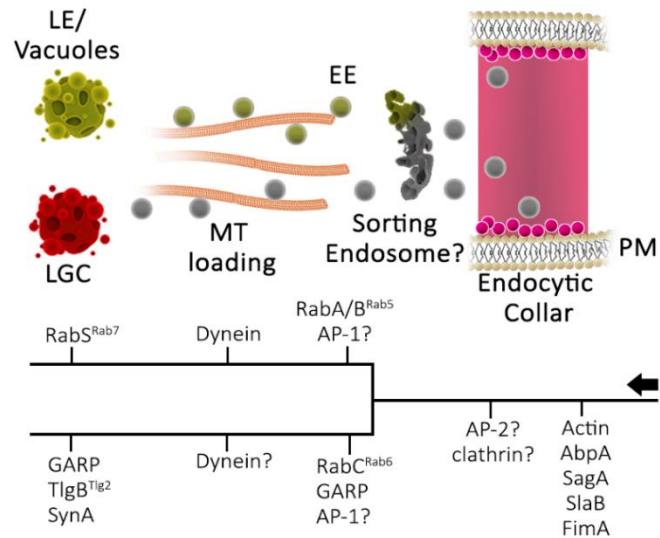


**Figure 1.32** A simplified schematic overview of the endocytic and retrograde pathway in *A. nidulans*, starting from right to left. Endocytic patches of filamentous fungi are localized predominately in the collar region (©Olga Martzoukou).

bundles with the SynA synaptobrevin as R-SNARE and co-localizes with PH<sup>OSBP</sup> (López-Berges et al., 2016; Pinar et al., 2013a). This SNARE bundle most probably mediates the fusion of endosome-derived retrograde traffic with the late Golgi, a pathway followed by proteins that are efficiently internalized at the subapical endocytic collar and recycle through the TGN before redirected for apical exocytosis to the PM (Abenza et al., 2009; Pantazopoulou and Peñalva, 2011; Taheri-Talesh et al., 2008). Genetic ablation of TlgB results in a minor effect on SynA localization except when combined with a mutation in the early Golgi syntaxin sedV (López-Berges et al., 2016). This indicates that when TlgB is absent, cargoes can recycle through early Golgi cisternae in a SedV<sup>Sed5</sup>-dependent manner and then move forward to the TGN by cisternal maturation (Steinberg et al., 2017). Moreover in mammalian cells, Rab6a'-mediated retrograde traffic from endosomes to the Golgi involves syntaxin 16 as well as syntaxin 5, the mammalian equivalents of Tlg2 and Sed5, respectively (Amessou et al., 2007). It has been suggested that RabC/Ypt6 plays a role in marking specific Golgi sites that accept endosome-derived carriers, at late (Tlg2-dependent) and early (Sed5-dependent) Golgi entry points (Siniosoglou and Pelham, 2001; Tsukada et al., 1999).

### 1.3.8 Endocytic recycling in polar cell growth

The basic mechanisms involved in membrane trafficking are very similar in all eukaryotic cell types. However, cell polarity and growth by apical extension of mammalian neurons or filamentous fungi is highly demanding in special trafficking mechanisms in the apical parts, compared to

subapical regions or non-polar cells, such as yeast cells. In the tips of polarized hyphal cells, a slightly subapical collar of endocytosis encircles an apical crescent where exocytosis predominates, although both processes can occur in subapical regions as well (Schultzhaus and Shaw, 2015; Valdez-Taubas and Pelham, 2003). Exocytosis and endocytosis are essential for hyphal growth and the tip growth apparatus can simply be thought of as a centre for apical delivering of exocytic vesicles and for recycling vesicular components. The spatial coupling of endocytosis and apex-directed exocytosis via a recycling route polarizes cargoes, maintaining the high exocytosis rate required for sustaining rapid hyphal extension (Peñalva, 2010; Upadhyay and Shaw, 2008).

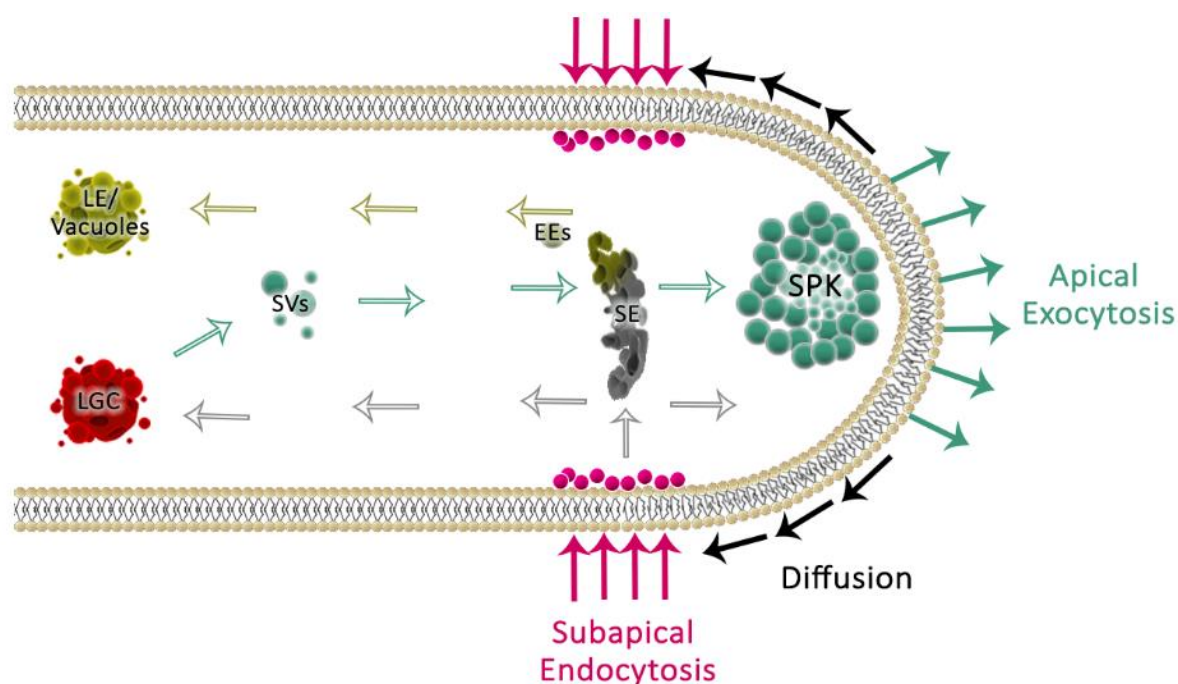


**Figure 1.33** Schematic overview of the endocytic recycling process in *A. nidulans*. The spatial coupling of subapical endocytosis with apex-directed exocytosis polarizes cargoes (©Olga Martzoukou).

Thus far only three cargoes of the endocytic recycling route have been identified in *A. nidulans*, including the synaptobrevin v-SNARE SynA, the phospholipid flippase DnfA and the chitin synthase ChsB (Abenza et al., 2009; Hernández-González et al., 2018; Lucena-Agell et al., 2015; Pantazopoulou and Peñalva, 2011; Peñalva, 2015; Schultzhaus et al., 2015; Taheri-Talesh et al., 2008; Valdez-Taubas and Pelham, 2003; Zhou et al., 2018). These polarized cargoes are incorporated into the PM during exocytosis and diffuse laterally in the membrane until encountered by the forward moving actin/AbpA collar. They are then internalized by endocytosis, recycled through endosomal and Golgi compartments and re-directed to the PM, most probably in a RabE-dependent manner (Hernández-González et al., 2018; Steinberg et al., 2017; Taheri-Talesh et al., 2008). In line with that observation, inactivation of basic regulators of the endocytic internalization machinery leads to lethality, seemingly due to a defect in polarity maintenance. It has been firmly established that

spatially coupled exocytosis and endocytosis are vital for the stabilization of polarity axes and thus for hyphal tip growth in *A. nidulans*, *A. oryzae*, *N. crassa*, and *A. gossypii* (Araujo-Bazán et al., 2008; Echaury-Espinosa et al., 2012; Higuchi et al., 2009; Jorde et al., 2011; Taheri-Talesh et al., 2008; Upadhyay and Shaw, 2008). Moreover, in *U. maydis* endocytic receptor recycling is essential during the early steps of pathogenicity (Fuchs et al., 2006). Several transmembrane cargoes, among which Snc1p (Valdez-Taubas and Pelham, 2003) and Wsc1p (Piao et al., 2007) follow the recycling pathway through the TGN, but things are different for filamentous fungi, as recycling of the Snc1p homologue SynA is RabC-independent (Pantazopoulou and Peñalva, 2011). However, a block in SynA endocytosis led to its uniform localization across the PM in *A. nidulans* (Hervás-Aguilar and Peñalva, 2010; Pantazopoulou and Peñalva, 2011), a phenotype similar to the one observed for DnfA, when its endocytic motif NPFxD was mutated (Schultzhause et al., 2015). Indirect endocytic recycling through the TGN is indisputably necessary for polarized growth. Therefore, it is likely that filamentous fungi have also developed a more direct recycling route, which remains uncharacterized.

One characteristic feature that qualifies *A. nidulans* as a model organism for intracellular traffic studies is that its hyphal tip cells grow exclusively by apical extension, which is supported by the highly polarized and continuous delivery of secretory vesicles to the apex. Special secretory organelles such as the unmatched fungal SPK constitute adaptations to this mode of growth, as secretory vesicles for example, accumulate there and organize into two strata before fusing with the apical membrane (see also 1.3.5). This apical extension appears to be transient rather than continuous, as the sites of vesicle fusion and polar growth direction are defined by the position of the SPK and cell end markers, such as the membrane-bound TeaR and its cytoskeleton-transported interacting partner, TeaA. Incessant delivery of vesicles that contain cell-end markers and recycled cargoes to the same polarity site, grants a stable supply of proteins necessary for growth. Disassembly and reassembly of temporary growth zones results in pulses of apical extension followed by small periods of growth arrest. Finally, the entire apex moves forward as new growth zones are established within the hyphal tip, at regions slightly offset from the earlier polarity site. In that way, loss of cell polarity is prevented as the previous growth zones are constantly turned over and polarized cargoes are efficiently recycled (Fischer et al., 2008; Ishitsuka et al., 2015; Takeshita et al., 2008).

### 1.3.9 Degradation Pathway

Upon co-translational insertion into the lipid bilayer of the endoplasmic reticulum (ER), newly synthesized membrane proteins are subject to a complex series of sorting, trafficking, quality

control and quality maintenance mechanisms in the secretory and endocytic pathways. A major control point is introduced from the moment cell surface proteins or cargoes reach the plasma membrane, as they are subject to tight downregulation (MacGurn, 2014). When not needed, these proteins are endocytosed and re-routed for degradation in the vacuole, directed through a series of sorting events and trafficking steps. Other control points include Golgi-to-endosome traffic, Golgi complex quality control and autophagy, which will not be discussed in detail here. A key regulator of many of these processes is the aforementioned ubiquitination, a post-translational modification which promotes rapid removal of fungal and mammalian membrane proteins via endocytosis, in response to various signals (see also 1.3.6).

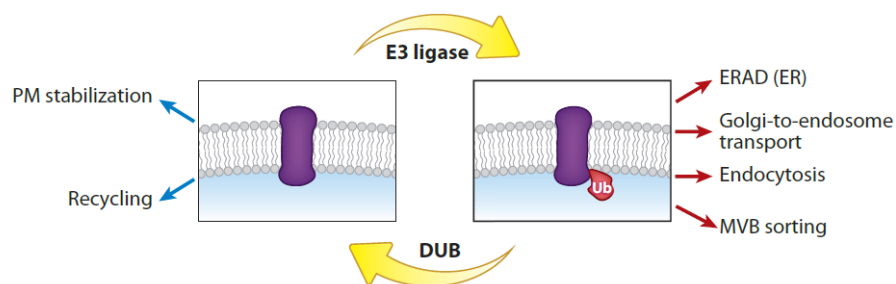


**Figure 1.34** The ubiquitin modification cycle of protein sorting from the plasma membrane and intracellular trafficking (MacGurn et al., 2012).

Ubiquitination is a reversible modification, and Ub is recycled after cleavage of the isopeptide bond by specific proteases termed De-Ubiquitinating enzymes (DUBs). For most transmembrane cargoes studied in yeast, cargo ubiquitination at the PM appears to be the primary determinant of endocytosis. The E3 ubiquitin ligase that mediates cargo ubiquitination and targeting for endocytosis, Rsp5, belongs to the Nedd4 HECT family and is a homologue of the *A. nidulans* HulA. An elaborate network of adaptors is responsible for mediating the interaction between the ubiquitin ligase and fungal PM proteins that do not contain PY motifs, as Rsp5<sup>HulA</sup> is recruited to cargoes with the help of arrestin-like soluble adaptors (Karachaliou et al., 2013; Lin et al., 2008; Nikko and Pelham, 2009). Interaction between ubiquitinated cargoes and adaptors possessing Ub-binding domains (e.g., epsin) mediates sorting into newly formed endocytic invaginations, which upon scission from the PM, fuse with the membrane of EEs. As mentioned earlier, some cargoes are recycled indirectly through the TGN or directly to the PM, while others are sorted for lysosomal/vacuolar delivery in a process that involves EE motility and includes maturation from an EE to a late endosome (LE) (Abenza et al., 2010, 2012).

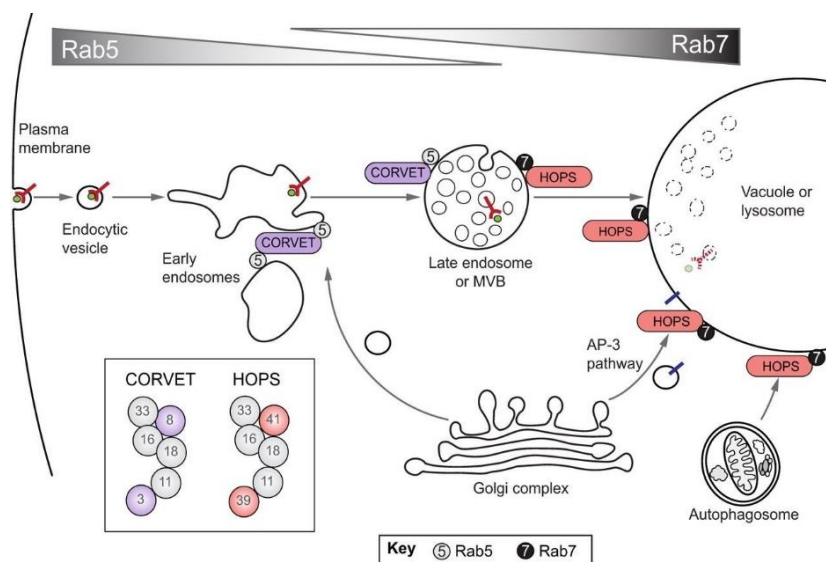


**Figure 1.35** Degradative pathway. Cargoes are endocytosed and transported into early endosomes. Rab5 recruits CORVET, which mediates homotypic fusion. During the early-to-late endosome maturation, Rab5 is substituted by Rab7 and CORVET by HOPS, which promotes homotypic fusion with the lysosomes/vacuoles (Balderhaar & Ungermann, 2013).

Of central importance for the biogenesis of endosomes and lysosomes in eukaryotic cells are certain associated membrane-tethering and fusion events that are mediated by CORVET/HOPS and SNARE complexes, respectively (Balderhaar and Ungermann, 2013; Krämer and Ungermann, 2011). CORVET ('class C core vacuole/endosome tethering') and HOPS ('homotypic fusion and protein sorting') complexes have been mainly, but not exclusively, characterized in yeast but are present also in *A. nidulans* (Abenza et al., 2010; López-Berges et al., 2017; Pinar et al., 2013b). These are heterohexameric protein complexes mediating the maturation of EEs into LEs, comprised of four common 'core' components, Vps11, Vps16, Vps18 and Vps33, and differing in two specific subunits, CORVET Vps8 and Vps3, and HOPS Vps39 and Vps41. They interact with Rab GTPases, mediate membrane tethering, and guide SNARE assembly that results in membrane fusion. Endocytic vesicles are tethered to EEs, where CORVET binds to the GTPase Rab5 and mediates endosome to endosome fusion. The HOPS complex on the other hand operates at the late endosome/multivesicular body (LE/MVB) stage as a Rab7 effector and mediates multiple fusion events including vacuolar homotypic fusion and vacuole protein sorting (Balderhaar and Ungermann, 2013; Bröcker et al., 2012; López-Berges et al., 2017).

The formation of a new LE is preceded by the generation of a Rab7 domain (Rink et al., 2005; Vonderheit and Helenius, 2005), which leads to the transient formation of a hybrid Rab5/Rab7 endosome. During maturation, membrane components and proteins responsible for fusion are exchanged, endosomes are localized to the perinuclear area, and the luminal pH is decreased. Moreover, a vacuolar morphology is acquired, to such an extent that early and late endosomes can be distinguished by electron microscopy (Abenza et al., 2012; Griffith and Reggiori, 2009; Huotari and Helenius, 2011; Prescianotto-Baschong and Riezman, 2002). Transmembrane proteins targeted to the vacuole can be sorted by not only cis-acting sorting signals, such as ubiquitin (Ub), but also

trans-acting factors like the Endosomal Sorting Complex Required for Transport (ESCRT) machinery (Henne et al., 2011) that operates in parallel on maturing endosomes (Arlt et al., 2015; Toshima et al., 2006).

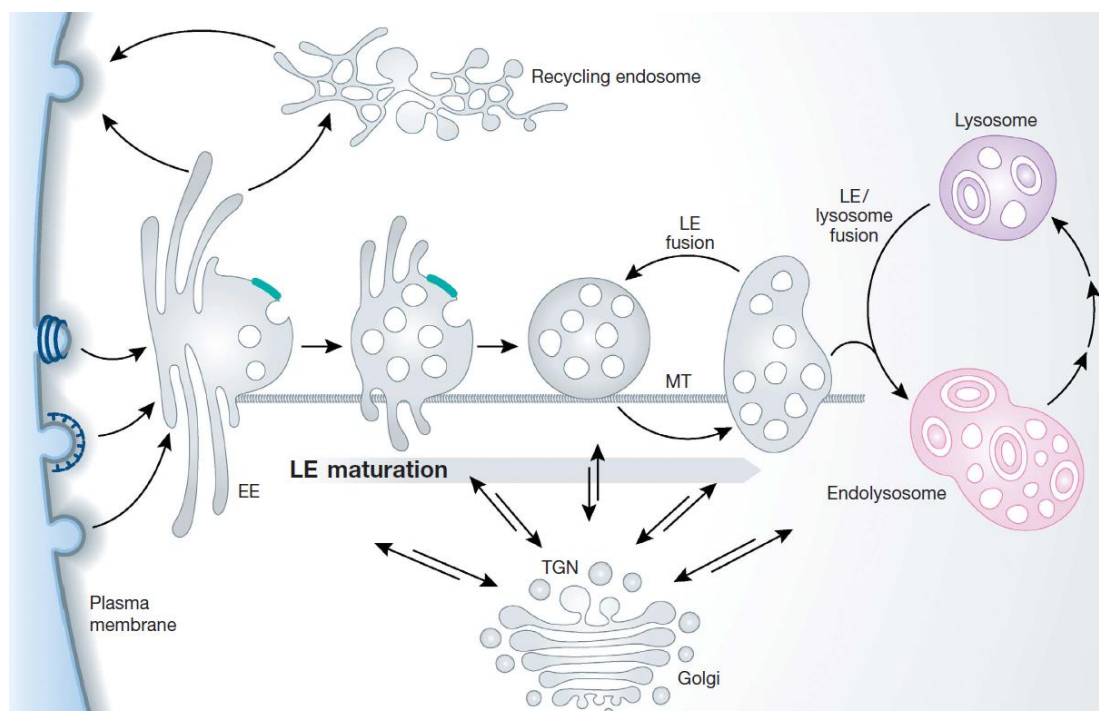


**Figure 1.36** The endosomal /degradative pathway. Following cargo internalization from the plasma membrane, entrance to the endocytic pathway results either in recycling or in targeting to the lysosome/vacuole for degradation through the endosomal system (Huotari and Helenius, 2011).

### 1.3.10 The cytoskeleton: General aspects and its role in fungal protein trafficking

The fungal cytoskeleton provides the framework for cell shape, hyphal branching, cytokinesis and morphogenesis. Protein trafficking also largely depends on *motorized movement* of the vesicles either on the *actin cytoskeleton* or on *microtubules*. Experimental evidence exists for both microtubule and actin cytoskeleton involvement in the intracellular transport of organelles and vesicles, cargo secretion to the PM and for actin participation in endocytosis from the PM. *Septins* have also been recognized as an important component of the cytoskeleton in a wide range of eukaryotic species. They participate in almost all known cytoskeletal functions in filamentous fungi, while a few extra functions have been attributed to them, including septation, chitin deposition, branching pattern regulation, preventing diffusion and conidiophore development.

### 1.3.10.1 Microtubules

Microtubules (MTs) are of central importance during mitosis, but in filamentous fungi they have some additional roles during interphase. They are important for the distribution of nuclei or other organelles and serve as tracks for transported vesicles (Takeshita et al., 2014; Xiang and Fischer, 2004). The discovery of gamma-tubulin (Oakley and Oakley, 1989) came from a genetic screen designed to identify genes important for MT function in *A. nidulans* and was found in all eukaryotes afterwards (Weil et al., 1986). Gamma-tubulin functions in microtubule nucleation and polar orientation found primarily in centrosomes and spindle pole bodies (SPB), which serve as fungal Microtubule Organizing Centers (MTOCs). SPBs are analogous to centrosomes in higher eukaryotes, but do not contain centrioles (Kilmartin, 2014; Seybold and Schiebel, 2013).

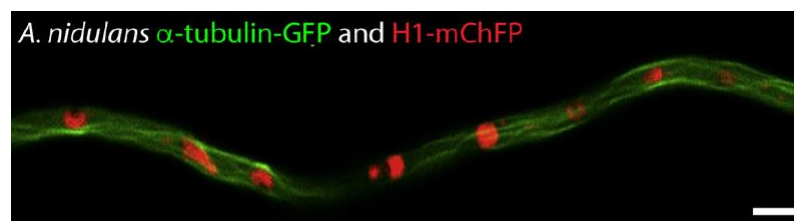


**Figure 1.37** Microtubules and nuclei visualized in *A. nidulans* with fluorescent tagged versions of  $\alpha$ -tubulin and H1 histone, respectively (Riquelme et al., 2018).

Two other members of the tubulin family, the dimer-forming Alpha-tubulin and Beta-tubulin are structural elements of the microtubule cytoskeleton but do not contribute to microtubule nucleation. MTs are tubular structures made of  $\alpha$  and  $\beta$ -tubulin heterodimers organized in 13 protofilaments, forming a hollow cylinder. Dimers polymerize at the (+) ends of MT by non-covalent bonding and ultimately form the protofilament structure. *In vivo* observations of *A. nidulans* revealed that MT plus ends originate from nuclei (MTOCs) but also from septa (sMTOCs), with the latter remaining to be elucidated (Konzack et al., 2005). Polarized microtubules are oriented in either anti-parallel or uniform arrays that exhibit a dynamic instability (Gardner et al., 2008). They continuously elongate for a period until they reach the cortex, and then depolymerize, until they recover and grow again (Ishitsuka et al., 2015).

For several eukaryotic cells –such as neurons of filamentous hyphae-, the regulation of size, shape and polarization is dependent on the fast, MT-based, long-range transport of vesicular carriers. Defects in microtubule-based transport are implicated in many neuropathologies (Hirokawa et al., 2010) and cause severe problems in vesicular trafficking and maintenance of apical growth (Fischer et al., 2008; Horio and Oakley, 2005; Sampson and Heath, 2005; Zhang et al., 2011). However, apical growth and mitosis do not compete for cellular resources. Presumably, the

population of cytoplasmic microtubules involved in polarized growth operates independently of that involved in mitosis (Riquelme et al., 2003).

Known MT-transported cargoes include endosomes, messenger RNA, secretory vesicles, peroxisomes, as well as nuclear pore complexes reflecting the diversity of metazoan systems (Abenza et al., 2009; Egan et al., 2012a; Gerst, 2008; Guimaraes et al., 2015; Lenz et al., 2006). Secretory vesicles containing components of the tip growth apparatus are transported along microtubules to the apical region in an acropetal manner, before being transferred to actin cables and delivered to the apical cortex of the hypha. This continuous flow of secretion carriers from the hyphal cell body to the tip is essential for cell wall and membrane extension (Fischer et al., 2008; A. Pantazopoulou et al., 2014; Taheri-Talesh et al., 2008; Zhou et al., 2018). Endosomes are transported bidirectionally along microtubules and apart from their role in lipid and membrane protein recycling, they seem to have a newly discovered role in subcellular transport: Serving as multipurpose platforms for a variety of ‘hitchhiking’ cargoes, such as lipids, proteins, mRNAs, ribosomes, and even whole organelles that achieve motility by connecting to moving ‘vehicle’ endosomes (Guimaraes et al., 2015; Haag et al., 2015; Salogiannis and Reck-Peterson, 2017).

Besides serving as tracks for vesicular traffic, microtubules are imperative in the maintenance of growth direction of hyphae and for holding the tip growth apparatus in position (Riquelme et al., 1998; Taheri-Talesh et al., 2008). TeaA, a cell end marker of *A. nidulans*, is specifically delivered to the apex by polymerizing microtubules with the help of the motor protein KipA and is anchored at the membrane by direct interaction with the prenylated TeaR, linking the MT and the actin cytoskeletons (Fischer et al., 2008; Ishitsuka et al., 2015; Takeshita et al., 2018, 2013). The interaction of the two cell end markers at the apical crescent triggers the recruitment of the formin SepA, which in turn initiates actin cable polymerization for targeted cargo exocytosis and

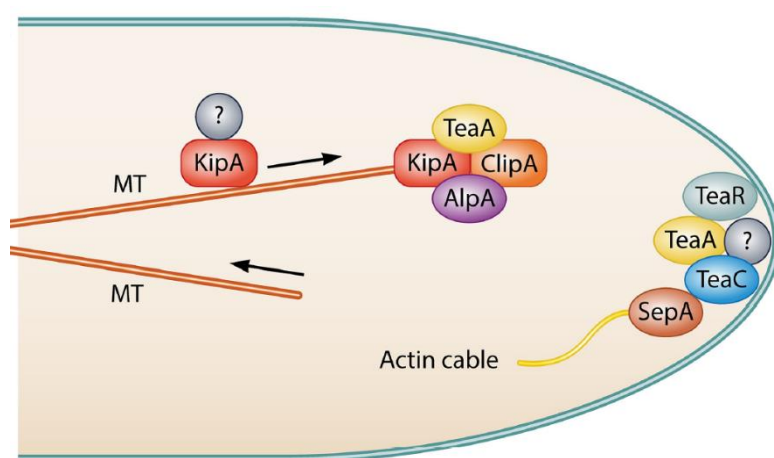


**Figure 1.38** Interaction of the microtubule and actin cytoskeleton at cortical sites is mediated by cell-end markers (Riquelme et al., 2018).

polarized growth (Higashitsuji et al., 2009). A suggested mechanism for MT guidance and pulling along actin filaments involves their capture at hyphal tips by MigA<sup>Kar9</sup>, which interacts with myosin V and probably enables trafficking toward the apex. MigA has an additional role in spindle positioning during mitosis via interaction with the



cortical protein ApsA, in the same way the homologue proteins, Kar9 and Num1 interact during mitosis in budding yeast (Fischer et al., 2008; Manck et al., 2015).

### 1.3.10.2 Actin

Actin cytoskeleton organization and functionality are of central importance in filamentous fungi apical growth, morphogenesis, exocytosis, endocytosis, and cytokinesis (Berepiki et al., 2011; Harris and Momany, 2004; Taheri-Talesh et al., 2008; Torralba et al., 1998; Upadhyay and Shaw, 2008; Virag and Griffiths, 2004). Actin polymerizes to form filaments (filamentous [F] actin) which assemble into different higher-order structures, such as actin rings, patches, and cables, which are required for distinct processes. Responsible for the regulation of F-actin structure and function are several Actin-Binding Proteins (ABPs), such as fimbrin, coronin, the Arp2/3 complex, and myosin II (Delgado-Álvarez et al., 2010; Riquelme et al., 2018; Taheri-Talesh et al., 2008).

Contractile actin rings guide septation during cytokinesis. The septal actomyosin tangle (SAT), a structure necessary for establishing the septation site, is a collection of F-actin cables associated with tropomyosin and a class II myosin. Soon after SAT formation the contractile actomyosin ring (CAR) assembles, driving the final step of cytokinesis. Although not every nuclear division generates a septum, mitotic signaling, cytokinesis and cell wall synthesis are processes linked with septation (Delgado-Álvarez et al., 2010; Gladfelter, 2006; Harris, 2001; Mouriño-Pérez, 2013; Seiler and Justa-Schuch, 2010).

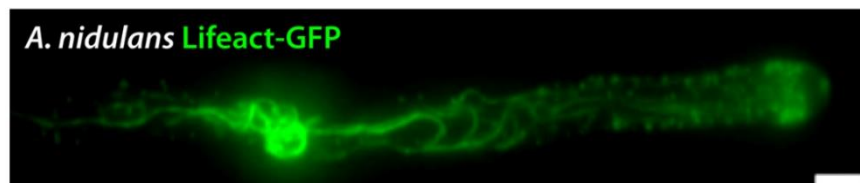


**Figure 1.39** Actin patches and cables at hyphal apical and subapical regions of *A.nidulans*, visualized with actin reporter Lifeact (Riquelme et al., 2018).

Patches of actin are predominantly found at the subapical collar region and secondly at peripheral foci, where the endocytic internalization machinery is also present -including AbpA, SlaB, fimbrin, the Arp2/3 complex and coronin- (Araujo-Bazán et al., 2008; Berepiki et al., 2011; Delgado-Álvarez et al., 2010; Schultzhaus et al., 2016). Endocytic patches mediate the endocytic recycling of polarity markers in an actin-dependent manner, as actin coat assembly at the last step of the internalization process allows for membrane invagination and vesicle budding to occur (Idrissi et al., 2008; Upadhyay and Shaw, 2008). Studies in filamentous and yeast-like fungi reveal the essentiality of an F-actin-associated protein, fimbrin, for efficient endocytosis (Kübler and Riezman, 1993;

Upadhyay and Shaw, 2008). Interestingly, *A. nidulans* and *N. crassa* fimbrin mutants exhibit severe defects in normal colony growth and general lipid endocytosis, traced with the lipophilic endocytic marker FM4-64 (Geli and Riezman, 1998; Upadhyay and Shaw, 2008). The Arp2/3 complex, a component essential for viability in most fungi, is located exclusively in actin patches where it nucleates F-actin branches (Egile et al., 2005).

In addition to actin patches, actin cables localize along fungal hyphae. They exhibit a dynamic behavior with cycles of elongation and shrinkage making visualization extremely difficult, but not impossible, especially with the development of new fluorescent markers such as tropomyosin (TpmA) and Lifeact (Bergs et al., 2016; Delgado-Álvarez et al., 2010; Schultzhaus et al., 2016; Taheri-Talesh et al., 2008). The presence of actin cables at the apical region of the hyphae is explained through their involvement in polarized transport, probably serving as tracks for the myosin V-dependent transport of various cargoes including secretory and endocytic vesicles, mRNAs, and Golgi equivalents (Berepiki et al., 2011; Pruyne and Bretscher, 2000; Taheri-Talesh et al., 2012). More specifically, F-actin is required at the hyphal apex to accept vesicles transported along microtubules and direct them to the sites of polarized exocytosis (Zhou et al., 2018). Assembled microfilaments are bundled into polarized cables with barbed plus ends, towards which motor proteins (myosins) move. Cable extension requires fimbrin and tropomyosin and proceeds in a direction opposite to that of vesicle transport (Berepiki et al., 2011; Pruyne et al., 1998).

The SPK, this intermediate sorting hub where secretory vesicles accumulate prior to apical membrane fusion, acts as a 'relay station' from long-distance vesicular transport along microtubules to short-distance actin-dependent movement to the apical PM at the hyphal tip (Berepiki et al., 2011; Harris et al., 2005). Given that hyphal polar growth can occur for a considerable amount of time in the absence of functional MTs, F-actin-mediated vesicle delivery could presumably suffice for hyphal extension (Torralba et al., 1998). However, it seems likely that the interdependence of actin and MT-based transport contributes to efficient apical delivery and therefore rapid hyphal growth (Takeshita et al., 2014). Additional experimental data strongly indicate that the integrity of both the SPK and the whole tip growth apparatus -including the SPK, the subapical endocytic ring, the polarisome, the exocyst and the apical crescent- is maintained by actin cables (Horio and Oakley, 2005; Riquelme and Sánchez-León, 2014; Taheri-Talesh et al., 2008).

### **1.3.10.3 Septins**

Septins were first discovered in temperature-sensitive screens for cell division defects in yeast (Hartwell, 1971), but only several years later were they recognized as an important component of the cytoskeleton in a spectrum of eukaryotic species (Versele and Thorner, 2005). The septin

family is conserved in most eukaryotes and includes GTPases, unique from other components of the cytoskeleton in that they heterooligomerize into complexes with defined stoichiometry, which in turn polymerize into long cytoskeletal filaments (Oh and Bi, 2011). Septins are crucial for shaping cell morphology and function as multimolecular protein-binding scaffolds that participate in a wide range of cellular processes including cytokinesis, cell migration, cell–pathogen interactions, as well as septation, chitin deposition, bud-site selection and polarity axes establishment at lateral branches in fungi (Berepiki and Read, 2013; Fung et al., 2014; Gladfelter, 2006; Steinberg et al., 2017). They associate directly with membranes, microtubules, and actin filaments, with effects on the dynamic properties of the cytoskeleton (Kremer et al., 2005; Spiliotis, 2018; Spiliotis and Gladfelter, 2012). In fact, septins colocalize with both actin and tubulin polymers in mammalian cells (Kinoshita et al., 1997; Nagata et al., 2003; Surka et al., 2002). The higher-order septin structures include elongated filaments, gauzes, rings at septation sites and bars, formed through end-on-end connections of septin oligomers (DeMay et al., 2011; Gladfelter, 2006; Juvvadi et al., 2011; Lindsey et al., 2010).

Five members of the septin family have been characterized in *A. nidulans*: AspA, -B, -C, -D and -E (Momany et al., 2001). The first four ‘core’ septins interact and form a complex critical for development, while AspE is necessary for the assembly of the higher-order structures (Hernández-Rodríguez et al., 2014). AspA and AspC interact with each other and show identical localization in discrete spots, bars and rings. They are important for normal development, especially for regulating germ tube and branch emergence, septation and conidiophore organization (Lindsey et al., 2010). The septin AspB also forms bars as well as filaments, and localizes to forming

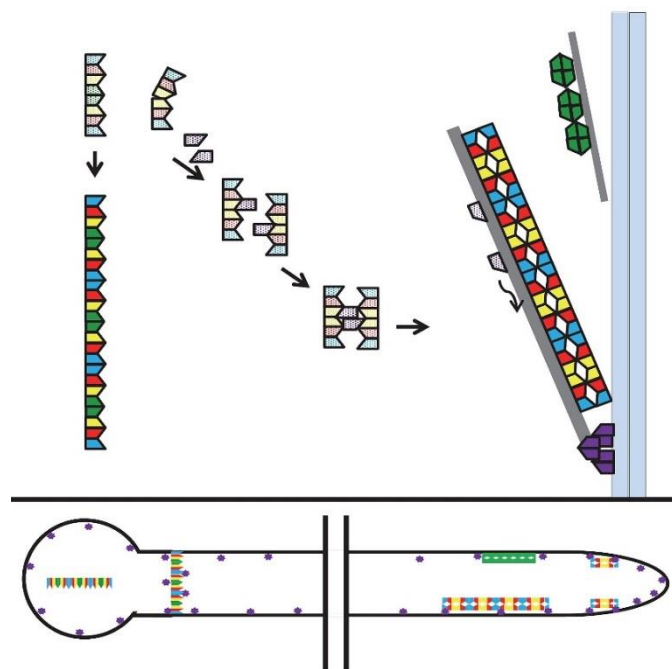


**Figure 1.40** Schematic representation of septin higher-order structure formation in *A.nidulans*. Blue: AspA; Red: AspC; Yellow: AspB; Green: AspD; Purple: AspE (Hernández-Rodríguez et al., 2014).

septa, emerging secondary germ tubes, branches and layers of the conidiophore. Strains carrying a temperature-sensitive mutation in *aspB* exhibit hyperbranching and defects in conidiation (Hernández-Rodríguez et al., 2012; Westfall and Momany, 2002).

### 1.3.11 Motor proteins

Cytoskeletal motor proteins are categorized into two types based on the “tracks” they move along: Actin motors such as myosin use microfilament tracks through interaction with actin, while microtubule motor proteins, like dynein and kinesin, move along MTs through interaction with tubulin. An additional classification of microtubule motors sorts them into plus-end motors and minus-end motors, depending on the direction in which they “walk” along the microtubule tracks.

#### 1.3.11.1 Microtubule motors

Two classes of MT-dependent motors, the minus end- directed dynein and the plus end- directed kinesins, are involved in organellar positioning and vesicular transport. In filamentous fungi only a single dynein motor is encoded, unlike the multiple -at least 10- kinesin genes (Schoch et al., 2003). Secretory vesicles are propelled along MTs for long distances by motorized movement of the conventional kinesin-1 (KinA in *A. nidulans*) toward hyphal tips (plus-end), whereas Kinesin-3 (UnCA in *A. nidulans*) and dynein (NudA in *A. nidulans*), function in the transport of early endosomes in the anterograde and retrograde direction, respectively (Abenza et al., 2009; Egan et al., 2012b; Peñalva et al., 2017; Takeshita et al., 2014; Zekert and Fischer, 2009). In fact, a recent superresolution analysis confirmed the previous results and revealed mechanistic details of the motorized movement of both vesicular populations (EEs and SVs), using as single cargo the chitin synthase ChsB. Transport events of KinA carrying SVs, exhibit fast movement (7 to 10  $\mu\text{m s}^{-1}$ ), contrastingly to the slower one (2 to 7  $\mu\text{m s}^{-1}$ ) of UnCA transferring EEs (Zhou et al., 2018). Molecular motors such as kinesin play roles in MT interaction with other cellular components and organelle transport (endosomes, secretory vesicles). In kinesin mutants of the filamentous fungus *N. crassa*, vesicles can reach the SPK although growth is slightly impaired and the SPK displays an erratic path.

Moreover, KinA is involved in nuclei positioning, MT dynamics and is necessary for the co-transport of dynein/dynactin complexes to the plus-end of MTs, carried along with SVs (Efimov, 2003; Requena et al., 2001; Zhang et al., 2003). The study of selected cargoes led to the observation that transport of *A. nidulans* Class III (ChsB) and V (CsmA) chitin synthases to the hyphal tips depends on the conventional kinesin (Takeshita et al., 2015) and that KIF13A, a member of the kinesin superfamily proteins in neurons, mediates selective cargo transport from the TGN to the plasma membrane via direct interaction with the  $\beta$ 1 subunit of the AP-1 adaptor (Nakagawa et al., 2000), a rare case in which AP-1 functions not only as a coat adaptor, but also as a motor adaptor.

Dynein motor complexes are much larger than kinesin and myosin (an actin motor), and drive intracellular transport toward the minus end of microtubules, at the MTOCs. In filamentous fungi, dynein is also implicated in nuclear distribution (Morris, 2003) additionally to the retrograde transport of vesicles and organelles (Seiler et al., 1999). Many genes involved in the *A. nidulans* dynein pathway have been isolated as *nud* (nuclear distribution) mutants leading to the identification of several associated components, including the dynein /dynactin complexes (Eckley et al., 1999; Holleran et al., 1998; King, 2000). Other isolated genes include NudF/Lis1 and NudE/Ro11, all localizing at comet-like structures that coincide with the MT plus-end loading zone and functioning in the cytoplasmic dynein pathway (Efimov, 2003; Zhang et al., 2003). Early endosome - but not secretory vesicle- dynein-based motility is regulated with the mediation of an additional adapter complex, known as Hook protein (HookA in *A. nidulans*). The Hook complex is anchored to the EE membrane and presumably upon interaction with dynein and kinesin-3, controls the activity or the attachment of both motors during bidirectional EE movement (Bielska et al., 2014; Steinberg, 2014; Zhang et al., 2014).

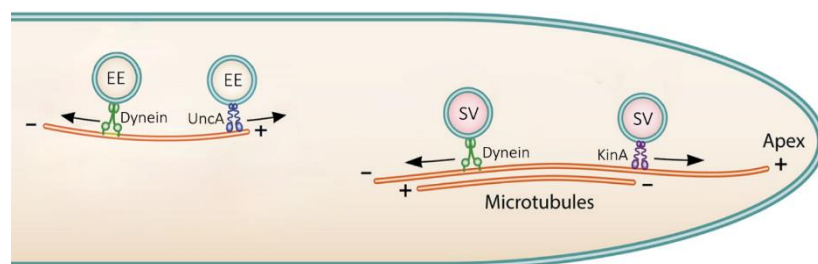


**Figure 1.41** Bidirectional motorized transport of early endosomes (EE) and secretory vesicles (SV) along microtubules (Adapted from Riquelme et al., 2018).

### 1.3.11.2 Actin motors

The genomes of the filamentous fungi *N. crassa* and *A. nidulans* contain a myosin I protein (MyoA, single-headed motor), a myosin II protein (MyoB, two headed motor implicated in actin-filament sliding), a myosin V (MyoE, two-headed motor implicated in vesicle transport), and an interesting filamentous fungus-specific allele, *csmA*, encoding a chimera of a myosin motor domain and a chitin synthase domain (Takeshita et al., 2002). Besides cortical actin patches, endocytosis of materials at the subapical ring of *A. nidulans* requires the activity of the myosin I MyoA, a protein also enriched in growing hyphal tips and at sites of septation (McGoldrick et al., 1995; Yamashita and May, 1998). MyoB can be found in contractile rings at forming septa and is critical for chitin deposition, septation, but not for hyphal elongation (Taheri-Talesh et al., 2012). The myosin-5 MyoE localizes to the Spk and moving cytoplasmic foci, and has been implicated in polarized growth as it mediates vesicle transport along actin cables in the apex-proximal area. Importantly, MyoE is

essential for polar hyphal extension and colony formation in the absence of all MT-based trafficking events (Taheri-Talesh et al., 2012; Zhang et al., 2011).

Connecting the puzzle pieces of vesicular trafficking reveals a dynamic picture of polarity maintenance during directional growth. Experimental data support a relay mechanism by which SVs are translocated by kinesin(s) (Lenz et al., 2006) on extending microtubules to the tip, where they are handed over to MyoE for the final step of transport to the PM (Pantazopoulou et al., 2014; Sharpless and Harris, 2002; Taheri-Talesh et al., 2012). This step involves association with F-actin cables, the assembly of which is nucleated by the formin SepA. Finally, SVs are either recycled back by dynein, or moved into the different SPK strata based on their molecular identity (macro- or micro-vesicles), where they are await briefly until the next calcium signal triggers exocytosis (Steinberg, 2007).

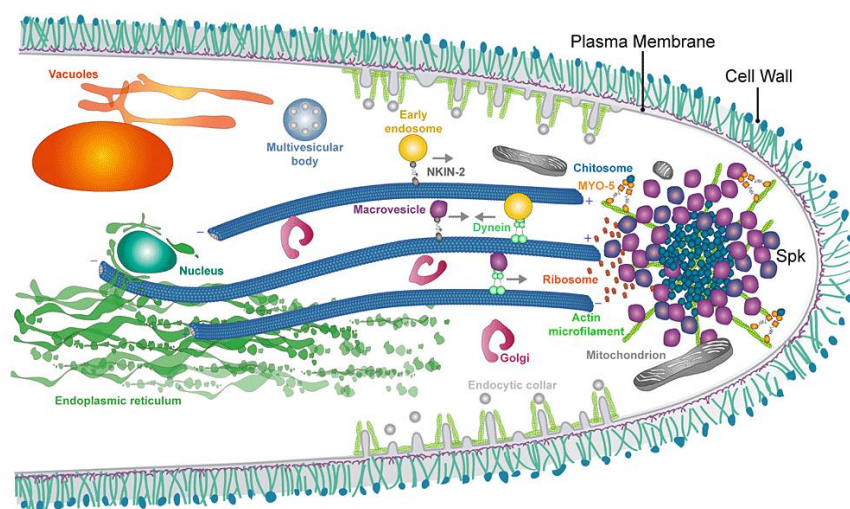


**Figure 1.42** Cartoon depicting the apical and subapical hyphal region of *A.nidulans* (Adapted from Riquelme and Martínez-Núñez, 2016).

## 1.4 AIMS OF THIS STUDY

The main idea of this dissertation is to gain insight on the intracellular trafficking pathways of the filamentous fungus *Aspergillus nidulans*, focusing on several distinct transport steps.

Our first aim is to study the role of UapA dimerization in ER-exit, by using selected ER-retained versions of the purine transporter, as well as pull-down assays and Bimolecular Fluorescence Complementantion (BiFC) assays (Chapter 3.1).

The second goal of our study is the investigation of the role of Adaptor Protein (AP) complexes and clathrin, in protein trafficking. More specifically, we will focus on the role of the three fungal multi-subunit complexes (AP-1, AP-2 and AP-3) in transporter vesicular traffic, using as a cargo the extensively studied transporter of the NAT/NCS2 family, UapA, as well as six more

transporters. In the same study, we will also investigate for the first time the role of clathrin light and heavy chains in the subcellular trafficking of transporters (Chapter 3.2).

Next, within the scope of this thesis, we will study the role of the AP-1 and AP-2 complexes in more detail. Thus, our third aim is to dissect the essential role of AP-1 in intracellular traffic and exocytosis of clathrin-coated vesicles, as well as in endosomal recycling. In parallel, we will elucidate the involvement of the cytoskeleton, motor proteins and Rab GTPases in these trafficking routes (Chapter 3.3).

For the last part of this work, we will investigate the role of the AP-2 complex in the endocytosis of selected cargoes and in apical membrane lipid and cell wall composition maintenance, along with a possible role for clathrin in these processes (Chapter 3.4).

The experimental work of this dissertation is separated in four parts, that fall within the general aim of studying established and emerging aspects of vesicular membrane protein trafficking.

## CHAPTER 2

## MATERIALS AND METHODS

## 2.1 STRAINS, CULTURE MEDIA, GROWTH AND STORAGE CONDITIONS

## 2.1.1 Strains used in this study

All strains carry the *veA1* mutation affecting sporulation. *pabaA1*, *pyroA4*, *riboB2*, *argB2*, *pyrG89*, *pantoB100*, *nicA2* and *inoB2* are auxotrophic mutations for p-aminobenzoic acid, pyridoxine, riboflavin, arginine, uracil/uridine, D-pantothenic acid nicotinic acid and inositol respectively. *yA2* and *wA4* are mutations resulting in yellow and white conidiospore colors respectively.

**Table 2.1** List of strains used in Chapter 3.1

Strain Genotype	References
<i>pabaA1</i>	wild-type reference strain
<i>uapA-K572R-gfp::argB uapAΔ azgAΔ uapCΔ:: AFpyrG pabaA1</i>	Gournas et al., 2010
<i>uapA100 pabaA1 pyroA4</i>	Ravagnani et al., 1997
<i>uapAΔ uapCΔ:: AFpyrG azgAΔ pabaA1</i>	Pantazopoulou et al., 2007
<i>uapA100 uapCΔ? azgAΔ pyroA4</i>	this study
<i>uapA-K572R-gfp uapA100 uapCΔ? azgAΔ</i>	this study
<i>alcA<sub>p</sub>-uapA-His uapAΔ uapCΔ:: AFpyrG azgAΔ pabaA1</i>	Lemuh et al., 2009
<i>alcA<sub>p</sub>-uapA-GFP uapAΔ uapCΔ:: AFpyrG azgAΔ pabaA1</i>	Gournas et al., 2010
<i>alcA<sub>p</sub>-uapA-GFP uapAΔ uapCΔ:: AFpyrG azgAΔ pantoB100</i>	this study
<i>alcA<sub>p</sub>-uapA-His alcA<sub>p</sub>-uapA-GFP uapAΔ uapCΔ:: AFpyrG azgAΔ</i>	this study
<i>uapA-YFPc uapAΔ uapCΔ:: AFpyrG azgAΔ pabaA1</i>	this study
<i>uapA-YFPn uapAΔ uapCΔ:: AFpyrG azgAΔ pabaA1</i>	this study
<i>uapA-YFPc uapA-YFPn uapAΔ uapCΔ:: AFpyrG azgAΔ pabaA1</i>	this study
<i>alcA<sub>p</sub>-uapA-YFPn uapAΔ uapCΔ:: AFpyrG azgAΔ pabaA1</i>	this study
<i>alcA<sub>p</sub>-uapA-YFPc alcA<sub>p</sub>-uapA-YFPn uapAΔ uapCΔ:: AFpyrG azgAΔ</i>	this study
<i>uapA-GFP uapAΔ uapCΔ:: AFpyrG azgAΔ pabaA1</i>	Pantazopoulou et al., 2007
<i>uapAΔ::uapA-GFP uapCΔ:: AFpyrG azgAΔ pabaA1 argB2 pantoB100</i>	this study
<i>alcA<sub>p</sub>-uapA-I74D-GFP alcA<sub>p</sub>-uapA-I74D-His uapAΔ uapCΔ:: AFpyrG azgAΔ pabaA1 argB2</i>	this study
<i>uapA-I74D-GFP uapAΔ uapCΔ:: AFpyrG azgAΔ pabaA1</i>	Amillis et al., 2011
<i>alcA<sub>p</sub>-uapA-I74D-YFPc alcA<sub>p</sub>-uapA-I74D-YFPn uapAΔ uapCΔ:: AFpyrG azgAΔ</i>	this study
<i>alcA<sub>p</sub>-uapA-I74D-YFPc alcA<sub>p</sub>-uapA-YFPn uapAΔ uapCΔ:: AFpyrG azgAΔ</i>	this study
<i>uapA-TMS14D-GFP uapAΔ uapCΔ:: AFpyrG azgAΔ pabaA1</i>	Vlanti et al., 2006
<i>alcA<sub>p</sub>-uapA-TMS14D-YFPc alcA<sub>p</sub>-uapA-TMS14D-YFPn uapAΔ uapCΔ:: AFpyrG azgAΔ</i>	this study
<i>alcA<sub>p</sub>-uapA-TMS14D-YFPc alcA<sub>p</sub>-uapA-YFPn uapAΔ uapCΔ:: AFpyrG azgAΔ</i>	this study
<i>alcA<sub>p</sub>-uapA-D44A/Y45A/D46A/Y47A-YFPc alcA<sub>p</sub>-uapA-D44A/Y45A/D46A/Y47A-YFPn uapAΔ uapCΔ:: AFpyrG azgAΔ</i>	this study
<i>alcA<sub>p</sub>-uapA-D44A/Y45A/D46A/Y47A-YFPc alcA<sub>p</sub>-uapA-YFPn uapAΔ uapCΔ:: AFpyrG azgAΔ</i>	this study
<i>alcA<sub>p</sub>-uapA-D44A/Y45A/D46A/Y47A-GFP uapAΔ uapCΔ:: AFpyrG azgAΔ</i>	this study
<i>alcA<sub>p</sub>-uapA-D44A/Y45A/D46A/Y47A-His alcA<sub>p</sub>-uapA-D44A/Y45A/D46A/Y47A-GFP uapAΔ uapCΔ:: AFpyrG azgAΔ</i>	this study
<i>prnB-GFP argB2 pabaA1 yA2</i>	Vangelatos et al., 2009
<i>prnB-YFPc::panB uapAΔ::uapA-YFPn::AFriboB uapCΔ::AFpyrG nkuAΔ::argB riboB2 pantoB100 pyroA4</i>	this study



**Table 2.2** List of strains used in Chapter 3.2

Strain Genotype	References
<i>pabaA1</i>	wild-type reference strain
<i>TNO2A7::nkuAΔ::argB pyrG89 pyroA4 riboB2</i>	Nayak <i>et al.</i> , 2006
<i>sagAΔ::AFriboB nkuAΔ::argB pyrG89 pyroA4 riboB2</i>	Karachaliou <i>et al.</i> , 2013
<i>thiA<sub>p</sub>::FLAG-ap1<sup>o</sup>::AFriboB nkuAΔ::argB pyrG89 pyroA4 riboB2</i>	This study
<i>ap2<sup>o</sup>Δ::AFriboB nkuAΔ::argB pyrG89 pyroA4 riboB2</i>	This study
<i>ap2<sup>h</sup>Δ::AFpyrG nkuAΔ::argB pyrG89 pyroA4 riboB2</i>	This study
<i>ap3<sup>o</sup>Δ::AFriboB nkuAΔ::argB pyrG89 pyroA4 riboB2</i>	This study
<i>thiA<sub>p</sub>-ap1<sup>o</sup>::AFriboB Ap2<sup>o</sup>Δ::AFriboB uapAΔ pabaA1</i>	This study
<i>ap2<sup>o</sup>Δ::AFriboB ap3<sup>o</sup>Δ::AFriboB uapAΔ uapCΔ::AFpyrG pabaA1</i>	This study
<i>uapA-GFP::AFriboB uapCΔ::AFpyrG nkuAΔ::argB pabaA1 pyroA4 riboB2</i>	Evangelinos <i>et al.</i> , 2016
<i>thiA<sub>p</sub>-ap1<sup>o</sup>::AFriboB uapAΔ::uapA-GFP</i>	This study
<i>ap2<sup>o</sup>Δ::AFriboB uapA-GFP uapCΔ::AFpyrG nkuAΔ::argB pabaA1</i>	This study
<i>ap3<sup>o</sup>Δ::AFriboB uapAΔ::uapA-GFP pabaA1</i>	This study
<i>alcA<sub>p</sub>::uapA-GFP::AFriboB uapCΔ::AFpyrG nkuAΔ::argB pabaA1 pyroA4 riboB2</i>	Evangelinos <i>et al.</i> , 2016
<i>alcA<sub>p</sub>::uapA-GFP::AFriboB ap2<sup>h</sup>Δ::AFpyrG riboB2 nkuAΔ::argB pyroA4</i>	This study
<i>prnBΔ::prnB-GFP argB2 pabaA1 yA2</i>	Tavoularis <i>et al.</i> , 2001
<i>agtAΔ::agtA-gfp::AFpyrG pyroA4</i>	Apostolaki <i>et al.</i> , 2009
<i>[fcyB-GFP]pBS-argB uapAΔ uapCΔ::AFpyrG azgAΔ argB2 pabaA1</i>	Vlanti and Diallinas, 2008
<i>[gpdA<sub>p</sub>::FurA-GFP]pGEM-panB uapAΔ uapCΔ::AFpyrG azgAΔ fcyBΔ::argB furDΔ::riboB furAΔ::riboB cntAΔ::riboB pantoB100 pabaA1</i>	Kryptou <i>et al.</i> , 2015
<i>[gpdA<sub>p</sub>::FurE-GFP]pGEM-panB uapAΔ uapCΔ::AFpyrG azgAΔ fcyBΔ::argB furDΔ::riboB furAΔ::riboB cntAΔ::riboB pantoB100 pabaA1</i>	Kryptou <i>et al.</i> , 2015
<i>[gpdA<sub>p</sub>::FurD-GFP]pGEM-panB uapAΔ uapCΔ::AFpyrG azgAΔ fcyBΔ::argB furDΔ::riboB furAΔ::riboB cntAΔ::riboB pantoB100 pabaA1</i>	Kryptou <i>et al.</i> , 2015
<i>prnB-GFP ap2<sup>o</sup>Δ::AFriboB nkuAΔ::argB</i>	This study
<i>agtA-GFP ap2<sup>o</sup>Δ::AFriboB nkuAΔ::argB pabaA1</i>	This study
<i>[fcyB-GFP]pBS-argB uapAΔ uapCΔ::AFpyrG azgAΔ ap2<sup>o</sup>Δ::AFriboB pabaA1 pyroA4</i>	This study
<i>[gpdA<sub>p</sub>::FurA-GFP]pGEM-panB ap2<sup>o</sup>Δ::AFriboB uapAΔ uapCΔ::AFpyrG azgAΔ fcyBΔ::argB furDΔ::riboB furAΔ::riboB cntAΔ::riboB pantoB100 pabaA1</i>	This study
<i>[gpdA<sub>p</sub>::FurE-GFP]pGEM-panB ap2<sup>o</sup>Δ::AFriboB uapAΔ uapCΔ::AFpyrG azgAΔ fcyBΔ::argB furDΔ::riboB furAΔ::riboB cntAΔ::riboB pantoB100 pabaA1</i>	This study
<i>[gpdA<sub>p</sub>::FurD-GFP]pGEM-panB ap2<sup>o</sup>Δ::AFriboB uapAΔ uapCΔ::AFpyrG azgAΔ fcyBΔ::argB furDΔ::riboB furAΔ::riboB cntAΔ::riboB pantoB100 pabaA1</i>	This study
<i>thiA<sub>p</sub>-claL::AFpyrG nkuAΔ::argB pyroA4 riboB2 pyrG89</i>	This study
<i>claLΔ::AFpyrG nkuAΔ::argB pyroA4 riboB2 pyrG89</i>	This study
<i>thiA<sub>p</sub>-claH::AFpyroA nkuAΔ::argB pyroA4 riboB2 pyrG89</i>	This study
<i>thiA<sub>p</sub>-claH::AFpyroA claH-(5xGA)GFP::AFpyrG nkuAΔ::argB pyrG89 pyroA4 riboB2</i>	This study
<i>uapA-GFP thiA<sub>p</sub>-claL::AFpyrG nkuAΔ::argB pyroA4 pyrG89</i>	This study
<i>thiA<sub>p</sub>-slaB::AFpyrG nkuAΔ::argB pyroA4 riboB2 pyrG89</i>	This study
<i>uapA-GFP thiA<sub>p</sub>-slaB::AFpyrG nkuAΔ::argB pyroA4 pyrG89</i>	This study

**Table 2.3** List of strains used in Chapter 3.3

Strain Genotype	References
<i>nkuAΔ::argB pyrG89 pyroA4 riboB2</i>	Nayak <i>et al.</i> , 2006
<i>H1-mRFP::AFriboB nkuAΔ::argB pyrG89 pyroA4</i>	Nayak <i>et al.</i> , 2010
<i>pyroA4[pyroA::gpdA<sup>m</sup><sub>p</sub>::mRFP-PH<sup>OSBP</sup>] inoB2 niiA4 wA4</i>	Pantazopoulou and Peñalva, 2009
<i>pyroA4[pyroA<sup>mut</sup>::gpdA<sup>m</sup><sub>p</sub>::mCherry-sedV] nkuAΔ::bar, wA4, niiA4 inoB2</i>	Pantazopoulou and Peñalva, 2011
<i>sagA-(5xGA)GFP::AFpyrG nkuAΔ::argB pyroA4 riboB2 pyrG89</i>	Karachaliou <i>et al.</i> , 2013
<i>slaB-GFP::AFpyrG nkuAΔ::argB pyrG89 pyroA4 argB2</i>	Araujo-Bazán <i>et al.</i> , 2008
<i>mCherry-synA::AFpyrG yA::AFpyroA GFP-tpmA fwA1 pyrG89 pyroA4 nicA2 nkuAΔ::argB</i>	Taheri-Talesh <i>et al.</i> , 2008
<i>abpA-mRFP::AFpyrG yA2 pabaA1 pyrG89</i>	Araujo-Bazán <i>et al.</i> , 2008
<i>GFP-ssA::AFpyrG nkuAΔ::bar pyrG89 pyroA4</i>	Taheri-Talesh <i>et al.</i> , 2008
<i>rab1<sup>A136D</sup>::AFpyrG pabaA1</i>	Pinar <i>et al.</i> , 2013

<i>sedV<sup>R238G</sup>::AFpyrG pyroA4 pyrG89 nkuAΔ::bar</i>	Pinar <i>et al.</i> , 2013
<i>alcA<sub>p</sub>::GFP-chsB::NCpyr4 nkuAΔ::argB pyrG89 pyroA4</i>	Takeshita <i>et al.</i> , 2013
<i>dnfA-GFP::AFpyrG nkuAΔ::argB pyrG89 pabaA1 pyroA4</i>	Schultzhaus <i>et al.</i> , 2015
<i>dnfB-GFP::AFpyrG nkuAΔ::argB pyrG89 pabaA1 pyroA4</i>	Schultzhaus <i>et al.</i> , 2015
<i>thiA<sub>p</sub>::FLAG-ap1<sup>o</sup>::AFriboB nkuAΔ::argB pyrG89 pyroA4 riboB2</i>	Martzoukou <i>et al.</i> , 2017
<i>thiA<sub>p</sub>::clal::AFpyrG nkuAΔ::argB pyroA4 riboB2 pyrG89</i>	Martzoukou <i>et al.</i> , 2017
<i>thiA<sub>p</sub>::FLAG-ap1<sup>o</sup>::AFriboB alcA<sub>p</sub>-uapA-GFP pabaA1</i>	Martzoukou <i>et al.</i> , 2017
<i>clal-(5xGA)GFP::AFpyrG nkuAΔ::argB pyroA4 riboB2 pyrG89</i>	Martzoukou <i>et al.</i> , 2017
<i>clalH-(5xGA)GFP::AFpyrG nkuAΔ::argB pyroA4 riboB2 pyrG89</i>	Martzoukou <i>et al.</i> , 2017
<i>clal-(5xGA)mRFP::AFpyrG nkuAΔ::argB pyroA4 riboB2 pyrG89</i>	Martzoukou <i>et al.</i> , 2017
<i>thiA<sub>p</sub>-clalH::AFpyroA dnfA-GFP::AFpyrG nkuAΔ::argB pyrG89 pabaA1 pyroA4</i>	Martzoukou <i>et al.</i> , 2017
<i>dnfA-GFP::AFpyrG ap2<sup>o</sup>Δ::AFriboB nkuAΔ::argB pyrG89 pyroA4</i>	Martzoukou <i>et al.</i> , 2017
<i>alcA<sub>p</sub>::mCherry-rabA::argB yA2 pantoB100 argB2</i>	Abenza <i>et al.</i> , 2010
<i>alcA<sub>p</sub>::mRFP-rabB::pyroA niiA4 nkuAΔ::bar inoB2 pyroA4 wA3</i>	Abenza <i>et al.</i> , 2011
<i>aspB-GFP::AFpyrG pyrG89 argB2 pabaB22 nkuAΔ::argB riboB2</i>	Westfall and Momany, 2002
<i>aspC-GFP::AFpyrG pabaA6 biA1</i>	Lindsey <i>et al.</i> , 2010
<i>aspD-GFP::AFpyrG argB2 riboB2</i>	Hernández-Rodríguez <i>et al.</i> , 2014
<i>aspE-GFP::AFpyrG riboB2</i>	Hernández-Rodríguez <i>et al.</i> , 2014
<i>alcA<sub>p</sub>::mCherry-tubA::pyroA nkuAΔ::argB pyrG89 pyroA4</i>	Takeshita <i>et al.</i> , 2013
<i>kinAΔ::pyr4 alcA<sub>p</sub>::GFP-kinA<sup>rigor</sup>::pyroA pyrG89 pyroA4 argB2</i>	Zekert and Fischer, 2009
<i>clalH-(5xGA)GFP::AFpyrG nkuAΔ::argB pyrG89 pyroA4 riboB2</i>	This study
<i>ap1<sup>o</sup>-(5xGA)GFP::AFpyrG nkuAΔ::argB pyrG89 pyroA4 riboB2</i>	This study
<i>ap1<sup>o</sup>-(5xGA)mRFP::AFpyrG nkuAΔ::argB pyrG89 pyroA4 riboB2</i>	This study
<i>alcA<sub>p</sub>::mRFP-rabB::pyroA4 ap1<sup>o</sup>-(5xGA)GFP::AFpyrG nkuAΔ::argB</i>	This study
<i>thiA<sub>p</sub>::FLAG-ap1<sup>o</sup>::AFriboB alcA<sub>p</sub>::mCherry-rabA::argB nkuAΔ::argB pantoB100 pyroA4</i>	This study
<i>alcA<sub>p</sub>::mRFP-rabB::pyroA thiA<sub>p</sub>::FLAG-ap1<sup>o</sup>::AFriboB nkuAΔ::argB riboB2 pyroA4 wA3</i>	This study
<i>thiA<sub>p</sub>::FLAG-ap1<sup>o</sup>::AFriboB GFP-ssoA::AFpyrG pabaA1</i>	This study
<i>thiA<sub>p</sub>::FLAG-ap1<sup>o</sup>::AFriboB pyroA4::[pyroA<sup>mut</sup>::gpdA<sup>m</sup><sub>p</sub>::mcherry-sedV] nkuAΔ::bar inoB2</i>	This study
<i>ap1<sup>o</sup>-(5xGA)GFP::AFpyrG pyroA4[pyroA<sup>mut</sup>::gpdA<sup>m</sup><sub>p</sub>::mcherry-sedV] nkuAΔ::argB pyrG89 pyroA4 inoB2</i>	This study
<i>thiA<sub>p</sub>::FLAG-ap1<sup>o</sup>::AFriboB sagA-(5xGA)GFP::AFpyrG nkuAΔ::argB pyrG89 pyroA4 riboB2</i>	This study
<i>thiA<sub>p</sub>::FLAG-ap1<sup>o</sup>::AFriboB slaB-GFP::AFpyrG nkuAΔ::argB pyrG89 pyroA4 riboB2</i>	This study
<i>thiA<sub>p</sub>::FLAG-ap1<sup>o</sup>::AFriboB abpA-mRFP::AFpyrG nkuAΔ::argB pyrG89 pyroA4 riboB2</i>	This study
<i>thiA<sub>p</sub>::FLAG-ap1<sup>o</sup>::AFriboB H1-mRFP::AFriboB</i>	This study
<i>thiA<sub>p</sub>::ap1<sup>h</sup>::AFriboB ap1<sup>o</sup>-(5xGA)GFP::AFpyrG nkuAΔ::argB pyrG89 pyroA4 riboB2</i>	This study
<i>thiA<sub>p</sub>::ap1<sup>o</sup>::AFriboB ap1<sup>o</sup>-(5xGA)GFP::AFpyrG nkuAΔ::argB pyrG89 pyroA4 riboB2</i>	This study
<i>thiA<sub>p</sub>::FLAG-ap1<sup>o</sup>::AFriboB alcA<sub>p</sub>::mCherry-tubA:pyroA</i>	This study
<i>kinAΔ::pyr4 pyroA4[alcA<sub>p</sub>::kinA<sup>rigor</sup>-GFP:pyroA] ap1<sup>o</sup>-(5xGA)mRFP::AFpyrG pyrG89</i>	This study
<i>ap1<sup>o</sup>-(5xGA)mRFP::AFpyrG clalH-(5xGA)GFP::AFpyrG nkuAΔ::argB pyroA4</i>	This study
<i>dnfA-GFP::AFpyrG ap1<sup>o</sup>-(5xGA)mRFP::AFpyrG nkuAΔ::argB pyrG89 pyroA4</i>	This study
<i>mCherry-synA::AFpyrG ap1<sup>o</sup>-(5xGA)GFP::AFpyrG nkuAΔ::argB pyrG89 pyroA4 nicA2</i>	This study
<i>thiA<sub>p</sub>::FLAG-ap1<sup>o</sup>::AFriboB ap2<sup>o</sup>Δ::AFpyroA dnfA-GFP::AFpyrG nkuAΔ::argB pyroA4</i>	This study
<i>thiA<sub>p</sub>::FLAG-ap1<sup>o</sup>::AFriboB dnfB-GFP::AFpyrG nkuAΔ::argB pyrG89 pyroA4</i>	This study
<i>thiA<sub>p</sub>::FLAGap1α::AFriboB clal-(5xGA)GFP::AFpyrG nkuAΔ::argB pyrG89 pyroA4 riboB2</i>	This study
<i>alcA<sub>p</sub>::mCherry-tubA::pyroA ap1<sup>o</sup>-(5xGA)GFP::AFpyrG nkuAΔ::argB pyrG89 pyroA4</i>	This study
<i>thiA<sub>p</sub>::rabE::AFriboB nkuAΔ::argB pyrG89 pyroA4 riboB2</i>	This study
<i>ap1<sup>o</sup>-(5xGA)GFP::AFpyrG thiA<sub>p</sub>::rabE::AFriboB nkuAΔ::argB pyrG89 pyroA4 riboB2</i>	This study
<i>ap1<sup>o</sup>-(5xGA)GFP::AFpyrG thiA<sub>p</sub>::clal::AFriboB nkuAΔ::argB pyrG89 pyroA4 riboB2</i>	This study
<i>aspB-GFP::AFpyrG thiA<sub>p</sub>::FLAG-ap1<sup>o</sup>::AFriboB nkuAΔ::argB pyrG89 riboB2 pyroA4</i>	This study
<i>aspC-GFP::AFpyrG thiA<sub>p</sub>::FLAG-ap1<sup>o</sup>::AFriboB pabaA6 pyroA4</i>	This study
<i>aspD-GFP::AFpyrG thiA<sub>p</sub>::FLAG-ap1<sup>o</sup>::AFriboB riboB2</i>	This study
<i>aspE-GFP::AFpyrG thiA<sub>p</sub>::FLAG-ap1<sup>o</sup>::AFriboB pyroA4</i>	This study
<i>thiA<sub>p</sub>::rabC::AFriboB nkuAΔ::argB pyrG89 pyroA4 riboB2</i>	This study
<i>thiA<sub>p</sub>::rabC::AFriboB ap1α-(5xGA)GFP::AFpyrG nkuAΔ::argB pyrG89 pyroA4 riboB2</i>	This study
<i>GFP-rabE::AFpyrG pyrG89 pyroA4 riboB2 nkuAΔ::argB</i>	This study
<i>ap1<sup>o</sup>-(5xGA)mRFP::AFpyrG GFP-rabE::AFpyrG nkuAΔ::argB</i>	This study
<i>thiA<sub>p</sub>::FLAG-ap1<sup>o</sup>::AFriboB yA::AFpyroA GFP-tpmA AFpyrG::mCherry-synA nkuAΔ::argB pyrG89</i>	This study
<i>ap1α-(5xGA)GFP::AFpyrG [pyroA-gpdAmp::mRFP-PHOSBP]pyroA4 nkuAΔ::argB pyrG89 inoB2</i>	This study

<i>pyroA4</i> [ <i>pyroA-gpdA</i> <sup>m</sup> <i> p</i> :: <i>mRFP-PH</i> <sup>OSBP</sup> ] <i>thiA</i> <sub>p</sub> :: <i>FLAG-ap1</i> <sup>σ</sup> :: <i>AFriboB</i>	This study
<i>thiA</i> <sub>p</sub> :: <i>FLAG-ap1</i> <sup>σ</sup> :: <i>AFriboB ap2</i> <sup>σ</sup> Δ:: <i>AFpyroA dnfA-GFP</i> :: <i>AFpyrG nkuAΔ</i> :: <i>argB pyroA4</i>	This study
<i>rab1</i> <sup>A136D</sup> :: <i>AFpyrG ap1</i> <sup>σ</sup> -(5xGA) <i>GFP</i> :: <i>AFpyrG pyroA4</i>	This study
<i>sedV</i> <sup>R238G</sup> :: <i>AFpyrG ap1</i> <sup>σ</sup> -(5xGA) <i>GFP</i> :: <i>AFpyrG nkuAΔ</i> :: <i>bar pyroA4</i>	This study
<i>thiA</i> <sub>p</sub> :: <i>FLAG-ap1</i> <sup>σ</sup> :: <i>AFriboB GFP-rabE</i> :: <i>AFpyrG AFpyrG</i> :: <i>mCherry-synA nkuAΔ</i> :: <i>argB pyrG89 pyroA4</i>	This study
<i>ap1</i> <sup>σ</sup> -(5xGA) <i>GFP</i> :: <i>AFpyrG uncAΔ</i> :: <i>AFriboB nkuAΔ</i> :: <i>argB pyrG89 riboB2 pyroA4</i>	This study
<i>thiA</i> <sub>p</sub> - <i>rabE</i> :: <i>AFriboB clal</i> -(5xGA) <i>GFP</i> :: <i>AFpyrG nkuAΔ</i> :: <i>argB pyrG89 riboB2 pyroA4</i>	This study
<i>thiA</i> <sub>p</sub> - <i>rabE</i> :: <i>AFriboB clalH</i> -(5xGA) <i>GFP</i> :: <i>AFpyrG nkuAΔ</i> :: <i>argB pyrG89 riboB2 pyroA4</i>	This study
<i>thiA</i> <sub>p</sub> - <i>clal</i> :: <i>AFriboB GFP-rabE</i> :: <i>AFpyrG nkuAΔ</i> :: <i>argB pyrG89 pyroA4 riboB2</i>	This study
<i>thiA</i> <sub>p</sub> - <i>rabE</i> :: <i>AFriboB AFpyrG</i> :: <i>mcherry-synA nkuAΔ</i> :: <i>argB pyrG89 pyroA4</i>	This study
<i>thiA</i> <sub>p</sub> - <i>rabE</i> :: <i>AFriboB AFpyrG</i> :: <i>alcA</i> <sub>p</sub> - <i>GFP-chsB nkuAΔ</i> :: <i>argB pyrG89 pyroA4 riboB2</i>	This study
<i>thiA</i> <sub>p</sub> - <i>ap1</i> <sup>σ</sup> :: <i>AFpyrG clalH</i> -(5xGA) <i>GFP</i> :: <i>AFpyrG argB2</i>	This study
<i>thiA</i> <sub>p</sub> - <i>ap1</i> <sup>σ</sup> :: <i>AFpyrG clal</i> -(5xGA) <i>GFP</i> :: <i>AFpyrG argB2</i>	This study
<i>thiA</i> <sub>p</sub> - <i>ap1</i> <sup>σ</sup> :: <i>AFpyrG clalH</i> -(5xGA) <i>GFP</i> :: <i>AFpyrG ap1</i> <sup>σ</sup> :: <i>argB argB2</i>	This study
<i>thiA</i> <sub>p</sub> - <i>ap1</i> <sup>σ</sup> :: <i>AFpyrG clal</i> -(5xGA) <i>GFP</i> :: <i>AFpyrG ap1</i> <sup>σ</sup> :: <i>argB argB2</i>	This study
<i>thiA</i> <sub>p</sub> - <i>ap1</i> <sup>σ</sup> :: <i>AFpyrG clalH</i> -(5xGA) <i>GFP</i> :: <i>AFpyrG ap1</i> <sup>σ</sup> - <i>N709A/G710A/F711A</i> :: <i>argB argB2</i>	This study
<i>thiA</i> <sub>p</sub> - <i>ap1</i> <sup>σ</sup> :: <i>AFpyrG clalH</i> -(5xGA) <i>GFP</i> :: <i>AFpyrG ap1</i> <sup>σ</sup> - <i>D632A/I633A/D634AN709A/G710A/ F711A</i> <i>argB2</i>	This study
<i>thiA</i> <sub>p</sub> - <i>ap1</i> <sup>σ</sup> :: <i>AFpyrG clal</i> -(5xGA) <i>GFP</i> :: <i>AFpyrG ap1</i> <sup>σ</sup> - <i>N709A/G710A/F711A</i> :: <i>argB argB2</i>	This study
<i>thiA</i> <sub>p</sub> - <i>ap1</i> <sup>σ</sup> :: <i>AFpyrG clal</i> -(5xGA) <i>GFP</i> :: <i>AFpyrG ap1</i> <sup>σ</sup> - <i>D632A/I633A/D634AN709A/G710A/ F711A</i> :: <i>argB argB2</i>	This study
<i>thiA</i> <sub>p</sub> - <i>ap1</i> <sup>σ</sup> :: <i>AFriboB dnfA-GFP</i> :: <i>AFpyrG alcA</i> <sub>p</sub> - <i>mRFP-RabB</i> :: <i>pyroA pyroA4 nkuAΔ</i> :: <i>argB pyrG89</i>	This study
<i>thiA</i> <sub>p</sub> - <i>ap1</i> <sup>σ</sup> :: <i>AFriboB dnfA-GFP</i> :: <i>AFpyrG alcA</i> <sub>p</sub> :: <i>mCherry-rabA</i> :: <i>argB pyroA4</i>	This study

**Table 2.4** List of strains used in Chapter 3.4

Strain Genotype	References
<i>TNO2A7</i> : <i>nkuAΔ</i> :: <i>argB pyrG89 pyroA4 riboB2</i>	Nayak <i>et al.</i> , 2006
<i>pyroA4</i> ::[ <i>pyroA</i> :: <i>gpdA</i> <sup>m</sup> <i> p</i> :: <i>mRFP-PH</i> <sup>OSBP</sup> ] <i>inoB2 niiA4 wA4</i>	Pantazopoulou and Peñalva, 2009
<i>sagA-GFP</i> :: <i>AFpyrG nkuAΔ</i> :: <i>argB pyroA4 riboB2 pyrG89</i>	Karachaliou <i>et al.</i> , 2013
<i>slaB-GFP</i> :: <i>AFpyrG Δnku</i> :: <i>argB pyrG89 pyroA4 argB2</i>	Araujo-Bazán <i>et al.</i> , 2008
<i>uapA-GFP</i> :: <i>AFriboB uapCΔ</i> :: <i>AFpyrG nkuAΔ</i> :: <i>argB pabaA1 pyroA4 riboB2</i>	Evangelinos <i>et al.</i> , 2016
<i>mCherry-synA</i> :: <i>AFpyrG yA</i> :: <i>AFpyroA GFP-tpmA fwA1 pyrG89 pyroA4 nicA2 nkuAΔ</i> :: <i>argB</i>	Taheri-Talesh <i>et al.</i> , 2008
<i>abpA-mRFP</i> :: <i>AFpyrG yA2 pabaA1 pyrG89</i>	Araujo-Bazán <i>et al.</i> , 2008
<i>dnfAΔ</i> :: <i>AFriboB nkuAΔ</i> :: <i>argB pyrG89 pyroA4</i>	Schultzhaus <i>et al.</i> , 2015
<i>dnfBΔ</i> :: <i>AFriboB nkuAΔ</i> :: <i>argB pyrG89 pyroA4</i>	Schultzhaus <i>et al.</i> , 2015
<i>dnfA-GFP</i> :: <i>AFpyrG nkuAΔ</i> :: <i>argB pyrG89 pabaA1 pyroA4</i>	Schultzhaus <i>et al.</i> , 2015
<i>dnfB-GFP</i> :: <i>AFpyrG nkuAΔ</i> :: <i>argB pyrG89 pabaA1 pyroA4</i>	Schultzhaus <i>et al.</i> , 2015
<i>stoAΔ</i> :: <i>AFpyrG argBΔ</i> :: <i>trpCΔB</i> or <i>argB2 pyrG89? pabaA1</i>	Takeshita <i>et al.</i> , 2012
<i>basA1, pyrG89</i>	Li <i>et al.</i> , 2007
<i>ap2</i> <sup>σ</sup> Δ:: <i>AFriboB nkuAΔ</i> :: <i>argB pyrG89 pyroA4 riboB2</i>	This study
<i>ap2</i> <sup>μ</sup> Δ:: <i>AFpyrG nkuAΔ</i> :: <i>argB pyrG89 pyroA4 riboB2</i>	This study
<i>ap2σ</i> -(5xGA) <i>GFP</i> :: <i>AFpyrG nkuAΔ</i> :: <i>argB pyrG89 pyroA4 riboB2</i>	This study
<i>ap2σ</i> -(5xGA) <i>mRFP</i> :: <i>AFpyrG nkuAΔ</i> :: <i>argB pyrG89 riboB2 pyroA4</i>	This study
<i>ap2</i> <sup>σ</sup> -(5xGA) <i>mRFP</i> :: <i>AFpyrG ap2</i> <sup>μ</sup> Δ:: <i>AFriboB nkuAΔ</i> :: <i>argB pyrG89 pyroA4 riboB2</i>	This study
<i>thiA</i> <sub>p</sub> - <i>slaB</i> :: <i>AFriboB nkuAΔ</i> :: <i>argB pyroA4 riboB2 pyrG89</i>	This study
<i>thiA</i> <sub>p</sub> - <i>clal</i> :: <i>AFpyrG nkuAΔ</i> :: <i>argB pyroA4 riboB2 pyrG89</i>	This study
<i>thiA</i> <sub>p</sub> - <i>clalH</i> :: <i>AFpyroA nkuAΔ</i> :: <i>argB pyroA4 riboB2 pyrG89</i>	This study
<i>dnfA-GFP</i> :: <i>AFpyrG thiA</i> <sub>p</sub> - <i>clalH</i> :: <i>AFpyroA nkuAΔ</i> :: <i>argB pyroA4 pabaA1 pyrG89</i>	This study
<i>dnfB-GFP</i> :: <i>AFpyrG thiA</i> <sub>p</sub> - <i>clalH</i> :: <i>AFpyroA nkuAΔ</i> :: <i>argB pyroA4 pabaA1 pyrG89</i>	This study
<i>thiA</i> <sub>p</sub> - <i>basA</i> :: <i>AFriboB nkuAΔ</i> :: <i>argB pyroA4 riboB2 pyrG89</i>	This study
<i>dnfA-GFP</i> :: <i>AFpyrG ap2</i> <sup>σ</sup> Δ:: <i>AFriboB nkuAΔ</i> :: <i>argB pyrG89 pyroA4</i>	This study
<i>dnfB-GFP</i> :: <i>AFpyrG ap2</i> <sup>σ</sup> Δ:: <i>AFriboB nkuAΔ</i> :: <i>argB pyrG89 pyroA4</i>	This study
<i>ap2</i> <sup>σ</sup> Δ:: <i>AFriboB dnfAΔ</i> :: <i>AFriboB pabaA1</i>	This study
<i>ap2</i> <sup>σ</sup> Δ:: <i>AFriboB dnfBΔ</i> :: <i>AFriboB pabaA1 pyroA4</i>	This study
<i>ap2</i> <sup>σ</sup> -(5xGA) <i>GFP</i> :: <i>AFpyrG dnfAΔ</i> :: <i>AFriboB nkuAΔ</i> :: <i>argB pyrG89 pyroA4</i>	This study
<i>ap2</i> <sup>σ</sup> -(5xGA) <i>GFP</i> :: <i>AFpyrG dnfBΔ</i> :: <i>AFriboB nkuAΔ</i> :: <i>argB pyrG89 pyroA4</i>	This study

<i>stoAΔ::AFpyrG ap2<sup>σ</sup>Δ::AFriboB pabaA1</i>	This study
<i>sagAΔ::AFriboB ap2<sup>σ</sup>Δ::AFriboB uapAΔ pabaA1 pyroA4</i>	This study
<i>slaB-GFP::AFpyrG ap2<sup>σ</sup>Δ::AFriboB nkuAΔ::argB pyroA4</i>	This study
<i>sagA-GFP::AFpyrG ap2<sup>σ</sup>Δ::AFriboB pabaA1 pyroA4</i>	This study
<i>ap2<sup>σ</sup>Δ::AFriboB abpA-mRFP::AFpyrG pabaA1</i>	This study
<i>ap2<sup>σ</sup>Δ mCherry-SynA GFP-TmpA yA2</i>	This study
<i>ap2<sup>σ</sup>-(5xGA)mRFP::AFpyrG sagA-GFP::AFpyrG pyroA4 riboB2</i>	This study
<i>ap2<sup>σ</sup>-(5xGA)mRFP::AFpyrG slaB-GFP::AFpyrG nkuAΔ::argB pyrG89 pyroA4 riboB2 pabaA1</i>	This study
<i>ap2<sup>σ</sup>-(5xGA)mRFP::AFpyrG dnfA-GFP::AFpyrG nkuAΔ::argB pyrG89 pyroA4</i>	This study
<i>ap2<sup>σ</sup>-(5xGA)mRFP::AFpyrG dnfB-GFP::AFpyrG nkuAΔ::argB pyrG89 pyroA4</i>	This study
<i>ap2σ-(5xGA)mRFP::AFpyrG claL-(5xGA)GFP::AFpyrG nkuAΔ::argB pyrG89 pyroA4</i>	This study
<i>claL-(5xGA)mRFP::AFpyrG ap2<sup>σ</sup>-(5xGA)GFP::AFpyrG nkuAΔ::argB pyroA4 riboB2 pyrG89</i>	This study
<i>claL-(5xGA)mRFP::AFpyrG nkuAΔ::argB pyroA4 riboB2 pyrG89</i>	This study
<i>claL-(5xGA)mRFP::AFpyrG uapAΔ::uapA-GFP nkuAΔ::argB pyroA4 pabaA1 pyrG89</i>	This study
<i>ap2<sup>σ</sup>-(5xGA)mRFP::AFpyrG uapAΔ::alcA<sub>p</sub>-uapA-GFP::AFriboB nkuAΔ::argB pabaA1 pyroA4 riboB2</i>	This study
<i>ap2<sup>σ</sup>-(5xGA)GFP::AFpyrG mCherry-synA::AFpyrG pyroA4</i>	This study
<i>ap2<sup>σ</sup>-(5xGA)GFP::AFpyrG abpA-mRFP::AFpyrG pyroA4</i>	This study
<i>ap2<sup>σ</sup>-(5xGA)mRFP::AFpyrG sagAΔ::AFriboB slaB-GFP::AFpyrG pyroA4</i>	This study
<i>ap2<sup>σ</sup>-(5xGA)mRFP::AFpyrG sagA-GFP::AFpyrG thiAp-slaB::AFriboB nkuAΔ::argB pyrG89 pyroA4 riboB2</i>	This study
<i>ap2σ-(5xGA)GFP::AFpyrG basA1 pyrG89 pyroA4</i>	This study
<i>thiA<sub>p</sub>-basA::AFpyrG ap2<sup>σ</sup>Δ::AFriboB nkuAΔ::argB pyrG89 riboB2 pyroA4</i>	This study
<i>thiA<sub>p</sub>-basA::AFriboB ap2σ-(5xGA)GFP::AFpyrG nkuAΔ::argB pyrG89 riboB2 pyroA4</i>	This study
<i>ap2<sup>σ</sup>-(5xGA)GFP::AFpyrG pyroA4::[pyroA::gpdA<sup>m</sup><sub>p</sub>::mRFP-PH<sup>OSBP</sup>]</i>	This study

### 2.1.2 Culture media

Standard complete (CM) and minimal media (MM) were used for *A. nidulans* growth. CM contains all the nutrients and auxotrophies required for fungal growth, whereas MM contains the minimum nutritional supplements possible, depending on the auxotrophic requirements of each strain, and a nitrogen source, according to the desired conditions. For solid growth mediums, 1-2% agar was added to the liquid medium, before autoclaving. Media and supplemented auxotrophies were at the concentrations given in FGSC (<http://www.fgsc.net>). Media and chemical reagents were obtained from Sigma-Aldrich (Life Science Chemilab SA, Hellas) or AppliChem (Bioline Scientific SA, Hellas).

**Table 2.5** Media used for *A. nidulans* growth

	Complete medium (CM)	Minimal medium (MM)	Sucrose medium (SM)
Salt solution	20 mL	20 mL	20 mL
Vitamin solution	10 mL	–	
D-Glucose	10 g	10 g	10 g
Casamino acids	1 g	–	–
Bactopeptone	2 g	–	–
Yeast extract	1 g	–	–
Sucrose	–	–	342,4 g
H <sub>2</sub> O <sub>dist</sub>	up to 1 L	up to 1 L	up to 1 L

**Table 2.6** Solutions for preparation of *A. nidulans* media

Salt solution		Vitamin solution		Trace Elements in 1 L H <sub>2</sub> O	
KCl	26 g	p-aminobenzoic acid	20 mg	Na <sub>2</sub> B <sub>4</sub> O <sub>7</sub> x 10 H <sub>2</sub> O	40 mg
MgSO <sub>4</sub> 7H <sub>2</sub> O	26 g	D-pantothenic acid	50 mg	CuSO <sub>4</sub> x 5 H <sub>2</sub> O	400 mg
KH <sub>2</sub> PO <sub>4</sub>	76 g	pyridoxine	50 mg	FeO <sub>4</sub> P x 4 H <sub>2</sub> O	714 mg
Trace elements	50 mL	riboflavin	50 mg	MnSO <sub>4</sub> x 1 H <sub>2</sub> O	728 mg
Chloroform	2 mL	biotine	1 mg	Na <sub>2</sub> MoO <sub>4</sub> x 2 H <sub>2</sub> O	800 mg
H <sub>2</sub> O <sub>dist</sub>	up to 1 L	H <sub>2</sub> O <sub>dist</sub>	up to 1 L	ZnSO <sub>4</sub> x 7 H <sub>2</sub> O	8 mg

The pH was adjusted to 6.8 with NaOH 1M. Nitrogen sources were used at final concentrations: urea 5 mM, NaNO<sub>3</sub> 10 mM, Ammonium L-(+)-tartrate 10 mM, purines 0.1 mg/mL. Amino acids (proline, L-glutamate) were used at 5 mM. Uracil and uridine were used at 5 mM and 10 mM respectively.

### 2.1.3 Growth and Storage conditions

For the inoculation of *A. nidulans* cultures, conidiospores were harvested from sporulating culture plates with the use of sterile toothpicks. Solid cultures were incubated in 37°C or 25°C for 2-4 days and liquid cultures were incubated overnight at 37°C or 25°C, 140-150 rpm. Repression of protein expression driven by the regulatable alcohol dehydrogenase (*alcA<sub>p</sub>*) promoter was achieved with the use of 1% glucose, whereas derepression occurred with the use of 0.1% (w/v) fructose as a sole carbon source. Induction of the same proteins was achieved by addition of 0.4% (v/v) ethanol in the non-repressing culture media. Repression of protein expression driven by the regulatable thiamine promoter (*thiA<sub>p</sub>*) was achieved with the use thiamine hydrochloride at a final concentration of 5–10 µM.

*Escherichia coli* bacterial cultures (strain DH5a) were grown on Luria-Bertani (LB) medium (Bacto Tryptone 10 g, NaCl 10 g, BactoYeast Extract 5 g for 1L). The pH was adjusted to 7.0 with NaOH 1M. After bacterial transformation, colony selection was achieved with the use of 100 µg/mL ampicillin. Solid cultures were incubated overnight at 37 °C. Liquid cultures were incubated in the same conditions, at 200 rpm.

Agar plates were stored at 4°C, to prevent a serious loss of fungal viability for some weeks. For long-term storage, glycerol stocks were prepared. *A. nidulans* conidiospores were harvested from ¼ of a fresh 100mm CM plate, in 1ml solution of 1:1 glycerol:PBS (NaCl 8 g, KCl 0,2 g, Na<sub>2</sub>PO<sub>4</sub> 1,44 g, KH<sub>2</sub>PO<sub>4</sub> 0,24 g, pH 7.4 with 1 N HCl), in a sterile eppendorf tube. The solution was mixed well and the glycerol stocks were stored for long periods at -80°C. For reviving stored fungal cultures, a small quantity of the stock was inoculated on appropriate media and then analyzed with growth tests to verify that no contamination had occurred.

## 2.2 GENETIC CROSSES AND PROGENY ANALYSIS

Petri dishes containing MM with the appropriate supplements were inoculated with spores from two different parental strains, in pairs, with a distance of 1cm between them. After incubation for 3 days at 37°C, small parts of media where a heterokaryon was formed, were removed with a sterile toothpick and transferred in small Petri dishes containing MM with nitrate and only the supplements required from both parental strains. Therefore, only heterokaryons were able to produce the missing supplements and grow. The plates were incubated for 3 days at 37°C, sealed with adhesive tape, and incubated for 14-20 days at 37°C. After that time, cleistothecia usually appeared (Todd et al., 2007).

The plates were unsealed and single cleistothecia (usually 8) were selected with a sterile toothpick. Surrounding cells were removed by rolling the cleistothecia on an agar plate. Finally, each cleistothecium was burst open by mechanical forces and the ascospores were released in an eppendorf tube containing 1 mL of sterile H<sub>2</sub>O<sub>dist.</sub> 10µL of each ascospore suspension was plated on selective minimal media and incubated for two days at 37°C, so that only recombinant progeny would grow. In order to obtain single colonies, usually 5µl of the suspension from one recombinant cleistothecium were plated. Several colonies were, then, selected and analyzed for their genetic background by growth tests under different conditions and comparison to well-studied controls.. Further progeny analysis included the use of fluorescence microscopy or polymerase chain reaction (PCR).

## 2.3 EPIFLUORESCENCE MICROSCOPY

Samples for wide-field epifluorescence microscopy and Total Internal Reflection Fluorescence Microscopy (TIRF-M) were prepared as follows: Germlings were incubated for 16–22 hr at 25° C in sterile 35 mm m-dishes, high glass bottom (*ibidi*, Germany) in 2 mL of liquid MM 1% glucose pH 4.6, containing the appropriate supplements and NaNO<sub>3</sub> as a nitrogen source. Culture was shifted when needed to various conditions for 2–4 h. For the observation of proteins expressed under the control of the *alcA<sub>p</sub>*, mycelia were grown for 14-16 h in MM with NaNO<sub>3</sub>, 0.1% (w/v) fructose as a sole carbon source and 0.4 % (v/v) ethanol either for 2 h or overnight. Repression of expression was achieved in MM supplemented with NaNO<sub>3</sub> and 1% (w/v) glucose. Filipin III and Calcofluor white were used for 5 min prior to observation at final concentrations of 1 µg/ml and 0.001% (w/v) respectively. FM4-64 and CMAC (7-amino-4-chloromethyl coumarin; Molecular Probes, Inc, USA) staining was according to Peñalva (2015) and Pantazopoulou et al. (2007), respectively. For FM4-64 staining in particular, germinated conidia were incubated on ice for 15 min with 10 mM

FM4-64 in MM, washed with 4-5 ml MM, and transferred to fresh 2 ml medium for 0–45 min chase time. For CMAC staining germinated conidia were incubated 25°C for 20 min with 1/1000 dilution of CMAC (5 mg/ml stock solution), washed with 4-5 ml MM, and transferred to fresh 2 ml medium. Benomyl, Latrunculin B and Brefeldin A were used at final concentrations of 2.5, 100, 100 µg/ml, respectively. For endocytosis, ammonium L-(+)-tartrate (10-20 mM) was added for 2 h before observation.

Images were obtained using an inverted Zeiss Axio Observer Z1 and an Axio Cam HR R3 camera. Contrast adjustment, area selection and color combining were made using the Zen lite 2012 software. Live imaging of plasma membrane ClaL was accomplished by TIRF microscopy. Hyphae were analyzed using a Leica AM TIRF MC set up on a Leica DMI6000 B microscope and a Leica 100X HCX PL APO 1.4 NA objective. For measurements of fluorescence intensity, the *Plot profile* command in ImageJ was used (<https://imagej.nih.gov/ij/>). For the quantification of colocalization, the Pearson's correlation coefficient (PCC) (Dunn et al., 2011) was calculated for a selected Region of interest (ROI), using the *coloc2* plugin of Fiji. Costes P-value was 1.00 (Costes et al., 2004), PSF was set to 1.2 and the number of iterations was 100. One sample t-test was performed to test the significance of differences in PCCs, using the Graphpad Prism software. Confidence interval was set to 95%. Colocalization results were also confirmed using the ICY colocalization studio plugin (<http://icy.bioimageanalysis.org/>) for selected regions of interest (ROIs). The Area Selection tool was used for the measurement of Vacuolar Surface (Total surface of vacuoles containing GFP/Hypha) and Vacuolar GFP Fluorescence (Total fluorescence intensity of vacuoles containing GFP/Hypha). Tukey's Multiple Comparison Test (One-Way ANOVA) using Graphpad Prism was performed to test the statistical significance of the results. Confidence interval was set to 95%. Scale bars were added using the FigureJ plugin of the ImageJ software (Mutterer and Zinck, 2013). Images were further processed and annotated in Adobe Photoshop CS4 Extended version 11.0.2.

## 2.4 NUCLEIC ACID MANIPULATIONS AND PLASMID CONSTRUCTIONS

Genomic DNA extraction from *A. nidulans* was as described in FGSC (<http://www.fgsc.net>). CM or MM culture plates were incubated for 4 days in 37°C. Conidiospores were harvested from 1/4 of the plate in 25 mL of liquid MM (containing NH<sub>4</sub><sup>+</sup> and the necessary supplements) and cultures were incubated overnight at 37°C, 140-150 rpm. The culture was then filtered through a blutex, dried and immediately frozen in liquid nitrogen. The mycelia were pulverized in a mortar with a pestle in the presence of liquid nitrogen and ~200 mg of the powder were transferred in a 2mL eppendorf tube, resuspended in 800 µL of DNA extraction buffer (Tris-HCl 0.2 M pH 8.0, Sodium

Dodecyl Sulfate (SDS) 1%, Ethylenediaminetetraacetic acid (EDTA) 1mM pH 8), mixed by vortexing and incubated on ice for 20 min. 800µL of pure phenol were added and the mixture was shaken vigorously at room temperature (RT) before centrifugation for 5 min at 12000 rpm, RT. The upper phase, containing the DNA, was transferred to a new eppendorf tube and equal volume of chloroform was added. Tube was shaken and centrifuged for 5 min at 12000 rpm, RT. The upper phase was recovered and transferred to a new 1.5 mL tube. The DNA was then precipitated by addition of equal volume of isopropanol and 1/10 volume of 3 M sodium acetate (pH=5.3). The mixture was gently mixed and centrifuged for 10 min at 12000 rpm, RT. The pellet was washed with 200 µL of 70% EtOH. After spinning for 2 min, EtOH was removed with a pipette and the pellet was dried for 5 min at 50°C. The pellet was then dissolved in 100µl of sterile distilled water, containing 0.2 mg/mL RNaseA and incubated at 37°C for 30 min. 2-3 µL of the DNA solution were analysed by agarose gel electrophoresis to quantify and check the quality of the extracted DNA.

For molecular cloning purposes, the appropriate amount of DNA was digested with 1 µl restriction enzyme, 1x restriction enzyme buffer and distilled water to a final volume of 20 µL at the enzyme's optimal temperature and for the time period specified by the manufacturer. Restriction enzymes were from Takara Bio or Minotech (Lab Supplies Scientific SA, Hellas). Conventional PCR reactions, high fidelity amplifications and site-directed mutagenesis were performed with KAPA *Taq* DNA and Kapa HiFi polymerases respectively (Kapa Biosystems, Roche Diagnostics, Hellas), according to manufacturer's instructions. Mutations were constructed by site-directed mutagenesis according to the instructions accompanying the QuikChange® Site-Directed Mutagenesis Kit (Agilent Technologies, Stratagene). The following formula was used for estimating the  $T_m$  of the primers:  $T_m = 69.3 + 0.41(\%GC) - 650/L - (\%mismatch)$ . After site-directed mutagenesis, 1µl of *DpnI* (TaKaRa) was used for incubation of the PCR product at 37°C for 2 h. For  $ap1^B$  site directed mutations, the relevant gene was cloned in the pBS-argB plasmid (Vlanti and Diallinas, 2008). Gene deletions and 'in locus' integrations of tagged gene fusions were generated by one step ligations or sequential cloning of the relevant fragments in the plasmids pBluescript SKII, or pGEM-T using oligonucleotides carrying additional restriction sites. When cloning with one restriction enzyme, alkaline phosphatase was used for 5 min at 37°C (TaKaRa). 0.5µl T4 DNA ligase (TaKaRa) was used for the ligation reaction, along with vector and insert at a 1:3 concentration ratio, 1x ligase buffer in 10 µl total volume, 25°C for 1.5 h. These plasmids were used as templates to amplify the relevant linear cassettes by PCR.

Agarose gel electrophoresis was performed for the analysis of the size and conformation of DNA in a sample, quantification of DNA, and the separation and extraction of DNA fragments. 1% agarose was dissolved in 1x TAE buffer (Composition for 1L 50X solution: 242 g Tris Base, 57.1 mL



glacial CH<sub>3</sub>COOH, 100 mL 0.5 M EDTA pH 8.0) and 0.5 mg/mL ethidium bromide (EtBr) were added before pouring the solution into a casting tray. DNA samples were mixed with loading buffer and loaded in the gel. To determine the size of the fragments, a molecular weight marker was loaded along with the samples and gels were run at 100V for 10-30 min. The gel was visualized under a UV transilluminator and DNA bands were either photographed or quickly excised from the gel for cloning purposes and purified as described in the manufacturer's instructions.

Plasmid preparation from *E. coli* strains and DNA bands gel extraction were performed using the Nucleospin Plasmid kit and the Nucleospin Extract II kit (Macherey-Nagel, Lab Supplies Scientific SA, Hellas). An aliquot was used for diagnostic digestions or PCR that would confirm the successful cloning of the desired DNA sequence, as well as the orientation of insertion. DNA sequences were determined by VBC-Genomics (Vienna, Austria). Southern blot analysis using specific gene probes and upstream or downstream fragments in the case of verifying gene deletions, was performed as described in Sambrook et al. (1989). [<sup>32</sup>P]-dCTP labeled molecules of gene specific probes were prepared using a random hexanucleotide primer kit following the supplier's instructions (Takara Bio, Lab Supplies Scientific SA, Hellas) and purified on MicroSpin S-200 HR columns (Roche Diagnostics, Hellas). Labeled [<sup>32</sup>P]-dCTP (3000 Ci / mmol) was purchased from the Institute of Isotops Co. Ltd, Miklós, Hungary.

## 2.5 TRANSFORMATION OF *Aspergillus nidulans*

Transformation was performed as described previously in Koukaki et al. (2003), using an *nkuA* DNA helicase deficient (TNO2A7; Nayak et al. 2006) recipient strain or derivatives for "in locus" integrations of gene fusions, or deletion cassettes by the *Aspergillus fumigatus* markers orotidine-59-phosphate decarboxylase (*AFpyrG*, *Afu2g0836*), GTP cyclohydrolase II (*AFriboB*, *Afu1g13300*), and a pyridoxine biosynthesis gene (*AFpyroA*, *Afu5g08090*), resulting in complementation of auxotrophies for uracil/uridine (*pyrG89*), riboflavin (*riboB2*), or pyridoxine (*pyroA4*), respectively. For generating "in locus" integrations of tagged *uapA* and *prnB* fusions, a  $\Delta uapA \Delta uapC::AfpYrG \Delta nkuA::argB \textit{riboB2 pantoB100 pyroA4}$  mutant strain was the recipient strain. Selection was based on complementation of the *riboB2* and *pantoB100* genetic auxotrophies for riboflavin and pantothenic acid, respectively. Mutants of *uapA-gfp*, *uapA-YFP* and *uapA-His* were constructed by transformation of a strain lacking the three major purine transporters *uapA*, *uapC* and *azgA* ( $\Delta ACZ$ ) based on the *A. nidulans* markers ornithine-carbamoyltransferase and para-aminobenzoic acid synthase, complementing the auxotrophic mutations for arginine (*argB2*) and p-aminobenzoin acid (*pabaA1*), respectively.

Filtered conidiospores were used to inoculate 200 ml liquid MM with  $\text{NH}_4^+$  and necessary supplements and the culture was incubated at 37°C for 4-4.5 h, 150 rpm. Entry of the conidia into the germinative phase was confirmed with microscopic observation, and the culture was centrifuged in sterile falcons at 4000rpm, 10min. Pellet resuspension in 20 ml of Solution I (1.2 M  $\text{MgSO}_4$ , 10 mM orthophosphate pH 5.8) was followed by incubation with 200mg of lytic enzyme (Glucanex), for 1.5-2 h at 30°C, 60 rpm. Protoplast concentration was achieved by centrifugation (4000 rpm, 10 min), followed by washing with 10 ml of Solution II (1 M Sorbitol, 10 mM Tris-HCl pH 7.5, 10 mM  $\text{CaCl}_2$ ) and resuspension in the same solution. Protoplasts, plasmid DNA (1.5 -2  $\mu\text{g}$ ) and  $\frac{1}{4}$  of the total volume of Solution III (60% (w/v) PEG6000, 10 mM Tris-HCl pH 7.5, 10 mM  $\text{CaCl}_2$ ) were added consecutively in an Eppendorf tube and incubated on ice for 15 min. Then 500  $\mu\text{L}$  of Solution III were added, mixed and incubated for another 15 min at RT, followed by centrifugation (6000 rpm, 10 min), wash and resuspension in 1 ml and 200  $\mu\text{l}$  of Solution II, respectively. For the last step, protoplasts were mixed with 4 ml of melted Top SM (Sucrose MM, 0.35% agar) and used to inoculate solid SM plates (1% agar). The appropriate negative control plate was used to transformation efficiency. After 4-5 days of incubation at 37°C, transformants were isolated by streaking on MM. Verification was achieved by PCR and Southern analysis. Combinations of mutations were constructed by standard genetic crossing.

## 2.6 PREPARATION AND TRANSFORMATION OF *Escherichia coli*

Competent DH5a *E. coli* cells were prepared by streaking from the glycerol stock on an LB agar plate and incubating at 37°C overnight. 5 ml of liquid LB medium were inoculated with a single colony from the plate and incubated at 37°C, 220 rpm overnight (16 h). Next, 0.5 ml of the overnight culture were used to inoculate 400 ml of LB medium for incubation at 37°C, 260 rpm until an  $\text{OD}_{600}$  of 0.45-0.55 was reached. After this the pellet was collected by centrifugation (4500 g, 4°C, 5 min), resuspended in ice-cold transformation buffer 1 (30 mM  $\text{CH}_3\text{COOK}$ , 10 mM  $\text{CaCl}_2$ , 50 mM  $\text{MnCl}_2$ , 100 mM  $\text{RbCl}_2$ , 15% glycerol, pH 5,8 with 1 M  $\text{CH}_3\text{COOH}$ ), 0.4x the original volume, and incubated for 5 min on ice. Next, centrifugation (4500 g, 5 min, 4°C) is followed by resuspension of the pellet in 1/25 original volume of ice-cold transformation buffer 2 (10 mM MOPS pH 6.5, 75 mM  $\text{CaCl}_2$ , 10 mM  $\text{RbCl}_2$ , 15% glycerol, pH 6.5 with 1 M KOH) and incubation for 15-60 min on ice. Aliquots of 200  $\mu\text{l}$  were distributed in sterile Eppendorf tubes and frozen at -80°C.

Transformation of *E. coli* was performed by addition of 0.01-0.5  $\mu\text{g}$  of plasmid DNA in 200  $\mu\text{l}$  of defrosted competent cells, mixing and incubation for 20-45 min on ice. A heat shock at 42°C for 90 sec is followed by incubation on ice for 2 min. After this, 1 ml LB is added in the tube and cells are incubated at 37°C for 45-60 min. Cell pellet is collected by centrifugation (8000 rpm, 2

min), resuspended in 100  $\mu$ l LB medium and spread on LB agar plates containing 100  $\mu$ g/ml ampicillin. After overnight incubation at 37°C, colonies can be selected and further analysed. The appropriate negative control plate was used to check antibiotic activity and transformation efficiency.

## 2.7 PROTEIN EXTRACTION AND PURIFICATION

Filtered conidiospores were used to inoculate 100 ml liquid MM with  $\text{NH}_4^+$  and necessary supplements and the culture was incubated at 37°C for 14-18 h, 25°C, 150 rpm. The culture was then filtered through a sterile blutex, dried and immediately frozen in liquid nitrogen. The mycelia were pulverized in a mortar with a pestle in the presence of liquid nitrogen 4-5 times and ~400 mg of the fine powder were transferred in a 2 mL eppendorf tube.

For Total Protein Extraction, the pulverized mycelium was resuspended in 800  $\mu$ l ice-cold Precipitation Buffer I [50 mM Tris-HCl pH 8.0, 50 mM NaCl, 12.5% (v/v) trichloroacetic acid (TCA), 1 mM PMSF, 1x Protease Inhibitors Cocktail (PIC)], vortexed and incubated for 10-30 min on ice. The pellet was collected by centrifugation (10 min, 13000 rpm, 4°C) and resuspended once in ice-cold ETOH 100% and twice in ice-cold acetone, with each step followed by a centrifugation for 5min, 13000 rpm, at 4°C. After the final centrifugation the supernatant was removed with a pipette and the pellet was air-dried for 30 min at 60°C. Next, the pellet was dissolved in Extraction Buffer I (100mM Tris-HCl pH=7.5, 50mM NaCl, 1% SDS, 1mM EDTA, 1x PIC, 1mM PMSF) and centrifuged (10-15 min, 13000 rpm, 4°C) before being transferred to pre-frozen 1.5 ml eppendorfs for storage at -80°C.

Membrane-Enriched Protein Extraction (adapted from Pantazopoulou et al., 2007), was mostly used before membrane protein purification for affinity chromatography (Chapter 3.1). The pulverized mycelium was collected in 2-6 eppendorfs and resuspended by addition of 2 ml ice-cold Extraction Buffer II in each tube (10 mM Tris-HCl pH 7.5, 100 mM NaCl, 5 mM  $\text{MgCl}_2$ , 0.3 M Sorbitol, 1 mM PMSF, 1 x PIC), mixed by vortexing and incubated for 20-30 min on ice. Supernatants were collected by centrifugation (3 min, 3000 rpm, 4°C) and transferred to pre-frozen eppendorfs. Precipitation of the membrane proteins was achieved by a centrifugation (1 h, 13000 rpm, 4°C) and pellets were resuspended in 80-100  $\mu$ l ice-cold Solubilisation Buffer (50 mM  $\text{NaH}_2\text{PO}_4$  pH 8.0, 150 mM NaCl, 1% (w/v) dodecyl- $\beta$ -D-maltoside (DDM), 1 mM PMSF, 1 x PIC). After this, suspensions were collected in one Eppendorf tube and stirred gently for 30 min on ice. A final centrifugation (20 min, 13.000rpm, 4°C) separates the solubilised membrane proteins in the supernatant, which is

collected and transferred in a new pre-frozen 1.5 ml Eppendorf tube. For long-term storage at  $-80^{\circ}\text{C}$ , glycerol is added at a final concentration of 20% (v/v).

Membrane protein purification was performed by a combination of Affinity Chromatography of His-tagged proteins (UapA-His<sub>10</sub>) and Gel Filtration Chromatography. For *Affinity Chromatography*, proteins of interest, genetically tagged with a sequence encoding for 10 histidine residues, were purified using the Protino Ni-NTA Columns (Macherey-Nagel GmbH). The flow rate of the mobile phase was kept consistent at 1 ml /min via a pump. Equilibration of the column was performed by 10-20 ml of Ni-column wash buffer (50 mM NaH<sub>2</sub>PO<sub>4</sub> pH 8.0, 300 mM NaCl, 0.01 % (w/v) DDM, 1 mM PMSF), containing 10 mM imidazole. The sample, containing 1-4 mg of solubilised protein in 1 ml Solubilisation Buffer was applied to the column and 2.5 ml of the flow-through were collected (fraction f<sub>0</sub>). After this, the column was washed abundantly with 10-20 ml of wash buffer, containing 20 mM imidazole and subsequently 50 mM imidazole, and two more 2.5 ml fractions were collected (f<sub>20</sub> and f<sub>50</sub>). Increasing concentrations of imidazole in the wash buffer (250 mM, 350 mM, 500 mM) resulted in the elution of bound proteins (His-tagged) and the corresponding 2.5 ml fractions were collected (f<sub>250</sub>, f<sub>350</sub>, f<sub>500</sub>). All eluents collected were put on ice. The column was washed abundantly with 500 mM imidazole and filled with 30% (v/v) EtOH before being stored at  $4^{\circ}\text{C}$ . For *Gel Filtration*, Sephadex G-25 columns were used. Each fraction collected from the Affinity Chromatography method, was loaded on a thoroughly washed with distilled water, Sephadex column. When the sample volume had entered the column, 3.5 ml of sterile distilled water were added to the column so that removal of salts and buffer exchange was performed. The protein was then eluted and frozen in 50 ml Eppendorf tubes at  $-80^{\circ}\text{C}$ . The samples were then concentrated by lyophilization for 2 days and resuspended in a buffer with 50 mM NaH<sub>2</sub>PO<sub>4</sub>, 10% glycerol, 0.1% w/v DDM, 1 mM PMSF, 1 x PIC, pH 7.5.

Protein quantification was done with the method of Bradford. 2 mL of Bradford Reagent (100 mg Coomassie Brilliant Blue G-250, 50 ml 100% EtOH, 100 ml H<sub>2</sub>PO<sub>4</sub>, 850 ml H<sub>2</sub>O) were mixed with 2  $\mu\text{L}$  of the protein extract and vortexed briefly, before being transferred to a cuvette. The spectrophotometer was calibrated with a 'blank' containing only the reagent, and then the optical density (OD) of samples was measured in duplicates, at 595 nm. Protein concentrations were quantified by comparing the OD values of the samples, against the BSA standard curve.

## 2.8 SDS-PAGE AND WESTERN BLOT

For SDS-page electrophoresis, proteins (30–50 mg estimated by Bradford assays) were incubated with 4x sample loading buffer (40% (v/v) glycerol, 250 mM Tris-HCl pH 6.8, 0.02% (w/v) bromophenol blue, 8% (v/v) SDS, 20% (v/v)  $\beta$ -mercaptoethanol) for 30 min at 37°C, loaded and separated in a 8–10% (w/v) polyacrylamide gel, with the use of electrophoresis running buffer (25mM Tris, 192 mM Glycine, 0.1% SDS pH 8.3) at 80 V through the stacking gel and 100 V through the separating gel. Next, proteins were transferred onto methanol-activated PVDF membranes (Macherey-Nagel, Lab Supplies Scientific SA, Hellas), with the use of Transfer Buffer (25mM Tris, 192 mM Glycine, 20% methanol), at 100V for 1.5-2 h. More specifically, the gel was placed in a cassette on top of a sponge and two filter papers, followed by the PVDF membrane, two more filter papers and another sponge. The cassette was inserted in a blotting apparatus (Mini PROTEAN™ Tetra Cell, Bio-Rad), filled with ice-cold Transfer Buffer, and electric current was applied. After transfer, the membrane was stored in TBS-T buffer (10 mM Tris-HCl pH 7.5, 150 mM NaCl) at 4°C. Blocking was performed with 2% (w/v) non-fat dry milk in TBS-T or 3% (w/v) BSA in TBS-Tween for 1h, RT, with gentle shaking. Immunodetection was performed with a primary anti-GFP monoclonal antibody (Roche Diagnostics, Hellas), an anti-FLAG M2 monoclonal antibody (Sigma-Aldrich), an anti-actin monoclonal (C4) antibody (MP Biomedicals Europe), all diluted at 1:2000, and a Penta-His HRP Conjugate antibody kit (Qiagen, SafeBlood BioAnalytica SA, Hellas) according to manufacturer's instructions. After 3x 10 min washing in TBS-T with vigorous shaking to remove non-specifically bound antibody, the membrane was incubated for 1 h with secondary goat anti-mouse IgG HRP-linked antibody (Cell Signaling Technology Inc, Bioline Scientific SA, Hellas), diluted in blocking buffer (1:1000-1:3500), at RT, with gentle shaking. The membrane was washed again 3 x 10 min as previously described, and blots were developed in a dark room with Kodak developing reagents, using the LumiSensor Chemiluminescent HRP Substrate kit (Genscript USA, Lab Supplies Scientific SA, Hellas) according to the manufacturer's instructions and SuperRX Fuji medical X-Ray films (FujiFILM Europe).

## CHAPTER 3

## RESULTS

## 3.1 PURINE TRANSPORTER DI-/OLIGOMERIZATION IS CRITICAL FOR ER-EXIT

Adapted from Martzoukou O, Karachaliou M, Yalelis V, Leung J, Bryne B, Amillis S, Diallinas G. *J Mol Biol.* 2015 Aug 14; 427(16):2679-96.

## 3.1.1 Rationale of the project

Polytopic transmembrane proteins, such as the UapA purine transporter of the NAT/NCS2 family, are co-translationally integrated in the ER membrane, prior to their packaging in COPII vesicles. ER-exit and the subsequent protein trafficking events, necessitate proper folding, which for certain cases includes successful dimerization or oligomerization of the protein molecules. By using as a cargo the extensively studied UapA transporter of *A. nidulans* and selected ER-retained mutant versions, we will assess the possibility of dimerization and investigate its role in ER-exit and membrane trafficking. For this purpose, we will perform co-immunoprecipitation and *in vivo* Bi-fluorescence assays. In the course of previous microscopy experiments of our group, it was demonstrated that the UapA-K572R mutant which cannot be ubiquitinated and thus internalized, exhibits vacuolar localization upon co-expression with the wild-type UapA, after endocytosis is triggered. Normally, UapA molecules are endocytosed in the presence of uric acid (UA) or ammonium ions ( $\text{NH}_4^+$ ). This *in trans* endocytosis of UapA-K572R suggested the association of UapA molecules in a homo-dimeric or oligomeric form (Gournas et al., 2010). Additionally, western blot immunodetection of the transporter, revealed biochemically uncharacterized high molecular weight bands, which probably corresponded to a putative di-/oligomeric form.

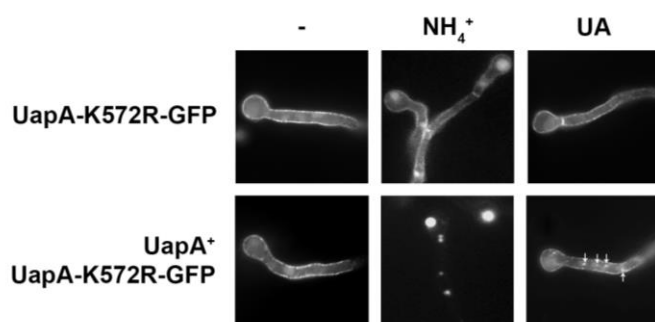


**Figure 3.1** *In trans* internalization of a GFP-tagged UapA mutant version (UapA-K572R-GFP) defective in endocytosis, upon co-expression with an untagged wt UapA (UapA<sup>+</sup>), expressed via the strong uapA100 promoter. Arrows indicate endosomes (Martzoukou et al., 2015).

### 3.1.2 Experimental process

#### 3.1.2.1 Biochemical evidence for UapA dimerization

In order to investigate UapA dimerization, we performed pull-down assays, using *A. nidulans* strains that co-express functional His-tagged and GFP-tagged transporter molecules (*alcA<sub>p</sub>-UapA-His<sub>10</sub>* and *alcA<sub>p</sub>-UapA-GFP*, respectively). Both UapA versions were expressed under the control of the regulatable *alcA* promoter. Affinity chromatography and Gel filtration was performed as described in the *Materials and Methods* chapter. The UapA-His version was tightly bound to the Ni<sup>2+</sup> column and when eluted with imidazole in the *f*<sub>250</sub> fraction, UapA-GFP was purified simultaneously, as indicated by Western blot analysis (Figure 3.2, left panel). Use of the anti-His antibody reveals a band at ~55 kDa, which corresponds to the monomeric form of UapA-His. Notice also a minor UapA-His specific band, at ~100 kDa, as well as a high molecular weight (HMW) band at >180 kDa, possibly indicating UapA oligomers or aggregates. With anti-GFP antibody, a band is detected at ~75 kDa, corresponding to monomeric UapA-GFP, whereas a HMW band is also visible. Contrastingly, when the same fraction of a strain expressing only UapA-His and not UapA-GFP was analysed, no signal was detected with the anti-GFP antibody (Figure 3.2, middle panel). The same result was observed when only UapA-GFP was expressed, which excludes the possibility of non-specific binding to the nickel column in the presence of 250 mM imidazole (Figure 3.2, right panel).

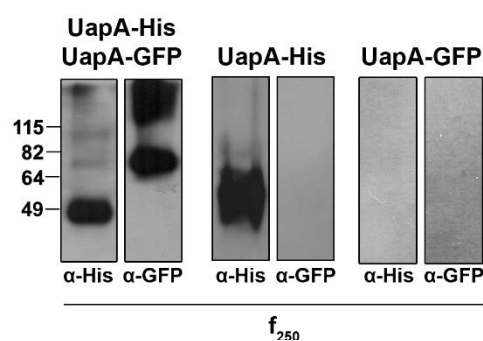


**Figure 3.2** Western blot analysis of *f*<sub>250</sub> of a strain co-expressing UapA-His and UapA-GFP or strains expressing only a single UapA version, as negative control. UapA-GFP co-purified with UapA-His, as indicated with the anti-GFP antibody (left panel). When expressed alone, UapA-His did not react with anti-GFP (middle panel), while UapA-GFP was not eluted at *f*<sub>250</sub> (right panel).

#### 3.1.2.2 In vivo evidence for UapA dimerization

To follow UapA dimerization *in vivo*, we developed a system for epifluorescence microscopic analysis via split-YFP reconstitution (Takeshita et al., 2008). More specifically, strains co-expressing UapA molecules tagged with each of the two halves of the Yellow Fluorescent Protein (YFP), were constructed (UapA-YFP<sub>C</sub>/UapA-YFP<sub>N</sub>) and compared to isogenic strains expressing UapA-GFP (positive control), or solely UapA-YFP<sub>C</sub> or UapA-YFP<sub>N</sub> (negative controls). Bimolecular fluorescence complementation (BiFC) reveals the topological proximity of the two differentially tagged UapA molecules, as a PM fluorescent signal is observed. Contrastingly, no YFP-reconstitution signal was

detected upon co-expression of UapA tagged with one half of the YFP protein and the proline transporter, PrnB, tagged with the other half (UapA-YFP<sub>N</sub>/PrnB-YFP<sub>C</sub>, grown on proline) (Figure 3.3, left panels). UapA dimerization persists upon ammonium (NH<sub>4</sub><sup>+</sup>) or substrate-elicited endocytosis (UA), until proteins reach the vacuolar membrane, as evidenced by CMAC staining. Interestingly, upon substrate addition UapA-YFP<sub>N</sub>/UapA-YFP<sub>C</sub> dimers are easily traceable in motile early endosomes and small vacuoles (Figure 3.3, right panels).

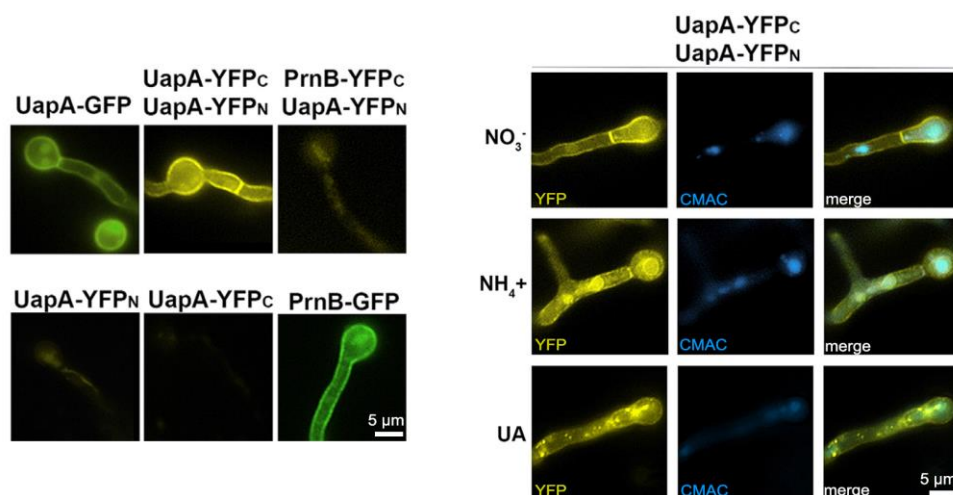


**Figure 3.3** Left panels: Reconstitution of YFP signal at the PM, due to the close association of co-expressed, differentially tagged, UapA molecules (UapA-YFP<sub>C</sub>/UapA-YFP<sub>N</sub>). UapA-GFP and PrnB-GFP are included as positive controls, whereas the non-dimerizing PrnB-YFP<sub>C</sub>/UapA-YFP<sub>N</sub> and the solely expressed UapA-YFP<sub>N</sub> or UapA-YFP<sub>C</sub>, are shown as negative controls. Right panels: Dimerization persists upon endocytosis (NH<sub>4</sub><sup>+</sup> or uric acid (UA) addition to the medium, and YFP signal coincides with large vacuoles (stained by CMAC) or motile EEs, respectively.

### 3.1.2.3 ER-retained UapA molecules do not dimerize properly

By using a combination of the previous techniques, we were able to investigate the importance of proper protein folding and ER-exit motifs, in transporter dimerization. More specifically, we used three previously constructed mutant versions of UapA that exhibit ER-retention, either due to lack of an ER-exit motif (DYDY/A), or due to partial misfolding (I74D and TMS14Δ). In the DYDY/A mutant, the Tyr-based amino terminal motif <sup>44</sup>DYDY<sup>47</sup>, which possibly serves as ER-export signal, is substituted with Ala residues. In the I74D mutant, Ile74 -located at the cytoplasmic limit of TMS1- is replaced with Asp, whereas in the TMS14Δ mutant, a 123 bp DNA fragment corresponding to TMS14 of UapA, has been deleted (Amillis et al., 2011; Vlanti et al., 2006). For BiFC assays, strains co-expressing under the *alcA<sub>p</sub>* promoter differentially tagged (YFP<sub>C</sub> or YFP<sub>N</sub>) ER-retained versions of UapA were constructed and analyzed with fluorescence microscopy. None of the strains showed YFP reconstitution signal in the ER when compared to isogenic GFP-tagged versions under the control of the same promoter (DYDY/A4-GFP, I74D-GFP και TMS14Δ-GFP)



(Figure 3.4, left panels), even though analogous signals have been reported in other studies (Zamyatnin et al., 2006). However, pull down assays of strains co-expressing UapA-DYDY/A-GFP/UapA-DYDY/A-His<sub>10</sub> or UapA-I74D-GFP/UapA-I74D-His<sub>10</sub>, reveal a physical interaction between the two differentially tagged (GFP, His<sub>10</sub>) molecules of each ER-retained mutant (Figure 3.4, right panels).

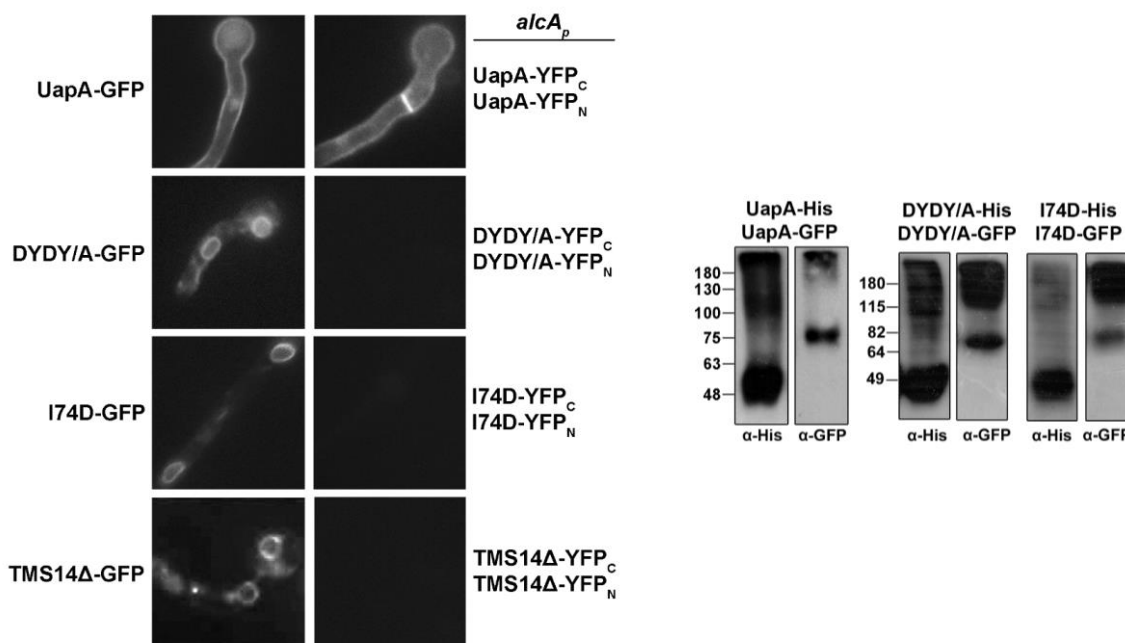


**Figure 3.4** Left panels: Inability for reconstitution of YFP signal in the ER, when differentially tagged versions (YFP<sub>C</sub> or YFP<sub>N</sub>) of ER-retained UapA mutants (DYDY/A, I74D, TMS14Δ) are co-expressed. UapA-GFP, DYDY/A-GFP, I74D-GFP, TMS14Δ-GFP, and the dimerizing UapA-YFP<sub>C</sub>/UapA-YFP<sub>N</sub> are included as positive controls. Right panels: Pull down assay of DYDY-A and I74D, reveals a physical interaction as the GFP-tagged version co-purifies with the His-tagged, for both ER-retained mutants.

### 3.1.3 Conclusions

We confirm the hypothesis that UapA oligomerizes (at least dimerizes) by using two different methods, a biochemical (pull down assay) and an *in vivo* method (BiFC). The split-YFP assay, not only provides evidence for the dimerization of UapA, but also enables the detection of the subcellular localization of the dimer. Upon triggering UapA endocytosis and during vacuolar sorting, the tight dimer formation is persistent, as evidenced by microscopic studies in the UapA-YFP<sub>C</sub>/UapA-YFP<sub>N</sub> strain. Moreover, by using ER-retained UapA mutants, either modified in their N-terminal motif or partially misfolded, we demonstrate that dimerization is associated with ER-exit. As these mutants seem to associate physically, but fail to associate properly in order to reconstitute YFP signal, our results reveal the essentiality of proper di-/oligomerization for transporter membrane trafficking.

## 3.2 THE AP COMPLEXES ARE DISPENSABLE FOR TRANSPORTER TRAFFICKING

Adapted from Martzoukou O, Amillis S, Zervakou A, Christoforidis S, Diallinas G. *Elife*. 2017 Feb 21; 6. pii: e20083.

### 3.2.1 Rationale of the project

The heterotetrameric Adaptor proteins (APs) are the major type of adaptors that mediate the formation of clathrin-coated vesicles in most eukaryotes, but had not been studied in *A. nidulans*. It has been reported that genetic disruption of any of the four AP subunits inactivates the function of the full complex (Robinson, 2004; 2015). The  $\beta$  subunits are particularly important for clathrin binding, whereas clathrin-binding motifs (L[L,I][D,E,N][L,F][D,E]) have been identified in the hinge domains of both  $\beta 1$  and  $\beta 2$  subunits of AP-1 and AP-2, respectively. *In silico* analysis performed in our lab, revealed that the AP  $\beta$  subunits of higher fungi lack an entire C-terminal domain, normally located close to the clathrin binding motif (Martzoukou et al., 2017). Based on this, we analyze the phenotypes of AP adaptors and clathrin genetic deletions and investigate whether they share common roles in transporter vesicular trafficking, using as a model cargo the extensively studied purine transporter UapA, as well as six other transporters belonging to different families. In this direction, we use microscopy to study the localization of fluorescent versions of transporters in AP<sup>+</sup> and AP<sup>-</sup> isogenic strains of all the fungal complexes (AP-1, AP-2, AP-3), as well as in corresponding clathrin strains (Cla<sup>+</sup> and Cla<sup>-</sup>).

### 3.2.2 Experimental process

#### 3.2.2.1 Lack of functional AP-1 and AP-2 complexes causes severe growth delay

In order to investigate the role of the three AP complexes in subcellular vesicular trafficking of transporters, we constructed three isogenic strains either carrying a deletion the  $\sigma$  subunit (*ap2 $\Delta$* , *ap3 $\Delta$* ) or expressing the same subunit (*thiA<sub>p</sub>-ap1 $\sigma$* ) under the control of the regulatable *thiA<sub>p</sub>* promoter (Apostolaki et al., 2012). Construction of a knockdown strain was necessary only in the case of the AP-1 complex, as the knock-out proved lethal (not shown). In order to exclude the possibility of any functional complementation between the  $\sigma$  subunits of different AP complexes, double AP-defective strains were also constructed via genetic crossing. AP-1 and AP-2 complexes, but not AP-3, proved to be essential for proper fungal growth, whereas in all cases, the phenotype was not enhanced when AP-deficiency was combined in the double AP-deficient strains (Figure 3.5). Microscopic morphology was consistent with the severe growth delay of these strains (Figure 3.5 A, bottom right insets), exhibiting hyperbranching, increased septa formation (Figure 3.5 B and C, respectively) and lack of canonical chitin distribution (Figure 3.5 D, calcofluor staining).

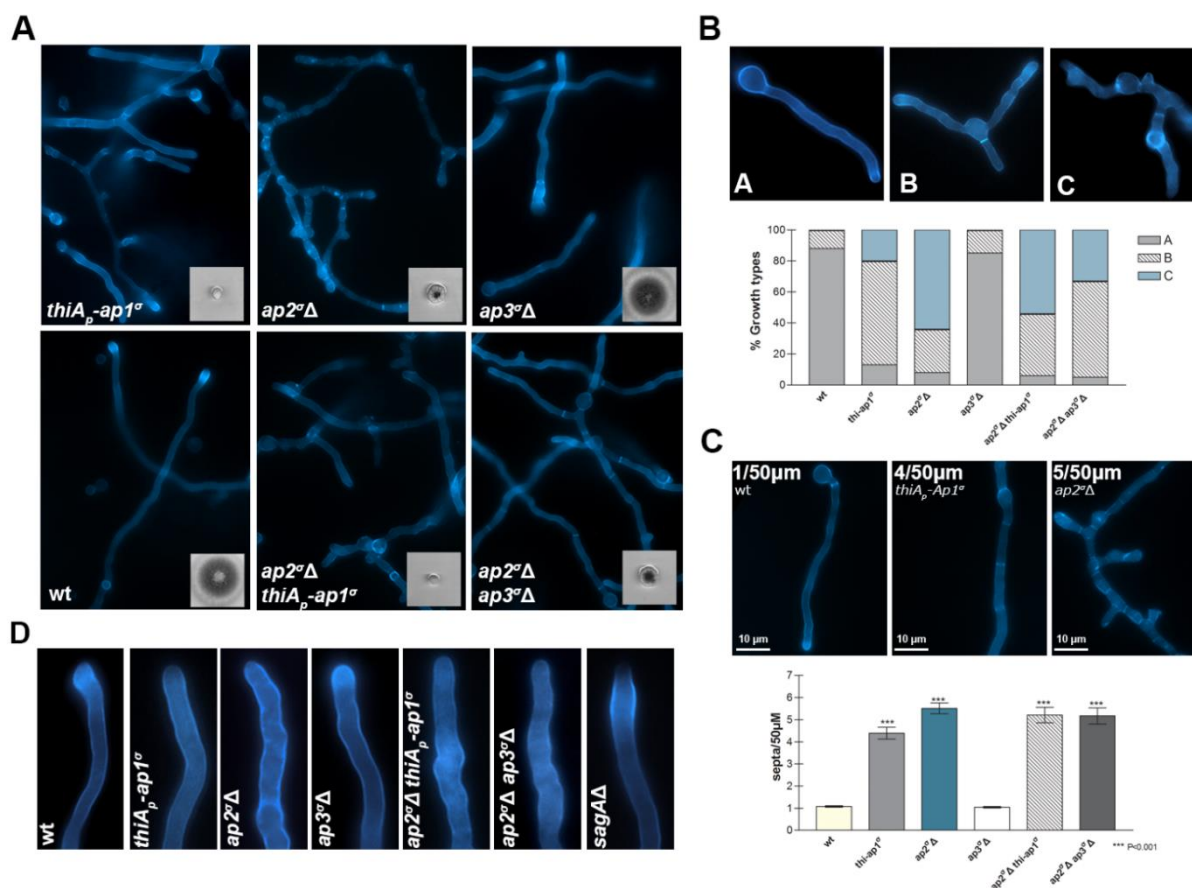


**Figure 3.5** (A) Colony growth (bottom right insets) and microscopic morphology with calcofluor staining, of strains lacking functional AP-1, AP-2 and AP-3 complexes (*thiA<sub>p</sub>-ap1<sup>o</sup>*, *ap2<sup>o</sup>Δ*, *ap3<sup>o</sup>Δ* respectively) and of double deficient strains (*thiA<sub>p</sub>-ap1<sup>o</sup>*, *ap2<sup>o</sup>Δ ap3<sup>o</sup>Δ*), compared to wild-type (wt). (B) Representative morphological phenotypes used for the categorization and quantification of hyper-branching patterns and corresponding quantitative analysis ( $n=31-100$  hyphae), revealing the specific effects of AP-1 and AP-2 deficiency in polar growth maintenance. (C) Representative types of increased septa formation of strains shown in A, and corresponding quantification performed for 50  $\mu\text{m}$  of hyphal length ( $n=27-32$  hyphae,  $P<0.001$  compared to wt), reveals the effect of AP-1 and AP-2 deficiency in septation. (D) Calcofluor deposition at the growing tip of strains shown in A, compared to a standard endocytic mutant, *sagAΔ*. Notice the reduced chitin accumulation at the collar region in the absence of functional AP-1 and AP-2 complexes, but not AP-3.

### 3.2.2.2 Lack of clathrin chains has versatile effects on growth rate and morphology

To study the role of clathrin with respect to transporter trafficking, we constructed strains that lack expression of the light (ClaL) or heavy chain (ClaH) of clathrin. Only the ClaL null mutant was viable (*claLΔ*) but exhibited problematic colony growth, thus we used conditional knock-down strains for both chains (*thiA<sub>p</sub>-claL*, *thiA<sub>p</sub>-claH*). Although *A. nidulans* growth was severely affected when either one of the clathrin chains was not expressed (Figure 3.6 A), microscopic morphology observation (Figure 3.6 B) uncovered the non-essentiality of the light chain in polar growth. Cells that lack ClaH, however, exhibited various morphological phenotypes, distinct from the ones

resulting from the absence of AP-1 and AP-2, such as abnormal hyphal width (a), isotropic expansion of the conidiospore head (b), tip swelling (c) and reduced hyphal size (d).



**Figure 3.6** (A) Colony growth and (B) microscopic morphology with calcofluor staining, of strains lacking expression of either the light or the heavy chain of clathrin (*thiA<sub>p</sub>-claL*, *claLΔ* and *thiA<sub>p</sub>-claH* respectively), compared to wild-type (wt). Microscopic morphology of hyphae lacking *Clal* is not severely changed, except for tip swelling, which occurred in a higher temperature (37°C). The observed morphological phenotypes for strains lacking *Clah* expression can be separated in four different types, appearing with almost the same frequency.

### 3.2.2.3 The AP complexes are dispensable for UapA exocytosis and endocytosis

Epifluorescence microscopic analysis was performed to study the role of AP complexes in UapA subcellular trafficking. In hyphae that do not express functional AP-1, AP-2 or AP-3 complexes (*thiA<sub>p</sub>-ap1<sup>σ</sup>*, *ap2<sup>σ</sup>Δ*, *ap3<sup>σ</sup>Δ* respectively), UapA-GFP was able to reach the PM under standard conditions (growth on NO<sub>3</sub>, Figure 3.7 upper panels), similar to the wt isogenic strain. When endocytosis was triggered by NH<sub>4</sub><sup>+</sup> addition (> 2h) to the culture media of the same strains, the transporter showed normal vacuolar localization due to internalization from the PM, as the fluorescent signal was decreased in the latter (Figure 3.7, lower panels). Strains lacking the standard endocytic factors *SagA* and *SlaB* (Araujo-Bazan *et al.*, 2008; Hervas-Aguilar and Penalva, 2010), are

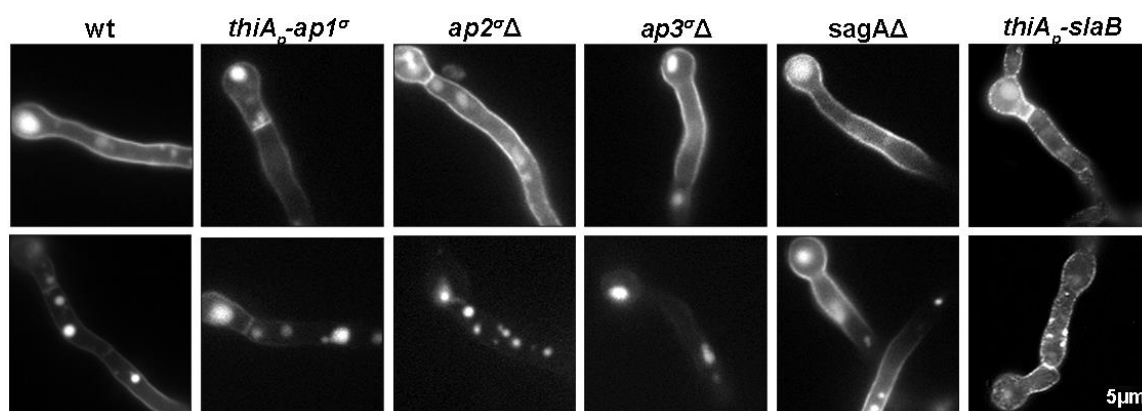


**Figure 3.7** Fluorescence microscopy analysis of UapA-GFP topology in the absence of functional AP complexes, compared to wt and endocytosis-deficient isogenic strains (*sagAΔ*, *thiA<sub>p</sub>-slaB*), under standard (nitrate, upper panels) and endocytic conditions (ammonium, lower panels).

also included as controls. Notice the persistence of PM fluorescence even in the presence of endocytic trigger. Our results show that all fungal AP complexes are not required for membrane trafficking of the purine transporter UapA.

### 3.2.2.4 Additional purine and amino-acid transporters do not require the AP-2 complex for endocytosis

To exclude the possibility that our results concerning endocytosis strictly apply for UapA, we tested six more transporters belonging to different protein families and exhibiting specificity for different substrates (PrnB, AgtA, FurA, FurD, FurE, FcyB) (Apostolaki et al., 2009; Kryptou et al., 2015; Tavoularis et al., 2001; Vlanti and Diallinas, 2008). We constructed strains carrying fluorescently tagged versions of these transporters in either wt or *ap2 $\Delta$*  isogenic genetic backgrounds, and performed microscopic analyses in standard and endocytic conditions, as previously described. FM4-64 staining, indicates the presence of all transporters in the vacuole, irrespective of AP-2 depletion, after the endocytic trigger was imposed (ammonium, >2h) (Figure

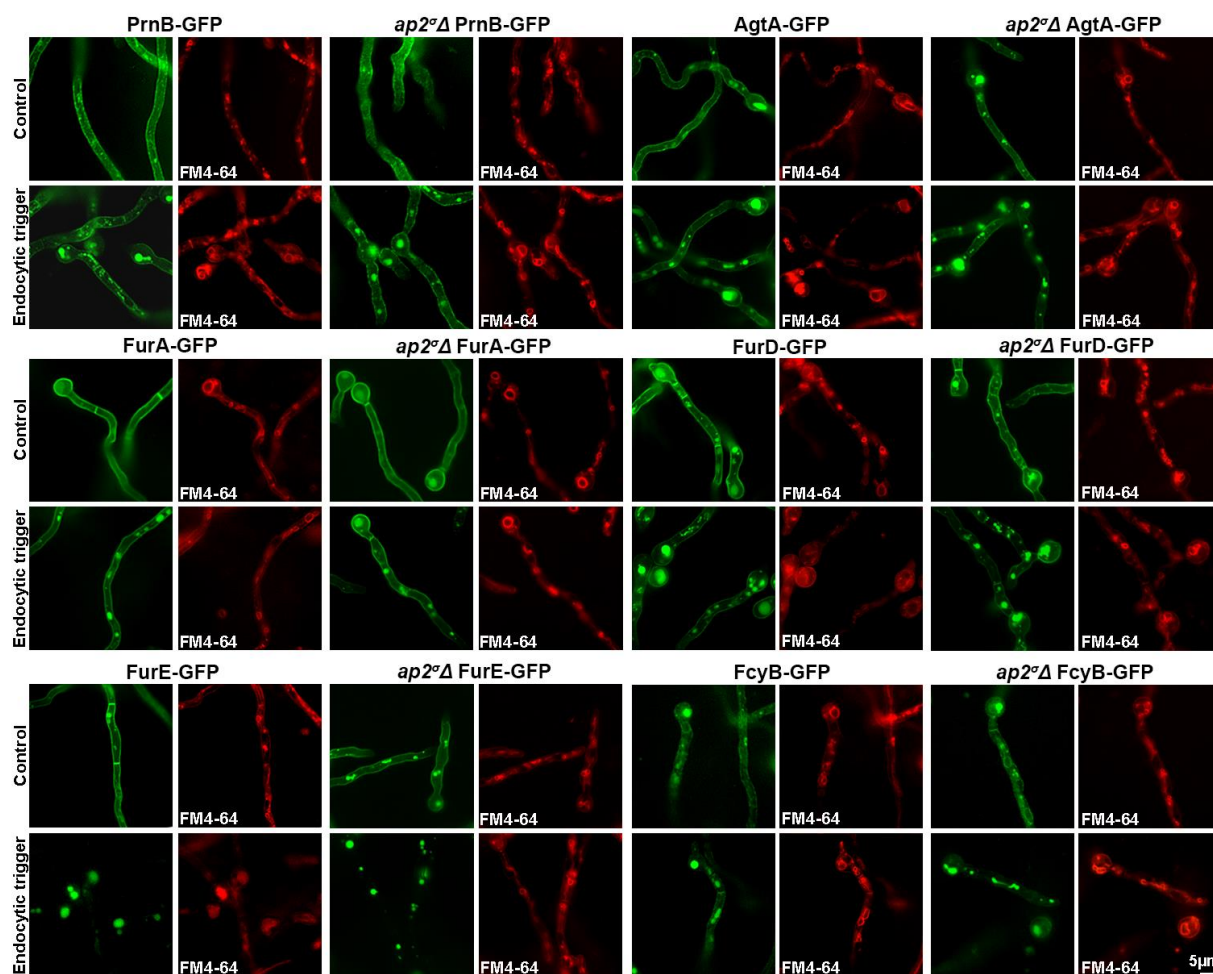


**Figure 3.8** Fluorescence microscopy analysis of six different transporters in the absence of a functional AP-2 complex, compared to wt isogenic strains. FM4-64 vacuolar staining is included.

3.8), whereas relevant quantification and statistical analysis confirms the aforementioned results (Figure 3.9 and *Materials and Methods*).

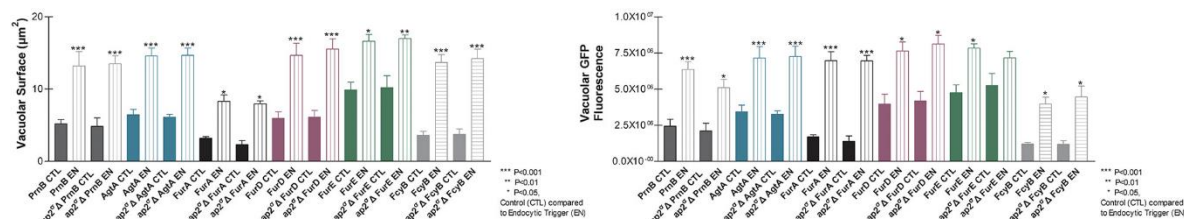


**Figure 3.9** Quantification of the results shown in Figure 3.8, confirms the physiological endocytosis of all the transporters, in the absence of the AP-2 complex. Measurements were performed for both Vacuolar Surface (left panel) and Vacuolar GFP Fluorescence (right panel). For details, see *Materials and Methods*.

### 3.2.2.5 Clathrin is essential for transporter trafficking

To determine whether clathrin has an AP-independent role in vesicular trafficking of the UapA transporter, we investigated its subcellular topology as previously, with a GFP-tagged transporter version expressed in a genetic background lacking either the light or the heavy chain of clathrin (*thiA<sub>p</sub>-claL* UapA-GFP and *thiA<sub>p</sub>-claH* UapA-GFP, respectively). Knockdown of ClaL expression (+thi, overnight: o/n) prevented the endocytic internalization of UapA, compared to the control (-thi, ClaL is expressed) where GFP-labeled vacuoles are observed (Figure 3.10, left panels). However, analogous experiments of *ab initio* thiamine addition could not be performed with ClaH, due to an apparent severe block in transporter exocytosis (Figure 3.10, right panels). Western blot analysis of total protein extracts from a strain expressing ClaH under the control of *thiA<sub>p</sub>* promoter, revealed a protein decrease to undetectable levels after 10 h of incubation with thiamine (not shown). Thus, in order to study the role of clathrin heavy chain in transporter endocytosis with epifluorescence microscopy, thiamine was added in the culture media (for 10 h), after a period of normal vegetative

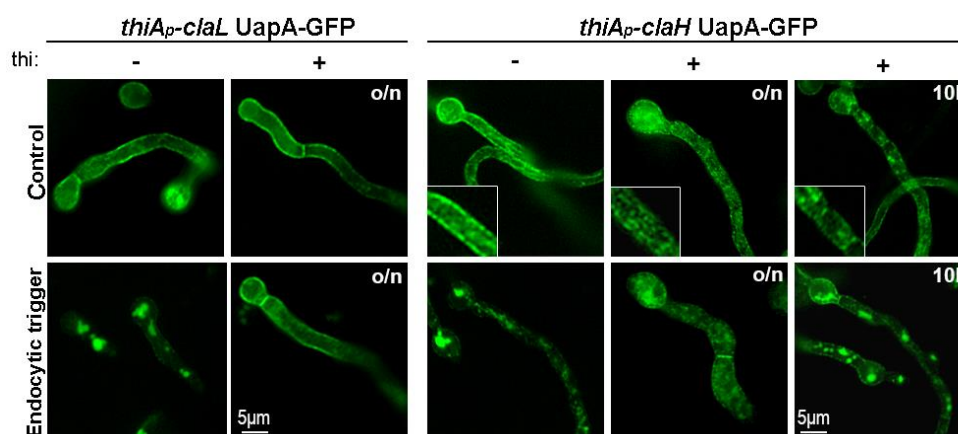


**Figure 3.10** Fluorescence microscopy showing the effects of clathrin depletion on the subcellular trafficking ('Control') and endocytosis (NH<sub>4</sub><sup>+</sup>, 2 h) of UapA-GFP. For more explanations see the text.

growth in the absence of thiamine (14 h). UapA was able to reach the PM before ClaH was depleted from the hypha, and upon ammonium-elicited endocytosis a significant fraction was not internalized. However, UapA-labeled cytoplasmic structures appeared even under standard conditions (nitrate), which could be derivatives of Golgi malfunction due to ClaH absence (Figure 3.10, right panels).

### 3.2.3 Conclusions

Investigation of the role of the AP complexes, showed that AP-1 and AP-2 are essential for fungal polar growth, whereas all three complexes are dispensable for transporter exocytosis and endocytosis. AP-1 and AP-2 also affect septation, branching pattern and cell wall deposition at the hyphal tip, as shown with calcofluor staining. Additionally, we demonstrate that both clathrin chains (ClaL and ClaH) are also required for rapid vegetative growth, even though the phenotypes resulting from their depletion are not similar to those observed for AP-deficient strains (AP-1 and AP-2). Lastly, one important finding was that transporter (UapA) endocytosis is clathrin-dependent but AP-2 independent, which could result from the evolutionary truncation of the  $\beta$ 2 subunit. The role of the AP-2 complex will be assessed in Chapter 3.4.

### 3.3 VESICULAR TRAFFICKING OF APICAL CARGOES REQUIRES THE AP-1

*Adapted from Martzoukou O, Diallinas G, Amillis S. **Genetics**. 2018 Jun 20; pii: genetics.301240.2018*

#### 3.3.1 Rationale of the project

The role of the essential AP-1 complex in *A. nidulans*, remained elusive, even though our previous results (Chapter 3.2) suggested an involvement in polar growth maintenance. Transporters exhibit AP-1-independent membrane transport, but in several organisms -mostly mammals- this complex, is involved in trafficking between the TGN and the endosomes (Robinson, 2015, 2004). Here we dissect the role of the AP-1 complex in vesicular trafficking, using AP-1<sup>+</sup> and AP-1<sup>-</sup> isogenic strains and several apical cargoes as markers, including the lipid flippases DnfA and DnfB, the chitin synthase ChsB and the endocytic factors SagA, SlaB, AbpA. We also use selected proteins involved in specialization of transport and fusion of secretory vesicles and endosomes, like the SNAREs SynA (v-SNARE) and SsoA (t-SNARE) and the Rab GTPases RabA, RabB (Early endosomes), RabE (post-Golgi and SVs), RabC (Retrograde transport), RabO (Golgi and SPK). Moreover, we assess the topological correlation of AP-1 with various subcellular organelles, like the Golgi network, the SPK, the cytoskeleton and with the heavy and light chains of clathrin (cis-Golgi: SedV, trans-Golgi: PH<sup>OSBP</sup>, SPK: Tropomyosin TpmA, MTs:  $\alpha$ -tubulin TubA, Septins: AspB, -C, -D, -E). Furthermore, to investigate in depth the association of AP-1 and clathrin, we construct strains carrying mutations in the putative clathrin binding boxes and in parallel we examine the role of RaBE with respect to clathrin, as it had not been studied before. Last but not least, recent research findings from other groups had indicated an additional role for AP-1, as a motor adaptor, that interacts directly with a member of the kinesin superfamily in neurons (Nakagawa *et al.*, 2000), thus we also test whether AP1 in *A. nidulans* correlates with two conventional kinesins, KinA and UnCA.

#### 3.3.2 Experimental process

##### 3.3.2.1 Subcellular localization and essentiality of the AP-1 complex

Our previous results highlighted the essentiality of AP-1 for proper colony growth, however we extended our study to include conditional knock-downs of two more subunits, the medium ( $\mu$ ) and the beta ( $\beta$ ), genetic disruption of which seems to affect growth in a similar way to the  $\sigma$  subunit. Western blot analysis confirms the total depletion of *ap1 $\sigma$*  in grown hyphae, when thiamine is added *ab initio* (o/n : overnight) (Figure 3.11 A). Calcofluor staining and microscopic observation of the *ap1 $\sigma$*  knock-down strain, confirms altered chitin deposition, increased septation and hyperbranching (Figure 3.11 B). We also address the question of the subcellular localization of AP-1



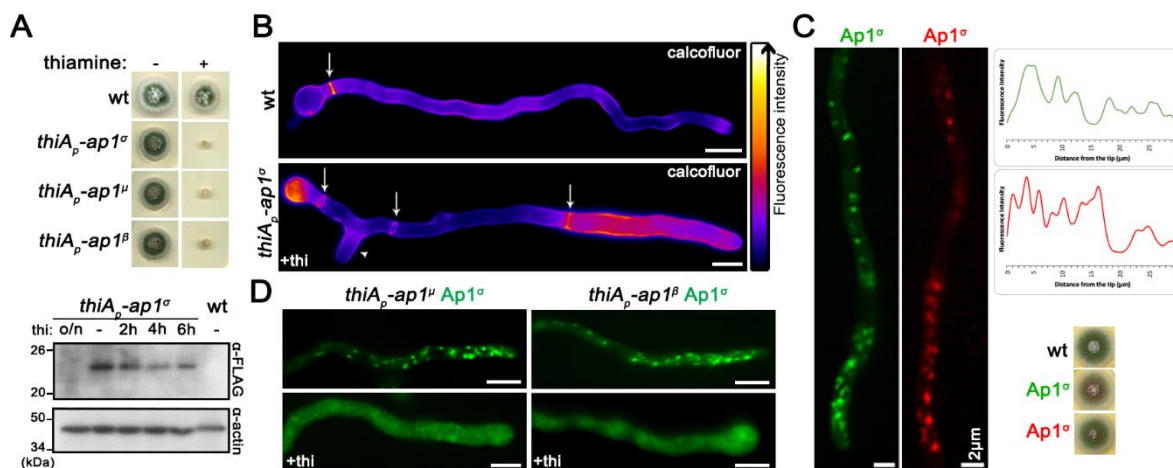


**Figure 3.11** (A) Growth tests of conditional knock-downs of the  $\sigma$ ,  $\mu$  and  $\beta$  AP-1 subunits (upper panel) and Western blot analysis of the FLAG- $Ap1^{\sigma}$  levels after addition of thiamine overnight (o/n) or for 2, 4, 6 h before mycelium harvesting and total protein extraction (lower panel). A strain expressing an untagged version of  $Ap1^{\sigma}$  is included as a control (wt). (B) Microscopic morphology of *thiAp-ap1 $\sigma$*  in the absence or presence of thiamine. Calcofluor staining and a 'fire' Look-up table (LUT, Image J software) are applied to make differences in chitin deposition more noticeable (arrows indicate septa, arrowhead points to an emerging branch). (C) Similar subcellular localization of functional (see growth tests, bottom right) AP-1  $\sigma$  subunits, tagged with GFP (left) and mRFP (right), reveals the polarized distribution of the complex (see also relevant quantitative analysis, upper right panel). (D) Microscopy studies of the  $Ap1^{\sigma}$ -GFP localization, the presence (upper panels) or absence (lower panels) of  $Ap1^{\mu}$  and  $Ap1^{\beta}$  subunits (left and right panels, respectively). Scale bars in B,C: 5  $\mu$ m.

by constructing strains expressing  $Ap1^{\sigma}$ -mRFP or  $Ap1^{\sigma}$ -GFP in a wild-type background, and show that functional GFP- or mRFP-tagged AP-1  $\sigma$  is localized in distinct cytoplasmic puncta, being more abundant in the apical region of hyphae (Figure 3.11 C). Moreover, to confirm the participation of all tested subunits in AP-1 complex formation, as well as the previously reported observation (Robinson, 2015) that inactivation of any subunit disrupts the whole complex, we use the thiamine-regulatable promoter *thiA<sub>p</sub>* to express  $Ap1^{\sigma}$ -GFP in *thiA<sub>p</sub>-ap1<sup>β</sup>* and *thiA<sub>p</sub>-ap1<sup>μ</sup>* isogenic backgrounds, in the absence (control) or presence of thiamine (repressed AP-1) (Figure 3.11 D). Our results are in line with complex disassembly in the absence of one subunit, as evidenced by the observed diffuse cytoplasmic signal (D).

### 3.3.2.2 AP-1 is required for proper apical protein localization

As mentioned in the introduction, apex-directed exocytosis of selected cargoes combined with their constitutive endocytosis at the collar region, creates polarization in hyphal growth, mostly evident by the accumulation of these proteins in an apical crescent. Based on our previous observations, AP-1 is essential for polarized growth, thus we used as markers, known, polarly localized cargoes to confirm the involvement of the adaptor in their subcellular trafficking. AP-1

deficient strains were tested for the localization of fluorescently tagged versions of the vesicular SNARE SynA and t-SNARE SsoA (Taheri-Talesh et al., 2008), the phospholipid flippases DnfA and DnfB (Schultzhaus et al., 2015), the class III chitin synthase ChsB (Takeshita et al., 2015) and the actin-interacting-protein TpmA (Taheri-Talesh et al., 2008). In all cases, AP-1 proved to be essential for the normal distribution of the proteins -in comparison to UapA, which is included as a negative control- as its depletion resulted in loss of polarity and appearance of bright cytoplasmic puncta. TpmA also lost its positioning, suggesting SPK destabilization with further implications for cytoskeleton organization (Figure 3.12, lower panels). We also test the localization of the collar-localized endocytic factors SagA, SlaB and AbpA (Araujo-Bazán et al., 2008; Hervás-Aguilar and Peñalva, 2010; Karachaliou et al., 2013), which appear mislocalized at the apical crescent, in the absence of AP-1.

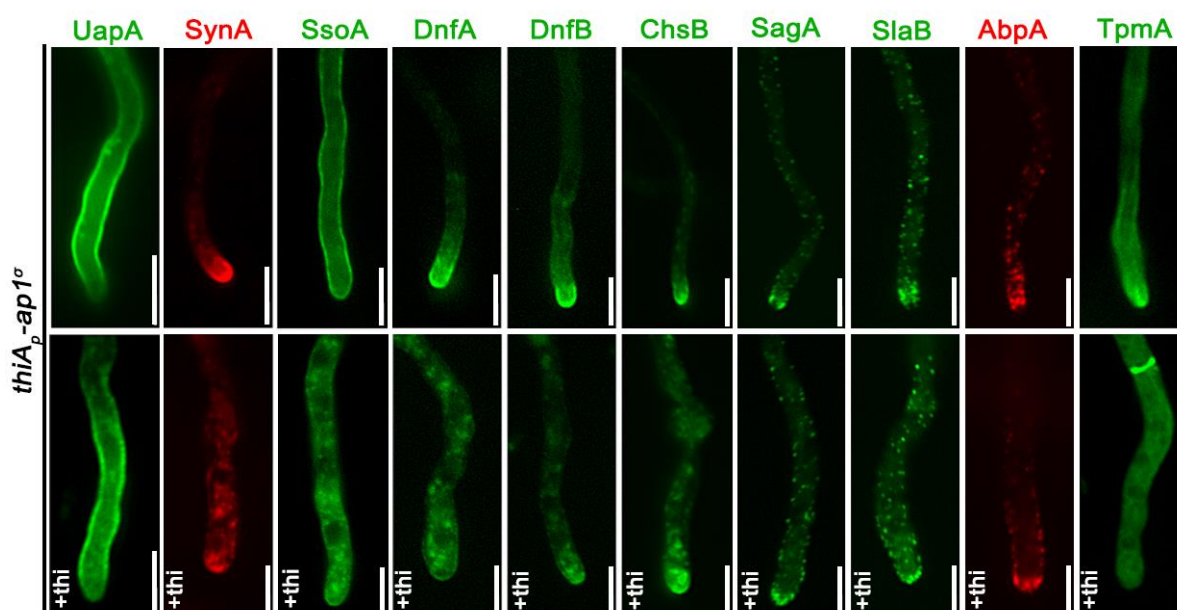


**Figure 3.12** Epifluorescence microscopic analysis of well-studied polar cargoes (upper panel) in conditions of AP-1 depletion (lower panels). All markers appear significantly affected, especially when compared to the purine transporter UapA whose trafficking is AP-1 independent (Chapter 3.2). Notice the loss of polarity, the appearance of various cytoplasmic structures (SynA, SsoA, DnfA, DnfB, ChsB), the abnormal localization of the endocytic collar (SagA, SlaB, AbpA) and the loss of SPK integrity (TpmA). For details on the role of proteins tested, see text. Scale bars: 5  $\mu$ m.

### 3.3.2.3 Late-Golgi cisternae transiently associate with AP-1 foci

To examine the possible association of AP-1 with the Golgi network, we use the extensively characterized markers SedV<sup>Sed5</sup> and PH<sup>OSBP</sup> for early- and late-Golgi, respectively (Pantazopoulou and Peñalva, 2009; Pinar et al., 2013a) (See also Chapter 1.3.4), for colocalization studies. Ap1<sup>o</sup> shows some topological correlation with the early-Golgi marker, SedV, but their colocalization degree is not high (n = 5; PCC = 0.35, P < 0.01). Time-series of a selected hyphal region, reveals that AP-1 foci 'decorate' SedV-labeled structures (Figure 3.13 A). In the case of PH<sup>OSBP</sup>, a significant degree of

colocalization is observed between the adaptor and the late-Golgi marker, also confirmed with quantitative analysis ( $n = 7$ ;  $PCC = 0.66$ ,  $P < 0.0001$ ). Corresponding time-series images indicate the coherent movement of the two proteins in all three dimensions, an association that appears to be dynamic and transient, as clearly shown by the progressive loss of colocalization (Figure 3.13 B).

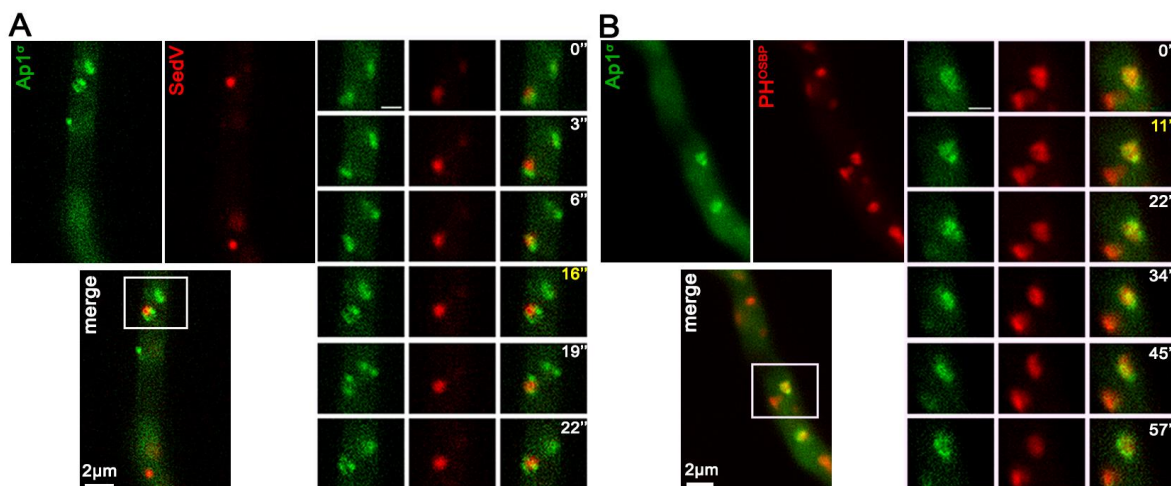


**Figure 3.13** Colocalization analysis of AP-1 and two Golgi markers, the early-Golgi SedV (A) and the late-Golgi PH<sup>OSBP</sup>. The degree of association of AP-1 with late-Golgi cisternae is relatively high, but the nature of their interaction appears to be transient and dynamic. Contrastingly, the adaptor exhibits very low colocalization with early-Golgi cisternae. Time-lapse images of a selected region are included for both markers, whereas the relative time of the uncropped image is highlighted in the corresponding time frame, in yellow. For more details and quantification of colocalization, see text.

#### 3.3.2.4 AP-1 localization is RabO- and RabC- dependent

To confirm the significant degree of association between AP-1 and the late-Golgi, we constructed strains that express the GFP-tagged version of the adaptor, in a genetic background of thermosensitive mutations that block Golgi trafficking in the restrictive temperature. SedV<sup>ts</sup> (SedV-R258G) affects the early-Golgi organization, whereas RabO<sup>ts</sup> (RabO-A163D) has an analogous impact on the late-Golgi (Pinar et al., 2013a). Shift to the non-permissive temperature leads to diffuse AP-1 signal in the case of late-, but not early-Golgi disorganization, as expected (Figure 3.14, left and middle panels). Conditional

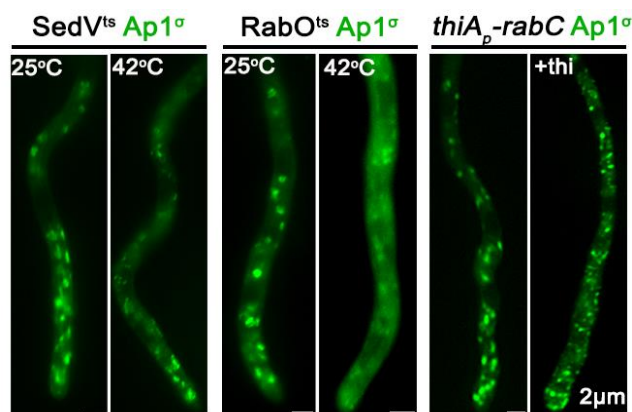


**Figure 3.14** Epifluorescence microscopy of AP-1 in genetic backgrounds that allow the conditional impairment of Golgi organization, upon shift to the restrictive temperature (42°C). SedV<sup>ts</sup> and RabO<sup>ts</sup> are thermosensitive mutations that affect early- and late-Golgi, respectively. The RabC-repressed altered localization of AP-1, further confirms an association of the adaptor with the late-Golgi.

knock-down of the RabC<sup>Rab6</sup> GTPase, which is also involved in Golgi homeostasis (Pantazopoulou and Peñalva, 2011), affects proper AP-1 localization, as the appearance of multiple small foci all over the hypha is observed (Figure 3.14, right panels).

### 3.3.2.5 Clathrin recruitment is mediated by AP-1 via specific C-terminal motifs

AP-1 has been indissolubly associated with clathrin in metazoa (Robinson, 2015), and based on the observation that the adaptor is localized transiently to the late-Golgi, we tested whether an interaction with clathrin occurs, in spite of the  $\beta 1$  truncation (see Chapter 3.2). To do so, we constructed strains co-expressing fluorescently tagged versions of the two proteins of interest (Ap-1 <sup>$\alpha$</sup> /ClaL and Ap-1 <sup>$\alpha$</sup> /ClaH). The degree of colocalization of Ap-1 <sup>$\alpha$</sup>  with both clathrin chains is high (claL: n= 9; PCC= 0.78, P< 0.0001; claH: n= 5; PCC= 0.76, P< 0.0001), and the patterns observed vary in size and shape. More specifically, AP-1 forms characteristic ‘horseshoe-like’ structures on top of ClaH foci, which are less prominent for ClaL foci (Figure 3.15, A and B). We also investigate the localization of AP-1 in the absence of ClaL and *vice versa*.

The topology of the adaptor appears unaffected by the depletion of ClaL (Figure 3.15 C, upper panels), but ClaL localization depends on the presence of a functional AP-1 (Figure 3.15 C, lower panels). The same picture is obtained when we follow the subcellular localization of both clathrin

chains in *ap1 <sup>$\beta$</sup>* -repressed strains (+thi), which appear dispersed in non-polar, small foci (Figure 3.15 D). Lastly, strains expressing (via plasmid integration events), Ap1 <sup>$\beta$</sup>  subunits mutated in one or two

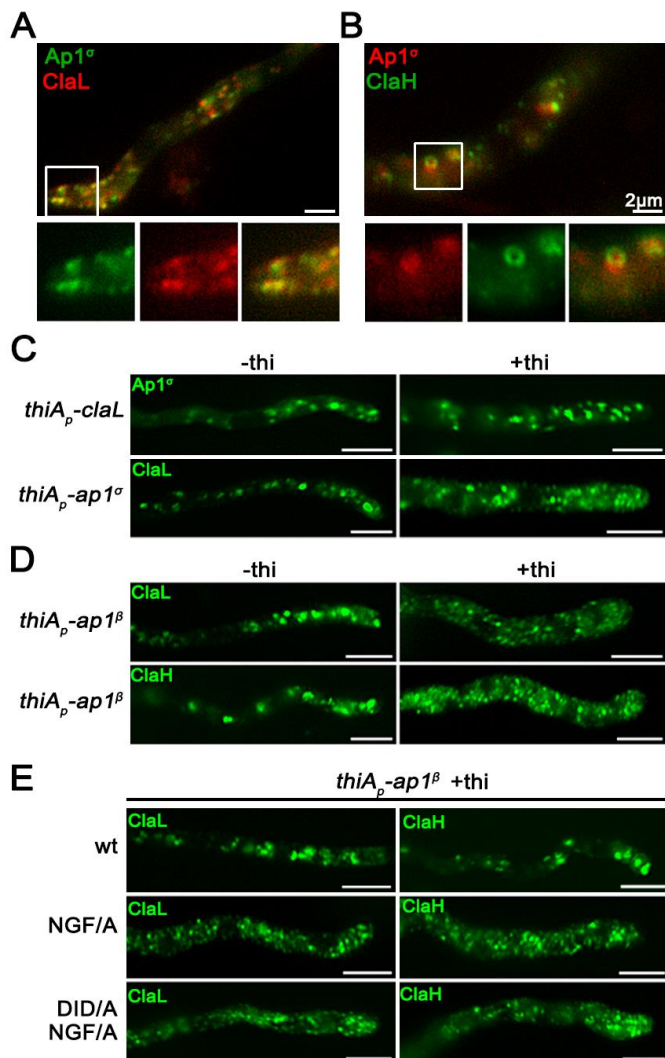


**Figure 3.15** (A and B) Colocalization analysis of AP-1 and clathrin light (ClaL) and heavy (ClaH) chains, respectively. (C) Subcellular localization of Ap1 <sup>$\alpha$</sup>  and ClaL in conditions of depletion of the latter or the former, respectively. (D) Repression of expression of *ap1 <sup>$\beta$</sup>*  (+thi) and its effect on the localization of ClaL (upper panel) or ClaH (lower panel). (E) Effect of mutations in clathrin-binding motifs <sup>709</sup>*NGF/A*<sup>711</sup> and <sup>632</sup>*DID/A*<sup>634</sup> on clathrin distribution. For details, see text. Scale bars in C, D, E: 5  $\mu$ m.

putative clathrin binding boxes (<sup>630</sup>LLDID<sup>634</sup> and <sup>707</sup>LLNGF<sup>711</sup>), have the same effect on ClaL and ClaH localization, as that of Ap1<sup>β</sup> depletion. Given the fact that these mutated motifs are expressed in a genetic background where wild-type β1 allele is not transcribed in the presence of thiamine, we suggest an interaction of AP-1<sup>β</sup> with clathrin, via these binding boxes (primarily via the <sup>707</sup>LLNGF<sup>711</sup>, based on the extent of clathrin mislocalization) (Figure 3.15 E).

### 3.3.2.6 AP-1 associates with post-Golgi exocytic carriers

To investigate whether AP-1 associates with post-Golgi membranes prior to their dissipation to secretory vesicles (SVs), we also study its localization relative to that of the RabE GTPase, which mediates the maturation of TGN to SVs (Pantazopoulou et al., 2014; Peñalva et al., 2017). Our results suggest a high degree of association between AP-1 and RabE-labeled SVs (n= 5; PCC= 0.72, P< 0.0001), more prominent at sites of branch emergence or at subapical regions (Figure 3.16 A). We also followed the localization of the two proteins in relevant knockdown mutants.

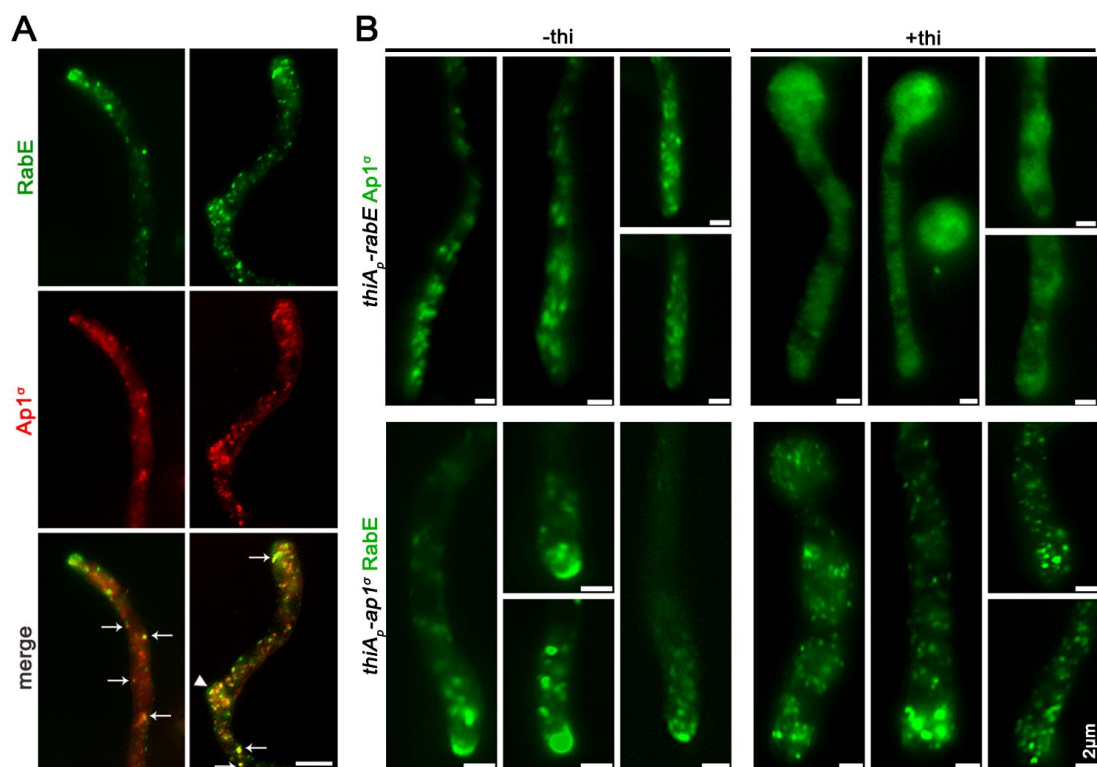


**Figure 3.16** (A) Colocalization analysis of RabE and AP-1 reveals their significant association in subapical foci (arrow) and in branch-emerging regions (arrowhead). (B) Subcellular localization of Ap1<sup>σ</sup> (upper panels) or RabE (lower panels) under wild-type conditions (-thi) and RabE or Ap1<sup>σ</sup> repression of expression (+thi), respectively. Notice the diffuse signal of AP-1 when RabE is depleted, as well as the appearance of small scattered RabE-labeled foci, when AP-1 is not functional.

Expression of *rabE* is necessary for punctate AP-1 distribution, since under fully repressed conditions the adaptor is localized in a diffuse cytoplasmic haze (Figure 3.16 B, upper panels). Contrastingly, a

functional AP-1 complex is required for the proper trafficking of RabE-labeled SVs, that fail to reach and assemble at the SPK when the adaptor is genetically repressed (Figure 3.16 B, lower panels).

### 3.3.2.7 AP-1 interacts with the microtubule network

To examine the possible association of the AP-1 and clathrin-coated SVs, with the cytoskeleton during trafficking along microtubule tracks, we perform colocalization analysis of AP-1 and the alpha-tubulin, TubA. As evidenced by the time-series images, motile AP-1 puncta dynamically decorate MTs (Figure 3.17 A). Additionally, incubation of the same strain with the anti-microtubule drug Benomyl, leads to an increase in diffuse cytoplasmic AP-1 signal, in line with a decrease in MT fluorescence (Figure 3.17 B, upper panel). Importantly, removal of Benomyl from the culture media restores both MT and AP-1 localization. Contrastingly, the depolymerization of actin cables due to Latrunculin B addition did not have a detectable effect of Ap1<sup>o</sup> polar localization (Figure 3.17 B, lower panel). The motor proteins that propel SV and EE movement along MTs in *A. nidulans*, are KinA and UncA, respectively (see also Chapter 1.3.11). Based on previous studies that

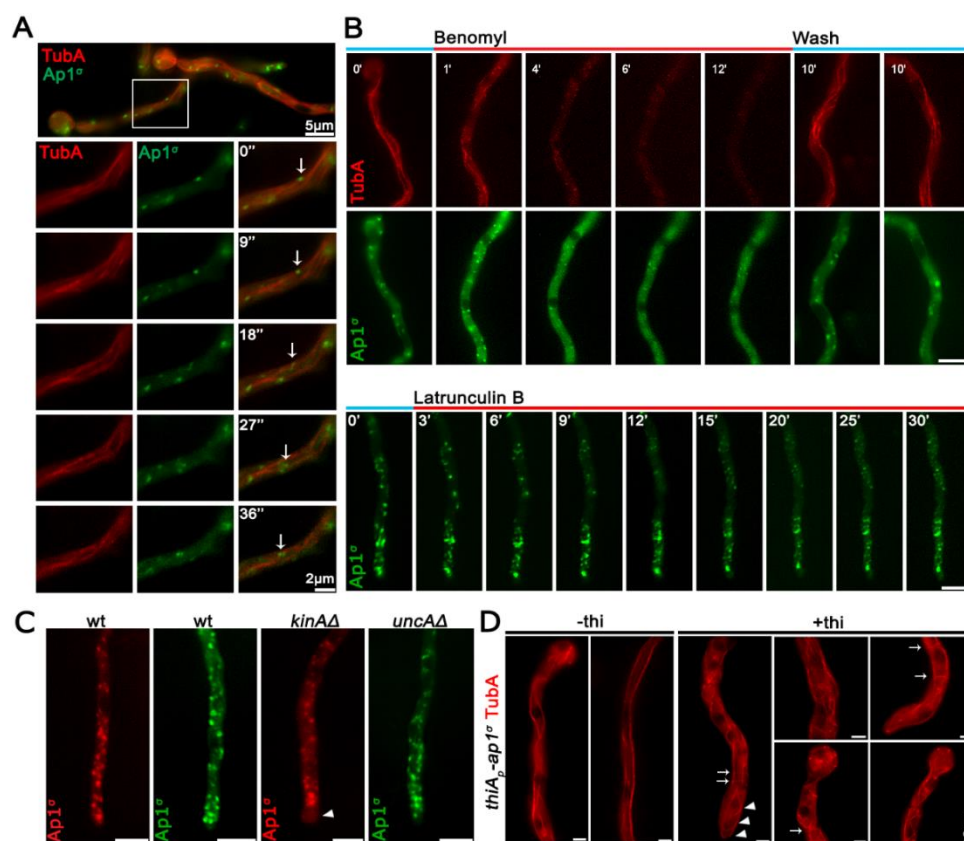


**Figure 3.17** (A) Colocalization analysis of Ap1<sup>o</sup> and alpha-tubulin (TubA). Time-series images highlight the movement of AP-1-labeled foci on MTs. (B) Benomyl treatment (upper panel) of the strain shown in A, confirms the association of AP-1 with MTs, whereas Latrunculin B treatment has no effect on AP-1 localization (lower panel). (C) Wild-type localization of AP-1 is affected in the absence of KinA, but not UncA. (D) TubA-labeled MTs are disorganized in hyphae lacking a functional AP-1 complex (+thi). Bars B,C: 5  $\mu$ m.

attribute a ‘motor-adaptor’ role to the AP-1 complex in polarized neuronal cells (Nakagawa *et al.*, 2000), we tested whether a kinesin is also implicated in the AP-1-mediated polar delivery of transport vesicles in *A. nidulans*. Our results show that AP-1 is unable to reach the apical area in the absence of the conventional kinesin, KinA (Figure 3.17 C). Instead, it accumulates in an area localized 1  $\mu\text{m}$  behind the apex, a phenotype characteristic of cargoes that utilize KinA as the main motor protein for their transport (Takeshita *et al.*, 2015). Importantly, the organization of the network of MTs appears to be disrupted when *ap1 $\sigma$*  is genetically repressed, as evidenced by mCherry-TubA fluorescent signal (Figure 3.17 D, +thi). Notice the curved MTs located close the tip (arrowhead), as well as distinct bright spots and several cross sections throughout the hypha (arrows).

### 3.3.2.8 AP-1 affects septin organization

We also studied another important component of the fungal cytoskeleton, septins (AspB-E), with respect to the role of AP-1 in *A.nidulans* (see also Chapter 1.3.10). Given the previously observed increased septum formation in AP-1-deficient hyphae (Chapter 3.2), we expected to see a phenotype in line with this observation. Our results confirm that upon AP-1 depletion, the three core Septins that participate in the formation of hetero-polymers (AspB, AspC, AspD), exhibit abnormally increased localization to cortical dots. These non-filamentous structures possibly mark positions of new septum formation, given also their appearance in pairs at opposite sides of the hypha.

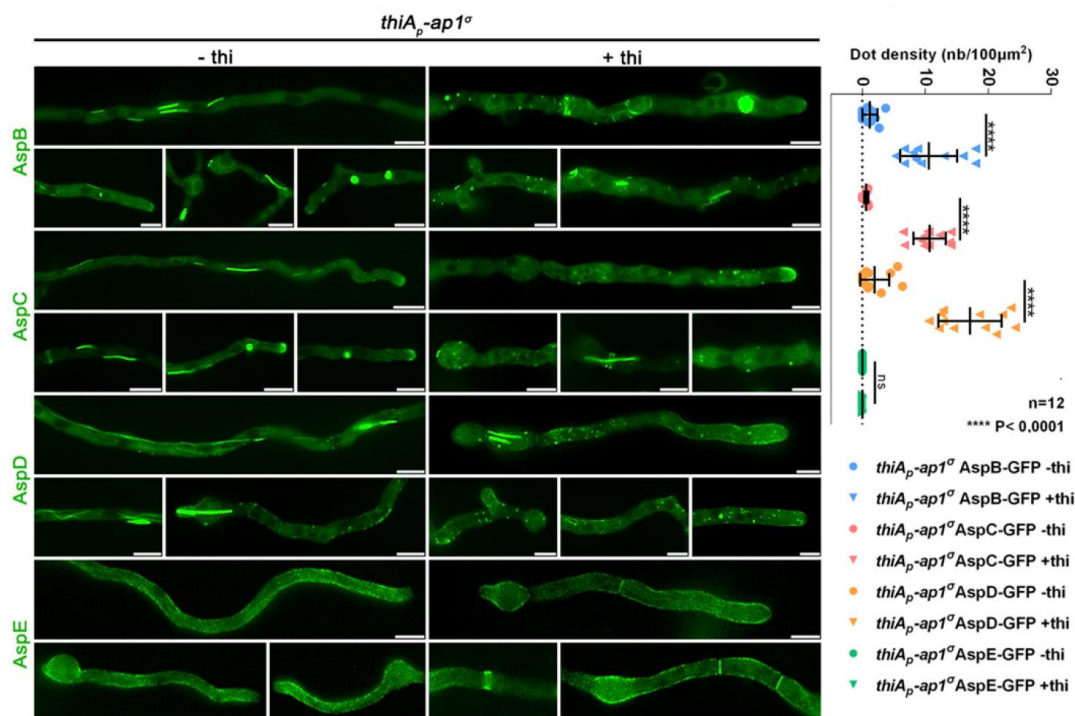


**Figure 3.18** Left panels: Septin localization in the presence (-thi) and absence (+thi) of a functional AP-1 complex. AspB, AspC and AspD appear more frequently in punctate structures described as ‘septin dots’, whereas the cortical AspE appears largely unaffected, except for its presence in the more abundant septa. Bars, 5  $\mu\text{m}$ . Right panel: Relevant quantification of dot density confirms our observations.

Importantly, AspE, which is not involved in the hetero-polymer, is not affected in a similar way by the repression of AP-1 (Figure 3.18).

### 3.3.2.9 Proper early endosome distribution and recycling require a functional AP-1

Studies of the subcellular localization of the early endosomal RabB<sup>Rab5</sup> GTPase compared to the localization of AP-1, reveal a transient association between the two markers, mostly evident in ring-like structures that appear in a subapical part of the hypha, close to the conidiospore head. In Figure 3.19, selected areas in small color boxes appear magnified in the center of each image, with corresponding coloration and numbering. Additionally, we investigate the interaction between AP-1 and EEs by constructing strains that express fluorescently tagged versions of the two Rab5 fungal homologues, RabA and RabB, in the absence of a functional adaptor. Our results show an increased accumulation of both endosomal markers in immotile puncta under conditions of repression (+thi) of *ap1<sup>o</sup>* (Figure 3.20, left panel). A time-course experiment of RabB under the same conditions, reveals that in fact, the motile endosomal subpopulation is not affected (Figure 3.20, middle panel). In AP-1 deficient hyphae, CMAC staining of RabB-labeled endosomes reveals the late-endosomal and/or vacuolar identity of a significant fraction (Figure 3.20, right panel).

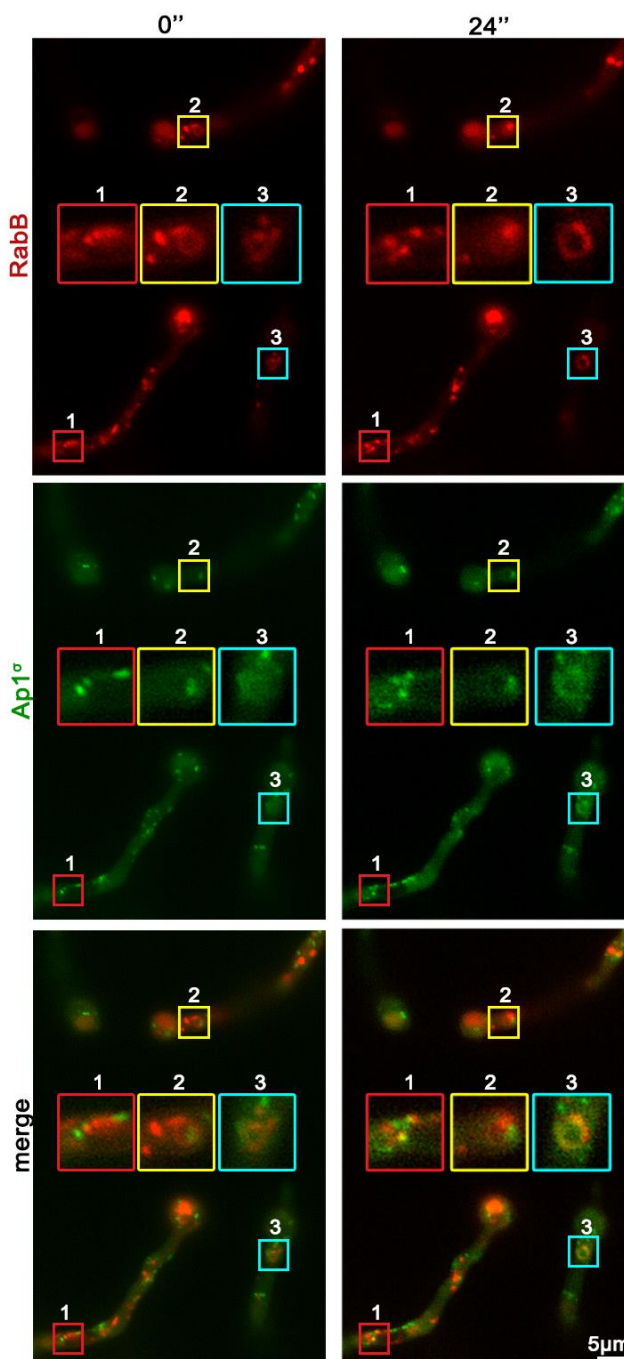


**Figure 3.19** Selected frames from a time-series, highlight the colocalization of AP-1 and RabB in transient ring-like structures.



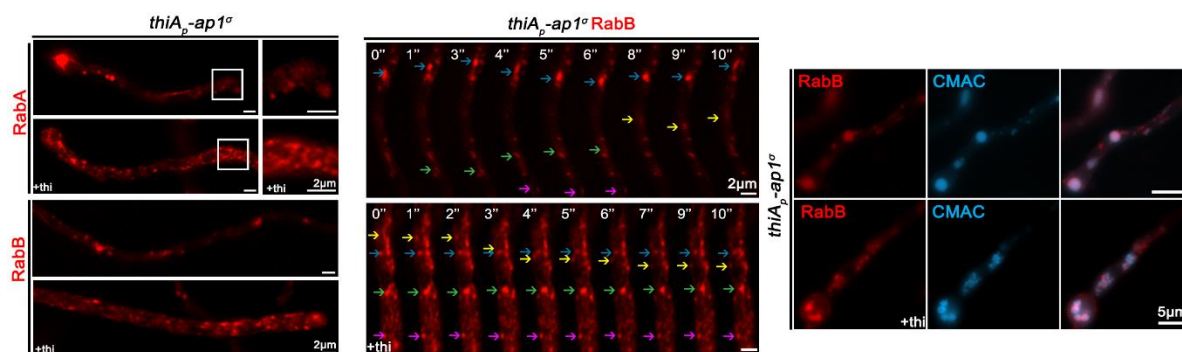


**Figure 3.20** Left panels: AP-1 repression (+*thi*) has a severe effect on early endosome morphology, as the immotile fraction of both RabA and RabB subpopulations is increased. Middle panels: Time-course analysis of RabB-labeled endosomes, under normal (-*thi*) or repressed (+*thi*) conditions for AP-1 expression. Each colored arrow ‘follows’ one endosomal spot throughout the time-series, from the moment it appears. Notice the increase in static puncta in the presence of thiamine. Right panels: CMAC vacuolar staining of RabB-labeled structures, in an AP-1-repressible strain. Notice the significant degree of staining in small RabB foci, when AP-1 is absent (+*thi*).

### 3.3.3 Conclusions

The AP-1 is essential for the polar localization of apical markers via its association with RabE<sup>Rab11</sup>-labeled secretory vesicles. It is transiently and dynamically associated with the late-Golgi and probably recruited during maturation to post-Golgi, thus subsequently acting downstream of RabE. AP-1, via specific C-terminal motifs, interacts and functions upstream of clathrin, in line with its established role in clathrin recruitment after cargo binding. Additionally, the adaptor participates in RabA/B<sup>Rab5</sup>-dependent endosomal recycling and is involved in the maturation of early endosomes. We also provide evidence that AP-1 associates with the microtubule cytoskeleton through the Kinesin-1 (KinA) and is critical for septin organization into higher order structures. By dissecting the role of the AP-1 complex, we rationalize its essentiality for the highly-demanding in cellular resources, polarized fungal growth.

### 3.4 THE AP-2 COMPLEX HAS A SPECIALIZED CLATHRIN-INDEPENDENT ROLE

Adapted from Martzoukou O, Amillis S, Zervakou A, Christoforidis S, Diallinas G. *Elife*. 2017 Feb 21;6. pii: e20083.

#### 3.4.1 Rationale of the project

AP-2 is involved in the formation of clathrin-coated vesicles at plasma membrane (PM) of most metazoan (Robinson, 2004, 2015), but its role in *A. nidulans* remained unclear. Our previous work demonstrated the AP-2 independent and clathrin-dependent transporter endocytosis (Chapter 3.2), thus in order to investigate the role of this essential complex we use as cargoes selected apical proteins involved in polarized growth, including the lipid flippases DnfA and DnfB, the v-SNARE SynA and the endocytic factors SagA, SlaB, and AbpA. Moreover, we determine the subcellular localization of the adaptor via colocalization analyses and we specifically exclude any topological correlation of AP-2 with clathrin, using TIRF microscopy. Lastly, to elucidate the role of the AP-2 complex in polar growth we construct double knockout strains of the adaptor and of factors involved in membrane lipid composition so as to test its genetic interactions by observing colony growth and microscopic morphology.

#### 3.4.2 Experimental process

##### 3.3.3.1 Subcellular localization of the AP-2 complex

To identify the subcellular site where AP-2 is localized, we constructed isogenic fluorescently tagged (with mRFP and GFP) versions of the  $\sigma$  subunit of AP-2, in wild-type background. The adaptor exhibits polar localization in the collar region of the hyphal tip, but is also present in small cortical puncta and at the septa. Genetic deletion of the  $\mu$  subunit, disrupts the localization of the tagged  $\sigma$  subunit, which appears in a diffuse cytoplasmic signal. This is in line with the notion that lack of a single AP subunit, inactivates the whole complex. Repression of ClaL (Clathrin light chain) expression however, has no detectable effect on AP-2 localization (Figure 3.21). A series of colocalization analyses is also performed, to study the positioning of

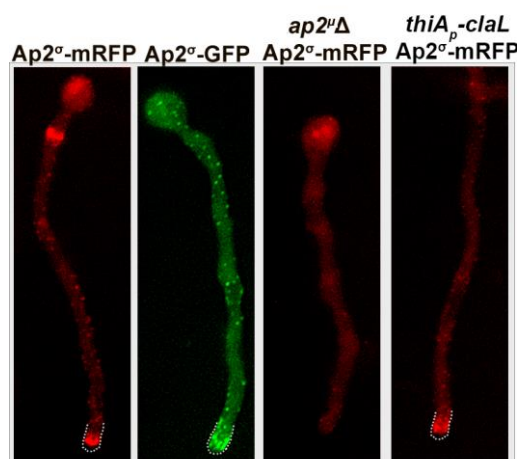


**Figure 3.21** Subcellular localization of mRFP- and GFP-tagged versions of the  $ap2^\sigma$  subunit appears identical (left panels).  $Ap2^\sigma$ -mRFP proper localization is lost to a diffuse cytoplasmic haze in an  $ap2^\sigma\Delta$  background, whereas it appears unaffected in  $claL$ -repressed conditions (right panels). Cell end is marked with a dotted line.

AP-2 with respect to endocytic factors (SagA and SlaB), an actin binding protein (AbpA), lipid flippases (DnfA and DnfB), clathrin (ClaL) and the UapA transporter, which was expected to show no-colocalization. Our results show a high degree of topological correlation between the adaptor and SagA (PCC=0.81), SlaB (PCC=0.77), DnfA (PCC=0.70), DnfB (PCC=0.74), AbpA (PCC=0.76) and SynA (PCC=0.69), but not with ClaL (PCC=0.35) or UapA (PCC=0.33) ( $P < 0.001$  in all cases). Colocalization with SynA, DnfA and DnfB occurs mostly in the collar region, and not at the apical crescent, whereas all the endocytic factors seem to colocalize with AP-2 in the collar and in actin patches.

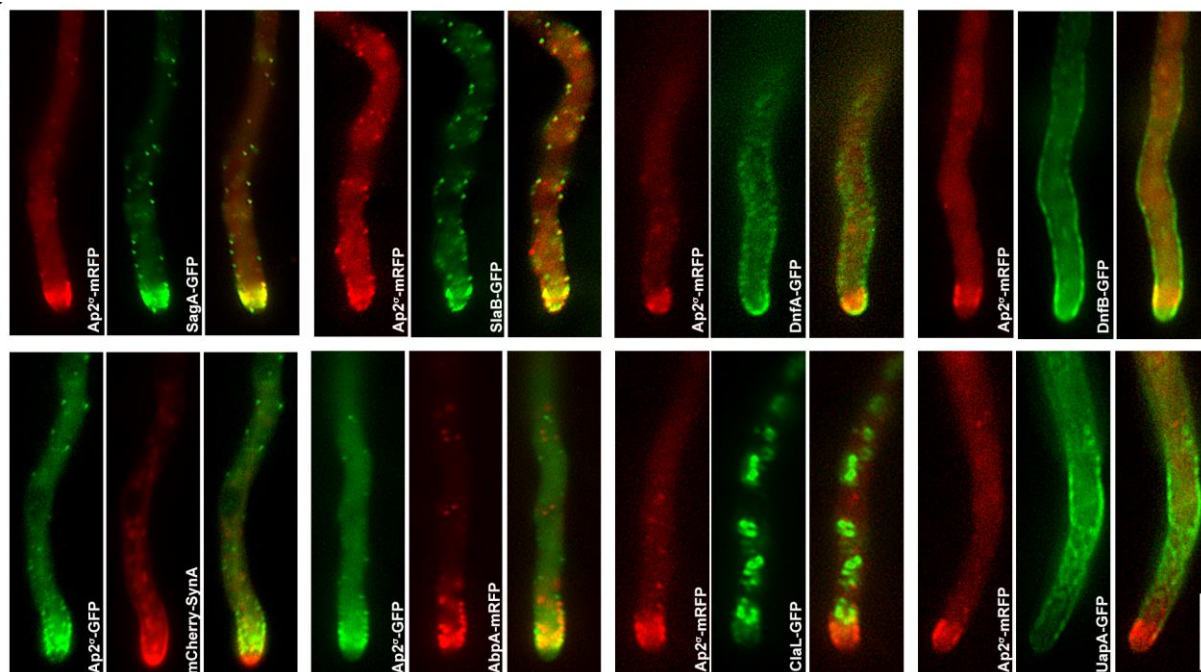


**Figure 3.22** Colocalization studies reveal the topological proximity of AP-2 with SagA, SlaB, DnfA, DnfB, SynA, AbpA, but not with ClaL or UapA. For details see text. Bar, 5  $\mu\text{m}$ .

### 3.3.3.2 AP-2 and clathrin exhibit completely distinct localization at the PM

To confirm the absence of colocalization between AP-2 and clathrin, we perform the same study using TIRF microscopy (in a collaboration with Prof. S. Christoforidis). This microscopy method allows us to visualize the PM signal, separately from the intracellular fluorescent signal. Strains expressing ClaL-GFP are tested first, and several Golgi-resembling structures seem to associate with the PM, but none of those is close to the collar region (Figure 3.23 A). Simultaneous visualization of AP-2 and ClaL with TIRF confirms the distinct localization of the two protein complexes in the PM (Figure 3.23 B), as evidenced by the relevant quantitative analysis (PCC=0.12,  $p < 0.05$ ).

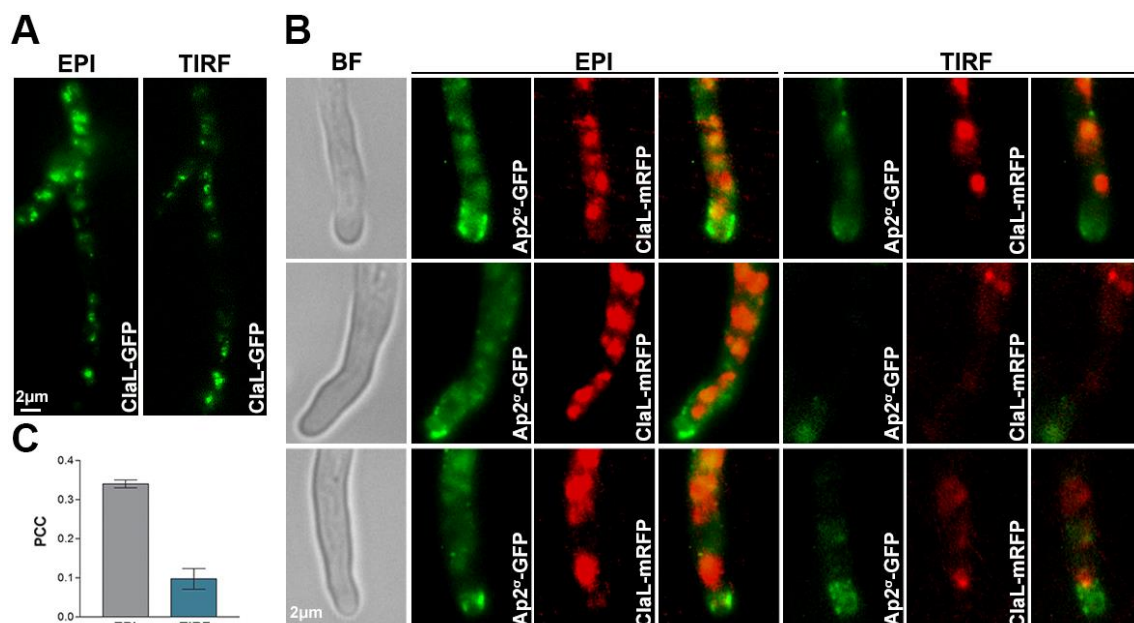
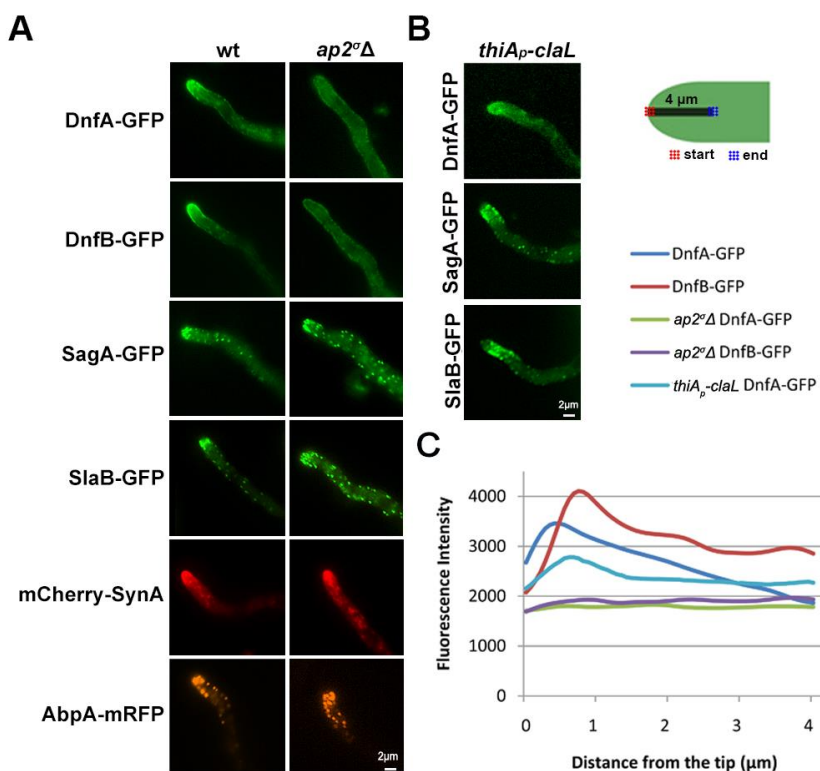


**Figure 3.23** (A) Epifluorescence (EPI) and respective TIRF images of ClaL-GFP. (B) TIRF microscopy study confirms the non-colocalization of the AP-2 complex and clathrin. Penetration depth is 110 nm. (C) Relevant quantitative analysis of B. [BF: Brightfield]

### 3.3.3.3 Lipid flippase endocytosis requires AP-2, but not clathrin

Loss of polar localization of the lipid flippases DnfA and DnfB is observed, in AP-2 deficient hyphae, compared to the wt. These proteins instead of marking the apical crescent, exhibit a homogenous low fluorescent signal across the PM. Interestingly, the apical localization of SagA, SlaB,

**Figure 3.24** (A) Epifluorescence microscopy of DnfA, DnfB, SagA, SlaB, SynA and AbpA in wt and AP-2<sup>-</sup> backgrounds. Notice the loss of apical signal solely for DnfA and DnfB. (B) DnfA, SagA and SlaB localization in ClaL-depleted hyphae. (C) Quantitative analysis of DnfA and DnfB fluorescence along 4 μm of hyphal tips, in wt, ap2<sup>Δ</sup> and claL-repressed isogenic backgrounds.



AbpA and SynA, are not affected by the depletion of AP-2 (Figure 3.24 A and C). In a genetic background where ClaL is repressed upon thiamine addition, all markers tested remain polarly localized, which further supports the distinct roles of AP-2 and clathrin (Figure 3.24 B and C).

### 3.3.3.4 AP-2 is involved in membrane lipid homeostasis

To investigate further the role of the AP-2 complex in polar growth, we test the genetic interactions of the adaptor with SagA, StoA, DnfA and DnfB by constructing double knockout strains. StoA, a stomatin homologue, is a protein involved in apical sterol-rich domain (SRD) maintenance (Takeshita *et al.*, 2012). BasA is another factor necessary for apical lipid maintenance, involved in the biosynthesis of sphingolipids. Here we use a thermosensitive mutation, namely *basA1*, at the restrictive temperature (42°C) to study its interaction with AP-2 in double-impaired strains. Growth

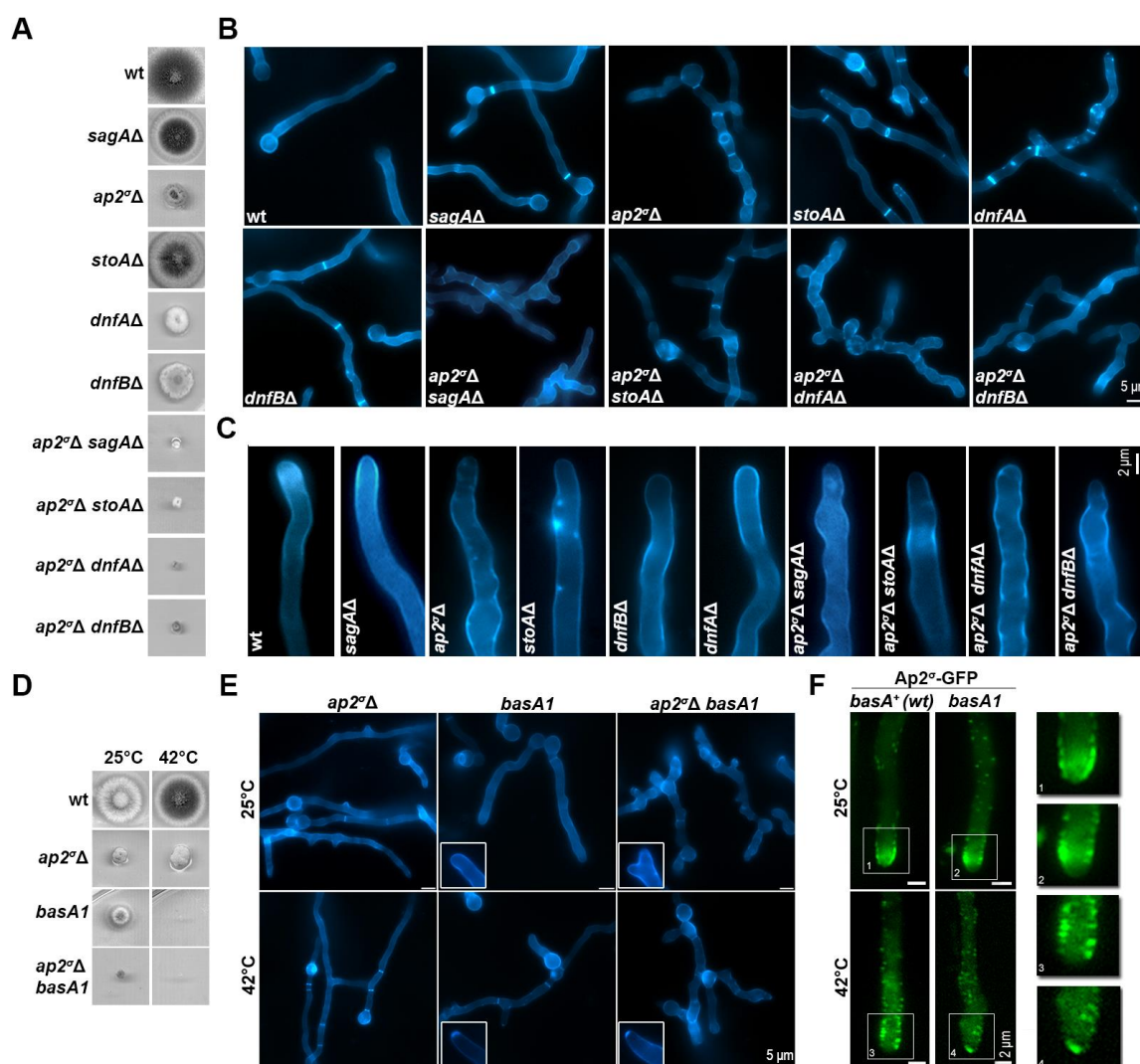


**Figure 3.25** (A,D) Growth of single and double null strains of *ap2 $\Delta$*  deletion combined with those of *sagA*, *stoA*, *dnfA*, *dnfB* and *basA1*. (B, C, E) Microscopic morphological phenotypes with calcofluor staining, of strains shown in A,B. (F) AP-2 localization in wild-type and *basA1* backgrounds, in the permissive (up, 25°C) and the restrictive temperature (down, 42°C). Zoom images of the hyphal tip are shown.

tests (Figure 3.25 A, D) reveal synthetic negative phenotypes in all cases, as colony growth was severely decreased. This phenotype is in line with microscopic observations (Figure 3.25 B, C, E), as the combined depletion of both AP-2 and all the aforementioned factors, leads to extreme hyperbranching, increased septation, and loss of the polar axis of growth, as evidenced by the appearance of ‘ruffled’ hyphae. Moreover, the localization of a GFP-tagged version of AP-2 in the absence of sphingolipid biosynthesis (*basA1*, 42°C) appears to have moved in an acropetal manner, from the endocytic collar to the cell end. Our results highlight the involvement of AP-2 in apical lipid maintenance, thus we also test the effect of its depletion on ergosterol. To do so, we use the fluorescent ergosterol marker Filipin III, which in a wild-type background typically stains the PM. A prominent loss of ergosterol polarity along with the appearance of random bright cortical foci is observed in the *ap2 $\Delta$*  and *stoA $\Delta$*  backgrounds, as well as in BasA- and SlaB-repressed conditions. On the contrary, lack of SagA, DnfA, DnfB and ClaL did not alter the polar distribution of ergosterol (Figure 3.26).

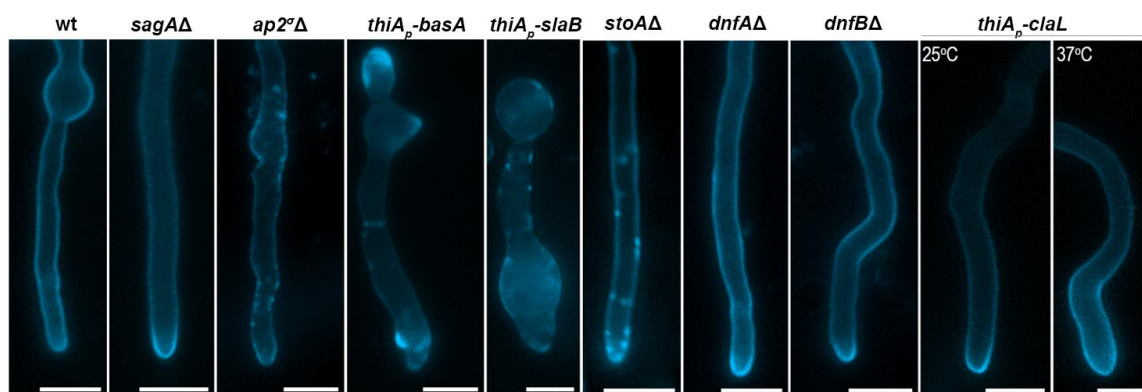


**Figure 3.26** Epifluorescence microscopy of ergosterol membrane localization in hyphae of strains carrying a genetic deletion or repression of specific factors, compared to wt. Notice the severe effect of AP-2, StoA, BasA and SlaB absence, on apical ergosterol deposition at the PM. Bar, 5  $\mu$ m.

### 3.4.3 Conclusions

The AP-2 complex is essential for polarity maintenance and growth in *A. nidulans*, due to its unique role in endocytosis. The adaptor is localized in the collar region, close to the hyphal apex, and in actin patches throughout the hypha. Genetic and cellular evidence, show an interaction between the AP-2 and specific proteins, such as the endocytic markers SagA and SlaB, the sphingolipid biosynthesis enzyme, BasA, the sterol-related protein, StoA, and components involved in the polar deposition of chitin. Most importantly however, it is necessary for the endocytic internalization and subsequent recycling of the lipid flippases DnfA and DnfB, as well as, apical lipid and cell wall maintenance. Thus, the role of the AP-2 complex in endocytosis of higher fungi, is specific and completely uncoupled from the respective role of clathrin in this process.

# CHAPTER 4

## DISCUSSION AND FUTURE RESEARCH

In this thesis, we studied several aspects concerning the molecular mechanisms underlying intracellular trafficking pathways of transmembrane proteins, specifically in the filamentous fungus *Aspergillus nidulans*. Whereas certain aspects of eukaryotic vesicular trafficking are in general well characterized, the mechanisms underlying the trafficking of transmembrane transporters and of apical cargoes exhibiting polar deposition, remain unclear. Through this study we dissected the role of AP complexes, AP-1 and AP-2, as well as that of clathrin, specific Rab GTPases or the fungal cytoskeleton, in cargo trafficking in *A. nidulans*. This study also addressed the role of cargo, and specifically transporter (UapA) dimerization, in initial steps of membrane traffic and particularly in exit from the ER.

In the first part of the thesis we aimed at understanding the molecular basis of cargo ER-exit and subcellular trafficking by utilizing the UapA transporter as a model cargo. Starting from the observation that UapA molecules can undergo *in trans* endocytosis (i.e. co-expression of a UapA version that is able to internalize, also promotes the endocytosis of UapA molecules that when expressed by themselves are defective in endocytosis), prompted us to investigate whether UapA oligomerizes. Using different methods, both biochemical and *in vivo*, we demonstrated a strong physical interaction between UapA monomers, as apparent oligomers/dimers remain stable until reaching the vacuolar membrane. Publication of the crystal structure of UapA and studies on specific dominant negative or positive mutations reported a year later in Alguel et al. (2016), confirmed that UapA dimerizes and that dimerization is necessary for function. Interestingly, specific ER-retained UapA mutants, arising from either a modification of a Tyr-based N-terminal motif (DYDY/A) or partial misfolding (I74D), also seem to oligomerize somehow, but do not seem associate properly and this in turn might cause their inability to exit the ER membrane. The exact role of UapA di-/oligomerization in ER-exit is still unknown and could be addressed in future studies. An important question to answer is whether the formation of dimers, confirmed by crystallization and other biochemical or biophysical methods, leads to dimer oligomerization and this in turn promotes ER-exit. Indeed, cargo oligomerization can elicit local membrane bending, as was shown by Springer et al. (2014). This process might also involve specific or general chaperones, recognizing the conserved ER-exit motif in the UapA N-tail. Importantly, a recent study confirmed the critical role of selected structural lipids in the stabilization or formation of the UapA dimer, via modulating transporter assembly and further showed that dimerization is necessary for function, but not for traffic and localization in the PM (Pyle et al., 2018). These results establish that early dimerization by itself is either not sufficient for

proper ER-exit or that it takes place later in the PM, further suggesting that the driving force for membrane bending and eventual ER-exit is oligomerization of monomers. In such traffic-related oligomerization of UapA, proper protein folding and interactions with lipids or chaperones through ER-exit motifs such as DYDY, might play critical roles that need to be investigated further.

In the next part of this thesis, we investigated the role of the fungal AP-complexes in transporter trafficking and turnover. Genetic depletion of AP-1 and AP-2, but not AP-3, resulted in growth and morphological phenotypes compatible with loss of polarity maintenance. More specifically, we observed hyperbranching and increased septation, as well as abnormal chitin deposition at the hyphal tip. Clathrin is also essential for fungal polar growth, as genetic knockdown of both the light and heavy chains causes severe growth delay, but had no effect on polarized chitin deposition, septa formation or branch emergence. ClaH in particular, has a critical role in Golgi function and cargo secretion, which is probably the main reason why the ClaH null mutation is lethal. The importance of ClaH in conventional secretion via the Golgi was also shown by Schultzhaus et al. (2017a). Interestingly, phylogenetic analyses performed in our lab indicated a C-terminal truncation of the appendage domain of the  $\beta$  subunits, in all the AP-complexes of higher fungi. Based on these observations, we followed the effect of depleting the AP complexes and clathrin, on transporter subcellular localization. We thus showed that AP-1, AP-2 and AP-3 are dispensable for transporter trafficking, endocytosis and turnover, unlike clathrin, which is required for these subcellular processes. Whether the heavy chain of clathrin (ClaH) is directly or indirectly involved in transporter exocytosis, remains unclear, given its essentiality for fungal polar growth and proper Golgi function. However, both clathrin chains (ClaL and ClaH) proved to have a direct role in transporter (UapA) internalization from the PM. To our knowledge, an AP-2 independent role of clathrin in endocytosis has not been shown rigorously before, although some evidence has been obtained in *S. cerevisiae* and mammals (Conner and Schmid, 2003; Motley et al., 2003; Traub, 2009). The direct establishment of necessary for fungal growth AP-independent trafficking pathways that became known through this study, raises several questions and provides hints on possible cryptic roles of the AP-complexes in other systems or specific cells. Based on the fact that in mammalian neurons, which also exhibit polarized growth, the  $\beta$ 2 subunit of AP-2 is not truncated, it would be interesting to know whether a functional differentiation of the adaptor and clathrin could occur via alternative splicing. Given the essentiality of AP-1 and AP-2 in fungal apical growth, but rather surprisingly their non-involvement in transporter trafficking, this thesis focused on the identification of other cargoes such as cortical and apical factors, and necessary interacting partners of AP-associated vesicular traffic. Within this concept, we functionally analyzed the AP-1 complex, which albeit extensively studied in metazoan cells and *S. cerevisiae*, and primarily implicated in a clathrin-



dependent TGN-to-endosome route, its role in other systems, including filamentous fungi had not been studied (Bonifacino, 2014; Hirst et al., 2012; Robinson 2015). Additionally, the fact that yeast AP-1 null mutants, unlike mammalian cells, are not lethal and exhibit only minor defects in PtdIns(3,5)P<sub>2</sub>-dependent processes and in the trafficking of the chitin synthase ChS3 (Arcones et al., 2016; Ma et al., 2009; Phelan et al., 2006; Valdivia et al., 2002; Yu et al. 2013), already indicated that AP complexes in different systems or cells might be serving different processes. For example, budding yeast possesses two functional AP-1 complexes with different medium subunits (Apm1 and Apm2), which recognize and sort distinct cargoes (Renard et al., 2010; Valdivia et al., 2002; Whitfield et al., 2016). Additionally, an interaction between the fungal-specific exomer complex and the AP-1 complex, was recently shown in fission yeast (Anton et al. 2018; Hoya et al., 2017). The heterotetrameric exomer is assembled at the late-Golgi and participates in the trafficking of specific proteins to the PM in response to stress signals (Wang et al., 2006). As already mentioned, the role of AP-1 had not been studied in filamentous fungi, which are characterized by a polarized mode of growth, only sustained through continuous endocytic recycling of selected cargoes such as the v-SNARE SynA, the chitin synthase ChsB or the lipid flippases DnfA and DnfB. Our results establish a fundamental role for AP-1 in apical cargo sorting to the PM of *A. nidulans*. Interestingly, AP-1 was also shown here to associate with clathrin (ClgL and ClgH), through specific short motifs in the C-terminal region of the  $\beta$ 1 subunit (LLNGF and LLDID). Although all AP  $\beta$  subunits of higher fungi are truncated in their C-terminal region (Martzoukou et al., 2017) the motifs identified herein resemble those previously reported to bind clathrin in yeast (Yeung and Payne, 2001). An additional important finding that is revealed through the present work, is the interaction of AP-1 with RabE<sup>Rab11</sup>-labeled post-Golgi secretory carriers. Association of the two proteins was shown previously only in a single report, where Rab11 and AP-1 colocalize with the reptilian reovirus p14 FAST protein at the mammalian TGN (Parmar and Duncan, 2016). In *A. nidulans*, transient late-Golgi equivalents mature to RabE<sup>Rab11</sup> exocytic carriers, whereas AP-1 and clathrin seem to be sequentially recruited during this maturation process and prior to microtubule-based trafficking towards the SPK. Among the transported cargoes are factors necessary for proper lipid composition (DnfA, DnfB), cell wall maintenance (ChsB) and SNARE proteins (SynA and SsoA). The involvement of the microtubule cytoskeleton is imperative in this intracellular trafficking process, in contrast to simpler unicellular eukaryotes such as yeasts that depend greatly on actin-based transport (Bretscher, 2003; Fischer et al., 2008; Moseley and Goode, 2006; Takeshita et al., 2014). The AP-1 complex, not only utilizes the MTs as tracks for the transport events it mediates, but also confers important alterations in the organization of the cytoskeleton, when depleted. The MT network appears overall stressed, with curved components at the hyphal tips, TubA-labeled foci close to the nuclei and increased cross

sections. This phenotype resembles the picture observed in the absence of cell end markers TeaA and TeaR, in line with the appearance of zigzagged hyphae in both depletion cases (Fischer et al., 2008; Takeshita and Fischer, 2011; Takeshita et al., 2013; Takeshita, 2018), thus it would be interesting to test if their trafficking is indeed AP-1-mediated. Septin polymerization and higher order structure formation is also disrupted, as evidenced with the appearance of increased cortical AspB, -C, and -D foci. Furthermore, we provide evidence for an association between AP-1 and the main SV kinesin, KinA. Similarly, in mammalian cells, a specific kinesin connects AP-1-coated SVs to MT cytoskeletal tracks, resembling the case of KIF13A in epithelial cells, where a direct interaction with the  $\beta 1$  subunit was shown (Nakagawa et al., 2000). Another case has been reported in HeLa cells, where the kinesin KIF5 provides the link between endosomes, MTs and an AP-1 accessory factor, Gadkin (Schmidt et al., 2009). Finally yet importantly, AP-1 transiently associates with Rab5-labeled endosomes in ring-like structures, whereas upon adaptor depletion a shift in the endosomal subpopulation is readily apparent. More specifically, as evidenced with CMAC staining, the increased number of immotile late endosomes present across the hypha reveals a block in the ‘sorting endosome-to-TGN’ and ‘sorting endosome-to-PM’ pathways. Thus, EEs are most probably redirected to the only “available” pathway –the degradative. This is also supported by the observation that upon RabC repression, AP-1 is mislocalized in small, non-polarized foci, of unknown molecular identity. It would be interesting to characterize more components of these foci (i.e. clathrin, Rab5,

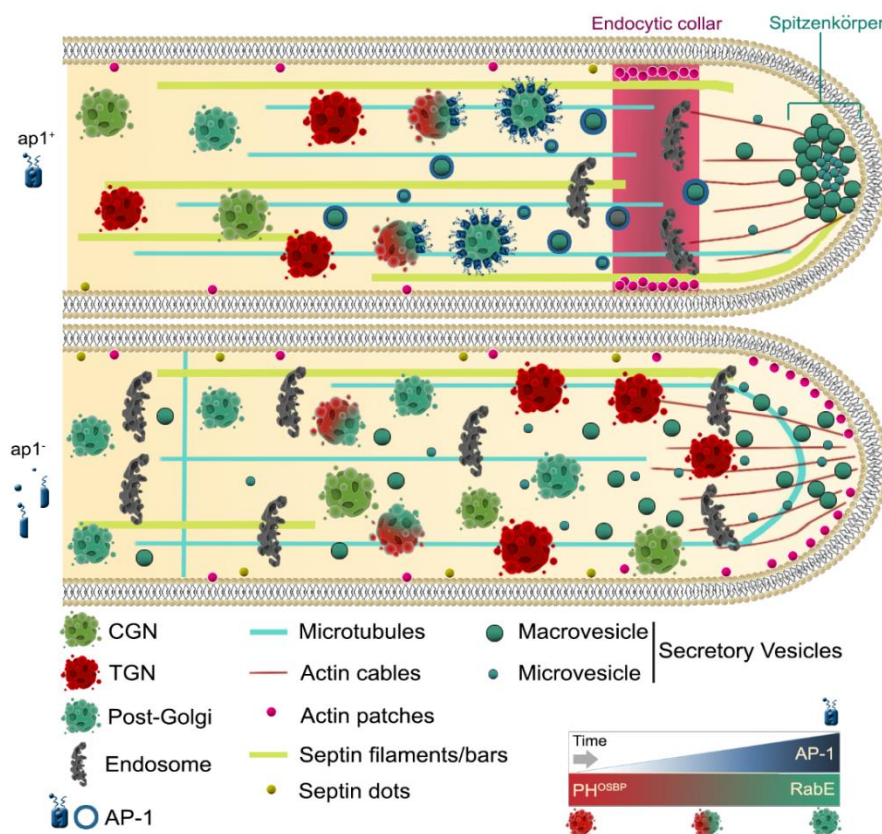


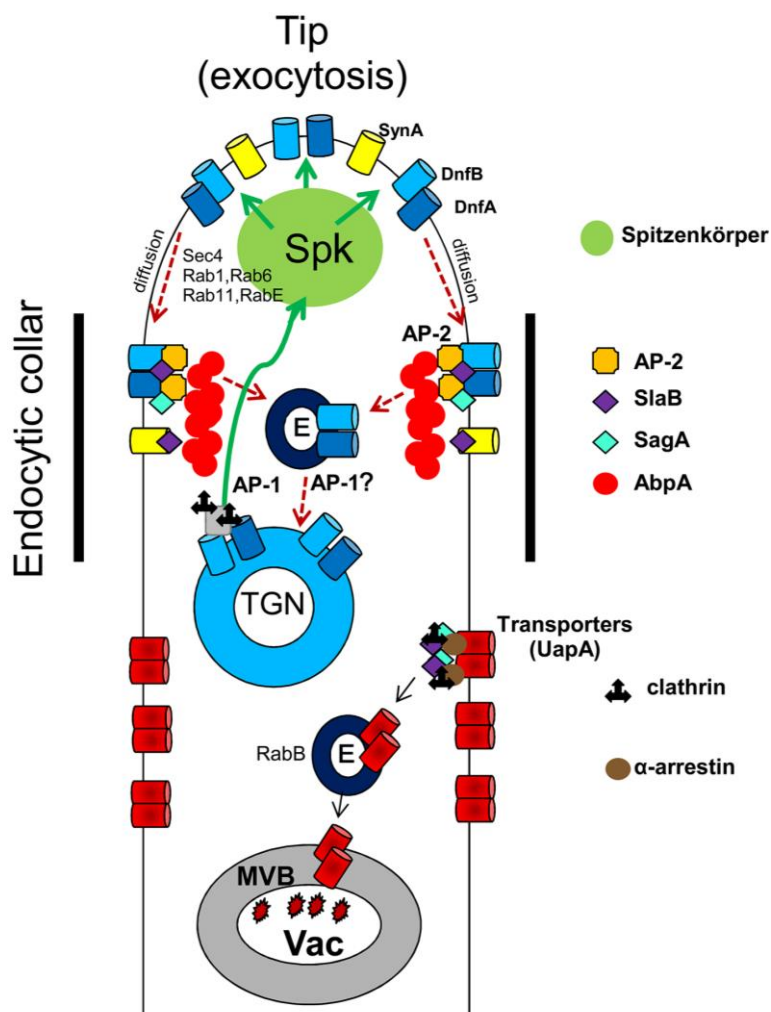
**Figure 4.1** Scheme summarizing the phenotypes observed in AP-1 depleted hyphae (lower panel), compared to wt (upper panel). Notice the cartoon at the bottom right side, indicating the recruitment of AP-1 during the TGN to post-Golgi maturation process. © Olga Martzoukou

recycling cargoes) and determine whether AP-1 is actually blocked in the sorting endosome. RabC, as mentioned in the Introduction, mediates the 'sorting endosome-to-TGN' recycling pathway in association with the GARP complex (Hernández-González et al., 2018). Even though the AP-1 complex associates with clathrin, it does not participate in transporter trafficking, in contrast to the heavy chain of clathrin (Clathrin) which proved to be critical for the proper sorting to the PM of seemingly all cargoes passing from the Golgi, that is, both transporters and polar cargoes necessary for apical growth (Martzoukou et al., 2017). Thus, it would be interesting to investigate further the molecular basis of trafficking of different cargoes, and how these might use distinct post-Golgi pathways to be sorted to their final membrane destination. The essentiality of AP-1 can be explained given its critical role in hyphal morphogenesis, cytoskeleton organization, apical cargo exocytosis and endosome recycling. This is in agreement with the notion that polar growth of filamentous fungi is maintained via the coupling of apex-directed exocytosis with subapical endocytosis, in an endocytic recycling process that polarizes cargoes related to PM and cell wall homeostasis.

The extensively studied AP-2 complex has been mostly associated with clathrin-dependent endocytosis from the PM in the majority of eukaryotic organisms. However, novel findings of this thesis reveal a specific role for the AP-2 complex, which acts independently of clathrin at the PM. This is clearly illustrated with colocalization studies using both widefield and TIRF microscopy, highlighting the completely distinct topology of the two protein complexes. AP-2 is localized in the actin-rich subapical collar of endocytosis, as well as in uniformly distributed endocytic patches, along with other known endocytic factors (SagA, SlaB, AbpA). Additionally, clathrin was shown to have no effect on the subapical endocytosis of two lipid flippases, which constitute the only known cargoes of the *A. nidulans* AP-2 complex to this day. In parallel, we investigated the effects of AP-2 function in apical membrane lipid and cell wall composition maintenance, processes where clathrin had no detectable involvement, as evidenced with filipin and calcofluor staining. This is further supported by the observation that proteins involved in sterol, sphingolipid, and phospholipid homeostasis (StoA, BasA and DnfA/DnfB respectively) are some of the genetic interactors of the AP-2 complex. The central role of AP-2 in subapical internalization is in agreement with previous reports showing that proper membrane lipid and cell wall composition is essential for fungal polar growth (Cheng et al., 2001; Takeshita et al., 2012). Importantly, through this work it is shown that an AP-2-dependent and clathrin-independent endocytic pathway operates in fungal hyphae, in line with the observation of Lau and Chou (2008) in HeLa cells, where AP-2 was shown to have post-endocytic trafficking functions in the non-clathrin, Arf6-mediated uptake of major histocompatibility complex (MHC) class I and  $\beta$ 1 integrin. Clathrin-independent endocytosis (CIE) has been previously associated with the maintenance of PM lipid composition (Shvets et al., 2015) and the endocytosis of GPI-anchored

proteins (Nichols, 2009), operating at sites of PM lipid rafts, caveolae or flotillin microdomains (Glebov et al., 2006; Kirkham et al., 2005), in some cases with the participation of dynamin (Lamaze et al., 2001). Thus, a more cargo-centric view of CIE and CME seems to arise from the above and other studies (Maldonado-Báez et al., 2013). In conclusion, despite the similarity in AP-1 and AP-2 phenotypic growth defects and their non-involvement in transporter trafficking, AP-1 is shown here to associate and function with clathrin at several post-Golgi membrane trafficking steps, while AP-2 acts independently of clathrin at the PM. Notwithstanding the fact that clathrin is not involved in the AP-2-driven polar cargo endocytosis, it is essential for AP-1-mediated apical cargo exocytosis and AP-independent transporter trafficking.

**Figure 4.2** Schematic model summarizing the roles of AP-1 and AP-2 complexes in a hypha of the filamentous fungus *A. nidulans*. Notice the clathrin-mediated pathway operating for transporter endocytosis from the PM, without the involvement of AP-2 (Adapted from Martzoukou et al., 2017). [E: endosome; TGN: trans-Golgi network; Vac: vacuole; MVB: multi-vesicular bodies; Spk: Spitzenkörper].



As mentioned earlier, the molecular mechanisms underlying transporter clathrin-dependent trafficking remain largely understudied. Filamentous fungi also require endocytic internalization all along their PM, serving the renewal or modification of membrane components in response to changing nutritional or stress conditions (Diallinas, 2014; Gournas et al., 2010; Karachaliou et al., 2013). This work opens a novel issue on how nonpolar cargoes, such as transporters, are sorted to,

and internalized from, the eukaryotic plasma membrane. Future research of our lab will focus on the identification of alternative clathrin adaptors, which could be involved in these trafficking pathways, such as GGA or the uncharacterized exomer complex of *A.nidulans* (Anton et al., 2018). Additionally, the molecular identity of the vesicles involved in these processes remains unidentified, with SVs and/or EEs being the more prominent candidates, although we cannot exclude the possibility that some transporters might be packaged in uncoated vesicles. In fact, a recent study reported the EE-mediated exocytosis of an enzyme in *A.nidulans*, which could also hold true for transporter sorting to the PM (Hernández-González et al., 2018b). We already know that transporters (UapA) do not require AP-1 for their trafficking to the PM, although the heavy chain of clathrin proved to be critical. But since AP-1 was shown in this thesis to interact with RabE, do transporters occupy SVs with clathrin coats recruited by an alternative adaptor, or is their transport completely RabE-independent? This question can be easily addressed by constructing RabE-depleted strains and performing microscopic analysis of the topology of UapA or other transporters. In case transporters do not require RabE for their exocytosis, the second exocytic Rab GTPase, RabD, could have an important role in this process. Moreover, the uncharacterized RabF, predicted to be involved in recycling, might also contribute to the vesicular trafficking of transporters. A similar approach could reveal whether other Rab GTPases or endosomes (RabC, RabO and RabA/RabB, RabF respectively) are involved in transporter trafficking pathways, including exocytosis and recycling. The requirement for MT- or actin-based transport is another critical point to address, along with the participation of relative motor proteins. Is KinA or UncA required for proper transporter positioning to the PM? Or could actin and MyoV, instead, play key roles in this process? Given the fact that transporters exhibit uniform PM distribution and internalization from seemingly random sites of the PM, we cannot exclude the possibility that their trafficking is nonpolar, thus MTs might be dispensable for these processes. This is further supported by the observation that MyoV, the fungal actin motor protein, can support polarized growth in *A. nidulans*, in the absence of any MT-based transport (Zhang et al., 2011). Studies in filamentous fungi have highlighted the importance of other aspects of intracellular trafficking, such as nontip directed exocytosis and unconventional secretion. For example, septum-directed exocytosis, though being poorly understood, also takes place in hyphae and requires the MT cytoskeleton, but not F-actin. Furthermore, some pathogenic fungi utilize MVB-mediated extracellular vesicle secretion (Shoji et al., 2014). A lot remains to be elucidated, concerning transporter vesicular trafficking, while these questions also apply to other nonpolar transmembrane cargoes, such as channels and receptors, for which PM sorting, endocytosis, or recycling remain elusive.

## CHAPTER 5

## REFERENCES

- Abeliovich, H., Grote, E., Novick, P., Ferro-Novick, S., 1998. Tlg2p, a yeast syntaxin homolog that resides on the Golgi and endocytic structures. *J. Biol. Chem.* 273, 11719–27.
- Abenza, J.F., Galindo, A., Pantazopoulou, A., Gil, C., de los Ríos, V., Peñalva, M.A., 2010. *Aspergillus* RabB<sup>Rab5</sup> integrates acquisition of degradative identity with the long distance movement of early endosomes. *Mol. Biol. Cell* 21, 2756–69.
- Abenza, J.F., Galindo, A., Pinar, M., Pantazopoulou, A., de los Rios, V., Penalva, M.A., 2012. Endosomal maturation by Rab conversion in *Aspergillus nidulans* is coupled to dynein-mediated basipetal movement. *Mol. Biol. Cell.* 23, 1889-901.
- Abenza, J.F., Pantazopoulou, A., Rodríguez, J.M., Galindo, A., Peñalva, M.A., 2009. Long-Distance Movement of *Aspergillus nidulans* Early Endosomes on Microtubule Tracks. *Traffic* 10, 57–75.
- Abramson, J., Smirnova, I., Kasho, V., Verner, G., Iwata, S., Kaback, H.R., 2003. The lactose permease of *Escherichia coli*: overall structure, the sugar-binding site and the alternating access model for transport. *FEBS Lett.* 555, 96–101.
- Alberts, B., Johnson, A., Lewis, J., Raff, M., Roberts, K., Walter, P., 2002. *Molecular biology of the cell.* Garland Science.
- Alcazar-Fuoli, L., Mellado, E., 2013. Ergosterol biosynthesis in *Aspergillus fumigatus*: its relevance as an antifungal target and role in antifungal drug resistance. *Front. Microbiol.* 3, 439.
- Alexopoulos, C.J., Mims, C.W., Blackwell, M., 1996. *Introductory Mycology*, 6th ed. John Wiley and Sons, New York. 43, 781.
- Alguel, Y., Amillis, S., Leung, J., Lambrinidis, G., Capaldi, S., Scull, N.J., Craven, G., Iwata, S., Armstrong, A., Mikros, E., Diallinas, G., Cameron, A.D., Byrne, B., 2016. Structure of eukaryotic purine/H<sup>+</sup> symporter UapA suggests a role for homodimerization in transport activity. *Nat. Commun.* 7, 11336.
- Alvarez, F.J., Douglas, L.M., Konopka, J.B., 2007. Sterol-rich plasma membrane domains in fungi. *Eukaryot. Cell* 6, 755–63.
- Amessou, M., Fradagrada, A., Falguieres, T., Lord, J.M., Smith, D.C., Roberts, L.M., Lamaze, C., Johannes, L., 2007. Syntaxin 16 and syntaxin 5 are required for efficient retrograde transport of several exogenous and endogenous cargo proteins. *J. Cell Sci.* 120, 1457–68.
- Amillis, S., Kosti, V., Pantazopoulou, A., Mikros, E., Diallinas, G., 2011. Mutational Analysis and Modeling Reveal Functionally Critical Residues in Transmembrane Segments 1 and 3 of the UapA Transporter. *J. Mol. Biol.* 411, 567–80.

- Anderson, R.G.W., Goldstein, J.L., Brown, M.S., 1977. A mutation that impairs the ability of lipoprotein receptors to localise in coated pits on the cell surface of human fibroblasts. *Nature* 270, 695–9.
- Angers, C.G., Merz, A.J., 2011. New links between vesicle coats and Rab-mediated vesicle targeting. *Semin. Cell Dev. Biol.* 22, 18–26.
- Anton, C., Taubas, J.V., Roncero, C., 2018. The Functional Specialization of Exomer as a Cargo Adaptor During the Evolution of Fungi. *Genetics* 208, 1483–98.
- Apostolaki, A., Erpapazoglou, Z., Harispe, L., Billini, M., Kafasla, P., Kizis, D., Peñalva, M.A., Scazzocchio, C., Sophianopoulou, V., 2009. AgtA, the dicarboxylic amino acid transporter of *Aspergillus nidulans*, is concertedly down-regulated by exquisite sensitivity to nitrogen metabolite repression and ammonium-elicited endocytosis. *Eukaryot. Cell* 8, 339–52.
- Apostolaki, A., Harispe, L., Calcagno-Pizarelli, A.M., Vangelatos, I., Sophianopoulou, V., Arst, H.N., Peñalva, M.A., Amillis, S., Scazzocchio, C., Scazzocchio, C., 2012. *Aspergillus nidulans* CkiA is an essential casein kinase I required for delivery of amino acid transporters to the plasma membrane. *Mol. Microbiol.* 84, 530–49.
- Araujo-Bazán, L., Peñalva, M.A., Espeso, E.A., 2008. Preferential localization of the endocytic internalization machinery to hyphal tips underlies polarization of the actin cytoskeleton in *Aspergillus nidulans*. *Mol. Microbiol.* 67, 891–905.
- Arcones, I., Sacristan, C., Roncero, C., 2016. Maintaining protein homeostasis: early and late endosomal dual recycling for the maintenance of intracellular pools of the plasma membrane protein Chs3. *Mol. Biol. Cell.* 27, 4021–4032.
- Argyrou, E., Sophianopoulou, V., Schultes, N., Diallinas, G., 2001. Functional characterization of a maize purine transporter by expression in *Aspergillus nidulans*. *Plant Cell* 13, 953–64.
- Arighi, C.N., Hartnell, L.M., Aguilar, R.C., Haft, C.R., Bonifacino, J.S., 2004. Role of the mammalian retromer in sorting of the cation-independent mannose 6-phosphate receptor. *J. Cell Biol.* 165, 123–33.
- Arlt, H., Auffarth, K., Kurre, R., Lisse, D., Piehler, J., Ungermann, C., 2015. Spatiotemporal dynamics of membrane remodeling and fusion proteins during endocytic transport. *Mol. Biol. Cell* 26, 1357–70.
- Arst, H.N., Cove, D.J., 1973. Nitrogen metabolite repression in *Aspergillus nidulans*. *Mol. Gen. Genet.* 126, 111–41.
- Arst, H.N., Hernández-González, M., Peñalva, M.A., Pantazopoulou, A., 2014. GBF/Gea mutant with a single substitution sustains fungal growth in the absence of BIG/Sec7. *FEBS Lett.* 588, 4799–806.
- Aspergillus & Aspergilliosis Website, 2018. <https://www.aspergillus.org.uk/> (accessed 11 July 2018).
- Axelrod, D.E., Gealt, M., Pastushok, M., 1973. Gene control of developmental competence in

*Aspergillus nidulans*. Dev. Biol. 34, 9–15.

- Baggett, J.J., D'Aquino, K.E., Wendland, B., 2003. The Sla2p talin domain plays a role in endocytosis in *Saccharomyces cerevisiae*. Genetics 165, 1661–74.
- Balderhaar, H.J. kleine, Ungermann, C., 2013. CORVET and HOPS tethering complexes - coordinators of endosome and lysosome fusion. J. Cell Sci. 126, 1307–16.
- Banks, I.R., Specht, C.A., Donlin, M.J., Gerik, K.J., Levitz, S.M., Lodge, J.K., 2005. A Chitin Synthase and Its Regulator Protein Are Critical for Chitosan Production and Growth of the Fungal Pathogen *Cryptococcus neoformans*. Eukaryot. Cell 4, 1902–12.
- Barlowe, C., 2003. Signals for COPII-dependent export from the ER: What's the ticket out? Trends Cell Biol. 13, 295-300.
- Barlowe, C., Helenius, A., 2016. Cargo Capture and Bulk Flow in the Early Secretory Pathway. Annu. Rev. Cell Dev. Biol. 32, 197–222.
- Barlowe, C., Orci, L., Yeung, T., Hosobuchi, M., Hamamoto, S., Salama, N., Rexach, M.F., Ravazzola, M., Amherdt, M., Schekman, R., 1994. COPII: a membrane coat formed by Sec proteins that drive vesicle budding from the endoplasmic reticulum. Cell 77, 895–907.
- Barnes, A.P., Polleux, F., 2009. Establishment of axon-dendrite polarity in developing neurons. Annu. Rev. Neurosci. 32, 347–81.
- Barrowman, J., Bhandari, D., Reinisch, K., Ferro-Novick, S., 2010. TRAPP complexes in membrane traffic: Convergence through a common Rab. Nat. Rev. Mol. Cell Biol. 11, 759-63.
- Becuwe, M., Léon, S., 2014. Integrated control of transporter endocytosis and recycling by the arrestin-related protein Rod1 and the ubiquitin ligase Rsp5. Elife 3, e03307.
- Behnia, R., Munro, S., 2005. Organelle identity and the signposts for membrane traffic. Nature 438, 597–604.
- Berepiki, A., Lichius, A., Read, N.D., 2011. Actin organization and dynamics in filamentous fungi. Nat. Rev. Microbiol. 9, 876-87.
- Berepiki, A., Read, N.D., 2013. Septins Are Important for Cell Polarity, Septation and Asexual Spore Formation in *Neurospora crassa* and Show Different Patterns of Localisation at Germ Tube Tips. PLoS One 8, e63843.
- Bergen, L.G., Morris, N.R., 1983. Kinetics of the nuclear division cycle of *Aspergillus nidulans*. J. Bacteriol. 156, 155–60.
- Bergs, A., Ishitsuka, Y., Evangelinos, M., Nienhaus, G.U., Takeshita, N., 2016. Dynamics of Actin Cables in Polarized Growth of the Filamentous Fungus *Aspergillus nidulans*. Front. Microbiol. 7, 682.
- Berro, J., Pollard, T.D., 2014. Local and global analysis of endocytic patch dynamics in fission yeast using a new 'temporal superresolution' realignment method. Mol. Biol. Cell 25, 3501–14.



- Bielska, E., Schuster, M., Roger, Y., Berepiki, A., Soanes, D.M., Talbot, N.J., Steinberg, G., 2014. Hook is an adapter that coordinates kinesin-3 and dynein cargo attachment on early endosomes. *J. Cell Biol.* 204, 989–1007.
- Blumental-Perry, A., Haney, C.J., Weixel, K.M., Watkins, S.C., Weisz, O.A., Aridor, M., 2006. Phosphatidylinositol 4-Phosphate Formation at ER Exit Sites Regulates ER Export. *Dev. Cell* 11, 671–82.
- Boettner, D.R., Chi, R.J., Lemmon, S.K., 2011. Lessons from yeast for clathrin-mediated endocytosis. *Nat. Cell Biol.* 14, 2–10.
- Bonifacino, J.S., 2014. Vesicular transport earns a Nobel. *Trends Cell Biol.* 24, 3–5.
- Bonifacino, J.S., 2004. The GGA proteins: Adaptors on the move. *Nat. Rev. Mol. Cell Biol.* 5, 23–32.
- Bonifacino, J.S., Glick, B.S., 2004. The Mechanisms of Vesicle Budding and Fusion. *Cell.* 116, 153–66.
- Bonifacino, J.S., Hierro, A., 2011. Transport according to GARP: Receiving retrograde cargo at the *trans*-Golgi network. *Trends Cell Biol.* 21, 159–67.
- Bonifacino, J.S., Lippincott-Schwartz, J., 2003. Coat proteins: shaping membrane transport. *Nat. Rev. Mol. Cell Biol.* 4, 409–14.
- Bonifacino, J.S., Traub, L.M., 2003. Signals for Sorting of Transmembrane Proteins to Endosomes and Lysosomes. *Annu. Rev. Biochem.* 72, 395–447.
- Borgia, P.T., Iartchouk, N., Riggle, P.J., Winter, K.R., Koltin, Y., Bulawa, C.E., 1996. The *chsB* Gene of *Aspergillus nidulans* Is Necessary for Normal Hyphal Growth and Development. *Fungal Genet. Biol.* 20, 193–203.
- Bowen, A.R., Chen-Wu, J.L., Momany, M., Young, R., Szaniszlo, P.J., Robbins, P.W., 1992. Classification of fungal chitin synthases. *Biochemistry* 89, 519–23.
- Bowman, S.M., Free, S.J., 2006. The structure and synthesis of the fungal cell wall. *BioEssays* 28, 799–808.
- Brach, T., Godlee, C., Moeller-Hansen, I., Boeke, D., Kaksonen, M., 2014. The initiation of clathrin-mediated endocytosis is mechanistically highly flexible. *Curr. Biol.* 24, 548–54.
- Brandhorst, D., Zwilling, D., Rizzoli, S.O., Lippert, U., Lang, T., Jahn, R., 2006. Homotypic fusion of early endosomes: SNAREs do not determine fusion specificity. *Proc. Natl. Acad. Sci.* 103, 2701–6.
- Breakspear, A., Langford, K.J., Momany, M., Assinder, S.J., 2007. CopA:GFP localizes to putative Golgi equivalents in *Aspergillus nidulans*. *FEMS Microbiol. Lett.* 277, 90–7.
- Bretscher, A., 2003. Polarized growth and organelle segregation in yeast. *J. Cell Biol.* 160, 811–16.
- Bröcker, C., Kuhlee, A., Gatsogiannis, C., Balderhaar, H.J. kleine, Hönscher, C., Engelbrecht-Vandré, S., Ungermann, C., Raunser, S., 2012. Molecular architecture of the multisubunit homotypic

- fusion and vacuole protein sorting (HOPS) tethering complex. *Proc. Natl. Acad. Sci. U. S. A.* 109, 1991–6.
- Brodsky, F.M., Chen, C.Y., Knuehl, C., Towler, M.C., Wakeham, D.E., 2001. Biological basket weaving: formation and function of clathrin-coated vesicles. *Annu. Rev. Cell Dev. Biol.* 17, 517–68.
- Bruggeman, J., Debets, A.J.M., Wijngaarden, P.J., DeVisser, J.A.G.M., Hoekstra, R.F., 2003. Sex slows down the accumulation of deleterious mutations in the homothallic fungus *Aspergillus nidulans*. *Genetics* 164, 479–85.
- Burd, C., Cullen, P.J., 2014. Retromer: a master conductor of endosome sorting. *Cold Spring Harb. Perspect. Biol.* 6, a016774.
- Caddick, M. X. 2004. Nitrogen regulation in mycelial fungi, p. 349-368. In R. Brambl, & G. A. Marzluf (Eds.), *The Mycota III, Biochemistry and Molecular Biology* (Vol. III, pp. 349-368). Berlin-Heidelberg: Springer-Verlag.
- Caddick, M.X., Jones, M.G., van Tonder, J.M., Le Cordier, H., Narendja, F., Strauss, J., Morozov, I.Y., 2006. Opposing signals differentially regulate transcript stability in *Aspergillus nidulans*. *Mol. Microbiol.* 62, 509–19.
- Cai, Y., Chin, H.F., Lazarova, D., Menon, S., Fu, C., Cai, H., Sclafani, A., Rodgers, D.W., De La Cruz, E.M., Ferro-Novick, S., Reinisch, K.M., 2008. The Structural Basis for Activation of the Rab Ypt1p by the TRAPP Membrane-Tethering Complexes. *Cell* 133, 1202–13.
- Cao, X., Ballew, N., Barlowe, C., 1998. Initial docking of ER-derived vesicles requires Uso1p and Ypt1p but is independent of SNARE proteins. *EMBO J.* 17, 2156–65.
- Carlsson, A.E., Shah, A.D., Elking, D., Karpova, T.S., Cooper, J.A., 2002. Quantitative Analysis of Actin Patch Movement in Yeast. *Biophys. J.* 82, 2333–43.
- Carr, C.M., Grote, E., Munson, M., Hughson, F.M., Novick, P.J., 1999. Sec1p binds to SNARE complexes and concentrates at sites of secretion. *J. Cell Biol.* 146, 333–44.
- Cazelle, B., Pokorska, A., Hull, E., Green, P.M., Stanway, G., Scazzocchio, C., 1998. Sequence, exon-intron organization, transcription and mutational analysis of *prnA*, the gene encoding the transcriptional activator of the *prn* gene cluster in *Aspergillus nidulans*. *Mol. Microbiol.* 28, 355–70.
- Chang, P.L.Y., Trevithick, J.R., 1974. How important is secretion of exoenzymes through apical cell walls of fungi? *Arch. Microbiol.* 101, 281–93.
- Champe, S. P., and L. D. Simon. 1992. Cellular differentiation and tissue formation in the fungus *Aspergillus nidulans*, p. 63–91. In E. F. Rossomando and S. Alexander (ed.), *Morphogenesis: an analysis of the developmental of biological form*. Marcel Dekker, Inc., New York, N.Y.
- Cheng, J., Park, T.-S., Fischl, A.S., Ye, X.S., 2001. Cell Cycle Progression and Cell Polarity Require Sphingolipid Biosynthesis in *Aspergillus nidulans*. *Mol Cell Biol* 21, 6198–209.
- Conibear, E., 2010. Converging views of endocytosis in yeast and mammals. *Curr. Opin. Cell Biol.* 22,

513–18.

- Conner, S.D., Schmid, S.L., 2003. Differential requirements for AP-2 in clathrin-mediated endocytosis. *J. Cell Biol.* 162, 773–80.
- Costes, S. V, Daelemans, D., Cho, E.H., Dobbin, Z., Pavlakis, G., Lockett, S., 2004. Automatic and quantitative measurement of protein-protein colocalization in live cells. *Biophys. J.* 86, 3993–4003.
- Coutinho, P., Parsons, M.J., Thomas, K.A., Hirst, E.M.A., Saúde, L., Campos, I., Williams, P.H., Stemple, D.L., 2004. Differential Requirements for COPI Transport during Vertebrate Early Development. *Dev. Cell* 7, 547–58.
- d’Enfert, C., Fontaine, T., 1997. Molecular characterization of the *Aspergillus nidulans treA* gene encoding an acid trehalase required for growth on trehalose. *Mol. Microbiol.* 24, 203–16.
- Daboussi, L., Costaguta, G., Payne, G.S., 2012. Phosphoinositide-mediated clathrin adaptor progression at the *trans*-Golgi network. *Nat. Cell Biol.* 14, 239–48.
- De Craene, J.-O., Soetens, O., André, B., 2001. The Npr1 Kinase Controls Biosynthetic and Endocytic Sorting of the Yeast Gap1 Permease. *J. Biol. Chem.* 276, 43939–48.
- De Haro, L., Quetglas, S., Iborra, C., Lévêque, C., Seagar, M., 2003. Calmodulin-dependent regulation of a lipid binding domain in the v-SNARE synaptobrevin and its role in vesicular fusion. *Biol. cell* 95, 459–64.
- de Koning, H., Diallinas, G., 2000. Nucleobase transporters. *Mol. Membr. Biol.* 17, 75–94.
- Delgado-Álvarez, D.L., Callejas-Negrete, O.A., Gómez, N., Freitag, M., Roberson, R.W., Smith, L.G., Mouriño-Pérez, R.R., 2010. Visualization of F-actin localization and dynamics with live cell markers in *Neurospora crassa*. *Fungal Genet. Biol.* 47, 573–86.
- Dell’Angelica, E.C., Klumperman, J., Stoorvogel, W., Bonifacino, J.S., 1998. Association of the AP-3 adaptor complex with clathrin. *Science* 280, 431–4.
- DeMay, B.S., Bai, X., Howard, L., Occhipinti, P., Meseroll, R.A., Spiliotis, E.T., Oldenbourg, R., Gladfelter, A.S., 2011. Septin filaments exhibit a dynamic, paired organization that is conserved from yeast to mammals. *J. Cell Biol.* 193, 1065–81.
- Dever, T.E., Glynias, M.J., Merrick, W.C., 1987. GTP-binding domain: three consensus sequence elements with distinct spacing. *Proc. Natl. Acad. Sci. U. S. A.* 84, 1814–18.
- DeWitt, N., 1999. Homologous recombination transgenic fungi. *Nat. Biotechnol.* 17, 523.
- Diallinas, G., 2008. *Aspergillus* transporters, in: *The Aspergilli. Genomics, Medical Applications, Biotechnology, and Research Methods.* pp. 297–316.
- Diallinas, G., Gorfinkiel, L., Arst, H.N., Cecchetto, G., Scazzocchio, C., 1995. Genetic and Molecular characterization of a gene encoding a wide specificity purine permease of *Aspergillus nidulans* reveals a novel family of transporters conserved in prokaryotes and. *J. Biol. Chem.* 270, 8610–

22.

- Diallinas, G., Gournas, C., 2008. Structure-function relationships in the nucleobase-ascorbate transporter (NAT) family. *Channels* 2, 1–10.
- Ding, J., Segarra, V.A., Chen, S., Cai, H., Lemmon, S.K., Ferro-Novick, S., 2016. Auxilin facilitates membrane traffic in the early secretory pathway. *Mol. Biol. Cell.* 27, 127–36.
- Doherty, G.J., McMahon, H.T., 2009. Mechanisms of Endocytosis. *Annu. Rev. Biochem.* 78, 857–902.
- Dores, M.R., Schnell, J.D., Maldonado-Baez, L., Wendland, B., Hicke, L., 2010. The Function of Yeast Epsin and Ede1 Ubiquitin-Binding Domains During Receptor Internalization. *Traffic* 11, 151–60.
- Douglas, L.M., Konopka, J.B., 2016. Plasma membrane organization promotes virulence of the human fungal pathogen *Candida albicans*. *J. Microbiol.* 54, 178–91.
- Doyle, T., Botstein, D., 1996. Movement of yeast cortical actin cytoskeleton visualized *in vivo*. *Proc. Natl. Acad. Sci. U. S. A.* 93, 3886–91.
- Drubin, D.G., Nelson, W.J., 1996. Origins of cell polarity. *Cell* 84, 335–44.
- Duncan, M.C., Costaguta, G., Payne, G.S., 2003. Yeast epsin-related proteins required for Golgi–endosome traffic define a  $\gamma$ -adaptin ear-binding motif. *Nat. Cell Biol.* 5, 77–81.
- Dunn, K.W., Kamocka, M.M., McDonald, J.H., 2011. A practical guide to evaluating colocalization in biological microscopy. *Am. J. Physiol. Cell Physiol.* 300, C723–42.
- Dunne, J.C., Kondylis, V., Rabouille, C., 2002. Ecdysone Triggers the Expression of Golgi Genes in *Drosophila* Imaginal Discs via Broad-Complex. *Dev. Biol.* 245, 172–86.
- Dupont, S., Lemetais, G., Ferreira, T., Cayot, P., Gervais, P., Beney, L., 2012. Ergosterol biosynthesis: a fungal pathway for life on land? *Evolution* 66, 2961–8.
- Eaton, S., 2008. Retromer retrieves wntless. *Dev. Cell* 14, 4–6.
- Echauri-Espinosa, R.O., Callejas-Negrete, O.A., Roberson, R.W., Bartnicki-García, S., Mouriño-Pérez, R.R., 2012. Coronin is a component of the endocytic collar of hyphae of *Neurospora crassa* and is necessary for normal growth and morphogenesis. *PLoS One* 7, e38237.
- Eckley, D.M., Gill, S.R., Melkonian, K.A., Bingham, J.B., Goodson, H. V, Heuser, J.E., Schroer, T.A., 1999. Analysis of dynactin subcomplexes reveals a novel actin-related protein associated with the *arp1* minifilament pointed end. *J. Cell Biol.* 147, 307–20.
- Efimov, V.P., 2003. Roles of NudE and NudF Proteins of *Aspergillus nidulans*: Insights from Intracellular Localization and Overexpression Effects. *Mol. Biol. Cell* 14, 871–88.
- Egan, M.J., McClintock, M.A., Reck-Peterson, S.L., 2012a. Microtubule-based transport in filamentous fungi. *Curr. Opin. Microbiol.* 15, 637–45.
- Egan, M.J., McClintock, M.A., Reck-Peterson, S.L., 2012b. Microtubule-based transport in filamentous fungi. *Curr. Opin. Microbiol.* 15, 637–45.

- Egile, C., Rouiller, I., Xu, X.-P., Volkmann, N., Li, R., Hanein, D., 2005. Mechanism of Filament Nucleation and Branch Stability Revealed by the Structure of the Arp2/3 Complex at Actin Branch Junctions. *PLoS Biol.* 3, e383.
- Ehrlich, M., Boll, W., van Oijen, A., Hariharan, R., Chandran, K., Nibert, M.L., Kirchhausen, T., 2004. Endocytosis by Random Initiation and Stabilization of Clathrin-Coated Pits. *Cell* 118, 591–605.
- Engel, A., Gaub, H.E., 2008. Structure and Mechanics of Membrane Proteins. *Annu. Rev. Biochem.* 77, 127–48.
- Engqvist-Goldstein, Å.E.Y., Drubin, D.G., 2003. Actin Assembly and Endocytosis: From Yeast to Mammals. *Annu. Rev. Cell Dev. Biol.* 19, 287–332.
- Epp, E., Nazarova, E., Regan, H., Douglas, L.M., Konopka, J.B., Vogel, J., Whiteway, M., 2013. Clathrin- and arp2/3-independent endocytosis in the fungal pathogen *Candida albicans*. *MBio* 4, e00476.
- Etxebeste, O., Espeso, E.A., 2016. Neurons show the path: tip-to-nucleus communication in filamentous fungal development and pathogenesis. *FEMS Microbiol. Rev.* 40, 610–24.
- Evangelinos, M., Martzoukou, O., Chorozián, K., Amillis, S., Diállinas, G., 2016. BsdA<sup>Bsd2</sup>-dependent vacuolar turnover of a misfolded version of the UapA transporter along the secretory pathway: prominent role of selective autophagy. *Mol. Microbiol.* 100, 893–911.
- Faini, M., Beck, R., Wieland, F.T., Briggs, J.A.G., 2013. Vesicle coats: structure, function, and general principles of assembly. *Trends Cell Biol.* 23, 279–88.
- Farhan, H., Weiss, M., Tani, K., Kaufman, R.J., Hauri, H.-P., 2008. Adaptation of endoplasmic reticulum exit sites to acute and chronic increases in cargo load. *EMBO J.* 27, 2043–54.
- Feigenson, G.W., 2006. Phase behavior of lipid mixtures. *Nat. Chem. Biol.* 2, 560–3.
- Fernandez, N., Puente, P., Leal, F., 1990. Fluid-phase endocytosis in yeasts other than *Saccharomyces cerevisiae*. *FEMS Microbiol. Lett.* 69, 7–11.
- Fewell, S.W., Brodsky, J.L., 2000. Entry into the Endoplasmic Reticulum: Protein Translocation, Folding and Quality Control. *Madame Curie Biosci. Database [Internet]. Austin (TX Landes Biosci.*
- FGSC, 2018. Fungal Genetics Stock Center <http://www.fgsc.net/> (accessed 11 July 2018).
- Fischer-Parton, S., Parton, R.M., Hickey, P.C., Dijksterhuis, J., Atkinson, H.A., Read, N.D., 2000. Confocal microscopy of FM4-64 as a tool for analysing endocytosis and vesicle trafficking in living fungal hyphae. *J. Microsc.* 198, 246–59.
- Fischer, R., Zekert, N., Takeshita, N., 2008. Polarized growth in fungi - Interplay between the cytoskeleton, positional markers and membrane domains. *Mol. Microbiol.* 68, 813–26.
- Fjorback, A.W., Seaman, M., Gustafsen, C., Mehmedbasic, A., Gokool, S., Wu, C., Militz, D., Schmidt, V., Madsen, P., Nyengaard, J.R., Willnow, T.E., Christensen, E.I., Mobley, W.B., Nykjaer, A., Andersen, O.M., 2012. Retromer Binds the FANSHY Sorting Motif in SorLA to Regulate Amyloid

- Precursor Protein Sorting and Processing. *J. Neurosci.* 32, 1467–80.
- Forster, R., Weiss, M., Zimmermann, T., Reynaud, E.G., Verissimo, F., Stephens, D.J., Pepperkok, R., 2006. Secretory Cargo Regulates the Turnover of COPII Subunits at Single ER Exit Sites. *Curr. Biol.* 16, 173–9.
- Friant, S., Pécheur, E.I., Eugster, A., Michel, F., Lefkir, Y., Nourrisson, D., Letourneur, F., 2003. Ent3p Is a PtdIns(3,5)P<sub>2</sub> effector required for protein sorting to the multivesicular body. *Dev. Cell* 5, 499–511.
- Fuchs, U., Hause, G., Schuchardt, I., Steinberg, G., 2006. Endocytosis is essential for pathogenic development in the corn smut fungus *Ustilago maydis*. *Plant Cell* 18, 2066–81.
- Fujiwara, M., Horiuchi, H., Ohta, A., Takagi, M., 1997. A Novel Fungal Gene Encoding Chitin Synthase with a Myosin Motor-like Domain. *Biochem. Biophys. Res. Commun.* 236, 75–78.
- Fukuda, K., Yamada, K., Deoka, K., Yamashita, S., Ohta, A., Horiuchi, H., 2009. Class III chitin synthase ChsB of *Aspergillus nidulans* localizes at the sites of polarized cell wall synthesis and is required for conidial development. *Eukaryot. Cell.* 8, 945–56.
- Fung, K.Y.Y., Dai, L., Trimble, W.S., 2014. Cell and Molecular Biology of Septins. *Int. Rev. Cell Mol. Biol.* 310, 289–339.
- Galagan, J.E., Calvo, S.E., Cuomo, C., Ma, L.-J., Wortman, J.R., Batzoglou, S., Lee, S.-I., Baştürkmen, M., Spevak, C.C., Clutterbuck, J., Kapitonov, V., Jurka, J., Scazzocchio, C., Farman, M., Butler, J., Purcell, S., Harris, S., Braus, G.H., Draht, O., Busch, S., D’Enfert, C., Bouchier, C., Goldman, G.H., Bell-Pedersen, D., Griffiths-Jones, S., Doonan, J.H., Yu, J., Vienken, K., Pain, A., Freitag, M., Selker, E.U., Archer, D.B., Peñalva, M. a, Oakley, B.R., Momany, M., Tanaka, T., Kumagai, T., Asai, K., Machida, M., Nierman, W.C., Denning, D.W., Caddick, M., Hynes, M., Paoletti, M., Fischer, R., Miller, B., Dyer, P., Sachs, M.S., Osmani, S. a, Birren, B.W., 2005. Sequencing of *Aspergillus nidulans* and comparative analysis with *A. fumigatus* and *A. oryzae*. *Nature* 438, 1105–15.
- Gardner, M.K., Hunt, A.J., Goodson, H. V., Odde, D.J., 2008. Microtubule assembly dynamics: new insights at the nanoscale. *Curr. Opin. Cell Biol.* 20, 64–70.
- Geli, M.I., Riezman, H., 1998. Endocytic internalization in yeast and animal cells: similar and different. *J. Cell Sci.* 111, 1031–7.
- Gerst, J.E., 2008. Message on the web: mRNA and ER co-trafficking. *Trends Cell Biol.* 18, 68–76.
- Gierz, G., Bartnicki-Garcia, S., 2001. A three-dimensional model of fungal morphogenesis based on the vesicle supply center concept. *J. Theor. Biol.* 208, 151–64.
- Gillingham, A.K., Munro, S., 2007. Identification of a guanine nucleotide exchange factor for Arf3, the yeast orthologue of mammalian Arf6. *PLoS One* 23, 579–611.
- Gilmore, R., Mandon, E.C., 2012. Understanding integration of  $\alpha$ -helical membrane proteins: the next steps. *Trends Biochem. Sci.* 37, 303–8.

- Giraud, C.G., Maccioni, H.J.F., 2003. Endoplasmic Reticulum Export of Glycosyltransferases Depends on Interaction of a Cytoplasmic Dibasic Motif with Sar1. *Mol. Biol. Cell* 14, 3753–66.
- Gladfelter, A.S., 2006. Control of filamentous fungal cell shape by septins and formins. *Nat. Rev. Microbiol.* 4, 223-9.
- Glebov, O.O., Bright, N.A., Nichols, B.J., 2006. Flotillin-1 defines a clathrin-independent endocytic pathway in mammalian cells. *Nat. Cell Biol.* 8, 46–54.
- Gomez-Navarro, N., Miller, E.A., 2016. COP-coated vesicles. *Curr. Biol.* 26, R54–7.
- Gonzalez, R., Gavrias, V., Gomez, D., Scazzocchio, C., Cubero, B., 1997. The integration of nitrogen and carbon catabolite repression in *Aspergillus nidulans* requires the GATA factor AreA and an additional positive-acting element, ADA. *EMBO J.* 16, 2937–44.
- Goode, B.L., Eskin, J.A., Wendland, B., 2015. Actin and endocytosis in budding yeast. *Genetics* 199, 315–58.
- Goudela, S., Reichard, U., Amillis, S., Diallinas, G., 2008. Characterization and kinetics of the major purine transporters in *Aspergillus fumigatus*. *Fungal Genet. Biol.* 45, 459–72.
- Gournas, C., Amillis, S., Vlanti, A., Diallinas, G., 2010. Transport-dependent endocytosis and turnover of a uric acid-xanthine permease. *Mol. Microbiol.* 75, 246-60.
- Gournas, C., Gkionis, S., Carquin, M., Twyffels, L., Tyteca, D., André, B., 2018. Conformation-dependent partitioning of yeast nutrient transporters into starvation-protective membrane domains. *Proc. Natl. Acad. Sci.* 115, e3145.
- Gournas, C., Oestreicher, N., Amillis, S., Diallinas, G., Scazzocchio, C., 2011. Completing the purine utilisation pathway of *Aspergillus nidulans*. *Fungal Genet. Biol.* 48, 840–48.
- Gow, N.A.R., 2016. Editorial for “the fungal cell wall” special issue. *Cell. Microbiol.* 18, 1187.
- Grant, B.D., Donaldson, J.G., 2009. Pathways and mechanisms of endocytic recycling. *Nat. Rev. Mol. Cell Biol.* 10, 597–608.
- Griffith, J., Reggiori, F., 2009. Ultrastructural Analysis of Nanogold-labeled Endocytic Compartments of Yeast *Saccharomyces cerevisiae* Using a Cryosectioning Procedure. *J. Histochem. Cytochem.* 57, 801–09.
- Guest, G.M., Lin, X., Momany, M., 2004. *Aspergillus nidulans* RhoA is involved in polar growth, branching, and cell wall synthesis. *Fungal Genet. Biol.* 41, 13-22.
- Guimaraes, S.C., Schuster, M., Bielska, E., Dagdas, G., Kilaru, S., Meadows, B.R.A., Schrader, M., Steinberg, G., 2015. Peroxisomes, lipid droplets, and endoplasmic reticulum “hitchhike” on motile early endosomes. *J. Cell Biol.* 211, 945-54.
- Guimarães, L.L., Toledo, M.S., Ferreira, F.A.S., Straus, A.H., Takahashi, H.K., 2014. Structural diversity and biological significance of glycosphingolipids in pathogenic and opportunistic fungi. *Front. Cell. Infect. Microbiol.* 4, 138.

- Guo, W., Grant, A., Novick, P., 1999a. Exo84p is an exocyst protein essential for secretion. *J. Biol. Chem.* 274, 23558–64.
- Guo, W., Roth, D., Walch-Solimena, C., Novick, P., 1999b. The exocyst is an effector for Sec4P, targeting secretory vesicles to sites of exocytosis. *EMBO J.* 18, 1071–80.
- Guo, Y., Au, W.-C., Shakoury-Elizeh, M., Protchenko, O., Basrai, M., Prinz, W.A., Philpott, C.C., 2010. Phosphatidylserine Is Involved in the Ferrichrome-induced Plasma Membrane Trafficking of Arn1 in *Saccharomyces cerevisiae*. *J. Biol. Chem.* 285, 39564–73.
- Guo, Y., Sirkis, D.W., Schekman, R., 2014. Protein Sorting at the *trans*-Golgi Network. *Annu. Rev. Cell Dev. Biol.* 30, 169–206.
- Gurtovenko, A.A., Vattulainen, I., 2007. Molecular Mechanism for Lipid Flip-Flops. *J. Phys. Chem. B* 111, 13554–9.
- Haag, C., Steuten, B., Feldbrügge, M., 2015. Membrane-Coupled mRNA Trafficking in Fungi. *Annu. Rev. Microbiol.* 69, 265–81.
- Harris, S.D., 2006. Cell Polarity in Filamentous Fungi: Shaping the Mold, in: *International Review of Cytology*. pp. 41–77.
- Harris, S.D., 2001. Septum formation in *Aspergillus nidulans*. *Curr. Opin. Microbiol.* 4, 736–9.
- Harris, S.D., Hofmann, A.F., Tedford, H.W., Lee, M.P., 1999. Identification and characterization of genes required for hyphal morphogenesis in the filamentous fungus *Aspergillus nidulans*. *Genetics* 151, 1015–25.
- Harris, S.D., Momany, M., 2004. Polarity in filamentous fungi: Moving beyond the yeast paradigm. *Fungal Genet. Biol.* 41, 391-400.
- Harris, S.D., Morrell, J.L., Hamer, J.E., 1994. Identification and characterization of *Aspergillus nidulans* mutants defective in cytokinesis. *Genetics* 136, 517–32.
- Harris, S.D., Read, N.D., Roberson, R.W., Shaw, B., Seiler, S., Plamann, M., Momany, M., 2005. Polarisome meets Spitzenkörper: Microscopy, genetics, and genomics converge. *Eukaryot. Cell* 4, 225-9.
- Harrison, M.S., Hung, C.-S., Liu, T. -t., Christiano, R., Walther, T.C., Burd, C.G., 2014. A mechanism for retromer endosomal coat complex assembly with cargo. *Proc. Natl. Acad. Sci.* 111, 267-72.
- Hartwell, L.H., 1971. Genetic control of the cell division cycle in yeast. IV. Genes controlling bud emergence and cytokinesis. *Exp. Cell Res.* 69, 265–76.
- Hatakeyama, R., Kamiya, M., Takahara, T., Maeda, T., 2010. Endocytosis of the aspartic acid/glutamic acid transporter Dip5 is triggered by substrate-dependent recruitment of the Rsp5 ubiquitin ligase via the arrestin-like protein Aly2. *Mol. Cell. Biol.* 30, 5598–607.
- Hayakawa, Y., Ishikawa, E., Shoji, J., Nakano, H., Kitamoto, K., 2011. Septum-directed secretion in the filamentous fungus *Aspergillus oryzae*. *Mol. Microbiol.* 81, 40-55.



- Henkart, M., Landis, D.M., Reese, T.S., 1976. Similarity of junctions between plasma membranes and endoplasmic reticulum in muscle and neurons. *J. Cell Biol.* 70, 338–47.
- Henne, W.M., Buchkovich, N.J., Emr, S.D., 2011. The ESCRT pathway. *Dev. Cell* 21, 77–91.
- Hernández-González, M., Bravo-Plaza, I., Pinar, M., de los Ríos, V., Arst, H.N., Peñalva, M.A., 2018. Endocytic recycling via the TGN underlies the polarized hyphal mode of life. *PLOS Genet.* 14, e1007291.
- Hernández-González, M., Pantazopoulou, A., Spanoudakis, D., Seegers, C.L.C., Peñalva, M.A., 2018b. Genetic dissection of the secretory route followed by a fungal extracellular glycosyl hydrolase. *Mol. Microbiol.* [epub ahead of print]. doi: 10.1111/mmi.14073
- Hernández-González, M., Peñalva, M.A., Pantazopoulou, A., 2015. Conditional inactivation of *Aspergillus nidulans sarA<sup>sar1</sup>* uncovers the morphogenetic potential of regulating endoplasmic reticulum (ER) exit. *Mol. Microbiol.* 95, 491–508.
- Hernández-Rodríguez, Y., Hastings, S., Momany, M., 2012. The septin *aspb* in *Aspergillus nidulans* forms bars and filaments and plays roles in growth emergence and conidiation. *Eukaryot. Cell* 11, 311–23.
- Hernández-Rodríguez, Y., Masuo, S., Johnson, D., Orlando, R., Smith, A., Couto-Rodriguez, M., Momany, M., 2014. Distinct septin heteropolymers co-exist during multicellular development in the filamentous fungus *Aspergillus nidulans*. *PLoS One* 9, e92819.
- Hervás-Aguilar, A., Peñalva, M.A., 2010. Endocytic machinery protein SlaB is dispensable for polarity establishment but necessary for polarity maintenance in hyphal tip cells of *Aspergillus nidulans*. *Eukaryot. Cell.* 9, 1504–18.
- Higashitsuji, Y., Herrero, S., Takeshita, N., Fischer, R., 2009. The Cell End Marker Protein TeaC Is Involved in Growth Directionality and Septation in *Aspergillus nidulans*. *Eukaryot. Cell* 8, 957–67.
- Higuchi, Y., Ashwin, P., Roger, Y., Steinberg, G., 2014. Early endosome motility spatially organizes polysome distribution. *J. Cell Biol.* 204, 343–57.
- Higuchi, Y., Shoji, J., Arioka, M., Kitamoto, K., 2009. Endocytosis is crucial for cell polarity and apical membrane recycling in the filamentous fungus *Aspergillus oryzae*. *Eukaryot. Cell* 8, 37–46.
- Hirata, T., Fujita, M., Nakamura, S., Gotoh, K., Motooka, D., Murakami, Y., Maeda, Y., Kinoshita, T., 2015. Post-Golgi anterograde transport requires GARP-dependent endosome-to-TGN retrograde transport. *Mol. Biol. Cell.* 26, 3071–84.
- Hirokawa, N., Niwa, S., Tanaka, Y., 2010. Molecular Motors in Neurons: Transport Mechanisms and Roles in Brain Function, Development, and Disease. *Neuron* 68, 610–38.
- Hirst, J., D. Barlow, L., Francisco, G.C., Sahlender, D.A., Seaman, M.N.J., Dacks, J.B., Robinson, M.S., 2011. The Fifth Adaptor Protein Complex. *PLoS Biol.* 9, e1001170.
- Hirst, J., Borner, G.H.H., Antrobus, R., Peden, A.A., Hodson, N.A., Sahlender, D.A., Robinson, M.S.,

2012. Distinct and overlapping roles for AP-1 and GGAs revealed by the “knocksideways” system. *Curr. Biol.* 22, 1711–6.
- Hohmann-Marriott, M.F., Uchida, M., van de Meene, A.M.L., Garret, M., Hjelm, B.E., Kokoori, S., Roberson, R.W., 2006. Application of electron tomography to fungal ultrastructure studies. *New Phytol.* 172, 208–20.
- Holleran, E.A., Karki, S., Holzbaur, E.L., 1998. The role of the dynactin complex in intracellular motility. *Int. Rev. Cytol.* 182, 69–109.
- Horio, T., Oakley, B.R., 2005. The Role of Microtubules in Rapid Hyphal Tip Growth of *Aspergillus nidulans*. *Mol. Biol. Cell* 16, 918–26.
- Hoshi, H.-O., Zheng, L., Ohta, A., Horiuchi, H., 2016. A Wiskott-Aldrich syndrome protein is involved in endocytosis in *Aspergillus nidulans*. *Biosci. Biotechnol. Biochem.* 80, 1802–12.
- Houbraken, J., de Vries, R.P., Samson, R. a, 2014. Modern taxonomy of biotechnologically important *Aspergillus* and *Penicillium* species., in: *Advances in Applied Microbiology*. Elsevier, pp. 199–249.
- Howard, J.P., Hutton, J.L., Olson, J.M., Payne, G.S., 2002. Sla1p serves as the targeting signal recognition factor for NPFX(1,2)D-mediated endocytosis. *J. Cell Biol.* 157, 315–26.
- Howard, R.J., 1981. Ultrastructural analysis of hyphal tip cell growth in fungi: Spitzenkörper, cytoskeleton and endomembranes after freeze-substitution. *J. Cell Sci.* 48, 89–103.
- Howes, M.T., Kirkham, M., Riches, J., Cortese, K., Walser, P.J., Simpson, F., Hill, M.M., Jones, A., Lundmark, R., Lindsay, M.R., Hernandez-Deviez, D.J., Hadzic, G., McCluskey, A., Bashir, R., Liu, L., Pilch, P., McMahon, H., Robinson, P.J., Hancock, J.F., Mayor, S., Parton, R.G., 2010. Clathrin-independent carriers form a high capacity endocytic sorting system at the leading edge of migrating cells. *J. Cell Biol.* 190, 675–91.
- Hoya, M., Yanguas, F., Moro, S., Prescianotto-Baschong, C., Doncel, C., de León, N., Curto, M.-Á., Spang, A., Valdivieso, M.-H., 2017. Traffic Through the Trans-Golgi Network and the Endosomal System Requires Collaboration Between Exomer and Clathrin Adaptors in Fission Yeast. *Genetics* 205, 673–90.
- Hsu, S.C., Hazuka, C.D., Roth, R., Foletti, D.L., Heuser, J., Scheller, R.H., 1998. Subunit composition, protein interactions, and structures of the mammalian brain Sec6/8 complex and septin filaments. *Neuron* 20, 1111–22.
- Hsu, S.C., Ting, A.E., Hazuka, C.D., Davanger, S., Kenny, J.W., Kee, Y., Scheller, R.H., 1996. The mammalian brain rsec6/8 complex. *Neuron* 17, 1209–19.
- Huotari, J., Helenius, A., 2011. Endosome maturation. *EMBO J.* 30, 3481–500.
- Hyde, R.J., Cass, C.E., Young, J.D., Baldwin, S.A., 2001. The ENT family of eukaryote nucleoside and nucleobase transporters: Recent advances in the investigation of structure/function relationships and the identification of novel isoforms, in: *Molecular Membrane Biology*. pp. 53–

63.

- ICY, 2018. ICY Bioimage Analysis Software. <http://icy.bioimageanalysis.org/> (accessed 11 July 2018).
- Idrissi, F.-Z., Grötsch, H., Fernández-Golbano, I.M., Presciatto-Baschong, C., Riezman, H., Geli, M.-I., 2008. Distinct acto/myosin-I structures associate with endocytic profiles at the plasma membrane. *J. Cell Biol.* 180, 1219–32.
- ImageJ, 2018. ImageJ image processing program. <https://imagej.nih.gov/ij/> (accessed 11 July 2018).
- Irazaqui, J.E., Lew, D.J., 2004. Polarity establishment in yeast. *J. Cell Sci.* 117, 2169–71.
- Ishitsuka, Y., Savage, N., Li, Y., Bergs, A., Grün, N., Kohler, D., Donnelly, R., Nienhaus, G.U., Fischer, R., Takeshita, N., 2015. Cell Biology: Superresolution microscopy reveals a dynamic picture of cell polarity maintenance during directional growth. *Sci. Adv.* 1, e1500947.
- Ito, Y., Uemura, T., Shoda, K., Fujimoto, M., Ueda, T., Nakano, A., 2012. cis-Golgi proteins accumulate near the ER exit sites and act as the scaffold for Golgi regeneration after brefeldin A treatment in tobacco BY-2 cells. *Mol. Biol. Cell.* 23, 3203–14.
- Jansen, R.-P., Niessing, D., Baumann, S., Feldbrügge, M., 2014. mRNA transport meets membrane traffic. *Trends Genet.* 30, 408–17.
- Jedd, G., Mulholland, J., Segev, N., 1997. Two new Ypt GTPases are required for exit from the yeast trans-Golgi compartment. *J. Cell Biol.* 137, 563–80.
- Jedd, G., Richardson, C., Litt, R., Segev, N., 1995. The Ypt1 GTPase is essential for the first two steps of the yeast secretory pathway. *J. Cell Biol.* 131, 583–90.
- Jones, L.A., Sudbery, P.E., 2010. Spitzenkörper, exocyst, and polarisome components in *Candida albicans* hyphae show different patterns of localization and have distinct dynamic properties. *Eukaryot. Cell* 9, 1455–65.
- Jorde, S., Walther, A., Wendland, J., 2011. The *Ashbya gossypii* fimbrin SAC6 is required for fast polarized hyphal tip growth and endocytosis. *Microbiol. Res.* 166, 137–45.
- Juvvadi, P.R., Fortwendel, J.R., Rogg, L.E., Steinbach, W.J., 2011. Differential localization patterns of septins during growth of the human fungal pathogen *Aspergillus fumigatus* reveal novel functions. *Biochem. Biophys. Res. Commun.* 405, 238–43.
- Kaksonen, M., Sun, Y., Drubin, D.G., 2003. A Pathway for Association of Receptors, Adaptors, and Actin during Endocytic Internalization. *Cell* 115, 475–87.
- Kaouass, M., Gamache, I., Ramotar, D., Audette, M., Poulin, R., 1998. The spermidine transport system is regulated by ligand inactivation, endocytosis, and by the Npr1p Ser/Thr protein kinase in *Saccharomyces cerevisiae*. *J. Biol. Chem.* 273, 2109–17.
- Karachaliou, M., Amillis, S., Evangelinos, M., Kokotos, A.C., Yalelis, V., Diallinas, G., 2013. The arrestin-like protein ArtA is essential for ubiquitination and endocytosis of the UapA transporter in response to both broad-range and specific signals. *Mol. Microbiol.* 88, 301–17.

- Karatza, P., Frillingos, S., 2005. Cloning and functional characterization of two bacterial members of the NAT/NCS2 family in *Escherichia coli*. *Mol. Membr. Biol.* 22, 251–61.
- Kartsonis, N.A., Nielsen, J., Douglas, C.M., 2003. Caspofungin: the first in a new class of antifungal agents. *Drug Resist. Updat.* 6, 197–218.
- Kasey, D.J., Casler, J.C., Glick, B.S., 2018. Budding yeast has a minimal endomembrane system. *Dev. Cell* 44, 56–72.
- Keller, N.P., Hohnt, T.M., 1997. Metabolic Pathway Gene Clusters in Filamentous Fungi. *Fungal Genet. Biol.* 7, 17–29.
- Kendrick, B., 1992. The fifth kingdom. Mycologue Publications, Newburyport, MA.
- Kilmartin, J. V., 2014. Lessons from yeast: the spindle pole body and the centrosome. *Philos. Trans. R. Soc. Lond. B. Biol. Sci.* 369, 20130456.
- King, S.M., 2000. The dynein microtubule motor. *Biochim. Biophys. Acta* 1496, 60–75.
- Kinoshita, M., Kumar, S., Mizoguchi, A., Ide, C., Kinoshita, A., Haraguchi, T., Hiraoka, Y., Noda, M., 1997. Nedd5, a mammalian septin, is a novel cytoskeletal component interacting with actin-based structures. *Genes Dev.* 11, 1535–47.
- Kirchhausen, T., 2000. Clathrin. *Annu. Rev. Biochem.* 69, 699–727.
- Kirk, P.M., Cannon, P.F., Minter, D.W., Stalpers, J.A., 2008. Dictionary of the Fungi, 10th ed. Wallingford: CABI.
- Kirkham, M., Parton, R.G., 2005. Clathrin-independent endocytosis: New insights into caveolae and non-caveolar lipid raft carriers. *Biochim. Biophys. Acta - Mol. Cell Res.* 1746, 350–63.
- Kobayashi, T., Beuchat, M.-H., Chevallier, J., Makino, A., Mayran, N., Escola, J.-M., Lebrand, C., Cosson, P., Kobayashi, T., Gruenberg, J., 2002. Separation and characterization of late endosomal membrane domains. *J. Biol. Chem.* 277, 32157–64.
- Kohli, M., Galati, V., Boudier, K., Roberson, R.W., Philippsen, P., 2008. Growth-speed-correlated localization of exocyst and polarisome components in growth zones of *Ashbya gossypii* hyphal tips. *J. Cell Sci.* 121, 3878–89.
- Konzack, S., Rischitor, P.E., Enke, C., Fischer, R., 2005. The Role of the Kinesin Motor KipA in Microtubule Organization and Polarized Growth of *Aspergillus nidulans*. *Mol. Biol. Cell* 16, 497–506.
- Kost, B., Lemichez, E., Spielhofer, P., Hong, Y., Tolias, K., Carpenter, C., Chua, N.H., 1999. Rac homologues and compartmentalized phosphatidylinositol 4, 5-bisphosphate act in a common pathway to regulate polar pollen tube growth. *J. Cell Biol.* 145, 317–30.
- Koukaki, M., Vlanti, A., Goudela, S., Pantazopoulou, A., Gioule, H., Tournaviti, S., Diallinas, G., 2005. The Nucleobase-ascorbate Transporter (NAT) Signature Motif in UapA Defines the Function of the Purine Translocation Pathway. *J. Mol. Biol.* 350, 499–513.

- Kourkoulou, A., Pittis, A.A., Diallinas, G., 2018. Evolution of substrate specificity in the Nucleobase-Ascorbate Transporter (NAT) protein family. *Microb. Cell* 5, 280–92.
- Krämer, L., Ungermann, C., 2011. HOPS drives vacuole fusion by binding the vacuolar SNARE complex and the Vam7 PX domain via two distinct sites. *Mol. Biol. Cell* 22, 2601–11.
- Kremer, B.E., Haystead, T., Macara, I.G., 2005. Mammalian septins regulate microtubule stability through interaction with the microtubule-binding protein MAP4. *Mol. Biol. Cell* 16, 4648–59.
- Kryptou, E., Evangelidis, T., Bobonis, J., Pittis, A.A., Gabaldón, T., Scazzocchio, C., Mikros, E., Diallinas, G., 2015. Origin, diversification and substrate specificity in the family of NCS1/FUR transporters. *Mol. Microbiol.* 96, 927–50.
- Kryptou, E., Kosti, V., Amillis, S., Myriantopoulos, V., Mikros, E., Diallinas, G., 2012. Modeling, Substrate Docking, and Mutational Analysis Identify Residues Essential for the Function and Specificity of a Eukaryotic Purine-Cytosine NCS1 Transporter. *J. Biol. Chem.* 287, 36792–803.
- Kübler, E., Riezman, H., 1993. Actin and fimbrin are required for the internalization step of endocytosis in yeast. *EMBO J.* 12, 2855–62.
- Kuehn, M.J., Herrmann, J.M., Schekman, R., 1998. COPII-cargo interactions direct protein sorting into ER-derived transport vesicles. *Nature* 391, 187–90.
- Kurokawa, K., Okamoto, M., Nakano, A., 2014. Contact of *cis*-Golgi with ER exit sites executes cargo capture and delivery from the ER. *Nat. Commun.* 5, 3653.
- Ladinsky, M.S., Wu, C.C., McIntosh, S., McIntosh, J.R., Howell, K.E., 2002. Structure of the Golgi and Distribution of Reporter Molecules at 20°C Reveals the Complexity of the Exit Compartments. *Mol. Biol. Cell* 13, 2810–25.
- Lamaze, C., Dujancourt, A., Baba, T., Lo, C.G., Benmerah, A., Dautry-Varsat, A., 2001. Interleukin 2 receptors and detergent-resistant membrane domains define a clathrin-independent endocytic pathway. *Mol. Cell* 7, 661–71.
- Lasiecka, Z.M., Winckler, B., 2011. Mechanisms of polarized membrane trafficking in neurons - focusing in on endosomes. *Mol. Cell. Neurosci.* 48, 278–87.
- Latgé, J.-P., 2007. The cell wall: a carbohydrate armour for the fungal cell. *Mol. Microbiol.* 66, 279–90.
- Lau, A.W., Chou, M.M., 2008. The adaptor complex AP-2 regulates post-endocytic trafficking through the non-clathrin Arf6-dependent endocytic pathway. *J. Cell Sci.* 121, 4008–17.
- Lee, B.N., Adams, T.H., 1994. Overexpression of *flbA*, an early regulator of *Aspergillus* asexual sporulation, leads to activation of *briA* and premature initiation of development. *Mol. Microbiol.* 14, 323–34.
- Lee, M.C.S., Miller, E.A., 2007. Molecular mechanisms of COPII vesicle formation. *Semin. Cell Dev. Biol.* 18, 424–34.

- Lee, M.C.S., Miller, E.A., Goldberg, J., Orci, L., Schekman, R., 2004. Bi-directional protein transport between the ER and Golgi. *Annu. Rev. Cell Dev. Biol.* 20, 87–123.
- Lee, S.C., Schmidtke, S., Dangott, L., Shaw, B.D., 2008. *Aspergillus nidulans* ArfB plays a role in endocytosis and polarized growth. *Eukaryot. Cell* 7, 1278–88.
- Lee, S.C., Shaw, B.D., 2008a. Localization and function of ADP ribosylation factor a in *Aspergillus nidulans*. *FEMS Microbiol. Lett.* 283, 216–22.
- Lee, S.C., Shaw, B.D., 2008b. ArfB links protein lipidation and endocytosis to polarized growth of *Aspergillus nidulans*. *Commun. Integr. Biol.* 1, 51–2.
- Lenardon, M.D., Munro, C.A., Gow, N.A.R., 2010. Chitin synthesis and fungal pathogenesis. *Curr. Opin. Microbiol.* 13, 416–23.
- Lenz, J.H., Schuchardt, I., Straube, A., Steinberg, G., 2006. A dynein loading zone for retrograde endosome motility at microtubule plus-ends. *EMBO J.* 25, 2275–86.
- Levine, T.P., Munro, S., 2002. Targeting of Golgi-specific pleckstrin homology domains involves both PtdIns 4-kinase-dependent and -independent components. *Curr. Biol.* 12, 695–704.
- Lewis, M.J., Nichols, B.J., Prescianotto-Baschong, C., Riezman, H., Pelham, H.R., 2000. Specific retrieval of the exocytic SNARE Snc1p from early yeast endosomes. *Mol. Biol. Cell* 11, 23–38.
- Li, S., Bao, D., Yuen, G., Harris, S.D., Calvo, A.M., 2007. *basA* regulates cell wall organization and asexual/sexual sporulation ratio in *Aspergillus nidulans*. *Genetics* 176, 243–53.
- Liang, W.J., Johnson, D., Jarvis, S.M., 2001. Vitamin C transport systems of mammalian cells, in: *Molecular Membrane Biology*. pp. 87–95.
- Liang, Y., Morozova, N., Tokarev, A.A., Mulholland, J.W., Segev, N., 2007. The role of Trs65 in the Ypt/Rab guanine nucleotide exchange factor function of the TRAPP II complex. *Mol. Biol. Cell* 18, 2533–41.
- Lichius, A., Yáñez-Gutiérrez, M.E., Read, N.D., Castro-Longoria, E., 2012. Comparative Live-Cell Imaging Analyses of SPA-2, BUD-6 and BNI-1 in *Neurospora crassa* Reveal Novel Features of the Filamentous Fungal Polarisome. *PLoS One* 7, e30372.
- Lin, C.H., MacGurn, J.A., Chu, T., Stefan, C.J., Emr, S.D., 2008. Arrestin-Related Ubiquitin-Ligase Adaptors Regulate Endocytosis and Protein Turnover at the Cell Surface. *Cell* 135, 714–725.
- Lindsey, R., Cowden, S., Hernández-Rodríguez, Y., Momany, M., 2010. Septins AspA and AspC are important for normal development and limit the emergence of new growth foci in the multicellular fungus *Aspergillus nidulans*. *Eukaryot. Cell* 9, 155–163.
- Lipatova, Z., Tokarev, A.A., Jin, Y., Mulholland, J., Weisman, L.S., Segev, N., 2008. Direct Interaction between a Myosin V Motor and the Rab GTPases Ypt31/32 Is Required for Polarized Secretion. *Mol. Biol. Cell* 19, 4177–4187.
- Liu, K., Hua, Z., Nepute, J.A., Graham, T.R., 2007. Yeast P4-ATPases Drs2p and Dnf1p are essential

- cargos of the NPF<sub>XD</sub>/Sla1p endocytic pathway. *Mol. Biol. Cell* 18, 487–500.
- Lockington, R., Scazzocchio, C., Sequeval, D., Mathieu, M., Felenbok, B., 1987. Regulation of alcR, the positive regulatory gene of the ethanol utilization regulon of *Aspergillus nidulans*. *Mol. Microbiol.* 1, 275–81.
- Loerke, D., Mettlen, M., Yarar, D., Jaqaman, K., Jaqaman, H., Danuser, G., Schmid, S.L., 2009. Cargo and dynamin regulate clathrin-coated pit maturation. *PLoS Biol.* 7, e57.
- López-Berges, M.S., Arst, H.N., Pinar, M., Peñalva, M.A., 2017. Genetic studies on the physiological role of CORVET in *Aspergillus nidulans*. *FEMS Microbiol. Lett.* 364, fnx065.
- López-Berges, M.S., Pinar, M., Abenza, J.F., Arst, H.N., Peñalva, M.A., 2016. The *Aspergillus nidulans* syntaxin PepA<sup>Pep12</sup> is regulated by two Sec1/Munc-18 proteins to mediate fusion events at early endosomes, late endosomes and vacuoles. *Mol. Microbiol.* 99, 199–216.
- Losev, E., Reinke, C.A., Jellen, J., Strongin, D.E., Bevis, B.J., Glick, B.S., 2006. Golgi maturation visualized in living yeast. *Nature* 441, 1002–6.
- Lu, F., Li, S., Jiang, Y., Jiang, J., Fan, H., Lu, G., Deng, D., Dang, S., Zhang, X., Wang, J., Yan, N., 2011. Structure and mechanism of the uracil transporter UraA. *Nature* 472, 243–6.
- Lucena-Agell, D., Galindo, A., Arst, H.N., Peñalva, M.A., 2015. *Aspergillus nidulans* ambient pH signaling does not require endocytosis. *Eukaryot. Cell.* 14, 545–53.
- Luckey, M., 2008. *Membrane Structural Biology*. Cambridge University Press, Cambridge.
- Luo, G., Zhang, J., Guo, W., 2014. The role of Sec3p in secretory vesicle targeting and exocyst complex assembly. *Mol. Biol. Cell* 25, 3813–22.
- Lutzoni, F., Kauff, F., Cox, C.J., McLaughlin, D., Celio, G., Dentinger, B., Padamsee, M., Hibbett, D., James, T.Y., Baloch, E., Grube, M., Reeb, V., Hofstetter, V., Schoch, C., Elizabeth, A.A., 2004. Assembling the fungal tree of life: progress, classification, and evolution of subcellular traits. *Am. J. Bot.* 91, 1446–80.
- Lynch-Day, M.A., Bhandari, D., Menon, S., Huang, J., Cai, H., Bartholomew, C.R., Brumell, J.H., Ferro-Novick, S., Klionsky, D.J., 2010. Trs85 directs a Ypt1 GEF, TRAPP<sub>III</sub>, to the phagophore to promote autophagy. *Proc. Natl. Acad. Sci. U. S. A.* 107, 7811–6.
- Ma, Y., Takeuchi, M., Sugiura, R., Sio, S.O., Kuno, T., 2009. Deletion mutants of AP-1 adaptin subunits display distinct phenotypes in fission yeast. *Genes to Cells* 14, 1015–28.
- MacGurn, J.A., 2014. Garbage on, garbage off: New insights into plasma membrane protein quality control. *Curr. Opin. Cell Biol.* 29, 92–8.
- MacGurn, J.A., Hsu, P.-C., Emr, S.D., 2012. Ubiquitin and Membrane Protein Turnover: From Cradle to Grave. *Annu. Rev. Biochem.* 81, 231–59.
- MacGurn, J.A., Hsu, P.-C., Smolka, M.B., Emr, S.D., 2011. TORC1 regulates endocytosis via Npr1-mediated phosphoinhibition of a ubiquitin ligase adaptor. *Cell* 147, 1104–17.

- Mahadev, R.K., Di Pietro, S.M., Olson, J.M., Piao, H.L., Payne, G.S., Overduin, M., 2007. Structure of Sla1p homology domain 1 and interaction with the NPFxD endocytic internalization motif. *EMBO J.* 26, 1963–71.
- Maldonado-Báez, L., Williamson, C., Donaldson, J.G., 2013. Clathrin-independent endocytosis: A cargo-centric view. *Exp. Cell Res.* 319, 2759–69.
- Manck, R., Ishitsuka, Y., Herrero, S., Takeshita, N., Nienhaus, G.U., Fischer, R., 2015. Genetic evidence for a microtubule-capture mechanism during polarised growth of *Aspergillus nidulans*. *J. Cell Sci.* 128, 3569–82.
- Markina-Iñarrairaegui, A., Pantazopoulou, A., Espeso, E.A., Peñalva, M.A., 2013. The *Aspergillus nidulans* Peripheral ER: Disorganization by ER Stress and Persistence during Mitosis. *PLoS One* 8, e67154
- Martin, R., Walther, A., Wendland, J., 2005. Ras1-Induced Hyphal Development in *Candida albicans* Requires the Formin Bni1. *Eukaryot. Cell* 4, 1712–1724.
- Martzoukou, O., Amillis, S., Zervakou, A., Christoforidis, S., Diallinas, G., 2017. The AP-2 complex has a specialized clathrin-independent role in apical endocytosis and polar growth in fungi. *Elife* 6, e20083.
- Martzoukou, O., Diallinas, G., Amillis, S., 2018. Secretory Vesicle Polar Sorting, Endosome Recycling and Cytoskeleton Organization Require the AP-1 Complex in *Aspergillus nidulans*. *Genetics* e301240.
- Martzoukou, O., Karachaliou, M., Yalelis, V., Leung, J., Byrne, B., Amillis, S., Diallinas, G., 2015. Oligomerization of the UapA Purine Transporter Is Critical for ER-Exit, Plasma Membrane Localization and Turnover. *J. Mol. Biol.* 427, 2679–96.
- Marzluf, G.A., 1997. Genetic regulation of nitrogen metabolism in the fungi. *Microbiol. Mol. Biol. Rev.* 61, 17–32.
- Matsuo, K., Higuchi, Y., Kikuma, T., Arioka, M., Kitamoto, K., 2013. Functional analysis of Abp1p-interacting proteins involved in endocytosis of the MCC component in *Aspergillus oryzae*. *Fungal Genet. Biol.* 56, 125–34.
- Matsuura-Tokita, K., Takeuchi, M., Ichihara, A., Mikuriya, K., Nakano, A., 2006. Live imaging of yeast Golgi cisternal maturation. *Nature* 441, 1007–10.
- Mayor, S., Pagano, R.E., 2007. Pathways of clathrin-independent endocytosis. *Nat. Rev. Mol. Cell Biol.* 8, 603–12.
- McGoldrick, C.A., Gruver, C., May, G.S., 1995. *myoA* of *Aspergillus nidulans* encodes an essential myosin I required for secretion and polarized growth. *J. Cell Biol.* 128, 577–87.
- McMahon, H.T., Wigge, P., Smith, C., 1997. Clathrin interacts specifically with amphiphysin and is displaced by dynamin. *FEBS Lett.* 413, 319–22.
- Meinecke, M., Boucrot, E., Camdere, G., Hon, W.-C., Mittal, R., McMahon, H.T., 2013. Cooperative



- recruitment of dynamin and BIN/amphiphysin/Rvs (BAR) domain-containing proteins leads to GTP-dependent membrane scission. *J. Biol. Chem.* 288, 6651–61.
- Mendoza, P., Díaz, J., Torres, V.A., 2014. On the role of Rab5 in cell migration. *Curr. Mol. Med.* 14, 235–45.
- Merhi, A., Andre, B., 2012. Internal Amino Acids Promote Gap1 Permease Ubiquitylation via TORC1/Npr1/14-3-3-Dependent Control of the Bul Arrestin-Like Adaptors. *Mol. Cell. Biol.* 32, 4510–22.
- Merrifield, C.J., Kaksonen, M., 2014. Endocytic accessory factors and regulation of clathrin-mediated endocytosis. *Cold Spring Harb. Perspect. Biol.* 6, a016733.
- Mills, I.G., Praefcke, G.J.K., Vallis, Y., Peter, B.J., Olesen, L.E., Gallop, J.L., Butler, P.J.G., Evans, P.R., McMahon, H.T., 2003. EpsinR. *J. Cell Biol.* 160, 213–22.
- Miserey-Lenkei, S., Colombo, M.I., 2016. Small RAB GTPases Regulate Multiple Steps of Mitosis. *Front. Cell Dev. Biol.* 4, 2.
- Mogelsvang, S., Marsh, B.J., Ladinsky, M.S., Howell, K.E., 2004. Predicting Function from Structure: 3D Structure Studies of the Mammalian Golgi Complex. *Traffic* 5, 338–45.
- Momany, M., 2005. Growth control and polarization. 43, S23-5.
- Momany, M., 2002. Polarity in filamentous fungi: Establishment, maintenance and new axes. *Curr. Opin. Microbiol.* 5, 580-5.
- Momany, M., Westfall, P.J., Abramowsky, G., 1999. *Aspergillus nidulans* swo mutants show defects in polarity establishment, polarity maintenance and hyphal morphogenesis. *Genetics* 151, 557–67.
- Momany, M., Zhao, J., Lindsey, R., Westfall, P.J., 2001. Characterization of the *Aspergillus nidulans* septin (*asp*) gene family. *Genetics* 157, 969-77.
- Morishita, M., Mendonsa, R., Wright, J., Engebrecht, J.A., 2007. Snc1p v-SNARE transport to the prospore membrane during yeast sporulation is dependent on endosomal retrieval pathways. *Traffic* 8, 1231-45.
- Morozova, N., Liang, Y., Tokarev, A.A., Chen, S.H., Cox, R., Andrejic, J., Lipatova, Z., Sciorra, V.A., Emr, S.D., Segev, N., 2006. TRAPP II subunits are required for the specificity switch of a Ypt–Rab GEF. *Nat. Cell Biol.* 8, 1263–69.
- Morris, N.R., 2003. Nuclear positioning: the means is at the ends. *Curr. Opin. Cell Biol.* 15, 54–9.
- Morris, N.R., Enos, A.P., 1992. Mitotic gold in a mold: *Aspergillus* genetics and the biology of mitosis. *Trends Genet.* 8, 32–7.
- Moseley, J.B., Goode, B.L., 2006. The yeast actin cytoskeleton: from cellular function to biochemical mechanism. *Microbiol. Mol. Biol. Rev.* 70, 605–45.

- Motley, A., Bright, N.A., Seaman, M.N.J., Robinson, M.S., 2003. Clathrin-mediated endocytosis in AP-2-depleted cells. *J. Cell Biol.* 162, 909–18.
- Motoyama, T., Fujiwara, M., Kojima, N., Horiuchi, H., Ohta, A., Takagi, M., 1997. The *Aspergillus nidulans* genes *chsA* and *chsD* encode chitin synthases which have redundant functions in conidia formation [corrected and republished article originally appeared in *Mol Gen Genet* 1996 Jun; 251:442-50]. *Mol. Gen. Genet.* 253, 520–8.
- Motoyama, T., Kojima, N., Horiuchi, H., Ohta, A., Takagi, M., 1994. Isolation of a chitin synthase gene (*chsC*) of *Aspergillus nidulans*. *Biosci. Biotechnol. Biochem.* 58, 2254–7.
- Mouriño-Pérez, R.R., 2013. Septum development in filamentous ascomycetes. *Fungal Biol. Rev.* 27, 1-9.
- Munn, A.L., 2001. Molecular requirements for the internalisation step of endocytosis: insights from yeast. *Biochim. Biophys. Acta* 1535, 236–57.
- Mutterer, J., Zinck, E., 2013. Quick-and-clean article figures with FigureJ. *J. Microsc.* 252, 89–91.
- Nagata, K.-I., Kawajiri, A., Matsui, S., Takagishi, M., Shiromizu, T., Saitoh, N., Izawa, I., Kiyono, T., Itoh, T.J., Hotani, H., Inagaki, M., 2003. Filament formation of MSF-A, a mammalian septin, in human mammary epithelial cells depends on interactions with microtubules. *J. Biol. Chem.* 278, 18538–43.
- Nakagawa, T., Setou, M., Seog, D.H., Ogasawara, K., Dohmae, N., Takio, K., Hirokawa, N., 2000. A novel motor, KIF13A, transports mannose-6-phosphate receptor to plasma membrane through direct interaction with AP-1 complex. *Cell* 1103, 569-81.
- Ng, A.Y.E., Ng, A.Q.E., Zhang, D., 2018. ER-PM Contacts Restrict Exocytic Sites for Polarized Morphogenesis. *Curr. Biol.* 28, 146-53.
- Nichols, B., 2009. Endocytosis of lipid-anchored proteins: excluding GEECs from the crowd. *J. Cell Biol.* 186, 457–9.
- Nielsen, E., Severin, F., Backer, J.M., Hyman, A.A., Zerial, M., 1999. Rab5 regulates motility of early endosomes on microtubules. *Nat. Cell Biol.* 1, 376–82.
- Nielsen, M.S., Gustafsen, C., Madsen, P., Nyengaard, J.R., Hermey, G., Bakke, O., Mari, M., Schu, P., Pohlmann, R., Dennes, A., Petersen, C.M., 2007. Sorting by the cytoplasmic domain of the amyloid precursor protein binding receptor SorLA. *Mol. Cell. Biol.* 27, 6842–51.
- Nikko, E., Pelham, H.R.B., 2009. Arrestin-Mediated Endocytosis of Yeast Plasma Membrane Transporters. *Traffic* 10, 1856–67.
- Nikko, E., Sullivan, J.A., Pelham, H.R.B., 2008. Arrestin-like proteins mediate ubiquitination and endocytosis of the yeast metal transporter Smf1. *EMBO Rep.* 9, 1216–21.
- Novick, P., Ferro, S., Schekman, R., 1981. Order of events in the yeast secretory pathway. *Cell* 25, 461–9.

- Novick, P., Field, C., Schekman, R., 1980. Identification of 23 complementation groups required for post-translational events in the yeast secretory pathway. *Cell* 21, 205–15.
- Nyathi, Y., Wilkinson, B.M., Pool, M.R., 2013. Co-translational targeting and translocation of proteins to the endoplasmic reticulum. *Biochim. Biophys. Acta - Mol. Cell Res.* 1833, 2392–402.
- O'Donnell, A.F., Apffel, A., Gardner, R.G., Cyert, M.S., 2010. Alpha-arrestins Aly1 and Aly2 regulate intracellular trafficking in response to nutrient signaling. *Mol. Biol. Cell* 21, 3552–66.
- Oakley, C.E., Oakley, B.R., 1989. Identification of  $\gamma$ -tubulin, a new member of the tubulin superfamily encoded by *mipA* gene of *Aspergillus nidulans*. *Nature* 338, 662–4.
- Oh, Y., Bi, E., 2011. Septin structure and function in yeast and beyond. *Trends Cell Biol.* 21, 141-48.
- Oshero, N., May, G.S., 2001. The molecular mechanisms of conidial germination. *FEMS Microbiol. Lett.* 199, 153–60.
- Pantazopoulou, A., 2016. The Golgi apparatus: insights from filamentous fungi. *Mycologia* 108, 603–22.
- Pantazopoulou, A., Diallinas, G., 2007. Fungal nucleobase transporters. *FEMS Microbiol. Rev.* 31, 657-75.
- Pantazopoulou, A., Peñalva, M., 2009. Organization and dynamics of the *Aspergillus nidulans* Golgi during apical extension and mitosis. *Mol. Biol. Cell* 20, 4335–47.
- Pantazopoulou, A., Peñalva, M.A., 2011. Characterization of *Aspergillus nidulans* RabC/Rab6. *Traffic* 12, 386-406.
- Pantazopoulou, A., Pinar, M., Xiang, X., Penalva, M.A., 2014. Maturation of late Golgi cisternae into RabE<sup>RAB11</sup> exocytic post-Golgi carriers visualized *in vivo*. *Mol. Biol. Cell* 25, 2428–43.
- Paoluzi, S., Castagnoli, L., Lauro, I., Salcini, A.E., Coda, L., Fre', S., Confalonieri, S., Pelicci, P.G., Di Fiore, P.P., Cesareni, G., 1998. Recognition specificity of individual EH domains of mammals and yeast. *EMBO J.* 17, 6541–50.
- Papadaki, G.F., Amillis, S., Diallinas, G., 2017. Substrate Specificity of the FurE Transporter Is Determined by Cytoplasmic Terminal Domain Interactions. *Genetics* 207, e300327.
- Parmar, H.B., Duncan, R., 2016. A novel tribasic Golgi export signal directs cargo protein interaction with activated Rab11 and AP-1–dependent Golgi–plasma membrane trafficking. *Mol. Biol. Cell* 27, 1320–31.
- Patterson, G.H., Hirschberg, K., Polishchuk, R.S., Gerlich, D., Phair, R.D., Lippincott-schwartz, J., 2008. Transport through the Golgi apparatus by rapid partitioning within a two-phase membrane system. *Cell* 133, 1055–67.
- Patwari, P., Lee, R.T., 2012. An expanded family of arrestins regulate metabolism. *Trends Endocrinol. Metab.* 23, 216–22.

- Pearson, C.L., Xu, K., Sharpless, K.E., Harris, S.D., 2004. MesA, a Novel Fungal Protein Required for the Stabilization of Polarity Axes in *Aspergillus nidulans*. *Mol. Biol. Cell* 15, 3658–72.
- Peden, A.A., Oorschot, V., Hesser, B.A., Austin, C.D., Scheller, R.H., Klumperman, J., 2004. Localization of the AP-3 adaptor complex defines a novel endosomal exit site for lysosomal membrane proteins. *J. Cell Biol.* 164, 1065–76.
- Peñalva, M.A., 2015. A lipid-managing program maintains a stout Spitzenkörper. *Mol. Microbiol.* 97, 1–6.
- Peñalva, M.A., 2005. Tracing the endocytic pathway of *Aspergillus nidulans* with FM4-64. *Fungal Genet. Biol.* 42, 963-75.
- Peñalva, M.Á., 2010. Endocytosis in filamentous fungi: Cinderella gets her reward. *Curr. Opin. Microbiol.* 13, 684–92.
- Peñalva, M.A., Zhang, J., Xiang, X., Pantazopoulou, A., 2017. Transport of fungal RAB11 secretory vesicles involves myosin-5, dynein/dynactin/p25, and kinesin-1 and is independent of kinesin-3. *Mol. Biol. Cell* 28, 947–61.
- Phelan, J.P., Millson, S.H., Parker, P.J., Piper, P.W., Cooke, F.T., 2006. Fab1p and AP-1 are required for trafficking of endogenously ubiquitylated cargoes to the vacuole lumen in *S. cerevisiae*. *J. Cell Sci.* 119, 4225–34.
- Piao, H.L., Machado, I.M.P., Payne, G.S., 2007. NPFXD-mediated endocytosis is required for polarity and function of a yeast cell wall stress sensor. *Mol. Biol. Cell* 18, 57–65.
- Pinar, M., Arst, H.N., Pantazopoulou, A., Tagua, V.G., de los Ríos, V., Rodríguez-Salarichs, J., Díaz, J.F., Peñalva, M.A., 2015. TRAPP2 regulates exocytic Golgi exit by mediating nucleotide exchange on the Ypt31 ortholog RabE<sup>RAB11</sup>. *Proc. Natl. Acad. Sci.* 112, 4346–51.
- Pinar, M., Pantazopoulou, A., Arst, H.N., Peñalva, M.A., 2013a. Acute inactivation of the *Aspergillus nidulans* Golgi membrane fusion machinery: Correlation of apical extension arrest and tip swelling with cisternal disorganization. *Mol. Microbiol.* 89, 228-48.
- Pinar, M., Pantazopoulou, A., Peñalva, M.A., 2013b. Live-cell imaging of *Aspergillus nidulans* autophagy: RAB1 dependence, Golgi independence and ER involvement. *Autophagy* 9, 1024–43.
- Pocha, S.M., Wassmer, T., Niehage, C., Hoflack, B., Knust, E., 2011. Retromer Controls Epithelial Cell Polarity by Trafficking the Apical Determinant Crumbs. *Curr. Biol.* 21, 1111–17.
- Prescianotto-Baschong, C., Riezman, H., 2002. Ordering of compartments in the yeast endocytic pathway. *Traffic* 3, 37–49.
- Prigent, M., Dubois, T., Raposo, G., Derrien, V., Tenza, D., Rossé, C., Camonis, J., Chavrier, P., 2003. ARF6 controls post-endocytic recycling through its downstream exocyst complex effector. *J. Cell Biol.* 163, 1111–21.
- Prosser, D.C., Drivas, T.G., Maldonado-Báez, L., Wendland, B., 2011. Existence of a novel clathrin-

- independent endocytic pathway in yeast that depends on Rho1 and formin. *J. Cell Biol.* 195, 657–71.
- Proszynski, T.J., Klemm, R.W., Gravert, M., Hsu, P.P., Gloor, Y., Wagner, J., Kozak, K., Grabner, H., Walzer, K., Bagnat, M., Simons, K., Walch-Solimena, C., 2005. A genome-wide visual screen reveals a role for sphingolipids and ergosterol in cell surface delivery in yeast. *Proc. Natl. Acad. Sci. U. S. A.* 102, 17981–6.
- Pruyne, D., Bretscher, A., 2000. Polarization of cell growth in yeast. *J. Cell Sci.* 113, 571–85.
- Pruyne, D.W., Schott, D.H., Bretscher, A., 1998. Tropomyosin-containing actin cables direct the Myo2p-dependent polarized delivery of secretory vesicles in budding yeast. *J. Cell Biol.* 143, 1931–45.
- Purushothaman, L.K., Arlt, H., Kuhlee, A., Raunser, S., Ungermann, C., 2017. Retromer-driven membrane tubulation separates endosomal recycling from Rab7/Ypt7-dependent fusion. *Mol. Biol. Cell.* 28, 783-91.
- Pyle, E., Kalli, A.C., Amillis, S., Hall, Z., Lau, A.M., Hanyaloglu, A.C., Diallinas, G., Byrne, B., Politis, A., 2018. Structural Lipids Enable the Formation of Functional Oligomers of the Eukaryotic Purine Symporter UapA. *Cell Chem. Biol.* 25, 1–9.
- Qualmann, B., Kessels, M.M., Kelly, R.B., 2000. Molecular links between endocytosis and the actin cytoskeleton. *J. Cell Biol.* 150, F111-6.
- Ramakrishnan, N.A., Drescher, M.J., Drescher, D.G., 2012. The SNARE complex in neuronal and sensory cells. *Mol. Cell. Neurosci.* 50, 58–69.
- Rasband, M.N., 2010. The axon initial segment and the maintenance of neuronal polarity. *Nat. Rev. Neurosci.* 11, 552–62.
- Raths, S., Rohrer, J., Crausaz, F., Riezman, H., 1993. end3 and end4: two mutants defective in receptor-mediated and fluid-phase endocytosis in *Saccharomyces cerevisiae*. *J. Cell Biol.* 120, 55–65.
- Ravagnani, A., Gorfinkiel, L., Langdon, T., Diallinas, G., Adjadj, E., Demais, S., Gorton, D., Arst, H.N., Scazzocchio, C., 1997. Subtle hydrophobic interactions between the seventh residue of the zinc finger loop and the first base of an HGATAR sequence determine promoter-specific recognition by the *Aspergillus nidulans* GATA factor AreA. *EMBO J.* 16, 3974–86.
- Reider, A., Wendland, B., 2011. Endocytic adaptors--social networking at the plasma membrane. *J. Cell Sci.* 124, 1613–22.
- Rein, U., Andag, U., Duden, R., Schmitt, H.D., Spang, A., 2002. ARF-GAP-mediated interaction between the ER-Golgi v-SNAREs and the COPI coat. *J. Cell Biol.* 157, 395–404.
- Renard, H.-F., Demaegd, D., Guerriat, B., Morsomme, P., 2010. Efficient ER Exit and Vacuole Targeting of Yeast Sna2p Require Two Tyrosine-Based Sorting Motifs. *Traffic* 11, 931–46.
- Requena, N., Alberti-Segui, C., Winzenburg, E., Horn, C., Schliwa, M., Philippsen, P., Liese, R., Fischer,

- R., 2001. Genetic evidence for a microtubule-destabilizing effect of conventional kinesin and analysis of its consequences for the control of nuclear distribution in *Aspergillus nidulans*. *Mol. Microbiol.* 42, 121–32.
- Ridley, A.J., Schwartz, M.A., Burridge, K., Firtel, R.A., Ginsberg, M.H., Borisy, G., Parsons, J.T., Horwitz, A.R., 2003. Cell Migration: Integrating Signals from Front to Back. *Science* 302, 1704–9.
- Rink, J., Ghigo, E., Kalaidzidis, Y., Zerial, M., 2005. Rab Conversion as a Mechanism of Progression from Early to Late Endosomes. *Cell* 122, 735–49.
- Riquelme, M., Aguirre, J., Bartnicki-García, S., Braus, G.H., Feldbrügge, M., Fleig, U., Hansberg, W., Herrera-Estrella, A., Kämper, J., Kück, U., Mouriño-Pérez, R.R., Takeshita, N., Fischer, R., 2018. Fungal Morphogenesis, from the Polarized Growth of Hyphae to Complex Reproduction and Infection Structures. *Microbiol. Mol. Biol. Rev.* 82, e00068-17.
- Riquelme, M., Fischer, R., Bartnicki-García, S., 2003. Apical growth and mitosis are independent processes in *Aspergillus nidulans*. *Protoplasma* 222, 211-5.
- Riquelme, M., Martínez-Núñez, L., 2016. Hyphal ontogeny in *Neurospora crassa*: a model organism for all seasons. *F1000Research* 5, 2801.
- Riquelme, M., Reynaga-Peña, C.G., Gierz, G., Bartnicki-García, S., 1998. What determines growth direction in fungal hyphae? *Fungal Genet. Biol.* 24, 101–9.
- Riquelme, M., Sánchez-León, E., 2014. The Spitzenkörper: A choreographer of fungal growth and morphogenesis. *Curr. Opin. Microbiol.* 20, 27-33.
- Robinson, D.G., Pimpl, P., 2014. Clathrin and post-Golgi trafficking: a very complicated issue. *Trends Plant Sci.* 19, 134–9.
- Robinson, M.S., 2015. Forty Years of Clathrin-coated Vesicles. *Traffic* 16, 1210-38.
- Robinson, M.S., 2004. Adaptable adaptors for coated vesicles. *Trends Cell Biol.* 14, 167–74.
- Robinson, M.S., Bonifacino, J.S., 2001. Adaptor-related proteins. *Curr Opin Cell Biol* 13, 444–53.
- Rothman, J.E., McNew, J.A., Parlati, F., Fukuda, R., Johnston, R.J., Paz, K., Paumet, F., Söllner, T.H., 2000. Compartmental specificity of cellular membrane fusion encoded in SNARE proteins. *Nature* 407, 153–9.
- Ruggiano, A., Foresti, O., Carvalho, P., 2014. ER-associated degradation: Protein quality control and beyond. *J. Cell Biol.* 204, 869–79.
- Salaün, C., James, D.J., Chamberlain, L.H., 2004. Lipid rafts and the regulation of exocytosis. *Traffic* 5, 255-64.
- Salogiannis, J., Reck-Peterson, S.L., 2017. Hitchhiking: A Non-Canonical Mode of Microtubule-Based Transport. *Trends Cell Biol.* 27, 141-50.
- Salom, D., Palczewski, K., 2011. Structural Biology of Membrane Proteins, in: Production of

- Membrane Proteins. Wiley-VCH Verlag GmbH & Co. KGaA, Weinheim, Germany, pp. 249–73.
- Sambrook, J., Fritsch, E.F. and Maniatis, T., 1989. Molecular cloning: a laboratory manual. Cold Spring Harbor Laboratory Press.
- Sampson, K., Heath, I.B., 2005. The dynamic behaviour of microtubules and their contributions to hyphal tip growth in *Aspergillus nidulans*. *Microbiology* 151, 1543–55.
- Sanchatjate, S., Schekman, R., 2006. Chs5/6 Complex: A Multiprotein Complex That Interacts with and Conveys Chitin Synthase III from the *Trans*-Golgi Network to the Cell Surface. *Mol. Biol. Cell* 17, 4157–66.
- Sandvig, K., Pust, S., Skotland, T., van Deurs, B., 2011. Clathrin-independent endocytosis: Mechanisms and function. *Curr. Opin. Cell Biol.* 23, 413-20.
- Sant, D.G., Tupe, S.G., Ramana, C. V., Deshpande, M. V., 2016. Fungal cell membrane—promising drug target for antifungal therapy. *J. Appl. Microbiol.* 121, 1498-510.
- Sato, K., Nakano, A., 2007. Mechanisms of COPII vesicle formation and protein sorting. *FEBS Lett.* 581, 2076-82.
- Scazzocchio, C., 2009. *Aspergillus*: A Multifaceted Genus, in: Schaechter, M. (Ed.), *Encyclopedia of Microbiology*. Elsevier, Oxford, pp. 401–21.
- Scazzocchio, C., 2006. *Aspergillus* genomes: secret sex and the secrets of sex. *Trends Genet.* 22, 521–5.
- Scazzocchio, C., 1992. Control of gene expression in the catabolic pathways of *Aspergillus nidulans*: a personal and biased account. *Biotechnology* 23, 43–68.
- Scazzocchio, C., Sdrin, N., Ong, G., 1982. Positive regulation in a eukaryote, a study of the *uaY* gene of *Aspergillus nidulans*: I. Characterization of alleles, dominance and complementation studies, and a fine structure map of the *uaY-oxpA* cluster. *Genetics* 100, 185–208.
- Schmidt, M.R., Maritzen, T., Kukhtina, V., Higman, V.A., Doglio, L., Barak, N.N., Strauss, H., Oschkinat, H., Dotti, C.G., Haucke, V., 2009. Regulation of endosomal membrane traffic by a Gadkin/AP-1/kinesin KIF5 complex. *Proc. Natl. Acad. Sci. U. S. A.* 106, 15344–9.
- Schneggenburger, R., Neher, E., 2005. Presynaptic calcium and control of vesicle fusion. *Curr. Opin. Neurobiol.* 15, 266–74.
- Schoch, C.L., Aist, J.R., Yoder, O.C., Gillian Turgeon, B., 2003. A complete inventory of fungal kinesins in representative filamentous ascomycetes. *Fungal Genet. Biol.* 39, 1–15.
- Schotman, H., Karhinen, L., Rabouille, C., 2009. Integrins mediate their unconventional, mechanical-stress-induced secretion via RhoA and PINCH in *Drosophila*. *J. Cell Sci.* 122, 2662–72.
- Schoustra, S.E., Debets, A.J.M., Slakhorst, M., Hoekstra, R.F., 2007. Mitotic recombination accelerates adaptation in the fungus *Aspergillus nidulans*. *PLoS Genet.* 3, e68.

- Schultzhaus, Z., Johnson, T., Shaw, B.D., 2017a. Clathrin localization and dynamics in *Aspergillus nidulans*. *Mol. Microbiol.* 103, 299–318.
- Schultzhaus, Z., Quintanilla, L., Hilton, A., Shaw, B.D., 2016. Live Cell Imaging of Actin Dynamics in the Filamentous Fungus *Aspergillus nidulans*. *Microsc. Microanal.* 22, 264–74.
- Schultzhaus, Z., Shaw, B.D., 2016. The flippase DnfB is cargo of fimbrin-associated endocytosis in *Aspergillus nidulans*, and likely recycles through the late golgi. *Commun. Integr. Biol.* 9, 1-3.
- Schultzhaus, Z., Yan, H., Shaw, B.D., 2015. *Aspergillus nidulans* flippase DnfA is cargo of the endocytic collar and plays complementary roles in growth and phosphatidylserine asymmetry with another flippase, DnfB. *Mol. Microbiol.* 97, 18-32.
- Schultzhaus, Z., Zheng, W., Wang, Z., Mouriño-Pérez, R., Shaw, B., 2017b. Phospholipid flippases DnfA and DnfB exhibit differential dynamics within the *A. nidulans* Spitzenkörper. *Fungal Genet. Biol.* 99, 26-8.
- Schultzhaus, Z.S., Shaw, B.D., 2015. Endocytosis and exocytosis in hyphal growth. *Fungal Biol. Rev.* 29, 43-53.
- Seaman, M.N.J., 2012. The retromer complex - endosomal protein recycling and beyond. *J. Cell Sci.* 125, 4693-702.
- Seaman, M.N.J., 2004. Cargo-selective endosomal sorting for retrieval to the Golgi requires retromer. *J. Cell Biol.* 165, 111–22.
- Sebastian, T.T., Baldrige, R.D., Xu, P., Graham, T.R., 2012. Phospholipid flippases: building asymmetric membranes and transport vesicles. *Biochim. Biophys. Acta* 1821, 1068–77.
- Seiler, S., Justa-Schuch, D., 2010. Conserved components, but distinct mechanisms for the placement and assembly of the cell division machinery in unicellular and filamentous ascomycetes. *Mol. Microbiol.* 78, 1058–76.
- Seiler, S., Plamann, M., Schliwa, M., 1999. Kinesin and dynein mutants provide novel insights into the roles of vesicle traffic during cell morphogenesis in *Neurospora*. *Curr. Biol.* 9, 779–85.
- Seybold, C., Schiebel, E., 2013. Spindle pole bodies. *Curr. Biol.* 23, R858–60.
- Sharpless, K.E., Harris, S.D., 2002. Functional Characterization and Localization of the *Aspergillus nidulans* Formin SEPA. *Mol. Biol. Cell* 13, 469–79.
- Shi, X., Sha, Y., Kaminskyj, S., 2004. *Aspergillus nidulans hypA* regulates morphogenesis through the secretion pathway. *Fungal Genet. Biol.* 41, 75–88.
- Shoji, J. ya, Kikuma, T., Kitamoto, K., 2014. Vesicle trafficking, organelle functions, and unconventional secretion in fungal physiology and pathogenicity. *Curr. Opin. Microbiol.* 20, 1-9.
- Shvets, E., Bitsikas, V., Howard, G., Hansen, C.G., Nichols, B.J., 2015. Dynamic caveolae exclude bulk



- membrane proteins and are required for sorting of excess glycosphingolipids. *Nat. Commun.* 6, 6867.
- Simon, S.M., 2008. Golgi Governance : The Third Way. *Cell* 133, 951–53.
- Simons, K., Ikonen, E., 1997. Functional rafts in cell membranes. *Nature* 387, 569-72.
- Siniossoglou, S., Peak-Chew, S.Y., Pelham, H.R., 2000. Ric1p and Rgp1p form a complex that catalyses nucleotide exchange on Ypt6p. *EMBO J.* 19, 4885–94.
- Siniossoglou, S., Pelham, H.R., 2001. An effector of Ypt6p binds the SNARE Tlg1p and mediates selective fusion of vesicles with late Golgi membranes. *EMBO J.* 20, 5991–8.
- Sioupouli, G., Lambrinidis, G., Mikros, E., Amillis, S., Diallinas, G., 2017. Cryptic purine transporters in *Aspergillus nidulans* reveal the role of specific residues in the evolution of specificity in the NCS1 family. *Mol. Microbiol.* 103, 319–32.
- Skruzny, M., Desfosses, A., Prinz, S., Dodonova, S.O., Gieras, A., Uetrecht, C., Jakobi, A.J., Abella, M., Hagen, W.J.H., Schulz, J., Meijers, R., Rybin, V., Briggs, J.A.G., Sachse, C., Kaksonen, M., 2015. An Organized Co-assembly of Clathrin Adaptors Is Essential for Endocytosis. *Dev. Cell.* 33, 150-62.
- Slepnev, V.I., De Camilli, P., 2000. Accessory factors in clathrin-dependent synaptic vesicle endocytosis. *Nat. Rev. Neurosci.* 1, 161–72.
- Smith, M.G., Swamy, S.R., Pon, L.A., 2001. The life cycle of actin patches in mating yeast. *J. Cell Sci.* 114, 1505–13.
- Smith, M.H., Ploegh, H.L., Weissman, J.S., 2011. Road to ruin: targeting proteins for degradation in the endoplasmic reticulum. *Science* 334, 1086–90.
- Söllner, T., Bennett, M.K., Whiteheart, S.W., Scheller, R.H., Rothman, J.E., 1993. A protein assembly-disassembly pathway in vitro that may correspond to sequential steps of synaptic vesicle docking, activation, and fusion. *Cell* 75, 409–18.
- Sorkin, A., 2004. Cargo recognition during clathrin-mediated endocytosis: a team effort. *Curr. Opin. Cell Biol.* 16, 392–99.
- Sparkes, I.A., Frigerio, L., Tolley, N., Hawes, C., 2009. The plant endoplasmic reticulum: a cell-wide web. *Biochem. J.* 423, 145–55.
- Specht, C.A., Liu, Y., Robbins, P.W., Bulawa, C.E., Iartchouk, N., Winter, K.R., Riggle, P.J., Rhodes, J.C., Dodge, C.L., Culp, D.W., Borgia, P.T., 1996. The *chsD* and *chsE* Genes of *Aspergillus nidulans* and Their Roles in Chitin Synthesis. *Fungal Genet. Biol.* 20, 153–67.
- Spiliotis, E.T., 2018. Spatial effects - site-specific regulation of actin and microtubule organization by septin GTPases. *J. Cell Sci.* 131, jcs207555.
- Spiliotis, E.T., Gladfelter, A.S., 2012. Spatial Guidance of Cell Asymmetry: Septin GTPases Show the Way. *Traffic* 13, 195-203.

- Springael, J.-Y., De Craene, J.-O., André, B., 1999. The Yeast Npi1/Rsp5 Ubiquitin Ligase Lacking Its N-Terminal C2 Domain Is Competent for Ubiquitination but Not for Subsequent Endocytosis of the Gap1 Permease. *Biochem. Biophys. Res. Commun.* 257, 561–6.
- Springer, S., Malkus, P., Borchert, B., Wellbrock, U., Duden, R., Schekman, R., 2014. Regulated Oligomerization Induces Uptake of a Membrane Protein into COPII Vesicles Independent of Its Cytosolic Tail. *Traffic* 15, 531–45.
- Stamenova, S.D., French, M.E., He, Y., Francis, S.A., Kramer, Z.B., Hicke, L., 2007. Ubiquitin binds to and regulates a subset of SH3 domains. *Mol. Cell* 25, 273–84.
- Steinberg, G., 2014. Endocytosis and early endosome motility in filamentous fungi. *Curr. Opin. Microbiol.* 20, 10–18.
- Steinberg, G., 2007. On the move: endosomes in fungal growth and pathogenicity. *Nat. Rev. Microbiol.* 5, 309–16.
- Steinberg, G., Peñalva, M.A., Riquelme, M., Wösten, H.A., Harris, S.D., 2017. Cell Biology of Hyphal Growth. *Microbiol Spectr.* 5, e0034.
- Stenbeck, G., Harter, C., Brecht, A., Herrmann, D., Lottspeich, F., Orci, L., Wieland, F.T., 1993. beta'-COP, a novel subunit of coatamer. *EMBO J.* 12, 2841–5.
- Sun, Y., Leong, N.T., Wong, T., Drubin, D.G., 2015. A Pan1/End3/Sla1 complex links Arp2/3-mediated actin assembly to sites of clathrin-mediated endocytosis. *Mol. Biol. Cell* 26, 3841–56.
- Surka, M.C., Tsang, C.W., Trimble, W.S., 2002. The mammalian septin MSF localizes with microtubules and is required for completion of cytokinesis. *Mol. Biol. Cell* 13, 3532–45.
- Swart, K., Debets, A.J.M., Slakhorst, M., Holub, E.F., Hoekstra, R.F., Bos, C.J., 2001. Genetic analysis in the asexual fungus *Aspergillus niger*. *Acta Biol. Hung.* 52, 335–43.
- Szul, T., Sztul, E., 2011. COPII and COPI Traffic at the ER-Golgi Interface. *Physiology* 26, 348–64.
- Szymkiewicz, I., Kowanetz, K., Soubeyran, P., Dinarina, A., Lipkowitz, S., Dikic, I., 2002. CIN85 Participates in Cbl-b-mediated Down-regulation of Receptor Tyrosine Kinases. *J. Biol. Chem.* 277, 39666–39672.
- Tabuchi, M., Yanatori, I., Kawai, Y., Kishi, F., 2010. Retromer-mediated direct sorting is required for proper endosomal recycling of the mammalian iron transporter DMT1. *J. Cell Sci.* 123, 756–66.
- Taheri-Talesh, N., Horio, T., Araujo-Bazán, L., Dou, X., Espeso, E.A., Peñ, M.A., Osmani, S.A., Oakley, B.R., 2008. The Tip Growth Apparatus of *Aspergillus nidulans*. *Mol. Biol. Cell* 19, 1439–49.
- Taheri-Talesh, N., Xiong, Y., Oakley, B.R., Yu, J.-H., 2012. The Functions of Myosin II and Myosin V Homologs in Tip Growth and Septation in *Aspergillus nidulans*. *PLoS One* 7, e31218.
- Tahirovic, S., Bradke, F., 2009. Neuronal polarity. *Cold Spring Harb. Perspect. Biol.* 1, a001644.
- Takeshita, N., 2018. Oscillatory fungal cell growth. *Fungal Genet. Biol.* 110, 10–4.

- Takeshita, N., Diallinas, G., Fischer, R., 2012. The role of flotillin FloA and stomatin StoA in the maintenance of apical sterol-rich membrane domains and polarity in the filamentous fungus *Aspergillus nidulans*. *Mol. Microbiol.* 83, 1136-52.
- Takeshita, N., Evangelinos, M., Zhou, L., Serizawa, T., Somera-Fajardo, R.A., Lu, L., Takaya, N., Nienhaus, G.U., Fischer, R., 2017. Pulses of Ca<sup>2+</sup> coordinate actin assembly and exocytosis for stepwise cell extension. *Proc. Natl. Acad. Sci.* 114, 5701–6.
- Takeshita, N., Fischer, R., 2011. On the role of microtubules, cell end markers, and septal microtubule organizing centres on site selection for polar growth in *Aspergillus nidulans*. *Fungal Biol.* 115, 506–17.
- Takeshita, N., Higashitsuji, Y., Konzack, S., Fischer, R., 2008. Apical Sterol-rich Membranes Are Essential for Localizing Cell End Markers That Determine Growth Directionality in the Filamentous Fungus *Aspergillus nidulans*. *Mol. Biol. Cell* 19, 339–51.
- Takeshita, N., Manck, R., Grün, N., de Vega, S.H., Fischer, R., 2014. Interdependence of the actin and the microtubule cytoskeleton during fungal growth. *Curr. Opin. Microbiol.* 20, 34-41.
- Takeshita, N., Mania, D., Herrero, S., Ishitsuka, Y., Nienhaus, G.U., Podolski, M., Howard, J., Fischer, R., 2013. The cell-end marker TeaA and the microtubule polymerase AlpA contribute to microtubule guidance at the hyphal tip cortex of *Aspergillus nidulans* to provide polarity maintenance. *J. Cell Sci.* 126, 5400–11.
- Takeshita, N., Ohta, A., Horiuchi, H., 2002. *csmA*, a gene encoding a class V chitin synthase with a myosin motor-like domain of *Aspergillus nidulans*, is translated as a single polypeptide and regulated in response to osmotic conditions. *Biochem. Biophys. Res. Commun.* 298, 103–9.
- Takeshita, N., Wernet, V., Tsuizaki, M., Grün, N., Hoshi, H.O., Ohta, A., Fischer, R., Horiuchi, H., 2015. Transportation of *Aspergillus nidulans* class III and V chitin synthases to the hyphal tips depends on conventional kinesin. *PLoS One* 10, e125937.
- Tavoularis, S., Scazzocchio, C., Sophianopoulou, V., 2001. Functional Expression and Cellular Localization of a Green Fluorescent Protein-Tagged Proline Transporter in *Aspergillus nidulans*. *Fungal Genet. Biol.* 33, 115–25.
- Taylor, M.J., Perrais, D., Merrifield, C.J., 2011. A high precision survey of the molecular dynamics of mammalian clathrin-mediated endocytosis. *PLoS Biol.* 9, e1000604.
- TCDB, 2018. Transporter Classification Database [http://www.tcdb.org/disease\\_explore.php](http://www.tcdb.org/disease_explore.php) Transporters and Diseases (accessed 11 July 2018).
- TerBush, D.R., Maurice, T., Roth, D., Novick, P., 1996. The Exocyst is a multiprotein complex required for exocytosis in *Saccharomyces cerevisiae*. *EMBO J.* 15, 6483–94.
- TerBush, D.R., Novick, P., 1995. Sec6, Sec8, and Sec15 are components of a multisubunit complex which localizes to small bud tips in *Saccharomyces cerevisiae*. *J. Cell Biol.* 130, 299–312.
- Todd, R.B., Hynes, M.J., Davis, M.A., 2007. Genetic manipulation of *Aspergillus nidulans*: Meiotic

- progeny for genetic analysis and strain construction. *Nat. Protoc.* 2, 811-21.
- Tokarev, A.A., Alfonso, A., Segev, N., 2009. Overview of Intracellular Compartments and Trafficking Pathways, in: *Trafficking Inside Cells*. Springer New York, New York, NY, pp. 3–14.
- Tomás, M., Martínez-Alonso, E., Ballesta, J., Martínez-Menárguez, J.A., 2010. Regulation of ER-Golgi intermediate compartment tubulation and mobility by COPI coats, motor proteins and microtubules. *Traffic* 11, 616–25.
- Torralba, S., Raudaskoski, M., Pedregosa, A.M., Laborda, F., 1998. Effect of cytochalasin A on apical growth, actin cytoskeleton organization and enzyme secretion in *Aspergillus nidulans*. *Microbiology* 144, 45–53.
- Toshima, J.Y., Toshima, J., Kaksonen, M., Martin, A.C., King, D.S., Drubin, D.G., 2006. Spatial dynamics of receptor-mediated endocytic trafficking in budding yeast revealed by using fluorescent alpha-factor derivatives. *Proc. Natl. Acad. Sci. U. S. A.* 103, 5793–8.
- Trahey, M., Hay, J.C., 2010. Transport vesicle uncoating: it's later than you think. *F1000 Biol. Rep.* 2, 47.
- TransportDB, 2018. Genomic Comparisons of Membrane Transport Systems. <http://www.membranetransport.org/> (accessed 11 July 2018).
- Traub, L.M., 2009. Tickets to ride: selecting cargo for clathrin-regulated internalization. *Nat. Rev. Mol. Cell Biol.* 10, 583–96.
- Trautwein, M., Schindler, C., Gauss, R., Dengjel, J., Hartmann, E., Spang, A., 2006. Arf1p, Chs5p and the ChAPs are required for export of specialized cargo from the Golgi. *EMBO J.* 25, 943–54.
- Travers, K.J., Patil, C.K., Wodicka, L., Lockhart, D.J., Weissman, J.S., Walter, P., 2000. Functional and genomic analyses reveal an essential coordination between the unfolded protein response and ER-associated degradation. *Cell* 101, 249–58.
- Tsukada, M., Will, E., Gallwitz, D., 1999. Structural and functional analysis of a novel coiled-coil protein involved in Ypt6 GTPase-regulated protein transport in yeast. *Mol. Biol. Cell* 10, 63–75.
- Ungewickell, E., Ungewickell, H., Holstein, S.E.H., Lindner, R., Prasad, K., Barouch, W., Martini, B., Greene, L.E., Eisenberg, E., 1995. Role of auxilin in uncoating clathrin-coated vesicles. *Nature* 378, 632–35.
- Upadhyay, S., Shaw, B.D., 2008. The role of actin, fimbrin and endocytosis in growth of hyphae in *Aspergillus nidulans*. *Mol. Microbiol.* 68, 690–705.
- Valdez-Taubas, J., Diallinas, G., Scazzocchio, C., Rosa, A.L., 2000. Protein expression and subcellular localization of the general purine transporter UapC from *Aspergillus nidulans*. *Fungal Genet. Biol.* 30, 105–13.
- Valdez-Taubas, J., Harispe, L., Scazzocchio, C., Gorfinkiel, L., Rosa, A.L., 2004. Ammonium-induced internalisation of UapC, the general purine permease from *Aspergillus nidulans*. *Fungal Genet. Biol.* 41, 42–51.

- Valdez-Taubas, J., Pelham, H.R.B., 2003. Slow Diffusion of Proteins in the Yeast Plasma Membrane Allows Polarity to Be Maintained by Endocytic Cycling. *Curr. Biol.* 13, 1636–40.
- Valdivia, R.H., Baggott, D., Chuang, J.S., Schekman, R.W., 2002. The yeast clathrin adaptor protein complex 1 is required for the efficient retention of a subset of late Golgi membrane proteins. *Dev. Cell* 2, 283–94.
- van der Rest, M.E., de Vries, Y., Poolman, B., Konings, W.N., 1995. Overexpression of Mal61p in *Saccharomyces cerevisiae* and characterization of maltose transport in artificial membranes. *J. Bacteriol.* 177, 5440–6.
- van der Sluijs, P., Hull, M., Webster, P., Mâle, P., Goud, B., Mellman, I., 1992. The small GTP-binding protein rab4 controls an early sorting event on the endocytic pathway. *Cell* 70, 729–40.
- van Meer, G., Voelker, D.R., Feigenson, G.W., 2008. Membrane lipids: where they are and how they behave. *Nat. Rev. Mol. Cell Biol.* 9, 112–24.
- Varshavsky, A., 2012. The Ubiquitin System, an Immense Realm. *Annu. Rev. Biochem.* 81, 167–76.
- Verdín, J., Bartnicki-Garcia, S., Riquelme, M., 2009. Functional stratification of the Spitzenkörper of *Neurospora crassa*. *Mol. Microbiol.* 74, 1044–53.
- Versele, M., Thorner, J., 2005. Some assembly required: yeast septins provide the instruction manual. *Trends Cell Biol.* 15, 414–24.
- Virag, A., Griffiths, A.J.F., 2004. A mutation in the *Neurospora crassa* actin gene results in multiple defects in tip growth and branching. *Fungal Genet. Biol.* 41, 213–25.
- Virag, A., Harris, S.D., 2006. Functional Characterization of *Aspergillus nidulans* Homologues of *Saccharomyces cerevisiae* Spa2 and Bud6. *Eukaryot. Cell* 5, 881–95.
- Vlanti, A., Amillis, S., Koukaki, M., Diallinas, G., 2006. A novel-type substrate-selectivity filter and ER-exit determinants in the UapA purine transporter. *J. Mol. Biol.* 357, 808–19.
- Vlanti, A., Diallinas, G., 2008. The *Aspergillus nidulans* FcyB cytosine-purine scavenger is highly expressed during germination and in reproductive compartments and is downregulated by endocytosis. *Mol. Microbiol.* 68, 959–77.
- Vonderheit, A., Helenius, A., 2005. Rab7 Associates with Early Endosomes to Mediate Sorting and Transport of Semliki Forest Virus to Late Endosomes. *PLoS Biol.* 3, e233.
- Waddle, J.A., Karpova, T.S., Waterston, R.H., Cooper, J.A., 1996. Movement of cortical actin patches in yeast. *J. Cell Biol.* 132, 861–70.
- Wang, C.-W., Hamamoto, S., Orci, L., Schekman, R., 2006. Exomer: A coat complex for transport of select membrane proteins from the trans-Golgi network to the plasma membrane in yeast. *J. Cell Biol.* 174, 973–83.
- Wang, J., Sun, H.-Q., Macia, E., Kirchhausen, T., Watson, H., Bonifacino, J.S., Yin, H.L., 2007. PI4P promotes the recruitment of the GGA adaptor proteins to the trans-Golgi network and

- regulates their recognition of the ubiquitin sorting signal. *Mol. Biol. Cell* 18, 2646–55.
- Weil, C.F., Oakley, C.E., Oakley, B.R., 1986. Isolation of mip (microtubule-interacting protein) mutations of *Aspergillus nidulans*. *Mol. Cell. Biol.* 6, 2963–8.
- Weinberg, J., Drubin, D.G., 2012. Clathrin-mediated endocytosis in budding yeast. *Trends Cell Biol.* 22, 1–13.
- Wendland, J., 2001. Comparison of morphogenetic networks of filamentous fungi and yeast. *Fungal Genet. Biol.* 34, 63-82.
- West, M., Zurek, N., Hoenger, A., Voeltz, G.K., 2011. A 3D analysis of yeast ER structure reveals how ER domains are organized by membrane curvature. *J. Cell Biol.* 193, 333–46.
- Westfall, P.J., Momany, M., 2002. *Aspergillus nidulans* septin AspB plays pre- and postmitotic roles in septum, branch, and conidiophore development. *Mol. Biol. Cell* 13, 110–8.
- Whitfield, S.T., Burston, H.E., Bean, B.D.M., Raghuram, N., Maldonado-Báez, L., Davey, M., Wendland, B., Conibear, E., 2016. The alternate AP-1 adaptor subunit Apm2 interacts with the Mil1 regulatory protein and confers differential cargo sorting. *Mol. Biol. Cell* 27, 588–98.
- Whyte, J.R.C., Munro, S., 2002. Vesicle tethering complexes in membrane traffic. *J. Cell Sci.* 115, 2627–37.
- Wolkow, T.D., Harris, S.D., Hamer, J.E., 1996. Cytokinesis in *Aspergillus nidulans* is controlled by cell size, nuclear positioning and mitosis. *J. Cell Sci.* 109, 2179–88.
- Wollman, R., Meyer, T., 2012. Coordinated oscillations in cortical actin and Ca<sup>2+</sup> correlate with cycles of vesicle secretion. *Nat. Cell Biol.* 14, 1261–1269.
- Wu, B., Guo, W., 2015. The Exocyst at a Glance. *J. Cell Sci.* 128, 2957–64.
- Wu, J., Miller, B.L., 1997. *Aspergillus* Asexual Reproduction and Sexual Reproduction Are Differentially Affected by Transcriptional and Translational Mechanisms Regulating stunted Gene Expression. *Mol. Cell. Biol.* 17, 6191–201.
- Wu, Y., Whiteus, C., Xu, C.S., Hayworth, K.J., Weinberg, R.J., Hess, H.F., De Camilli, P., 2017. Contacts between the endoplasmic reticulum and other membranes in neurons. *Proc. Natl. Acad. Sci. U. S. A.* 114, E4859–67.
- Xiang, X., Fischer, R., 2004. Nuclear migration and positioning in filamentous fungi. *Fungal Genet. Biol.* 41, 411–9.
- Xiang, X., Plamann, M., 2003. Cytoskeleton and motor proteins in filamentous fungi. *Curr. Opin. Microbiol.* 6, 628-33.
- Xing, Y., Böcking, T., Wolf, M., Grigorieff, N., Kirchhausen, T., Harrison, S.C., 2010. Structure of clathrin coat with bound Hsc70 and auxilin: mechanism of Hsc70-facilitated disassembly. *EMBO J.* 29, 655–65.

- Yamashita, A., Singh, S.K., Kawate, T., Jin, Y., Gouaux, E., 2005. Crystal structure of a bacterial homologue of Na<sup>+</sup>/Cl<sup>-</sup>-dependent neurotransmitter transporters. *Nature* 437, 215–23.
- Yamashita, R.A., May, G.S., 1998. Constitutive activation of endocytosis by mutation of *myoA*, the myosin I gene of *Aspergillus nidulans*. *J. Biol. Chem.* 273, 14644–8.
- Yamashita, R.A., Osherov, N., May, G.S., 2000. Localization of Wild Type and Mutant Class I Myosin Proteins in *Aspergillus nidulans* Using GFP-Fusion Proteins. *Cell Motil. Cytoskelet.* 45, 163–72.
- Yang, Y., El-Ganiny, A.M., Bray, G.E., Sanders, D.A.R., Kaminskyj, S.G.W., 2008. *Aspergillus nidulans* hypB encodes a Sec7-domain protein important for hyphal morphogenesis. *Fungal Genet. Biol.* 45, 749–59.
- Yernool, D., Boudker, O., Jin, Y., Gouaux, E., 2004. Structure of a glutamate transporter homologue from *Pyrococcus horikoshii*. *Nature* 431, 811–18.
- Yeung, B.G., Payne, G.S., 2001. Clathrin Interactions with C-Terminal Regions of the Yeast AP-1 beta and gamma Subunits are Important for AP-1 Association with Clathrin Coats. *Traffic* 2, 565–76.
- Yildirim, M. a, Goh, K.-I., Cusick, M.E., Barabási, A.-L., Vidal, M., 2007. Drug-target network. *Nat. Biotechnol.* 25, 1119–26.
- Youn, J.-Y., Friesen, H., Kishimoto, T., Henne, W.M., Kurat, C.F., Ye, W., Ceccarelli, D.F., Sicheri, F., Kohlwein, S.D., McMahon, H.T., Andrews, B.J., 2010. Dissecting BAR Domain Function in the Yeast Amphiphysins Rvs161 and Rvs167 during Endocytosis. *Mol. Biol. Cell* 21, 3054–69.
- Yu, X., Yang, G., Yan, C., Baylon, J.L., Jiang, J., Fan, H., Lu, G., Hasegawa, K., Okumura, H., Wang, T., Tajkhorshid, E., Li, S., Yan, N., 2017. Dimeric structure of the uracil:proton symporter UraA provides mechanistic insights into the SLC4/23/26 transporters. *Cell Res.* 27, 1020–33.
- Yu, Y., Li, C., Kita, A., Katayama, Y., Kubouchi, K., Udo, M., Imanaka, Y., Ueda, S., Masuko, T., Sugiura, R., 2013. Sip1, an AP-1 Accessory Protein in Fission Yeast, Is Required for Localization of Rho3 GTPase. *PLoS One* 8, e68488.
- Zamyatnin, A.A., Solovyev, A.G., Bozhkov, P. V., Valkonen, J.P.T., Morozov, S.Y., Savenkov, E.I., 2006. Assessment of the integral membrane protein topology in living cells. *Plant J.* 46, 145–54.
- Zeigerer, A., Gilleron, J., Bogorad, R.L., Marsico, G., Nonaka, H., Seifert, S., Epstein-Barash, H., Kuchimanchi, S., Peng, C.G., Ruda, V.M., Conte-Zerial, P. Del, Hengstler, J.G., Kalaidzidis, Y., Koteliansky, V., Zerial, M., 2012. Rab5 is necessary for the biogenesis of the endolysosomal system *in vivo*. *Nature* 485, 465–70.
- Zekert, N., Fischer, R., 2009. The *Aspergillus nidulans* Kinesin-3 UncA Motor Moves Vesicles along a Subpopulation of Microtubules. *Mol. Biol. Evol.* 20, 673–84.
- Zerial, M., McBride, H., 2001. Rab proteins as membrane organizers. *Nat. Rev. Mol. Cell Biol.* 2, 107–17.
- Zhang, J., Li, S., Fischer, R., Xiang, X., 2003. Accumulation of cytoplasmic dynein and dynactin at microtubule plus ends in *Aspergillus nidulans* is kinesin dependent. *Mol. Biol. Cell* 14, 1479–88.

- Zhang, J., Qiu, R., Arst, H.N., Peñalva, M.A., Xiang, X., 2014. HookA is a novel dynein–early endosome linker critical for cargo movement *in vivo*. *J. Cell Biol.* 204, 1009–26.
- Zhang, J., Tan, K., Wu, X., Chen, G., Sun, J., Reck-Peterson, S.L., Hammer, J.A., Xiang, X., 2011. *Aspergillus* myosin-V supports polarized growth in the absence of microtubule-based transport. *PLoS One* 6, e28575
- Zhang, X.-M., Ellis, S., Sriratana, A., Mitchell, C.A., Rowe, T., 2004. Sec15 Is an Effector for the Rab11 GTPase in Mammalian Cells. *J. Biol. Chem.* 279, 43027–34.
- Zhou, L., Evangelinos, M., Wernet, V., Eckert, A.F., Ishitsuka, Y., Fischer, R., Nienhaus, G.U., Takeshita, N., 2018. Superresolution and pulse-chase imaging reveal the role of vesicle transport in polar growth of fungal cells. *Sci. Adv.* 4, e1701798.




## CHAPTER 6

## APPENDIX

6.1 *Curriculum vitae*

## PERSONAL INFORMATION

Olga Martzoukou

 Athinas 2, 14121 Athens (Greece) +306944338427 o.martzoukou@biol.uoa.gr

Date of birth 18 Dec 1988

## WORK EXPERIENCE

Mar 2017–Jun 2018

**Biologist****Faculty of Biology, National and Kapodistrian University of Athens**PhD Fellow. Research project: "*Secretory Vesicle Polar Sorting, Endosome Recycling and Cytoskeleton Organization Require the AP-1 Complex in Aspergillus nidulans*".

May 2016–Feb 2017

**Biologist****Faculty of Biology, National and Kapodistrian University of Athens**PhD Fellow. Research project: "*The AP-2 complex has a specialized endocytic role serving polar growth by apical extension in filamentous fungi: specialization by evolutionary truncation*".

Mar 2015–Apr 2016

**Biologist****Faculty of Biology, National and Kapodistrian University of Athens**PhD Fellow. Research project: "*Transporter oligomerization, trafficking & turnover: novel insights from a model microbial eukaryote*".

Jun 2014–Feb 2015

**Biologist****"Alexander Fleming" Biomedical Sciences Research Center**PhD Fellow. Title of Project: "*Development of genetic and genomic analyses technologies using the transposon MINOS and applications in model organisms*" (MINOS-Thales).

Director: Dr. Savvakis, Supervisor: Prof. Diallinas.

Sep 2011–Apr 2012

**Undergraduate student****Biomedical Research Foundation of the Academy of Athens**BSc thesis. Division of Basic Neuroscience, Field of Neurodegenerative Disorders. Research project: "*The role of Calcium dishomeostasis in the toxicity of ASYN in SH-SY5Y human neuroblastoma cells*".

Supervisors: Assoc. Prof. Papazafiri, Investigator/Assoc. Prof. Vekrellis

## EDUCATION AND TRAINING

Sep 2006–May 2014

**B.Sc., General Biology (With Honours)**

Faculty of Biology, School of Science, National and Kapodistrian University of Athens, Αθήνα (Greece)

Upper Second-Class Honours (2:1) (8.24/10). Ranked 1st in graduating class - Pronounced the

Graduate's Oath at the Graduate Student Oath Ceremony.

May 2014–Jul 2018

### PhD Candidate

Molecular Microbiology Laboratory, Department of Botany, Faculty of Biology,  
School of Science, National and Kapodistrian University of Athens, Athens  
(Greece)

PhD thesis title: "A study of membrane protein trafficking, endocytosis and degradation  
through the development of new genetic and biochemical tools"

Supervisor: Prof. G. Diallinas

### PERSONAL SKILLS

---

Mother tongue

Greek

Foreign languages

English

Certificate of Proficiency in English (ECPE) - C2 level

French

DELFL 1er degré, (Unités A1-A4) - B2 level

Russian

Elementary proficiency

Job-related skills

- Basic molecular biology, microbiology and genetics techniques (UV mutagenesis, Molecular cloning, Bacterial transformation, *A. nidulans* protoplast transformation)
- Genomic DNA, plasmid DNA and protein isolation
- SDS-PAGE, agarose gel electrophoresis
- Western blotting, silver staining, Ni<sup>2+</sup>-affinity Chromatography
- Immunoprecipitation
- PCR (conventional, primer design)
- Epifluorescence microscopy
- SH-SY5Y cell culture

Digital skills

- Excellent knowledge of Microsoft Windows, Microsoft Office
- Excellent knowledge of Adobe Photoshop, Adobe Bridge
- ImageJ, ICY, Graphpad Prism, Pymol, ZEN
- Bioinformatics tools (BLAST, MultAlin, ClustalW, Perl, ExpASY)

### ADDITIONAL INFORMATION

---

Publications

- **Martzoukou O.**, Diallinas G, Amillis S. Secretory Vesicle Polar Sorting, Endosome Recycling and Cytoskeleton Organization Require the AP-1 Complex in *Aspergillus nidulans*. **Genetics**. 2018 Jun 20.
- **Martzoukou O.**, Amillis S., Zervakou A., Christoforidis S., Diallinas G. The AP-2 complex has a specialized clathrin-independent role in apical endocytosis and polar growth in fungi. **eLIFE**. 2017 Feb 21.
- Evangelinos M., **Martzoukou O.**, Choroziou K., Amillis S., Diallinas G. BsdA<sup>Bsd2</sup>-dependent vacuolar turnover of a misfolded version of the UapA transporter along the secretory pathway: prominent role of selective autophagy. **Mol Microbiol**. 2016 Feb 24.
- **Martzoukou O.**, Karachaliou M., Yaelis V., Leung J., Byrne B., Amillis S., Diallinas G. Oligomerization of the UapA Purine Transporter Is Critical for ER-Exit, Plasma Membrane Localization and Turnover. **J Mol Biol**. 2015 Aug 14.

## Seminars

- **FEBS Advanced microscopy course 2017** (Van Leeuwenhoek Centre for Advanced Microscopy, Amsterdam, The Netherlands, 11-16 Jun, 2017) "Functional imaging of cellular signals", Awarded YTF travel grant.
- **RIIP International Course 2016** (Hellenic Pasteur Institute, Athens Greece, Jul 4-8, 2016) "Cell Biology and infection: Digital Image Processing/Analysis Tools for Quantitative Light Microscopy Imaging"

## Honours and awards

- **Doctoral Scholarship** May 2017 - May 2018. Hellenic State Scholarships Foundation (IKY) - National Strategic Reference Framework (NSRF 2014-2020).
- **Travel Grant** Jun 2017. YTF Grant for my participation in the FEBS Advanced Course "Functional imaging of cellular signals", held in Amsterdam, The Netherlands.
- **Travel Grant** Nov 2016. Hellenic Society for Biochemistry and Molecular Biology (HSBMB) - Travel Grant for my participation in the 67th Panhellenic Conference of the Hellenic Society for Biochemistry and Molecular Biology held in Ioannina, Greece.
- **Travel Grant** Feb 2016. COST-Proteostasis Network - Travel grant for my participation in the 7th autophagy & proteasome workshop, held in Clermont-Ferrand, France.
- **ACCI Essay Award – 2<sup>nd</sup> Prize** 2011. Athens Chamber of Commerce and Industry - "Competitiveness and social cohesion, the big challenge".

## Conferences

- 14th European Conference on Fungal Genetics (Haifa, Israel, 25-28 Feb 2018) "Roles of the AP-2 and AP-1 complexes in apical cargo sorting, endocytosis and polar growth in fungi", [G.Diallinas](#), [O.Martzoukou](#), [A.Zervakou](#), [S.Amillis](#)
- EMBO Conference - Cell Biology of the Neuron: Polarity Plasticity and Regeneration (Heraklion Crete, 7-10 May 2017), "The AP-2 complex has a specialized clathrin-independent role in polarity maintenance in Fungi" [O.Martzoukou](#), [S.Amillis](#), [A.Zervakou](#), [S.Christoforidis](#), [G.Diallinas](#)
- 67th Panhellenic Conference of the HSBMB (Ioannina, 25th-27th Nov, 2016), [Travel Grant for Poster Presentation](#), P110: "The AP-2 complex has a specialized endocytic role serving polar growth by apical extension in filamentous fungi: specialization by evolutionary truncation" [O.Martzoukou](#), [S.Amillis](#), [A.Zervakou](#), [G.Diallinas](#)
- Unconventional Protein and Membrane Traffic Independent Meeting (Lecce, Italy, 4 - 7 Oct 2016) "Unconventional clathrin-independent role of the AP-2 complex in apical endocytosis and polar growth in fungi" [O.Martzoukou](#), [S.Amillis](#), [A.Zervakou](#), [G.Diallinas](#)
- 34<sup>th</sup> Small Meeting on Yeast Transport and Energetics (MAICH, Crete Greece, Aug 29-Sep 1 2016), [Oral Presentation](#): "The AP-2 complex has a specialized endocytic role serving polar growth by apical extension in filamentous fungi: specialization by evolutionary truncation" [O.Martzoukou](#), [S.Amillis](#), [A.Zervakou](#), [G.Diallinas](#)
- 7<sup>th</sup> Autophagy & Proteasome Workshop (Clermont-Ferrand, France, 6-8 Apr 2016), [Travel Grant for Poster Presentation](#): "BsdA-dependent vacuolar turnover of a misfolded version of the UapA transporter along the secretory pathway: Prominent role of selective autophagy" [M. Evangelinos](#), [O. Martzoukou](#), [K. Choroziou](#), [S. Amillis](#), [G. Diallinas](#)
- 6<sup>th</sup> Mikrobiokosmos Conference (National Hellenic Research Foundation, Athens, Apr 3-5, 2015), [Poster Presentation](#): "Oligomerization of the UapA purine transporter is critical for ER-exit and plasma membrane localization" [O.Martzoukou](#), [M.Karachaliou](#), [S. Amillis](#), [V. Yalelis](#), [J. Leung](#), [B. Byrne](#), [G. Diallinas](#)
- 65th Panhellenic Conference of the HSBMB (Thessaloniki, Thessaloniki Concert Hall, 28th -30th November, 2014), [Oral Presentation](#), ID 18: "*Oligomerization of the UapA purine transporter is critical for ER-exit and sorting into plasma membrane microdomains*" [O.Martzoukou](#), [M.Karachaliou](#), [S. Amillis](#), [V. Yalelis](#), [J. Leung](#), [B. Byrne](#), [G. Diallinas](#)
- 1<sup>st</sup> Proteostasis Meeting 2014, COST Proteostasis Network (Valencia, Centro de Investigación Principe Felipe, 5-7 Nov 2014), Short T-4 WG4: "*The role of transmembrane cargo oligomerization in ER-exit and membrane organization*" [O. Martzoukou](#), [M. Karachaliou](#), [M. Evangelinos](#), [S. Amillis](#), [G. Diallinas](#)
- 33<sup>rd</sup> Scientific Conference of HSBC (Edessa May 19-21, 2011), [Oral and Poster Presentation](#): "Dysregulation of Ca<sup>2+</sup> homeostasis contributes to a-synuclein conferred toxicity to human SH-SY5Y neuroblastoma cells" [O. Martzoukou](#), [K. Melachroinou](#), [K. Vekrellis](#), [P. Papazafiri](#)

## 6.2 LIST OF OLIFONUCLEOTIDES USED IN THIS STUDY

Oligonucleotides	Sequence 5'-3'
<b><i>ap2<sup>o</sup>Δ::AFpyrG / ap2<sup>o</sup>Δ::AFriboB</i></b>	
ap2σ 5' SphI F	CGCGGCATGCGAAGAATCGCGTTAATGTCTCGGG
ap2σ 5' SpeI R	CGCGACTAGTCTTGTCTGATGGCCCGCGGTGCTC
ap2σ 3' SpeI F	CGCGACTAGTTTATTGTTTCATGTGATAAGTGAACGG
ap2σ 3' NdeI R	CGCGCATATGGAGATACCAGGAGTAGCCCC
AFriboB SpeI F	CGCGACTAGTAAGCTTGATATCACAATCAGC
AFriboB SpeI R	CGCGACTAGTCCCGGGCTGCAGGAATTCGATAAG
AFpyrG SpeI F	CGCGACTAGTGCCTCAAACAATGCTCTTCACCCTC
AFpyrG SpeI R	CGCGACTAGTACTGTCTGAGAGGAGGCACTGATGCG
<b><i>ap2<sup>o</sup>-(5xGA)GFP::AFpyrG / ap2<sup>o</sup>-(5xGA)mRFP::AFpyrG</i></b>	
ap2 <sup>o</sup> 5' KpnI F	CGCGGGTACCGTCGTAATATAACTCGTACAGCAATC
ap2 <sup>o</sup> 3' ORF SpeI NS R	CGCGACTAGTCTCCAGTTTATCCAGATGTTCTAGCC
ap2 <sup>o</sup> 3' SpeI F	CGCGACTAGTTTATTGTTTCATGTGATAAGTGAACGGCTGC
ap2 <sup>o</sup> 3' NotI R	CGCGGCGGCCGCGAGATACCAGGAGTAGCCCCGCTG
5xGA SpeI F	CGCGACTAGTGGAGCTGGTGCAGGCGCTGGAGCCGGTGCC
AFpyrG SpeI R	CGCGACTAGTACTGTCTGAGAGGAGGCACTGATGCG
<b><i>ap2<sup>h</sup>Δ::AFpyrG / ap2<sup>h</sup>Δ::AFriboB</i></b>	
ap2 <sup>h</sup> 5' KpnI F	CGCGGGTACCCCTTACCCTCATCCGACTCCGAAC
ap2 <sup>h</sup> 5' SpeI R	CGCGACTAGTTTTGCGATTAGGCGTGGTGGTAAGG
ap2 <sup>h</sup> 3' SpeI F	CGCGACTAGTGGCTGATGCTAACATATATATTTGCG
ap2 <sup>h</sup> 3' NotI R	CGCGGCGGCCGCCCACTCCCACTGATGACAGTCAATG
AFriboB SpeI F	CGCGACTAGTAAGCTTGATATCACAATCAGC
AFriboB SpeI R	CGCGACTAGTCCCGGGCTGCAGGAATTCGATAAG
AFpyrG SpeI F	CGCGACTAGTGCCTCAAACAATGCTCTTCACCCTC
AFpyrG SpeI R	CGCGACTAGTACTGTCTGAGAGGAGGCACTGATGCG
<b><i>ap3<sup>o</sup>Δ::AFpyrG</i></b>	
ap3 <sup>o</sup> 5' ApaI F	CGCGGGGCCCGAGTCCGCACTCAGCAGCTC
ap3 <sup>o</sup> 5' SpeI R	CGCGACTAGTTTCGGATATAGGCTGATGGTG
ap3 <sup>o</sup> 3' SpeI F	CGCGACTAGTGGTTGTACAGCTTCTCCGTG
ap3 <sup>o</sup> 3' NdeI R	CGCGCATATGGGGAAGGAAAACAACCAGCTC
<b><i>thiA<sub>p</sub>-ap1<sup>o</sup>::AFriboB</i></b>	
ap1 <sup>o</sup> 5' ApaI F	CGCGGGGCCCGCAGGACTGCTGTTAGGGAGC
ap1σ 5' SphI R	CGCGGCATGCTTTGCGATTGTGGGAAAAGTCGTGG
ap1 <sup>o</sup> ORF SacII F	CGGCCCGCGATGGCAATTCAGTAAGACTTGAATGC
ap1 <sup>o</sup> 3' NotI R	CGCGGCGGCCGCGGGTAAGTATCCCTGTTGTCTTAGC
AFriboB SphI F	CCCGGGCATGCAAGCTTGATATCACAATCAGC
AFriboB SphI R	CCCGGGCATGCCCCGGGCTGCAGGAATTCGATAAG

thiA <sub>p</sub> SphI F	CGGGCATGCCGACCTGGCACCTACAGAAGAATCC
thiA <sub>p</sub> FLAG SacII R	CGCGCCGCGGCTTGTTCATCGTCGTCCTTGTAGTCCAT GTTGACTCAGTTCAATGGTTCGACTATAG
<b><i>claLΔ::AFpyrG</i></b>	
claL 5' NcoI F	CGGCCATGGCCCTCGCATAATCGCATCCTCTAC
claL 5' SpeI R	CGCGACTAGTCCTCCTTGAATATAGGATATACGACG
claL 3' SpeI F	CGCGACTAGTCTGCTGATTCCCTAATATTCTGGCC
claL 3' NotI R	CGCGGCGGCCGCCAGGTCAAAGCCGAGGTTGAAG
AFpyrG SpeI F	CGCGACTAGTGCCTCAAACAATGCTCTTCACCCTC
AFpyrG SpeI R	CGCGACTAGTACTGTCTGAGAGGAGGCACTGATGCG
<b><i>thiA<sub>p</sub>-claL::AFpyrG / thiA<sub>p</sub>-claL::AFriboB</i></b>	
claL 5' NcoI F	CGGCCATGGCCCTCGCATAATCGCATCCTCTAC
claL 5' SpeI R	CGCGACTAGTCCTCCTTGAATATAGGATATACGACG
claL ORF SpeI F	CGCGACTAGTATGGCTGACCGCTTCCCGTCGTTG
claL 3' NotI R	CGCGGCGGCCGCCAGGTCAAAGCCGAGGTTGAAG
thiA <sub>p</sub> XbaI F	CGCGTCTAGACGACCTGGCACCTACAGAAGAATCC
thiA <sub>p</sub> SpeI R	CGCGACTAGTGTGACTCAGTTCAATGGTTCGAC
AFpyrG SpeI F	CGCGACTAGTGCCTCAAACAATGCTCTTCACCCTC
AFpyrG XbaI R	CGCGTCTAGAACTGTCTGAGAGGAGGCACTGATGCG
AFriboB SpeI F	CGCGACTAGTAAGCTTGATATCACAATCAGC
AFriboB XbaI R	CGCGTCTAGACCCGGGCTGCAGGAATTCGATAAG
<b><i>claL-(5xGA)GFP::AFpyrG</i></b>	
ClaL 5' NcoI F	CGGCCATGGCCCTCGCATAATCGCATCCTCTAC
ClaL ORF NS SpeI R	CGCGACTAGTAACCCCGCTAGCGCCAGGCGCTC
ClaL 3' SpeI F	CGCGACTAGTCTGCTGATTCCCTAATATTCTGGCC
ClaL 3' NotI R	CGCGGCGGCCGCCAGGTCAAAGCCGAGGTTGAAG
5xGA SpeI F	CGCGACTAGTGGAGCTGGTGCAGGCGCTGGAGCCGGTGCC
AFpyrG SpeI R	CGCGACTAGTACTGTCTGAGAGGAGGCACTGATGCG
<b><i>claHΔ::AFpyrG</i></b>	
ClaH 5' ApaI F	CGCGGGGCCCCGCAAGTACCTTGTCTTCAAATGG
ClaH 5' SpeI R	GATGACTAGTGTGACGCTGTGAAGTTG
ClaH ORF2 SpeI F	CGCGACTAGTGAAGAACTGGGTGATATTGTCCGACC
ClaH ORF2 NotI R	CGCGGCGGCCGCGCAGTGGCAACAACCTGGTCAATGAGAG
AFpyrG SpeI F	CGCGACTAGTGCCTCAAACAATGCTCTTCACCCTC
AFpyrG SpeI R	CGCGACTAGTACTGTCTGAGAGGAGGCACTGATGCG
<b><i>thiA<sub>p</sub>-claH::AFpyroA</i></b>	
ClaH 5' ApaI F	CGCGGGGCCCCGCAAGTACCTTGTCTTCAAATGG
ClaH 5' SpeI R	GATGACTAGTGTGACGCTGTGAAGTTG
ClaH ORF SpeI F	CGCGACTAGTATGGCTCCTCTTCCCATCAAATCAC

ClaH ORF NotI R	CGCGGCGGCCGCTTGTGATTGTCTCTGGCGTCCTC
AFpyroA XbaI F	CGCGTCTAGAGGACATCAGATGCTGGATTAC
AFpyroA SpeI R	CGCGACTAGTGCAGTGTCTACATAATGAAGG
thiA <sub>p</sub> XbaI F	CGCGTCTAGACGACCTGGCACCTACAGAAGAATCC
thiA <sub>p</sub> SpeI R	CGCGACTAGTGTGACTCAGTTCAATGGTTCGAC
<b><i>thiA<sub>p</sub>-basA::AFpyrG / thiA<sub>p</sub>-basA::AFriboB</i></b>	
basA 5' ApaI F	GCGCGGGCCCGAGCGTACTCTTCAGGTGACCCTTG
basA 5' SpeI R2	CGCGACTAGTGCAACGTCAATTAGGACGTCGG
basA ORF SpeI F	CGCGACTAGTATGGCTACAAACACAACCTTGCTCTATGATC
basA 3' NotI R	CGCGGCGGCCGCCGTGGATCGGTTAGGCATGCATATG
thiA <sub>p</sub> XbaI F	CGCGTCTAGACGACCTGGCACCTACAGAAGAATCC
thiA <sub>p</sub> SpeI R	CGCGACTAGTGTGACTCAGTTCAATGGTTCGAC
AFpyrG SpeI F	CGCGACTAGTGCCTCAAACAATGCTCTTCACCCTC
AFpyrG XbaI R	CGCGTCTAGAACTGTCTGAGAGGAGGCACTGATGCG
AFriboB SpeI F	CGCGACTAGTAAGCTTGATATCACAATCAGC
AFriboB XbaI R	CGCGTCTAGACCCGGGCTGCAGGAATTCGATAAG
<b><i>thiA<sub>p</sub>-slaB::AFpyrG / thiA<sub>p</sub>-slaB::AFriboB</i></b>	
slaB 5 KpnI F2	CGCGGGTACCCGATGATTGAGATATCCCGCCGGTC
slaB 5 SpeI R3	CGCGACTAGTCAGACCTCCTAAAGTCCGCGGGTCTTG
slaB ORF SpeI F2	CGCGACTAGTATGAGTCGGTAGGTAATTGGGGACTG
slaB ORF SacI R	CGCGGAGCTCCATACTTGCTTCTCCATGTGTTGAC
thiA <sub>p</sub> XbaI F	CGCGTCTAGACGACCTGGCACCTACAGAAGAATCC
thiA <sub>p</sub> SpeI R	CGCGACTAGTGTGACTCAGTTCAATGGTTCGAC
AFpyrG SpeI F	CGCGACTAGTGCCTCAAACAATGCTCTTCACCCTC
AFpyrG XbaI R	CGCGTCTAGAACTGTCTGAGAGGAGGCACTGATGCG
AFriboB SpeI F	CGCGACTAGTAAGCTTGATATCACAATCAGC
AFriboB XbaI R	CGCGTCTAGACCCGGGCTGCAGGAATTCGATAAG
<b><i>(alcA<sub>p</sub>)-uapA-YFP<sub>C</sub>/uapA-YFP<sub>N</sub></i></b>	
YFP <sub>C</sub> F	CGTCTAGAGGCCGACAAGCAGAAGAAC
YFP <sub>C</sub> R	CGTCTAGAGCTTGTACAGCTCGTCCATG
YFP <sub>N</sub> F	CGTCTAGAGGTGAGCAAGGGCGAGGAG
YFP <sub>N</sub> R	CGTCTAGAGCATGATATAGACGTTGTGGCTG
3'UTR BglII R	GCAGATCTGCAATAACTCAACCGCCTTCCC
alcA NotI F	CGCGGCGGCCGCTAAGTCCCTTCGATTTCTCC
alcA BamHI R	CGGGATCCATTTGAGGCGAGGTGATAG
exp Bam F	CGCGGGATCCCTCCATCCATTCAACCGAC
GFP SpeIR	CGACTAGTTTACTTGTACAGCTCGTCCATG
<b><i>alcA<sub>p</sub>-uapA-His</i></b>	
expBam F	CGCGGGATCCCTCCATCCATTCAACCGAC
Ctail His Spe R	CCGACTAGTTAATGATGATGATGATGATGGTGGTGGTGGTGTCTAGAGACTTCAGCAG GCATGATTGCG

uapAXbaR NS II	GCTCTAGAGCCTGCTTGTCTGATACTC
<b><i>alcA<sub>p</sub>-DYDY/A-GFP</i></b>	
expBam F	CGCGGGATCCCTCCATCCATTCAACCGAC
uapAXbaR NS II	GCTCTAGAGCCTGCTTGTCTGATACTC
GFP Xba F2	CGTCTAGAATGGTGAGCAAGGGCGAG
GFP SpeI R	CGACTAGTTTACTTGTACAGCTCGTCCATG
<b><i>PrnB-YFPc</i></b>	
PrnB ORF XhoI F	CGCGCTCGAGCATGGCCTCTATTGTCTGGTTTGTC
PrnB ORF EcoRV R	CGCGGATATCAAAAATCCACCACCAGACTCGCTCC
YFPc link EcoRV F	CGCGGATATCGGAGGTATGGCCGACAAGCAGAAGAACG
GFP Pst R	AA CTGCAG TTA CTT GTA CAG CTC GTC CAT GC
panB PstI F	CGCGCTGCAGGGATTGGGAGGTGACACAG
PrnB 3 BamHI F	CGCGGGATCCATAGACGACTATATATATAACAGGACTATATACTG
PrnB 3 NotI R	CGCGGCGGCCCGCCGAGATTACCTCCAATGGCAGTG
<b><i>pGEM ap1<sup>σ</sup>-(5xGA)GFP::AFpyrG / pGEM ap1<sup>σ</sup>-(5xGA)mRFP::AFpyrG</i></b>	
ap1 <sup>σ</sup> 5' Apal F	CGCGGGGCCCCATTTCTAGGGATGTGGCTGCAGG
ap1 <sup>σ</sup> 3' ORF XbaI NS R	CGCGTCTAGACATGATCTTCGTAACCACATCTTCCTC
ap1 <sup>σ</sup> 3' XbaI F	CGCGTCTAGAGAGCGTCATCAGTGATACGCTTC
ap1 <sup>σ</sup> 3' NotI R	CGCGGCGGCCCGGGCGTGAGGATACCATCATCGAATG
5xGA XbaI F	CGCGTCTAGAGGAGCTGGTGCAGGCGCTGGAGCCGGTGCC
AFpyrG XbaI R	CGCGTCTAGAACTGTCTGAGAGGAGGCACTGATGCG
<b><i>pBS SKII claH<sup>-(5xGA)GFP::AFpyrG</sup></i></b>	
claH ORF KpnI F	CGCGGGTACCCTGGACCAGCTCGCAGAACTGAAG
claH ORF NS SpeI R	CGCGACTAGTGAAAGGACGGAACCCCGTGGCCTG
claH 3' SpeI F	CGCGACTAGTGCTCGCCTTGTCTTTTTGAGGGGTAG
claH 3' NotI R	CGCGGCGGCCCGGACAATCAGATTGACAGGGAGGG
5xGA SpeI F	CGCGACTAGTGAGCTGGTGCAGGCGCTGGAGCCGGTGCC
AFpyrG SpeI R	CGCGACTAGTACTGTCTGAGAGGAGGCACTGATGCG
<b><i>pGEM thiA<sub>p</sub>::ap1<sup>H</sup>::AFriboB</i></b>	
ap1 <sup>H</sup> 5' Apal F	CGCGGGGCCCCGATACGAGCGTTCCAGGACCGCTTC
ap1 <sup>H</sup> 5' SpeI R	CGCGACTAGTGCACTTGCCACAACCTCCAGTATTC
ap1 <sup>H</sup> ORF SpeI F	CGCGACTAGTATGGCATCGGCGGTTTTCTTCCTAG
ap1 <sup>H</sup> ORF NotI R	CGCGGCGGCCCGCCAGTTCTGCGGCATAAGAACTC
AFriboB SpeI R	CCGGACTAGTCCCGGGCTGCAGGAATTCGATAAG
thiA <sub>p</sub> SpeI R	CGCGACTAGTGTGACTCAGTTCAATGGTTTCGAC
<b><i>pGEM thiA<sub>p</sub>::ap1<sup>B</sup>::AFriboB</i></b>	
ap1 <sup>B</sup> 5' Apal F	CGCGGGGCCCCAAGGCCGATTGGAACCGAGC
ap1 <sup>B</sup> 5' SpeI R	CGCGACTAGTGCCCTACTAGCTCTTCAGTCATAC
ap1 <sup>B</sup> ORF SpeI F	CGCGACTAGTATGGATTGTTGTGGACAGGGGAAG
ap1 <sup>B</sup> ORF NotI R	CGCGGCGGCCCGCCACCAGAGAACAACCTCGGAATACC
AFriboB SpeI R	CCGGACTAGTCCCGGGCTGCAGGAATTCGATAAG
thiA <sub>p</sub> SpeI R	CGCGACTAGTGTGACTCAGTTCAATGGTTTCGAC
<b><i>pGEM thiA<sub>p</sub>::rabE::AFriboB</i></b>	
rabE 5' Apal F	CGCGGGGCCCCGAGTGCGGAATATGCCTCCACCTG
rabE 5' SpeI R	CGCGACTAGTAGCGAACAGTTAGATACACCGAGGG
rabE ORF SpeI F	CGCGACTAGTATGGCTAACGACGAGTATGATGTGAG
rabE 3' NotI R	CGCGGCGGCCCGCTAACGGCTGAGCTAGGTTACTG

AFriboB SpeI R	CCGGACTAGTCCCGGGCTGCAGGAATTCGATAAG
thiA <sub>p</sub> SpeI R	CGCGACTAGTGTTGACTCAGTTCAATGGTTTCGAC
<b>pGEM thiA<sub>p</sub>::rabC::AFriboB</b>	
rabC 5' ApaI F	CGCGGGGCCCCAACGGTTATGGACGAAGTATGCGG
rabC 5' XbaI R	CGCGTCTAGAGGGGACAAGAGGTCAAATGTAAAGTC
rabC ORF XbaI F	CGCGTCTAGAATGGCTTCAGCATCAACGGCCGGG
rabC 3' NotI R	CGCGGCGGCCGCGGGTAGTTGAGCTCAACGCATCG
AFriboB XbaI R	CCGGTCTAGACCCGGGCTGCAGGAATTCGATAAG
thiA <sub>p</sub> XbaI R	CGCGTCTAGAGTTGACTCAGTTCAATGGTTTCGAC
<b>pGEM uncA::AFriboB</b>	
uncA 5' ApaI F	CGCGGGGCCCCCGGCATAAGCTCTTCCTGCTATG
uncA 5' SpeI R	CGCGACTAGTGGAGCGGACAACAAATTGCGCACG
uncA 3' SpeI F	CGCGACTAGTCGCCGATGAAGATCTACACTGGAATG
uncA 3' NotI R	CGCGGCGGCCGCTGGTGTGAAGTCGTCTGTCGTC
AFriboB SpeI F	CCGGACTAGTAAGCTTGATATCACAATCAGCTTTTC
AFriboB SpeI R	CCGGACTAGTCCCGGGCTGCAGGAATTCGATAAG
<b>pGEM GFP-rabE::AFpyrG</b>	
rabE 5' ApaI F	CGCGGGGCCCCGAGTGCAGGAATATGCCTCCACCTG
rabE 5' SpeI R	CGCGACTAGTAGCGAACAGTTAGATACACCGAGGG
rabE ORF SpeI F	CGCGACTAGTATGGCTAACGACGAGTATGATGTGAG
rabE ORF SpeI R	CGCGACTAGTTTAAACAGCATCCACCCTTGTCTCGG
rabE 3' SpeI F	CGCGACTAGTCGTCAACAACGATTTGCGGTTCTG
rabE 3' NotI R2	CGCGGCGGCCGCTGTCCAGACCAAAGACCTCCGG
sGFP XbaI F	CGCGTCTAGAATGGTGAGCAAGGGCGAGGAG
sGFP SpeI NS R	CGCGACTAGTCTGTACAGCTCGTCCATGCC
AFpyrG SpeI F	CGCGACTAGTGCCTCAAACAATGCTCTTACCCTC
AFpyrG XbaI R	CGCGTCTAGAACTGTCTGAGAGGAGGCACTGATGCG
<b>pBS SKII ap1<sup>β</sup>-argB</b>	
ap1 <sup>β</sup> 5' BamHI F	CGCGGGATCCCCATACGATACACCCAAGGCGAAG
ap1 <sup>β</sup> 3' NotI R	CGCGGCGGCCGCCATTGGCGGCTTCAGACACCAC
argB PstI F	CGCGCTGCAGGCTTTATTTTCGCGGTTTTTTGGGG
argB PstI R	CGCGCTGCAGGTCGACCTACAGCCATTGCG
<b>Mutagenesis oligos</b>	
ap1 <sup>β</sup> 632DID <sup>634</sup> /A F	CAATGTGGAGAACCTTCTGGCGCCGCTTTCGATGGCACTGCGCCTGC
ap1 <sup>β</sup> 632DID <sup>634</sup> /A R	GCAGGCGCAGTGCCATCGAAAGCGGCCCGCCAGAAGGTTCTCCACATTG
ap1 <sup>β</sup> 709NGF <sup>711</sup> /A F	GTGCGGGCGCTGACCTTCTCGCGCCGCTTCTGGGTTGGATCTTCCGGC
ap1 <sup>β</sup> 709NGF <sup>711</sup> /A R	GCCGAAAGATCCAACCCAGAAGCGGCCGCGAGAAGGTCAGCGCCCGCAC

*ap1<sup>α</sup>-(5xGA)GFP::AFpyrG*, *clh-(5xGA)GFP::AFpyrG*, *ap1<sup>α</sup>-(5xGA)mRFP::AFpyrG*, *ap2<sup>α</sup>-(5xGA)GFP::AFpyrG*, *clal-(5xGA)GFP::AFpyrG* and *ap2<sup>α</sup>-(5xGA)mRFP::AFpyrG* constructs carry a 5x Gly-Ala (5xGA) linker, amplified together with GFP or mRFP and *AFpyrG* from plasmids p1439, or p1491 respectively (Szewczyk et al. 2006)

### 6.3 REPRINTS OF ORIGINAL PUBLICATIONS





# Oligomerization of the UapA Purine Transporter Is Critical for ER-Exit, Plasma Membrane Localization and Turnover

Olga Martzoukou<sup>1</sup>, Mayia Karachaliou<sup>1</sup>, Vassilis Yalilis<sup>1</sup>, James Leung<sup>2</sup>, Bernadette Byrne<sup>2</sup>, Sotiris Amillis<sup>1</sup> and George Diallinas<sup>1</sup>

<sup>1</sup> - Faculty of Biology, University of Athens, Panepistimioupolis 15784, Athens, Greece

<sup>2</sup> - Division of Molecular Biology, Imperial College, London SW7 2AZ, UK

Correspondence to George Diallinas: [diallina@biol.uoa.gr](mailto:diallina@biol.uoa.gr)

<http://dx.doi.org/10.1016/j.jmb.2015.05.021>

Edited by I. B. Holland

## Abstract

Central to the process of transmembrane cargo trafficking is the successful folding and exit from the ER (endoplasmic reticulum) through packaging in COPII vesicles. Here, we use the UapA purine transporter of *Aspergillus nidulans* to investigate the role of cargo oligomerization in membrane trafficking. We show that UapA oligomerizes (at least dimerizes) and that oligomerization persists upon UapA endocytosis and vacuolar sorting. Using a validated bimolecular fluorescence complementation assay, we provide evidence that a UapA oligomerization is associated with ER-exit and turnover, as ER-retained mutants due to either modification of a Tyr-based N-terminal motif or partial misfolding physically associate but do not associate properly. Co-expression of ER-retained mutants with wild-type UapA leads to *in trans* plasma membrane localization of the former, confirming that oligomerization initiates in the ER. Genetic suppression of an N-terminal mutation in the Tyr motif and mutational analysis suggest that transmembrane  $\alpha$ -helix 7 affects the oligomerization interface. Our results reveal that transporter oligomerization is essential for membrane trafficking and turnover and is a common theme in fungi and mammalian cells.

© 2015 Elsevier Ltd. All rights reserved.

## Introduction

In eukaryotes, polytopic transmembrane proteins, such as transporters, channels and receptors, are co-translationally integrated in the ER (endoplasmic reticulum) membrane and subsequently follow a vesicular secretory pathway for targeting to their final destination, this being the plasma or organellar membranes [1,2]. Central to the process of transmembrane protein exit from the ER is the concentrative packaging of protein cargoes in cytoplasmically budding COPII vesicles [3–8]. Assembly of the COPII coat on the ER membrane occurs in a stepwise fashion, beginning with recruitment of the GTPase Sar1, which recruits the heterodimeric Sec23/24. The Sec23/24 makes additional interactions directly with the membrane. Sec24 serves as the principle cargo binding adaptor. Following pre-budding complex formation, heterodimers of Sec13/31 are recruited via interaction between Sec23 and Sec31, and this interaction drives membrane curvature. In addition to

the need for proper cargo folding [7,9,10], the process of ER-exit also requires the presence of specific ER-exit motifs on the cytoplasm-facing side of cargo proteins, usually in their N- or C-terminal region. Such short motifs include di-basic, tri-basic, di-acidic, di-leucine or tyrosine-based signals, several of which interact with the Sec23p–Sec24p complex in a Sar1p-dependent way [3,11–14]. Disruption of these motifs, similar to cargo misfolding, leads to ER retention. After vesicle formation, downstream events lead to uncoating of transport vesicles and recycling of the COPII coat components [4,8]. COPII vesicle membrane cargoes are sorted in the *cis*-Golgi and eventually in the *trans*-Golgi network, an important sorting station where cargoes are packaged into distinct transport vesicles and eventually targeted to various membrane destinations [15]. Although our understanding of COPII-mediated vesicle formation has developed substantially over the past two decades, many details of this process remain unresolved.

The short cargo motifs required for ER-exit are believed to interact mainly with one of three binding sites on the COPII coat component, Sec24 [16]. The majority of ER-exported membrane proteins, however, carry no known export signal in their sequence. Thus, either new signals remain to be identified or something else drives their recruitment into COPII vesicles. As many membrane proteins form oligomers prior to export from the ER, combinatorial signals have been postulated to link oligomerization to efficient export [17]. For a yeast COPII binding cargo receptor protein and its mammalian homologue (Emp47p, a type I membrane protein), oligomerization is required for its export from the ER but is not required for efficient binding of COPII subunits in the pre-budding complex [18]. This shows that oligomerization acts downstream from the cargo–Sec24 interaction. Very recently, Springer *et al.* showed that regulated oligomerization induces the packaging of a membrane protein into COPII vesicles independently of any putative ER-exit motif [19]. Oligomerization or assembly of cargo proteins seems important for ER-exit of some other cargo proteins, including SNARE molecules or G-protein-coupled receptors [20–22]. Oligomerization of neurotransmitter (e.g., dopamine and serotonin) transporters has also been shown to occur in the ER and is maintained both at the cell surface and during trafficking between the plasma membrane and endosomes [23–30]. The human blood–brain barrier glucose transport protein GLUT1 also forms homodimers and homotetramers in detergent micelles and in cell membranes, which in turn seems to determine its function [31].

In this work, we use the *Aspergillus nidulans* purine transporter UapA as a model transmembrane cargo to investigate the role of cargo oligomerization in ER-exit, plasma membrane localization and turnover. UapA is an H<sup>+</sup>/uric acid-xanthine symporter consisting of 14 transmembrane segments (TMS) and cytoplasmic N- and C-termini. It is the founding member of the ubiquitously conserved Nucleobase-Ascorbate Transporter family [32–34]. The choice of UapA follows from the uniquely detailed current knowledge of its structure, function and regulation of expression, together with preliminary genetic evidence suggesting that UapA might oligomerize [35]. Inactive UapA mutants, unlike active wild-type UapA, cannot be endocytosed in response to substrate transport but can do so when co-expressed with active UapA. The simplest explanation for this phenomenon, called *in trans* endocytosis, is that UapA molecules oligomerize (at least dimerize) in the plasma membrane so that it is sufficient to have only a fraction of active molecules to recruit or activate the endocytic machinery and thus internalize both active and non-active UapA molecules [35,36]. Here, we provide multiple lines of evidence that UapA dimerizes (oligomerizes) in the ER membrane and

provide evidence for a link among oligomerization, ER-exit and subsequent membrane trafficking. Our results are discussed in relation to similar findings concerning the role of oligomerization of mammalian transporters.

## Results

### Biophysical evidence for UapA dimerization

We have recently isolated a specific mutant with exceptional stability for performing biophysical studies [37]. This mutant has a missense mutation replacing a Gly with a Val residue in TMS10, in addition to a deletion removing the first 11 N-terminal amino acids. A GFP-tagged version of UapA-G411VΔ1-11 is normally secreted and localized in the plasma membrane of *A. nidulans* or *Saccharomyces cerevisiae* (data not shown). The mutant exhibits highly reduced transport activity but retains substrate binding, strongly indicating that the gross folding of the transporter is not significantly affected [38]. UapA-G411VΔ1-11 was purified after heterologous expression in *S. cerevisiae* and used in static light-scattering measurements. As shown in Fig. 1, the measured molecular mass for UapA-G411VΔ1-11 is  $140 \pm 4.2$  kDa. Given that the predicted molecular mass of the monomeric form of UapA-G411VΔ1-11 is 60,138 kDa, our data support that UapA can form dimers.

### *In vivo* indirect evidence for UapA oligomerization in the plasma membrane

We have shown before that endocytosis of non-active UapA molecules occurs when these are co-expressed with active UapA molecules. This phenomenon of *in trans* endocytosis occurs even when the active UapA molecule cannot, by itself, be endocytosed due to the presence of mutation Lys572Arg, which prevents Hula/ArtA-dependent ubiquitination [35,36]. To further investigate whether the non-ubiquitylated mutant version UapA-K572R can be itself endocytosed *in trans* when expressed with active UapA molecules, we constructed a GFP-tagged UapA-K572R (UapA-K572R-GFP) and expressed it in a genetic background that hyper-expresses untagged wild-type UapA molecules due to a promoter mutation [39]. Results in Fig. 2 show that UapA-K572R-GFP is efficiently internalized upon imposing endocytic conditions (ammonium or uric acid addition), solely when co-expressed with wild-type UapA molecules. As UapA-K572R-GFP is a non-ubiquitylated version of UapA and ubiquitination is absolutely necessary for endocytosis, the most rational explanation for our results is that the mutant molecules are internalized due to their tight dimerization/oligomerization with wild-type UapA molecules.

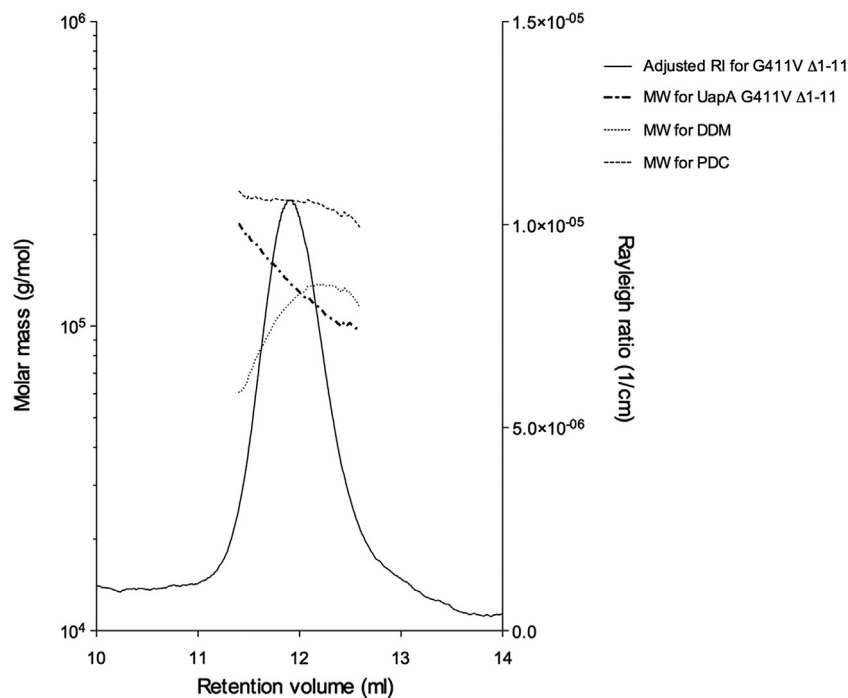


**Fig. 1.** Light-scattering measurements of purified UapA-G411V $\Delta$ 1-11. The measurements from the refractive index detector for UapA-G411V $\Delta$ 1-11 and the DDM micelle are indicated in black broken and dotted lines, respectively. The measurements from the refractive index detector for the total protein–detergent micelle are shown in the gray broken line. The measured molecular mass for UapA-G411V $\Delta$ 1-11 is  $140 \pm 4.2$  kDa. The predicted molecular mass of the monomeric form of UapA-G411V $\Delta$ 1-11 is 60,138 kDa. The data strongly suggest that the UapA is dimeric in DDM solution.

### BiFC assays support UapA oligomerization

Bimolecular fluorescence complementation (BiFC), as well as its version referred to as split-YFP assay, allows the *in vivo* detection of oligomerization through reconstitution of a fluorescent protein that has previously been bisected [40]. Here, we used this system to investigate further UapA dimerization/oligomerization *in vivo*. We constructed three isogenic strains, two expressing UapA-tagged C-terminally with either the N-terminal or the C-terminal part of YFP (UapA-YFP<sub>N</sub> and UapA-YFP<sub>C</sub>, respectively) and one co-expressing UapA-YFP<sub>N</sub> and UapA-YFP<sub>C</sub>, simultaneously. Co-expression of UapA-YFP<sub>C</sub> and UapA-YFP<sub>N</sub> in a strain lacking endogenous uric acid transporters (*uapAΔ uapCΔ*) resulted in growth on uric acid, sensitivity to substrate analogues (oxypurinol and 2-thioxanthine) (Fig. 3a) and prominent reconstitution of YFP fluorescence in the plasma membrane (Fig. 3b). In contrast, no significant YFP fluorescence signal was detected when the two halves of YFP were expressed as separate fusions with UapA (Fig. 3b).

To our knowledge, BiFC has not been used before as an assay for oligomerization of polytopic membrane proteins. Thus, one might argue that reconstitution of fluorescent YFP is not a formal proof for oligomerization but might rather reflect proximal

localization of proteins restricted in the environment of the plasma membrane. As shown later in this manuscript, evidence against this argument comes from experiments showing that specific mutant versions of UapA do not reconstitute split-YFP in analogous assays. For further reinforcing the validity of the BiFC assays for detecting UapA oligomerization, we adapted the BiFC experiment for detecting possible interactions of UapA with another plasma membrane transporter, namely, the L-proline transporter PrnB [41]. We co-expressed UapA-YFP<sub>N</sub> with PrnB-YFP<sub>C</sub> (see Materials and Methods) and tested for YFP reconstitution, as previously described. The right panel in Fig. 3b shows that no fluorescence was obtained, strongly supporting the idea that YFP reconstitution via UapA molecules reflects a specific association, most evidently dimerization.

In the experiments shown in Fig. 3, UapA-YFP expression was driven by the native *uapA* promoter, which allows continuous and relatively low level UapA synthesis. We also constructed analogous strains where the expression of UapA-YFP<sub>C</sub> and UapA-YFP<sub>N</sub> was driven by the controllable *alcA<sub>p</sub>* promoter [42]. The *alcA<sub>p</sub>-UapA-YFP<sub>C</sub>/alcA<sub>p</sub>-UapA-YFP<sub>N</sub>* strain could grow on uric acid, similarly to a control strain expressing *alcA<sub>p</sub>-UapA-GFP* (Fig. 3c). This is also reflected in very similar xanthine transporter rates

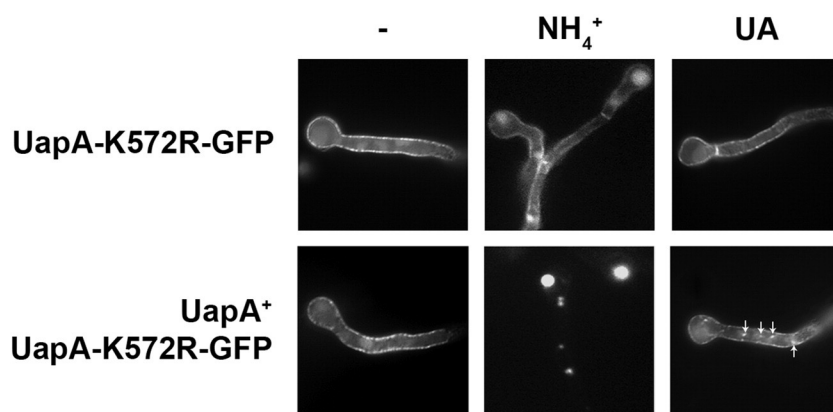


**Fig. 2.** *In trans* endocytosis of a non-ubiquitinated UapA mutant co-expressed with wild-type UapA. UapA-K572R-GFP is a UapA mutant that cannot be ubiquitinated and endocytosed in response to ammonium or substrate (UA; uric acid) addition in the growth medium. The figure shows an epifluorescence microscopy analysis of a strain expressing UapA-K572R-GFP alone or co-expressed with wild-type UapA in the genetic background of *uapA100*. *uapA100* is a promoter mutation leading to a 3-fold increase in UapA protein levels. The subcellular localization of UapA-K572R-GFP is followed under control conditions and endocytic conditions (ammonium or UA addition). Arrows indicate the vacuolar staining of UapA-K572R-GFP.

in the two strains (Fig. 3d). Most importantly, a strong YFP signal was observed, associated with the plasma membrane in the strain co-expressing *alcA<sub>p</sub>-UapA-YFP<sub>C</sub>* and *alcA<sub>p</sub>-UapA-YFP<sub>N</sub>*, solely under inducing conditions for *alcA<sub>p</sub>*, (0.1% fructose, ethanol for 4 h). Under repressing conditions (1% glucose for 3 h), no YFP fluorescence was visible (Fig. 3e). The reconstitution of YFP when attached to separate UapA molecules suggests that UapA dimerizes so that the C-tails of the two monomers are in close distance necessary to reconstitute YFP.

We also tested whether UapA-YFP<sub>N</sub>/UapA-YFP<sub>C</sub> apparent oligomerization, shown by reconstitution of YFP, persists upon endocytosis. Figure 3f shows that UapA-YFP<sub>N</sub>/UapA-YFP<sub>C</sub> internalization is evident in the presence of NH<sub>4</sub><sup>+</sup> or excess substrate. In the presence of ammonium, YFP fluorescence is still associated with the plasma membrane but is also visible in large vacuoles (detected by CMAC). Diffuse low fluorescence is apparent within the vacuolar lumen, which suggests that the two parts of YFP dissociate upon turnover of UapA. In the presence of substrate (uric acid), UapA internalization is also evident in addition to motile early endosomes and small vacuoles, as has been shown previously for wild-type UapA-GFP [35]. These results show that UapA dimerization persists during endocytosis, in early endosomes and all along the endosomal pathway until internalization into the vacuolar lumen.

### Pull-down assays support UapA oligomerization

To provide further direct evidence for UapA oligomerization, we also performed pull-down assays using membrane protein extracts of a strain co-expressing differentially tagged UapA molecules. A strain co-

expressing from the *alcA<sub>p</sub>* promoter GFP- and His<sub>10</sub>-tagged versions of UapA was constructed. Protein samples were purified with a Ni-NTA column under non-denaturing conditions and the eluted fractions were analyzed by SDS polyacrylamide gel silver staining (Fig. 4a, left panel). Western blot analysis with anti-His antibody identified, in the eluted fractions at 250 mM imidazole, a major band at ~55 kDa, which corresponds to monomeric UapA-His [43]. A second minor band of estimated size close to 110 kDa, probably corresponding to UapA-His dimers, was also evident (Fig. 4a). Western blot analysis of the eluted UapA-specific fraction with anti-GFP antibody showed a prominent band migrating at the position corresponding to monomeric UapA-GFP (~75 kDa), thus demonstrating that UapA-GFP co-purified with UapA-His, very probably as a result of dimerization (Fig. 4b). This is further confirmed in the negative control strain where UapA-GFP is expressed without UapA-His. In this case, the eluted imidazole fraction (250 mM) from a Ni-NTA column does not contain UapA-GFP. A very similar result was obtained with an inverse pull-down assay where UapA-GFP was first precipitated with anti-GFP antibodies on ProtA-Sepharose beads, followed by co-immunoprecipitation of UapA-His detected with anti-His antibody, confirming the dimerization/oligomerization of UapA molecules (see Supplementary Fig. S1).

The data shown in Fig. 4a and b were obtained using protein expressed from the *alcA<sub>p</sub>* promoter induced with ethanol for 4 h before collecting total membrane protein extracts. This means that UapA molecules are continuously synthesized so that, in addition to the plasma membrane, UapA is also localized in the ER, the Golgi and trafficking vesicles. We repeated the pull-down experiment with protein

extracts isolated after repression of *de novo* UapA synthesis. Under these conditions, detectable UapA-GFP molecules are solely associated with the plasma membrane [44]. Results in Fig. 4c were practically identical with those of Fig. 4b supporting that UapA-His/UapA-GFP dimerization persists in the plasma membrane. Under these conditions, we again obtained, besides monomeric UapA species, additional higher molecular weight (MW) bands, which might represent dimers/oligomers or aggregates of UapA-GFP that are SDS resistant.

We also tested whether the presence of substrates during growth affects the apparent UapA-His/UapA-GFP dimerization. Figure 4d shows no effect of substrate on the pull-down result. This is in line with the results in Fig. 3f, which showed that apparent UapA dimers persist during internalization and until turnover in the vacuolar lumen. The reduced amount of both UapA-His and UapA-GFP after prolonged presence of substrate is probably due to internalization and the subsequent vacuolar turnover [35].

### Identification of a cytoplasmic N-terminal signal necessary for ER-exit of UapA

ER retention of polytopic membrane proteins is usually due to partial misfolding or the lack of functional ER-exit signals. To identify possible ER-exit signals in UapA, we carried out a systematic mutational analysis of the N-terminal cytoplasmic region of UapA-GFP. This segment that is 68 amino acids long is the most likely location of ER-exit and trafficking motifs, as deletion of the cytoplasmic C-terminal region has absolutely no effect in these processes [35]. Deletions and Ala scanning mutagenesis revealed a short sequence (Asp44-Tyr45-Asp46-Tyr47) and particularly a single residue within it, Tyr47, as being critical for ER-exit and thus essential for detectable UapA transport activity and growth on uric acid (Fig. 5). Substitution of the entire Asp-Tyr-Asp-Tyr sequence with Ala residues (DYDY<sub>47</sub>/A<sub>4</sub>) leads to dramatic turnover of UapA associated with retention in perinuclear ER membranes. This effect seems to be mainly due to replacement of Tyr47, as the single mutation Y47A leads to a similar effect to that seen for the quadruple DYDY<sub>47</sub>/A<sub>4</sub> mutant. Importantly, direct transport assays showed that over-expressed UapA-Y47A conserves a normal  $K_m$  value for physiological substrates (see Fig. 5d). This is highly suggestive that the gross folding of the UapA-Y47A polypeptide is not affected. In turn, this confirms that reduced ER-exit and increased turnover in this mutant are not due to misfolding.

To further understand the nature of the defect in Y47A, we made systematic substitutions of Tyr47 and showed that Tyr can be functionally substituted with Phe, but not with other residues (Fig. 5e). Thus, the presence of an aromatic amino acid at position 47 is necessary for proper ER-exit and expression

in the plasma membrane of UapA. The Asp-Tyr-Asp-Tyr consensus sequence, including Tyr47, is highly conserved in all fungal homologues of UapA (Fig. S2).

### ER-retained mutants of UapA physically associate but do not reconstitute split-YFP

We investigated whether mutations affecting ER-exit also affect oligomerization. To that end, we used three UapA mutant versions. The first two, UapA-I74D and UapA- $\Delta$ TMS14, were examples of partially misfolded mutants [45,46]. The third is UapA-DYDY<sub>47</sub>/A<sub>4</sub>, as described above. We used UapA-DYDY<sub>47</sub>/A<sub>4</sub> rather than the UapA-Y47A, as ER-exit is more drastically affected in this mutant than in UapA-Y47A.

We performed BiFC assays for UapA-I74D, UapA- $\Delta$ TMS14 and UapA-DYDY<sub>47</sub>/A<sub>4</sub>, as described for wild-type UapA. All strains made (see **Materials and Methods**) had the expected growth phenotypes (Fig. S3). None of the mutants tested showed significant YFP reconstitution, strongly suggesting that all relevant mutation impair dimerization/oligomerization (Fig. 6a). In apparent contradiction with the BiFC assays, pull-down assays showed that mutant molecules of UapA-DYDY<sub>47</sub>/A<sub>4</sub> or UapA-I74D physically associate (Fig. 6b). However, in UapA mutants, it is evident that the amount of monomeric UapA-GFP co-precipitated is relatively reduced, in favor of an increase in a high MW signal, when compared with the analogous ratio in the wild-type control. Although the quantification of monomeric to higher MW oligomers or aggregates in different strains is difficult to estimate rigorously, mainly due to different half-lives of wild-type and mutant UapA molecules, in light of the BiFC assays, our results strongly support the idea that the physical association in the mutants is topologically different from the interaction in the wild-type UapA.

### *In trans* exocytosis of ER-retained UapA mutants supports early oligomerization in the ER

We performed BiFC assays using strains in which the mutant versions of UapA (UapA-I74D-YFP<sub>C</sub>, UapA- $\Delta$ TMS14-YFP<sub>C</sub> or UapA-DYDY<sub>47</sub>/A<sub>4</sub>-YFP<sub>C</sub>) were co-expressed with a wild-type UapA (UapA-YFP<sub>N</sub>). In all cases, the strains grew well on uric acid, showing that there was no dominant negative effect of the mutant version on the wild-type UapA (Fig. 7a). Figure 7b shows that YFP fluorescence is reconstituted in UapA-I74D-YFP<sub>C</sub>/UapA-YFP<sub>N</sub> and UapA-DYDY<sub>47</sub>/A<sub>4</sub>-YFP<sub>C</sub>/UapA-YFP<sub>N</sub>, but not in UapA- $\Delta$ TMS14-YFP<sub>C</sub>/UapA-YFP<sub>N</sub>. Most importantly, fluorescence is associated with the plasma membrane. The reconstitution of split-YFP shows that UapA-I74D-YFP<sub>C</sub> or UapA-DYDY<sub>47</sub>/A<sub>4</sub>-YFP<sub>C</sub> molecules are able to dimerize or physically associate with wild-type UapA

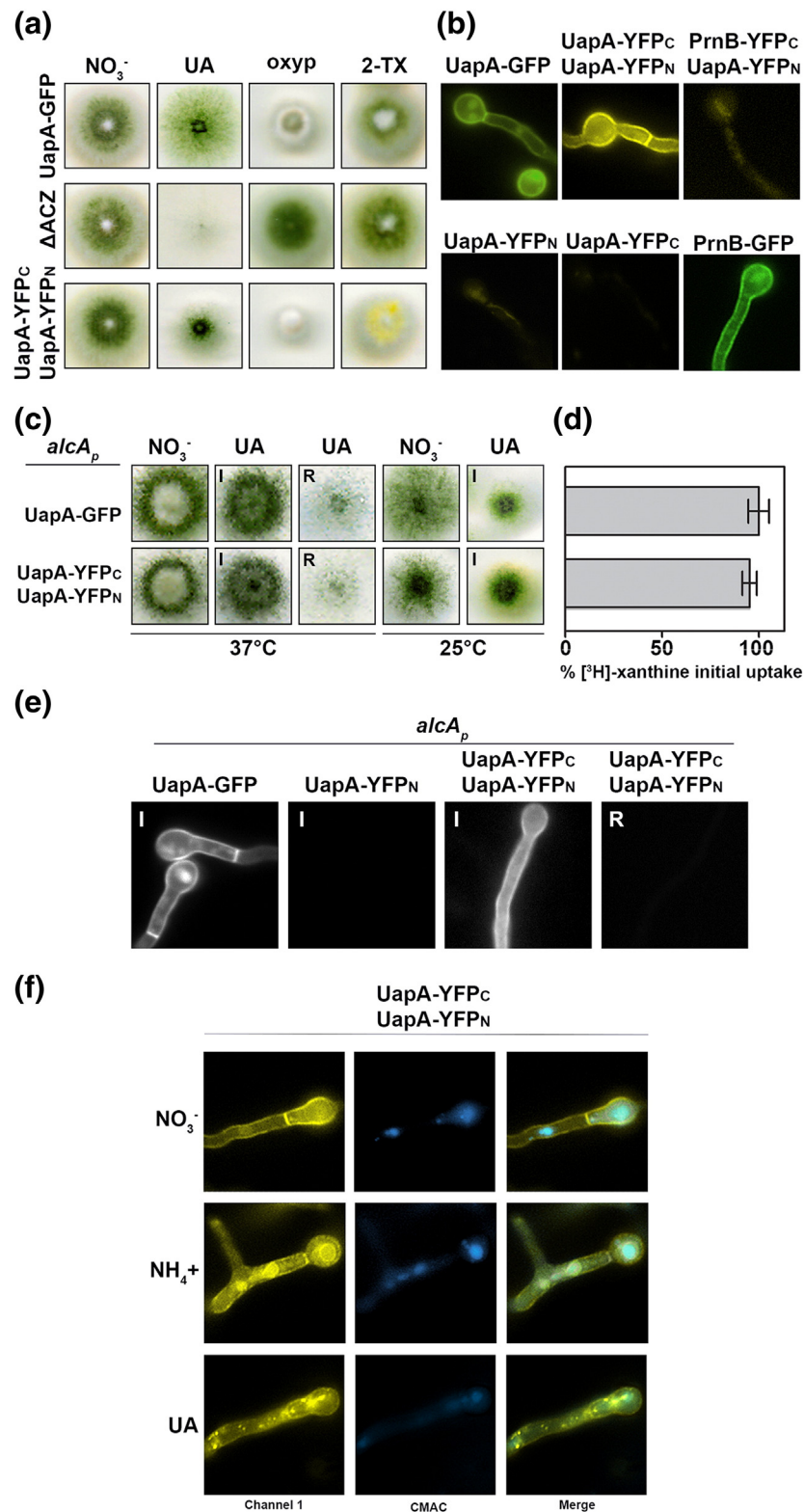
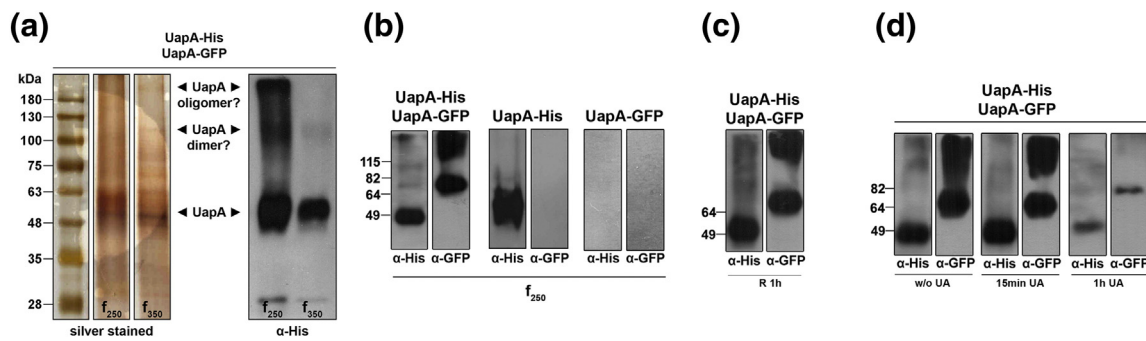


Fig. 3. (legend on next page)



**Fig. 4.** Direct biochemical evidence for UapA oligomerization in a strain co-expressing UapA-His<sub>10</sub> and UapA-GFP. (a) Solubilized total membrane protein preparations from the strain co-expressing UapA-His<sub>10</sub> and UapA-GFP under inducing conditions were applied to Ni-NTA columns, eluted with increasing concentrations of imidazole (only f<sub>250</sub> and f<sub>350</sub> fractions are shown) and analyzed by SDS polyacrylamide gel electrophoresis, followed by silver staining or immunoblotting with an anti-His antibody. A prominent band reacting with the anti-His antibody in the fraction eluted at 250 mM is detected. The size of this band is estimated to be ~55 kDa, which corresponds to monomeric UapA-His [43]. A less prominent anti-His specific band appearing at just over the 100 kDa might correspond to a dimeric form of UapA. (b) The f<sub>250</sub> fraction of the strain co-expressing UapA-His and UapA-GFP also reacts with the anti-GFP. In contrast, the same fraction from a strain expressing solely UapA-His does not react with the anti-GFP antibody, as expected. (c) Western blot analysis, using anti-GFP antibody, of similarly eluted UapA-His fractions isolated from the UapA-His<sub>10</sub>/UapA-GFP strain grown under repressing conditions (1 h glucose). Under this condition, *de novo* synthesis is blocked and thus preformed UapA molecules are solely present in the plasma membrane. (d) Western blot analysis, using anti-GFP antibody, of eluted UapA-His fractions isolated from the UapA-His<sub>10</sub>/UapA-GFP strain incubated for 4 h under inducing conditions, in the presence of substrate (uric acid) for 15 min or 1 h before cell harvesting. In all cases, protein samples are heated at 37 °C for 30 min before loading onto the SDS-PAGE gel.

molecules. In UapA-DYDY<sub>47</sub>/A<sub>4</sub>-YFP<sub>C</sub>/UapA-YFP<sub>N</sub>, fluorescence is also visibly associated with perinuclear ER membrane rings. This confirms that oligomerization occurs in the ER membrane and persists in the plasma membrane. The absence of YFP reconstitution in UapA-ΔTMS14-YFP<sub>C</sub>/UapA-

YFP<sub>N</sub> was to be expected, as the deletion of the last transmembrane domain (TMS14) should orientate the C-terminus toward the extracellular side of the membrane, thus preventing its association with the C-terminus of wild type. Thus, the UapA-ΔTMS14-YFP<sub>C</sub>/UapA-YFP<sub>N</sub> experiment also serves as a

**Fig. 3.** *In vivo* evidence for UapA oligomerization using BiFC. (a) Growth test of the UapA-YFP<sub>C</sub>/UapA-YFP<sub>N</sub> transformant, as compared to a control strain expressing UapA-GFP and a mutant lacking all major purine transporters (ΔACZ). All strains shown are otherwise isogenic and thus grow similarly on standard nitrogen sources (e.g., NaNO<sub>3</sub>). Strains expressing a functional UapA grow on uric acid (UA) as sole nitrogen source and are sensitive to oxypurinol (OX) or 2-thioxanthine (2-TX) (green/yellowish conidiospores), whereas the mutant lacking UapA shows very leaky growth on UA and is resistant to OX and 2-TX (green conidiospores). The growth profile of UapA-YFP<sub>C</sub>/UapA-YFP<sub>N</sub> is compatible with a functional UapA and in fact shows higher expression of UapA compared to UapA-GFP, as judged mostly by increased sensitivity to OX and 2-TX. Given that the single chimeric transporter UapA-YFP<sub>C</sub> or UapA-YFP<sub>N</sub> is also functional (results not shown), the YFP tags do not affect, within the limit of growth tests, UapA function. Strains are grown at 25 °C. (b) Epifluorescence microscopic analysis of the strains expressing either UapA-YFP<sub>C</sub> or UapA-YFP<sub>N</sub>, or co-expressing UapA-YFP<sub>C</sub>/UapA-YFP<sub>N</sub>, compared to an isogenic strain expressing UapA-GFP. Strains co-expressing UapA-YFP<sub>N</sub>/PmB-YFP<sub>C</sub>, grown on proline, are also shown as a negative control. (c and d) Growth test and radiolabeled [<sup>3</sup>H]xanthine transport activity of a strain co-expressing *alcA<sub>p</sub>*-UapA-YFP<sub>C</sub>/*alcA<sub>p</sub>*-UapA-YFP<sub>N</sub>. The panel on the left confirms that the *alcA<sub>p</sub>*-UapA-YFP<sub>C</sub>/*alcA<sub>p</sub>*-UapA-YFP<sub>N</sub> strain grows similarly to isogenic *alcA<sub>p</sub>*-UapA-GFP. Notice that UapA-mediated full growth on UA is only observed under inducing conditions (I; fructose, ethanol) for the *alc<sub>p</sub>* promoter, while only marginal growth is observed under repressing (R; glucose) conditions. The panel on the right confirms that *alcA<sub>p</sub>*-UapA-YFP<sub>C</sub>/*alcA<sub>p</sub>*-UapA-YFP<sub>N</sub> and *alcA<sub>p</sub>*-UapA-GFP have comparable transport activities. Transport activities are expressed as % of initial uptake rate, considering the rate of UapA-GFP as 100%. Results represent averages of three experiments, each experiment carried out in triplicate, with standard deviation <20%. (e) Epifluorescence microscopic analysis of strains expressing *alcA<sub>p</sub>*-UapA-GFP or *alcA<sub>p</sub>*-UapA-YFP<sub>N</sub>, or co-expressing *alcA<sub>p</sub>*-UapA-YFP<sub>C</sub>/*alcA<sub>p</sub>*-UapA-YFP<sub>N</sub>. For *alcA<sub>p</sub>*-UapA-GFP or *alcA<sub>p</sub>*-UapA-YFP<sub>N</sub> strains, only inducing conditions (I; fructose, ethanol) are shown, whereas for the *alcA<sub>p</sub>*-UapA-YFP<sub>C</sub>/*alcA<sub>p</sub>*-UapA-YFP<sub>N</sub> strain, both repressing (R; glucose) and inducing (I) conditions are shown. (f) Epifluorescence microscopic analysis of strains co-expressing UapA-YFP<sub>C</sub>/UapA-YFP<sub>N</sub> under standard conditions (nitrate as nitrogen source) or under endocytic conditions [addition of ammonium or substrate (uric acid) for 4 h in samples grown with nitrate]. Channel 1 shows reconstitution of YFP by UapA-YFP<sub>N</sub>/UapA-YFP<sub>C</sub> dimerization, while CMAC staining is used for vacuole detection. Endocytosis triggered by ammonium leads to rapid sorting of UapA-YFP<sub>N</sub>/UapA-YFP<sub>C</sub> apparent dimers in large vacuoles, whereas substrate-triggered endocytosis results in sorting of UapA-YFP<sub>N</sub>/UapA-YFP<sub>C</sub> in motile early endosomes and small vacuoles.

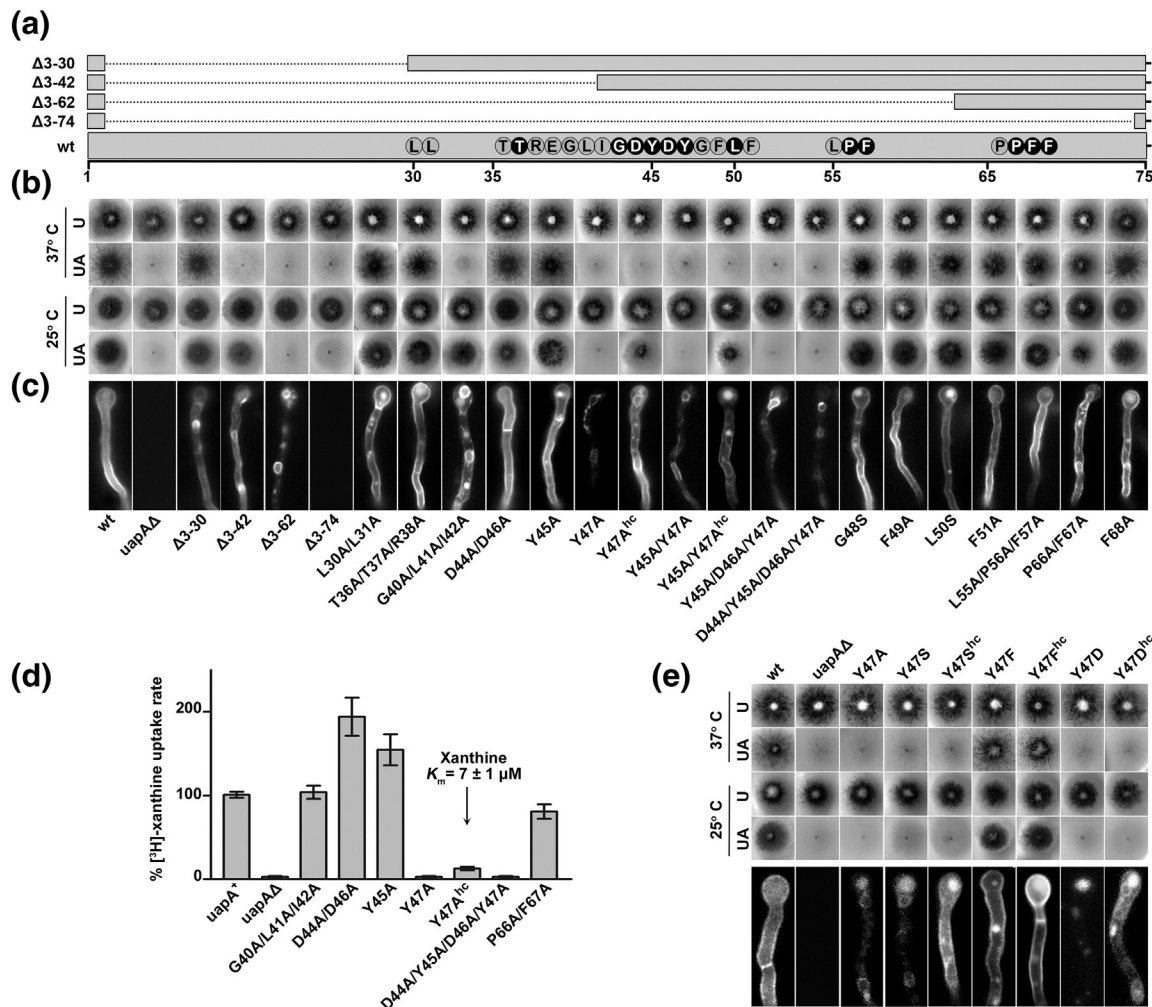


**Fig. 5.** Identification of an N-terminal motif necessary for ER-exit of UapA. (a) Schematic representation of the N-terminal region of UapA, highlighting the amino acid residues conserved and mutated. Overlapping deletions of the N-terminal region are also depicted. hc means expression from high-copy plasmids. (b) Growth test of N-terminal UapA mutants. All mutants shown, unless otherwise stated, arise from functional single-copy plasmid integration events. In all cases, UapA is functionally tagged with GFP. hc stands for plasmid high-copy transformants that over-express the mutant form of UapA. This constitutes a standard tool for further testing the subcellular localization and transport activity of selected mutants that are expressed at very low levels, as is the case here of Y47A. Mutants are tested on MM either with a standard nitrogen source unrelated to UapA function (urea) or on uric acid, the main physiological substrate of UapA, as sole nitrogen source, at 25 °C and 37 °C. Positive and negative controls (wt and  $\Delta$ UapA) are isogenic strains expressing wild-type UapA and a strain lacking all major purine transporters (*uapA $\Delta$  uapC $\Delta$  azgA $\Delta$* ), respectively. Notice that the inability for growth on uric acid is always associated with substitution of Tyr47 or deletions removing an N-terminal part including Tyr47 ( $\Delta$ 3-42,  $\Delta$ 3-62 and  $\Delta$ 3-74). The triple substitution G40A/L41A/I42A also led to apparent loss of UapA, but only at 37 °C. (c) Epifluorescence microscopy of N-terminal UapA mutants. Mutants with apparent ER retention, reduced localization in the plasma membrane and vacuolar sorting are always associated with substitution Y47A or the deletion of an N-terminal segment including Tyr47. Deletion  $\Delta$ 3-30 shows a degree of vacuolar turnover, whereas the double substitution P66A/F67A shows partial ER retention. The deletion of the entire N-terminal region leads to no fluorescence. These results are in agreement with growth tests and uptake assays. (d) Transport activities, expressed as % of initial uptake rates, of selected mutants (see Fig. 3 legend). (e) Systematic mutational analysis of Tyr47. Growth tests and epifluorescence microscopy analysis of Tyr47 substitutions show that only substitution Y47F restores the secretion of UapA to the plasma membrane and, consequently, also restores its apparent transport activity (experimental details are as above).

negative control in BiFC assays. *In trans* sorting of UapA-DYDY<sub>47</sub>/A<sub>4</sub>-GFP in the plasma membrane upon co-expression with over-expressed (from a

high-copy plasmid transformant) wild-type UapA further confirmed the formation of UapA dimers (Fig. 7c).



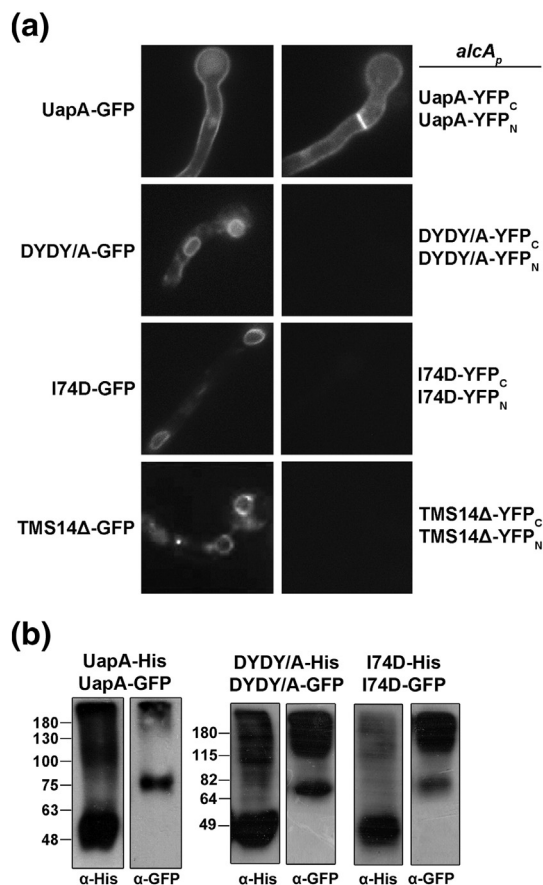


**Fig. 6.** UapA mutants retained in the ER do not dimerize properly. (a) BiFC assays of wild-type UapA and mutants UapA-DYDY/A<sub>4</sub>, UapA-I74D and UapA-ΔTMS14. Strains co-expressing from the *alcA<sub>p</sub>* promoter the mutant forms of UapA, tagged with either YFP<sub>N</sub> or YFP<sub>C</sub>, are shown. Isogenic strains expressing from *alcA<sub>p</sub>* the same mutant versions UapA, or a wild-type UapA, tagged with GFP, are also included as controls. No reconstitution of YFP was detected in any of the mutants tested. (b) Pull-down experiments in strains co-expressing UapA-DYDY/A<sub>4</sub>-GFP/UapA-DYDY/A<sub>4</sub>-His<sub>10</sub> or UapA-I74D-GFP/UapA-I74D-His<sub>10</sub>. Notice the reduced amount of monomeric co-precipitated UapA-GFP relative to higher MW species, possibly UapA aggregates (see the text).

### Genetic suppression of Y47A reveals the importance of TMS7 and TMS11 in ER-exit of UapA

We obtained two different intragenic suppressors, namely, V298A and F437C, the former restoring the defects caused by Y47A much more strongly than the latter (Fig. 8a). Val298 and Phe437 are located in the middle of TMS7 and the outward-facing end of TMS11 (Fig. 8b), respectively, both being quite well conserved residues in UapA homologues (Fig. S4). Both mutations restored UapA-mediated transport rates (Fig. 8c). Functional restoration was in line with restoration of ER-exit and plasma membrane

localization, as evidenced by both standard epifluorescence analysis and BiFC assays (Fig. 8d). Strains expressing the suppressor mutations in the absence of the original mutation (UapA-V298A or UapA-F437C) conferred growth phenotypes, subcellular localization and transport activities, similar to wild-type UapA (data not shown). Thus, suppression of Y47A is probably not due to allele-specific interactions of Tyr47 with Val298 or Phe437 but is rather a bypass of the effect of Y47A.

### Gly residues in TMS7 are critical for wild-type-like oligomerization, ER-exit and turnover of UapA

Three independent observations suggested that TMS7 might be part of or affects the oligomerization interface. Firstly, the crystal structure of the bacterial UapA homologue UraA shows that TMS7 has the highest *B*-factors of all the transmembrane segments, indicating that this region of UraA is the most flexible, and therefore, it is a candidate for intermolecular interactions [47]. Secondly, TMS7 is predicted to form a bend  $\alpha$ -helix, one part facing the lipid bilayer and the other one facing toward the TMS13 and TMS14, which are candidates for dimerization domains (Y. Alguel, A. Cameron, G. Diallinas and B. Byrne, unpublished results). Thirdly, TMS7 includes several Gly residues (Gly301, Gly305 and Gly313) in the form of GX<sub>3</sub>G or GX<sub>7</sub>G motifs (X being hydrophobic residues), known to be critical for inter-helical interactions in membrane proteins [48–50].

To test the importance of the Gly residues in TMS7 of UapA, we made a series of substitutions to Ala or Leu residues and functionally analyzed the corresponding mutants. In all cases, we constructed the single, double and triple substitutions. Results are shown in Fig. 9a. All substitutions to Leu, except G313L, led to apparent loss of UapA activity as judged from growth tests. In addition, none of the mutants correctly localized to the plasma membrane. Furthermore, a low UapA-GFP signal was also detected in vacuoles in several mutants. Single substitutions of Gly301, Gly305 and Gly313 to Ala did not significantly affect UapA localization and transport activity. However, double and triple substitutions scored as apparent loss-of-function mutations. In these cases, we detected dramatic vacuolar turnover and some ER retention. The fact that Ala substitutions were better tolerated than Leu substitutions was in line with observations that G/AX<sub>3</sub>G/A or G/AX<sub>7</sub>/A motifs can also function as weaker helical interaction motifs [48].

We tested whether UapA molecules carrying the triple Ala substitution (UapA-GGG/A<sub>3</sub>) could dimerize. Figure 9b shows that no YFP reconstitution is obtained in strains co-expressing UapA-GGG/A<sub>3</sub>-YFP<sub>N</sub> and UapA-GGG/A<sub>3</sub>-YFP<sub>C</sub>. Relevant pull-down assays showed that, in the GGG/A<sub>3</sub> mutant, UapA molecules still associate despite the fact that the ratio of monomeric UapA-GGG/A<sub>3</sub>-GFP *versus*

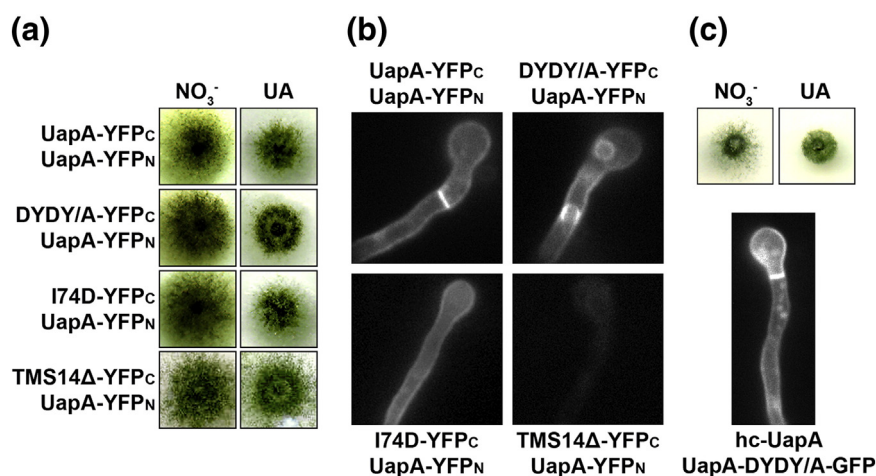


**Fig. 7.** *In trans* exocytosis of ER-retained UapA mutants. (a) Growth tests of strains co-expressing UapA-I74D-YFP<sub>C</sub>, UapA-ΔTMS14-YFP<sub>C</sub> or UapA-DYDY/A<sub>4</sub>-YFP<sub>C</sub> with a wild-type UapA-YFP<sub>N</sub>. As expected, all strains grow on UA. (b) BiFC assays of the same strains shown in (a). Notice YFP fluorescence reconstitution in the plasma membrane of strains co-expressing UapA-I74D or UapA-DYDY/A<sub>4</sub> with wild-type UapA while there is no YFP signal detected in UapA-ΔTMS14/UapA. In UapA-DYDY/A<sub>4</sub>/UapA, YFP signal is also detected in the perinuclear ER. (c) Growth test and epifluorescence analysis of a strain co-expressing UapA-DYDY<sub>47</sub>/A<sub>4</sub>-GFP and wild-type UapA. Notice the sorting of UapA-DYDY<sub>47</sub>/A<sub>4</sub>-GFP in the plasma membrane. In this case, the high expression of wild-type UapA (in relation to UapA-DYDY<sub>47</sub>/A<sub>4</sub>-GFP) was achieved by selecting a transformant that harbors three copies of the relative plasmid (hc-UapA).

high MW aggregates is reduced compared to wild-type UapA (Fig. 9c). Using the inverse pull-down assay where UapA-GFP is precipitated with anti-GFP antibodies on ProtA-Sepharose beads, followed by co-immunoprecipitation of UapA-His detected with anti-His, we confirmed that UapA molecules associate, but again the ratio of monomeric UapA-GGG/A<sub>3</sub>-GFP *versus* high MW aggregates seemed somehow reduced (see Supplementary Fig. S1).

Finally, we also showed that UapA-GGG/A<sub>3</sub> can be sorted to the plasma membrane upon co-expression with wild-type UapA (Fig. 9d). This is in line with partial restoration of UapA-mediated growth on uric acid. Overall, the results obtained with the mutant lacking the Gly residues in TMS7 are very similar to those obtained with the other ER-retained mutants studied here (UapA-DYDY/A<sub>4</sub> and UapA-I74D).

#### Intragenic complementation of plasma membrane localization in ER-retained mutants

We also constructed strains co-expressing UapA-GGG/A<sub>3</sub> with UapA-DYDY/A<sub>4</sub>-GFP and performed growth tests and epifluorescence analysis (Fig. 10). These strains could not grow on uric acid, as expected, but showed partial restoration of plasma membrane localization, never seen when these two UapA versions are expressed by themselves. This partial intragenic complementation is readily explained by dimerization, constituting further strong evidence that dimerization/oligomerization of UapA is functionally linked to ER-exit and plasma membrane localization and stability.

## Discussion

Four independent assays showed that UapA forms, at least, homodimers in the ER and that oligomerization persists along the secretion pathway, in the plasma membrane and during endocytosis. Of these assays, the *in vivo* reconstitution of split-YFP proved ideal to detect minor topological changes in the association of UapA molecules. A similar strategy has been used to show transporter oligomerization in a handful of previous reports [51–55]. However, to our knowledge, this is the first time BiFC has been shown to detect highly specific transporter dimerization/oligomerization; no reconstitution of split-YFP was detected in *specific* UapA mutants or when one part of YFP was tagged in another plasma membrane transporter.

UapA, in common with most ion-driven polytopic symporters, functions as a monomer. This is based on genetic, biochemical and structural data. Although we cannot rule out that dimerization might have a subtle effect on transport kinetics *per se*, it seems much more reasonable to assume that oligomerization affects membrane trafficking, plasma membrane localization and protein stability, as proposed for several mammalian transporters (discussed also later). Recent evidence also supports the and further oligomerization of the mammalian SVCT2 vitamin C transporter, which belongs to the same protein family as UapA [56].

We examined whether UapA mutants showing problematic ER-exit associated with increased turnover can dimerize. We made use of two kinds of ER-retained

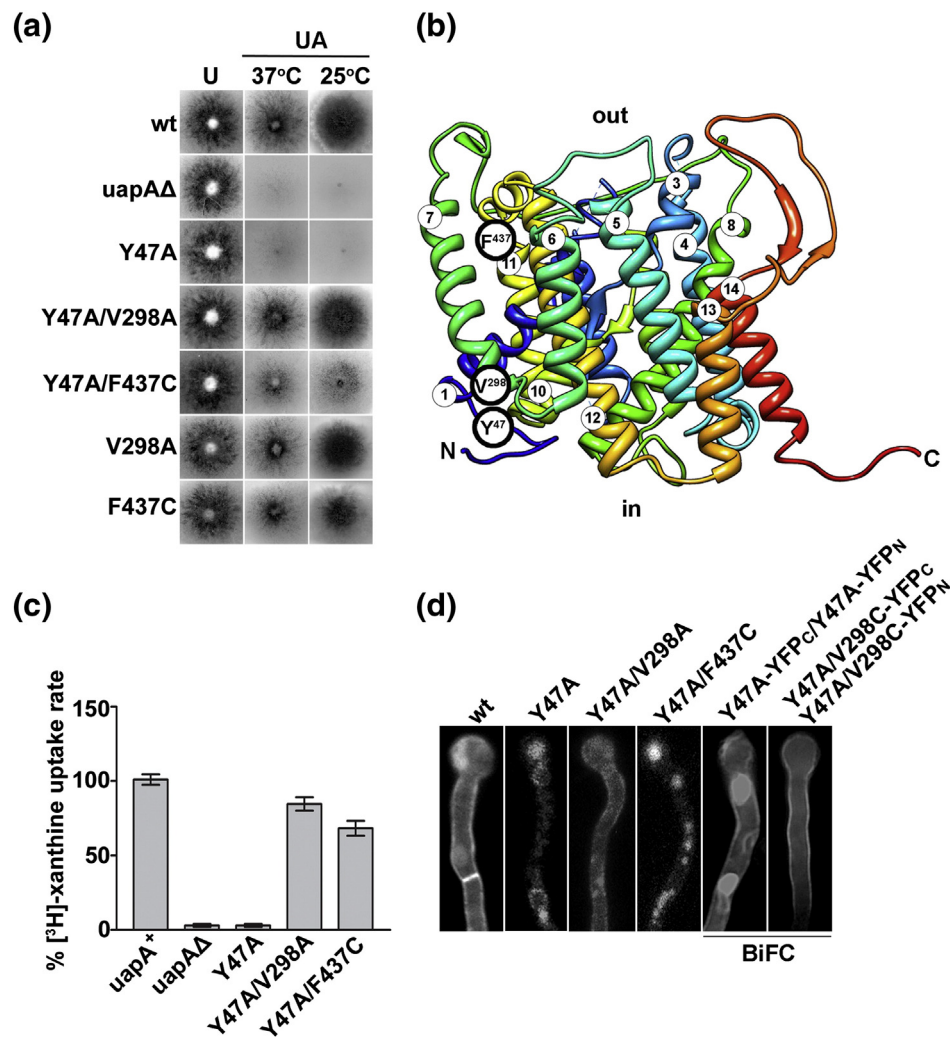


**Fig. 8.** Specific mutations in TMS7 and TMS11 genetically suppress the ER-exit defect of UapA-Y47A. (a) Growth tests of the two genetic suppressors compared to the original mutant. Notice that suppressor mutation V298A is stronger than F437C. (b) Identity (V298A and F437C) and topology of the two genetic suppressor mutations of UapA-Y47A. (c) Transport rates in suppressors and original mutant. (d) Epifluorescence microscopy of suppressors and original mutant and BiFC assays of UapA-Y47A and UapA-Y47A/V298A, showing the restoration of plasma membrane localization in the latter.

mutants. The first are due to partial misfolding, whereas the second are due to the lack of the N-terminal DYDY<sub>47</sub> motif, which does not seem to affect gross UapA folding. However, the two types of mutants showed similar characteristics: ER retention, increased vacuolar turnover, non-reconstitution of split-YFP fluorescence and a modified mode of association in pull-down assays. Importantly, the ER-retained mutant versions of UapA, co-expressed with wild-type UapA, were sorted in the plasma membrane. This phenomenon of *in trans* sorting seems analogous to the *in trans* endocytosis of UapA mutants, detected here (Fig. 2) and previously [35], and is most easily explained by the formation of dimers. More impressively, co-expression of different ER-retained mutants of UapA restored plasma membrane localization, which constitutes further strong evidence for dimerization (see Fig. 10).

The isolation of genetic suppressors of ER-retained mutants mapping in TMS7 and TMS11 suggested that these lipid-facing transmembrane domains of UapA [34], especially TMS7 which includes the strongest suppressor and functionally essential GX<sub>3</sub>G motifs, must be involved in critical helical interactions. Our results strongly favor the involvement of TMS7 in homo-oligomerization. At present, we cannot propose a model on how and how many UapA monomers associate, but it seems that functional UapA association requires both helical interactions within the plasma membrane and interactions involving the cytoplasmic terminal regions of UapA. The latter interactions might in fact be crucial to the molecular cross-talk with the ER-exit machinery. Ongoing efforts to obtain the crystal structure of UapA will give a definitive answer to this issue

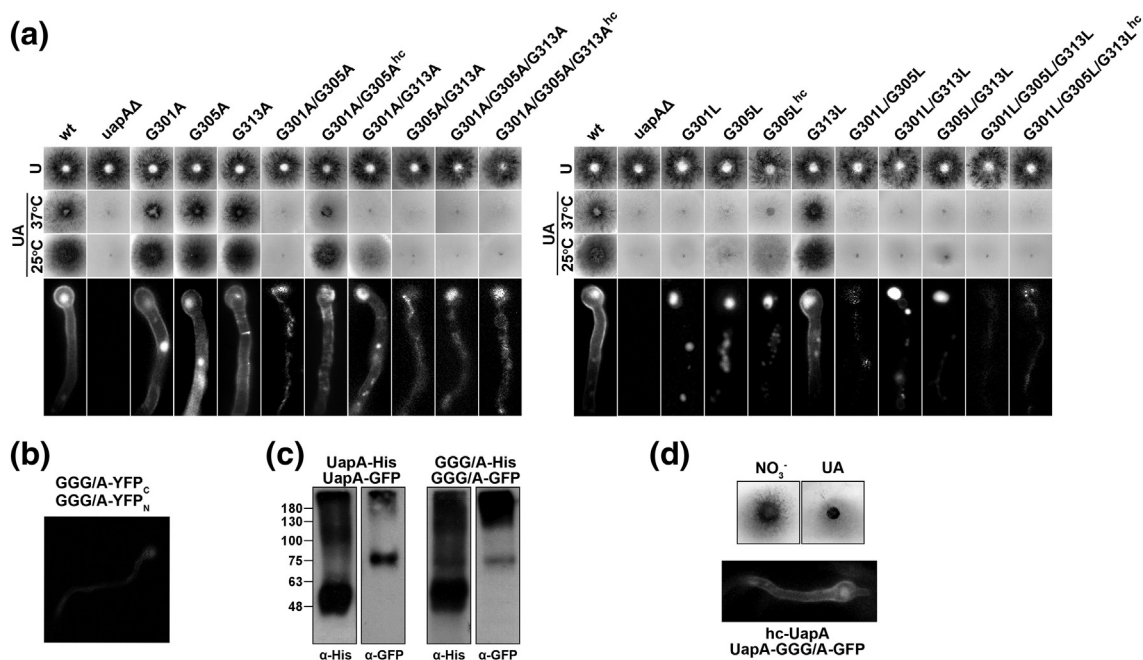


**Fig. 9.** Gly residues in TMS7 are critical for proper UapA dimerization, topology and turnover. (a) Growth tests and epifluorescence microscopy of mutants carrying Ala or Leu substitution in Gly residues of TMS7. (b) BiFC assay of UapA-GGG/A<sub>3</sub>-YFP<sub>N</sub> with UapA-GGG/A<sub>3</sub>-YFP<sub>C</sub>. No reconstituted YFP signal is detected. (c) Pull-down assays of protein extracts from strains co-expressing UapA-GGG/A<sub>3</sub>-GFP with UapA-GGG/A<sub>3</sub>-His and a wild-type relative control strain. (d) Growth tests and epifluorescence microscopy of a strain co-expressing UapA-GGG/A<sub>3</sub>-GFP with multi-copy wild-type UapA (hc-UapA).

(Y. Alguel, B. Byrne and A. Cameron, personal communication).

One basic question to answer is how the cytoplasmic N-terminal DYDY<sub>47</sub> motif affects ER-exit. Does it interact with the packaging COPII machinery? We failed to detect an interaction with either Sec23 or Sec24 (results not shown). Alternatively,

the DYDY<sub>47</sub> motif might interact with a chaperone, specific for UapA packaging into COPII vesicles. ER membrane chaperones, involved in ER-exit of specific protein families, have been found in fungi [57–60]. In particular, Shr3p in *S. cerevisiae* is necessary for the correct association and concentrative ER-exit of all 18 amino acid transporters of the

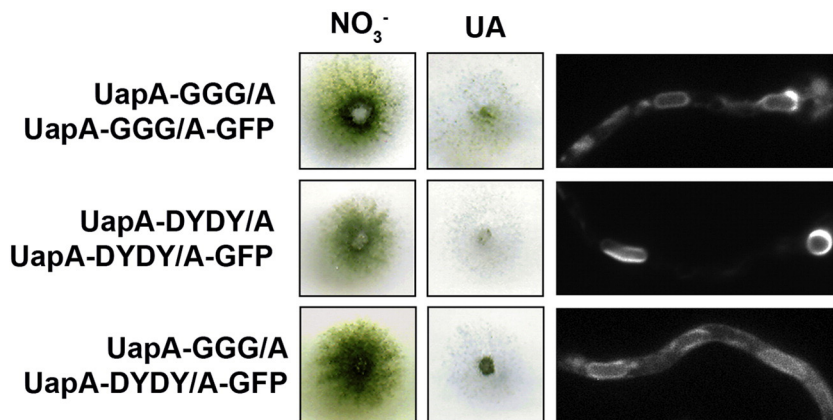


**Fig. 10.** Intragenic complementation of ER-retained mutants. Growth tests and epifluorescence microscopy of a strain co-expressing UapA-GGG/A<sub>3</sub> with UapA-DYDY/A<sub>4</sub>-GFP. Control strains co-expressing either UapA-GGG/A<sub>3</sub> with UapA-GGG/A<sub>3</sub>-GFP or UapA-DYDY/A<sub>4</sub> with UapA-DYDY/A<sub>4</sub>-GFP are also shown. Partial re-localization of UapA-DYDY/A<sub>4</sub>-GFP was observed only upon co-expression with UapA-GGG/A<sub>3</sub>. Notice that there is no significant growth on UA, suggesting that both versions of UapA lack significant transport activity.

APC family. Interestingly, in the absence of Shr3p, amino acid transporters integrate in the ER membrane and fold correctly, but the monomers form aggregates and consequently fail to exit the ER membrane. However, we still cannot exclude that the cytoplasmic N-terminal DYDY<sub>47</sub> motif interacts with specific sequences of UapA, eliciting a topological effect, and thus promoting dimerization/oligomerization and ER-exit.

Our results are very similar to findings obtained on the role of oligomerization in the membrane trafficking of neurotransmitter transporters in mammals. Both the dopamine (DAT) [24–26] and serotonin (SERT) [23,28,30] transporters have been found to dimerize and eventually oligomerize into higher-order assemblies. The evidence for oligomerization in these cases comes from co-immunoprecipitation experiments, cross-linking and fluorescence resonance energy transfer but also from dominant-negative phenotypes obtained when mutants were co-expressed with wild-type proteins. Fluorescence resonance energy transfer signals in DAT were detected at the plasma membrane and in intracellular membrane compartments [25]. The similarity of our results with those of the neurotransmitter transporters is impressive. In both cases, wild-type oligomers are formed in the ER and then maintained both at the plasma membrane and during trafficking between the plasma membrane and endosomes. In addition, in both cases, co-expression of mutant and wild-type proteins led to negative (ER retention) or positive (plasma membrane localization) *in trans* sorting. Interestingly, it has also been proposed that oligomerization of DAT at the plasma membrane is reduced upon substrate binding and transport, and this in turn led to speculation that substrate-elicited endocytosis operates by loosening oligomerization. The evidence for that comes from a reduction in surface DAT determined by biotinylation and reduction in DAT oligomerization as assessed by cross-linking [27,29]. In UapA, the presence of substrates did not abolish oligomerization, as assessed by pull-down assays and the persistence of strong split-YFP fluorescent signals in endosomes and the vacuolar membrane upon endocytosis. Our findings do not answer the question whether UapA dimers further assemble into higher oligomeric complexes as seen for DAT and SERT.

Several logical assumptions suggest how oligomerization might have evolved to be a critical link among proper folding, quality control, ER-exit, membrane trafficking and turnover. Firstly, correct folding and maturation of a protein are required for oligomerization, ensuring that only correctly folded proteins enter the secretory pathway. Secondly, oligomerization can induce a conformational change that might increase the affinity for a specific ER membrane microdomain, which might then lead to further oligomerization owing to increased concentration in such a domain and eventually to concentrative ER-exit [19]. Thirdly,

homo-oligomerized cargoes could travel as highly specific membrane microdomains and remain so in their final membrane destination. This in turn provides a mechanistic solution to how specific transporters (or channels or receptors) could be sorted and turned over by endocytosis or direct sorting from the Golgi, in response to substrate excess or other specific physiological signals, without affecting the turnover of other transporters.

## Materials and Methods

### Media, strains, growth conditions and *A. nidulans* transformation

Standard complete and minimal media (MM) for *A. nidulans* were used<sup>†</sup>. *Escherichia coli* was grown on Luria-Bertani medium. Media and chemical reagents were obtained from Sigma-Aldrich (Life Science Chemilab SA, Hellas) or Appli-Chem (Bioline Scientific SA, Hellas). *A. nidulans* transformation was performed as described previously [60]. A  $\Delta$ azgA  $\Delta$ uapA  $\Delta$ uapC::AfpYrG pabaA1 argB2 mutant strain [61] was the recipient strain in transformations with plasmids carrying differentially tagged wild-type or mutant versions of UapA (see below). Selection was based on complementation of the pabaA1 and argB2 genetic auxotrophies for *p*-aminobenzoic acid and arginine. Transformants expressing either single-copy or multi-copy plasmid integration events were identified by PCR and Southern analysis. A  $\Delta$ uapA  $\Delta$ uapC::AfpYrG  $\Delta$ nkuA::argB riboB2 pantoB100 pyroA4 mutant strain [36] was the recipient strain for generating “in locus” integrations of tagged uapA and prnB fusions (see below), based on complementation of the riboB2 and pantoB100 genetic auxotrophies for riboflavin and pantothenic acid, respectively. Growth tests were performed at 25 °C or 37 °C, at pH 6.8.

### Standard nucleic acid manipulations

Genomic DNA extraction from *A. nidulans* was as described in Fungal Genetics Stock Center<sup>‡</sup>. Plasmid preparation from *E. coli* strains and DNA bands were purified from agarose gels using the Nucleospin Plasmid Kit and the Nucleospin ExtractII Kit according to the manufacturer's instructions (Macherey-Nagel, Lab Supplies Scientific SA, Hellas). DNA sequences were determined by VBC-Genomics (Vienna, Austria). Mutations were constructed by site-directed mutagenesis according to the instructions accompanying the QuikChange® Site-Directed Mutagenesis Kit (Agilent Technologies, Stratagene). Southern blot analysis was performed as described in Ref. [62]. [<sup>32</sup>P]dCTP labeled molecules of uapA, argB or pabaA specific probes were prepared using a random hexanucleotide primer kit following the supplier's instructions (Takara Bio, Lab Supplies Scientific SA, Hellas) and purified on MicroSpin™ S-200 HR columns, following the supplier's instructions (Roche Diagnostics, Hellas). Labeled [<sup>32</sup>P]dCTP (3000 Ci mmol<sup>-1</sup>) was purchased from the Institute of Isotopes Co. Ltd, Miskolc, Hungary. Restriction enzymes were from Takara Bio (Lab Supplies Scientific SA, Hellas). Conventional PCR reactions were performed with KAPATaq DNA polymerase (Kapa Biosystems, Lab Supplies Scientific

SA, Hellas). Amplification of products and site-directed mutagenesis were performed with Kapa HiFi (Kapa Biosystems, Lab Supplies Scientific SA, Hellas).

### Plasmid constructions

Plasmid pAN510 and derivatives pAN510exp, pAN510exp-GFP, pAN510-GFP and pBS-argB-alcA<sub>p</sub> are described in previous articles [44,63–65]. These plasmids are derivatives from the original pAN510 plasmid [38,66] and were constructed by disrupting a XbaI site of the pBluescript polylinker and introducing a BamHI site next to the start codon of *uapA*, by site-directed mutagenesis. Given that there is a natural XbaI site after the stop codon of *uapA*, the *uapA* coding sequence could be exchanged by BamHI/XbaI double digestion. In pAN520exp, the *argB* sequence has been replaced by *pabaA* from pBS-pabaA [64]. The *alcA<sub>p</sub>* 480-bp sequence was used to replace the native *uapA* promoter sequence in the derivative plasmids of the type pAN510. All point mutations were constructed by site-directed mutagenesis on plasmid pAN510-GFP or, in the case of multiple mutations, on already mutated versions of this plasmid. N-terminal truncations of UapA ( $\Delta$ 3-30,  $\Delta$ 3-42,  $\Delta$ 3-62 and  $\Delta$ 3-74) were constructed by introducing a BamHI restriction site at the desirable position and subcloning of the ORF (open reading frame) in pAN510exp-GFP. For BiFC analyses, the N-terminal half of yellow fluorescent protein (YFP<sub>N</sub>; 154 amino acids of YFP) or the C-terminal half of YFP (YFP<sub>C</sub>; 86 amino acids of YFP) was amplified from plasmids PDV7 and PDV8 [67] and cloned into pAN510exp, pAN510exp-alcA<sub>p</sub>, pAN520exp or pAN520exp-alcA<sub>p</sub> at the native XbaI site (XbaI/SpeI compatible end ligation), followed by cloning of the *uapA* ORF carrying the desirable mutations. The same approach (XbaI/SpeI compatible end ligation) was followed for the construction of plasmid pAN510exp-alcA<sub>p</sub>-His. Plasmids expressing the UapA-YFP<sub>N</sub> and PrmB-YFP<sub>C</sub> were used as templates to generate gene replacement cassettes by PCR and were constructed by sequential cloning of the relevant ORFs together with approximately 1.5-kb upstream/downstream regions and the auxotrophic markers *riboB* (AN0670) and *pantoB* (AN1778), respectively.

### Total protein extraction and Western blot analysis

Cultures for total protein extraction were grown in MM supplemented with nitrate at 25 °C for 16 h. Total protein extraction was performed as previously described [68]. Equal sample loading was estimated by Bradford assays and Coomassie staining. Total proteins (30 µg) were separated by SDS-PAGE [10% (w/v) polyacrylamide gel] and electrobotted (Mini PROTEAN™ Tetra Cell, Bio-Rad) onto PVDF membranes (Macherey-Nagel, Lab Supplies Scientific SA, Hellas) for immunodetection. The membrane was treated with 2% (w/v) non-fat dried milk and immunodetection was performed with a primary mouse anti-GFP monoclonal antibody (Roche Diagnostics, Hellas), a secondary goat anti-mouse IgG HRP-linked antibody (Cell Signaling Technology Inc., Biotline Scientific SA, Hellas) and a Penta-His HRP Conjugate antibody kit (Qiagen, SafeBlood BioAnalytica SA, Hellas). Blots were developed by the chemiluminescent method using the LumiSensor Chemiluminescent HRP Substrate kit (Genscript USA, Lab Supplies Scientific SA,

Hellas) and SuperRX Fuji medical X-ray films (FujiFILM Europe, Lab Supplies Scientific SA, Hellas).

### Membrane-enriched extraction for purification

The membrane-enriched extraction protocol (adapted from Ref. [43]) was used prior to membrane protein purification by affinity chromatography. To increase protein yield, we performed the extraction procedure in 6–10 eppendorf tubes, containing mycelia of the same strain. The mycelia powder was resuspended in 2 mL of ice-cold extraction buffer (10 mM Tris-HCl, pH 7.5, 100 mM NaCl, 5 mM MgCl<sub>2</sub>, 0.3 M sorbitol, 1 mM PMSF and 1 × Protease Inhibitor Cocktail), mixed by vortexing and incubated on ice for 20–30 min. The samples were then centrifuged for 3 min, at 3000 rpm, 4 °C, to remove cell debris and the supernatants were transferred in pre-frozen eppendorf tubes. Membrane proteins were then precipitated by centrifuging the samples for 1 h at 13,000 rpm, 4 °C. The pellets were resuspended in 80–100 µL of ice-cold solubilization buffer. The suspensions were collected in eppendorf tubes and solubilized, as described below.

### Purification of membrane proteins and affinity chromatography

UapA purification was performed by combining affinity chromatography of a His-tagged recombinant version, UapA-His<sub>10</sub>, with gel filtration chromatography. The procedure followed is an adaptation of the method described in Ref. [43]. Prior to chromatographic purification of UapA-His<sub>10</sub>, crude membrane protein extracts are solubilized by resuspending in solubilization buffer [50 mM NaH<sub>2</sub>PO<sub>4</sub>/Na<sub>2</sub>HPO<sub>4</sub>, pH 8.0, 150 mM NaCl, 1% (w/v) dodecyl-β-D-maltoside (DDM), 1 mM PMSF and 1 × Protease Inhibitor Cocktail]. The sample was stirred gently for 30 min on ice and then centrifuged for 20 min at 12,000g, 4 °C, to separate the solubilized from the insoluble proteins. The supernatant (solubilized proteins) was then transferred to a pre-frozen eppendorf tube and glycerol was added to a final concentration of 20% (v/v) and gently mixed. The detergent-solubilized protein sample was stored at –80 °C for further use or loaded directly onto Protino Ni-NTA Columns (Macherey-Nagel GmbH) for purification. The mobile phase was delivered in a consistent flow rate of 1 mL/min via a pump. The column was first equilibrated with 10–20 column volumes of Ni-column wash buffer [50 mM NaH<sub>2</sub>PO<sub>4</sub>, pH 8.0, 300 mM NaCl, 0.01% (w/v) DDM and 1 mM PMSF], containing 10 mM imidazole. A total of 1–4 mg of protein in 1 mL of detergent solubilization buffer were applied to the column and 2.5 mL of the flow-through was collected and put on ice (fraction f<sub>0</sub>). The column was washed abundantly (10–20 column volumes) with wash buffer containing 20 mM imidazole and subsequently with another containing 50 mM imidazole to remove unbound and loosely bound molecules. A total of 2.5 mL of each eluent were collected and put on ice (fractions f<sub>20</sub> and f<sub>50</sub>). Bound protein was eluted with increasing concentrations of imidazole in the column wash buffer (250 mM, 350 mM and 500 mM) and 2.5 mL of each eluent was collected and put on ice (fractions f<sub>250</sub>, f<sub>350</sub> and f<sub>500</sub>). The column was washed abundantly with the 500 mM imidazole wash buffer and filled with 30% (v/v) EtOH before storing at 4 °C. Desalting and concentration of purified

proteins (UapA-His<sub>10</sub>) was achieved by gel filtration in Sephadex G-25 columns. A total of 2.5 mL of each fraction eluted from the Ni-NTA column were loaded onto the Sephadex column, which was previously washed abundantly with distilled water. After the sample volume had completely entered the column, 3.5 mL of sterile distilled water was added to the column and the protein was eluted and frozen at  $-80^{\circ}\text{C}$ . The frozen protein samples were then concentrated by overnight lyophilization. The freeze-dried samples were resuspended in a buffer containing 50 mM NaH<sub>2</sub>PO<sub>4</sub>/Na<sub>2</sub>HPO<sub>4</sub>, 10% glycerol, 0.1% (w/v) DDM, 1 mM PMSF and 1× Protease Inhibitor Cocktail, adjusted to pH 7.5 and analyzed electrophoretically and immunologically.

### Kinetic analysis

[<sup>3</sup>H]xanthine (33 Ci mmol<sup>-1</sup>; Moravek Biochemicals, California, USA) uptake in MM was assayed in germinating conidiospores of *A. nidulans* concentrated at 10<sup>7</sup> conidiospores/100 μL, at 37 °C, pH 6.8, as recently described in detail [69]. All transport assays were carried out in at least three independent experiments, with three replicates for each concentration or time point. Standard deviation was <20%.

### Epifluorescence microscopy

Samples for standard epifluorescence microscopy were prepared as previously described [35,36]. In brief, germlings incubated on coverslips in liquid MM supplemented with NaNO<sub>3</sub> as nitrogen source for 12–14 h at 25 °C were observed on an Axioplan Zeiss phase contrast epifluorescent microscope and the resulting images were acquired with a Zeiss-MRC5 digital camera using the AxioVs40 V4.40.0 software. Image processing, contrast adjustment and color combining were made using the Adobe Photoshop CS4 Extended version 11.0.2 software or the ImageJ software. Images were converted to RGB and annotated using Photoshop CS4 before being saved to TIFF. For inverted fluorescence microscopy, germlings were incubated in sterile 35-mm micro-dishes, high glass bottom (*ibidi*, Germany) in liquid MM supplemented with NaNO<sub>3</sub> as nitrogen source for 16–18 h at 25 °C. Images were obtained with an AxioCam HR R3 camera using the Zen lite 2012 software either as single images or in stacks of 10–12 optical sections along z-axis with a Z step size at 0.31 μm. Contrast adjustment, area selection and color combining were made using the Zen 2012 software. Images exported as tiffs were annotated and further processed in Adobe Photoshop CS4 Extended version 11.0.2 software for brightness adjustment, rotation and alignment. A desaturated and inverted version of the image was also created in each case, so as to achieve better visualization.

### Static light-scattering measurements of purified UapA

UapA-G411VΔ1-11, a thermostabilised version of the UapA, was expressed and isolated as described previously [37]. The oligomeric state of the UapA-G411VΔ1-11 construct at a detected protein concentration of 1.4 mg/mL in sample buffer (20 mM Tris-HCl, pH 7.5, 150 mM NaCl, 5% glycerol, 500 mM xanthine and 0.03% DDM) was

assessed with a Malvern Viscotek TDMax Tetra detection system, including static light scattering, UV and refractive index detectors, connected downstream of a Superdex-200 10/30 gel-filtration column previously equilibrated in sample buffer. The protein is initially separated on the gel-filtration column prior to further analysis. The data were analyzed with the Omnisec software (Malvern) following the manufacturer's protocols and used to calculate the MW of the protein particles in the individual fractions eluting from the column. In this case, the detergent micelles present in the sample contribute to the size of the protein particles. The system was calibrated first with buffer containing DDM detergent alone at the same concentration as the test sample [0.03% (w/v) DDM<sub>LA</sub>] and the size of the detergent micelles was calculated. This is then subtracted from the MW of the protein-detergent complex to provide an accurate assessment of the size of the protein particles.

### Selection of genetic suppressors

UV exposure conditions used for the mutagenesis of the strain expressing UapA-Y47A were determined based on a specifically constructed cell survival curve. According to the resulting cell survival curve, the time for achieving >98% lethality in 10<sup>7</sup> conidiospores, which was used for this work, was estimated at 4 min 30 s. UV exposure of conidiospore suspensions in 0.01% Tween in Petri dishes was performed at a standard distance of 20 cm from an Osram HNS30 UV-B/C lamp. Mutagenized conidiospores were plated in standard MM supplemented with 0.5 mM uric acid as sole nitrogen source and necessary vitamins. Suppressors appeared as distinct well conidiating colonies after 7 days of incubation at 25 °C.

### Acknowledgments

We are grateful to Joseph Strauss for hosting in his laboratory and supporting Sotiris Amillis during the systematic mutational analysis of the UapA. We thank Anna Vlanti for assisting in the construction of some mutants. We also thank Vassilis Bitsikas for critical comments. Olga Martzoukou and work in the laboratory of George Djalinas were supported by a research grant from Fondation Santé. Mayia Karachaliou was supported by the European Union (European Social Fund) and Greek national funds through the Operational Program "Education and Lifelong Learning" of the National Strategic Reference Framework Research Funding Program: Heracleitus II, Investing in Knowledge Society through the European Social Fund, Investing in Knowledge Society through the European Social Fund. Work in the laboratory of Bernadette Byrne and James Leung was supported by the European Community's Seventh Framework Program FP7/2007-2013 under Grant Agreement No. HEALTH-F4-2007-201924, EDICT Consortium and Biotechnology and Biological Sciences Research Council grant BB/K017292/1.

## Appendix A. Supplementary data

Supplementary data to this article can be found online at <http://dx.doi.org/10.1016/j.jmb.2015.05.021>.

Received 5 March 2015;

Received in revised form 27 May 2015;

Accepted 28 May 2015

Available online xxx

### Keywords:

transport;  
membrane sorting;  
trafficking;  
bimolecular fluorescence;  
endocytosis

† Media and supplemented auxotrophies were at the concentrations given in <http://www.fgsc.net>.

‡ <http://www.fgsc.net>.

### Abbreviations used:

BiFC, bimolecular fluorescence complementation; MW, molecular weight; MM, minimal media; DDM, dodecyl- $\beta$ -D-maltoside.

## References

- [1] Nyathi Y, Wilkinson BM, Pool MR. Co-translational targeting and translocation of proteins to the endoplasmic reticulum. *Biochim Biophys Acta* 2013;1833:2392–402.
- [2] D'Arcangelo JG, Stahmer KR, Miller EA. Vesicle-mediated export from the ER: COPII coat function and regulation. *Biochim Biophys Acta* 2013;1833:2464–72.
- [3] Barlowe C. Signals for COPII-dependent export from the ER: what's the ticket out? *Trends Cell Biol* 2003;13:295–300.
- [4] Sato K, Nakano A. Mechanisms of COPII vesicle formation and protein sorting. *FEBS Lett* 2007;581:2076–82.
- [5] Fath S, Mancias JD, Bi X, Goldberg J. Structure and organization of coat proteins in the COPII cage. *Cell* 2007;129:1325–36.
- [6] Budnik A, Stephens DJ. ER exit sites-localization and control of COPII vesicle formation. *FEBS Lett* 2009;583:3796–803.
- [7] Copic A, Latham CF, Horlbeck MA, D'Arcangelo JG, Miller EA. ER cargo properties specify a requirement for COPII coat rigidity mediated by Sec13p. *Science* 2012;335:1359–62.
- [8] Gillon AD, Latham CF, Miller EA. Vesicle-mediated ER export of proteins and lipids. *Biochim Biophys Acta* 2012;1821:1040–9.
- [9] Ruggiano A, Foresti O, Carvalho P. Quality control: ER-associated degradation: protein quality control and beyond. *J Cell Biol* 2014;204:869–79.
- [10] Stolz A, Ernst A, Dikic I. Cargo recognition and trafficking in selective autophagy. *Nat Cell Biol* 2014;16:495–501.
- [11] Wang X, Matteson J, An Y, Moyer B, Yoo JS, Bannykh S, et al. COPII-dependent export of cystic fibrosis transmembrane conductance regulator from the ER uses a di-acidic exit code. *J Cell Biol* 2004;167:65–74.
- [12] Renard HF, Demaegd D, Guerriat B, Morsomme P. Efficient ER exit and vacuole targeting of yeast Sna2p require two tyrosine-based sorting motifs. *Traffic* 2010;11:931–46.
- [13] Dong C, Nichols CD, Guo J, Huang W, Lambert NA, Wu G. A triple arg motif mediates  $\alpha$ (2B)-adrenergic receptor interaction with Sec24C/D and export. *Traffic* 2012;13:857–68.
- [14] Otsu W, Kurooka T, Otsuka Y, Sato K, Inaba M. A new class of endoplasmic reticulum export signal PhiXPhiXPhi for transmembrane proteins and its selective interaction with Sec24C. *J Biol Chem* 2013;288:18521–32.
- [15] Guo Y, Sirkis DW, Schekman R. Protein Sorting at the trans-Golgi Network. *Annu Rev Cell Dev Biol* 2014;30:169–206.
- [16] Russell C, Stagg SM. New insights into the structural mechanisms of the COPII coat. *Traffic* 2010;11:303–10.
- [17] Sato K, Nakano A. Oligomerization of a cargo receptor directs protein sorting into COPII-coated transport vesicles. *Mol Biol Cell* 2003;14:3055–63.
- [18] Sato K, Nakano A. Emp47p and its close homolog Emp46p have a tyrosine-containing endoplasmic reticulum exit signal and function in glycoprotein secretion in *Saccharomyces cerevisiae*. *Mol Biol Cell* 2002;13:2518–32.
- [19] Springer S, Malkus P, Borchert B, Wellbrock U, Duden R, Schekman R. Regulated oligomerization induces uptake of a membrane protein into COPII vesicles independent of its cytosolic tail. *Traffic* 2014;15:531–45.
- [20] Lu X, Zhang Y, Shin YK. Supramolecular SNARE assembly precedes hemifusion in SNARE-mediated membrane fusion. *Nat Struct Mol Biol* 2008;5:700–6.
- [21] Van Craenenbroeck K. GPCR oligomerization: contribution to receptor biogenesis. *Subcell Biochem* 2012;63:43–65.
- [22] Wu G. Identification of endoplasmic reticulum export motifs for G protein-coupled receptors. *Methods Enzymol* 2013;521:189–202.
- [23] Kilic F, Rudnick G. Oligomerization of serotonin transporter and its functional consequences. *Proc Natl Acad Sci U S A* 2000;97:3106–11.
- [24] Hastrup H, Sen N, Javitch JA. The human dopamine transporter forms a tetramer in the plasma membrane: cross-linking of a cysteine in the fourth transmembrane segment is sensitive to cocaine analogs. *J Biol Chem* 2003;278:45045–8.
- [25] Sorkina T, Doolen S, Galperin E, Zahniser NR, Sorkin A. Oligomerization of dopamine transporters visualized in living cells by fluorescence resonance energy transfer microscopy. *J Biol Chem* 2003;278:28274–83.
- [26] Torres GE, Carneiro A, Seamans K, Fiorentini C, Sweeney A, Yao WD, et al. Oligomerization and trafficking of the human dopamine transporter. Mutational analysis identifies critical domains important for the functional expression of the transporter. *J Biol Chem* 2003;278:2731–9.
- [27] Chen N, Reith ME. Substrates dissociate dopamine transporter oligomers. *J Neurochem* 2008;105:910–20.
- [28] Fjorback AW, Pla P, Müller HK, Wiborg O, Saudou F, Nyengaard JR. Serotonin transporter oligomerization documented in RN46A cells and neurons by sensitized acceptor emission FRET and fluorescence lifetime imaging microscopy. *Biochem Biophys Res Commun* 2009;380:724–8.
- [29] Li Y, Cheng SY, Chen N, Reith ME. Interrelation of dopamine transporter oligomerization and surface presence as studied with mutant transporter proteins and amphetamine. *J Neurochem* 2010;114:873–85.
- [30] Anderluh A, Klotzsch E, Reismann AW, Brameshuber M, Kudlacek O, Newman AH, et al. Single molecule analysis reveals coexistence of stable serotonin transporter monomers and oligomers in the live cell plasma membrane. *J Biol Chem* 2014;289:4387–99.
- [31] De Zutter JK, Levine KB, Deng D, Carruthers A. Sequence determinants of GLUT1 oligomerization: analysis by



- homology-scanning mutagenesis. *J Biol Chem* 2013;288:20734–44.
- [32] Diallinas G, Gournas C. Structure–function relationships in the nucleobase-ascorbate transporter (NAT) family: lessons from model microbial genetic systems. *Channels (Austin)* 2008;2:363–72.
- [33] Gournas C, Papageorgiou I, Diallinas G. The nucleobase-ascorbate transporter (NAT) family: genomics, evolution, structure–function relationships and physiological role. *Mol Biosyst* 2008;4:404–16.
- [34] Kosti V, Lambrinidis G, Myriantopoulos V, Diallinas G, Mikros E. Identification of the substrate recognition and transport pathway in a eukaryotic member of the nucleobase-ascorbate transporter (NAT) family. *PLoS ONE* 2012;7:e41939.
- [35] Gournas C, Amillis S, Vlanti A, Diallinas G. Transport-dependent endocytosis and turnover of a uric acid-xanthine permease. *Mol Microbiol* 2010;75:246–60.
- [36] Karachaliou M, Amillis S, Evangelinos M, Kokotos AC, Yalelis V, Diallinas G. The arrestin-like protein ArtA is essential for ubiquitination and endocytosis of the UapA transporter in response to both broad-range and specific signals. *Mol Microbiol* 2013;88:301–17.
- [37] Leung J, Cameron AD, Diallinas G, Byrne B. Stabilizing the heterologously expressed uric acid-xanthine transporter UapA from the lower eukaryote *Aspergillus nidulans*. *Mol Membr Biol* 2013;30:32–42.
- [38] Koukaki M, Vlanti A, Goudela S, Pantazopoulou A, Gioule H, Tournaviti S, et al. The nucleobase-ascorbate transporter (NAT) signature motif in UapA defines the function of the purine translocation pathway. *J Mol Biol* 2005;350:499–513.
- [39] Diallinas G, Scazzocchio C. A gene coding for the uric acid-xanthine permease of *Aspergillus nidulans*: inactivational cloning, characterization, and sequence of a *cis*-acting mutation. *Genetics* 1989;122:341–50.
- [40] Hu CD, Chinenov Y, Kerppola TK. Visualization of interactions among bZIP and Rel family proteins in living cells using bimolecular fluorescence complementation. *Mol Cell* 2002;9:789–98.
- [41] Vangelatos I, Vlachakis D, Sophianopoulou V, Diallinas G. Modelling and mutational evidence identify the substrate binding site and functional elements in APC amino acid transporters. *Mol Membr Biol* 2009;26:356–70.
- [42] Felenbok B. The ethanol utilization regulon of *Aspergillus nidulans*: the alcA-alcR system as a tool for the expression of recombinant proteins. *J Biotechnol* 1991;17:11–7.
- [43] Lemuh ND, Diallinas G, Frilingos S, Mermelekas G, Karagouni AD, Hatzinikolaou DG. Purification and partial characterization of the xanthine-uric acid transporter (UapA) of *Aspergillus nidulans*. *Protein Expr Purif* 2009;63:33–9.
- [44] Pantazopoulou A, Lemuh ND, Hatzinikolaou DG, Drevet C, Cecchetto G, Scazzocchio C, et al. Differential physiological and developmental expression of the UapA and AzgA purine transporters in *Aspergillus nidulans*. *Fungal Genet Biol* 2007;44:627–40.
- [45] Amillis S, Kosti V, Pantazopoulou A, Mikros E, Diallinas G. Mutational analysis and modeling reveal functionally critical residues in transmembrane segments 1 and 3 of the UapA transporter. *J Mol Biol* 2011;411:567–80.
- [46] Vlanti A, Amillis S, Koukaki M, Diallinas G. A. A novel-type substrate-selectivity filter and ER-exit determinants in the UapA purine transporter. *J Mol Biol* 2006;357:808–19.
- [47] Lu F, Li S, Jiang Y, Jiang J, Fan H, Lu G, et al. Structure and mechanism of the uracil transporter UraA. *Nature* 2011;472:243–6.
- [48] Kleiger G, Grothe R, Mallick P, Eisenberg D. GXXXG and AXXXA: common alpha-helical interaction motifs in proteins, particularly in extremophiles. *Biochemistry* 2002;41:5990–7.
- [49] Senes A, Engel DE, DeGrado WF. Folding of helical membrane proteins: the role of polar, GxxxG-like and proline motifs. *Curr Opin Struct Biol* 2004;14:465–79.
- [50] Mueller BK, Subramaniam S, Senes A. A frequent, GxxxG-mediated, transmembrane association motif is optimized for the formation of interhelical C<sup>α</sup>-H hydrogen bonds. *Proc Natl Acad Sci U S A* 2014;111:E888–95.
- [51] Haider AJ, Briggs D, Self TJ, Chilvers HL, Holliday ND, Kerr ID. Dimerization of ABCG2 analysed by bimolecular fluorescence complementation. *PLoS ONE* 2011;6:e25818.
- [52] Chang MH, Chen AP, Romero MF. NBCE1A dimer assemble visualized by bimolecular fluorescence complementation. *Am J Physiol Renal Physiol* 2014;306:F672–80.
- [53] Lasry I, Golan Y, Berman B, Amram N, Glaser F, Assaraf YG. In situ dimerization of multiple wild type and mutant zinc transporters in live cells using bimolecular fluorescence complementation. *J Biol Chem* 2014;289:7275–92.
- [54] Li N, Cui Z, Fang F, Lee JY, Ballatori N. Heterodimerization, trafficking and membrane topology of the two proteins, Ost alpha and Ost beta, that constitute the organic solute and steroid transporter. *Biochem J* 2007;407:363–72.
- [55] McFarlane HE, Shin JJ, Bird DA, Samuels AL. Arabidopsis ABCG transporters, which are required for export of diverse cuticular lipids, dimerize in different combinations. *Plant Cell* 2010;22:3066–75.
- [56] Salazar K, Cerda G, Martínez F, Sarmiento JM, González C, Rodríguez F, et al. SVCT2 transporter expression is post-natally induced in cortical neurons and its function is regulated by its short isoform. *J Neurochem* 2014;130:693–706.
- [57] Gilstring CF, Melin-Larsson M, Ljungdahl PO. Shr3p mediates specific COPII coatomer-cargo interactions required for the packaging of amino acid permeases into ER-derived transport vesicles. *Mol Biol Cell* 1999;10:3549–65.
- [58] Martínez P, Ljungdahl PO. The SHR3 homologue from *S. pombe* demonstrates a conserved function of ER packaging chaperones. *J Cell Sci* 2000;113:4351–62.
- [59] Kota J, Ljungdahl PO. Specialized membrane-localized chaperones prevent aggregation of polytopic proteins in the ER. *J Cell Biol* 2005;168:79–88.
- [60] Erpapazoglou Z, Kafasla P, Sophianopoulou V. The product of the SHR3 orthologue of *Aspergillus nidulans* has restricted range of amino acid transporter targets. *Fungal Genet Biol* 2006;43:222–33.
- [61] Koukaki M, Giannoutsou E, Karagouni A, Diallinas G. A novel improved method for *Aspergillus nidulans* transformation. *J Microbiol Methods* 2003;55:687–95.
- [62] Sambrook J, Russell DW. *Molecular cloning: a laboratory manual*. Cold Spring Harbor, New York: Cold Spring Harbor Laboratory Press; 2001.
- [63] Diallinas G, Valdez J, Sophianopoulou V, Rosa A, Scazzocchio C. Chimeric purine transporters of *Aspergillus nidulans* define a domain critical for function and specificity conserved in bacterial, plant and metazoan homologues. *EMBO J* 1998;17:3827–37.
- [64] Vlanti A, Diallinas G. The *Aspergillus nidulans* FcyB cytosine-purine scavenger is highly expressed during germination and in reproductive compartments and is downregulated by endocytosis. *Mol Microbiol* 2008;68:959–77.
- [65] Papageorgiou I, Gournas C, Vlanti A, Amillis S, Pantazopoulou A, Diallinas G. Specific interdomain synergy

- in the UapA transporter determines its unique specificity for uric acid among NAT carriers. *J Mol Biol* 2008;382:1121–35.
- [66] Gorfinkiel L, Diallinas G, Scazzocchio C. Sequence and regulation of the *uapA* gene encoding a uric acid-xanthine permease in the fungus *Aspergillus nidulans*. *J Biol Chem* 1993;268:23376–81.
- [67] Takeshita N, Higashitsuji Y, Konzack S, Fischer R. Apical sterol-rich membranes are essential for localizing cell end markers that determine growth directionality in the filamentous fungus *Aspergillus nidulans*. *Mol Biol Cell* 2008;19:339–51.
- [68] Galanopoulou K, Scazzocchio C, Galinou ME, Liu W, Borbolis F, Karachaliou M, et al. Purine utilization proteins in the Eurotiales: cellular compartmentalization, phylogenetic conservation and divergence. *Fungal Genet Biol* 2014;69: 96–108.
- [69] Kryptou E, Diallinas G. Transport assays in filamentous fungi: kinetic characterization of the UapC purine transporter of *Aspergillus nidulans*. *Fungal Genet Biol* 2014;63:1–8.

# BsdA<sup>Bsd2</sup>-dependent vacuolar turnover of a misfolded version of the UapA transporter along the secretory pathway: prominent role of selective autophagy

Minoas Evangelinos, Olga Martzoukou, Koar Choroizian, Sotiris Amillis and George Dhallinas\*

Faculty of Biology, University of Athens, Panepistimioupolis 15784, Athens, Greece.

## Summary

Transmembrane proteins translocate cotranslationally in the endoplasmic reticulum (ER) membrane and traffic as vesicular cargoes, via the Golgi, in their final membrane destination. Misfolding in the ER leads to protein degradation basically through the ERAD/proteasome system. Here, we use a mutant version of the purine transporter UapA ( $\Delta R481$ ) to show that specific misfolded versions of plasma membrane cargoes undergo vacuolar turnover prior to localization in the plasma membrane. We show that non-endocytic vacuolar turnover of  $\Delta R481$  is dependent on BsdA<sup>Bsd2</sup>, an ER transmembrane adaptor of Hula<sup>Rsp5</sup> ubiquitin ligase. We obtain *in vivo* evidence that BsdA<sup>Bsd2</sup> interacts with Hula<sup>Rsp5</sup> and  $\Delta R481$ , primarily in the ER. Importantly, accumulation of  $\Delta R481$  in the ER triggers delivery of the selective autophagy marker Atg8 in vacuoles along with  $\Delta R481$ . Genetic block of autophagy (*atg9* $\Delta$ , *rabO<sup>ts</sup>*) reduces, but does not abolish, sorting of  $\Delta R481$  in the vacuoles, suggesting that a fraction of the misfolded transporter might be redirected for vacuolar degradation via the Golgi. Our results support that multiple routes along the secretory pathway operate for the detoxification of *Aspergillus nidulans* cells from misfolded membrane proteins and that BsdA is a key factor for marking specific misfolded cargoes.

## Introduction

In eukaryotes, polytopic transmembrane proteins face strict folding controls, most of which operate during their translocation in the membrane of the ER directly from ribosomes. It is in fact the process of cotranslational ER translocation that imposes special challenges for folding, given that translation operates at higher rates compared to protein folding (Nyathi *et al.*, 2013). Fine protein quality control systems for detecting misfolded proteins in the ER have evolved for detoxifying cells from potentially deleterious polypeptides (Smith *et al.*, 2011; Gardner *et al.*, 2013; Ruggiano *et al.*, 2014). Proper folding is also an absolute requirement for subsequent packaging into COPII secretory vesicles, ER-exit and, eventually, targeting to the plasma or organellar membranes (Sato and Nakano, 2007; D'Arcangelo *et al.*, 2013). Protein misfolding in the ER membrane can occur stochastically, but also in response to stress conditions (e.g. higher temperature, oxidation, drugs or nutrient starvation), or due to mutations affecting cargo intrinsic folding, or in some cases, specific *cis*-acting sequences necessary for the molecular cross-talk of cargoes and sorting chaperones (Schubert *et al.*, 2000; Kincaid and Cooper, 2007; Kawaguchi *et al.*, 2010; Lukacs and Verkman, 2012).

In most cases, misfolded proteins or proteins that do not properly fold within a certain time are targeted for ER-associated degradation (ERAD), which efficiently retrotranslocates them from the ER into the cytosol for degradation via the ubiquitin-proteasome system (Smith *et al.*, 2011; Gardner *et al.*, 2013). Lys48-linked ubiquitylation of the misfolded cargo acts as the primary molecular signal for ERAD (Rotin and Staub, 2011; Lemus and Goder, 2014). Distinct overlapping ERAD pathways, associated with different RING-type E3 ubiquitin ligases (e.g. Hrd1 and Doa10), are selective for different cargoes (Smith *et al.*, 2011). Despite ERAD, accumulation of misfolded proteins in the ER causes stress. To cope with ER stress, cells have evolved an unfolded protein response (UPR) (Ellgaard and Helenius, 2003; Walter and Ron, 2011; Brodsky, 2012). The UPR coordinates the increase in ER-folding capacity through a broad

\*For correspondence. E-mail dhallina@biol.uoa.gr; Tel. (+30) 210 7274649; Fax (+30) 210 7274702.

transcriptional up-regulation of ER-folding, lipid biosynthesis and ERAD machinery (Travers *et al.*, 2000), with a decrease in folding load through selective mRNA degradation and translational repression (Hollien and Weissman, 2006). In addition, a distinct ER Quality Control (ERQC) mechanism, called HIP (Hrd1p independent-proteolysis), has been described in *Saccharomyces cerevisiae* (Haynes *et al.*, 2002). HIP eliminates misfolded proteins from the ER in a manner that requires vesicular transport from the ER to the Golgi apparatus. Once in the *cis*-Golgi compartment, the misfolded cargo is modified by 1,6-mannose addition before Lys63-type ubiquitylation by the HECT-type ubiquitin ligase Rsp5p and subsequent degradation by the proteasome. It was proposed that the misfolded protein might interact with the proteasome in the vicinity of the Golgi, or it may be transported back to the ER where it presumably translocates in the proteasome. Very recently it has also been shown that in *S. cerevisiae* the proteasome acquires a role in the endocytic-vacuolar pathway during cold response (Isasa *et al.*, 2016).

Some misfolded proteins escape the ERQC and are degraded in the vacuole/lysosome. Such misfolded protein cargoes are caught primarily in the Golgi apparatus and then sorted into the multivesicular bodies (MVB)/vacuolar pathway, in a process called Golgi Quality Control (GQC). Details of the mechanism of GQC remain poorly understood (Hegde and Ploegh, 2010; Wang *et al.*, 2011). In *S. cerevisiae*, HECT- (Rsp5) and RING-type (Tul1) ubiquitin ligases seem to be involved in GQC (Lewis and Pelham, 2009). Both ubiquitin ligase systems seem to recognize exposed polar transmembrane regions, thus targeting partially misfolded proteins for vacuolar degradation (Lewis and Pelham, 2009).

Misfolded transmembrane proteins can also be found in the plasma membrane, either because they have escaped all other control points, or due to conditions imposed after these proteins have reached the plasma membrane (Lin *et al.*, 2008; Wang *et al.*, 2011). These proteins are also subject to quality control and degraded via ubiquitylation, endocytosis and sorting into the MVB/vacuole. Plasma Membrane Quality Control (PMQC) involves Rsp5-dependent ubiquitylation. It seems that GQC and PMQC, and probably other peripheral quality control pathways, all converge at the MVB endosomal compartment.

Still another possible pathway for detoxifying cells from misfolded proteins is autophagy. General autophagy is a starvation-elicited, non-selective, degradative pathway, which supplies cells with essential macromolecules for survival (Kruse *et al.*, 2006; Mizushima *et al.*, 2008). However, there is also nutrient-independent selective autophagy, the main function of which is to enforce intracellular quality control by selective disposal of protein aggregates and damaged organelles (Mizush-

ima *et al.*, 2008). Selective autophagy of misfolded proteins is known as Quality Control (QC) autophagy (Lee and Yao, 2010; Yao, 2010). Unlike starvation-induced autophagy, QC autophagy distinguishes its substrates by recognizing their ubiquitylated forms. In this process, receptors need to tether the ubiquitylated cargo to nascent autophagosomes. E3 ubiquitin ligases are involved in ubiquitylation of QC autophagic substrates. Interestingly, K63-linked rather than K48-linked ubiquitin chains could also be part of a defining ubiquitin code for QC autophagic substrates (Yao, 2010).

Supporting Information Figure S1 summarizes the putative turnover pathways of membrane proteins.

The filamentous ascomycete *Aspergillus nidulans* with its amenability to *in vivo* multidimensional microscopy is becoming one of the best genetically tractable systems to study cellular processes related to membrane trafficking and proteostasis (Peñalva, 2010; Abenza *et al.*, 2012; Peñalva *et al.*, 2012; Pantazopoulou *et al.*, 2014; Pinar *et al.*, 2015). In this work, we use a specific mutant version of the UapA purine/H<sup>+</sup> symporter (Gournas *et al.*, 2008, 2010; Diallinas and Gournas, 2008), which exhibits partial ER-retention associated with vacuolar turnover (Kosti *et al.*, 2010), for identifying mechanisms responsible for its degradation. We show that this mutant, called  $\Delta$ R481, is turned-over by both ERAD and selective autophagy, operating prior to plasma membrane localization and endocytosis. Interestingly, in mutants genetically blocked in autophagy, a fraction of  $\Delta$ R481 seems to be degraded by sorting from the Golgi to the vacuole. We demonstrate that the non-endocytic vacuolar turnover of  $\Delta$ R481 is dependent on BsdA<sup>Bsd2</sup>, a functional adaptor of the Hula<sup>Rsp5</sup> ubiquitin ligase. Our results support that eukaryotic cells use multiple parallel QC systems to ensure detoxification from misfolded proteins all along the secretory pathway.

## Results

### *Misfolded UapA mutants show partial ER-retention and reduced steady-state protein levels, associated with both ERAD and vacuolar turnover*

The UapA uric acid-xanthine/H<sup>+</sup> symporter is one of the most extensively studied transporters in eukaryotes (see reviews Diallinas and Gournas, 2008; Gournas *et al.*, 2008; Diallinas, 2014). It is a polytopic membrane protein possessing 14  $\alpha$ -helical transmembrane segments (TMSs) and cytoplasmic N- and C-terminal tails. Using fully functional GFP-tagged versions of UapA, we have shown that UapA molecules are exclusively sorted in the plasma membrane (PM), apparently through the secretion pathway, involving ER-exit and passage through the Golgi compartment (Pantazopoulou *et al.*, 2007; Gournas *et al.*, 2010).

Functional UapA or UapA-GFP allows full growth on uric acid or xanthine as sole nitrogen source, as these purines are efficiently catabolized to ammonium in *A. nidulans* (Gournas *et al.*, 2011). Basal low-level turnover operates via endocytosis and sorting to the MVB/vacuolar compartment (Gournas *et al.*, 2010). Massive UapA endocytosis and prominent vacuolar degradation can be elicited in response to a shift in rich nitrogen source media, or in the presence of excess substrates (Gournas *et al.*, 2010; Karachaliou *et al.*, 2013). No other turnover pathway, besides endocytosis, is currently known to operate for wild-type UapA. Finally, there is no current evidence that UapA recycles, under any conditions tested, from the endosomes back to the PM.

Several loss-of-function mutations of UapA show nearly normal plasma membrane localization with moderately increased vacuolar turnover (Koukaki *et al.*, 2005; Pantazopoulou and Diallinas, 2006; Vlanti *et al.*, 2006; Papageorgiou *et al.*, 2008; Kosti *et al.*, 2010). However, a smaller number of specific mutations located within or in the cytoplasmic borders of TMSs leads to massive vacuolar turnover of UapA, often associated with partial ER retention, and no or little plasma membrane localization. Vacuolar sorting of the corresponding mutant versions of UapA-GFP has been confirmed by the co-localization with 7-amino-4-chloromethylcoumarin (CMAC), whereas partial ER retention is evidenced by fluorescent labelling of perinuclear ER rings (Pantazopoulou and Diallinas, 2006; Vlanti *et al.*, 2006; Kosti *et al.*, 2010; Amillis *et al.*, 2011; Martzoukou *et al.*, 2015; see below). Prominent examples of such, apparently misfolded, UapA versions are shown in Fig. 1A and concern mutations located in TMS1 (I74N, H86A), TMS7 (G301L/G313L) or TMS13 ( $\Delta$ R481, AGR481). In some of these mutants, low plasma membrane localization of UapA is also observed, as for example in H86A.

The subcellular co-localization of these mutants with vacuoles has been shown before. Figure 1B shows the vacuolar localization of a selected mutant, namely  $\Delta$ R481, using the lipophilic dye FM4-64 and CMAC (Peñalva, 2005).  $\Delta$ R481-GFP associated fluorescent structures show short range slow motility in the periphery of perinuclear ER rings (Video S1A). This contrasts the situation when we follow vacuolar sorting via early endosomal sorting of wild-type UapA after endocytosis (Gournas *et al.*, 2010; Karachaliou *et al.*, 2013; Video S1B). This observation suggested that a major fraction of  $\Delta$ R481 is degraded in the vacuole by a pathway other than endocytosis. Similar evidence for non-endocytic turnover of other apparently misfolded UapA mutants was obtained (not shown). Subsequent work described in this article concerns mutant  $\Delta$ R481, taken as a model misfolded version of UapA and used for identifying the

mechanism(s) of vacuolar turnover by an apparently non-endocytic route.

The subcellular localization of wild-type UapA and  $\Delta$ R481 reflects expression from the *uapA* native promoter, which is rather moderate at the onset of germination and drops to lower levels during vegetative growth of *A. nidulans* (Amillis *et al.*, 2004; Gournas *et al.*, 2010). To better analyze the nature of  $\Delta$ R481 turnover, we made use of the controllable strong promoter of the alcohol dehydrogenase gene (*alcA<sub>p</sub>*) (Felenbok, 1991), which allowed us to perform promoter shut-off experiments. Transcription from *alcA<sub>p</sub>* in the presence of a non-repressible carbon source (e.g. fructose) leads to continuous UapA expression (see Fig. 1C, left panel). Efficient repression of UapA transcription, evidenced as lack of UapA-GFP fluorescence, can be achieved when samples are shifted to glucose (Pantazopoulou *et al.*, 2007). When  $\Delta$ R481-GFP is expressed from the *alcA<sub>p</sub>* promoter under non-repressible conditions, fluorescence is mostly associated with perinuclear ER membranes, a membranous network and vacuoles similar to the picture obtained when expressed from the native promoter (Fig. 1C, right panels). However, low GFP fluorescence is also associated with the cell periphery, which suggested that when  $\Delta$ R481-GFP is continuously expressed via *alcA<sub>p</sub>*, a fraction of it eventually reaches the plasma membrane (~20% compared to the wild-type UapA).

We followed the steady-state levels of  $\Delta$ R481-GFP compared to wild-type UapA-GFP by Western blot analysis, using an anti-GFP antibody. We detected significantly lower steady-state levels of intact  $\Delta$ R481-GFP compared to wild-type UapA-GFP, both during the 3-hour induction of the *alcA<sub>p</sub>* (pulse) (31% versus 100%) and after a 2-hour cycloheximide (CHX) chase period, blocking total protein synthesis (6% versus 33%) (Fig. 1D). Similar results were also obtained in transcriptional pulse-chase experiments, in which *alcA<sub>p</sub>* transcription of UapA-GFP or  $\Delta$ R481-GFP is induced (I) for 3 h (pulse) followed by a 2-hour transcriptional repression (R) of *alcA<sub>p</sub>* by the addition of glucose (chase, results not shown). These results suggested that  $\Delta$ R481-GFP, compared to wild-type UapA-GFP, is susceptible to more rapid turnover. In addition, this experiment revealed that the vacuolar degradation of  $\Delta$ R481 might be higher than that of wild-type UapA, as evidenced by the higher accumulation of free GFP in the strain expressing  $\Delta$ R481-GFP compared to wild-type UapA-GFP (i.e. 92% versus 74%). Detection of free GFP in Western analyses is a standard indirect measure for vacuolar degradation of GFP-tagged membrane proteins, due to the low rate of turnover of the GFP in the vacuoles (Shintani and Klionsky, 2004; Pinar *et al.*, 2013a).

To investigate the possible involvement of ERAD in the non-vacuolar turnover, we compared changes in the

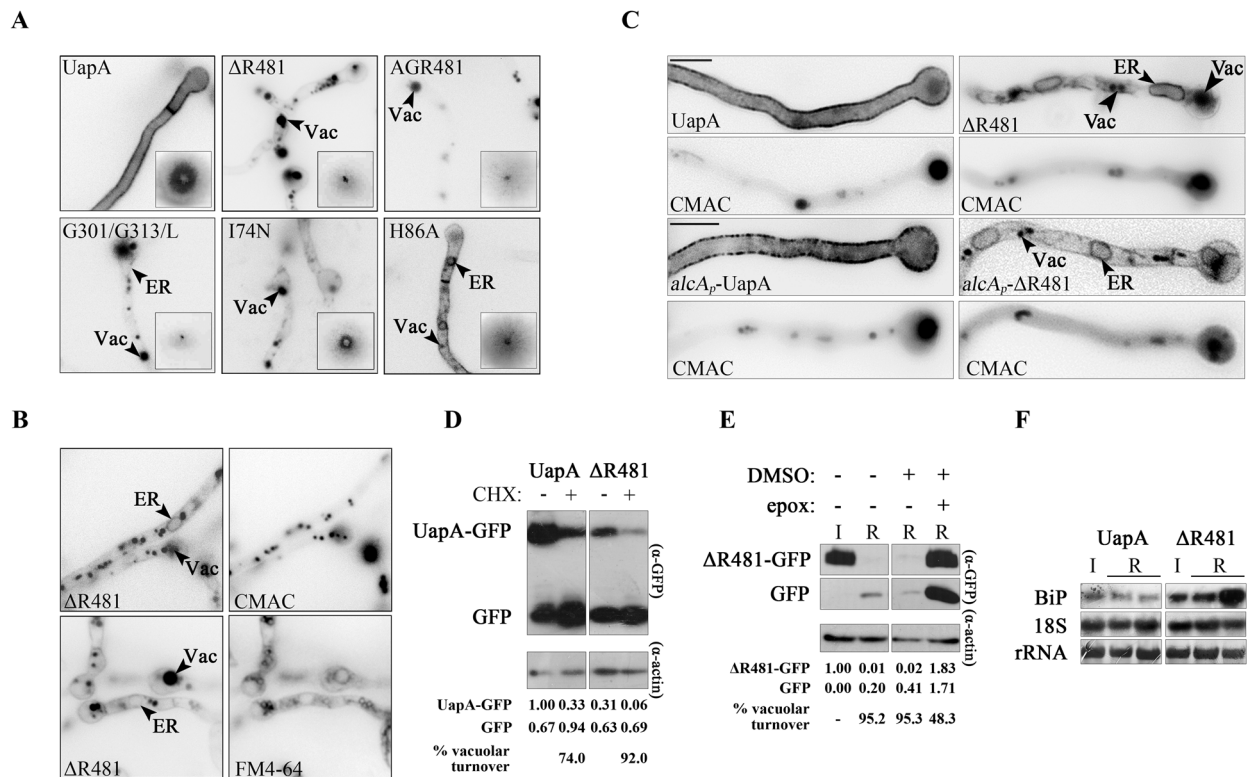


**Fig. 1.** Misfolded UapA mutants show partial ER-retention and reduced steady-state protein levels, associated with both ERAD and vacuolar turnover.

**A.** Epifluorescence microscopy showing the localization of selected, GFP-tagged, mutants of UapA (TMS13- $\Delta R481$ , TMS13-AGR481, TMS7-G301/G313L, TMS1-I74N and TMS1-H86A) in vacuoles (Vac) and perinuclear ER rings, contrasting the PM localization of the wild-type UapA. Inserts at the left bottom side show UapA-dependent growth on uric acid as sole nitrogen of *A. nidulans* strains expressing the relevant UapA versions. Conidiospore production reflects efficiency of nitrogen source uptake, thus, revealing UapA transporter activity (for details of strains see Experimental procedures and Supporting Information Table S1).

**B.** Epifluorescence inverted microscopy showing the subcellular co-localization of mutant  $\Delta R481$  with CMAC- and FM4-64-stained vacuoles.

**C.** Epifluorescence inverted microscopy showing the localization of GFP-tagged wild-type UapA and mutant  $\Delta R481$  expressed from the native or the  $alcA_p$  promoter. Note that upon expression from the  $alcA_p$  promoter all (99.6%) hyphal cells show a degree of PM localization of  $\Delta R481$ -GFP, contrasting the low percentage (21%) of cells with PM localization of  $\Delta R481$ -GFP when expression is driven by the native promoter. Notice also that the fraction of  $\Delta R481$ -GFP localized in the PM upon  $alcA_p$ -driven expression is  $20 \pm 6\%$  of that of the wild-type  $alcA_p$ -UapA-GFP, as estimated using Image J in 10 different hyphae. Lower panels show CMAC staining of vacuoles. Scale bars represent  $5 \mu\text{m}$ .

**D.** Western blot analysis, using anti-GFP antibody, of wild-type UapA or mutant  $\Delta R481$ , expressed from  $alcA_p$ , in the absence or after adding cycloheximide (CHX), which is used to shut-off *de novo* protein synthesis. Lowest panel shows a control for protein loading using anti-actin antibody. Relative steady-state levels of the different proteins/polypeptides, estimated as described in Experimental procedures, is shown at the bottom.

**E.** Western blot analysis after a 3-hour induction (I) followed by a 2-hour transcriptional repression (R), in the presence of the non-reversible ERAD inhibitor epoxomicin or DMSO as control. Untreated samples have been also included as controls. Relative protein quantification is as in D.

**F.** Northern blot analysis detecting BiP mRNA steady-state levels in strains expressing wild-type UapA or mutant  $\Delta R481$ , under  $alcA_p$  inducing (3 h) or repressing conditions (3 h induction followed by 1 or 2 h of repression respectively). RNA loading controls are shown in the lower panels.

steady-state levels of  $\Delta R481$  after a 2-hour treatment with epoxomicin, a selective non-reversible proteasome inhibitor (Meng *et al.*, 1999). Indeed, Fig. 1E shows that pharmacological block of ERAD significantly inhibited the turnover of  $\Delta R481$  ( $\sim 49\%$ ). Importantly however, even when ERAD is blocked, the remaining  $\sim 51\%$  of  $\Delta R481$  is degraded in the vacuole, as evidenced by the levels of free GFP.

The observed ER retention and ERAD of  $\Delta R481$  strongly suggested that  $\Delta R481$  is a partially misfolded version of UapA. This was confirmed by the observation that the  $alcA_p$ -driven expression of  $\Delta R481$ , but not of

wild-type UapA, induced 3.5-fold the transcription of BiP (Fig. 1F), an ER-associated chaperone, the over-expression of which is directly associated with UPR (Walter and Ron, 2011).

#### *Vacuolar turnover of $\Delta R481$ occurs primarily by non-endocytic mechanism(s) involving Hula-dependent activity*

Vacuolar turnover of wild-type UapA through endocytosis and MVB/endosomal sorting requires ubiquitylation at a

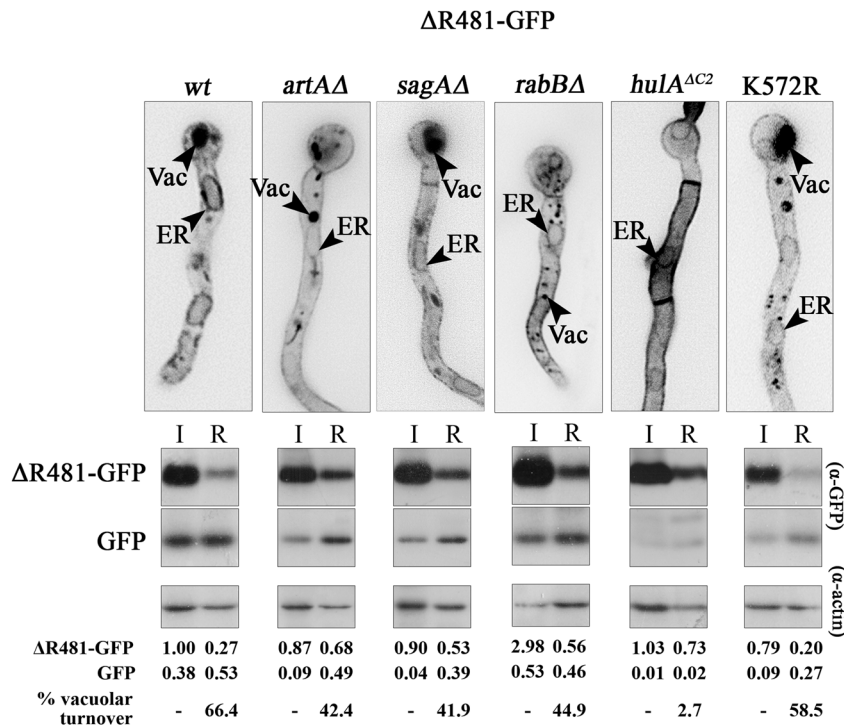


**Fig. 2.** Vacuolar turnover of ΔR481 necessitates Hula-dependent ubiquitylation and occurs independently from endocytosis. Upper panel: Epifluorescence inverted microscopy showing the localization of ΔR481-GFP in different isogenic genetic backgrounds (*artAΔ*, *sagAΔ*, *rabBΔ* or *hulaΔC2*) or of a version of ΔR481-GFP carrying mutation K572R. Lower panel: Relative Western blot analysis, using anti-GFP antibody and conditions described in Fig. 1E, of the same strains shown in the upper panel. Protein loading (actin levels) and relative quantification is shown at the bottom. Notice that only expression in *hulaΔC2* blocks vacuolar sorting and degradation of ΔR481.

single C-terminal Lys residue (Lys572) catalyzed by the HECT-type ubiquitin ligase Hula<sup>Rsp5</sup> (Gournas *et al.*, 2010). Hula-dependent ubiquitylation of UapA requires the activity of the arrestin-like adaptor ArtA (Karachaliou *et al.*, 2013). Upon ubiquitylation, UapA molecules are recruited to endocytic vesicles and are internalized in a process that requires the Saga<sup>End3</sup> actin-binding protein. To test a possible contribution of endocytosis in the vacuolar degradation of ΔR481, we followed its subcellular localization in mutant strains lacking functional Hula<sup>Rsp5</sup>, ArtA and Saga proteins, or by using a version of ΔR481, which cannot be ubiquitylated due to the mutation K572R.

Our results show that in mutant strains deficient in UapA endocytosis (*artAΔ* or *sagAΔ*), ΔR481 still shows ER retention and significant, albeit reduced, vacuolar degradation (Fig. 2). The fact that blocking endocytosis reduces, but does not abolish the level of vacuolar degradation suggested that only the fraction of ΔR481 that reaches the plasma membrane is vulnerable to endocytosis, whilst the rest is degraded by a non-endocytic mechanism. Given the rather unlikely possibility that endocytosis of misfolded UapA versions might depend on arrestin-like adaptors or factors other than ArtA or Saga, we also used a *rabBΔ* mutant strain, lacking the early endosomal GTPase RabB<sup>Rab5</sup>. Deletion of RabB<sup>Rab5</sup> prevents the MVB sorting and vacuolar delivery of plasma membrane transporters during endocytosis (Abenza *et al.*, 2010). Results shown in Fig. 2 confirm that a genetic block (*rabBΔ*) of the endocytic sorting of

ΔR481 in vacuoles has only a partial effect on the levels of ΔR481 vacuolar degradation, similar to what was observed in *artAΔ* and *sagAΔ* strains (turnover rates 41.9–44.9%). Vacuolar degradation of ΔR481 was however totally blocked in the absence of a fully functional Hula<sup>Rsp5</sup> ubiquitin ligase (*hulaΔ* strain), as evidenced by the near absence of vacuoles or free GFP in relevant Western blot after 3 h induction (I) followed by a 2-hour transcriptional repression of the *alcA<sub>p</sub>* (R) (2.7% turnover). Interestingly, the version of ΔR481 carrying substitution K572R was efficiently turned-over (58.5%), similarly to the original ΔR481 (66.4%). This shows that action of Hula, unlike that employed in the endocytic turnover of UapA, is unrelated to ubiquitination of K572. This strongly supported that a major mechanism of ΔR481 degradation operates prior to PM localization and independently of endocytosis.

Independence of the non-endocytic vacuolar degradation of ΔR481 from Lys572, but dependence on Hula<sup>Rsp5</sup>, suggested that other Lys residues in ΔR481 might be exposed to Hula<sup>Rsp5</sup>-dependent ubiquitylation, or that Hula<sup>Rsp5</sup> has an indirect effect on ΔR481. To test this, we mutated simultaneously all cytoplasmic-facing Lys residues present in the N-tail (K21R, K22R, K59R, K60R, K73R) and the C-tail (K572R) of UapA in ΔR481 and tested whether this modification blocks its turnover. Supporting Information Figure S2A shows that ΔR481 lacking all six Lys residues present in cytoplasmically exposed protein termini (i.e. 6KR) is still significantly degraded in

vacuoles. This suggests that either HulA<sup>Rsp5</sup> does not ubiquitylate  $\Delta$ R481 or a 'cryptic' Lys residue from a transmembrane segment or cytoplasmic loops, or even from the GFP tag itself, is exposed and acts as the acceptor of ubiquitin. In the last case, this would be a consequence of the presence of the  $\Delta$ R481 mutation, as the GFP tag is not a target for ubiquitylation in the wild-type UapA (Karachaliou *et al.*, 2013). To explore further these two possibilities, we performed Western blot analysis adapted for detecting ubiquitylated forms of UapA, as in Gournas *et al.* (2010). We could not however detect ubiquitylation of  $\Delta$ R481 compared to wild-type UapA (Supporting Information Fig. S2B). This implies that either  $\Delta$ R481 is not directly ubiquitylated or that our assays are not sufficiently sensitive to detect ubiquitylation of the fraction of  $\Delta$ R481 that undergoes vacuolar degradation.

#### Non-endocytic vacuolar degradation of $\Delta$ R481 requires BsdA<sup>Bsd2</sup>

Our results suggested that a major fraction of  $\Delta$ R481 is turned-over by HulA-dependent ubiquitylation and sorting to the vacuole from a secretory compartment, most probably the ER, the Golgi or the endosomal network, rather than the plasma membrane via endocytosis. We searched for putative adaptors mediating the interaction of HulA with  $\Delta$ R481 at the ER/Golgi/endosome interface. For this, we made use of knowledge coming *S. cerevisiae*. Two were the most obvious candidates. These are the homologues of the Bsd2 or Ear1 proteins. These proteins are required for Rsp5-dependent ubiquitylation and sorting of specific cargo proteins, including misfolded transporters, into the MVB/vacuole (Hettema *et al.*, 2004; Léon *et al.*, 2008; Nikko and Pelham, 2009). We identified *in silico* single homologues of both *S. cerevisiae* proteins in *A. nidulans*, which we named BsdA<sup>Bsd2</sup> (AN5668, 36% identity) and EarA<sup>Ear1</sup> (AN0831, 50% identity), and constructed by standard reverse genetics the relevant knockout strains (*bsdA* $\Delta$  and *earA* $\Delta$ ). *bsdA* $\Delta$  has a mildly delayed rate of growth in the presence of subtoxic concentrations of CdCl<sub>2</sub> and produces fewer conidiospores at 42°C, compared to an isogenic control strain (Supporting Information Fig. S3). A similar, but stronger, mutant phenotype has been observed for *bsd2* $\Delta$  in *S. cerevisiae* (Liu *et al.*, 1997). The growth phenotype of *earA* $\Delta$  is moderately distinct from that of an isogenic *earA*<sup>+</sup> strain and has no effect on  $\Delta$ R481-GFP turnover (results not shown), thus no further work was performed with this mutant.

The absence of a functional BsdA<sup>Bsd2</sup> (*bsdA* $\Delta$ ) suppressed vacuolar sorting and increased relocalization of  $\Delta$ R481 in the plasma membrane, whilst ER retention was still evident (Fig. 3A). This also suggested that lack of a

functional BsdA does not suppress misfolding and ER retention. Lack of a functional BsdA<sup>Bsd2</sup> had also no apparent effect on wild-type UapA localization. Western blot analysis further showed that the high vacuolar turnover of  $\Delta$ R481 in the wild-type background (*bsdA*<sup>+</sup>) is significantly, but not totally, blocked in the absence of a functional BsdA<sup>Bsd2</sup> (22.8% turnover in *bsdA* $\Delta$ , versus 55.7% in *bsdA*<sup>+</sup> background; see Fig. 3C). We tested whether the remaining vacuolar degradation is the product of endocytosis, given that  $\Delta$ R481 molecules expressed from the *alcA<sub>p</sub>* reach the PM and are thus eligible to endocytic turnover. We followed the subcellular localization of  $\Delta$ R481 in the *bsdA* $\Delta$  *artA* $\Delta$  and *bsdA* $\Delta$  *sagA* $\Delta$  double mutants. In both cases, within the limits of epifluorescence microscopy,  $\Delta$ R481 was entirely localized in the plasma membrane with no evidence for vacuolar sorting (Fig. 3B, upper panel). The non-localization of  $\Delta$ R481 with the vacuoles in *bsdA* $\Delta$  *artA* $\Delta$  or *bsdA* $\Delta$  *sagA* $\Delta$  mutants becomes even more evident under conditions where *de novo* protein synthesis is blocked with cycloheximide (CHX). Under these conditions, already synthesized  $\Delta$ R481 molecules have exited the ER (no perinuclear rings detected) and followed an apparently normal trafficking route towards the plasma membrane or the vacuoles (Fig. 3B, lower panel). Western blot analysis following degradation of  $\Delta$ R481 after a 3-hour transcriptional induction (I) and a 2-hour transcriptional repression (R) of *alcA<sub>p</sub>* (Fig. 3C) confirms that in the double *bsdA* $\Delta$  *artA* $\Delta$  or *bsdA* $\Delta$  *sagA* $\Delta$  mutants very little turnover of  $\Delta$ R481 takes place (13.9–15.2%). Notice that in these mutants, despite the absence of detectable vacuolar sorting, as judged by epifluorescence microscopy, we still detect low amounts of free GFP in westerns, which is taken as minor vacuolar degradation.

We further showed that the function of BsdA is irrelevant to endocytosis, as in a *bsdA* $\Delta$  background, plasma membrane sorted  $\Delta$ R481 is drastically endocytosed in the presence of ammonium (Fig. 3D), a standard signal triggering UapA internalization from the PM (Gournas *et al.*, 2010). Internalization from PM is however completely blocked in the double *bsdA* $\Delta$  *artA* $\Delta$  mutant (Fig. 3D and Video S2), thus,  $\Delta$ R481 endocytosis is absolutely dependent on a functional ArtA, the same adaptor recruited during the endocytosis of wild-type UapA. This result dismisses the possibility that  $\Delta$ R481 requires other arrestin-like proteins for its endocytic turnover.

Overall, our results showed that blocking the BsdA<sup>Bsd2</sup>-dependent turnover pathway, which apparently operates from secretory compartments, impairs vacuolar degradation of  $\Delta$ R481 molecules and promotes relocalization in the plasma membrane. Consequently, in a *bsdA* $\Delta$  background  $\Delta$ R481 molecules are sorted in the plasma membrane and from there a fraction of them undergo ArtA-, SagA- and RabB-dependent endocytosis



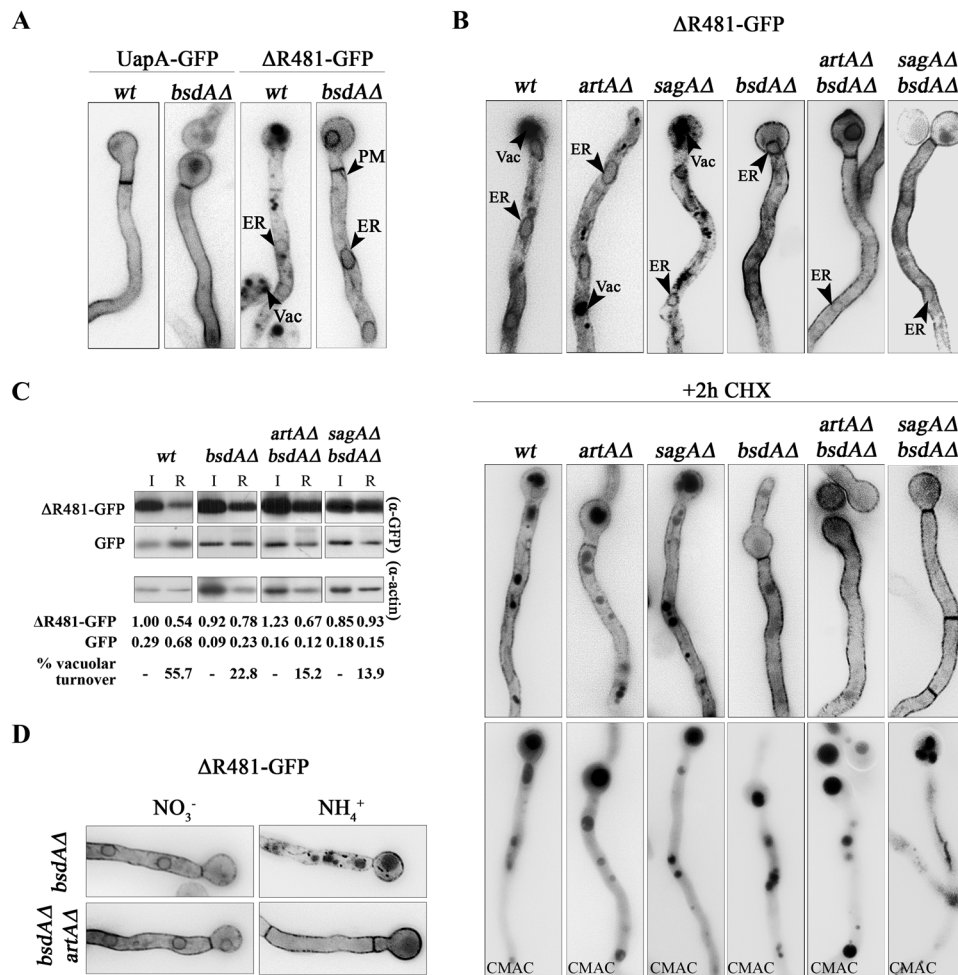


**Fig. 3.** Non-endocytic vacuolar degradation of ΔR481 requires BsdA<sup>Bsd2</sup>.

**A.** Epifluorescence inverted microscopy showing the localization of GFP-tagged wild-type UapA or mutant ΔR481 in *bsdA*<sup>+</sup> and *bsdAΔ* isogenic backgrounds. Notice that ΔR481-GFP vacuolar turnover is apparently blocked in *bsdAΔ*, but ER localization persists.

**B.** Epifluorescence inverted microscopy showing the localization ΔR481-GFP in different isogenic genetic backgrounds (*artAΔ*, *sagAΔ*, *bsdAΔ*, *artAΔ bsdAΔ* or *sagAΔ bsdAΔ*). Notice, in the upper panel, that total block in ΔR481-GFP vacuolar turnover is obtained only in the double *artAΔ bsdAΔ* or *sagAΔ bsdAΔ* mutants. The lower panel shows the same samples after addition of cycloheximide (CHX) for 2 h for blocking *de novo* protein synthesis. Under this treatment already-synthesized ΔR481-GFP is localized in vacuoles and the PM, as the ER-retained fraction is apparently degraded or/and sorted to the PM. Again, notice that total block of vacuolar degradation of ΔR481-GFP is obtained only in the double *artAΔ bsdAΔ* or *sagAΔ bsdAΔ* mutants. The lowest panel shows vacuoles stained with CMAC.

**C.** Western blot analysis, using anti-GFP antibody of ΔR481-GFP expressed in wild-type, *artAΔ bsdAΔ* or *sagAΔ bsdAΔ* genetic backgrounds. Total protein was extracted after a 3-hour transcriptional induction (I) followed by an additional 2-hour transcriptional repression of the *alcA<sub>p</sub>*. Protein loading (actin levels) and relative quantification is shown at the bottom.

**D.** Epifluorescence inverted microscopy detecting the subcellular localization of ΔR481-GFP in *bsdAΔ* or *bsdAΔ artAΔ* isogenic mutants, under control (NO<sub>3</sub><sup>-</sup>) or endocytic conditions (NH<sub>4</sub><sup>+</sup>).

and vacuolar sorting. Thus, simultaneous genetic blocks of the endocytic flux of ΔR481 (in *artAΔ*, *sagAΔ* or *rabBΔ* strains) and of the *bsdA*-dependent pathway impairs vacuolar degradation. Note that, despite the total plasma membrane localization of ΔR481 in the *bsdAΔ artAΔ* or *bsdAΔ sagAΔ* backgrounds, we could not detect any measurable transport activity, reflected in the lack of growth on uric acid as a sole nitrogen source, showing ΔR481 is still a misfolded and inactive version of UapA (Supporting Information Fig. S4).

#### BsdA<sup>Bsd2</sup> is an ER transmembrane adaptor of Hula

To detect the subcellular localization of BsdA, we constructed both N- and C-terminally GFP-tagged versions. Strains expressing these constructs were analyzed with epifluorescence microscopy. The N-terminally tagged GFP-BsdA version showed very little cytoplasmic and rather diffuse fluorescence, incompatible with a transmembrane protein (not shown). Instead, the C-terminal GFP-tagged version of BsdA gave a strong fluorescent signal labelling perinuclear ER membranes and an extended,

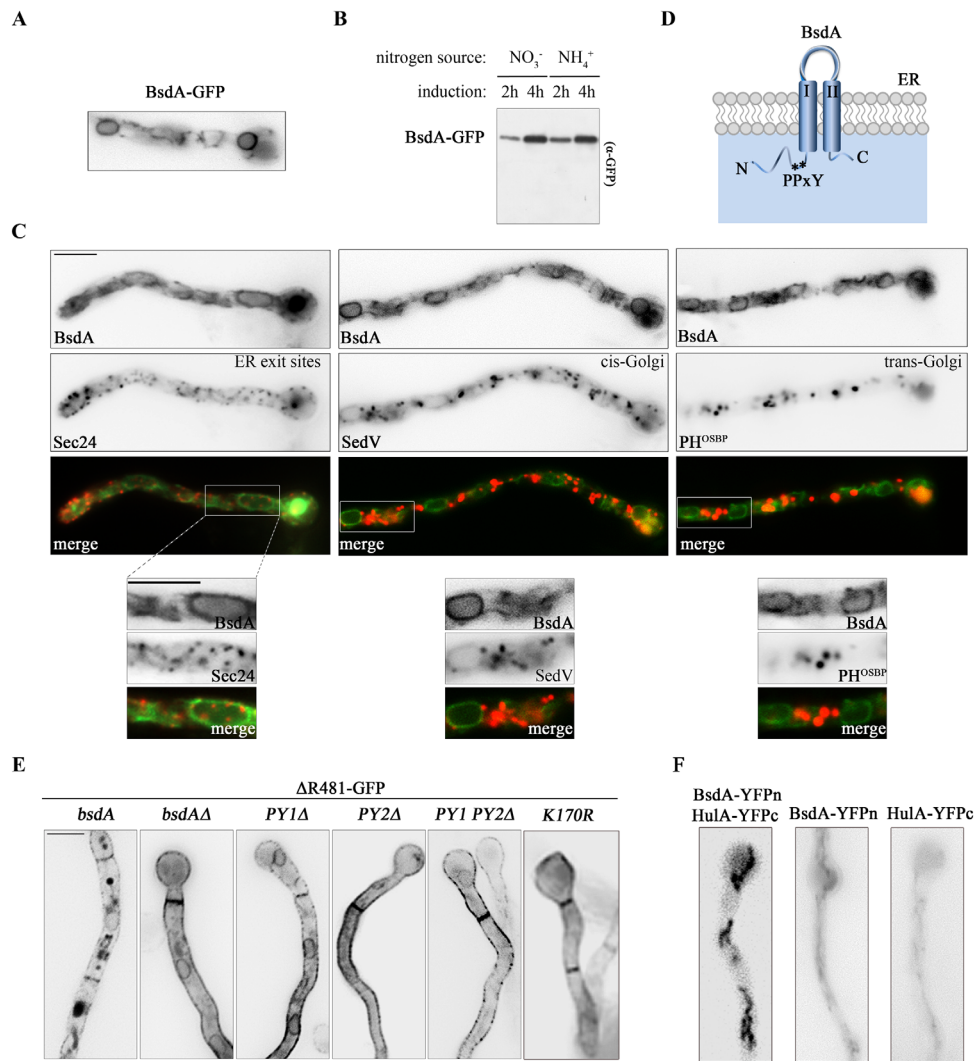


**Fig. 4.** BsdA<sup>Bsd2</sup> is a protein of the ER membrane.

A. Epifluorescence inverted microscopy showing the subcellular localization of BsdA-GFP expressed from *alcA<sub>p</sub>* promoter. A similar picture is obtained when BsdA-GFP is expressed from its native promoter.

B. Western blot analysis, using anti-GFP antibody, of an intact GFP-tagged BsdA protein, expressed under induced conditions from *alcA<sub>p</sub>*, in the presence of ammonium or nitrate ions as sole nitrogen sources.

C. Epifluorescence inverted microscopy investigating the co-localization of BsdA-GFP with ER exit sites (Sec24-mRFP) and *cis*- (SedV-mCherry) or *trans*- (mRFP-PH<sup>OSBP</sup>) Golgi markers (for strain details see Experimental procedures). Scale bars represent 5  $\mu\text{m}$ .

D. Schematic topology of BsdA<sup>Bsd2</sup> showing the presence of two putative transmembrane segments (marked as I, II), the cytoplasmic N- and C-tails and the cytoplasmic PY motifs.

E. Epifluorescence inverted microscopy showing the essential role of the PY motifs and Lys170 of BsdA-GFP, in respect to the vacuolar sorting of  $\Delta$ R481-GFP.

F. Direct *in vivo* evidence for the interaction of BsdA-YFPn and HulA-YFPc via a relative BiFC assay (see text). Notice that no reconstituted split-YFP fluorescence is detected in control strains expressing either BsdA-YFPn or HulA-YFPc.

rather immotile cytoplasmic membrane network, apparently the ER membrane network (Fig. 4A). Western blot analysis of BsdA-GFP using an anti-GFP antibody confirmed the presence of a single polypeptide at the expected molecular weight (Fig. 4B). Absence of a free GFP fragment in this Western blot analysis, characteristic of vacuolar proteolysis of transmembrane proteins, further suggested that the GFP tag has no significant effect on

BsdA folding and thus no effect on its subcellular localization. BsdA-GFP showed practically no co-localization with Sec24-mRFP, a marker of the ER exit sites (ERes), or with *cis*- or *trans*-Golgi markers, such as syntaxin mCherry-SedV (Pinar *et al.*, 2013a) and mRFP-PH<sup>OSBP</sup> (Pantazopoulou and Peñalva, 2009) respectively (Fig. 4C; for strain construction details see Experimental procedures). The significance of this becomes apparent later.

*In silico* prediction of the topology of BsdA supports the existence of two transmembrane domains (TMD) and a rather long cytoplasmic N-tail. This is somehow different from Bsd2p in *S. cerevisiae*, which has three putative TMDs (Hetteema *et al.*, 2004), but similar to nearly all homologous proteins in Aspergilli of known genome sequences (<http://www.aspgd.org/>). The N-tail of BsdA hosts two putative PPXY motifs (Figs 4D and Supporting Information Fig. S5), through which BsdA apparently recruits Hula<sup>Rsp5</sup>, as assumed by the interaction of Bsd2p with Rsp5p in *S. cerevisiae* (Hetteema *et al.*, 2004; Sullivan *et al.*, 2007). We obtained direct evidence for the functional importance of both PY elements by directed mutagenesis (for details see Experimental procedures).  $\Delta R481$  turnover was significantly blocked in strains expressing Ala substituted versions of either or both PY elements (Fig. 4E), similarly to strains carrying a *bsdA* $\Delta$  null mutant. Furthermore, BsdA has been identified as ubiquitylated protein in the ubiquitome of *A. nidulans* (Chu *et al.*, 2016). This work identified Lys170, just upstream from the PY elements, as the ubiquitin acceptor residue. We obtained direct evidence for the importance of Lys170 in BsdA function, based on the observation that mutation K170R blocked the turnover of  $\Delta R481$ , similarly to *bsdA* $\Delta$  null or PY mutants (Fig. 4E). However, we failed to detect ubiquitylated forms of BsdA using an anti-ubiquitin antibody (not shown).

We obtained direct evidence for the *in vivo* interaction of BsdA and Hula. This was achieved by using a bifluorescence complementation (BiFC) assay, which detects the reconstitution of fluorescence by the association of the two parts of split-YFP (YFPn and YFPc; Martzoukou *et al.*, 2015) when tagged in BsdA and Hula respectively (for details see Experimental procedures). This is shown in Fig. 4F where fluorescence is clearly detected in cytoplasmic structures in a strain coexpressing BsdA-YFPn and Hula-YFPc, but not in control strains expressing either BsdA-YFPn or Hula-YFPc. The site of this subcellular interaction is discussed later.

#### *BsdA<sup>Bsd2</sup> interacts with $\Delta R481$ , but not with wild-type UapA, in the ER*

All evidence supported that BsdA interacts with  $\Delta R481$ . We examined the localization of BsdA-GFP in respect to that of  $\Delta R481$ -mRFP. Figure 5A shows that the two proteins partially co-localize in cytoplasmic structures, often found in the periphery of perinuclear ER rings or next to the PM, but also in vacuoles (mostly evident in the spore head). Notice also the dynamic reshaping of the co-localization structure in the middle of the hyphae, highlighted with an arrowhead in Fig. 5A. This resembles the formation of autophagosomes, an observation

that will be later confirmed. It is also important to notice that in the strain expressing BsdA-GFP,  $\Delta R481$ -mRFP showed significant vacuolar degradation as expected for a *bsdA*<sup>+</sup> strain, confirming that the BsdA-GFP chimeric protein is functional.

We obtained direct evidence for the interaction of BsdA with  $\Delta R481$  by using the BiFC assay that follows the reconstitution of split-YFP, as we described above for the interaction of BsdA and Hula, and previously for the homodimerization of UapA (Martzoukou *et al.*, 2015). We constructed a strain expressing simultaneously  $\Delta R481$ -YFPn and BsdA-YFPc, as well as control strains expressing each construct alone (see Experimental procedures). Figure 5B shows that split-YFP fluorescence is reconstituted, only in the  $\Delta R481$ -YFPn/BsdA-YFPc strain, in perinuclear ER membrane rings (2 h) and other cytoplasmic structures (4 h), as well as, in vacuoles (6 h). The interaction of BsdA with  $\Delta R481$  is dynamic and transient, given that fluorescence was associated with distinct subcellular compartments depending on the time period of *de novo* synthesis of the two protein partners. Importantly, no reconstituted YFP fluorescence was detected in a strain coexpressing wild-type UapA-YFPn with BsdA-YFPc, or in control strains expressing either  $\Delta R481$ -YFPn or BsdA-YFPc alone (Fig. 5B, right panels). We further investigated the site(s) of  $\Delta R481$ -YFPn/BsdA-YFPc interaction by co-localization studies with Golgi markers (for strain construction see Experimental procedures). Results in Fig. 5C are suggestive of limited apparent co-localization of  $\Delta R481$ /BsdA with the Golgi. This was in line with the no co-localization of  $\Delta R481$ -GFP with Golgi markers, as shown in Fig. 5D. The significance of this becomes apparent later.

#### *Selective autophagy is involved in the vacuolar turnover of $\Delta R481$*

The only currently known pathway for vacuolar degradation of ER trapped proteins is selective autophagy (see Introduction). We investigated the role of selective autophagy in the turnover of  $\Delta R481$  through co-localization studies with Atg8, a key selective autophagy marker. This ubiquitin-like protein, which is localized in phagophore assembly sites (PAS), mature phagophores and autophagosomes, plays a central role in autophagy in *S. cerevisiae* (Nakatogawa *et al.*, 2007) and *A. nidulans* (Pinar *et al.*, 2013b), and is widely accepted as a prototypical protein marker for autophagy. We first checked whether under the conditions used for the experiments concerning the localization and turnover of  $\Delta R481$  (i.e. minimal media with nitrate as sole nitrogen source) starvation-dependent selective autophagy is elicited. For this, we followed the subcellular localization of mCherry-Atg8 in a wild-type

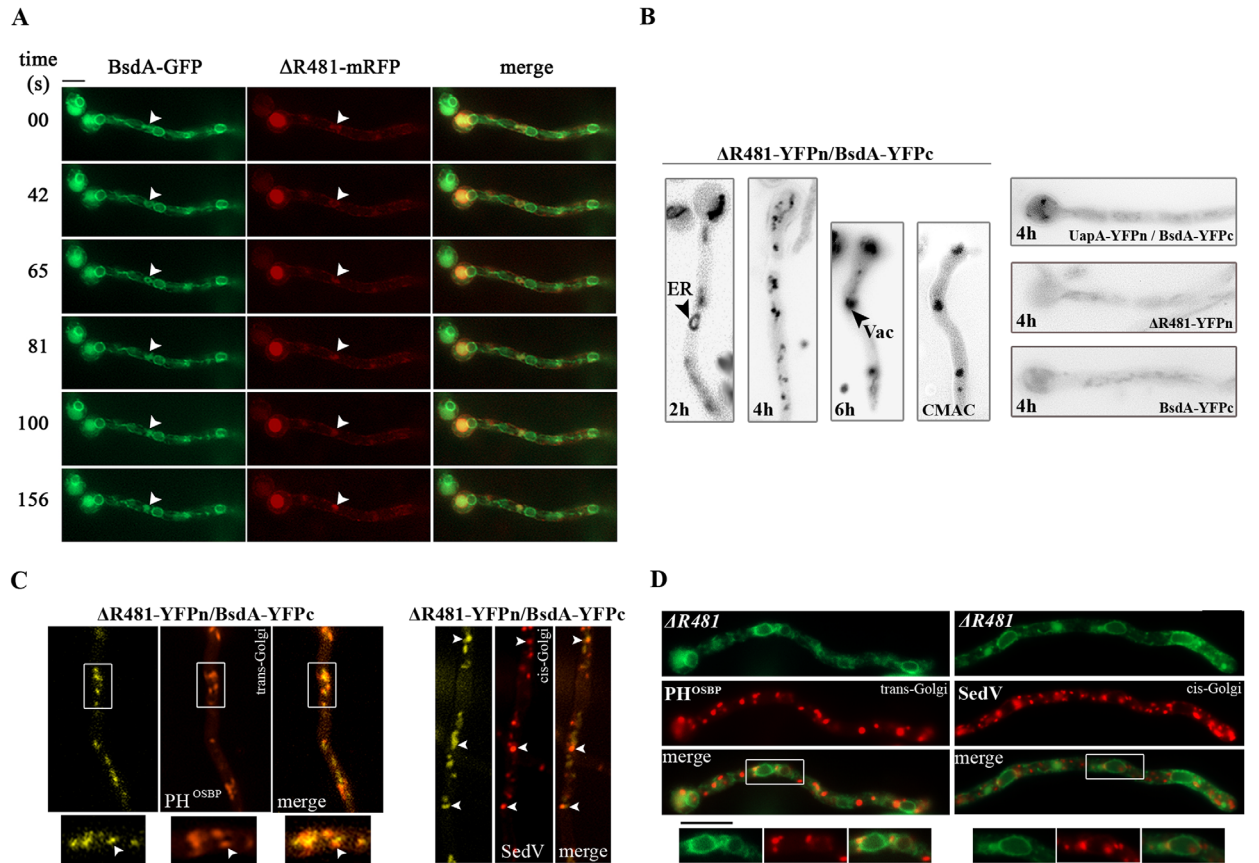


**Fig. 5.** BsdA<sup>Bsd2</sup> interacts with ΔR481, but not with wild-type UapA, in the ER.

A. Epifluorescence inverted microscopy showing the partial co-localization of BsdA-GFP and ΔR481-mRFP in perinuclear ER membrane rings, cytoplasmic structures peripheral to the ER, and in vacuoles. The picture shows snapshots from a time lapse movie of 2 min. Notice the dynamic reshaping of the BsdA-GFP/ΔR481-mRFP highlighted with arrowhead. This structure resembles the formation of autophagosomes (see Fig. 6).

B. Direct *in vivo* evidence for the interaction of ΔR481-YFPn with BsdA-YFPc via a relative BiFC assay after 2, 4 or 6 h of *de novo* synthesis of the two partner proteins (see text). Notice that at 2 h this interaction labels ER perinuclear rings, whereas at 6 h ΔR481-YFPn/BsdA-YFPc co-localize with vacuoles (CMAC). Notice also that no reconstituted split-YFP fluorescence is detected in control strains expressing either ΔR481-YFPn or BsdA-YFPc alone, or in a strain co-expressing wild-type UapA-YFPn with BsdA-YFPc.

C. Epifluorescence inverted microscopy showing very minor apparent co-localization of reconstituted split-YFP fluorescence of ΔR481-YFPn/BsdA-YFPc with *cis*- or *trans*-Golgi markers (SedV and PH<sup>OSBP</sup> respectively; see text).

D. Epifluorescence inverted microscopy showing non-co-localization of ΔR481-GFP with *cis*- (SedV-mCherry) or *trans*- (mRFP- PH<sup>OSBP</sup>) Golgi markers. Scale bars represent 5 μm.

strain expressing wild-type UapA (i.e. no UapA mutant). Figure 6A shows the absence of apparent selective autophagy, as judged by the presence of a cytoplasmic red fluorescent haze and only 1 or 2 bright foci per hypha, apparently PAS, which, as expected, do not co-localize with vacuoles (Kimura *et al.*, 2011; Pinar *et al.*, 2013b).

In contrast to the above picture, expression of ΔR481-GFP elicited significant progressive formation of ΔR481-GFP-positive, mCherry-Atg8 labelled autophagosomes, and, finally vacuolar degradation of both ΔR481-GFP and mCherry-Atg8 (Fig. 6B and C). This is in line with the observation that in autophagy Atg8 is degraded in the vacuoles (Kimura *et al.*, 2011; Pinar *et al.*, 2013b). The shape of the ΔR481-GFP and mCherry-Atg8 puncta is characteristic of mature autophagosomes, showing

the progressive closure of autophagosomal membranes (Fig. 6C). Importantly, the co-localization of ΔR481-GFP and mCherry-Atg8 in vacuoles was nearly absolute, suggesting that autophagy is the primary mechanism for ΔR481-GFP vacuolar turnover.

To further test whether sorting of mCherry-Atg8 to the vacuoles elicited by ΔR481-GFP requires a functional BsdA protein, we also performed co-localization studies of mCherry-Atg8 with ΔR481-GFP in a *bsdAΔ* genetic background. Figure 6D shows that expression of ΔR481-GFP in the absence of BsdA triggers some selective autophagy, as judged by the detection of a few Atg8-marked autophagosomes. Importantly, in this case, none of these autophagosomes contained ΔR481-GFP, in sharp contrast to what was observed in a *bsdA*<sup>+</sup>

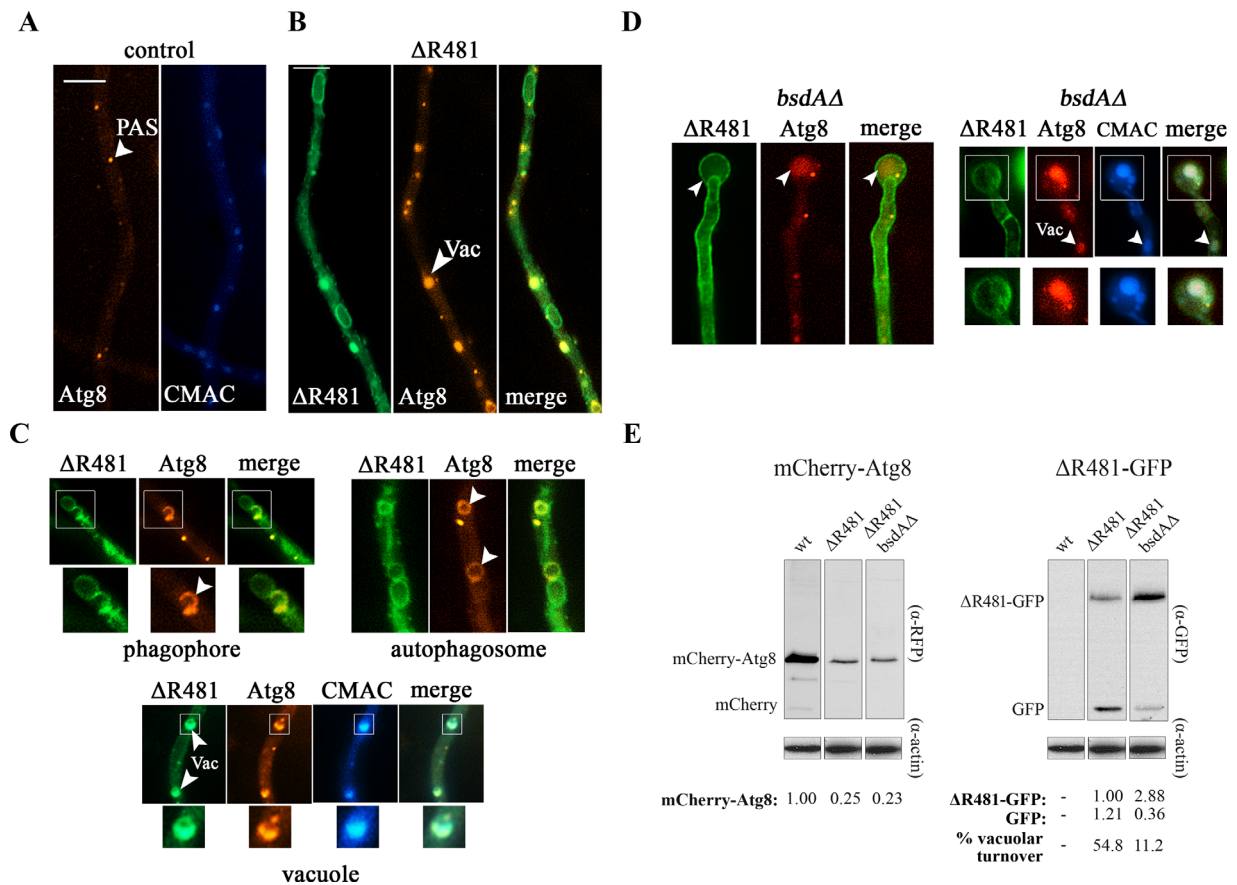


**Fig. 6.** Vacuolar turnover of  $\Delta R481$  occurs by BsdA-dependent selective autophagy.

A. Epifluorescence inverted microscopy showing that autophagy is not elicited, under growth conditions used, when no misfolded version of UapA-GFP is expressed. Notice the presence of some mCherry-Atg8 specific PAS, but the absence of mature autophagosomes. Notice also that the mCherry-Atg8 marker does not co-localize with vacuoles.

B. Induction of autophagosomes by  $\Delta R481$ -GFP and co-localization of  $\Delta R481$ -GFP, mCherry-Atg8 and vacuoles (CMAC).

C. Highlights of co-localization of  $\Delta R481$ -GFP with mCherry-Atg8 depicting the characteristic formation of phagophores, autophagosomes and vacuoles stained CMAC. Scale bars represent 5  $\mu\text{m}$ .

D. Epifluorescence inverted microscopy showing that in a *bsdA* $\Delta$  mutant, mCherry-Atg8 specific PAS and a few mature autophagosomes are formed when  $\Delta R481$ -GFP is expressed, but in this case  $\Delta R481$  does not co-localize with either mCherry-Atg8 or vacuoles (CMAC).

E. Western blot analysis, using anti-mCherry or anti-GFP antibodies, showing that expression of  $\Delta R481$ -GFP for 5 h results in increased, but BsdA-independent, turnover of mCherry-Atg8. Protein loading (actin levels) and relative quantification is shown at the bottom.

background. This suggests that whilst the accumulation of the misfolded version of UapA ( $\Delta R481$ -GFP) in the ER membrane might act as a signal for selective autophagy, a functional BsdA protein is necessary for the specific turnover of the misfolded cargo.

Previous observations have shown that when autophagy is active, Atg8 undergoes vacuolar turnover (Pinar *et al.*, 2013b). We performed a Western blot analysis following the steady-state levels of mCherry-Atg8, either when there is no misfolded mutant expressed (control) or when  $\Delta R481$ -GFP is expressed in *bsdA*<sup>+</sup> ( $\Delta R481$ ) and *bsdA* $\Delta$  ( $\Delta R481$  *bsdA* $\Delta$ ) isogenic backgrounds. Figure 6E shows that the steady-state level of mCherry-Atg8 is significantly higher in the control strain treated in the same conditions, whereas expression of  $\Delta R481$ -GFP significantly elicits the turnover of mCherry-Atg8. However,

mCherry-Atg8 turnover seems independent of BsdA, as it is also observed in the *bsdA* $\Delta$  strain expressing  $\Delta R481$ . Figure 6E (right panel) also confirms that significant vacuolar degradation of  $\Delta R481$ -GFP is BsdA-dependent. Overall, our results suggested that whilst the presence of a misfolded version of UapA trapped in the ER membrane elicits selective autophagy, the BsdA protein is not necessary for triggering autophagy, but is rather essential for the subsequent specific turnover of  $\Delta R481$ -GFP through sorting into autophagosomes.

#### Genetic blocks in autophagy reduce, but do not abolish, $\Delta R481$ vacuolar turnover

To further show the importance of selective autophagy in  $\Delta R481$  turnover, we followed  $\Delta R481$  subcellular

localization and vacuolar degradation in strains genetically blocked in autophagy. For this we used a null mutant of Atg9, a key factor absolutely essential for autophagy (Mari and Reggiori, 2005; Stanley *et al.*, 2014), and a temperature sensitive (*ts*) mutant of RabO (Pinar *et al.*, 2013b). The advantage of RabO<sup>ts</sup> (A136D) stems from the fact that in this mutant blocks in autophagy and Golgi can be uncoupled depending on temperature. At 25–28°C, hyphae show relatively normal secretion, but are completely blocked in autophagy, whereas at 37°C both autophagy and Golgi traffic are blocked.

Figure 7A shows that in an *atg9Δ* background, ΔR481 is significantly sorted in the PM, but still a fraction of it is degraded in the vacuoles (39.6% turnover). Whilst, in principle, the vacuolar sorting of ΔR481 in *atg9Δ* could be due to endocytosis of the fraction that reached the PM, we obtained evidence that this is not the case, as in the double mutant *atg9Δ art4Δ*, which is also blocked in endocytosis, we measured a practically identical number of vacuoles (5–6 per 40 μm of hyphal length). The most probable explanation for this is that when selective autophagy is blocked, a fraction of ΔR481 is redirected towards the Golgi, and from there sorted to the endosomal/MVB pathway for vacuolar degradation prior to PM localization.

The above hypothesis predicted that in the RabO<sup>ts</sup> mutant, ΔR481 turnover would be totally blocked at 37°C, but partially so at 25°C. Results shown in Fig. 7B confirm the total absence of ΔR481 vacuolar turnover in the *rabO<sup>ts</sup>* mutant when cells are shifted to the non-permissive temperature (37°C) prior to and during the 3-hour induction of ΔR481 *de novo* synthesis, whereas low vacuolar degradation goes on during the induction at the permissive temperature (25°C). More specifically, in the *rabO<sup>ts</sup>* mutant at 37°C, ΔR481 is present in cytoplasmic structures that resemble ER aggregates (Pinar *et al.*, 2013a), which do not co-localize with vacuoles (Fig. 7B, right panel). We could not however obtain intact membrane proteins from the *rabO<sup>ts</sup>* mutant when the 3-hour induction (I) followed by the 2-hour repression (R) of *alcA<sub>p</sub>* was carried out at the non-permissive temperature (37°C), whereas at the permissive temperature (25°C), we had similar levels of intact ΔR481-GFP between the control and the *rabO<sup>ts</sup>*, but the vacuolar degradation of ΔR481 was reduced (31.4% turnover). Thus, the picture at 25°C in the *rabO<sup>ts</sup>* mutant is similar to that obtained in the *atg9Δ* mutant (31.4% compared to 39.6% turnover), supporting that selective autophagy is the major mechanism for the down-regulation of ΔR481.

Since however ΔR481 turnover seems to operate at a low level in *rabO<sup>ts</sup>* and *atg9Δ* mutants, we used a standard Golgi traffic mutant, which has a normal ability for autophagy, to investigate a possible role of Golgi in

ΔR481 turnover. The mutant used is a conditional SedV<sup>ts</sup> mutant showing a block in ER to Golgi protein sorting at the non-permissive (> 37°C) temperature (Pinar *et al.*, 2013a). Importantly, and similar to the experiment with *rabO<sup>ts</sup>*, cells were shifted to the non-permissive temperature (37°C) prior to induction of ΔR481 *de novo* synthesis. Figure 7C shows that lack of a functional SedV at 37°C does not seem to block the vacuolar degradation of ΔR481, as judged by epifluorescence microscopic analysis. A low reduction at the level of vacuolar degradation is only detected in Western blot analysis of *sedV<sup>ts</sup>* at 25°C (63% turnover, versus 81% in the *sedV<sup>+</sup>* strain), whilst we could not obtain analogous data from the Western analysis at 37°C, due to protein degradation. Similar results were obtained when *de novo* protein synthesis was blocked with cycloheximide (Supporting Information Fig. S6).

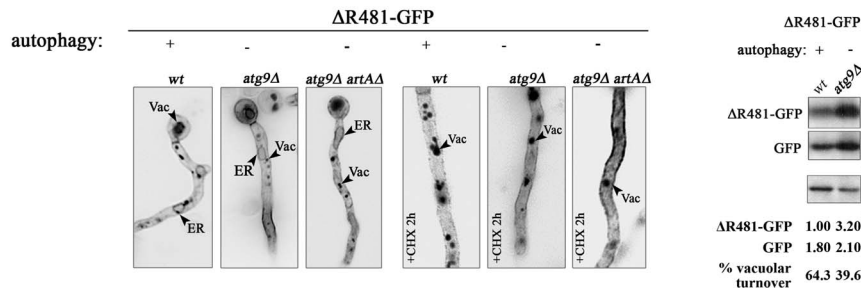
Thus, all evidence pointed to the idea that when selective autophagy is active, ΔR481 degradation from the Golgi is probably minor. This contrasts the picture when autophagy is blocked (*atg9Δ* or *rabO<sup>ts</sup>* at 25°C), where a significant degree of vacuolar turnover might indeed operate through the Golgi and the MVB/endosomal route.

## Discussion

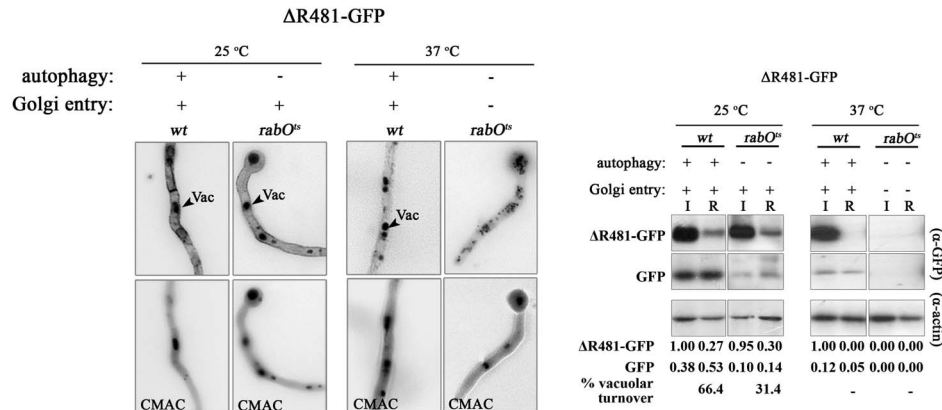
Eukaryotic transporters and other polytopic transmembrane proteins face the challenge of cotranslational folding, a process characterized by high complexity as it not only takes place within specific microdomains of the ER membrane including the translocase complex and a specific lipid environment, but also because it needs to adapt the rate of translation to the much slower process of polypeptide folding. Improper folding might 'easily' occur due to stochastic errors, stressful conditions or mutations affecting the local folding of specific domains. As a result, it is not surprising that complex control mechanisms have evolved to sense misfolding and either assist folding, or reduce the expression and/or degrade misfolded proteins. ERAD, activation of UPR, selective autophagy and Golgi QC, constitute main mechanisms for releasing cells from the toxic effects of misfolded proteins. Here we provided evidence that all the above described processes are orchestrated to detoxify *A. nidulans* from potential deleterious versions of the UapA transporter, the contribution of each turnover mechanism being depended on whether one or more of the other turnover pathways is blocked.

The first novel issue concerning the turnover of ΔR481 is that a significant fraction of it escapes ERAD and is degraded in the vacuole. Sorting of misfolded membrane proteins in vacuoles could, in principle, occur directly from the ER via selective autophagy through the

A



B



C

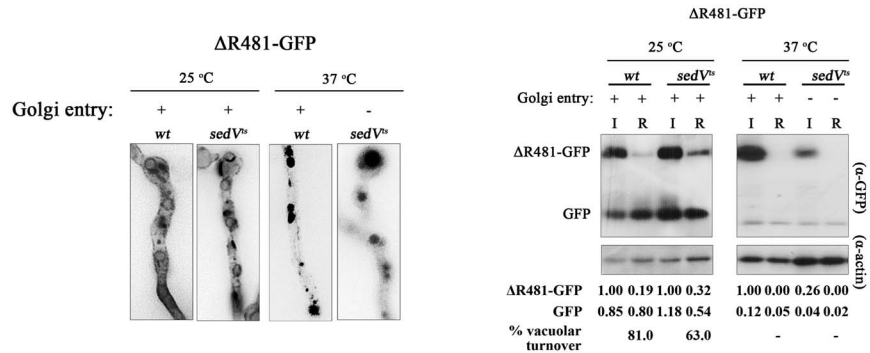


**Fig. 7.** Genetic blocks in autophagy reduce, but do not abolish, ΔR481 vacuolar turnover.

A. Left panel: Epifluorescence inverted microscopy showing the reduction of ΔR481-GFP vacuolar turnover in *atg9Δ* and *atg9Δ art4Δ* mutants. The relative number of vacuoles, as detected by both GFP fluorescence or CMAC staining, in *atg9Δ* and *atg9Δ art4Δ* was estimated to be practically identical (5–6 vacuoles per 40 μm of hyphal length). Right panel: Western blot analysis, using anti-GFP, confirming the role of Atg9 in ΔR481-GFP vacuolar turnover. Protein loading (actin levels) and relative quantification is shown at the bottom.

B. Left panel: Epifluorescence inverted microscopy revealing the role of RabO in ΔR481 vacuolar turnover. Shift to the non-permissive temperature was 1 h before inducing ΔR481 synthesis (see Experimental procedures). Right panel: Western blot analysis confirming the role of RabO-dependent autophagy in ΔR481-GFP vacuolar turnover. More specifically, when only autophagy is blocked (25°C), a significant fraction of ΔR481-GFP is rescued from degradation and sorted into the PM, similarly to what is observed in the *atg9Δ* strain. When both autophagy and Golgi traffic are blocked (37°C), ΔR481-GFP labels apparent ER aggregates and is never sorted in vacuoles. Shift to the non-permissive temperature (37°C) was imposed 1 h before the induction of ΔR481-GFP synthesis. At 37°C, intact ΔR481-GFP could not be detected in relative Western analysis. Protein loading (actin levels) and relative quantification is shown at the bottom.

C. Left panel: Epifluorescence inverted microscopy showing the non-effect of a conditional genetic block in Golgi traffic (*sedV<sup>ts</sup>* at 37°C), imposed prior to induction of ΔR481-GFP synthesis, in ΔR481-GFP vacuolar turnover. Right panel: Western blot analysis, using anti-GFP, of mutant ΔR481 in wild-type and *sedV<sup>ts</sup>* isogenic genetic backgrounds, confirming the non-involvement of Golgi traffic in ΔR481 turnover when autophagy is active. Protein loading (actin levels) and relative quantification is shown at the bottom. For more details see Experimental procedures and the text.

Golgi/endosomal apparatus, or by internalization from the plasma membrane. We showed that ΔR481 molecules escaping ERAD may follow all three routes, each of which contributes to turnover depending on the

genetic background used and the level of ΔR481 expression. For example, when ΔR481 is expressed from its native, low-strength promoter, very little of it reaches the PM as most of it has been degraded during

secretion by ERAD, selective autophagy, and probably via some Golgi to endosome sorting. When  $\Delta R481$  is strongly expressed from the *alcA<sub>p</sub>* promoter, a fraction of it (~20% compared to the wild-type) reaches the plasma membrane in all hyphal cells and thus becomes vulnerable to endocytosis, most evident in mutants deficient in endocytosis. When autophagy is blocked (*atg9 $\Delta$*  or *rabO<sup>ts</sup>* at 25°C), a mechanism for vacuolar degradation seems to operate through the Golgi/MVB/Endosome route. When Golgi traffic is blocked (*sedV<sup>ts</sup>*), selective autophagy seems to be the major detectable mechanism for vacuolar sorting. When both autophagy and Golgi traffic are blocked (*rabO<sup>ts</sup>* at 37°C),  $\Delta R481$  never reaches the vacuole and remains in aggregated ER membranes.

The second important finding of this work is the key role of BsdA in the non-endocytic vacuolar turnover of  $\Delta R481$ . Lack of a functional *bsdA*, either by total deletion (*bsdA $\Delta$* ) or via specific missense mutations affecting its two PY elements or the Lys necessary for ubiquitylation, totally suppresses the non-endocytic vacuolar degradation of  $\Delta R481$ . The non-endocytic, BsdA-dependent vacuolar degradation of  $\Delta R481$  can, in principle, operate via two mechanisms: selective autophagy or sorting from the Golgi to the Endosome/MVB pathway. We provided direct evidence for the involvement of selective autophagy in  $\Delta R481$  degradation (Fig. 6). Furthermore, we provided genetic evidence that when autophagy is blocked,  $\Delta R481$  degradation might operate via the Golgi/Endosome/MVB route (Fig. 7). Noticeably however, we showed BsdA is not an essential autophagic factor as its genetic absence does not eliminate the formation of autophagosomes and has no significant impact on the vacuolar turnover of Atg8. It rather seems that BsdA is a specific factor necessary for the degradation of a certain type of misfolded cargoes, such as  $\Delta R481$ . In other words, BsdA acts downstream from the primary trigger of selective autophagy in order to 'mark' misfolded cargoes that have escaped ERAD. This 'marking' implicates Hula activity, as loss-of-function mutations in *hula*, similar to *bsdA* mutations, block the vacuolar turnover of  $\Delta R481$ . Unfortunately, we could not directly identify the molecular target of Hula-ubiquitylation, although we obtained some indirect evidence that this might be related to BsdA ubiquitylation. In anyway, the functions of BsdA and Hula are absolutely necessary for the vacuolar degradation of  $\Delta R481$  by selective autophagy and seemingly via Golgi to endosome/vacuole sorting.

Given that in *S. cerevisiae* Bsd2p substrates are either transporters of potential toxic metals or misfolded versions of transporters, it has been proposed that Bsd2p might have a general role in the QC of membrane proteins (Hetteima *et al.*, 2004; Stimpson *et al.*,

2006; Nikko and Pelham, 2009). Our findings on BsdA support the proposed biochemical role of Bsd2p, but also point to a more specific and cargo-centric role and further reveal the involvement of selective autophagy. It is reasonable to propose that BsdA or Bsd2p, being transmembrane proteins themselves, recognize misfolded transmembrane domains in the ER, and through recruitment of Hula/Rsp5 'mark' the problematic cargoes for subsequent degradation, prior to PM sorting. Notably however, in *S. cerevisiae* Bsd2p has been proposed to act at the Golgi/Endosome interface rather than the ER (Hetteima *et al.*, 2004), as our present work showed for BsdA. The apparent difference in the subcellular localization of Bsd2p or BsdA might reflect a real functional difference of the two proteins. In line with their different localization, Bsd2p and BsdA also differ in their number of putative transmembrane domains, Bsd2p having three (Hetteima *et al.*, 2004) and BsdA two. However, an earlier report challenges the above scenario, as it provided direct biochemical evidence that Bsd2p, similar to BsdA, is an ER-associated protein (Liu *et al.*, 1997).

As a final conclusion, our work shows that several distinct mechanisms (ERAD, QC autophagy, GQC and endocytosis) might be employed in the turnover of misfolded versions of membrane cargoes.

## Experimental procedures

### *Media, strains, growth conditions and transformation*

Standard complete and minimal media (MM) for *A. nidulans* were used. Media and supplemented auxotrophies were used at the concentrations given in FGSC (<http://www.fgsc.net>). *Escherichia coli* was grown on Luria-Bertani medium. Media and chemical reagents were obtained from Sigma-Aldrich (Life Science Chemilab SA, Hellas) or AppliChem (Bioline Scientific SA, Hellas). Carbon sources were used at the final concentrations: Glucose 1% (w/v), Fructose 0.1% (w/v). Nitrogen sources were used at the final concentrations: NaNO<sub>3</sub> 10 mM, Ammonium L-(+)-tartrate 10 mM, uric acid 0.5 mM. Ethanol was used at a final concentration of 0.4% (v/v). Cycloheximide, CdCl<sub>2</sub> and epoxomicin were used at final concentrations of 50 µg/ml, 25 µM and 500 nM respectively. *Aspergillus nidulans* transformation was performed as described previously in Koukaki *et al.* (2003). An *nkuA* DNA helicase deficient strain (TNO2A7; Nayak *et al.*, 2006) was the recipient strain for generating 'in locus' integrations of tagged gene fusions, or gene deletions by the *A. fumigatus* markers orotidine-5'-phosphate-decarboxylase (AFpyrG, Afu2g0836) or GTP-cyclohydrolase II (AF*riboB*, Afu1g13300), resulting in complementation of auxotrophies for uracil/uridine (*pyrG89*) or riboflavin (*riboB2*) respectively. A *uapA $\Delta$  uapC $\Delta$ ::AFpyrG azgA $\Delta$  pabaA1 argB2* ( $\Delta ACZ$ ; Pantazopoulou *et al.*, 2007) mutant strain was the recipient strain in transformations with plasmids carrying tagged wild-type or mutant versions



of UapA. Transformants were verified by PCR and Southern analysis. Combinations of mutations were constructed by standard genetic crossing. Growth tests were performed at 25, 37 or 42°C, at pH 6.8. *A. nidulans* strains used are listed in Supporting Information Table S1.

#### Standard nucleic acid manipulations and plasmid constructions

Genomic DNA extraction from *A. nidulans* was as described in FGSC (<http://www.fgsc.net>). Plasmid preparation from *E. coli* strains and DNA extraction from agarose gels was performed using the Nucleospin Plasmid kit and the Nucleospin Extract II kit according to the manufacturer's instructions (Macherey-Nagel, Lab Supplies Scientific SA, Hellas). DNA sequences were determined by VBC-Genomics (Vienna, Austria). Point mutations were constructed by site-directed mutagenesis according to the instructions accompanying the Quik-Change® Site-Directed Mutagenesis Kit (Agilent Technologies, Stratagene). Southern and northern blot analysis using specific gene probes for *uapA*, *argB*, *bipA*, *18S* and upstream or downstream fragments in the case of verifying gene deletions, was performed as described in Sambrook *et al.* (1989). [<sup>32</sup>P]-dCTP labelled molecules of gene specific probes were prepared using a random hexanucleotide primer kit following the supplier's instructions (Takara Bio, Lab Supplies Scientific SA, Hellas) and purified on MicroSpin™ S-200 HR columns (Roche Diagnostics, Hellas). Labelled [<sup>32</sup>P]-dCTP (3000 Ci mmol<sup>-1</sup>) was purchased from the Institute of Isotopes Co. Ltd., Miskolc, Hungary. Restriction enzymes were from Takara Bio (Lab Supplies Scientific SA, Hellas). Conventional PCRs, high fidelity amplifications and site-directed mutagenesis were performed using KAPA Taq DNA and Kapa HiFi polymerases respectively (Kapa Biosystems, Lab Supplies Scientific SA, Hellas). Gene deletions and 'in locus' integrations of tagged gene fusions were generated by one step ligations or sequential cloning of the relevant fragments in the plasmids pBluescript SK II, or pGEM using oligonucleotides carrying additional restriction sites. These plasmids were used as templates to amplify the relevant linear cassettes by PCR. For primers and information related to these constructs see Supporting Information Table S2. More specifically, the gene deletion cassettes for *bsdA* and *earA* were constructed using primer pairs 1–2/3–4/5–6 and 7–8/9–10/11–12 respectively. For the construction of the fusion cassette *bsdA-gfp::AFpyrG* (primer pairs 13–15/16–19/20–21) the *gfp* ORF together with *AFpyrG* was amplified from plasmid p1439 (Szewczyk *et al.*, 2006). For the construction of the fusion cassette *alcA<sub>p</sub>-bsdA-gfp::AFpyrG* (primer pairs 22–23/24–27/28–29/30–31) and *alcA<sub>p</sub>-gfp-bsdA::AFpyrG* (primer pairs 32–33/34–36/39–40/41–42) driven under the controllable *alcA<sub>p</sub>* promoter, an intermediate plasmid was first constructed, where the *bsdA* ORF (primer pairs 25–26 or 35–36) was exchanged with the *uapA* ORF in the plasmid pBS-*alcA<sub>p</sub>-uapA-gfp*, also carrying an arginine auxotrophy complementation marker (*argB*) (Pantazopoulou *et al.*, 2007; Gournas *et al.*, 2010). This plasmid and a derivative where the *argB* selection marker was exchanged with *pabaA* (complementing

*pabaA1*; p-aminobenzoic acid auxotrophy; Martzoukou *et al.*, 2015) was used for the construction of plasmids pBS-*alcA<sub>p</sub>-uapA-yfp<sub>N</sub>* (Martzoukou *et al.*, 2015), pBS-*alcA<sub>p</sub>-bsdA-yfp<sub>N</sub>* (primer pairs 71–72/73–74), pBS-*alcA<sub>p</sub>-bsdA-yfp<sub>C</sub>* (primer pairs 71–72/75–76) and for the construction of *bsdA* point mutations (primer pairs 77–78/79–80/81–82). These plasmids were either used directly for transformation based complementation of *argB2* or *pabaA1* auxotrophies (as in the case of split YFP constructs) or served as templates to amplify and subsequently clone the inserted fragments in plasmids carrying the relevant endogenous 5' and 3' UTRs and other auxotrophic markers for targeted integration (as in the case of *bsdA* point mutations; primer pairs 14–70/22–23/28–29/30–31). *yfp<sub>N/C</sub>* were amplified from plasmids pDV7 and pDV8 (Takeshita *et al.*, 2008). For the construction of pBS-*alcA<sub>p</sub>-ΔR481-His* the *uapA-ΔR481* ORF was exchanged with the wt *uapA* in the plasmid pBS-*alcA<sub>p</sub>-uapA-His* (Martzoukou *et al.*, 2015). The *yfp<sub>C</sub>-hula::AFriboB* fusion cassette was constructed using primer pairs 59–60/61–62/63–64/65–66. The *sec24-mRFP::AFpyrG* cassette (primer pairs 43–44/45–46/47–48) also carries a Gly-Ala linker repeat (5xGA) in frame between the ORF and the fluorescent tag, amplified together with *AFpyrG* from plasmid p1491 (Szewczyk *et al.*, 2006). For the construction of *uapA-gfp::AFriboB* (primer pairs 49–50/53–54/55–56/57–58) and *alcA<sub>p</sub>-uapA-gfp::AFriboB* (primer pairs 49–50/51–52/53–54/55–56/57–58) and mutants, a native *Bgl*III site 806bp upstream of the *uapA* translation initiation codon served as insertion point for *alcA<sub>p</sub>* and *AFriboB*. The construction of all other *uapA* mutations is described previously (Pantazopoulou *et al.*, 2007; Gournas *et al.*, 2010; Kosti *et al.*, 2010; Martzoukou *et al.*, 2015).

#### Protein extraction, purification and Western blot analysis

Cultures for total protein extraction were grown in MM supplemented with glucose and NaNO<sub>3</sub> as a nitrogen source at 25°C for 16 h, thus repressing transcription of the *alcA<sub>p</sub>* and synthesis of the studied protein, and then shifted to MM supplemented with fructose, ethanol and NaNO<sub>3</sub> at 25°C for 3 h for eliciting *de novo* synthesis of UapA or ΔR481 through induction of the *alcA<sub>p</sub>* promoter. Total protein synthesis was then inhibited (chased) for 2 h by addition of cycloheximide. In other experiments, a modified transcriptional pulse-chase assay was used. Cultures for total protein extraction were grown in MM supplemented with glucose and NaNO<sub>3</sub> at 25°C for 16 h, thus repressing transcription of the *alcA<sub>p</sub>* and synthesis of the studied protein. Then, cultures were shifted to MM supplemented with fructose, ethanol and NaNO<sub>3</sub> at 25°C for 3 h for eliciting *de novo* synthesis of UapA or ΔR481 through induction of the *alcA<sub>p</sub>* promoter (pulse). This corresponds to the induced conditions termed 'I' in all figures of this work. Immediately after collecting samples for the induced conditions, cultures were shifted in MM glucose and NaNO<sub>3</sub> at 25°C for an additional 2-hour period to repress transcription from *alcA<sub>p</sub>* (chase), thus allowing us to examine protein stability of ΔR481 in distinct genetic backgrounds (termed 'R' in all figures). To test the effect of the thermosensitive, *rabO<sup>ts</sup>* or *sedV<sup>ts</sup>* mutations on the degradation of ΔR481, the same

assay was further modified to ensure that the transcriptional pulse-chase will be performed entirely at the non-permissive conditions. For that, an extra step of incubation in MM supplemented with glucose and NaNO<sub>3</sub> (repressed condition of *alcAp*) at the non-permissive temperature (37°C) for 1 h was included to block Golgi traffic prior of transcriptional induction in MM supplemented with fructose, ethanol and NaNO<sub>3</sub>, at 37°C for 3 h (pulse). Cell lysates were collected (I) and immediately cultures were shifted to MM supplemented with glucose and NaNO<sub>3</sub> at 37°C, thus initiating the chase period by repression of the *alcA<sub>p</sub>* transcription. For control, the same assay was entirely performed at 25°C. To investigate the contribution of the proteasome in the degradation of ΔR481, the transcriptional pulse assay was followed by a 2-hour chase period, in which the proteasome activity was inhibited in specific samples. For that, 500 nM of the proteasome inhibitor epoxomicin (or DMSO as control) was added immediately after shifting to MM supplemented with glucose and NaNO<sub>3</sub> at 25°C. To investigate the role of autophagy in the degradation of ΔR481, we compare changes in the steady-state levels of mCherry-Atg8 in strains expressing wild-type UapA or the mutant ΔR481-GFP. Cultures were grown in MM supplemented with glucose and NaNO<sub>3</sub> at 25°C for 16 h, thus repressing transcription of the *alcA<sub>p</sub>*, and then shifted to MM supplemented with fructose, ethanol and NaNO<sub>3</sub> at 25°C for 5 h inducing the transcription of the *alcA<sub>p</sub>* promoter. Total and membrane-enriched protein extraction was performed as described previously (Apostolaki et al., 2012; Karachaliou et al., 2013). Equal sample loading was estimated by Bradford assays and Coomassie staining. Total proteins (30–50 μg) were separated by SDS-PAGE (8–10% w/v polyacrylamide gel) and electroblotted (Mini PROTEAN™ Tetra Cell, BIORAD) onto PVDF membranes (Macherey-Nagel, Lab Supplies Scientific SA, Hellas). UapA-His<sub>10</sub> purification was carried out as in Martzoukou et al. (2015) using Protino Ni-NTA Columns (Macherey-Nagel GmbH, Lab Supplies Scientific SA). Immunodetection was performed with a primary rabbit anti-RFP polyclonal antibody (Rockland Immunochemicals Inc.), a primary mouse anti-GFP monoclonal antibody (Roche Diagnostics, Hellas), a primary mouse anti-actin monoclonal (C4) antibody (MP Biomedicals Europe, Lab Supplies Scientific SA), or a mouse anti-Ubiquitin monoclonal antibody (Ub-P4D1 HRP Conjugate; Santa Cruz Biotechnology, SafeBlood BioAnalytica SA), a mouse Penta-His HRP Conjugate antibody kit (Qiagen, SafeBlood BioAnalytica SA, Hellas) and a secondary goat anti-rabbit IgG HRP-linked antibody (Sigma-Aldrich, Life Science Chemilab SA, Hellas), or a goat anti-mouse IgG HRP-linked antibody (Cell Signaling Technology Inc, Bioline Scientific SA, Hellas). Blots were developed by the chemiluminescent method using the LumiSensor Chemiluminescent HRP Substrate kit (Genscript USA, Lab Supplies Scientific SA, Hellas) and SuperRX Fuji medical X-Ray films (FujiFILM Europe). Relative steady-state levels of intact UapA-GFP, ΔR481-GFP, Atg8-mCherry or free GFP, were estimated using standard ImageJ analysis tool, normalized to actin levels. Present vacuolar degradation was estimated as relative quantity of free GFP/relative quantity of the sum of free GFP + ΔR481-GFP.

### Epifluorescence microscopy and BiFC assays

Samples for standard epifluorescence microscopy were prepared as previously described (Gournas et al., 2010; Karachaliou et al., 2013). In brief, germlings were incubated on coverslips in liquid MM supplemented with NaNO<sub>3</sub> and glucose 0.1% for experiments with the native *uapA* promoter or fructose 0.1% for experiments with the *alcA<sub>p</sub>* promoter for 16–22 h at 25°C and were observed on an Axioplan Zeiss phase contrast epifluorescent microscope. The resulting images were acquired with a Zeiss-MRC5 digital camera using the AxioVs40 V4.40.0 software. For inverted fluorescence microscopy, germlings were incubated in sterile 35 mm μ-dishes, high glass bottom (*ibidi*, Germany) in liquid MM supplemented with NaNO<sub>3</sub> and glucose for experiments with the native *uapA* promoter or fructose for experiments with the *alcA<sub>p</sub>* promoter for 16–22 h at 25°C. In chase experiments performed only with *alcA<sub>p</sub>* constructs, germlings were incubated in liquid MM supplemented with NaNO<sub>3</sub> and fructose to allow moderate continuous transcription of the *alcA<sub>p</sub>*. Immediately after the microscopic observation of the samples, *de novo* protein synthesis was blocked with the addition of cycloheximide (CHX) for 2 h, allowing us to follow *in vivo* the degradation route of ΔR481. To test the effect of the thermosensitive *rabO<sup>ts</sup>* or *sedV<sup>ts</sup>* mutations on the degradation of misfolded ΔR481, germlings were incubated in glucose, repressing transcription of the *alcA<sub>p</sub>* promoter for 18–22 h at 25°C, transferred to 37°C for 1 h to block Golgi traffic, and then shifted in fructose plus ethanol medium for inducing transcription of *alcAp-ΔR481* for 3 h at 37°C (pulse). In the case of *sedV<sup>ts</sup>* immediately after the microscopic observation of the samples, *de novo* protein synthesis was blocked with the addition of cycloheximide (CHX) for 2 h at 37°C, allowing us to follow *in vivo* the degradation route of ΔR481 (chase). For controls, the same assay was performed, entirely at 25°C. For BiFC assays, germlings were incubated in liquid MM supplemented with glucose and NaNO<sub>3</sub> as nitrogen source for 16 h and then shifted in fructose plus ethanol medium for 2–6 h at 4°C prior observation. Images were obtained with an AxioCam HR R3 camera using the Zen lite 2012 software either as single images, or in stacks of 10–12 optical sections along z-axis with a Z step size at 0.31 μm. Contrast adjustment, area selection and color combining were made using the Zen 2012 software. Images exported as TIFFs were annotated and further processed in Adobe Photoshop CS4 Extended version 11.0.2 or the ImageJ software for brightness adjustment, rotation and alignment. A desaturated and inverted version of the image was also created in each case, so as to achieve better visualization.

### Acknowledgements

We thank Vasiliki Kosti and Irene Roussounelou for preliminary experiments concerning the role of the BsdA and help in microscopy. We thank Miguel Angel Peñalva and Areti Pantazopoulou for strains expressing ER, Golgi and autophagy markers and I. Trougakos for epoxomicin. This work was supported by a research grant from *Fondation Santé* (2015) and work from COST Action (PROTEOSTASIS BM1307) and by COST (European Cooperation in Science and Technology).

## References

- Abenza, J.F., Galindo, A., Pantazopoulou, A., Gil, C., de los Ríos, V., and Peñalva, M.A. (2010) *Aspergillus* RabB Rab5 integrates acquisition of degradative identity with the long distance movement of early endosomes. *Mol Biol Cell* **21**: 2756–2769.
- Abenza, J.F., Galindo, A., Pinar, M., Pantazopoulou, A., de los Ríos, V., and Peñalva, M.A. (2012) Endosomal maturation by Rab conversion in *Aspergillus nidulans* is coupled to dynein-mediated basipetal movement. *Mol Biol Cell* **23**: 1889–1901.
- Amillis, S., Cecchetto, G., Sophianopoulou, V., Koukaki, M., Scazzocchio, C., and Diallinas, G. (2004) Transcription of purine transporter genes is activated during the isotropic growth phase of *Aspergillus nidulans* conidia. *Mol Microbiol* **52**: 205–216.
- Amillis, S., Kosti, V., Pantazopoulou, A., Mikros, E., and Diallinas, G. (2011) Mutational analysis and modeling reveal functionally critical residues in transmembrane segments 1 and 3 of the UapA transporter. *J Mol Biol* **411**: 567–580.
- Apostolaki, A., Harispe, L., Calcagno-Pizarelli, A.M., Vangelatos, I., Sophianopoulou, V., Arst, H.N. Jr., et al. (2012) *Aspergillus nidulans* CkiA is an essential casein kinase I required for delivery of amino acid transporters to the plasma membrane. *Mol Microbiol* **84**: 530–549.
- Brodsky, J.L. (2012) Cleaning up: ER-associated degradation to the rescue. *Cell* **151**: 1163–1167.
- Chu, X.L., Feng, M.G., and Ying, S.H. (2016) Qualitative ubiquitome unveils the potential significances of protein lysine ubiquitination in hyphal growth of *Aspergillus nidulans*. *Curr Genet* **62**: 191–201. doi:10.1007/s00294-015-0517-7
- D'Arcangelo, J.G., Stahmer, K.R., and Miller, E.A. (2013) Vesicle-mediated export from the ER: COPII coat function and regulation. *Biochim Biophys Acta* **1833**: 2464–2472.
- Diallinas, G. (2014) Understanding transporter specificity and the discrete appearance of channel-like gating domains in transporters. *Front Pharmacol* **5**: 207.
- Diallinas, G., and Gournas, C. (2008) Structure-function relationships in the nucleobase-ascorbate transporter (NAT) family: lessons from model microbial genetic systems. *Channels (Austin)* **2**: 363–372.
- Ellgaard, L., and Helenius, A. (2003) Quality control in the endoplasmic reticulum. *Nat Rev Mol Cell Biol* **4**: 181–191.
- Felenbok, B. (1991) The ethanol utilization regulon of *Aspergillus nidulans*: the alcA-alcR system as a tool for the expression of recombinant proteins. *J Biotechnol* **17**: 11–17.
- Gardner, B.M., Pincus, D., Gotthardt, K., Gallagher, C.M., and Walter, P. (2013) Endoplasmic reticulum stress sensing in the unfolded protein response. *Cold Spring Harb Perspect Biol* **5**: a013169.
- Gournas, C., Papageorgiou, I., and Diallinas, G. (2008) The nucleobase-ascorbate transporter (NAT) family: genomics, evolution, structure-function relationships and physiological role. *Mol Biosyst* **4**: 404–416.
- Gournas, C., Amillis, S., Vlant, A., and Diallinas, G. (2010) Transport-dependent endocytosis and turnover of a uric acid-xanthine permease. *Mol Microbiol* **75**: 246–260.
- Gournas, C., Oestreicher, N., Amillis, S., Diallinas, G., and Scazzocchio, C. (2011) Completing the purine utilisation pathway of *Aspergillus nidulans*. *Fungal Genet Biol* **48**: 840–848.
- Haynes, C.M., Caldwell, S., and Cooper, A.A. (2002) An HRD/DER-independent ER quality control mechanism involves Rsp5p-dependent ubiquitination and ER-Golgi transport. *J Cell Biol* **158**: 91–101.
- Hegde, R.S., and Ploegh, H.L. (2010) Quality and quantity control at the endoplasmic reticulum. *Curr Opin Cell Biol* **22**: 437–446.
- Hettema, E.H., Valdez-Taubas, J., and Pelham, H.R. (2004) Bsd2 binds the ubiquitin ligase Rsp5 and mediates the ubiquitination of transmembrane proteins. *EMBO J* **23**: 1279–1288.
- Hollien, J., and Weissman, J.S. (2006) Decay of endoplasmic reticulum-localized mRNAs during the unfolded protein response. *Science* **313**: 104–107.
- Isasa, M., Suñer, C., Díaz, M., Puig-Sàrries, P., Zuin, A., Bichman, A., et al. (2016) Cold temperature induces the reprogramming of proteolytic pathways in yeast. *J Biol Chem* **291**: 1664–1675.
- Karachaliou, M., Amillis, S., Evangelinos, M., Kokotos, A.C., Yaelis, V., and Diallinas, G. (2013) The arrestin-like protein ArtA is essential for ubiquitination and endocytosis of the UapA transporter in response to both broad-range and specific signals. *Mol Microbiol* **88**: 301–317.
- Kawaguchi, S., Hsu, C.L., and Ng, D.T. (2010) Interplay of substrate retention and export signals in endoplasmic reticulum quality control. *PLoS One* **5**: e15532.
- Kimura, S., Maruyama, J., Kikuma, T., Arioka, M., and Kitamoto, K. (2011) Autophagy delivers misfolded secretory proteins accumulated in endoplasmic reticulum to vacuoles in the filamentous fungus *Aspergillus oryzae*. *Biochem Biophys Res Commun* **406**: 464–470.
- Kincaid, M.M., and Cooper, A.A. (2007) Misfolded proteins traffic from the endoplasmic reticulum (ER) due to ER export signals. *Mol Biol Cell* **18**: 455–463.
- Kosti, V., Papageorgiou, I., and Diallinas, G. (2010) Dynamic elements at both cytoplasmically and extracellularly facing sides of the UapA transporter selectively control the accessibility of substrates to their translocation pathway. *J Mol Biol* **397**: 1132–1134.
- Koukaki, M., Giannoutsou, E., Karagouni, A., and Diallinas, G. (2003) A novel improved method for *Aspergillus nidulans* transformation. *J Microbiol Methods* **55**: 687–695.
- Koukaki, M., Vlant, A., Goudela, S., Pantazopoulou, A., Gioule, H., Tournaviti, S., and Diallinas, G. (2005) The nucleobase-ascorbate transporter (NAT) signature motif in UapA defines the function of the purine translocation pathway. *J Mol Biol* **350**: 499–513.
- Kruse, K.B., Brodsky, J.L., and McCracken, A.A. (2006) Autophagy: an ER protein quality control process. *Autophagy* **2**: 135–137.
- Lee, J.Y., and Yao, T.P. (2010) Quality control autophagy: a joint effort of ubiquitin, protein deacetylase and actin cytoskeleton. *Autophagy* **6**: 555–557.
- Lemus, L., and Goder, V. (2014) Regulation of endoplasmic reticulum-associated protein degradation (ERAD) by ubiquitin. *Cells* **3**: 824–847.
- Léon, S., Erpapazoglou, Z., and Haguenaer-Tsapis, R. (2008) Ear1p and Ssh4p are new adaptors of the

- ubiquitin ligase Rsp5p for cargo ubiquitylation and sorting at multivesicular bodies. *Mol Biol Cell* **19**: 2379–2388.
- Lewis, M.J., and Pelham, H.R. (2009) Inefficient quality control of thermosensitive proteins on the plasma membrane. *PLoS One* **4**: e5038.
- Lin, C.H., MacGurn, J.A., Chu, T., Stefan, C.J., and Emr, S.D. (2008) Arrestin-related ubiquitin-ligase adaptors regulate endocytosis and protein turnover at the cell surface. *Cell* **135**: 714–722.
- Liu, X.F., Supek, F., Nelson, N., and Culotta, V.C. (1997) Negative control of heavy metal uptake by the *Saccharomyces cerevisiae* BSD2 gene. *J Biol Chem* **272**: 11763–11769.
- Lukacs, G.L., and Verkman, A.S. (2012) CFTR: folding, misfolding and correcting the  $\Delta$ F508 conformational defect. *Trends Mol Med* **18**: 81–91.
- Mari, M., and Reggiori, F. (2007) Atg9 trafficking in the yeast *Saccharomyces cerevisiae*. *Autophagy* **3**: 145–148.
- Martoukou, O., Karachaliou, M., Yalilis, V., Leung, J., Byrne, B., Amillis, S., and Diallinas, G. (2015) Oligomerization of the UapA purine transporter is critical for ER-exit, plasma membrane localization and turnover. *J Mol Biol* **427**: 2679–2696.
- Meng, L., Mohan, R., Kwok, B.H., Elofsson, M., Sin, N., and Crews, C.M. (1999) Epoxomicin, a potent and selective proteasome inhibitor, exhibits in vivo antiinflammatory activity. *Proc Natl Acad Sci U S A* **96**: 10403–10408.
- Mizushima, N., Levine, B., Cuervo, A.M., and Klionsky, D.J. (2008) Autophagy fights disease through cellular self-digestion. *Nature* **451**: 1069–1075.
- Nakatogawa, H., Ichimura, Y., and Ohsumi, Y. (2007) Atg8, a ubiquitin-like protein required for autophagosome formation, mediates membrane tethering and hemifusion. *Cell* **130**: 165–78.
- Nayak, T., Szewczyk, E., Oakley, C.E., Osmani, A., Ukil, L., Murray, S.L., et al. (2006). A versatile and efficient gene-targeting system for *Aspergillus nidulans*. *Genetics* **172**: 1557–1566.
- Nikko, E., and Pelham, H.R. (2009) Arrestin-mediated endocytosis of yeast plasma membrane transporters. *Traffic* **10**: 1856–1867.
- Nyathi, Y., Wilkinson, B.M., and Pool, M.R. (2013) Co-translational targeting and translocation of proteins to the endoplasmic reticulum. *Biochim Biophys Acta* **1833**: 2392–2402.
- Pantazopoulou, A., and Diallinas, G. (2006) The first transmembrane segment (TMS1) of UapA contains determinants necessary for expression in the plasma membrane and purine transport. *Mol Membr Biol* **23**: 337–348.
- Pantazopoulou, A., and Peñalva, M.A. (2009) Organization and dynamics of the *Aspergillus nidulans* Golgi during apical extension and mitosis. *Mol Biol Cell* **20**: 4335–4347.
- Pantazopoulou, A., Lemuh, N.D., Hatzinikolaou, D.G., Drevet, C., Cecchetto, G., Scazzocchio, C., and Diallinas, G. (2007) Differential physiological and developmental expression of the UapA and AzgA purine transporters in *Aspergillus nidulans*. *Fungal Genet Biol* **44**: 627–640.
- Pantazopoulou, A., Pinar, M., Xiang, X., and Peñalva, M.A. (2014) Maturation of late Golgi cisternae into RabE (RAB11) exocytic post-Golgi carriers visualized in vivo. *Mol Biol Cell* **25**: 2428–2443.
- Papageorgiou, I., Gournas, C., Vlantzi, A., Amillis, S., Pantazopoulou, A., and Diallinas, G. (2008) Specific inter-domain synergy in the UapA transporter determines its unique specificity for uric acid among NAT carriers. *J Mol Biol* **382**: 1121–1135.
- Peñalva, M.A. (2005) Tracing the endocytic pathway of *Aspergillus nidulans* with FM4-64. *Fungal Genet Biol* **42**: 963–975.
- Peñalva, M.Á. (2010) Endocytosis in filamentous fungi: *Candida* gets her reward. *Curr Opin Microbiol* **13**: 684–692.
- Peñalva, M.A., Galindo, A., Abenza, J.F., Pinar, M., Calcagno-Pizarelli, A.M., Arst, H.N., and Pantazopoulou, A. (2012) Searching for gold beyond mitosis: mining intracellular membrane traffic in *Aspergillus nidulans*. *Cell Logist* **2**: 2–14.
- Pinar, M., Pantazopoulou, A., Arst, H.N. Jr, and Peñalva, M.A. (2013a) Acute inactivation of the *Aspergillus nidulans* Golgi membrane fusion machinery: correlation of apical extension arrest and tip swelling with cisternal disorganization. *Mol Microbiol* **89**: 228–248.
- Pinar, M., Pantazopoulou, A., and Peñalva, M.A. (2013b) Live-cell imaging of *Aspergillus nidulans* autophagy: RAB1 dependence, Golgi independence and ER involvement. *Autophagy* **9**: 1024–1043.
- Pinar, M., Arst, H.N. Jr., Pantazopoulou, A., Tagua, V.G., de Los Ríos, V., Rodríguez-Salarichs, J., et al. (2015) TRAPP2 regulates exocytic Golgi exit by mediating nucleotide exchange on the Ypt31 ortholog RabERAB11. *Proc Natl Acad Sci U S A* **112**: 4346–4351.
- Rotin, D., and Staub, O. (2011) Role of the ubiquitin system in regulating ion transport. *Pflugers Arch* **461**: 1–21.
- Ruggiano, A., Foresti, O., and Carvalho, P. (2014) Quality control: ER-associated degradation: protein quality control and beyond. *J Cell Biol* **204**: 869–879.
- Sambrook, J., Fritsch, E., and Maniatis, T. (1989) *Molecular Cloning: A Laboratory Manual*. Cold Spring Harbor, NY: Cold Spring Harbor Laboratory Press.
- Sato, K., and Nakano, A. (2007) Mechanisms of COPII vesicle formation and protein sorting. *FEBS Lett* **581**: 2076–2082.
- Schubert, U., Anton, L.C., Gibbs, J., Norbury, C.C., Yewdell, J.W., and Bennink, J.R. (2000) Rapid degradation of a large fraction of newly synthesized proteins by proteasomes. *Nature* **404**: 770–774.
- Shintani, T., and Klionsky, D.J. (2004) Cargo proteins facilitate the formation of transport vesicles in the cytoplasm to vacuole targeting pathway. *J Biol Chem* **279**: 29889–29894.
- Smith, M.H., Ploegh, H.L., and Weissman, J.S. (2011) Road to ruin: targeting proteins for degradation in the endoplasmic reticulum. *Science* **334**: 1086–1090.
- Stanley, R.E., Ragusa, M.J., and Hurley, J.H. (2014) The beginning of the end: how scaffolds nucleate autophagosome biogenesis. *Trends Cell Biol* **24**: 73–81.
- Stimpson, H.E., Lewis, M.J., and Pelham, H.R. (2006) Transferrin receptor-like proteins control the degradation of a yeast metal transporter. *EMBO J* **25**: 662–672.
- Sullivan, J.A., Lewis, M.J., Nikko, E., and Pelham, H.R. (2007) Multiple interactions drive adaptor-mediated recruitment of the ubiquitin ligase rsp5 to membrane proteins in vivo and in vitro. *Mol Biol Cell* **18**: 2429–2440.

- Szewczyk, E., Nayak, T., Oakley, C.E., Edgerton, H., Xiong, Y., Taheri-Talesh, N., *et al.* (2006) Fusion PCR and gene targeting in *Aspergillus nidulans*. *Nat Protoc* **1**: 3111–3120.
- Takeshita, N., Higashitsuji, Y., Konzack, S., and Fischer, R. (2008) Apical sterol-rich membranes are essential for localizing cell end markers that determine growth directionality in the filamentous fungus *Aspergillus nidulans*. *Mol Biol Cell* **19**: 339–351.
- Travers, K.J., Patil, C.K., Wodicka, L., Lockhart, D.J., Weissman, J.S., and Walter, P. (2000) Functional and genomic analyses reveal an essential coordination between the unfolded protein response and ER-associated degradation. *Cell* **101**: 249–258.
- Vlanti, A., Amillis, S., Koukaki, M., and Diallinas, G. (2006) A novel-type substrate-selectivity filter and ER-exit determinants in the UapA purine transporter. *J Mol Biol* **357**: 808–819.
- Walter, P., and Ron, D. (2011) The unfolded protein response: from stress pathway to homeostatic regulation. *Science* **334**:1081–1086.
- Wang, S., Thibault, G., and Ng, D.T. (2011) Routing misfolded proteins through the multivesicular body (MVB) pathway protects against proteotoxicity. *J Biol Chem* **286**: 29376–29387.
- Yao, T.P. (2010) The role of ubiquitin in autophagy-dependent protein aggregate processing. *Genes Cancer* **1**: 779–786.

### Supporting information

Additional supporting information may be found in the online version of this article at the publisher's web-site.

# The AP-2 complex has a specialized clathrin-independent role in apical endocytosis and polar growth in fungi

Olga Martzoukou<sup>1</sup>, Sotiris Amillis<sup>1</sup>, Amalia Zervakou<sup>1</sup>, Savvas Christoforidis<sup>2,3</sup>, George Diallinas<sup>1\*</sup>

<sup>1</sup>Department of Biology, National and Kapodistrian University of Athens, Athens, Greece; <sup>2</sup>Institute of Molecular Biology and Biotechnology-Biomedical Research, Foundation for Research and Technology, Ioannina, Greece; <sup>3</sup>Laboratory of Biological Chemistry, Department of Medicine, School of Health Sciences, University of Ioannina, Ioannina, Greece

**Abstract** Filamentous fungi provide excellent systems for investigating the role of the AP-2 complex in polar growth. Using *Aspergillus nidulans*, we show that AP-2 has a clathrin-independent essential role in polarity maintenance and growth. This is in line with a sequence analysis showing that the AP-2  $\beta$  subunit ( $\beta 2$ ) of higher fungi lacks a clathrin-binding domain, and experiments showing that AP-2 does not co-localize with clathrin. We provide genetic and cellular evidence that AP-2 interacts with endocytic markers SlaB<sup>End4</sup> and SagA<sup>End3</sup> and the lipid flippases DnfA and DnfB in the sub-apical collar region of hyphae. The role of AP-2 in the maintenance of proper apical membrane lipid and cell wall composition is further supported by its functional interaction with BasA (sphingolipid biosynthesis) and StoA (apical sterol-rich membrane domains), and its essentiality in polar deposition of chitin. Our findings support that the AP-2 complex of dikarya has acquired, in the course of evolution, a specialized clathrin-independent function necessary for fungal polar growth.

DOI: 10.7554/eLife.20083.001

\*For correspondence: diallina@biol.uoa.gr

**Competing interests:** The authors declare that no competing interests exist.

**Funding:** See page 22

**Received:** 27 July 2016

**Accepted:** 07 February 2017

**Published:** 21 February 2017

**Reviewing editor:** Randy Schekman, Howard Hughes Medical Institute, University of California, Berkeley, United States

© Copyright Martzoukou et al. This article is distributed under the terms of the [Creative Commons Attribution License](#), which permits unrestricted use and redistribution provided that the original author and source are credited.

## Introduction

The five distinct Adaptor Protein (AP or adaptin) complexes are heterotetrameric adaptors that recruit membrane cargoes and coat proteins during vesicle formation at various subcellular locations for membrane trafficking in eukaryotes (Nakatsu and Ohno, 2003; Robinson, 2004, 2015). AP-1 is necessary for the formation of clathrin-coated vesicles that traffic between the *trans*-Golgi network (TGN) and early endosomes. AP-2 is involved in the formation of clathrin-coated endocytic vesicles from the plasma membrane (PM). AP-3 is involved in, apparently, clathrin-independent vesicle formation in the Golgi for traffic to endosomes and lysosomes or vacuoles. AP-4 and AP-5 seem to have more specialized roles in vesicle transport of specific cargoes from the TGN to endosomes and/or the cell surface (Hirst et al., 2013). All AP complexes are composed of two different subunits of high molecular weight ~100 kDa (called  $\alpha$ ,  $\beta$  or  $\gamma$  adaptins), one subunit of medium size ( $\mu$ , 47–50 kDa), and one low-molecular-weight subunit ( $\sigma$ , 17–19 kDa). The five AP complexes have been shown to have a wide eukaryote distribution, supporting that all were present in the Last Eukaryote Common Ancestor (LECA) (Barlow et al., 2014). Noticeably, however, each AP complex, except AP-1, has been lost in various lineages. Fungi possess homologues of all AP-1, AP-2 and AP-3 subunits, but the great majority of them, have lost AP-4 and AP-5. This loss concerns all Dikarya (Ascomycetes and Basidiomycetes) and most primitive fungi. AP-4 or AP-5 subunits are however present in the glomeromycete *Rhizophagus irregularis* and chytrid fungi *Spizellomyces punctatus* and

*Batrachomyces dendrobatidis*, as well as, the sister group of all fungi, *Fusiclona alba*. Notably, all eukaryotes studied possess clathrin, except for the Microsporidia intracellular parasites. Interestingly, the microsporidian *Encephalitozoon cuniculi* maintains AP subunits without having clathrin (Barlow et al., 2014), suggesting an unknown clathrin-independent role of AP complexes.

The role of the AP-2 complex in clathrin-mediated endocytosis is well established in mammals. By contrast, its role in endocytosis in unicellular eukaryotes, such as the yeasts *Saccharomyces cerevisiae*, *Schizosaccharomyces pombe* and *Candida albicans* has been questioned. An early systematic biochemical and genetic characterization of AP complexes in *S. cerevisiae* provided evidence that AP complexes are dispensable for clathrin function (Yeung et al., 1999). Similarly, Huang et al. (1999) have shown that AP deletion strains did not display the phenotypes associated with clathrin deficiency, including slowed growth and endocytosis, defective late Golgi protein retention and impaired cytosol to vacuole/autophagy function. Subsequently however, AP-2 has been localized to endocytic sites that are associated with clathrin, and have a cargo-specific function in killer toxin K28 endocytosis, making it likely that AP-2 functions with clathrin (Carroll et al., 2009, 2012). Furthermore, AP-2 has been shown to be critical for hyphal growth in *C. albicans* and polarized cell responses in *S. cerevisiae*, and in particular to be necessary for relocalization of the cell wall stress sensor Mid2 to the tip of a mating projection following pheromone addition (Chapa-y-Lazo et al., 2014). Additionally, an interaction between the mu ( $\mu$ ) subunit of AP-2 and the cell wall integrity pathway component Pkc1 was reported to affect recruitment of the AP-2 complex to endocytic sites (Chapa-y-Lazo and Ayscough, 2014). In another systematic screen to identify proteins required for cargo internalization, clathrin was shown to have a critical role for synaptobrevin homologue Snc1 endocytosis, but the role of AP-2 was not investigated (Burston et al., 2009). In a more recent study it has been shown that clathrin contributes to the regularity of vesicle scission and vesicle size, but is not required for elongating or shaping the endocytic membrane invagination, but again the role of AP-2 was not studied (Kukulski et al., 2016). Finally, in *S. pombe*, the AP-2  $\alpha$  component (Apl3p) was shown to interact physically with clathrin light chain (Clc1p), and genetically with both Clc1p and the endocytic factor Sla2p and additionally *apl3 $\Delta$*  null mutants showed altered dynamics of endocytic sites associated with abnormal cell wall synthesis and morphogenesis (de León et al., 2016; de León and Valdivieso, 2016).

The apparently moderate role of AP-2 for growth in yeasts might reflect the fact that endocytosis in general is not essential for growth in unicellular fungi. In contrast to yeasts, the extreme polar growth of filamentous fungi, taking place by apical extension, is absolutely dependent on efficient and continuous endocytosis. Seminal studies on endocytosis and its relationship to growth have been performed in the basidiomycete *Ustilago maydis* (Steinberg, 2014) and the ascomycete *Aspergillus nidulans* (Peñalva, 2010), two emerging cell biology model systems.

Two aspects of endocytosis have been studied in detail in *A. nidulans*. The first relates to the essential role of apical endocytosis in hyphal tube extension and polar growth (Araujo-Bazán et al., 2008; Taheri-Talesh et al., 2008; Hervas-Aguilar and Penalva, 2010; Peñalva, 2010). It has been rigorously shown that polar growth maintenance is based on the spatial and functional coupling of rapid and continuous apical secretion and endocytosis in the hyphal tip region. Apically localized cargoes, as exemplified by the v-SNARE synaptobrevin homologue SynA, are internalized from a 'collar' region immediately below the hyphal tip and sorted in early endosomes (EEs). EEs can mature into Late Endosomes (LE) or Multivesicular Bodies (MVB) and be sorted into vacuoles, or recycle back, apparently via the *trans*-Golgi network (TGN) onto the PM. These post-endocytic trafficking processes taking place at the hyphal tips seem to be essential for the normal rate of secretion and proper growth. SlaB<sup>End4</sup> and actin polymerization are major factors for apical endocytosis.

A second aspect of endocytosis in *A. nidulans* is related to its role in PM transporter down-regulation in response to physiological or stress signals (Gournas et al., 2010; Karachaliou et al., 2013). Unlike endocytosis related to apical cargoes taking place mostly at hyphal tips, transporter internalization takes place homogeneously all along the hyphal membrane and necessitates cargo ubiquitination. Transporter ubiquitination requires a group of cargo-specific  $\alpha$ -arrestin like proteins, acting as adaptors of the HECT-type ubiquitin ligase Hula<sup>Rsp5</sup>. Transporter ubiquitination is followed by internalization and sorting into EEs and the MVB/vacuolar pathway for terminal degradation. Transporter internalization, similar to apical endocytosis, requires actin polymerization and functional endocytic factors SagA<sup>End3</sup> or SlaB<sup>End4</sup>.

Curiously, the role of clathrin or AP-2 in apical or transporter endocytosis had not, until very recently, been investigated in *A. nidulans*, or other filamentous fungi. An exception is a very recent report that studied clathrin dynamics in *A. nidulans*, following basically the subcellular localization and role in growth, of the clathrin heavy chain, ClaH (Schultzhaus et al., 2017b). This report showed that ClaH is localized mostly in late (*trans*) Golgi and secondarily to tentative endocytic sites, and although absolutely essential for growth, it does not seem to be involved in endocytosis. The later conclusion was, however, solely supported by studies concerning the internalization of the FM4-64 lipophilic marker, rather than specific endocytic cargoes. This report did not investigate the role of AP-2, or any AP complex, in relation to clathrin or to *A. nidulans* growth.

In this work, we investigate the role of the AP-2 complex and clathrin in polar growth and endocytosis in *A. nidulans*. We present evidence that the roles of AP-2 and clathrin are distinct, apparently due to an evolutionary truncation of the clathrin-binding domain in the  $\beta$  subunit of AP-2 in all higher fungi. We further provide evidence that AP-2 has a specialized, clathrin-independent role related to maintaining proper apical lipid and cell wall composition and thus promoting polar growth.

## Results

### Fungal AP complexes possess evolutionary truncated $\beta$ subunits

A recent evolutionary analysis studied the distribution and origin of all AP complex subunits in fungi (Barlow et al., 2014). The conclusion from this thorough study was that all fungi possess AP-1, AP-2 or AP-3 subunits, but most, and apparently all Dikarya, have lost AP-4 or AP-5. Given our interest on the role of AP1-3 complexes in membrane traffic and particularly of AP-2 in endocytosis in *A. nidulans*, we carried out a similar analysis with particular emphasis on *Aspergillus* species. **Figure 1—figure supplement 1** shows that all *Aspergilli* possess highly similar homologous AP1-3 subunits, which can be unambiguously assigned into the distinct AP complexes. *Aspergillus* AP subunits are also phylogenetically highly related to homologues from all major fungal groups, as well as, selected model organisms (**Figure 1—figure supplement 2**). Importantly, AP subunits of a given complex are more similar to those of the orthologous complex in distantly related species, than to subunits of other AP complexes of the same species, in line with the acquisition of different functional roles of AP-1,-2 or -3 complexes in cargo membrane traffic.

A major and somehow surprising finding concerning the  $\beta$  subunits of not only *Aspergillus* species, but most fungi (all dikarya) came from the sequence analyses we performed. We observed that the  $\beta$  subunits of all three AP complexes do not contain the C-terminal part, of approximately 332 amino acid residues, which however is present in some primitive fungi, such as the chytrids *Rozella allomycis*, *Allomyces macrogynus* *Batrachochytrium dendrobatidis*, *Spizellomyces punctatus* and *Macrophomina phaseolina* and in the fungal sister group *Fonticula alba* (all sharing 35–40% identity with human  $\beta$  subunits) (**Figure 1A**). The C-terminal domain of the  $\beta$  subunit is conserved in several Amoebozoa (25–36% identity), Rhizaria (31% identity), Alveolata (29% identity in *Plasmodium* or *Toxoplasma* species), Choanoflagellates (34–44% identity), Mesomycetozoea (44–50% identity), Algae (30% identity), and in the great majority of plants (38% identity) and Metazoa (58–60% identity) (**Figure 1B** and data not shown). Some prominent losses, except fungi, were identified in *Trypanosoma* and *Leishmania* species and in Excavata. Importantly, the lost part corresponds to an essential part of  $\beta$  appendage, which includes two C-terminal domains (pfam02883 and pfam09066) involved in clathrin binding and polymerization, and consequently necessary for the translocation of endocytic accessory proteins to a membrane bud site (Mousavi et al., 2004; Lemmon and Traub, 2012). A hydrophobic patch present in the lost domain also binds to a subset of D $\Phi$ [F/W] motif-containing proteins that are bound by the alpha-adaptin appendage domain (epsin, AP180) (Lemmon and Traub, 2012). Thus, fungal AP complexes might be incapable of interacting, at least via a ‘canonical’ association, with clathrin. Microsporidia, which are probably the only known eukaryotes lacking clathrin, also lack the clathrin binding domains in their AP complexes (Barlow et al., 2014). A major prediction from these observations is that, in fungi, clathrin-dependent processes, such as endocytosis and vesicle budding, might be AP-complex independent, while any role of the AP complexes might in turn be clathrin-independent. Obviously this prediction does not exclude that AP-2 or AP-1 complexes might still have the potential to interact with clathrin through unknown binding sequences in the  $\beta$  subunit or domains in other subunits, as for example reported for AP-1



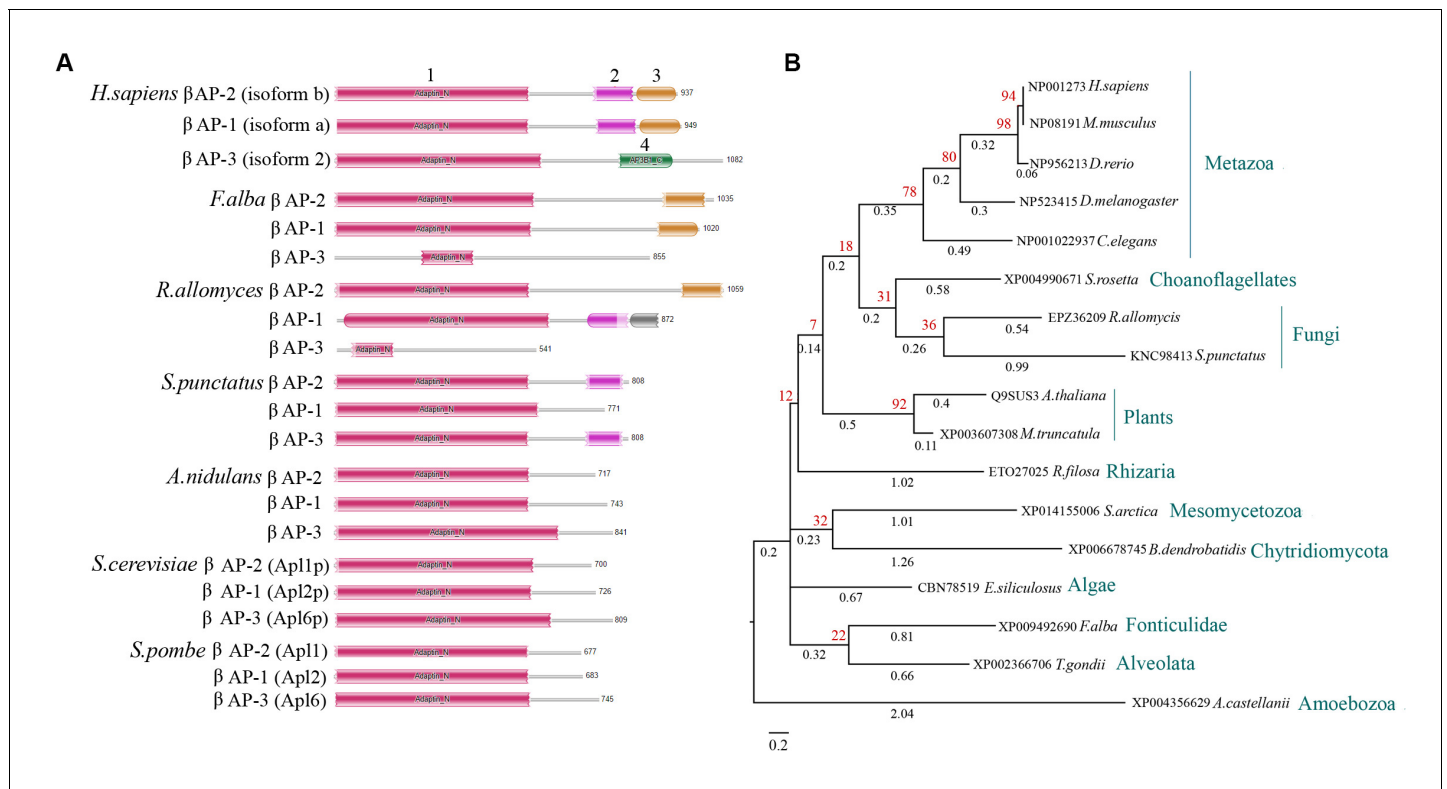


**Figure 1.** The β subunit of fungal AP complexes lacks clathrin-binding domains. **(A)** Cartoon depicting the absence in the β subunits of AP complexes of higher fungi (*A. nidulans*, *S. cerevisiae* or *S. pombe*) of a C-terminal region that includes putative clathrin binding domains. The cartoon includes the human AP1-3 β subunits as examples of canonical AP complexes, as well as, selected primitive fungi (*Rozella allomyces* and *Spizellomyces punctatus*) and *F. alba*, as examples of lower eukaryotes conserving degenerate versions of putative clathrin binding domains. One signifies the N-terminal adaptin domain (pfam01602, ~534 amino acids) common in all AP complexes. Two is the α-adaptin C2 domain (pfam02883, ~111 amino acids) present in the β subunits of AP-2 and AP-1, required for binding to clathrin. Three is the β2-adaptin appendage (pfam09066, ~112 amino acid residues) present in the β subunits of AP-2 and AP-1, required for binding to clathrin. Four is the so-called clathrin adaptor protein complex β1 subunit domain, found in AP-3 complexes, probably required for Golgi association (pfam14796, ~148 amino acids). **(B)** Phylogenetic relationships of the C-terminal region of the β subunit of AP-2 that includes clathrin-binding domains. The tree includes selected organisms representing major taxonomic groups, from the amoeba *A. castellanii* to metazoa such as *C. elegans* and *H. sapiens*. The tree was reconstructed with the maximum-likelihood method and bootstrap-method testing (shown in red). The branch scale used was 0.2 and the branch lengths (shown in black) reflect the expected number of substitutions per site.

DOI: 10.7554/eLife.20083.002

The following figure supplements are available for figure 1:

**Figure supplement 1.** Phylogenetics of the four subunits of AP1, AP-2 and AP-3 of Aspergilli with three model organisms used as out-groups.

DOI: 10.7554/eLife.20083.003

**Figure supplement 2.** Phylogenetics of the four subunits of AP-1, AP-2 and AP-3 of major fungal groups with out-groups from model organisms.

DOI: 10.7554/eLife.20083.004

in *S. cerevisiae* (Yeung and Payne, 2001). However, subsequent experimental evidence presented herein strongly support a clathrin-independent role of AP-2 in *A. nidulans* polar growth.

### AP-1 and AP-2, but not AP-3, complexes are critical for polarity maintenance and *A. nidulans* growth

To investigate the role of AP complexes in cargo membrane traffic and endocytosis in *A. nidulans* we constructed three null mutants, each carrying a deletion of the gene encoding the σ subunit of AP-1 (AN7682; *apaS*), AP-2 (AN0722; *apbS*) or AP-3 (AN5519; *apcS*) (<http://www.aspergillusgenome.org/> and Osmani and Goldman, 2008). Our primary interest was to examine the role of AP-2 in endocytosis, which however also necessitated the knock-out of the σ subunits of AP-1 and AP-3 in addition to that of AP-2, for excluding any possible functional complementation due to the similarity

of the three  $\sigma$  subunits. Genetic disruption of the  $\sigma$  subunits, similarly to disruption of any of the four AP subunits, has been reported to inactivate the function of the full adaptor complex (Robinson, 2004, 2015). Isogenic null mutants were constructed and named *thiA<sub>p</sub>-ap1 $\sigma$* , *ap2 $\sigma$*  $\Delta$  or *ap3 $\sigma$*  $\Delta$  (see Materials and methods). For the *ap1 $\sigma$*  gene, given its knock-out proved lethal (results not shown), we constructed a conditional knock-down strain using the thiamine-repressible promoter, *thiA<sub>p</sub>* (Apostolaki et al., 2012). The  $\sigma$  subunit null mutant strains were analyzed phenotypically and microscopically.

Knocking-down *ap1 $\sigma$*  or deleting *ap2 $\sigma$*  severely affected growth rate and colony morphology, whereas the *ap3 $\sigma$*  $\Delta$  mutant exhibited only a very minor delay in growth rate (inserts in Figure 2A). The double mutant strains *ap2 $\sigma$*  $\Delta$ *thiA<sub>p</sub>-ap1 $\sigma$*  and *ap2 $\sigma$*  $\Delta$ *ap3 $\sigma$*  $\Delta$ , constructed via standard genetic crossing, had growth rates similar to the single *thiA<sub>p</sub>-ap1 $\sigma$*  or *ap2 $\sigma$*  $\Delta$  mutant, showing that the defect in *ap2 $\sigma$*  $\Delta$  is independent of AP-1 or AP-3 complexes. All mutants tested remained sensitive to selected antifungals, such as 5-fluorouracil, 5-fluorocytosine or 8-azaguanine, similar to wild-type isogenic controls, suggesting that the expression and/or turnover of transporters specific for these antifungals is not affected (not shown).

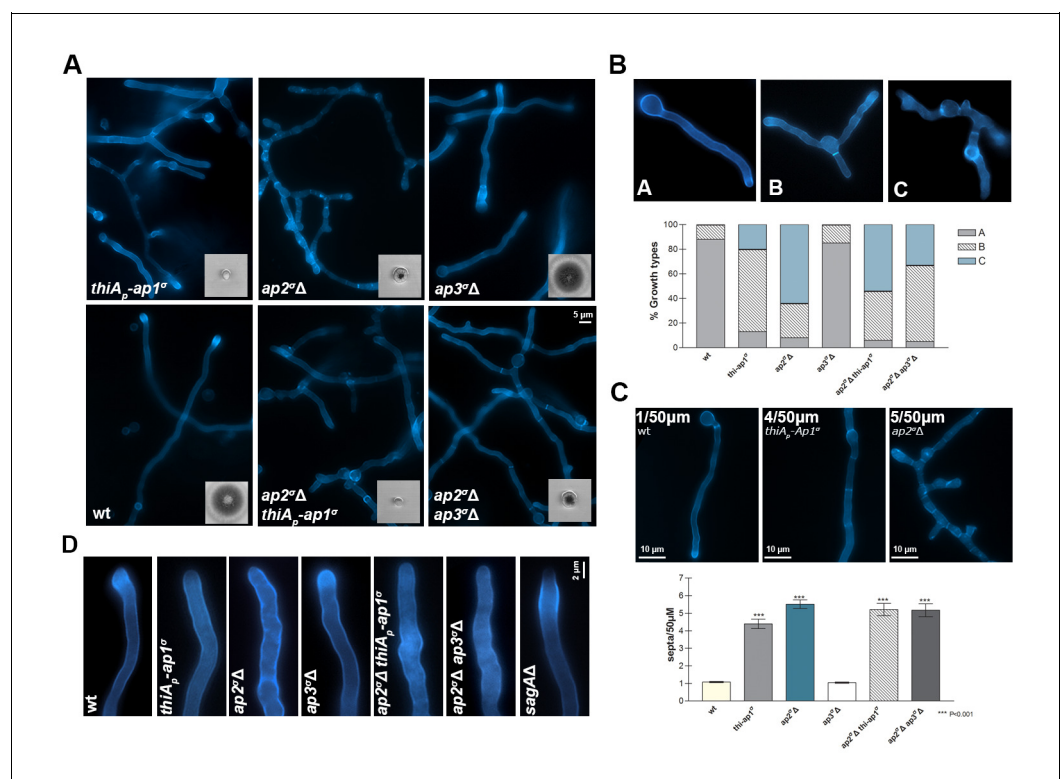


**Figure 2.** AP-1 and AP-2, but not AP-3, complexes are critical for *A. nidulans* growth. (A) Colony growth (bottom left inserts) and microscopic morphology (20 hr hyphal cells stained with calcofluor) of isogenic *thiA<sub>p</sub>-ap1 $\sigma$* , *ap2 $\sigma$*  $\Delta$ , *ap3 $\sigma$*  $\Delta$ , *ap2 $\sigma$*  $\Delta$  *thiA<sub>p</sub>-ap1 $\sigma$*  and *ap2 $\sigma$*  $\Delta$  *ap3 $\sigma$*  $\Delta$  mutant strains, compared to wild-type (wt). Biological/Technical replicates: 4/25, 3/12, 3/15, 3/10, 2/10, 2/10 for wild-type and mutant strains, respectively. For the definition of the two categories of replicates see Materials and methods. (B) Representative types of morphological phenotypes related to unipolar or multipolar germination (upper panel) and relative quantitative analysis of  $n = 100$  hyphae of wild-type and  $n = 84, 58, 60, 48$  and  $31$  hyphae of *thiA<sub>p</sub>-ap1 $\sigma$* , *ap2 $\sigma$*  $\Delta$ , *ap3 $\sigma$*  $\Delta$ , *ap2 $\sigma$*  $\Delta$  *thiA<sub>p</sub>-ap1 $\sigma$*  and *ap2 $\sigma$*  $\Delta$  *ap3 $\sigma$*  $\Delta$ , respectively (lower panel). Replicates as in (A). (C) Representative types of septa formation (upper panel) and relative quantitative analysis of  $n = 32$  hyphae of wild-type and  $n = 32, 23, 32, 32$  and  $27$  hyphae of *thiA<sub>p</sub>-ap1 $\sigma$* , *ap2 $\sigma$*  $\Delta$ , *ap3 $\sigma$*  $\Delta$ , *ap2 $\sigma$*  $\Delta$  *thiA<sub>p</sub>-ap1 $\sigma$*  and *ap2 $\sigma$*  $\Delta$  *ap3 $\sigma$*  $\Delta$  respectively (lower panel). Replicates as in (A).  $p < 0.001$  for *thiA<sub>p</sub>-ap1 $\sigma$* , *ap2 $\sigma$*  $\Delta$ , *ap2 $\sigma$*  $\Delta$  *thiA<sub>p</sub>-ap1 $\sigma$*  and *ap2 $\sigma$*  $\Delta$  *ap3 $\sigma$*  $\Delta$ , compared to wt. See Materials and methods for statistical analysis methods and statistical tests used. (D) Calcofluor deposition at the tip of growing hyphae in AP mutants and wild-type. A standard endocytic mutant, *sagA* $\Delta$ , showing reduced calcofluor staining at the tip is included for comparison. For experimental details see Materials and methods. Replicates as in (A).

DOI: 10.7554/eLife.20083.005

We examined the microscopic morphology of the mutants constructed. *thiA<sub>p</sub>-ap1<sup>σ</sup>* and *ap2<sup>σ</sup>Δ*, but not *ap3<sup>σ</sup>Δ*, showed altered hyphal morphology, characterized by anomalous polar tube hyper-branching and shorter coenocytic compartments, that is, reduced septa distances (**Figure 2A**). This effect was confirmed by quantification of the distinct microscopic morphological phenotypes and septa frequencies, as shown in **Figure 2B and C**. We also tested calcofluor deposition at the apex of polar tips in AP complex mutants, relatively to wild-type. Calcofluor stains chitin and the absence of intense calcofluor-staining at the tip indicates abnormal cell wall synthesis, related to problematic recycling of chitin synthases. This has been observed in mutants blocked in apical endocytosis (**Higuchi et al., 2009**). Calcofluor localization was totally depolarized in *thiA<sub>p</sub>-ap1<sup>σ</sup>* and *ap2<sup>σ</sup>Δ*, similar to what was observed in the endocytic mutant *SagA* (**Figure 2D**). Thus, the overall picture obtained with *thiA<sub>p</sub>-ap1<sup>σ</sup>* and *ap2<sup>σ</sup>Δ* mutants was that of defective maintenance of polarity (**Momany, 2002; Steinberg, 2014**).

## AP complexes are dispensable for membrane traffic and endocytosis of transporters

We investigated the role of the AP complexes on membrane cargo traffic and endocytosis by following the subcellular localization of a GFP-tagged transporter, namely UapA. UapA is an extensively studied uric acid-xanthine/H<sup>+</sup> symporter, which has been used as a model cargo for studying the regulation of exocytosis and endocytosis of polytopic membrane proteins in *A. nidulans* (**Pantazopoulou et al., 2007; Gournas et al., 2010; Karachaliou et al., 2013**). After synthesis and translocation in the ER, fully functional GFP-tagged UapA molecules follow a vesicular secretion pathway to localize homogeneously and stably in the PM of hyphal cells. However, UapA molecules undergo ubiquitylation-dependent endocytosis and vacuolar degradation in response to substrate excess or to the presence of rich nitrogen sources (NH<sub>4</sub><sup>+</sup> or glutamine). This picture remained unaffected when we followed the subcellular localization of UapA-GFP in isogenic *thiA<sub>p</sub>-ap1<sup>σ</sup>*, *ap2<sup>σ</sup>Δ* or *ap3<sup>σ</sup>Δ* mutant backgrounds (**Figure 3A**). The same picture is obtained under conditions of de novo or continuous UapA-GFP synthesis, or when signals triggering endocytosis are imposed after repression of UapA-GFP synthesis (data not shown). The non-essentiality of the AP-1 and AP-3 complexes in UapA traffic was somehow expected, because transporter exocytosis occurs by direct fusion of post-Golgi vesicles with the PM, and seemingly does not involve sorting from the Golgi to the endosomal compartment. However, the dispensability of AP-2, an adaptor involved in the formation of endocytic vesicles in other systems, for UapA-GFP endocytosis was somehow unexpected and contrasted the picture observed in standard endocytic mutants (*sagAΔ* or *thiA<sub>p</sub>-slaB*), where UapA internalization from the PM was totally blocked (see right panels in **Figure 3A** and **Figure 3—figure supplement 1** for the construction of *thiA<sub>p</sub>-slaB*). The non-involvement of AP-2 in UapA endocytosis was further confirmed by time-lapse experiments, performed in the *ap2<sup>σ</sup>Δ* mutant strain and an isogenic wild-type control (*ap2<sup>σ</sup>+*), which showed that UapA-GFP internalization initiates at 15 min and becomes more prominent 20–30 min after NH<sub>4</sub><sup>+</sup> addition in both strains (**Figure 3B**).

The non-involvement of AP-2 in UapA endocytosis raised issues worthy to be investigated. Firstly, we tested whether the endocytosis of other evolutionary, structurally and functionally distinct transporters is also AP-2 independent. **Figure 3C,E and F** show that this is indeed the case, as all six transporters tested are internalized with the same efficiency and rate, in both *ap2<sup>σ</sup>Δ* and *ap2<sup>σ</sup>+* backgrounds, in response to endocytic signals (**Tavoularis et al., 2001; Vlanti and Diallinas, 2008; Apostolaki et al., 2009; Kryptou et al., 2015**). Noticeably, different transporters exhibit different stabilities and endocytic ‘sensitivities’, but as quantification confirmed (**Figure 3E and F**), in all cases AP-2 proved dispensable for their proper internalization rate and turnover. We also examined whether the genetic elimination of a different AP-2 subunit, other than σ2, also leads to similar results in respect to transporter endocytosis. We deleted the gene encoding the μ2 subunit of the AP-2 complex, and subsequently constructed *ap2<sup>σ</sup>Δ ap2<sup>μ</sup>Δ* double mutants and strains expressing UapA-GFP in the *ap2<sup>μ</sup>Δ* background. The *ap2<sup>σ</sup>Δ*, *ap2<sup>μ</sup>Δ* and *ap2<sup>σ</sup>Δ ap2<sup>μ</sup>Δ* mutants had identical phenotypes, characterized by loss of polarity maintenance and poor growth rate (**Figure 3—figure supplement 2**). UapA-GFP endocytosis operated normally in the *ap2<sup>μ</sup>Δ* background, similar to what was observed in the *ap2<sup>σ</sup>Δ* or wild-type isogenic backgrounds (**Figure 3D**). Overall, these results confirmed that AP-2 is dispensable for transporter endocytosis.

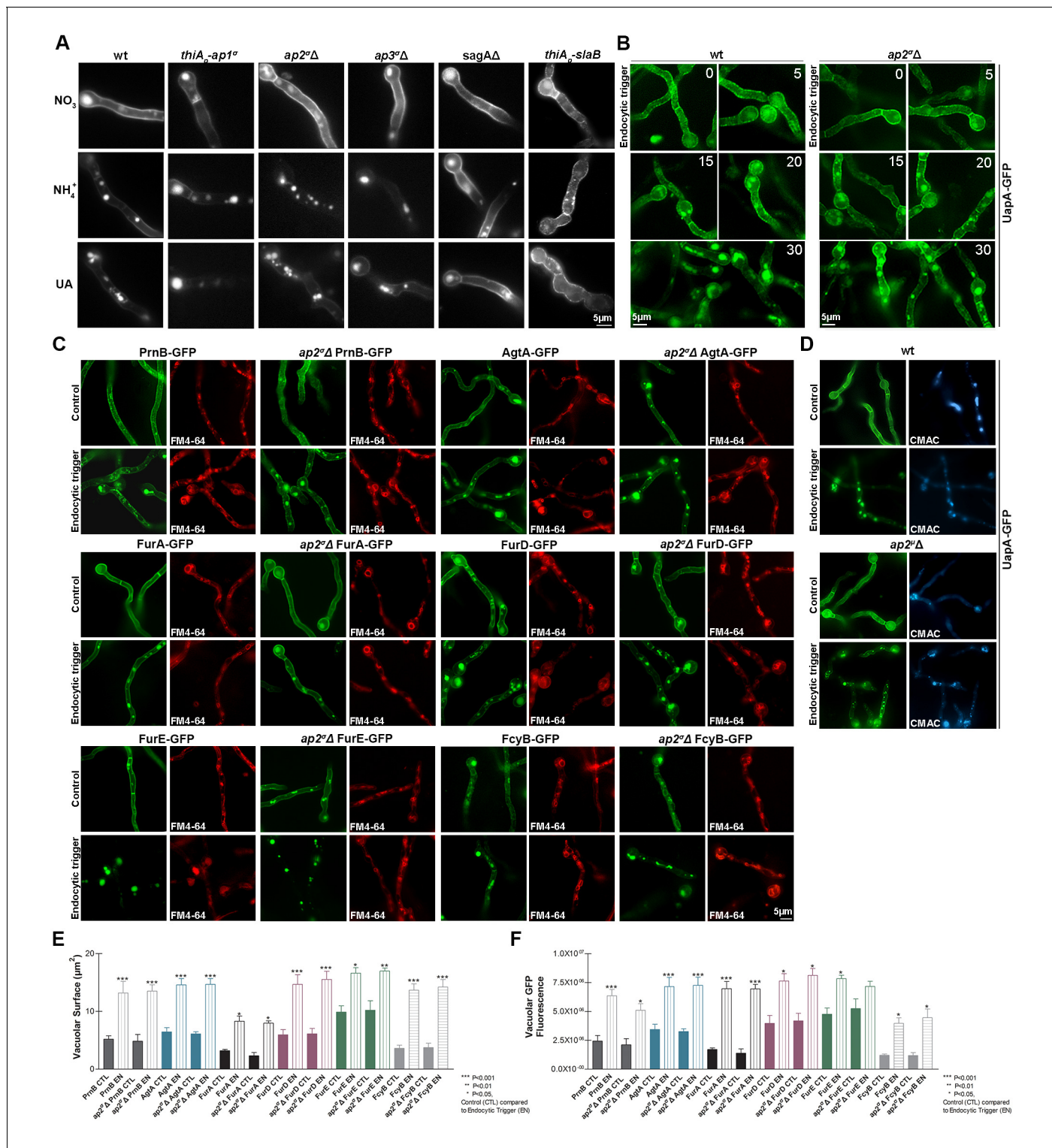


**Figure 3.** AP complexes are dispensable for transporter membrane traffic and endocytosis. All panels show Epifluorescence microscopy analyses of 18–20 hr growing hyphal cells in supplemented Minimal Media. (A) Subcellular localization of UapA-GFP under standard growing conditions (NO<sub>3</sub><sup>-</sup> as sole N source) and in response to endocytic signals (standard conditions followed by 2 hr addition of either NH<sub>4</sub><sup>+</sup> or uric acid, UA) in AP (*thiA<sub>p</sub>-ap1<sup>σ</sup>*, *ap2<sup>Δ</sup>*, *ap3<sup>Δ</sup>*) or endocytic mutants (*sagAΔ* and *thiA<sub>p</sub>-slaB*), compared to isogenic wild-type. Biological/Technical replicates: 2/10. (B) Time course (min) of NH<sub>4</sub><sup>+</sup>-elicited endocytosis of UapA-GFP in a *ap2<sup>Δ</sup>* genetic background. An identical picture is obtained in a wild-type (*ap2<sup>+</sup>*) background (Gournas et al., 2010). Biological/Technical replicates: 2/10. (C) Subcellular localization of six GFP-tagged transporters belonging to distinct protein families (PrnB, AgtA, FurA, FurD, FurE and FcyB; for details see text) in response to endocytic trigger (2 hr NH<sub>4</sub><sup>+</sup>). Staining with FM4-64 is included to Figure 3 continued on next page

Figure 3 continued

show that in the presence of  $\text{NH}_4^+$  all transporters are eventually sorted for degradation in the vacuoles, similarly to what was observed with UapA. Biological/Technical replicates: 2/20, 2/20, 2/15, 2/15, 2/15 and 3/10. (D) Relative subcellular localization of UapA-GFP in response to endocytic trigger (2 hr  $\text{NH}_4^+$ ) in wild-type and *ap2 $\Delta$*  genetic backgrounds. CMAC staining highlights terminal sorting in the vacuoles in the presence of  $\text{NH}_4^+$ . Notice that UapA-GFP is normally endocytosed in *ap2 $\Delta$* , similarly to *ap2 $\Delta$*  or the wild-type strain. Biological/Technical replicates: 2/12. See also **Figure 3—figure supplement 2**. (E–F) Quantitative analysis of transporter endocytosis presented in (C) as depicted by measurements of vacuolar surface or vacuolar GFP fluorescence. n = 5 hyphae per condition (Control or Endocytosis). For the method of measurements, statistical analysis and other experimental details see Materials and methods. Replicates as in (C).

DOI: [10.7554/eLife.20083.006](https://doi.org/10.7554/eLife.20083.006)

The following figure supplements are available for figure 3:

**Figure supplement 1.** Phenotypic characterization of a conditional null mutant of SlaB constructed using the *thiA<sub>p</sub>* repressible promoter.

DOI: [10.7554/eLife.20083.007](https://doi.org/10.7554/eLife.20083.007)

**Figure supplement 2.** Phenotypic characterization of conditional *ap2 $\Delta$*  null mutants constructed using standard reverse genetics and genetic crossing.

DOI: [10.7554/eLife.20083.008](https://doi.org/10.7554/eLife.20083.008)

## Clathrin and AP-2 have distinct roles in *A. nidulans* growth and transporter endocytosis

We showed that AP-2 is essential for polarity maintenance, but dispensable for transporter trafficking and endocytosis. To investigate the role of clathrin in these processes, we constructed relevant null or conditional mutants of the heavy (ClaH) and light (ClaL) chains of clathrin. The ClaH null mutant (*claH*) was not viable as it could only be rescued in heterokaryotic transformants (Osmani et al., 2006). The ClaL null mutant (*claL*) was viable, but severely affected in growth (Figure 4A). The corresponding conditional mutants were based on the use of the highly repressible *thiA<sub>p</sub>* promoter (Apostolaki et al., 2012). In the absence of thiamine (repressor), strains expressing *thiA<sub>p</sub>-claH* or *thiA<sub>p</sub>-claL* grew similar to wild-type isogenic control strains (not shown), whereas in the presence of thiamine *thiA<sub>p</sub>-claH* did not grow to form colonies, while *thiA<sub>p</sub>-claL* formed very small compact colonies, compatible with a severe growth defect (Figure 4A). Schultzhaus et al. (2017b), recently reported very similar growth phenotypes. We further examined the thiamine-repressible mutants under the microscope (Figure 4B). The *thiA<sub>p</sub>-claL* strain showed normal hyphae morphology and polar growth in the absence of thiamine, but prominent hypha tip swelling under *ab initio* repression of ClaL, that is, in the continuous presence of thiamine, especially at 37°C. This phenotype, which was confirmed by quantification (Figure 4C–E), might be associated with genetic blocks in apical endocytosis of specific cargoes. Knock-down of ClaL did not however modify the polar deposition of calcofluor staining, which suggests normal chitin synthesis (Higuchi et al., 2009; Takeshita et al., 2012), and neither affected polarity maintenance. The *thiA<sub>p</sub>-claH* strain also showed normal hyphae morphology and polar growth in the absence of thiamine, but contrastingly, hyphae morphology was severely affected in the continuous presence of thiamine, becoming flattened and often showing swelling of tips or conidiospore heads, or becoming thinner and smaller in overall size, an indication of progressive lethality (Figure 4B and F). Still however, polarity maintenance was preserved when ClaH was repressed. Thus, in no case the phenotypes resulting from the absence of clathrin, either ClaH or ClaL, resembled those obtained in the absence of AP-2.

We also asked whether clathrin has a role in transporter endocytosis. Knockdown of ClaL expression blocked ammonium-elicited endocytosis of the UapA transporter, but knockdown of ClaH expression showed a more complex picture (Figure 4G). More specifically, in the latter case, when thiamine was added from the beginning of growth, UapA-GFP showed a rather diffuse and cytoplasmic appearance, instead of the normal cortical marking of the PM (notice the magnified area in the relevant insert in Figure 4G). This picture was obtained independently from the presence or absence of the endocytic trigger. Under the light of the recent publication of Schultzhaus et al. (2017b), which showed that ClaH is principally localized in the late Golgi, but also based on our own independent results on the effect of ClaH on other apical markers, described later in this work, it seems that *ab initio* knockdown of ClaH severely affects secretion of cargoes, including transporters. This leads to apparent Golgi and endosome collapse and progressive lethality, which could easily explain why we detect UapA-GFP in cytosolic structures, rather than in the PM. In addition, a block in transporter secretion would also create a cellular stress signal resulting in further internalization and turnover of transporters.

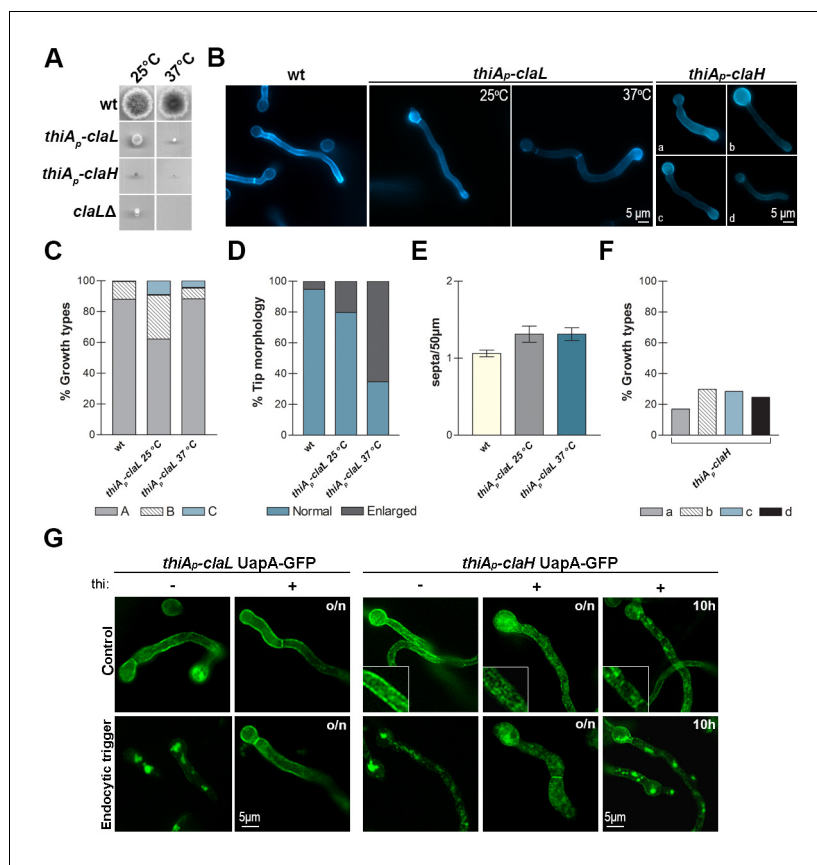


**Figure 4.** Clathrin is essential for growth and transporter secretion or/and endocytosis. (A, B) Colony growth phenotypes and microscopic morphology (hyphal cells stained with calcofluor) of ClaL knock-out (*claΔ*) or conditionally knocked-down (*thiA<sub>p</sub>-claL* and *thiA<sub>p</sub>-claH*) mutants. Representative types of morphological phenotypes (a-d) of *thiA<sub>p</sub>-claH* are shown (B, right panel). For details see text. Biological/Technical replicates in (B): 4/25, 2/20 and 2/100, for the three strains respectively. Unless otherwise stated, thiamine was added *ab initio* (16 hr) at a final concentration of 10 µg ml<sup>-1</sup>. (C–E) Quantitative analysis of growth phenotypes (categorized as in Figure 2 in A,B or C), tip morphology and number of septa, in *thiA<sub>p</sub>-claL* (thiamine-repressed) and an isogenic wild-type control (wt). (C) Analysis of n = 100 hyphae of wild-type and n = 45, 94 hyphae of *thiA<sub>p</sub>-claL* at 25°C and 37°C respectively. (D) Analysis of n = 95, 69, 95 hyphal tips of wt, *thiA<sub>p</sub>-claL* at 25°C and 37°C respectively. (E) Analysis of n = 32 hyphae of wt and knock-down strains. Replicates as in (B). (F) Relative quantitative analysis of growth types shown in (B), of n = 200 hyphae of *thiA<sub>p</sub>-claH* (thiamine-repressed). Replicates as in (B). (G) Epifluorescence microscopy showing the relative subcellular localization of UapA-GFP under control or endocytic conditions (2 hr NH<sub>4</sub><sup>+</sup>) in isogenic wild-type and *thiA<sub>p</sub>-claL* or *thiA<sub>p</sub>-claH* genetic backgrounds. Notice that repression of *claL* expression (o/n thiamine) blocks UapA-GFP endocytic turnover, *ab initio* repression of *claH* expression (o/n thiamine) severely blocks UapA-secretion to the PM, whereas *claH* repression (10 hr thiamine) after pre-secretion of UapA-GFP into the PM (14 hr) leads to an apparent block in secretion, but a fraction of UapA-GFP still remains in the PM. For more explanations see the text. Biological/Technical replicates: 4/10, 3/15 for *thiA<sub>p</sub>-claL* UapA-GFP and *thiA<sub>p</sub>-claH* UapA-GFP, respectively.

DOI: [10.7554/eLife.20083.009](https://doi.org/10.7554/eLife.20083.009)

The following figure supplements are available for figure 4:

**Figure supplement 1.** Western blot analysis of *thiA<sub>p</sub>-claH*-GFP.

DOI: [10.7554/eLife.20083.010](https://doi.org/10.7554/eLife.20083.010)

**Figure supplement 2.** Time course of FM4-64 internalization in wild-type and mutant strains.

DOI: [10.7554/eLife.20083.011](https://doi.org/10.7554/eLife.20083.011)

To allow secretion and proper localization of UapA-GFP to the PM to take place, and subsequently to check the role of ClaH in endocytosis, we decided to repress *claH* expression by adding thiamine after a period of pre-growth (14 hr) in the absence of thiamine. For this, we directly tested whether 5 or 10 hr repression of *claH* via the *thiA* promoter is sufficient for depleting ClaH, by performing and quantifying immunoblot assays using anti-GFP or anti-actin antibodies against total protein extracts from a strain expressing ClaH-GFP. Results shown in **Figure 4—figure supplement 1** confirmed that addition of thiamine for  $\geq 10$  hr dramatically reduced ClaH. In contrast, 5 hr addition of thiamine had no effect on ClaH steady state levels, apparently because the relevant polypeptide is quite stable. Based on these immunoblots, we examined the effect of ClaH on UapA-GFP endocytosis by using at least a 10 hr period of *claH* repression, after pre-secretion of UapA-GFP into the PM. In this case, a significant fraction of UapA-GFP remained PM-associated despite the appearance of UapA-specific cytoplasmic structures and increased vacuolar degradation, which are however expected outcomes resulting from a block in Golgi functioning and transporter secretion (**Figure 4G**, extreme right panel).

Overall, our results strongly suggest that although both chains of clathrin seem essential for transporter (UapA-GFP) endocytosis, they do have distinct roles in transporter secretion. ClaL is dispensable for Golgi functioning and transporter secretion towards the PM, while ClaH seems absolutely essential for Golgi functioning and cargo secretion. These results further support that clathrin and the AP-2 complex have distinct roles in respect to both cargo secretion and transporter endocytosis.

Notably, we also found that FM4-64 endocytosis is not affected by deletions of genes encoding AP-2 complex subunits, clathrin or the endocytic factors SagA and SlaB, suggesting still another pathway of endocytosis in *A. nidulans* (**Figure 4—figure supplement 2**).

## AP-2, but not clathrin, is essential for the polar localization of lipid flippases DnfA and DnfB

Guided by the fact that lack of a functional AP-2 complex (*ap2<sup>Δ</sup>* or *ap2<sup>H</sup>* mutants) leads to defective polarity maintenance and dramatically reduced growth, we tested whether AP-2 has a specific role in the polar localization of well-studied apical cargoes, such as the v-SNARE SynA (**Valdez-Taubas and Pelham, 2003; Pantazopoulou and Peñalva, 2011**) or the DnfA and DnfB flippases (**Schultzhaus et al., 2015**). These are the only presently known recycling cargoes of the endocytic collar shown rigorously to be involved in polar growth (**Peñalva, 2015**). In parallel, we examined the role of AP-2 in the polar localization of the endocytic markers, SlaB (**Araujo-Bazán et al., 2008; Herivas-Aguilar and Penalva, 2010**) and SagA (**Karachaliou et al., 2013**), or of AbpA, which marks the sites of actin polymerization (**Araujo-Bazán et al., 2008**). Appropriate strains were constructed by standard genetic crossing. **Figure 5A** shows that in the *ap2<sup>Δ</sup>* genetic background there is total depolarization of DnfA and DnfB, as these proteins now mark the hyphal PM rather homogeneously (see also **Figure 5E, Figure 5—figure supplement 1A**). In contrast, absence of a functional AP-2 did not detectably affect the polar localization of SagA, SlaB, SynA or AbpA. Quantification of polarized versus non-polarized localization of these markers confirmed our conclusions (**Figure 5B**). The same overall results were obtained when we used the *ap2<sup>H</sup>* mutant rather than *ap2<sup>Δ</sup>* (results not shown).

We tested the role of clathrin (ClaL) in the polar localization of DnfA, SlaB and SagA. **Figure 5C** shows that in a *thiA<sub>p</sub>-claL* strain repressed *ab initio* for ClaL expression, all markers tested remain polarly localized, marking principally the collar region behind the tip (see also **Figure 5E**). We also tested the role of ClaH in DnfA or DnfB localization (**Figure 5D** and **Figure 5—figure supplement 1B**). In a *thiA<sub>p</sub>-claH* genetic background, *ab initio* (that is, o/n) addition of thiamine led to cytoplasmic distribution of DnfA-GFP or DnfB-GFP, which in this case mark large, often bulbous, bodies and a membrane-like network (upper and lower left panels in **Figure 5D**), resembling the picture obtained when we followed UapA-GFP in the absence of ClaH (see **Figure 4G**), or when Golgi/endosomes collapse in response to the presence of Brefeldin A (BFA) (middle panels in **Figure 5D**). We further showed that addition of BFA in the culture medium of a strain expressing ClaH (de-repressed *thiA<sub>p</sub>-claH*) leads to reversible de-polarization of DnfA-GFP (lower panel in **Figure 5—figure supplement 2**), but to irreversible de-polarization of DnfA-GFP and progressive apparent hyphae death (that is, hyphae cells become thinner) when ClaH expression is repressed (upper panel in **Figure 5—figure supplement 2**). This picture is in very good agreement with the reversibility of the negative effect of BFA on Golgi function, which has been rigorously studied in **Pantazopoulou and Penalva**

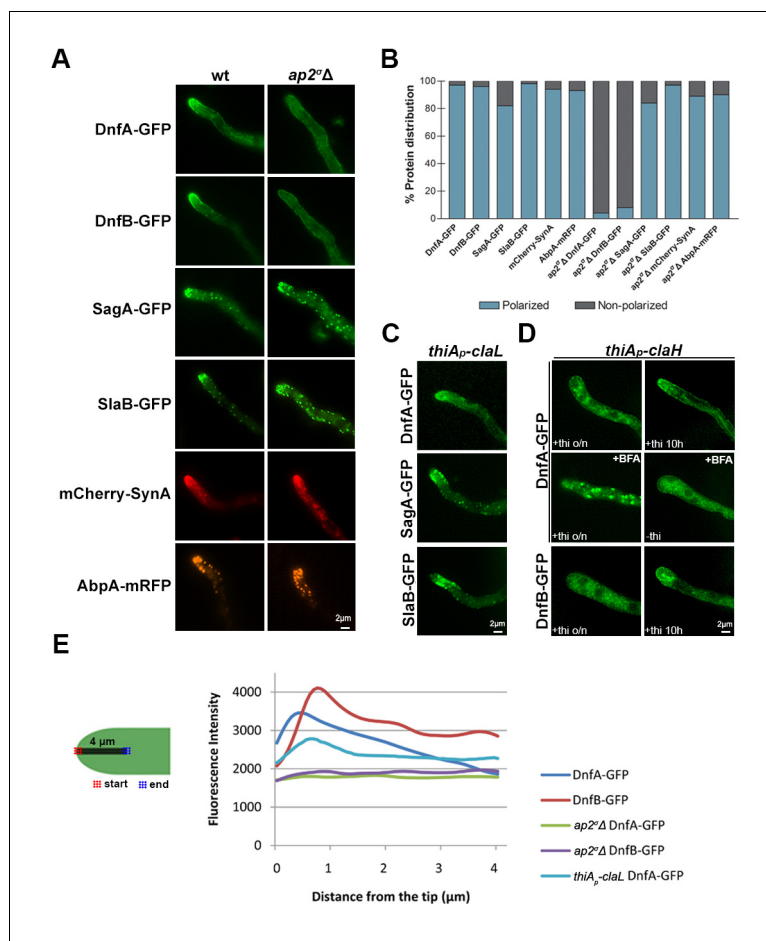


**Figure 5.** AP-2 is essential for the polar localization of lipid flippases DnfA and DnfB. (A) Epifluorescence microscopy showing the subcellular localization of apical markers DnfA, DnfB, SagA, SlaB, SynA and AbpA in wild-type and *ap2 $\Delta$*  genetic backgrounds. DnfA and DnfB are lipid flippases, SagA and SlaB are factors involved in the formation of endocytic vesicles, AbpA is an actin-polymerization marker, and SynA is a v-SNARE marking the apical tip (for more details see the text). Notice that lack of a functional AP-2 complex leads to detectable depolarization of solely DnfA and DnfB. Representative phenotypes selected from 30–40 hyphae for wt and mutant strains. Biological replicates: 4. (B) Quantitative analysis of protein (apical marker) distribution (polarized versus non-polarized) of  $n = 58, 56, 51, 40, 32, 43$  and  $48, 50, 37, 60, 45, 61$  hyphal tips of DnfA-GFP, DnfB-GFP, SagA-GFP, SlaB-GFP, mCherry-SynA, AbpA-mRFP in wild-type and *ap2 $\Delta$*  genetic backgrounds, respectively. Replicates as in (A). (C) Epifluorescence microscopy of the subcellular localization of DnfA, SagA and SlaB in a *thiA<sub>p</sub>-claL* genetic background. Notice that ClaL repression (o/n thiamine) does not affect DnfA, SagA or SlaB polarization. Representative phenotypes selected from 20–30 hyphae for each strain. Biological replicates: 3. (D) Epifluorescence microscopy of the subcellular localization of DnfA or DnfB in a *thiA<sub>p</sub>-claH* genetic background. Notice that *ab initio* ClaH repression (o/n thiamine) affects DnfA or DnfB polarization (upper and lower left panels), apparently due to Golgi collapse (see text), while in samples repressed (10 hr thiamine) after a period of pre-growth (16 hr), a degree of polarization is retained (upper and lower right panels). The middle panel depicts DnfA localization in the presence of the Golgi inhibitor Brefeldin A (BFA), under ClaH repressed (o/n thiamine, 150 min BFA) or de-repressed conditions (25 min BFA). Notice the apparent block in DnfA-GFP secretion (also refer to **Figure 5—figure supplement 1** and the text for more details). Biological/Technical replicates: 3/50, 2/50 for *thiA<sub>p</sub>-claH* DnfA-GFP and *thiA<sub>p</sub>-claH* DnfB-GFP respectively. (E) Quantitative analysis of fluorescence intensity of DnfA-GFP or DnfB-GFP in wt, *ap2 $\Delta$*  or *thiA<sub>p</sub>-claL* (thiamine-repressed), along 4  $\mu\text{m}$  of hyphal tips. For details of fluorescence intensity measurements see Materials and methods. DOI: [10.7554/eLife.20083.012](https://doi.org/10.7554/eLife.20083.012)

The following figure supplements are available for figure 5:

**Figure supplement 1.** Subcellular localization of DnfA-GFP or DnfB-GFP in wild-type, *ap2 $\Delta$* , *thiA<sub>p</sub>-claL* or *thiA<sub>p</sub>-claH* isogenic backgrounds. DOI: [10.7554/eLife.20083.013](https://doi.org/10.7554/eLife.20083.013)

Figure 5 continued on next page



Figure 5 continued

**Figure supplement 2.** Time course of Brefeldin A effect on DnfA-GFP subcellular localization in a *thiA<sub>p</sub>-claH* mutant.

DOI: [10.7554/eLife.20083.014](https://doi.org/10.7554/eLife.20083.014)

(2009). Importantly, our results show that normal Golgi secretion is necessary for maintaining the polar localization of DnfA-GFP.

When ClaH was depleted, by thiamine addition for 10 hr, following a period of pre-growth (16 hr) that allows a fraction of DnfA-GFP or DnfB-GFP to be secreted and polarly localized, a degree of polarization of both flippases was preserved in some hyphae, but in general the polar localization of DnfA-GFP or DnfB-GFP was disrupted (see upper and lower right panels in **Figure 5D** and also **Figure 5—figure supplement 1B**). This picture, however, did not constitute a surprise, given the effect of BFA in DnfA-GFP polar localization. It is rather compatible with the idea that a severe block in conventional cargo secretion, obtained either by BFA or by the depletion of ClaH, leads to an inability to maintain the apical localization of markers, such as DnfA, and apparently DnfB.

In summary, our results strongly suggest that the depletion of clathrin does not directly affect the pre-established polarization of flippases. While the dispensability of ClaL in apical cargo localization is clear, the non-essential role of ClaH on flippase polarization establishment is more difficult to formally confirm because depletion of ClaH affects Golgi function and secretion, and thus polarization maintenance. Our results are in agreement with results reported in **Schultzhaus et al. (2017a); (2017b)**, which establish that ClaH is localized principally in late Golgi, only weakly in the apical collar region and is excluded from the hyphal tip. Overall, these results further showed that AP-2 and clathrin have distinct roles in cargo subcellular localization in *A. nidulans*.

### AP-2 co-localizes with DnfA, DnfB, AbpA, SagA and SlaB, but not with clathrin or UapA

We performed a series of co-localization studies examining the subcellular positioning of AP-2 in relationship to several membrane cargoes, including endocytic proteins (SagA and SlaB), actin polymerization markers (AbpA), apical markers (DnfA, DnfB and SynA) or transporters (UapA). For that we constructed strains expressing functional Ap2<sup>σ</sup>-GFP or Ap2<sup>σ</sup>-mRFP, and crossed these with strains expressing GFP- or RFP-tagged apical markers. **Figure 6A** shows that, in a wild-type background, Ap2<sup>σ</sup>-GFP or Ap2<sup>σ</sup>-mRFP has a polar cortical distribution, marking mostly the endocytic collar of growing tips, but also the septa. The apical and cortical localization of Ap2<sup>σ</sup>-GFP was 'replaced' by a rather diffuse cytoplasmic fluorescent signal in an *ap2<sup>μ</sup>Δ* genetic background, showing that disruption of the full AP-2 complex by deleting a single subunit also disrupts its physiological localization. Noticeably, apical localization of Ap2<sup>σ</sup>-GFP remained unaffected in a genetic background lacking clathrin light chain (repressed *thiA<sub>p</sub>-claL*). Kymograph analysis further showed that the AP-2 complex marking the apical region, including the collar, is rather static. This also suggests that AP-2 is not localized in highly motile early endosomes (EEs). Additionally, no significant co-localization of Ap2<sup>σ</sup>-GFP was obtained with a marker of the TGN (PH<sup>OSBP</sup>) (**Figure 6—figure supplement 1**).

AP-2 co-localized cortically, with a high statistical significance ( $p < 0.001$ ), with SagA (80.7%), SlaB (77.4%), DnfA (70.1%), DnfB (77.0%), AbpA (75.8%) and SynA (68.8%). We also quantified and statistically confirmed that co-localization of AP-2 with apical markers (DnfA and SynA) occurs basically in the collar region, rather than the apical tip (lower panel in **Figure 6C**). Noticeably, co-localization of AP-2/SlaB or AP-2/SagA was modified in genetically deleted *sagAΔ* or *thiA<sub>p</sub>-slaB* backgrounds, respectively, becoming less polarized and more extending away from the tip (**Figure 6D**). Importantly, AP-2 did not co-localize with clathrin (ClaL) or UapA (**Figure 6B,C**). In fact ClaL and UapA, in contrast to all other apical markers, do not localize significantly in the collar region, where apical endocytosis occurs.

Given the importance of confirming the non-colocalization of AP-2 and clathrin for the present work, we obtained additional evidence to support this finding. **Figure 6—figure supplement 2**, panel A, shows that strains expressing the chimeric ClaL-mRFP or ClaL-GFP proteins grow similar to wild-type, contrasting the severe growth defects associated with the lack of ClaL expression. This

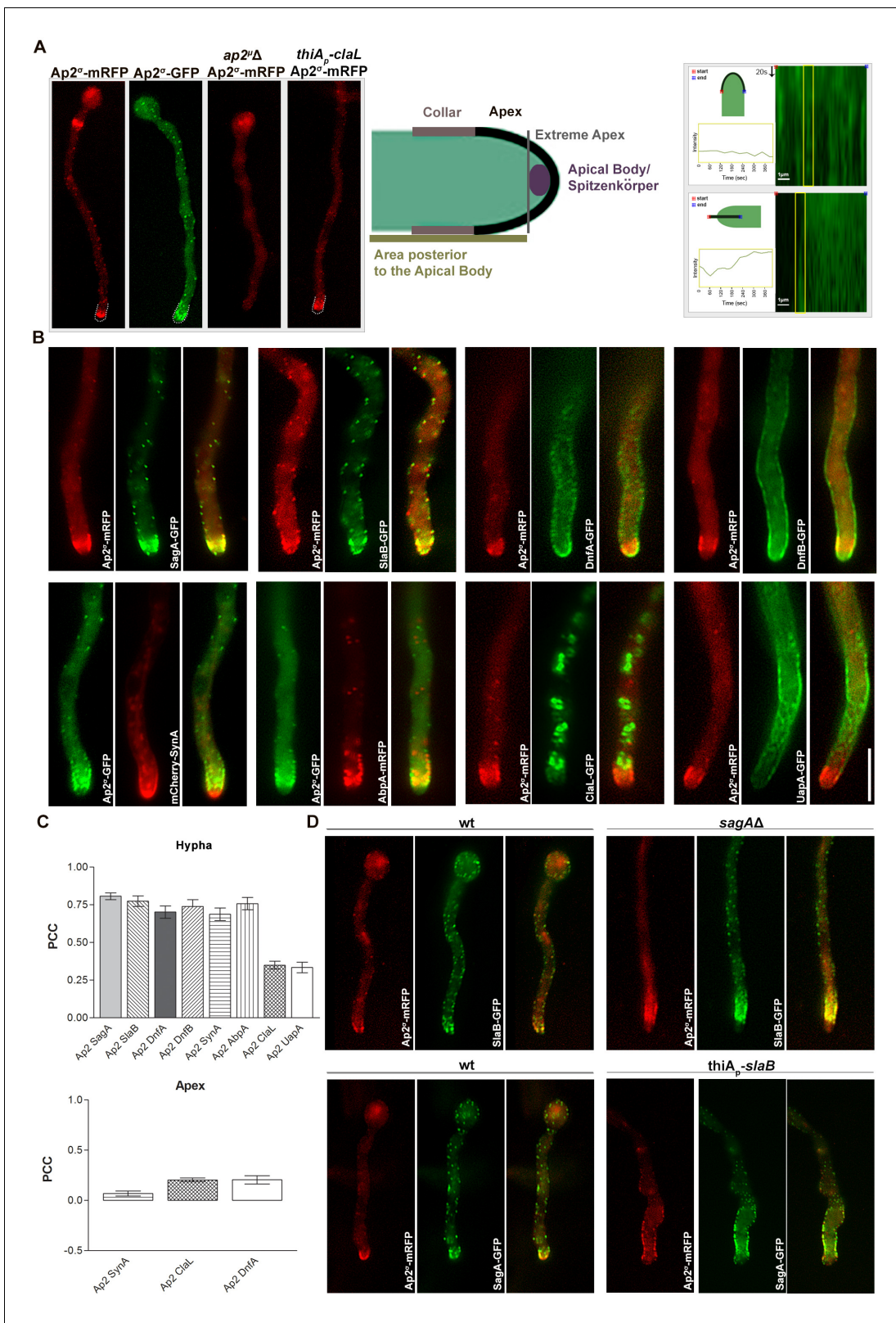


**Figure 6.** AP-2 shows polar co-localization with DnfA, DnfB, SagA and SlaB, but not with clathrin or UapA. (A) Subcellular localization of functional Ap2<sup>σ</sup>-mRFP or Ap2<sup>σ</sup>-GFP in wild-type background, or of Ap2<sup>σ</sup>-mRFP in *ap2<sup>σ</sup>Δ* or *thiA<sub>p</sub>-claL* backgrounds. Notice that the absence of a functional μ subunit leads to non-polar and non-cortical fluorescent signal of Ap2<sup>σ</sup>-mRFP, whereas Ap2<sup>σ</sup>-mRFP remains apically localized in the absence of clathrin (left panel). Biological/Technical replicates: 5/10, 5/10, 3/6 and 3/12, respectively. Cartoon depicting the hyphal tip of *A. nidulans* (middle panel). Figure 6 continued on next page

Figure 6 continued

Kymograph analysis showing the rather static localization of Ap2<sup>σ</sup>-GFP at the hyphal tip (right panel). Biological/Technical replicates: 2/3. (B) Subcellular localization experiments related the possible co-localization of Ap2<sup>σ</sup>-mRFP or Ap2<sup>σ</sup>-GFP with GFP- or mRFP-tagged SagA, SlaB, DnfA, DnfB, SynA, AbpA, ClaL and UapA. Notice the apparent cortical co-localization, especially at the collar region, of AP-2 with SagA, SlaB, DnfA, DnfB, SynA and AbpA, but not with ClaL or UapA. Biological replicates: 2, Technical replicates: 5–7. (C) Quantification of co-localization by calculating Pearson's Correlation Coefficient (PCC) for n = 5 hyphae, confirming significant co-localization of AP-2 with SagA, SlaB, DnfA, DnfB, SynA and AbpA. P-values are p < 0.0001 for co-localization of AP-2 with SagA, SlaB, DnfA, DnfB, SynA, AbpA, p = 0.0002 and p = 0.0007 for ClaL and UapA respectively (upper panel). Quantification of co-localization by calculating Pearson's Correlation Coefficient (PCC) specifically at the apical region of tips for n = 7, 10, 6 tip regions of strains co-expressing fluorescent-tagged AP-2 and DnfA, SynA, ClaL respectively, showing that AP-2 does not co-localize with SynA, ClaL or DnfA (lower panel). P-values are 0.0026, 0.0250 and 0.0001 respectively. See Materials and methods for statistical analysis methods and statistical tests used. (D) Subcellular co-localization of Ap2<sup>σ</sup>-mRFP with SlaB-GFP or SagA-GFP in *sagAΔ* or *thiA<sub>p</sub>-slaB* backgrounds, respectively. Notice the relative depolarization of Ap2<sup>σ</sup>-mRFP/SlaB-GFP in *sagAΔ* and of Ap2<sup>σ</sup>-mRFP/SagA-GFP in *thiA<sub>p</sub>-slaB*. Representative phenotypes selected from 20 hyphae for wt and mutant strains. Biological replicates: 2, Technical replicates: 10.

DOI: [10.7554/eLife.20083.015](https://doi.org/10.7554/eLife.20083.015)

The following figure supplements are available for figure 6:

**Figure supplement 1.** Epifluorescence microscopy following the in parallel localization of Ap2<sup>σ</sup>-GFP and the TGN marker mRFP-PH<sup>OSBP</sup>.

DOI: [10.7554/eLife.20083.016](https://doi.org/10.7554/eLife.20083.016)

**Figure supplement 2.** Evidence for the functionality and proper subcellular localization of GFP- or mRFP-tagged ClaL.

DOI: [10.7554/eLife.20083.017](https://doi.org/10.7554/eLife.20083.017)

constitutes good evidence that GFP- or RFP-tagged versions of ClaL are functional. Additionally, panel B shows that the localization of ClaL-GFP or ClaL-mRFP is identical and compatible with the expected localization for clathrin, as in both cases ClaL marks Golgi-like structures and cortical foci. Panel C further shows a rather weak association of ClaL with subcortical patches close to the collar endocytic region. The apparent prominent localization of ClaL in Golgi-like structures is in full agreement with results in *Schultzhaus et al. (2017b)*, who have shown that ClaH-GFP localizes principally in the late Golgi, and has only a weak association with the sub-apical collar region. In the same article, the authors have further shown that ClaH and ClaL co-localize. Finally, the functionality of ClaL-mRFP was also confirmed by showing that strains expressing ClaL-mRFP are fully active in respect to UapA-GFP endocytosis (panel D), contrasting the block of UapA endocytosis when ClaL is not functional (see *Figure 4G*).

To further test the distribution of AP-2 and clathrin between plasma membrane and internal vesicles, as well as, to assess more rigorously the degree of possible co-localization between these two protein complexes, we analysed the localization of Ap2<sup>σ</sup>-GFP and ClaL-mRFP by TIRF microscopy, followed by relevant quantification analysis (*Figure 7*). Practically no co-localization of the two polypeptides was observed (PPC = 0.12) in the PM. Only a minor fraction of the two polypeptides colocalized (PPC = 0.34) intracellularly. These data are in perfect line with the rest of our findings, confirming that the function of AP-2 in apical endocytosis is clathrin-independent.

Overall, our results are also in line with the following notions. First, AP-2 seems to synergize with endocytic factors SlaB and SagA at the endocytic collar, at sites of actin polymerization, marked by AbpA. Second, disruption of SagA or SlaB, but not of AP-2, somehow depolarizes the localization of this endocytic complex. Third, AP-2 is very probably the cargo-recognition (for example, DnfA and DnfB) partner of this complex. Finally, AP-2 and clathrin are involved in mutually exclusive endocytic or secretion pathways, also supporting a cargo-centric view of membrane trafficking (*Maldonado-Báez et al., 2013*).

## Further genetic and cellular evidence that AP-2 is involved in apical lipid maintenance

To further establish the role of AP-2 we tested its genetic interactions with SagA, DnfA and DnfB, but also with proteins involved in apical lipid maintenance, namely StoA and BasA. StoA is a stomatin homologue involved in the maintenance of apical sterol-rich membrane domains (SRDs) and polarity in *A. nidulans* (*Takeshita et al., 2012*). In metazoa, stomatins are oligomeric, lipid raft-associated proteins with scaffolding functions necessary for the maintenance of specific lipid composition in membranes, but their molecular function is still unclear (*Lapatsina et al., 2012*). BasA is required for phytosphingosine biosynthesis and is essential for fungal viability. A previously reported

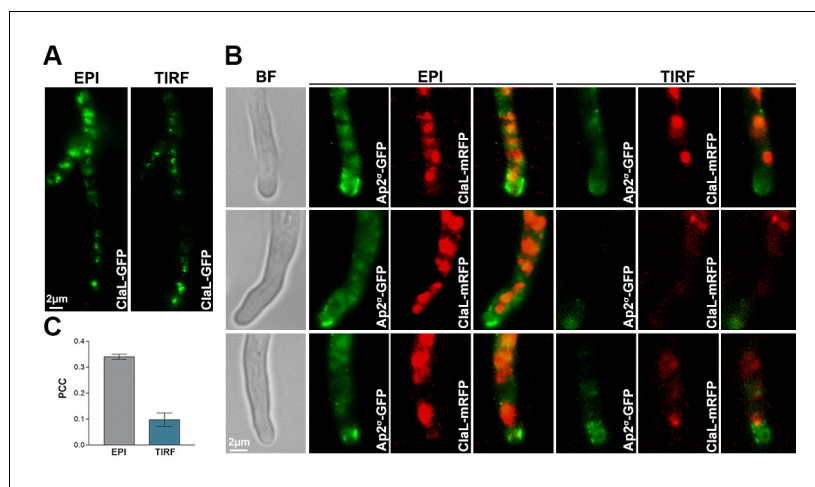


**Figure 7.** TIRF Microscopy confirms the non-colocalization of clathrin and AP-2. (A) Epifluorescence images and respective TIRF (Total Internal Reflection Fluorescence) microscopy of ClaL-GFP, confirming that a fraction of ClaL is associated with the PM. The penetration depth for TIRF was set to 110 nm. Biological/Technical replicates: 2/10. (B) Additional subcellular localization experiments investigated the possible co-localization of Ap2<sup>σ</sup>-GFP with ClaL-mRFP. Epifluorescence microscopy (EPI) confirms the very low cortical co-localization of AP-2 with ClaL, similar to that observed when the two proteins were inversely tagged (see **Figure 6C**). Respective TIRF microscopy shows no co-localization of the two proteins in the plasma membrane. The penetration depth for TIRF was set to 150 nm. Biological replicates: 3, Technical replicates: 8. BF: Brightfield. (C) Quantification of co-localization by calculating Pearson's Correlation Coefficient (PCC) for  $n = 3$  hyphae, of a strain co-expressing GFP-tagged AP-2 and ClaL-mRFP. The corresponding P-values are  $p < 0.0001$  and  $p < 0.05$  for the PCCs calculated by epifluorescence microscopy and by TIRF, respectively. See Materials and methods for statistical analysis methods and statistical tests used.

DOI: [10.7554/eLife.20083.018](https://doi.org/10.7554/eLife.20083.018)

thermosensitive missense mutation in *basA* (*basA1*) resulted in an aberrant cell wall thickening and growth arrest at 42°C (*Li et al., 2007*). For the present work, we used null mutants of *SagA* (*Karachaliou et al., 2013*), *DnfA*, *DnfB* (*Schultzhaus et al., 2015*) and *StoA* (*Takeshita et al., 2012*), and either *basA1* or a conditional knock-down mutant of *basA*, constructed herein using the *thiA<sub>p</sub>* promoter. These mutants were all crossed with the *ap2<sup>σ</sup>Δ* strain. Growth phenotypes of the resulting double mutants compared to single mutants are shown in **Figure 8A and D**. In all cases, double mutants showed reduced growth compared to single mutants (that is, synthetic negative phenotypes), strongly suggesting that the function of AP-2 is related to that of *SagA*, *DnfA* and *DnfB*, as expected based on the subcellular localization experiments, but also to *StoA* and *BasA*. Microscopic examination of the morphology of the mutants confirmed that the defects in AP-2 and *SagA*, *DnfA*, *DnfB*, *StoA* or *BasA* were additive (**Figure 8B,C and E**). Finally, **Figure 8F** shows that the localization of AP-2<sup>σ</sup>-GFP in a *basA1* genetic background is not anymore in the collar region, but instead marks internal structures just behind the tip. All above observations were confirmed by relevant quantitative analysis, as shown in **Figure 8G and H**.

Given that AP-2 was related to *BasA*, and thus sphingolipid localization, we tested whether AP-2 also affects the localization of ergosterol, the partner of sphingolipids in lipid rafts. To do so, we used filipin III, an established fluorescent ergosterol marker (*Van Leeuwen et al., 2008*). In wild-type *A. nidulans* and other filamentous fungi, filipin stains the PM, but with a predominant polar deposition at the hyphal apex (*Li et al., 2006*). We observed significant depolarization, often associated with the appearance of discrete cortical foci and abnormal filipin staining in the *ap2<sup>σ</sup>Δ*, as well as, in *thiA<sub>p</sub>-slaB*, *stoAΔ* and *thiA<sub>p</sub>-basA* mutant backgrounds. In contrast, we observed a polar localization of filipin in *thiA<sub>p</sub>-claL*, *dnfAΔ*, *dnfBΔ* and *sagAΔ* mutant strains, similar to wild-type (**Figure 9A**). Quantification of these results, by measuring the strength of the filipin fluorescent signal along the tip, confirmed the critical role of AP-2, as well as, of *BasA*, *SlaB* or *StoA*, in the apical positioning of ergosterol (**Figure 9B**). These results further supported that AP-2 has a specific role in lipid apical localization, distinct from clathrin, necessary polar growth.

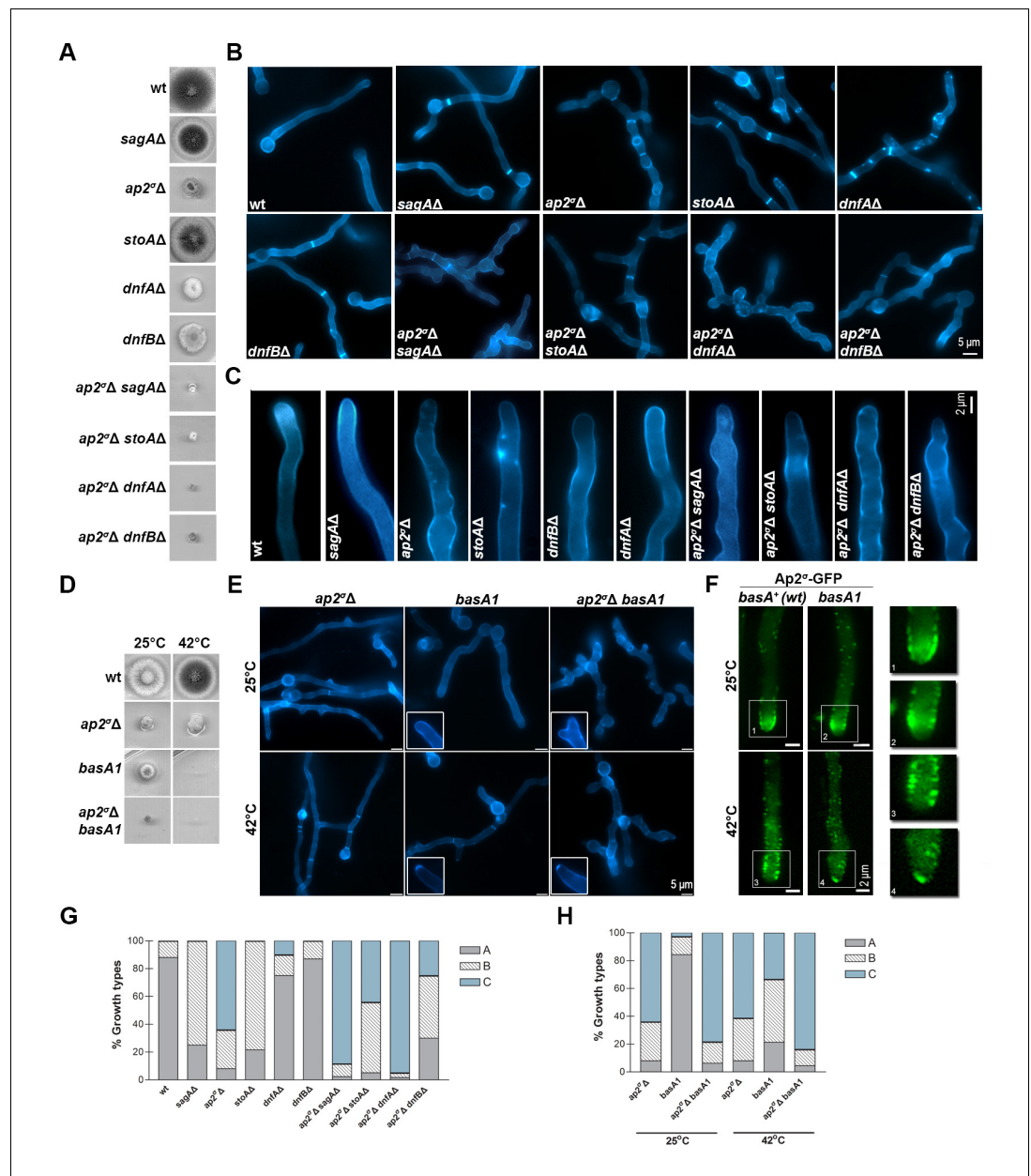


**Figure 8.** AP-2 interacts genetically with endocytic factors and proteins involved in apical lipid maintenance. (A) Growth phenotypes of single and double null mutants related to AP-2 and SagA, StoA, DnfA and DnfB. (B) Microscopic morphology of hyphal cells, stained with calcofluor, of strains shown in (A). Representative phenotypes selected from 100 hyphae for wt and 20–50 hyphae for mutant strains. Biological/Technical replicates: 4/25, 3/10, 3/15, 2/20, 2/15, 2/15, 3/10, 2/20, 2/15 and 2/15, respectively. (C) Apical deposition of calcofluor in strains shown in (A) and (B). Biological/Technical replicates as in (B). (D, E) Growth phenotypes and microscopic morphology of *ap2<sup>Δ</sup>*, *basA1<sup>ts</sup>* and *ap2<sup>Δ</sup> basA1<sup>ts</sup>* strains. Inserts highlight the modification of calcofluor deposition from the collar region to the extreme apex in *basA1<sup>ts</sup>* strains under the non-permissive temperature (42°C). Representative phenotypes selected from 45 hyphae for *ap2<sup>Δ</sup>* and mutant strains. Biological/Technical replicates: 3/15. (F) Localization at the extreme apex, rather than in the collar region, of AP-2 in a *basA1<sup>ts</sup>* genetic background. Notice that a similarly modified localization of calcofluor (chitin) was obtained in the *basA1<sup>ts</sup>* at 42°C (see relevant inserts in **Figure 7E**). Representative phenotypes selected from 30 hyphae. Biological replicates: 2, Technical replicates: 15. (G–H) Quantitative analysis of growth types shown in (B) and (E), categorized as in **Figure 2** in A, B or C. (G) Analysis of *n* = 100 hyphae of wild-type and *n* = 32, 58, 51, 40, 92, 43, 59, 58, 100 hyphae of mutant strains. (H) Analysis of *n* = 25, 77, 65 and *n* = 75, 42, 68 hyphae of *ap2<sup>Δ</sup>*, *basA1*, *ap2<sup>Δ</sup> basA1* at 25°C and 37°C respectively.

DOI: 10.7554/eLife.20083.019

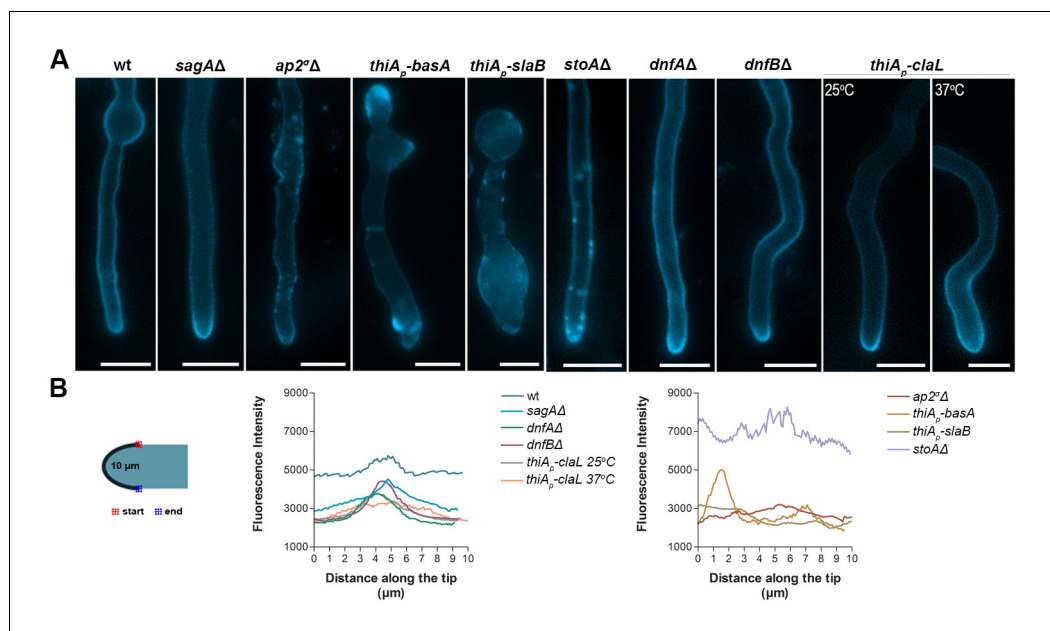


**Figure 9.** AP-2 is critical for ergosterol membrane localization. (A) Apical filipin staining of ergosterol in hyphal cells of wild-type and mutants. Notice the significant alterations and loss or reduction in apical staining in *ap2<sup>Δ</sup>*, *thiA<sub>p</sub>-basA*, *thiA<sub>p</sub>-slaB* and *stoAΔ* genetic backgrounds. Representative phenotypes selected from  $n = 20$  hyphae for wt and mutant strains. Biological replicates: 2, Technical replicates: 20. Scale bars represent 5 μm. (B) Quantitative analysis of fluorescence intensity of filipin staining along the surface of hyphae tips. The region measured is depicted in the cartoon on the left.

DOI: 10.7554/eLife.20083.020

## Discussion

In mammals, the AP-2 appendages of  $\alpha 2$  and  $\beta 2$  subunits orchestrate endocytosis through hierarchical interactions with clathrin, other endocytic proteins and PM lipids. The appendage of the  $\beta 2$  subunit specifically interacts with clathrin (Keyel et al., 2008; Thieman et al., 2009). Lower eukaryotes, like free living filamentous fungi, face the challenge of rapid and polarized growth via apical extension, a process that is absolutely dependent on efficient endocytosis and recycling of chaperones and enzymes, related to PM and cell wall deposition at the growing tip (Peñalva, 2010, 2015; Peñalva et al., 2012). Fungi also need both basal and conditionally elicited endocytosis all along their hyphal PM, serving the renewal or modification of membrane components in response to changing nutritional or stress conditions, best exemplified by the endocytic turnover of transporters (Gournas et al., 2010; Karachaliou et al., 2013; Diallinas, 2014). The role of AP-2 and that of clathrin in the endocytosis of apical cargoes or transporters had not been studied in filamentous fungi, until recently.

Here we showed that AP-2 is dispensable for transporter endocytosis and conventional apical secretion, but essential for polarity maintenance and the polar localization of membrane lipid or cell wall components. In parallel, we showed that clathrin (both ClaH and ClaL) is also essential for *A. nidulans* growth and that ClaH has a critical role in Golgi function and cargo secretion, which is probably the main reason why the ClaH null mutation is lethal. The importance of ClaH in conventional secretion via the Golgi was also recently reported by Schultzhaus et al. (2017b). An essential role of clathrin in the endocytosis of transporters is also well supported by our results. Importantly, we also showed that the function of ClaL is unrelated to polarity maintenance or the polar localization of lipid or cell wall-related apical cargoes, which contrasts its essential role in transporter endocytosis. Our results also supported that the effect of ClaH depletion in maintaining the polar localization of apical cargoes is due to malfunctioning of Golgi-dependent secretion, rather than a direct effect on the polar localization establishment, similarly to what is observed when BFA is added to growing cells. These results, together with the absence of any significant overlap in the PM localization of

clathrin and AP-2, and the distinct phenotypes of clathrin and AP-2 mutants, confirmed that clathrin and AP-2 are recruited in distinct, cargo-dependent, trafficking pathways.

Led by the observation that genetic knock-out of AP-2 resulted in phenotypes compatible with loss of polarity maintenance, we followed the effect of deleting AP-2 on the subcellular localization of well-established apical markers. We thus showed that AP-2 co-localizes apically with endocytic factors SlaB and SagA at sites of actin polymerization in the sub-apical collar region. Subsequently, we provided direct evidence that AP-2 has a role on the apical localization and function of DnfA and DnfB flippases, and affects ergosterol (filipin) and cell wall (calcofluor) deposition at the tip. We finally showed that AP-2 interacts functionally with other proteins involved in apical lipid maintenance and scaffolding (BasA and StoA). The key role of AP-2 in apical endocytosis is in line with previous results showing that proper membrane lipid and cell wall composition is essential for fungal polar growth (Cheng *et al.*, 2001; Takeshita *et al.*, 2012). A speculative model on the role of AP-2 and other relevant factors in apical endocytosis and polarity maintenance is shown in Figure 10. This model also considers recent findings on the recycling of apical markers described in Schultzhaus *et al.* (2015); (2016); (2017b) and Peñalva (2015).

An AP-2 independent role of clathrin in endocytosis is not novel, as it has been reported before in mammals and yeast (Conner and Schmid, 2003; Motley *et al.*, 2003; Sorkin, 2004; Traub, 2009; Brach *et al.*, 2014). To our knowledge, however, the opposite is a novel finding, as no other report has shown a major clathrin-independent role of the AP-2 complex. A role, albeit minor, for AP-2 in maintaining normal post-endocytic trafficking of major histocompatibility complex class I (MHCI) proteins and beta1 integrin is the only reported case of a clathrin-independent role of AP-2 (Lau and Chou, 2008). Interestingly, Microsporidia possess AP complexes, but not clathrin, which further shows that AP complexes can function without clathrin. The fact that no canonical clathrin binding domains were identified in the  $\beta 1$  and  $\beta 2$  subunits of primitive fungi supports the notion that Dikarya have lost clathrin-binding domains during their evolution. The experimental support of a clathrin-independent role of AP-2 in endocytosis was in good agreement with the *in silico* observation that the  $\beta 2$  subunit of AP-2 of all higher fungi lacks the entire C-terminal  $\beta$  appendage, which includes known clathrin binding domains. Interestingly, clathrin binding domains are also missing from the AP-1  $\beta$  subunit ( $\beta 1$ ) of all Dikarya, suggesting that in fungi AP-1 might also function independently of clathrin, very probably being involved in the recycling via the TGN compartment of specific apical proteins. Thus AP-2 and AP-1 might function in the same pathway for apical cargo recycling. Interestingly, AP-1 has been reported to function independently of clathrin in phagocytosis in murine macrophages (Braun *et al.*, 2007). This has been correlated with the presence of two isoforms of the  $\gamma$ -adaptin subunit of AP-1 in macrophages (Santambrogio *et al.*, 2005), and it has been proposed that the cleaved form of AP-1 is the one associated with vesicles present under phagocytic cups (Braun *et al.*, 2007).

Our findings strongly suggest the existence of clathrin-independent endocytosis (CIE) related to polar growth in *A. nidulans*. Over the last years, there has been an increasing interest concerning CIE, not only because it is the mode of entry of bacterial toxins and cell surface proteins (Maldonado-Báez *et al.*, 2013; Mayor *et al.*, 2014), but also because it has raised strong debates concerning its physiological significance. In a recent report, Bitsikas *et al.* (2014), provided evidence that clathrin-independent pathways do not, in fact, contribute significantly to endocytic flux. However, in cases where it has been supported experimentally, CIE seems to be specialized for the maintenance of PM lipid composition (Shvets *et al.*, 2015) and the endocytosis of proteins anchored to the membrane by glycosyl phosphatidylinositol (GPI) (Nichols, 2009; Bitsikas *et al.*, 2014). Additionally, in some cases CIE has also been reported to depend on specific PM lipid rafts and/or microdomains, such as caveolae or flotillins (Glebov *et al.*, 2006), despite some recent contradicting reports supporting that caveolae and flotillins function in organizing PM domains, rather being *bona fide* endocytic factors (Parton and del Pozo, 2013). Finally, some CIE pathways also depend on dynamin (Lamaze *et al.*, 2001). An apparent conclusion from the above and other studies is that distinctions and variations in both clathrin-dependent endocytosis (CME) or CIE seem to arise from the endocytic cargo being examined (Maldonado-Báez *et al.*, 2013). Our work suggests that AP-2 is a key cargo-specific recognition factor in apical CIE in fungi.

For long, yeasts were thought to depend solely on CME. However, recent evidence demonstrated the existence of a CIE pathway that depends on the GTPase Rho1, Rom1/2, formin Bni1 and  $\alpha$ -arrestins (Prosser and Wendland, 2012; Prosser *et al.*, 2011, 2015). In addition, a CIE pathway

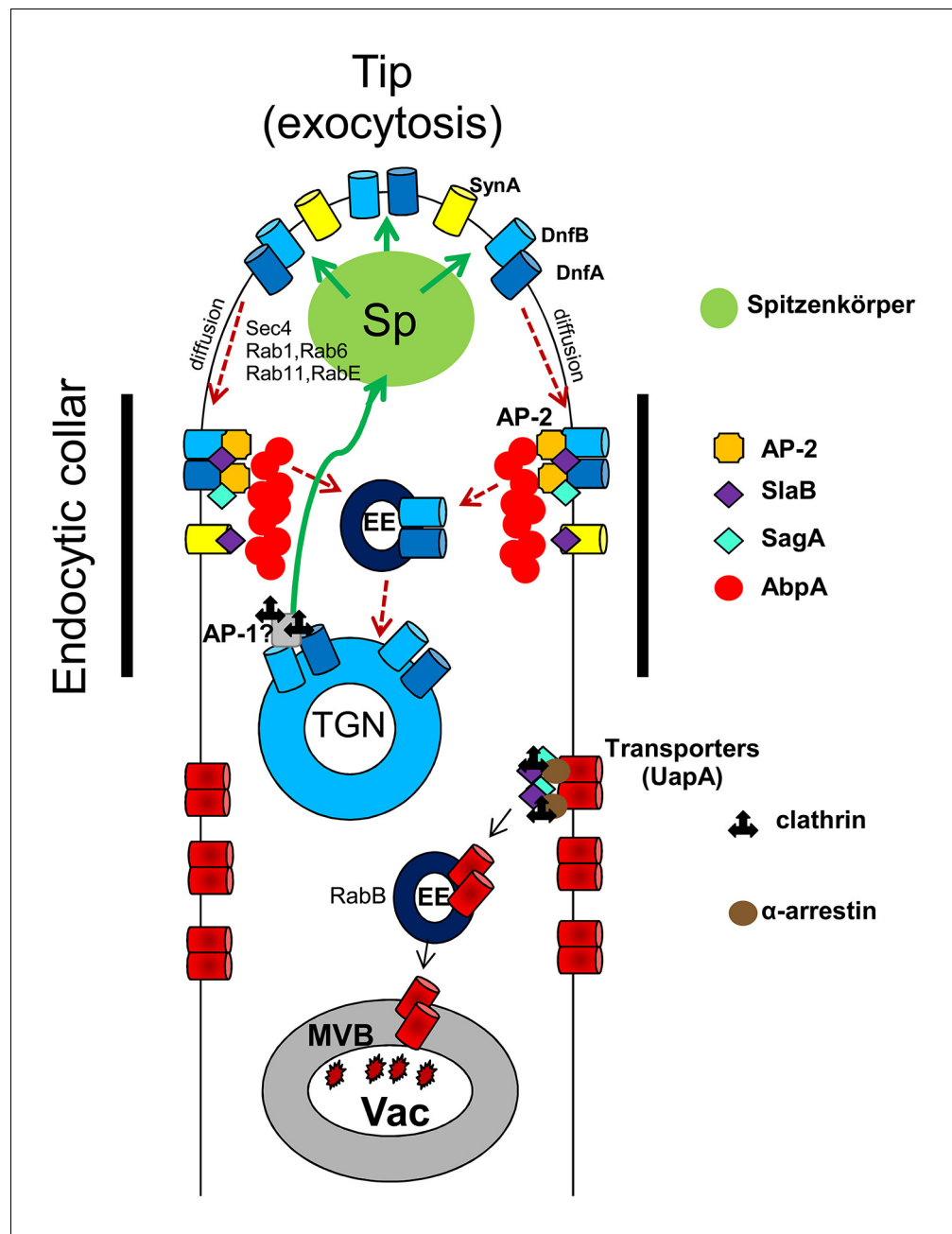


**Figure 10.** A speculative model highlighting the role of AP-2 in DnfA and DnfB endocytosis at the apical region of *A. nidulans* growing hyphal cells. After reaching the PM, DnfA and DnfB diffuse laterally to the collar region where they are recognized by AP-2 and undergo actin polymerization-dependent endocytosis with the help of SagA and SlaB. Endocytic vesicles are sorted in the Early Endosomes (EEs) and from there DnfA and DnfB undergo retrograde traffic to the TGN, the Spitzenkörper (a vesicle sorting region in filamentous ascomycetes; [Pantazopoulou et al., 2014](#)) and eventually reach the PM ([Schultzhaus et al., 2015](#); [Peñalva, 2015](#)). Extrapolating from the observation that AP-1 loss-of-function mutants are severely defective in polarity maintenance and growth, similar to AP-2 mutants, we predict that AP-1 is involved in the retrograde exocytosis (green arrows) of DnfA, DnfB and other cargoes essential for lipid or cell wall (for example, chitin synthases) maintenance. The model does not exclude that a fraction of DnfA and DnfB and other cargoes endocytosed by the AP-2 pathway would undergo degradation after being sorted into degradative EEs that are destined to the vacuole. The model also depicts that transporters and possibly other non-polar membrane proteins are not cargoes of the AP-2 pathway, but instead undergo clathrin- and  $\alpha$ -arrestin-dependent endocytosis, followed by sorting into degradative EEs and eventual degradation in the vacuole (Vac). The model also suggests that SlaB

*Figure 10 continued on next page*



Figure 10 continued

and SagA endocytic factors might have roles in both the AP-2 and clathrin endocytic pathways. Finally, the model shows that SynA (V-Snare) is not a cargo of the AP-2 pathway. The roles of some other factors in exocytosis (Sec4, Rab11, Rab1, Rab6 and RabE) or sorting (RabB) of cargoes, is based on the work of the group of M.A. Peñalva (Peñalva, 2015).

DOI: 10.7554/eLife.20083.021

was discovered in *Candida albicans* (Epp et al., 2013). Interestingly, in yeast,  $\alpha$ -arrestins are important for cargo selection in both the CME and CIE, but seem to function by distinct mechanisms in each pathway, as in the CIE pathway, unlike CME, their function is independent of the Rsp5 ubiquitin ligase (Lin et al., 2008; Nikko et al., 2008; Prosser et al., 2015). Although the involvement of AP-2 in CIE in yeast has not been examined, the involvement of  $\alpha$ -arrestins differentiates it from the apical CIE pathway we identify herein, as none of the *A. nidulans* arrestin knock-out mutants shows defects in polarity maintenance and growth (Karachaliou et al., 2013). This however does not exclude the possibility that the apical CIE pathway in *A. nidulans* shares other factors of the CIE pathway identified in yeast (for example, Rho1, Rom1/2 or formin Bni1). In fact, SepA (orthologue of Bni1; Harris et al., 1997; Sharpless and Harris, 2002), is necessary for septum formation and polarity maintenance, and RhoA<sup>Rho1</sup> plays a role in polarity, proper branching pattern, and cell wall deposition (Guest et al., 2004), phenotypes related to the proposed AP-2 function.

The present work does not intend to explore the mechanistic details of the AP-2 pathway in *A. nidulans* or identify the entire set of factors involved. However it shows, for the first time, the existence of a clathrin-independent pathway related to polarity maintenance in filamentous fungi, and most importantly identifies AP-2 as a key factor for the apical recycling of enzymes, lipids and cell wall components necessary for fungal growth. From the evolutionary point of view, our work suggests that in higher fungi the function of the AP-2 complex has been uncoupled, probably via a specific gene truncation, from clathrin-mediated endocytosis, and that this uncoupling seems to serve specific cellular challenges of fungal polar growth.

## Materials and methods

### Media, strains, growth conditions and transformation

Standard complete and minimal media (MM) for *A. nidulans* were used. Media and supplemented auxotrophies were at the concentrations given in FGSC (<http://www.fgsc.net>) (RRID: SCR\_008143). Media and chemical reagents were obtained from Sigma-Aldrich (Life Science Chemilab SA, Hellas) or AppliChem (Bioline Scientific SA, Hellas). Glucose 1% (w/v) was used as a carbon source. NaNO<sub>3</sub> at 10 mM was used as a nitrogen source. Thiamine hydrochloride was used at a final concentration of 5–10  $\mu$ M. *A. nidulans* transformation was performed as described previously in Koukaki et al. (2003). An *nkuA* DNA helicase deficient strain (TNO2A7; Szewczyk et al., 2007; Nayak et al., 2006) was the recipient strain for generating ‘in locus’ integrations of tagged gene fusions, or gene deletions by the *A. fumigatus* markers orotidine-5'-phosphate-decarboxylase (AFpyrG, Afu2g0836) or GTP-cyclohydrolase II (AFriboB, Afu1g13300), resulting in complementation of auxotrophies for uracil/uridine (*pyrG89*) or riboflavin (*riboB2*) respectively. Transformants were verified by PCR and Southern analysis. Combinations of mutations were constructed by standard genetic crossing. *A. nidulans* strains used are listed in **Supplementary file 1**.

### Standard nucleic acid manipulations and plasmid constructions

Genomic DNA extraction from *A. nidulans* was as described in FGSC (<http://www.fgsc.net>) (RRID: SCR\_008143). Plasmid preparation from *E. coli* strains and DNA bands gel extraction were done using the Nucleospin Plasmid kit and the Nucleospin Extract II kit (Macherey-Nagel, Lab Supplies Scientific SA, Hellas). DNA sequences were determined by VBC-Genomics (Vienna, Austria). Southern blot analysis using specific gene probes and upstream or downstream fragments in the case of verifying gene deletions, was performed as described in Sambrook et al. (1989). [<sup>32</sup>P]-dCTP labeled molecules of gene specific probes were prepared using a random hexanucleotide primer kit following the supplier's instructions (Takara Bio, Lab Supplies Scientific SA, Hellas) and purified on

MicroSpin S-200 HR columns (Roche Diagnostics, Hellas). Labeled [ $^{32}\text{P}$ ]-dCTP (3000 Ci mmol $^{-1}$ ) was purchased from the Institute of Isotops Co. Ltd, Miskolc, Hungary. Restriction enzymes were from Takara Bio (Lab Supplies Scientific SA, Hellas). Conventional PCR reactions, high fidelity amplifications and site-directed mutagenesis were performed with KAPA Taq DNA and Kapa HiFi polymerases respectively (Kapa Biosystems, Lab Supplies Scientific SA, Hellas). Gene deletions and 'in locus' integrations of tagged gene fusions were generated by one step ligations or sequential cloning of the relevant fragments in the plasmids pBluescript SKII, or pGEM-T using oligonucleotides carrying additional restriction sites. These plasmids were used as templates to amplify the relevant linear cassettes by PCR. For primers and information related to these constructs see **Supplementary file 2**.

### Total protein extraction and western blot analysis

Cultures for total protein extraction were grown in MM supplemented with NaNO $_3$  at 25° C. Thiamine hydrochloride was used at a final concentration of 5–10  $\mu\text{M}$ . Total protein extraction was performed as previously described (**Galanopoulou et al., 2014**). Equal sample loading was estimated by Bradford assays. Total proteins (30–50  $\mu\text{g}$ ) were separated in polyacrylamide gels (8–10 % w/v) and electroblotted (Mini PROTEAN Tetra Cell, BIORAD) onto PVDF membranes (Macherey-Nagel, Lab Supplies Scientific SA, Hellas). Immunodetection was performed with a primary mouse anti-GFP monoclonal antibody (Roche Diagnostics), a mouse anti-actin monoclonal (C4) antibody (MP Biomedicals Europe) and a secondary goat anti-mouse IgG HRP-linked antibody (Cell Signaling Technology Inc, Bioline Scientific SA, Hellas). Blots were developed using the LumiSensor Chemiluminescent HRP Substrate kit (Genscript USA, Lab Supplies Scientific SA, Hellas) and SuperRX Fuji medical X-Ray films (FujiFILM Europe). Quantification of ClaH-GFP or actin levels using ImageJ were estimated separately and relative to each other and are given as ratios, where in each case the lowest value was arbitrarily set as 1.

### Phylogenetic analysis

BLASTp searches were performed on the NCBI database (RRID: SCR\_004870) to identify which organisms acquire a C-terminal domain on  $\beta$  AP-2 subunit, with *H. sapiens*  $\beta$  AP-2 as query. The selected sequences were retrieved and, with the use of UniProt database (RRID: SCR\_002380), the C-terminal domains were identified and selected from each sequence. The phylogenetic tree reconstruction of the C-terminal domains was performed on MEGA6 software (RRID: SCR\_000667) (**Tamura et al., 2013**) with the maximum-likelihood method and bootstrap testing for 150 replications. The substitution model was WAG and the ML heuristic method selected was Nearest-Neighbor-Interchange (NNI). NCBI sequences used for figure illustrations; *H. sapiens* (NP\_001273:  $\beta$ AP-2, NP\_001118:  $\beta$ AP-1 and NP\_004635:  $\beta$  AP-3), *F. alba* (XP\_009492690:  $\beta$  AP-2, XP\_009492179:  $\beta$  AP-1 and XP\_009495754:  $\beta$  AP-3), *R. allomyces* (EPZ36209:  $\beta$  AP-2, EPZ33551:  $\beta$  AP-1 and EPZ35993:  $\beta$  AP-3), *S. punctatus* (KNC98413:  $\beta$  AP-2, KNC96576:  $\beta$  AP-1 and KND02292:  $\beta$  AP-3), *A. nidulans* (CBF70501:  $\beta$  AP-2, CBF83537:  $\beta$  AP-1 and CBF90059:  $\beta$  AP-3), *S. cerevisiae* (NP\_012538:  $\beta$  AP-2, NP\_012787:  $\beta$  AP-1 and NP\_011777:  $\beta$  AP-3), and *S. pombe* (NP\_596435:  $\beta$  AP-2, NP\_595274:  $\beta$  AP-1 and NP\_593796:  $\beta$  AP-3). The illustrations were taken from HMMER (RRID: SCR\_005305) homology (search mode) of EBI database (RRID: SCR\_002872) where the sequences were subjected and subsequently manipulated.

### Inverted epifluorescence microscopy, TIRF-M live imaging and statistical analysis

Samples for wide-field epifluorescence microscopy and Total Internal Reflection Fluorescence Microscopy (TIRF-M) were prepared as previously described (**Evangelinos et al., 2016**). Germlings were incubated in sterile 35 mm  $\mu$ -dishes, high glass bottom (*ibidi*, Germany) in liquid MM for 16–22 hr at 25° C. Filipin III and Calcofluor white were used for 5 min prior to observation at final concentrations of 1  $\mu\text{g ml}^{-1}$  and 0001% (w/v) respectively. FM4-64 and CMAC staining was according to **Peñalva (2015)** and **Evangelinos et al. (2016)**, respectively. Brefeldin A was used at a final concentration of 100  $\mu\text{g ml}^{-1}$ . Images were obtained using a Zeiss Axio Observer Z1/Axio Cam HR R3 camera. Contrast adjustment, area selection and color combining were made using the Zen lite 2012 software. Live imaging of plasma membrane ClaL was accomplished by TIRF-M. Hyphae were analyzed using a Leica AM TIRF MC set up on a Leica DMI6000 B microscope and a Leica 100X HCX PL

APO 1.4 NA objective. Biological replicates correspond to different samples, while technical replicates correspond to different hyphae observed and/or photographed within each sample. For kymograph generation and all measurements of fluorescence intensity, the *Reslice* and *Plot profile* commands in ImageJ (RRID: SCR\_003070) were used, respectively (<https://imagej.nih.gov/ij/>). For the statistical analysis in **Figure 2**, Tukey's Multiple Comparison test was performed (One-way ANOVA), using the Graphpad Prism software (RRID: SCR\_002798). Confidence interval was set to 95%. For quantifying colocalization (**Dunn et al., 2011**), Pearson's correlation coefficient (PCC) above thresholds, for a selected Region of interest (ROI) was calculated, using the *coloc2* plugin of Fiji (RRID: SCR\_002285). Costes P-value was 1.00 for all the images tested (**Costes et al., 2004**). PSF was set to 1.2 and the number of iterations was 100. One sample t-test was performed to test the significance of differences in PCCs, using the Graphpad Prism software. Confidence interval was set to 95%. Colocalization results were also confirmed using the ICY (RRID: SCR\_010587) colocalization studio plugin (pixel-based method) (<http://icy.bioimageanalysis.org/>) for ROIs that included either the foci and the tip area which were selected using the Spot Detector plugin, or the extreme apex area, selected using the Area Selection tool. The same tool was also used for the measurement of Vacuolar Surface (Total surface of vacuoles containing GFP/Hypha) and Vacuolar GFP Fluorescence (Total fluorescence intensity of vacuoles containing GFP/Hypha) in **Figure 3E–F**, while Tukey's Multiple Comparison Test (One-Way ANOVA) using Graphpad Prism was performed to test the statistical significance of the results. Scale bars were added using the FigureJ plugin of the ImageJ (RRID: SCR\_003070) software (**Mutterer and Zinck, 2013**). Images were further processed and annotated in Adobe Photoshop CS4 Extended version 11.0.2 (RRID: SCR\_002078).

## Acknowledgements

We thank Brian Shaw for the DnfA and DnfB strains and Norio Takeshita for the StoA strain. We also thank Spiros Efthimiopoulos for Brefeldin A. This work was supported by the *Fondation Santé*, to which we are grateful.

---

## Additional information

### Funding

Funder	Author
Fondation Sante	George Diallinas

The funders had no role in study design, data collection and interpretation, or the decision to submit the work for publication.

### Author contributions

OM, Data curation, Software, Formal analysis, Investigation, Methodology; SA, Data curation, Investigation, Methodology, Writing—original draft; AZ, Software, Investigation; SC, Resources, Methodology; GD, Conceptualization, Resources, Formal analysis, Supervision, Funding acquisition, Validation, Visualization, Writing—original draft, Project administration, Writing—review and editing

### Author ORCIDs

George Diallinas,  <http://orcid.org/0000-0002-3426-726X>

---

## Additional files

### Supplementary files

- Supplementary file 1. Strains used in this study.  
DOI: [10.7554/eLife.20083.022](https://doi.org/10.7554/eLife.20083.022)
- Supplementary file 2. Oligonucleotides used in this study for cloning purposes.  
DOI: [10.7554/eLife.20083.023](https://doi.org/10.7554/eLife.20083.023)

## References

- Apostolaki A**, Erpapazoglou Z, Harispe L, Billini M, Kafasla P, Kizis D, Peñalva MA, Scazzocchio C, Sophianopoulou V. 2009. AgtA, the dicarboxylic amino acid transporter of *Aspergillus nidulans*, is concertedly down-regulated by exquisite sensitivity to nitrogen metabolite repression and ammonium-elicited endocytosis. *Eukaryotic Cell* **8**:339–352. doi: [10.1128/EC.00270-08](https://doi.org/10.1128/EC.00270-08), PMID: [19168757](https://pubmed.ncbi.nlm.nih.gov/19168757/)
- Apostolaki A**, Harispe L, Calcagno-Pizarelli AM, Vangelatos I, Sophianopoulou V, Arst HN, Peñalva MA, Amillis S, Scazzocchio C. 2012. *Aspergillus nidulans* CkiA is an essential casein kinase I required for delivery of amino acid transporters to the plasma membrane. *Molecular Microbiology* **84**:530–549. doi: [10.1111/j.1365-2958.2012.08042.x](https://doi.org/10.1111/j.1365-2958.2012.08042.x), PMID: [22489878](https://pubmed.ncbi.nlm.nih.gov/22489878/)
- Araujo-Bazán L**, Peñalva MA, Espeso EA. 2008. Preferential localization of the endocytic internalization machinery to hyphal tips underlies polarization of the actin cytoskeleton in *Aspergillus nidulans*. *Molecular Microbiology* **67**:891–905. doi: [10.1111/j.1365-2958.2007.06102.x](https://doi.org/10.1111/j.1365-2958.2007.06102.x), PMID: [18179595](https://pubmed.ncbi.nlm.nih.gov/18179595/)
- Barlow LD**, Dacks JB, Wideman JG. 2014. From all to (nearly) none: tracing adaptin evolution in fungi. *Cellular Logistics* **4**:e28114. doi: [10.4161/cl.28114](https://doi.org/10.4161/cl.28114), PMID: [24843829](https://pubmed.ncbi.nlm.nih.gov/24843829/)
- Bitsikas V**, Corrêa IR, Nichols BJ. 2014. Clathrin-independent pathways do not contribute significantly to endocytic flux. *eLife* **3**:e03970. doi: [10.7554/eLife.03970](https://doi.org/10.7554/eLife.03970), PMID: [25232658](https://pubmed.ncbi.nlm.nih.gov/25232658/)
- Brach T**, Godlee C, Moeller-Hansen I, Boeke D, Kaksonen M. 2014. The initiation of clathrin-mediated endocytosis is mechanistically highly flexible. *Current Biology* **24**:548–554. doi: [10.1016/j.cub.2014.01.048](https://doi.org/10.1016/j.cub.2014.01.048), PMID: [24530066](https://pubmed.ncbi.nlm.nih.gov/24530066/)
- Braun V**, Deschamps C, Raposo G, Benaroch P, Benmerah A, Chavrier P, Niedergang F. 2007. AP-1 and ARF1 control endosomal dynamics at sites of FcR mediated phagocytosis. *Molecular Biology of the Cell* **18**:4921–4931. doi: [10.1091/mbc.E07-04-0392](https://doi.org/10.1091/mbc.E07-04-0392), PMID: [17914058](https://pubmed.ncbi.nlm.nih.gov/17914058/)
- Burston HE**, Maldonado-Báez L, Davey M, Montpetit B, Schluter C, Wendland B, Conibear E. 2009. Regulators of yeast endocytosis identified by systematic quantitative analysis. *The Journal of Cell Biology* **185**:1097–1110. doi: [10.1083/jcb.200811116](https://doi.org/10.1083/jcb.200811116), PMID: [19506040](https://pubmed.ncbi.nlm.nih.gov/19506040/)
- Carroll SY**, Stimpson HE, Weinberg J, Toret CP, Sun Y, Drubin DG. 2012. Analysis of yeast endocytic site formation and maturation through a regulatory transition point. *Molecular Biology of the Cell* **23**:657–668. doi: [10.1091/mbc.E11-02-0108](https://doi.org/10.1091/mbc.E11-02-0108), PMID: [22190733](https://pubmed.ncbi.nlm.nih.gov/22190733/)
- Carroll SY**, Stirling PC, Stimpson HE, Giesselmann E, Schmitt MJ, Drubin DG. 2009. A yeast killer toxin screen provides insights into a/b toxin entry, trafficking, and killing mechanisms. *Developmental Cell* **17**:552–560. doi: [10.1016/j.devcel.2009.08.006](https://doi.org/10.1016/j.devcel.2009.08.006), PMID: [19853568](https://pubmed.ncbi.nlm.nih.gov/19853568/)
- Chapa-y-Lazo B**, Allwood EG, Smaczynska-de Rooij II, Snape ML, Ayscough KR. 2014. Yeast endocytic adaptor AP-2 binds the stress sensor Mid2 and functions in polarized cell responses. *Traffic* **15**:546–557. doi: [10.1111/tra.12155](https://doi.org/10.1111/tra.12155), PMID: [24460703](https://pubmed.ncbi.nlm.nih.gov/24460703/)
- Chapa-Y-Lazo B**, Ayscough KR. 2014. Apm4, the mu subunit of yeast AP-2 interacts with Pkc1, and mutation of the Pkc1 consensus phosphorylation site Thr176 inhibits AP-2 recruitment to endocytic sites. *Communicative & Integrative Biology* **7**:e28522. doi: [10.4161/cib.28522](https://doi.org/10.4161/cib.28522), PMID: [25346786](https://pubmed.ncbi.nlm.nih.gov/25346786/)
- Cheng J**, Park TS, Fischl AS, Ye XS. 2001. Cell cycle progression and cell polarity require sphingolipid biosynthesis in *Aspergillus nidulans*. *Molecular and Cellular Biology* **21**:6198–6209. doi: [10.1128/MCB.21.18.6198-6209.2001](https://doi.org/10.1128/MCB.21.18.6198-6209.2001), PMID: [11509663](https://pubmed.ncbi.nlm.nih.gov/11509663/)
- Conner SD**, Schmid SL. 2003. Differential requirements for AP-2 in clathrin-mediated endocytosis. *The Journal of Cell Biology* **162**:773–780. doi: [10.1083/jcb.200304069](https://doi.org/10.1083/jcb.200304069), PMID: [12952931](https://pubmed.ncbi.nlm.nih.gov/12952931/)
- Costes SV**, Daelemans D, Cho EH, Dobbin Z, Pavlakis G, Lockett S. 2004. Automatic and quantitative measurement of protein-protein colocalization in live cells. *Biophysical Journal* **86**:3993–4003. doi: [10.1529/biophysj.103.038422](https://doi.org/10.1529/biophysj.103.038422), PMID: [15189895](https://pubmed.ncbi.nlm.nih.gov/15189895/)
- de León N**, Hoya M, Curto MA, Moro S, Yanguas F, Doncel C, Valdivieso MH. 2016. The AP-2 complex is required for proper temporal and spatial dynamics of endocytic patches in fission yeast. *Molecular Microbiology* **100**:409–424. doi: [10.1111/mmi.13327](https://doi.org/10.1111/mmi.13327), PMID: [26749213](https://pubmed.ncbi.nlm.nih.gov/26749213/)
- de León N**, Valdivieso MH. 2016. The long life of an endocytic patch that misses AP-2. *Current Genetics* **62**:765–770. doi: [10.1007/s00294-016-0605-3](https://doi.org/10.1007/s00294-016-0605-3), PMID: [27126383](https://pubmed.ncbi.nlm.nih.gov/27126383/)
- Dereeper A**, Guignon V, Blanc G, Audic S, Buffet S, Chevenet F, Dufayard JF, Guindon S, Lefort V, Lescot M, Claverie JM, Gascuel O. 2008. Phylogeny.fr: robust phylogenetic analysis for the non-specialist. *Nucleic Acids Research* **36**:W465–W469. doi: [10.1093/nar/gkn180](https://doi.org/10.1093/nar/gkn180), PMID: [18424797](https://pubmed.ncbi.nlm.nih.gov/18424797/)
- Diallinas G**. 2014. Understanding transporter specificity and the discrete appearance of channel-like gating domains in transporters. *Frontiers in Pharmacology* **5**:207. doi: [10.3389/fphar.2014.00207](https://doi.org/10.3389/fphar.2014.00207), PMID: [25309439](https://pubmed.ncbi.nlm.nih.gov/25309439/)
- Dunn KW**, Kamocka MM, McDonald JH. 2011. A practical guide to evaluating colocalization in biological microscopy. *AJP: Cell Physiology* **300**:C723–C742. doi: [10.1152/ajpcell.00462.2010](https://doi.org/10.1152/ajpcell.00462.2010)
- Epp E**, Nazarova E, Regan H, Douglas LM, Konopka JB, Vogel J, Whiteway M. 2013. Clathrin- and Arp2/3-independent endocytosis in the fungal pathogen *Candida albicans*. *mBio* **4**:e00476-13. doi: [10.1128/mBio.00476-13](https://doi.org/10.1128/mBio.00476-13), PMID: [23982070](https://pubmed.ncbi.nlm.nih.gov/23982070/)
- Evangelinos M**, Martzoukou O, Choroziyan K, Amillis S, Diallinas G. 2016. BsdA(Bsd2)-dependent vacuolar turnover of a misfolded version of the UapA transporter along the secretory pathway: prominent role of selective autophagy. *Molecular Microbiology* **100**:893–911. doi: [10.1111/mmi.13358](https://doi.org/10.1111/mmi.13358), PMID: [26917498](https://pubmed.ncbi.nlm.nih.gov/26917498/)
- Galanopoulou K**, Scazzocchio C, Galinou ME, Liu W, Borbolis F, Karachaliou M, Oestreicher N, Hatzinikolaou DG, Diallinas G, Amillis S. 2014. Purine utilization proteins in the eurotiales: cellular compartmentalization,

- phylogenetic conservation and divergence. *Fungal Genetics and Biology* **69**:96–108. doi: [10.1016/j.fgb.2014.06.005](https://doi.org/10.1016/j.fgb.2014.06.005), PMID: [24970358](https://pubmed.ncbi.nlm.nih.gov/24970358/)
- Glebov OO**, Bright NA, Nichols BJ. 2006. Flotillin-1 defines a clathrin-independent endocytic pathway in mammalian cells. *Nature Cell Biology* **8**:46–54. doi: [10.1038/ncb1342](https://doi.org/10.1038/ncb1342), PMID: [16341206](https://pubmed.ncbi.nlm.nih.gov/16341206/)
- Gournas C**, Amillis S, Vlanti A, Diallinas G. 2010. Transport-dependent endocytosis and turnover of a uric acid-xanthine permease. *Molecular Microbiology* **75**:246–260. doi: [10.1111/j.1365-2958.2009.06997.x](https://doi.org/10.1111/j.1365-2958.2009.06997.x), PMID: [20002879](https://pubmed.ncbi.nlm.nih.gov/20002879/)
- Guest GM**, Lin X, Momany M. 2004. Aspergillus nidulans RhoA is involved in polar growth, branching, and cell wall synthesis. *Fungal Genetics and Biology* **41**:13–22. doi: [10.1016/j.fgb.2003.08.006](https://doi.org/10.1016/j.fgb.2003.08.006), PMID: [14643255](https://pubmed.ncbi.nlm.nih.gov/14643255/)
- Harris SD**, Hamer L, Sharpless KE, Hamer JE. 1997. The Aspergillus nidulans sepA gene encodes an FH1/2 protein involved in Cytokinesis and the maintenance of cellular polarity. *The EMBO Journal* **16**:3474–3483. doi: [10.1093/emboj/16.12.3474](https://doi.org/10.1093/emboj/16.12.3474), PMID: [9218790](https://pubmed.ncbi.nlm.nih.gov/9218790/)
- Hervás-Aguilar A**, Peñalva MA. 2010. Endocytic machinery protein SlaB is dispensable for polarity establishment but necessary for polarity maintenance in hyphal tip cells of Aspergillus nidulans. *Eukaryotic Cell* **9**:1504–1518. doi: [10.1128/EC.00119-10](https://doi.org/10.1128/EC.00119-10), PMID: [20693304](https://pubmed.ncbi.nlm.nih.gov/20693304/)
- Higuchi Y**, Shoji JY, Arioka M, Kitamoto K. 2009. Endocytosis is crucial for cell polarity and apical membrane recycling in the filamentous fungus Aspergillus oryzae. *Eukaryotic Cell* **8**:37–46. doi: [10.1128/EC.00207-08](https://doi.org/10.1128/EC.00207-08), PMID: [19028995](https://pubmed.ncbi.nlm.nih.gov/19028995/)
- Hirst J**, Irving C, Borner GH. 2013. Adaptor protein complexes AP-4 and AP-5: new players in endosomal trafficking and progressive spastic paraplegia. *Traffic* **14**:153–164. doi: [10.1111/tra.12028](https://doi.org/10.1111/tra.12028), PMID: [23167973](https://pubmed.ncbi.nlm.nih.gov/23167973/)
- Huang KM**, D'Hondt K, Riezman H, Lemmon SK. 1999. Clathrin functions in the absence of heterotetrameric adaptors and AP180-related proteins in yeast. *The EMBO Journal* **18**:3897–3908. doi: [10.1093/emboj/18.14.3897](https://doi.org/10.1093/emboj/18.14.3897), PMID: [10406795](https://pubmed.ncbi.nlm.nih.gov/10406795/)
- Karachaliou M**, Amillis S, Evangelinos M, Kokotos AC, Yalalis V, Diallinas G. 2013. The arrestin-like protein ArtA is essential for ubiquitination and endocytosis of the UapA transporter in response to both broad-range and specific signals. *Molecular Microbiology* **88**:301–317. doi: [10.1111/mmi.12184](https://doi.org/10.1111/mmi.12184), PMID: [23490137](https://pubmed.ncbi.nlm.nih.gov/23490137/)
- Keyel PA**, Thieman JR, Roth R, Erkan E, Everett ET, Watkins SC, Heuser JE, Traub LM. 2008. The AP-2 adaptor beta2 appendage scaffolds alternate cargo endocytosis. *Molecular Biology of the Cell* **19**:5309–5326. doi: [10.1091/mbc.E08-07-0712](https://doi.org/10.1091/mbc.E08-07-0712), PMID: [18843039](https://pubmed.ncbi.nlm.nih.gov/18843039/)
- Koukaki M**, Giannoutsou E, Karagouni A, Diallinas G. 2003. A novel improved method for Aspergillus nidulans transformation. *Journal of Microbiological Methods* **55**:687–695. doi: [10.1016/S0167-7012\(03\)00208-2](https://doi.org/10.1016/S0167-7012(03)00208-2), PMID: [14607411](https://pubmed.ncbi.nlm.nih.gov/14607411/)
- Kryptou E**, Evangelidis T, Bobonis J, Pittis AA, Gabaldón T, Scazzocchio C, Mikros E, Diallinas G. 2015. Origin, diversification and substrate specificity in the family of NCS1/FUR transporters. *Molecular Microbiology* **96**:927–950. doi: [10.1111/mmi.12982](https://doi.org/10.1111/mmi.12982), PMID: [25712422](https://pubmed.ncbi.nlm.nih.gov/25712422/)
- Kukulski W**, Picco A, Specht T, Briggs JA, Kaksonen M. 2016. Clathrin modulates vesicle scission, but not invagination shape, in yeast endocytosis. *eLife* **5**:e16036. doi: [10.7554/eLife.16036](https://doi.org/10.7554/eLife.16036), PMID: [27341079](https://pubmed.ncbi.nlm.nih.gov/27341079/)
- Lagache T**, Sauvonnnet N, Danglot L, Olivo-Marin JC. 2015. Statistical analysis of molecule colocalization in bioimaging. *Cytometry Part A* **87**:568–579. doi: [10.1002/cyto.a.22629](https://doi.org/10.1002/cyto.a.22629)
- Lamaze C**, Dujeancourt A, Baba T, Lo CG, Benmerah A, Dautry-Varsat A. 2001. Interleukin 2 receptors and detergent-resistant membrane domains define a clathrin-independent endocytic pathway. *Molecular Cell* **7**:661–671. doi: [10.1016/S1097-2765\(01\)00212-X](https://doi.org/10.1016/S1097-2765(01)00212-X), PMID: [11463390](https://pubmed.ncbi.nlm.nih.gov/11463390/)
- Lapatsina L**, Brand J, Poole K, Daumke O, Lewin GR. 2012. Stomatin-domain proteins. *European Journal of Cell Biology* **91**:240–245. doi: [10.1016/j.ejcb.2011.01.018](https://doi.org/10.1016/j.ejcb.2011.01.018), PMID: [21501885](https://pubmed.ncbi.nlm.nih.gov/21501885/)
- Lau AW**, Chou MM. 2008. The adaptor complex AP-2 regulates post-endocytic trafficking through the non-clathrin Arf6-dependent endocytic pathway. *Journal of Cell Science* **121**:4008–4017. doi: [10.1242/jcs.033522](https://doi.org/10.1242/jcs.033522), PMID: [19033387](https://pubmed.ncbi.nlm.nih.gov/19033387/)
- Lemmon SK**, Traub LM. 2012. Getting in touch with the clathrin terminal domain. *Traffic* **13**:511–519. doi: [10.1111/j.1600-0854.2011.01321.x](https://doi.org/10.1111/j.1600-0854.2011.01321.x), PMID: [22239657](https://pubmed.ncbi.nlm.nih.gov/22239657/)
- Li S**, Bao D, Yuen G, Harris SD, Calvo AM. 2007. basA regulates cell wall organization and asexual/sexual sporulation ratio in Aspergillus nidulans. *Genetics* **176**:243–253. doi: [10.1534/genetics.106.068239](https://doi.org/10.1534/genetics.106.068239), PMID: [17409079](https://pubmed.ncbi.nlm.nih.gov/17409079/)
- Li S**, Du L, Yuen G, Harris SD. 2006. Distinct ceramide synthases regulate polarized growth in the filamentous fungus Aspergillus nidulans. *Molecular Biology of the Cell* **17**:1218–1227. doi: [10.1091/mbc.E05-06-0533](https://doi.org/10.1091/mbc.E05-06-0533), PMID: [16394102](https://pubmed.ncbi.nlm.nih.gov/16394102/)
- Lin CH**, MacGurn JA, Chu T, Stefan CJ, Emr SD. 2008. Arrestin-related ubiquitin-ligase adaptors regulate endocytosis and protein turnover at the cell surface. *Cell* **135**:714–725. doi: [10.1016/j.cell.2008.09.025](https://doi.org/10.1016/j.cell.2008.09.025), PMID: [18976803](https://pubmed.ncbi.nlm.nih.gov/18976803/)
- Maldonado-Báez L**, Williamson C, Donaldson JG. 2013. Clathrin-independent endocytosis: a cargo-centric view. *Experimental Cell Research* **319**:2759–2769. doi: [10.1016/j.yexcr.2013.08.008](https://doi.org/10.1016/j.yexcr.2013.08.008), PMID: [23954817](https://pubmed.ncbi.nlm.nih.gov/23954817/)
- Mayor S**, Parton RG, Donaldson JG. 2014. Clathrin-independent pathways of endocytosis. *Cold Spring Harbor Perspectives in Biology* **6**:a016758. doi: [10.1101/cshperspect.a016758](https://doi.org/10.1101/cshperspect.a016758), PMID: [24890511](https://pubmed.ncbi.nlm.nih.gov/24890511/)
- Momany M**. 2002. Polarity in filamentous fungi: establishment, maintenance and new axes. *Current Opinion in Microbiology* **5**:580–585. doi: [10.1016/S1369-5274\(02\)00368-5](https://doi.org/10.1016/S1369-5274(02)00368-5), PMID: [12457701](https://pubmed.ncbi.nlm.nih.gov/12457701/)
- Motley A**, Bright NA, Seaman MN, Robinson MS. 2003. Clathrin-mediated endocytosis in AP-2-depleted cells. *The Journal of Cell Biology* **162**:909–918. doi: [10.1083/jcb.200305145](https://doi.org/10.1083/jcb.200305145), PMID: [12952941](https://pubmed.ncbi.nlm.nih.gov/12952941/)

- Mousavi SA, Malerød L, Berg T, Kjekken R. 2004. Clathrin-dependent endocytosis. *Biochemical Journal* **377**:1–16. doi: [10.1042/bj20031000](https://doi.org/10.1042/bj20031000), PMID: [14505490](https://pubmed.ncbi.nlm.nih.gov/14505490/)
- Mutterer J, Zinck E. 2013. Quick-and-clean article figures with FigureJ. *Journal of Microscopy* **252**:89–91. doi: [10.1111/jmi.12069](https://doi.org/10.1111/jmi.12069), PMID: [23906423](https://pubmed.ncbi.nlm.nih.gov/23906423/)
- Nakatsu F, Ohno H. 2003. Adaptor protein complexes as the key regulators of protein sorting in the post-Golgi network. *Cell Structure and Function* **28**:419–429. doi: [10.1247/csf.28.419](https://doi.org/10.1247/csf.28.419), PMID: [14745134](https://pubmed.ncbi.nlm.nih.gov/14745134/)
- Nayak T, Szewczyk E, Oakley CE, Osmani A, Ukil L, Murray SL, Hynes MJ, Osmani SA, Oakley BR. 2006. A versatile and efficient gene-targeting system for *Aspergillus nidulans*. *Genetics* **172**:1557–1566. doi: [10.1534/genetics.105.052563](https://doi.org/10.1534/genetics.105.052563), PMID: [16387870](https://pubmed.ncbi.nlm.nih.gov/16387870/)
- Nichols B. 2009. Endocytosis of lipid-anchored proteins: excluding GEECs from the crowd. *The Journal of Cell Biology* **186**:457–459. doi: [10.1083/jcb.200907119](https://doi.org/10.1083/jcb.200907119), PMID: [19687254](https://pubmed.ncbi.nlm.nih.gov/19687254/)
- Nikko E, Sullivan JA, Pelham HR. 2008. Arrestin-like proteins mediate ubiquitination and endocytosis of the yeast metal transporter Smf1. *EMBO Reports* **9**:1216–1221. doi: [10.1038/embor.2008.199](https://doi.org/10.1038/embor.2008.199), PMID: [18953286](https://pubmed.ncbi.nlm.nih.gov/18953286/)
- Osmani A, Goldman GH. 2008. *The Aspergilli: Genomics, Medical Aspects, Biotechnology, and Research Methods*. CRC Press. p 177–197.
- Osmani AH, Oakley BR, Osmani SA. 2006. Identification and analysis of essential *Aspergillus nidulans* genes using the heterokaryon rescue technique. *Nature Protocols* **1**:2517–2526. doi: [10.1038/nprot.2006.406](https://doi.org/10.1038/nprot.2006.406), PMID: [17406500](https://pubmed.ncbi.nlm.nih.gov/17406500/)
- Pantazopoulou A, Lemuh ND, Hatzinikolaou DG, Drevet C, Cecchetto G, Scazzocchio C, Diallinas G. 2007. Differential physiological and developmental expression of the UapA and AzgA purine transporters in *Aspergillus nidulans*. *Fungal Genetics and Biology* **44**:627–640. doi: [10.1016/j.fgb.2006.10.003](https://doi.org/10.1016/j.fgb.2006.10.003), PMID: [17126042](https://pubmed.ncbi.nlm.nih.gov/17126042/)
- Pantazopoulou A, Penalva MA. 2009. Organization and dynamics of the *Aspergillus nidulans* golgi during apical extension and mitosis. *Molecular Biology of the Cell* **20**:4335–4347. doi: [10.1091/mbc.E09-03-0254](https://doi.org/10.1091/mbc.E09-03-0254)
- Pantazopoulou A, Peñalva MA. 2011. Characterization of *Aspergillus nidulans* RabC/Rab6. *Traffic* **12**:386–406. doi: [10.1111/j.1600-0854.2011.01164.x](https://doi.org/10.1111/j.1600-0854.2011.01164.x)
- Pantazopoulou A, Pinar M, Xiang X, Penalva MA. 2014. Maturation of late golgi cisternae into RabERAB11 exocytic post-Golgi carriers visualized in vivo. *Molecular Biology of the Cell* **25**:2428–2443. doi: [10.1091/mbc.E14-02-0710](https://doi.org/10.1091/mbc.E14-02-0710), PMID: [24943841](https://pubmed.ncbi.nlm.nih.gov/24943841/)
- Parton RG, del Pozo MA. 2013. Caveolae as plasma membrane sensors, protectors and organizers. *Nature Reviews Molecular Cell Biology* **14**:98–112. doi: [10.1038/nrm3512](https://doi.org/10.1038/nrm3512), PMID: [23340574](https://pubmed.ncbi.nlm.nih.gov/23340574/)
- Peñalva MA, Galindo A, Abenza JF, Pinar M, Calcagno-Pizarelli AM, Arst HN, Pantazopoulou A. 2012. Searching for gold beyond mitosis: mining intracellular membrane traffic in *Aspergillus nidulans*. *Cellular Logistics* **2**:2–14. doi: [10.4161/cl.19304](https://doi.org/10.4161/cl.19304), PMID: [22645705](https://pubmed.ncbi.nlm.nih.gov/22645705/)
- Peñalva MA. 2015. A lipid-managing program maintains a stout Spitzenkörper. *Molecular Microbiology* **97**:1–6. doi: [10.1111/mmi.13044](https://doi.org/10.1111/mmi.13044), PMID: [25921726](https://pubmed.ncbi.nlm.nih.gov/25921726/)
- Peñalva MÁ. 2010. Endocytosis in filamentous fungi: cinderella gets her reward. *Current Opinion in Microbiology* **13**:684–692. doi: [10.1016/j.mib.2010.09.005](https://doi.org/10.1016/j.mib.2010.09.005), PMID: [20920884](https://pubmed.ncbi.nlm.nih.gov/20920884/)
- Pinar M, Pantazopoulou A, Arst HN, Peñalva MA. 2013. Acute inactivation of the *Aspergillus nidulans* golgi membrane fusion machinery: correlation of apical extension arrest and tip swelling with cisternal disorganization. *Molecular Microbiology* **89**:228–248. doi: [10.1111/mmi.12280](https://doi.org/10.1111/mmi.12280), PMID: [23714354](https://pubmed.ncbi.nlm.nih.gov/23714354/)
- Prosser DC, Drivas TG, Maldonado-Báez L, Wendland B. 2011. Existence of a novel clathrin-independent endocytic pathway in yeast that depends on Rho1 and formin. *The Journal of Cell Biology* **195**:657–671. doi: [10.1083/jcb.201104045](https://doi.org/10.1083/jcb.201104045), PMID: [22065638](https://pubmed.ncbi.nlm.nih.gov/22065638/)
- Prosser DC, Pannunzio AE, Brodsky JL, Thorner J, Wendland B, O'Donnell AF. 2015.  $\alpha$ -Arrestins participate in cargo selection for both clathrin-independent and clathrin-mediated endocytosis. *Journal of Cell Science* **128**:4220–4234. doi: [10.1242/jcs.175372](https://doi.org/10.1242/jcs.175372), PMID: [26459639](https://pubmed.ncbi.nlm.nih.gov/26459639/)
- Prosser DC, Wendland B. 2012. Conserved roles for yeast Rho1 and mammalian RhoA GTPases in clathrin-independent endocytosis. *Small GTPases* **3**:229–235. doi: [10.4161/sgtp.21631](https://doi.org/10.4161/sgtp.21631), PMID: [23238351](https://pubmed.ncbi.nlm.nih.gov/23238351/)
- Robinson MS. 2004. Adaptable adaptors for coated vesicles. *Trends in Cell Biology* **14**:167–174. doi: [10.1016/j.tcb.2004.02.002](https://doi.org/10.1016/j.tcb.2004.02.002), PMID: [15066634](https://pubmed.ncbi.nlm.nih.gov/15066634/)
- Robinson MS. 2015. Forty years of clathrin-coated vesicles. *Traffic* **16**:1210–1238. doi: [10.1111/tra.12335](https://doi.org/10.1111/tra.12335), PMID: [26403691](https://pubmed.ncbi.nlm.nih.gov/26403691/)
- Sambrook J, Fritsch E, Maniatis T. 1989. *Molecular Cloning: A Laboratory Manual*. Cold Spring Harbour, New York: Cold Spring Harbour Press.
- Santambrogio L, Potolicchio I, Fessler SP, Wong SH, Raposo G, Strominger JL. 2005. Involvement of caspase-cleaved and intact adaptor protein 1 complex in Endosomal remodeling in maturing dendritic cells. *Nature Immunology* **6**:1020–1028. doi: [10.1038/ni1250](https://doi.org/10.1038/ni1250), PMID: [16170319](https://pubmed.ncbi.nlm.nih.gov/16170319/)
- Schultzhaus Z, Johnson TB, Shaw BD. 2017b. Clathrin localization and dynamics in *Aspergillus nidulans*. *Molecular Microbiology* **103**:299–318. doi: [10.1111/mmi.13557](https://doi.org/10.1111/mmi.13557), PMID: [27741567](https://pubmed.ncbi.nlm.nih.gov/27741567/)
- Schultzhaus Z, Shaw BD. 2016. The flippase DnfB is cargo of fimbrin-associated endocytosis in *Aspergillus nidulans*, and likely recycles through the late golgi. *Communicative & Integrative Biology* **9**:e1141843. doi: [10.1080/19420889.2016.1141843](https://doi.org/10.1080/19420889.2016.1141843), PMID: [27195062](https://pubmed.ncbi.nlm.nih.gov/27195062/)
- Schultzhaus Z, Yan H, Shaw BD. 2015. *Aspergillus nidulans* flippase DnfA is cargo of the endocytic collar and plays complementary roles in growth and phosphatidylserine asymmetry with another flippase, DnfB. *Molecular Microbiology* **97**:18–32. doi: [10.1111/mmi.13019](https://doi.org/10.1111/mmi.13019), PMID: [25846564](https://pubmed.ncbi.nlm.nih.gov/25846564/)

- Schultzhaus Z**, Zheng W, Wang Z, Mouriño-Pérez R, Shaw B. 2017a. Phospholipid flippases DnfA and DnfB exhibit differential dynamics within the *A. nidulans* Spitzenkörper. *Fungal Genetics and Biology* **99**:26–28. doi: [10.1016/j.fgb.2016.12.007](https://doi.org/10.1016/j.fgb.2016.12.007), PMID: [28034798](https://pubmed.ncbi.nlm.nih.gov/28034798/)
- Sharpless KE**, Harris SD. 2002. Functional characterization and localization of the *Aspergillus nidulans* formin SEPA. *Molecular Biology of the Cell* **13**:469–479. doi: [10.1091/mbc.01-07-0356](https://doi.org/10.1091/mbc.01-07-0356), PMID: [11854405](https://pubmed.ncbi.nlm.nih.gov/11854405/)
- Shvets E**, Bitsikas V, Howard G, Hansen CG, Nichols BJ. 2015. Dynamic caveolae exclude bulk membrane proteins and are required for sorting of excess glycosphingolipids. *Nature Communications* **6**:6867. doi: [10.1038/ncomms7867](https://doi.org/10.1038/ncomms7867), PMID: [25897946](https://pubmed.ncbi.nlm.nih.gov/25897946/)
- Sorkin A**. 2004. Cargo recognition during clathrin-mediated endocytosis: a team effort. *Current Opinion in Cell Biology* **16**:392–399. doi: [10.1016/j.ceb.2004.06.001](https://doi.org/10.1016/j.ceb.2004.06.001), PMID: [15261671](https://pubmed.ncbi.nlm.nih.gov/15261671/)
- Steinberg G**. 2014. Endocytosis and early endosome motility in filamentous fungi. *Current Opinion in Microbiology* **20**:10–18. doi: [10.1016/j.mib.2014.04.001](https://doi.org/10.1016/j.mib.2014.04.001), PMID: [24835422](https://pubmed.ncbi.nlm.nih.gov/24835422/)
- Szewczyk E**, Nayak T, Oakley CE, Edgerton H, Xiong Y, Taheri-Talesh N, Osmani SA, Oakley BR. 2007. Fusion PCR and gene targeting in *Aspergillus nidulans*. *Nature Protocols* **1**:3111–3120. doi: [10.1038/nprot.2006.405](https://doi.org/10.1038/nprot.2006.405)
- Taheri-Talesh N**, Horio T, Araujo-Bazán L, Dou X, Espeso EA, Peñalva MA, Osmani SA, Oakley BR. 2008. The tip growth apparatus of *Aspergillus nidulans*. *Molecular Biology of the Cell* **19**:1439–1449. doi: [10.1091/mbc.E07-05-0464](https://doi.org/10.1091/mbc.E07-05-0464), PMID: [18216285](https://pubmed.ncbi.nlm.nih.gov/18216285/)
- Takeshita N**, Diallinas G, Fischer R. 2012. The role of flotillin FloA and stomatin StoA in the maintenance of apical sterol-rich membrane domains and polarity in the filamentous fungus *Aspergillus nidulans*. *Molecular Microbiology* **83**:1136–1152. doi: [10.1111/j.1365-2958.2012.07996.x](https://doi.org/10.1111/j.1365-2958.2012.07996.x), PMID: [22329814](https://pubmed.ncbi.nlm.nih.gov/22329814/)
- Tamura K**, Stecher G, Peterson D, Filipinski A, Kumar S. 2013. MEGA6: molecular evolutionary genetics analysis version 6.0. *Molecular Biology and Evolution* **30**:2725–2729. doi: [10.1093/molbev/mst197](https://doi.org/10.1093/molbev/mst197), PMID: [24132122](https://pubmed.ncbi.nlm.nih.gov/24132122/)
- Tavoularis S**, Scazzocchio C, Sophianopoulou V. 2001. Functional expression and cellular localization of a green fluorescent Protein-Tagged proline transporter in *Aspergillus nidulans*. *Fungal Genetics and Biology* **33**:115–125. doi: [10.1006/fgbi.2001.1280](https://doi.org/10.1006/fgbi.2001.1280)
- Thieman JR**, Mishra SK, Ling K, Doray B, Anderson RA, Traub LM. 2009. Clathrin regulates the association of PIPKγ661 with the AP-2 adaptor beta2 appendage. *Journal of Biological Chemistry* **284**:13924–13939. doi: [10.1074/jbc.M901017200](https://doi.org/10.1074/jbc.M901017200), PMID: [19287005](https://pubmed.ncbi.nlm.nih.gov/19287005/)
- Traub LM**. 2009. Tickets to ride: selecting cargo for clathrin-regulated internalization. *Nature Reviews Molecular Cell Biology* **10**:583–596. doi: [10.1038/nrm2751](https://doi.org/10.1038/nrm2751), PMID: [19696796](https://pubmed.ncbi.nlm.nih.gov/19696796/)
- Valdez-Taubas J**, Pelham HR. 2003. Slow diffusion of proteins in the yeast plasma membrane allows polarity to be maintained by endocytic cycling. *Current Biology* **13**:1636–1640. doi: [10.1016/j.cub.2003.09.001](https://doi.org/10.1016/j.cub.2003.09.001), PMID: [13678596](https://pubmed.ncbi.nlm.nih.gov/13678596/)
- Van Leeuwen MR**, Smant W, de Boer W, Dijksterhuis J. 2008. Filipin is a reliable in situ marker of ergosterol in the plasma membrane of germinating conidia (spores) of *Penicillium discolor* and stains intensively at the site of germ tube formation. *Journal of Microbiological Methods* **74**:64–73. doi: [10.1016/j.mimet.2008.04.001](https://doi.org/10.1016/j.mimet.2008.04.001), PMID: [18485505](https://pubmed.ncbi.nlm.nih.gov/18485505/)
- Vlanti A**, Diallinas G. 2008. The *Aspergillus nidulans* FcyB cytosine-purine scavenger is highly expressed during germination and in reproductive compartments and is downregulated by endocytosis. *Molecular Microbiology* **68**:959–977. doi: [10.1111/j.1365-2958.2008.06198.x](https://doi.org/10.1111/j.1365-2958.2008.06198.x), PMID: [18384518](https://pubmed.ncbi.nlm.nih.gov/18384518/)
- Yeung BG**, Payne GS. 2001. Clathrin interactions with C-terminal regions of the yeast AP-1 beta and gamma subunits are important for AP-1 association with clathrin coats. *Traffic* **2**:565–576. doi: [10.1034/j.1600-0854.2001.20806.x](https://doi.org/10.1034/j.1600-0854.2001.20806.x), PMID: [11489214](https://pubmed.ncbi.nlm.nih.gov/11489214/)
- Yeung BG**, Phan HL, Payne GS. 1999. Adaptor complex-independent clathrin function in yeast. *Molecular Biology of the Cell* **10**:3643–3659. doi: [10.1091/mbc.10.11.3643](https://doi.org/10.1091/mbc.10.11.3643), PMID: [10564262](https://pubmed.ncbi.nlm.nih.gov/10564262/)

# Secretory Vesicle Polar Sorting, Endosome Recycling and Cytoskeleton Organization Require the AP-1 Complex in *Aspergillus nidulans*

Olga Martzoukou, George Diallinas,<sup>1</sup> and Sotiris Amillis<sup>1</sup>

Department of Biology, National and Kapodistrian University of Athens, Panepistimioupolis, 15784, Greece

ORCID IDs: 0000-0001-5445-484X (O.M.); 0000-0002-3426-726X (G.D.)

**ABSTRACT** The AP-1 complex is essential for membrane protein traffic via its role in the pinching-off and sorting of secretory vesicles (SVs) from the *trans*-Golgi and/or endosomes. While its essentiality is undisputed in metazoa, its role in simpler eukaryotes seems less clear. Here, we dissect the role of AP-1 in the filamentous fungus *Aspergillus nidulans* and show that it is absolutely essential for growth due to its role in clathrin-dependent maintenance of polar traffic of specific membrane cargoes toward the apex of growing hyphae. We provide evidence that AP-1 is involved in both anterograde sorting of RabE<sup>Rab11</sup>-labeled SVs and RabA/B<sup>Rab5</sup>-dependent endosome recycling. Additionally, AP-1 is shown to be critical for microtubule and septin organization, further rationalizing its essentiality in cells that face the challenge of cytoskeleton-dependent polarized cargo traffic. This work also opens a novel issue on how nonpolar cargoes, such as transporters, are sorted to the eukaryotic plasma membrane.

**KEYWORDS** fungi; traffic; secretion; Rab GTPases; transport; microtubules

**A**LL eukaryotic cells face the challenge of topological sorting of their biomolecules to their proper subcellular destinations. In particular, newly synthesized membrane proteins, which are translationally translocated into the membrane of the endoplasmic reticulum (ER), follow complex, dynamic, and often overlapping, trafficking routes, embedded in the lipid bilayer of “secretory” vesicles, to be sorted to their final target membrane (Feyder *et al.* 2015; Viotti 2016). In vesicular membrane trafficking, the nature of the protein cargo and relevant adaptor proteins play central roles in deciding the routes followed and the final destination of cargoes. Despite the emerging evidence of alternative, or nonconventional, trafficking routes, cargo passage through a continuously maturing early-to-late Golgi is considered to be part of the major mechanism and the most critical step in membrane protein sorting. Following exit from the *trans*-Golgi network (TGN, also known as late-Golgi), cargoes packed in distinct vesicles travel to their final destination,

which, in most cases, is the plasma membrane or the vacuole. This anterograde vesicular movement can be direct or via the endosomal compartment, and, in any case, assisted by motor proteins and the cytoskeleton (Bard and Malhotra 2006; Cai *et al.* 2007; Anitei and Hoflack 2011; Hunt and Stephens 2011; Guo *et al.* 2014). Membrane protein cargoes at the level of late Golgi can also follow the opposite route, getting sorted into retrograde vesicles, recycling back to an earlier compartment. Acquiring a “ticket” for a specific route implicates adaptors and accessory proteins, several of which are also associated with clathrin (Nakatsu and Ohno 2003; Robinson 2004, 2015).

Apart from the COPI and COPII vesicle coat adaptors that mediate traffic between the ER and the early Golgi compartment (Lee *et al.* 2004; Zanetti *et al.* 2011), of particular importance are the heterotetrameric AP (formally named after assembly polypeptide and later as adaptor protein) complexes, comprising of two large subunits (also called adaptins;  $\beta$ -adaptin and  $\gamma$ - or  $\alpha$ -adaptin), together with a medium-sized ( $\mu$ ) and a small ( $\sigma$ ) subunit (Robinson 2004, 2015). Other adaptors, some of which display similarity to AP subunits, such as the GGAs, epsin-related proteins, or components of the exomer and retromer complexes, are also critical for the sorting of specific cargoes (Bonifacino 2004,

Copyright © 2018 by the Genetics Society of America

doi: <https://doi.org/10.1534/genetics.118.301240>

Manuscript received April 2, 2018; accepted for publication June 19, 2018; published Early Online June 20, 2018.

<sup>1</sup>Corresponding authors: Department of Biology, National and Kapodistrian University of Athens, Panepistimioupolis, 15784 Athens, Greece. E-mail: diallina@biol.uoa.gr; and samillis@biol.uoa.gr



2014; Robinson 2015; Spang 2015; Anton *et al.* 2018). Importantly, the various cargo sorting routes often overlap, and might share common adaptors (Hoya *et al.* 2017). Among the major AP complexes (Bonifacino 2014; Nakatsu *et al.* 2014), AP-1 and AP-2, which in most cells work to propel vesicle formation through recruitment of clathrin, are the most critical for cell homeostasis and function (Robinson 2004, 2015). In brief, AP-2 is involved in vesicle budding for protein endocytosis from the PM, whereas AP-1 is involved in vesicle pinching-off from the TGN and/or endosomal compartments, although in the latter case it is still under debate whether secretory vesicles (SVs) derive from the TGN, from the endosome, or from both (Nakatsu *et al.* 2014; Robinson 2015). AP-1 was also shown to be responsible for retrograde transport from early endosomes (EEs) in both yeast and mammalian cells, but also to guide recycling pathways from the endosome to the plasma membrane in yeast (Spang 2015). The undisputed essentiality of AP-1 and AP-2 in mammalian cells is, however, less obvious in simple unicellular eukaryotes, such as the yeasts *Saccharomyces cerevisiae* or *Schizosaccharomyces pombe*, where null mutants in the genes encoding AP subunits are viable, with only relatively minor growth or morphological defects (Phan *et al.* 1994; Huang *et al.* 1999; Meyer *et al.* 2000; Valdivia *et al.* 2002; Ma *et al.* 2009; Yu *et al.* 2013; Arcones *et al.* 2016). In sharp contrast, the growth of AP-1 and AP-2 null mutants in the filamentous fungus *Aspergillus nidulans* is severely arrested after spore germination (Martzoukou *et al.* 2017, and results presented therein), reflecting blocks in essential cellular processes, probably similar to mammalian cells.

In recent years, *A. nidulans* has emerged as a powerful system for studying membrane cargo traffic (Momany 2002; Taheri-Talesh *et al.* 2008; Steinberg *et al.* 2017). This is due not only to its powerful classical and reverse genetic tools, but also to its specific cellular characteristics and manner of growth. *A. nidulans* is made of long cellular compartments (hyphae), characterized by polarized growth, in a process starting with an initial establishment of a growth site, followed by polarity maintenance and cell extension through the regulated continuous supply of vesicles toward the apex. A vesicle sorting terminal at the hyphal apex, termed Spitzenkörper (Spk), is thought to generate an exocytosis gradient, which, when coupled with endocytosis from a specific hotspot behind the site of growth, termed endocytic collar, is able to sustain apical growth (Peñalva 2015; Schultzhause and Shaw 2015; Pantazopoulou 2016; Steinberg *et al.* 2017). Apical trafficking of cargoes, traveling from the ER through the different stages of early (*cis*-) and late (*trans*-) Golgi toward their final destination, and apical cargo endocytosis/recycling, are essential for growth, as null mutations blocking either Golgi function, microtubule (MT) organization, or apical cargo recycling are lethal or severely deleterious (Fischer *et al.* 2008; Takeshita and Fischer 2011; Peñalva 2015; Pantazopoulou 2016; Steinberg *et al.* 2017). Curiously, the role of AP complexes in *A. nidulans* or any other filamentous fungus, has not been studied, with the exception of our recent

work on AP-2 (Martzoukou *et al.* 2017). In the latter study, we showed that the AP-2 of *A. nidulans* has a rather surprising clathrin-independent essential role in polarity maintenance and growth, related to the endocytosis of specific polarized cargoes involved in apical lipid and cell wall composition maintenance. This was in line with the observation that AP-2  $\beta$  subunit ( $\beta 2$ ) lacks the ability to bind clathrin, which itself has been shown to be essential for the endocytosis of distinct cargoes, as, for example, various transporters (Martzoukou *et al.* 2017; Schultzhause *et al.* 2017). In the current study, we focus on the role of the AP-1 complex in cargo trafficking in *A. nidulans*. We provide evidence that AP-1 is essential for fungal polar growth via its dynamic role in post-Golgi secretory vesicle polar sorting, proper MT organization, and endosome recycling.

## Materials and Methods

### Media, strains, growth conditions, and transformation

Standard complete and minimal media for *A. nidulans* were used (details in FGSC, <http://www.fgsc.net>). Media and chemical reagents were obtained from Sigma-Aldrich (Life Science Chemilab SA, Hellas) or AppliChem (Bioline Scientific SA, Hellas). Glucose 0.1–1% (w/v) was used as a carbon source. NaNO<sub>3</sub> and NH<sub>4</sub><sup>+</sup> (ammonium tartrate dibasic) were used as nitrogen sources at 10 mM. Thiamine hydrochloride (thi) was used at a final concentration of 10  $\mu$ M. Transformation was performed as described previously in Koukaki *et al.* (2003), using an *nkuA* DNA helicase deficient (TNO2A7; Nayak *et al.* 2006) recipient strain or derivatives for “in locus” integrations of gene fusions, or deletion cassettes by the *Aspergillus fumigatus* markers orotidine-5'-phosphate-decarboxylase (*AFpyrG*, Afu2g0836), GTP-cyclohydrolase II (*AFriboB*, Afu1g13300), and a pyridoxine biosynthesis gene (*AFpyroA*, Afu5g08090), resulting in complementation of auxotrophies for uracil/uridine (*pyrG89*), riboflavin (*riboB2*), or pyridoxine (*pyroA4*), respectively. Transformants were verified by PCR and Southern analysis. Combinations of mutations and tagged strains with fluorescent epitopes were generated by standard genetic crossing. The *Escherichia coli* strain used was DH5 $\alpha$ . *A. nidulans* strains used in this study are listed in Supplemental Material, Table S1 (see also File S7).

### Nucleic acid manipulations and plasmid constructions

Genomic DNA was extracted from *A. nidulans* as described in FGSC (<http://www.fgsc.net>). Plasmid preparation and DNA gel extraction were performed using the Nucleospin Plasmid kit and the Nucleospin Extract II kit (Macherey-Nagel, Lab Supplies Scientific SA, Hellas). Restriction enzymes were from Takara Bio or Minotech (Lab Supplies Scientific SA, Hellas). DNA sequences were determined by Eurofins-Genomics (Vienna, Austria). Southern blot analysis using specific gene probes was performed as described in Sambrook *et al.* (1989), using [<sup>32</sup>P]-dCTP labeled molecules prepared by a

random hexanucleotide primer kit and purified on MicroSpin S-200 HR columns (Roche Diagnostics, Hellas). Labeled [<sup>32</sup>P]-dCTP (3000 Ci mmol<sup>-1</sup>) was purchased from the Institute of Isotopes Co. Ltd, Miskolc, Hungary. Conventional PCR reactions, high fidelity amplifications, and site-directed mutagenesis were performed using KAPA Taq DNA, and Kapa HiFi polymerases (Kapa Biosystems, Roche Diagnostics, Hellas). Gene fusion cassettes were generated by one-step ligations or sequential cloning of the relevant fragments in the plasmids pBluescript SKII or pGEM-T using oligonucleotides carrying additional restriction sites. These plasmids were used as templates to amplify the relevant linear cassettes by PCR. For *ap1<sup>β</sup>* site directed mutations, the relevant gene was cloned in the pBS-argB plasmid (Vlanti and Diallinas 2008). For primers, see Table S2.

### Protein extraction and western blots

Cultures for total protein extraction were grown in minimal media supplemented with NaNO<sub>3</sub> or NH<sub>4</sub><sup>+</sup> at 25°. Total protein extraction was performed as previously described (Papadaki *et al.* 2017). Total proteins (30–50 μg estimated by Bradford assays) were separated in a polyacrylamide gel (8–10% w/v) onto PVDF membranes (Macherey-Nagel, Lab Supplies Scientific SA, Hellas). Immunodetection was performed with a primary anti-FLAG M2 monoclonal antibody (Sigma-Aldrich), an anti-actin monoclonal (C4) antibody (MP Biomedicals Europe) and a secondary HRP-linked antibody (Cell Signaling Technology Inc, Bioline Scientific SA, Hellas). Blots were developed using the LumiSensor Chemiluminescent HRP Substrate kit (Genscript USA, Lab Supplies Scientific SA, Hellas) and SuperRX Fuji medical X-Ray films (FujiFILM Europe).

### Microscopy and statistical analysis

Samples for wide-field epifluorescence microscopy were prepared as previously described (Martzoukou *et al.* 2017). Germlings were incubated in sterile 35 mm μ-dishes, high glass bottom (*ibidi*, Germany) in liquid minimal media for 16–22 hr at 25°. Benomyl, Latrunculin B, Brefeldin A, and Calcofluor white were used at final concentrations of 2.5, 100, 100 μg ml<sup>-1</sup>, 0.001% (w/v), respectively. FM4-64 and CMAC staining was according to Peñalva (2005) and Evangelinos *et al.* (2016), respectively. Images were obtained using an inverted Zeiss Axio Observer Z1 with appropriate filters (motorized turret with position change <200 ms, according to the manufacturer) and an Axio Cam HR R3 camera. Contrast adjustment, area selection, and color combining were made using the Zen lite 2012 software. Sum Intensity Projections of selected frames were created using the “Z project” command of ImageJ software. ImageJ Plot profile was used for measurements of fluorescence intensity (<https://imagej.nih.gov/ij/>). For quantifying colocalization, Pearson’s correlation coefficient (PCC) above thresholds, for a selected region of interest (ROI) was calculated using the ICY colocalization studio plugin (pixel-based method) (<http://icy.bioimageanalysis.org/>). One sample *t*-test was

performed to test the significance of differences in PCCs, using Graphpad Prism software. Confidence interval (C.I.) was set to 95%. For quantifying dot density in Figure 6, ROIs were selected using the Area Selection tool and the Spot Detector plugin of ICY. Tukey’s multiple comparison test was performed (one-way ANOVA) using Graphpad Prism software for statistical analyses. C.I. was set to 95%. Scale bars were added using the FigureJ plugin of ImageJ software. Images were further processed and annotated in Adobe Photoshop CS4 Extended version 11.0.2.

### Data availability

Strains constructed in this work are available upon request. Supplementary material has been uploaded to figshare. Supplemental material available at Figshare: <https://doi.org/10.25386/genetics.6619922>.

## Results

### The AP-1 complex localizes polarly in distinct cytoplasmic structures and is essential for growth

In *A. nidulans*, the AP-1 adaptor complex is encoded by the genes AN7682 (*ap-1<sup>σ</sup>*), AN4207 (*ap-1<sup>γ</sup>*), AN3029 (*ap-1<sup>β</sup>*), and AN8795 (*ap-1<sup>μ</sup>*). In a previous study, a knockout of the gene encoding the AP-1 σ subunit proved lethal, therefore we employed a conditional knock-down strain (Martzoukou *et al.* 2017), using the thiamine-repressible promoter *thiA<sub>p</sub>* (Apostolaki *et al.* 2012). The phenotypic analysis of this strain showed that repression of *ap1<sup>σ</sup>* results in severely retarded colony growth, reflected at the microscopic level in wider and shorter hyphae with increased numbers of side branches and septa. Figure 1, A and B highlights these results, further showing that *thiA<sub>p</sub>*-dependent full repression of not only *ap1<sup>σ</sup>*, but also *ap1<sup>β</sup>* and *ap1<sup>μ</sup>*, results in lack of growth. Notably, besides increased numbers of side branches and septa, staining level and cortical localization of calcofluor white are modified upon repression of AP-1<sup>σ</sup>, suggesting altered chitin deposition (Figure 1B). Given that the genetic disruption of three AP-1 subunits appears to affect growth in *A. nidulans* similarly, and also that the inactivation of any subunit has been reported to disrupt the full complex in other organisms (Robinson 2015 and refs therein), the AP-1<sup>σ</sup> subunit was chosen to further investigate the role of the AP-1 complex in intracellular cargo trafficking pathways. Figure 1C shows that expression of functional GFP- or mRFP-tagged AP-1<sup>σ</sup> has distinct localization in cytoplasmic puncta, the motility of which resembles a Brownian motion, being more abundant in the apical region of hyphae and apparently absent from the Spk. The distinct localization of AP-1<sup>σ</sup> localization, which resembles the distribution of Golgi markers (see below), is lost and replaced by a fluorescent cytoplasmic haze when the β or μ subunits are knocked-down (Figure 1D). Noticeably, the majority of these foci are not stained by FM4-64 or CMAC (Figure 1, E and F), strongly suggesting that they are distinct from endosomes and vacuoles.

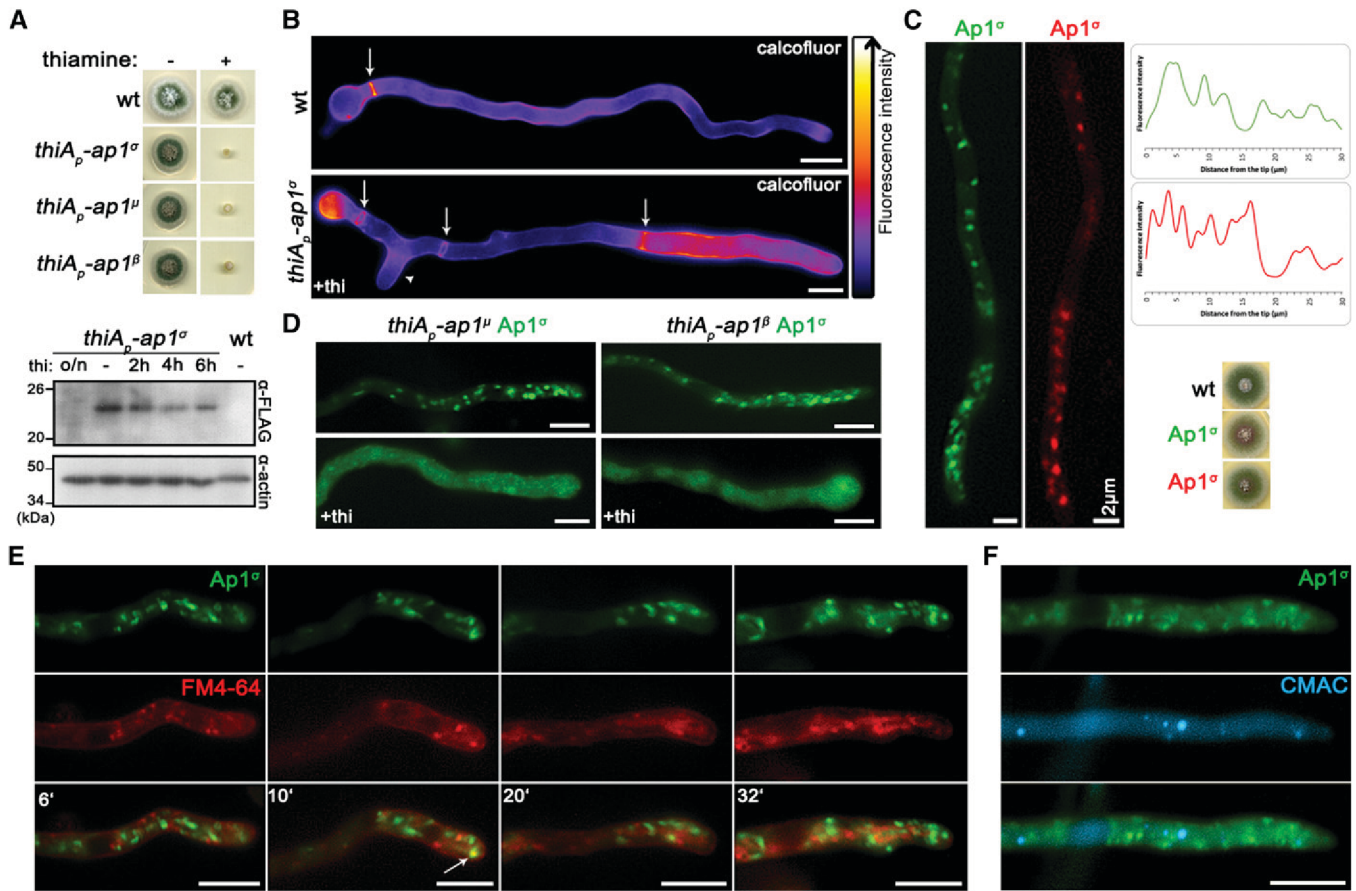


**Figure 1** The AP-1 complex localizes in distinct polarly distributed structures and is essential for growth. (A) Upper panel: Growth of isogenic strains carrying thi-repressible alleles of *ap1 $\sigma$* , *ap1 $\mu$* , and *ap1 $\beta$*  (*thiA $_p$ -ap1 $\sigma$* , *thiA $_p$ -ap1 $\mu$* , and *thiA $_p$ -ap1 $\beta$* ) compared to wild-type (*wt*) in the absence (–) or presence (+) of thi. Lower panel: Western blot analysis comparing protein levels of FLAG-Ap1 $\sigma$  in the absence (0 hr) or presence of thi, added for 2, 4, 6, or 16 hr (overnight culture, o/n). *wt* is a standard wild-type strain (untagged *ap1 $\sigma$* ) which is included as a control for the specificity of the  $\alpha$ -FLAG antibody. Equal loading is indicated by actin levels. (B) Microscopic morphology of hyphae in a strain repressed for *ap1 $\sigma$*  expression (+thi, lower panel) compared to *wt* (upper panel) stained with calcofluor white. Septal rings and side branches are indicated by arrows and arrowheads. Notice the differences in the calcofluor deposition at the hyphal head, tip, and the sub apical segment (Lookup table [LUT] fire [Image], National Institutes of Health) (C) Subcellular localization of Ap1 $\sigma$ -GFP and Ap1 $\sigma$ -mRFP in isogenic strains and relative quantitative analysis of fluorescence intensity (right upper panel), highlighting the polar distribution of Ap1 $\sigma$ . Growth tests showing that the tagged versions of Ap1 $\sigma$  are functional (right lower panel). (D) Subcellular localization of Ap1 $\sigma$ -GFP in isogenic strains carrying thi-repressible alleles of *ap1 $\mu$*  (left panels) or *ap1 $\beta$*  (right panels) in the absence (upper panels) or presence of thi (+thi, o/n). Note that repression of expression of either the  $\mu$  or the  $\beta$  subunit leads to diffuse cytoplasmic fluorescence of Ap1 $\sigma$ . (E) Subcellular localization of Ap1 $\sigma$ -GFP in the presence of FM4-64, which labels dynamically endocytic steps (PM, EEs, late endosomes/vacuoles). Notice that Ap1 $\sigma$ -GFP structures do not colocalize with FM4-64, except a few cases observed in the subapical region (indicated with an arrow at the 10 min picture). (F) Subcellular localization of Ap1 $\sigma$ -GFP in the presence of the vacuolar stain 7-amino-4-chloromethylcoumarin (Blue CMAC). No Ap1 $\sigma$ -GFP/CMAC colocalization is observed. Unless otherwise stated, Bar, 5  $\mu$ m. Except (C) where the hyphal apex is at the lower side, in all other cases the hyphal apex is at the right side of the image series.

**Knockdown of AP-1 affects the localization of polarly localized cargoes**

As mentioned in the Introduction, polarized growth of fungal hyphae is sustained by the continuous delivery of cargo-containing SVs toward the hyphal apex, and accumulation at the Spk before fusion with the plasma membrane (PM). Once localized in the PM at the hyphal apex, several cargoes diffuse laterally and become recycled through the actin-patch-enriched subapical regions of the endocytic collar, balancing exocytosis with endocytosis (Harris *et al.* 2005; Steinberg 2007; Berepiki *et al.* 2011; Takeshita *et al.* 2014; Peñalva *et al.* 2017; Steinberg *et al.* 2017; Zhou *et al.* 2018). In order

to study the potential implications of the AP-1 complex in these processes, we monitored the localization of specific established apical and collar markers in conditions where the *ap-1 $\sigma$*  expression has been fully repressed. These markers include the secretory v-SNARE SynA and t-SNARE SsoA (Taheri-Talesh *et al.* 2008), the phospholipid flippases DnfA and DnfB that partially localize in the Spk (Schultzhaus *et al.* 2015), the class III chitin synthase ChsB known to play a key role in hyphal tip growth and cell wall integrity maintenance (Yanai *et al.* 1994; Takeshita *et al.* 2015), the tropomyosin TpmA decorating actin at the Spk and on actin cables at the hyphal tip (Taheri-Talesh *et al.* 2008), and, finally, the

endocytic patch specific marker AbpA marking the sites of actin polymerization (Araujo-Bazán *et al.* 2008), along with the endocytic markers SlaB and SagA (Araujo-Bazán *et al.* 2008; Hervás-Aguilar and Peñalva 2010; Karachaliou *et al.* 2013). Additionally, we also tested the localization of the UapA xanthine-uric acid transporter, which our previous work suggested is not affected by the loss of function of the AP-1 complex (Martzoukou *et al.* 2017).

Figure 2 and Figure S1 highlight our results, which show that the localization of all markers tested is affected in the absence of AP-1 $\sigma$ , with the only clear exception being the plasma membrane transporter UapA. Additionally, the general positioning of nuclei also appears unaffected as indicated by labeled histone 1 (Nayak *et al.* 2010). Of the markers tested, SynA, DnfA, DnfB, and ChsB significantly lose their polar distribution (Figure 2 and Figure S1A) and do not seem to properly reach the Spk, concomitant with their increased presence in distinct, rather static, cytoplasmic puncta of various sizes. The nonpolar distribution of SsoA is generally conserved, but its cortical positioning is reduced and replaced by numerous cytoplasmic puncta. The cytoplasmic puncta that appear under AP-1 $\sigma$  depletion show very minor cargo-dependent colocalization with vacuoles stained with CMAC, mostly evident with chitin synthase ChsB (Figure S1B; see also later). Finally, collar-associated markers (SagA, SlaB, and AbpA) appear “moved” in an acropetal manner toward the hyphal tip. TpmA has also lost its proper localization at the hyphal tip, suggesting defective stabilization of actin filaments at the level of the Spk (Bergs *et al.* 2016). For relative quantification of fluorescence intensity see also Figure S1A.

Previous studies have shown that mutations preventing endocytosis of polar markers result in a uniform rather than polarized distribution of cargoes at the PM (Schultzhaus *et al.* 2015; Schultzhaus and Shaw 2016; Martzoukou *et al.* 2017). In contrast, when exocytosis is impaired due to the absence of clathrin, several cargoes show predominantly noncortical cytoplasmic localization (Martzoukou *et al.* 2017). Thus, our present observations strongly suggest that secretion and/or recycling is the process blocked in the absence of the AP-1 complex, while endocytosis remains functional. The latter is further supported by the fact that repression of AP-1 in the absence of a functional AP-2 complex, results in significant apparent cortical retention of specific cargoes, such as DnfA, despite the concurrent subapical accumulation of cytoplasmic DnfA-labeled structures (Figure 2B), which notably do not colocalize with endocytic membranes stained by FM4-64 (Figure S2).

#### **AP-1 associates transiently with the trans-golgi**

In *A. nidulans*, the process of maturation of Golgi has been extensively studied (Peñalva 2010; Pantazopoulou 2016; Steinberg *et al.* 2017). The markers syntaxin SedV<sup>Sed5</sup> and the human oxysterol-binding protein PH domain (PH<sup>OSBP</sup>) are well-established markers to follow the dynamics of early/*cis*-Golgi (Pinar *et al.* 2013) and late/*trans*-Golgi compartments (Pantazopoulou and Peñalva 2009), respectively.

Here we examined the possible association of the AP-1 complex with Golgi compartments using these markers. Figure 3A shows that AP-1 $\sigma$  exhibits no colocalization, despite some topological proximity, with the early-Golgi, although in some cases it orbits around SedV marker (see also File S1). In contrast, most AP-1 $\sigma$  labeled structures show a significant degree of apparent association with PH<sup>OSBP</sup>, which suggests that AP-1 partially colocalizes with the late-Golgi (Figure 3B, see also File S2). Notably, the degree of association of AP-1 with PH<sup>OSBP</sup> has a transient character, as seen by the apparent progressive loss of colocalization. The increased association of AP-1 $\sigma$  with late-Golgi is further supported by the effect of Brefeldin A, which leads to transient Golgi collapse in aggregated bodies, several of which included the AP-1 marker (Figure 3C). Thermosensitive mutations in SedV (SedV-R258G) or the regulatory GTPase RabO<sup>Rab1</sup> (RabO-A136D) are known to lead to early-Golgi, or both early- and late-Golgi, disorganization upon shift to the restrictive temperature (Pinar *et al.* 2013). These mutations led to AP-1 $\sigma$  subcellular distribution modification, further supporting the association of AP-1 with late-, but not with early-Golgi. In particular, in SedV-R258G, AP-1 $\sigma$  localization was less affected, whereas in RabO-A136D AP-1 $\sigma$  fluorescence was significantly delocalized from distinct puncta to a cytoplasmic haze (Figure 3D). Finally, knockdown of RabC<sup>Rab6</sup>, another small GTPase responsible for Golgi network organization, also results in smaller AP-1 $\sigma$  foci (Figure 3D), resembling the fragmented Golgi equivalents observed for PH<sup>OSBP</sup> in a *rabCΔ* genetic background (Pantazopoulou and Peñalva 2011). Importantly, knockdown of AP-1 had a moderate but detectable effect on the overall picture of early- or late-Golgi markers, which in this case seem relocated in the subapical region of the hypha, thus showing increased polarization (Figure 3E and Figure S3). The significance of this observation is discussed later.

#### **AP-1 associates with clathrin via specific C-terminal motifs**

AP-1 and AP-2 association with clathrin is considered as a key interaction mediating the recognition of cargo prior to clathrin cage assembly in metazoa (Robinson 2015). Clathrin-binding motifs, or boxes, have been identified in the hinge regions of the  $\beta$  subunits (Dell’Angelica *et al.* 1998). In *A. nidulans*, clathrin light and heavy chains have been recently visualized (Martzoukou *et al.* 2017; Schultzhaus *et al.* 2017) and shown to dynamically decorate the late-Golgi, also coalescing after Brefeldin A treatment (Schultzhaus *et al.* 2017). Given that AP-1 was shown here to associate with late-Golgi, we tested whether it also associates with clathrin light and/or heavy chains, despite having a truncated C-terminal region (Martzoukou *et al.* 2017). Figure 4, A and B suggests a high degree of colocalization of AP-1 $\sigma$  with both clathrin light chain, ClaL, and heavy chain, ClaH. In the case of ClaL, foci are often detected comigrating with AP-1 $\sigma$ , which, once formed, move to all dimensions coherently (see also File S3). In the case of ClaH, “horseshoe”-like structures appear

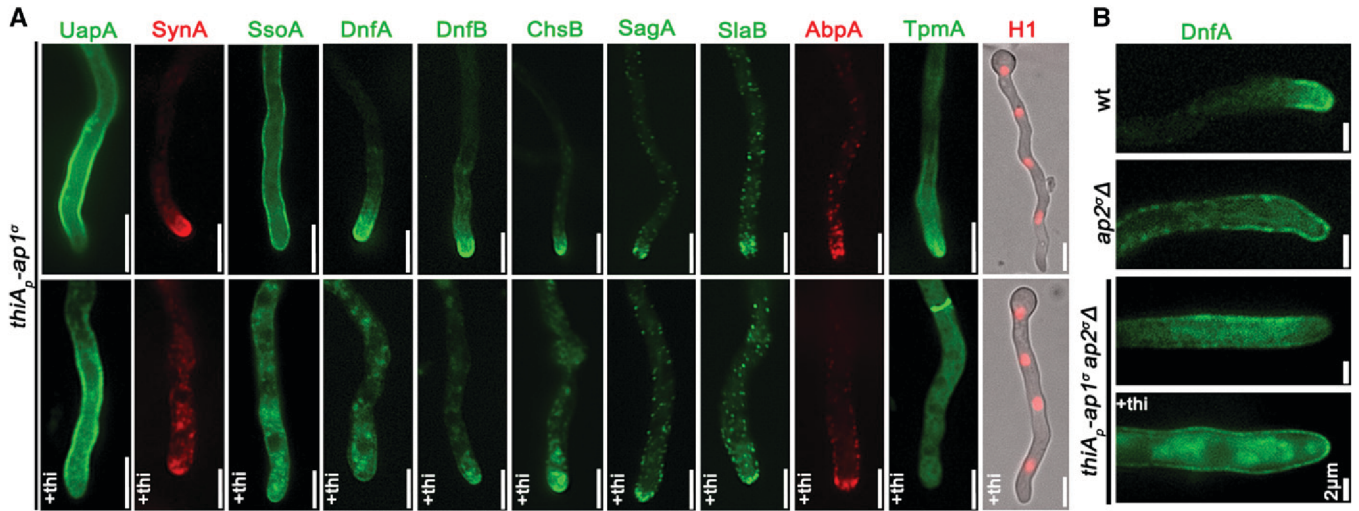


**Figure 2** Lack of expression of AP-1 affects the topology of polar cargoes. (A) Comparison of the cellular localization of specific GFP- or mRFP/mCherry-tagged protein cargoes under conditions where  $ap1^\sigma$  is expressed (upper panel) or fully repressed by thi (lower panel, +thi). The cargoes tested are the UapA transporter, the SNAREs SynA and SsoA, phospholipid flippases DnfA and DnfB, chitin synthase ChsB, endocytic markers SagA and SlaB, the actin-polymerization marker AbpA, tropomyosin TpmA, and histone H1 (*i.e.*, nuclei). Notice that when  $ap1^\sigma$  is fully repressed polar apical cargoes are depolarized and mark numerous relatively static cytoplasmic puncta. Hyphal apex is at the lower side of the image series. (B) Localization of DnfA-GFP in strains carrying the  $ap2^\sigma\Delta$  null allele, or the  $ap2^\sigma\Delta$  null allele together with the repressible  $thiA_p-ap1^\sigma$  allele, or an isogenic wild-type control (*wt*:  $ap2^\sigma+$   $ap1^\sigma+$ ). Note that loss of polar distribution due to defective apical endocytosis observed in the  $ap2^\sigma\Delta$  strains (Martzoukou *et al.* 2017) persists when AP-1 $\sigma$  is also repressed, indicating that, in the latter case, the majority of accumulating internal structures are due to problematic exocytosis of DnfA. Hyphal apex at the right side of the image series. Unless otherwise stated, Bar, 5  $\mu$ m.

to coalesce predominantly, which again are characterized by coherent movement with AP-1 $\sigma$  (see also File S4).

We also followed the localization of clathrin in the absence of AP-1, and vice versa, the localization of AP-1 in the absence of clathrin. Results in Figure 4C (upper panel) show that repression of ClaL expression does not affect the wild-type localization of AP-1 $\sigma$ . In contrast, repression of AP-1 $\sigma$  leads to a prominent increase in rather static, ClaL-containing, cytoplasmic puncta (Figure 4C, lower panel). This suggests AP-1 functions upstream from ClaL, in line with the established role of AP-1 in clathrin recruitment after cargo binding at late-Golgi or endosomal membranes.

Since our results supported a physical and/or functional association of AP-1 with clathrin, we addressed how this could be achieved given that the *A. nidulans* AP-1 $\beta$ , which is the subunit that binds clathrin in metazoa and yeast (Gallusser and Kirchhausen 1993), lacks canonical clathrin binding domains in its C-terminal region, but still possesses putative clathrin boxes ( $^{630}$ LLDID $^{634}$  and  $^{707}$ LLNGF $^{711}$ ). Noticeably, these motifs resemble the LLDLF or LLDFD sequences, found at the extreme C-terminus of yeast AP-1 $\beta$ , which have been shown to interact with clathrin (Yeung and Payne 2001). First, we showed that total repression of AP-1 $\beta$  expression leads to a prominent increase in static ClaL or ClaH puncta, compatible with altered clathrin localization (Figure 4D). Then, we asked whether the putative clathrin boxes in AP-1 $\beta$  play a role in the proper localization of clathrin. To do so, the  $^{707}$ LLNGF $^{711}$  or/and  $^{630}$ LLDID $^{634}$  motifs of AP-1 $\beta$  were mutated in a genetic background that also possesses a wild-type  $ap-1^\beta$  allele expressed via the repressible  $thiA_p$  promoter.

These strains allowed us to follow the localization of clathrin (*claL* or *claH*) when wild-type or mutant versions of  $ap-1^\beta$  were expressed. Figure 4E shows that mutations in  $^{707}$ LLNGF $^{711}$ , and to a much lesser extent  $^{630}$ LLDID $^{634}$ , lead to modification of clathrin localization, similar to the picture obtained under total repression of AP-1 $\beta$ . Notably, the mutated versions of AP-1 $\beta$  partially restore the growth defects of repressed AP-1 $\beta$  (Figure S5). This suggests that interaction with clathrin via these boxes is not the primary determinant for the essentiality of AP-1 in fungal growth.

#### AP-1 associates with Rabe<sup>Rab11</sup>-labeled SVs

The results obtained thus far suggested that the AP-1 complex is involved in post-Golgi anterograde trafficking of SVs. In *A. nidulans*, such vesicles deriving from the late-Golgi, traffic along MT tracks toward regulated discharge at the apical plasma membrane level (Berepiki *et al.* 2011; Peñalva *et al.* 2017; Steinberg *et al.* 2017; Zhou *et al.* 2018). The small GTPase Rabe<sup>Rab11</sup>, which is recruited along with its regulators, and precedes and very probably mediates late-Golgi exit of SVs toward the hyphal tip, plays a pivotal role in these early processes (Pantazopoulou *et al.* 2014; Pinar *et al.* 2015; Peñalva *et al.* 2017). Post-Golgi RabE labeled structures, including the Spk, do not colocalize with endosomes stained by FM4-64 or late-endosome/vacuoles stained by CMAC (Figure 5, A and B). In contrast, they show a significant degree of association with AP-1 $\sigma$ , suggesting that the majority of these vesicles are coated by AP-1 (Figure 5C). This is particularly prominent on foci of subapical regions

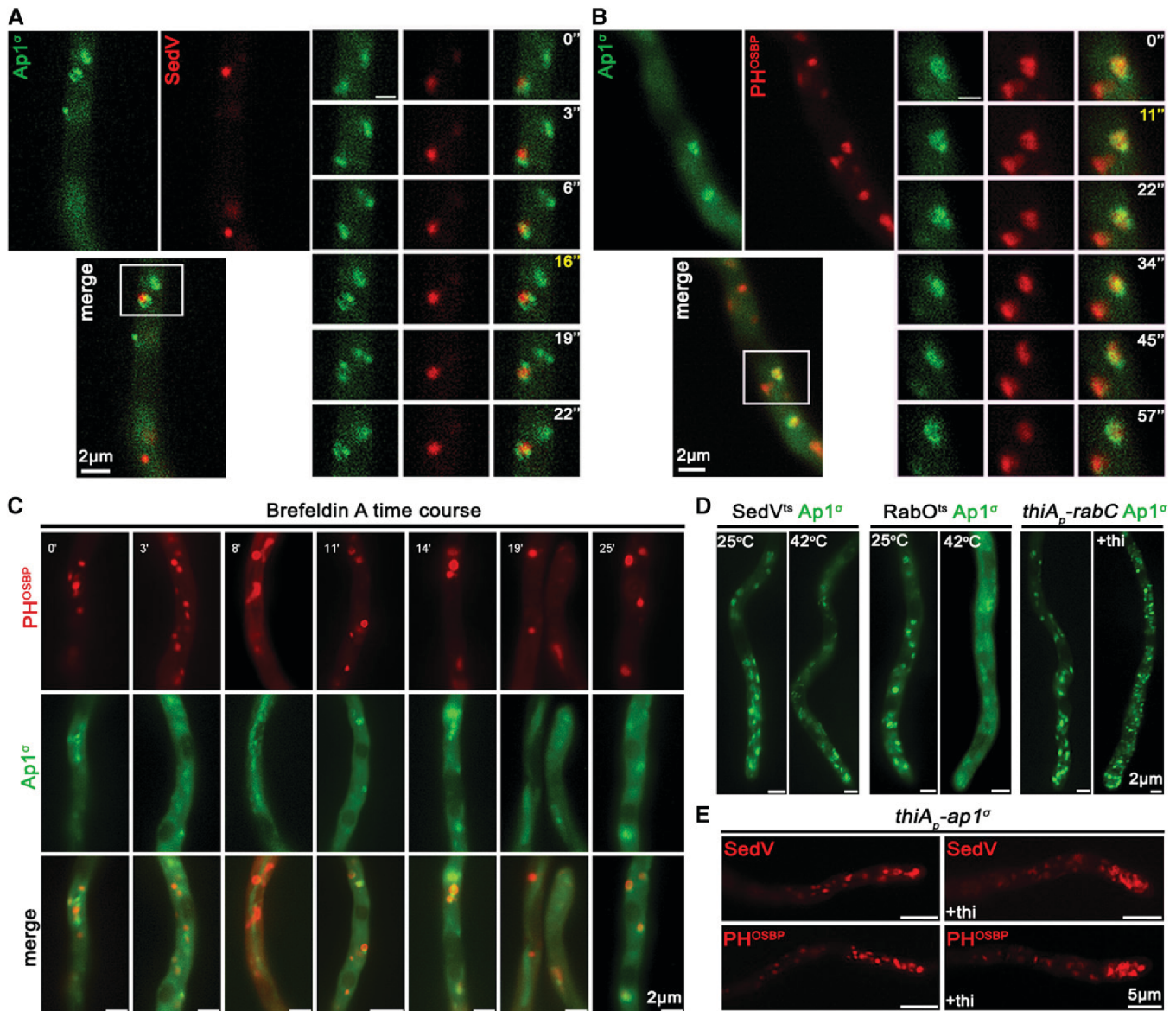


**Figure 3** AP-1 associates transiently with the late-Golgi. (A and B) Subcellular localization of Ap1 $\sigma$ -GFP relative to *cis*- (SedV-mCherry) and *trans*-Golgi (PH<sup>OSBP</sup>-mRFP) markers. Notice that Ap1 $\sigma$  colocalizes significantly with the *trans*-Golgi marker PH<sup>OSBP</sup> ( $n = 7$ ; PCC = 0.66,  $P < 0.0001$ ), but not with the *cis*-Golgi marker SedV ( $n = 5$ ; PCC = 0.35,  $P < 0.01$ ). This colocalization is dynamic and transient, as shown in selected time-lapse images on the right panels (for relevant videos, see also File S1 and File S2). (C) Subcellular localization of Ap1 $\sigma$  and PH<sup>OSBP</sup> in the presence of the inhibitor Brefeldin A, showing that a fraction of Brefeldin bodies (*i.e.*, collapsed Golgi membranes) includes both markers, further supporting a transient AP-1/late Golgi association. (D) Subcellular localization of Ap1 $\sigma$  in SedV<sup>ts</sup> or RabO<sup>ts</sup> thermosensitive mutants or a strain carrying a repressible *rabC* allele. These strains are used as tools for transiently blocking proper Golgi function. Notice that at the restrictive temperature (42 $^{\circ}$ C), Ap1 $\sigma$  fluorescence becomes increasingly diffuse, mostly in the RabO<sup>ts</sup> mutant, whereas, under RabC-repressed conditions, small Ap1 $\sigma$ -labeled puncta increase in number. These results are compatible with the notion that AP-1 proper localization necessitates wild-type Golgi dynamics. (E) Distribution of early- and late-Golgi markers SedV and PH<sup>OSBP</sup> relative to *ap1* $\sigma$  expression or repression (+*thi*). Notice the effect of accumulation of Golgi toward the hyphal apex under repressed conditions. Image series in (A–C) present subapical regions of hyphae, whereas in (D) the hyphal apex is at the lower image side and in (E) at the right image side.

(Figure 5C, left panels) and also at sites of newly emerging branches (Figure 5C, middle panels).

We further examined the association of AP-1 and RabE by following their localization in relevant knockdown mutants. Given that the knockout of RabE proved lethal (results not shown), we monitored AP-1 localization in a knockdown strain where *rabE* expression can be totally repressed via

the *thiA<sub>p</sub>* promoter. Similarly, we followed RabE localization in an analogous AP-1 knockdown mutant. Figure 5D (upper panel) shows that, when RabE is fully repressed, AP-1 fluorescence appears mostly as a cytoplasmic haze, suggesting that AP-1 acts downstream of RabE. In contrast, when AP-1 is repressed, RabE does not reach the Spk, while most fluorescence dissolves into scattered static puncta (Figure 5D,

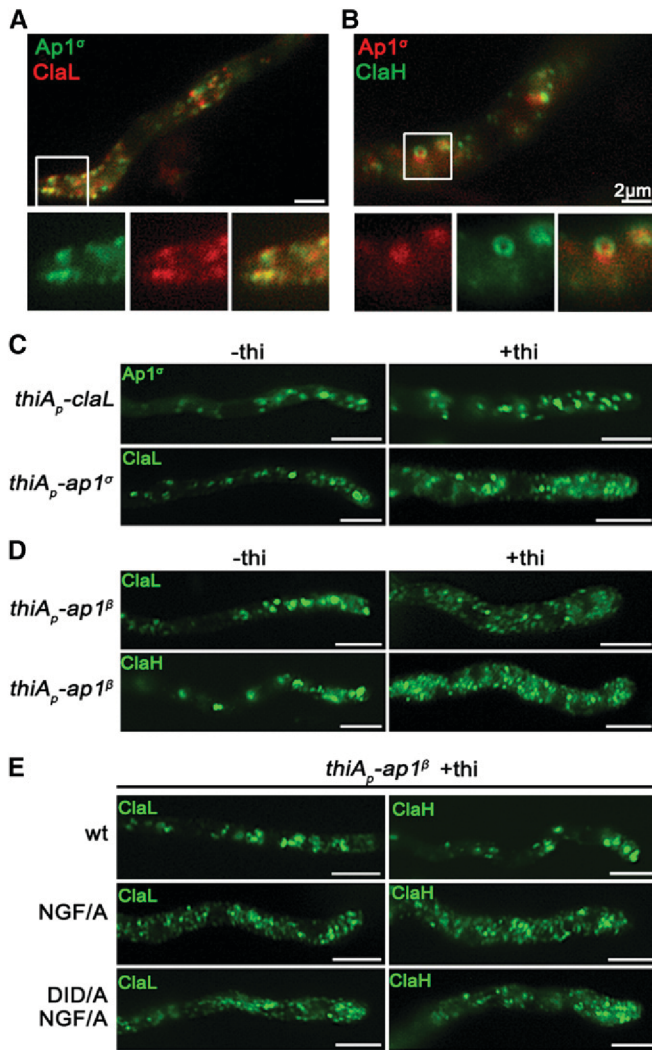


**Figure 4** C-terminal motifs in AP-1 $\beta$  are essential for wild-type clathrin localization. (A and B) Subcellular localization of Ap1 $\sigma$  relative to that of clathrin light (ClaL) and heavy (ClaH) chains. Notice the significant colocalization of AP-1 with both clathrin chains (claL:  $n = 9$ ; PCC = 0.78,  $P < 0.0001$ ) (claH:  $n = 5$ ; PCC = 0.76,  $P < 0.0001$ ), also highlighted by the comigration of the two markers in the relevant videos (File S3 and File S4, see also Figure S4). Hyphal apex is at the left side of (A), whereas in (B) a subapical hyphal region is presented. (C and D) Subcellular distribution of Ap1 $\sigma$  and clathrin light chain ClaL under conditions where *claL* or *ap1 $\sigma$*  are expressed/repressed, respectively (-thi/+thi). Note that repression of ClaL expression has no significant effect on Ap1 $\sigma$ -GFP localization, whereas repression of Ap1 $\sigma$  expression leads to more diffuse ClaL fluorescence with parallel appearance of increased numbers of cytoplasmic puncta. A similar picture is obtained when clathrin light and heavy chain localization are monitored under conditions of expression/repression of *ap1 $\beta$* . These results are compatible with the idea that clathrin localization is dependent on the presence of AP-1, but not vice versa. Hyphal apex is at the right side of the image series. (E) Effect of AP-1 $\beta$  C-terminal mutations modifying putative clathrin-binding motifs (<sup>709</sup>NGF/A<sup>711</sup> and <sup>632</sup>DID/A<sup>634</sup>) on ClaL and ClaH distribution. Notice that replacement of <sup>709</sup>NGF<sup>711</sup>, and to a lesser extent, of <sup>632</sup>DID<sup>634</sup>, by alanines, leads to modification of clathrin subcellular localization, practically identical to the picture observed in (D) when Ap1 $\beta$  expression is fully repressed. Hyphal apex is at the right side of the image series. Unless otherwise stated, Bar, 5  $\mu$ m.

lower panel). This strongly suggests that polar secretion of RabE and apparently of SVs is blocked.

Furthermore, upon repression of *rabE*, crucial apical markers like SynA or ChsB lose their polar distribution, failing to reach their proper destination at the cell cortex (Figure 5E, upper panels). This inhibition of targeting appears more dramatic than the one observed when AP-1 is repressed (see Figure 2), thus indicating the existence of possible alternative RabE-dependent, but AP-1 independent routes. In addition, clathrin labeled structures also lose their wild-type distribution under *rabE* repression conditions, resulting in scattered small puncta (Figure 5E, lower panels), resembling the phenotype observed for ClaL in the absence of a functional AP-1 complex (see Figure 4, C and D). Similar polar localization defects are observed in RabE-labeled SVs in strains repressed for clathrin light chain, suggesting that the majority of SVs requires a clathrin coat to reach the Spk (Figure 5F). Given the fact that, unlike RabE, neither AP-1 $\sigma$  nor clathrin appear to occupy the Spk, it seems that SVs are uncoated from AP-1 and clathrin prior to their localization in Spk, and thus before actin-dependent localization at the apical PM.

We also tested the relative localization of an apical marker (SynA) and RabE in a genetic background where Ap1 $\sigma$  expression can be repressed. When Ap1 $\sigma$  is expressed, SynA and RabE colocalize significantly, mostly evident in the Spk, whereas when Ap1 $\sigma$  is repressed, colocalization persists but shows a more dispersed pattern and is practically absent from the Spk (Figure 5G and Figure S6B). This strongly suggests the AP-1 is essential for anterograde movement of post-Golgi vesicles.

#### AP-1 associates with the MT cytoskeleton

Previous studies have shown that RabE-labeled SVs utilize MT tracks and kinesin-1 for their anterograde traffic, and, when present at the Spk, use myosin-5 and actin cables to be delivered at the apical PM or eventually move back in retrograde direction powered by dynein motors (Zhang *et al.* 2011; Egan *et al.* 2012; Peñalva *et al.* 2017; Steinberg *et al.* 2017; Zhou *et al.* 2018). Here, we examined the possible association of AP-1 with specific dynamic elements of the cytoskeleton involved in cargo traffic. Figure 6A shows that AP-1 puncta decorate MTs labeled by alpha-tubulin, TubA. Notably, the path of motile AP-1 puncta is, in most cases, dictated by the direction of the MTs (see also File S5). The association with the MT network is further supported by the effect of the anti-MT drug Benomyl, which results in an almost complete, but reversible, disassembly of MTs with a parallel increase in Ap1 $\sigma$ -GFP labeled cytoplasmic haze (Figure 6B, upper panel, mostly evident at 4–6 min). In contrast, inhibition of F-actin dynamics via Latrunculin B treatment shows that actin depolymerization does not lead to detectable modification of AP-1 localization (Figure 6B lower panel). This result is in agreement with the observation that AP-1 is excluded from the actin polymerization area.

Kinesins are motor proteins involved in the transport of SVs, EEs, organelles, and also mRNA and dynein motors

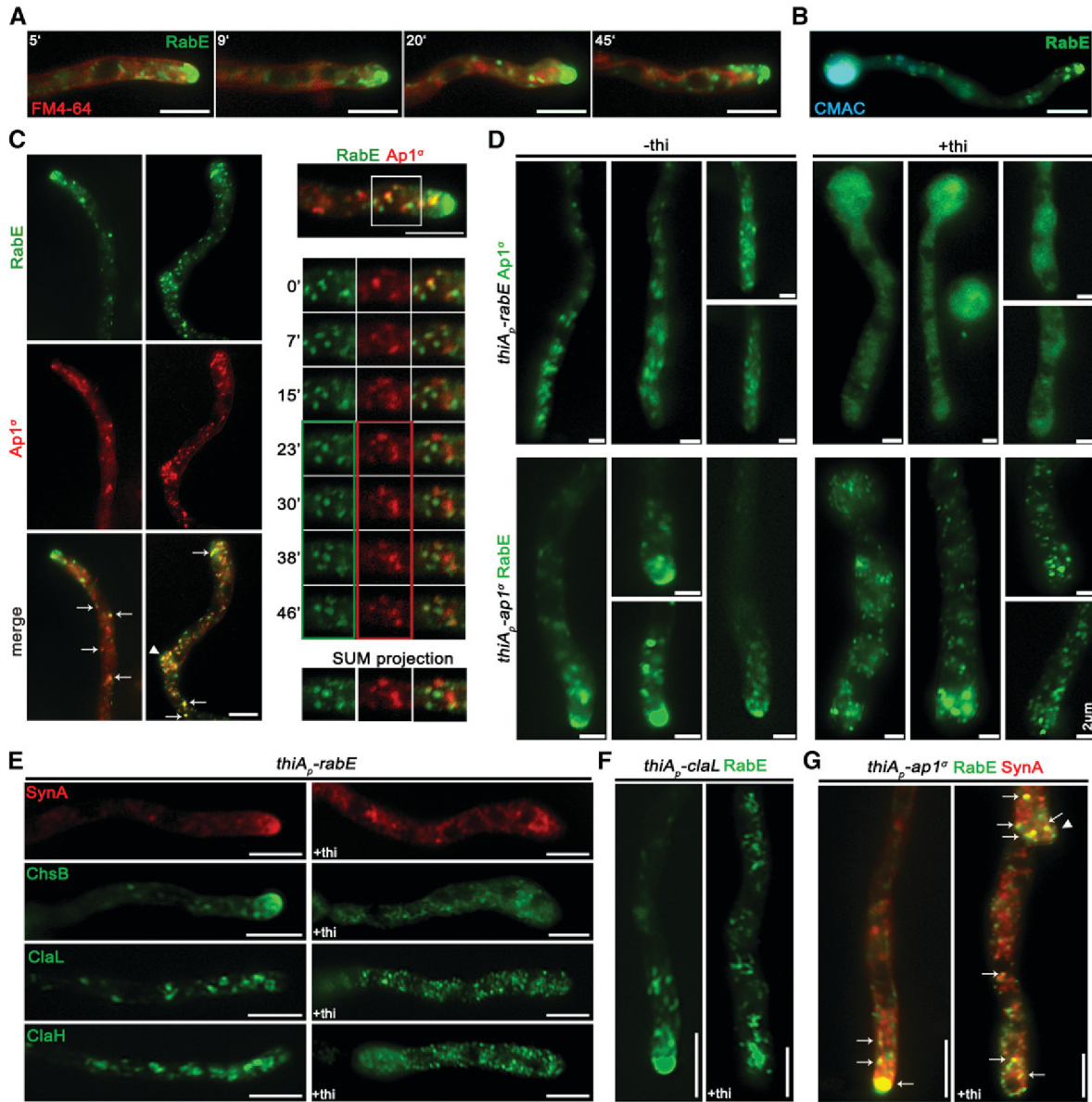


**Figure 5** AP-1 associates with RabE<sup>Rab11</sup>-labeled SVs. (A and B) Time course of RabE-GFP localization in the presence of FM4-64 (see also Figure S6A) or CMAC, indicating the nonendocytic character for RabE-labeled structures. Hyphal apex is at the right side of the image series. (C) Left panel: subcellular localization of Ap1<sup>σ</sup>-mRFP and RabE-GFP, showing significant colocalization in several fluorescent cytoplasmic puncta (arrows) throughout the hyphae but more prominent at subapical regions and sites of branch emergence (arrowheads) ( $n = 5$ ; PCC = 0.72,  $P < 0.0001$ ). Notice that colocalization is apparently excluded at the level of Spk, where RabE is prominent, whereas Ap1<sup>σ</sup> is not. Hyphal apex is at the upper side of the image series. Right panel: localization of Ap1<sup>σ</sup>-mRFP and RabE-GFP in a selected area sliced in time frames. Colored boxes indicate the slices used for SUM projection. Hyphal apex is at the right side of the image series. (D) Subcellular localization of Ap1<sup>σ</sup>-GFP or RabE-GFP in strains carrying thiamine-repressible *thiA<sub>p</sub>-rabE* or *thiA<sub>p</sub>-ap1<sup>σ</sup>* alleles respectively, observed under conditions of expression (-thi) or repression (+thi). Note that, in the absence of *rabE* expression, Ap1<sup>σ</sup>-labeled fluorescence appears as a cytoplasmic haze rather than distinct puncta (upper panels), while in the absence of *ap1<sup>σ</sup>* expression, RabE fluorescence disappears from the Spk, and is associated with numerous scattered bright puncta along the hypha (lower panels—43.24% uniform distribution, and intensity of puncta, 37.84% more than two brighter puncta close to the apex are observed, 18.9% one brighter mislocalized punctum at the apex is observed,  $n = 37$ ). Hyphal apex is at the lower side of the image series. (E) Subcellular localization of SynA, ChsB, ClaL, and ClaH in strains carrying the thiamine-repressible *thiA<sub>p</sub>-rabE* allele, observed under conditions of expression (-thi) or repression (+thi) of *rabE*. Note that, in all cases, the wild-type distribution of fluorescence is severely affected, resulting in loss of polarized structures and appearance of an increased number of scattered bright foci, the latter being more evident in ClaL and ClaH. Hyphal apex is at the right side of the image series. (F) Localization of RabE-GFP in a strain carrying a thiamine-repressible *thiA<sub>p</sub>-claL* allele, observed under conditions of expression (-thi) or repression (+thi) of *claL*. Notice the disappearance of RabE from the Spk and its association with numerous scattered bright clusters along the hypha—a picture similar to that obtained in absence of *ap1<sup>σ</sup>* expression in (D). Hyphal apex is at the lower side of the image series. (G) Colocalization analysis of SynA and RabE in a strain carrying a thiamine-repressible *thiA<sub>p</sub>-ap1<sup>σ</sup>* allele (see also Figure S6B). Note that, when Ap1<sup>σ</sup> is expressed, SynA and RabE colocalize intensively at the Spk but also elsewhere along the hypha, whereas when Ap1<sup>σ</sup> expression is repressed (+thi), both fluorescent signals disappear from the Spk and appear mostly in numerous scattered and rather immotile puncta, several of which show double fluorescence. Hyphal apex is at the lower side of the image series. Unless otherwise stated, Bar, 5  $\mu$ m.



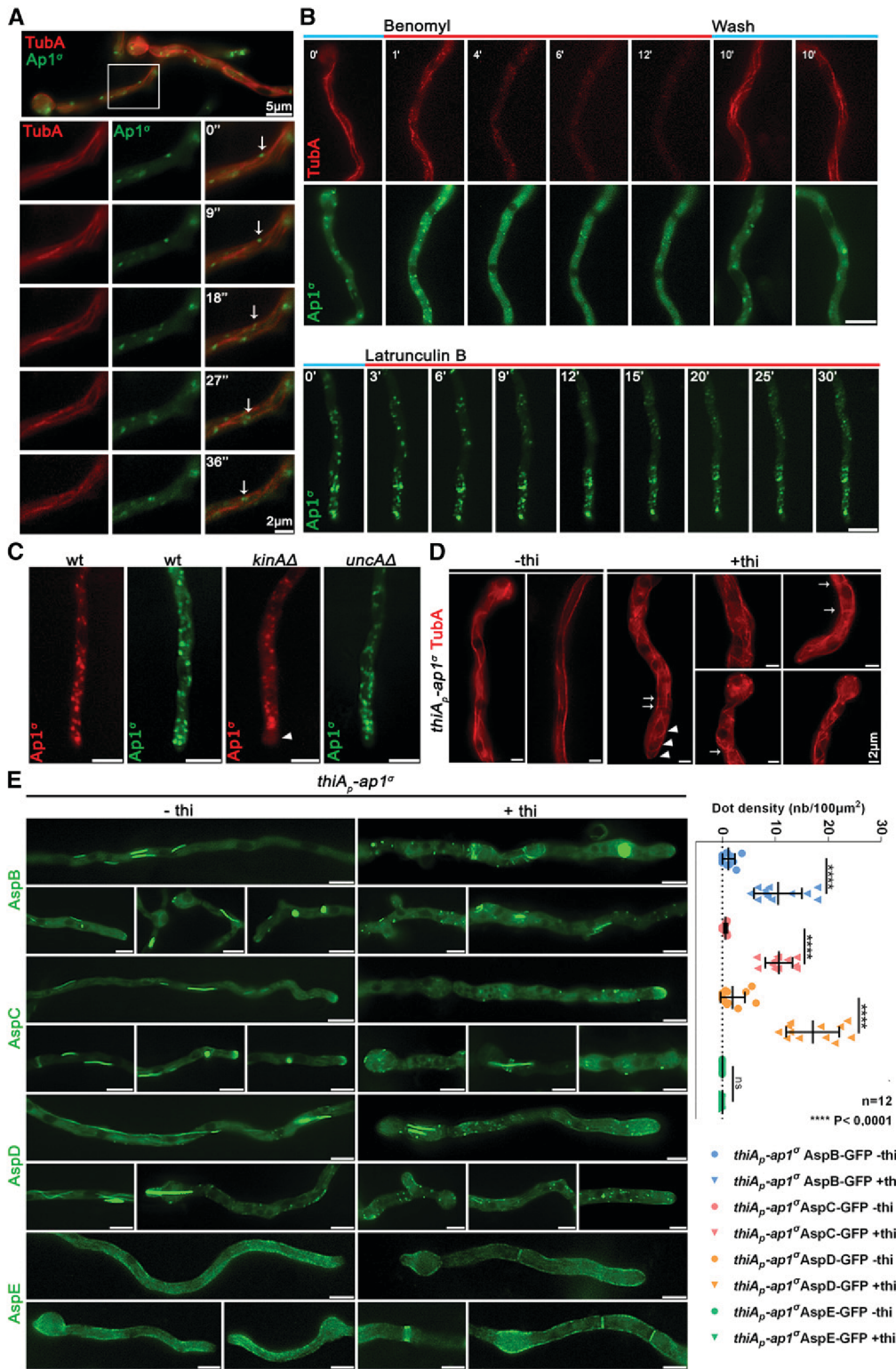


**Figure 6** AP-1 associates with the cytoskeleton and affects septin organization. (A) Relative Ap1<sup>σ</sup>-GFP and mCherry-TubA (α-tubulin) subcellular localization. Notice Ap1<sup>σ</sup> fluorescent foci decorating dynamically TubA-labeled MTs, as highlighted with arrows in the selected time-lapse images on the lower panels (see also File S5). Hyphal apex is at the right side of the image series. (B) Time course of treatment of strains expressing Ap1<sup>σ</sup> and TubA with the anti-MT drug Benomyl (upper panels). Notice that Benomyl elicits an almost complete, but reversible, disassociation of Ap1<sup>σ</sup> and TubA, resulting in diffuse cytoplasmic fluorescent signals. In contrast, treatment with the anti-actin drug Latrunculin B does not elicit a significant change in the polar distribution of Ap1<sup>σ</sup> (lower panels). Hyphal apex is at the lower side of the image series. (C) Subcellular localization of AP-1 in wt and in strains lacking the kinesins KinA and UncaA, respectively. Notice the absence of apical labeling of AP-1 in the *kinAΔ* strain, indicated with an arrowhead. Hyphal apex is at the lower side of the image series. (D) Subcellular organization of the MT network, as revealed by TubA-labeling, in a strain carrying a thiamine-repressible *thiA<sub>p</sub>-ap1<sup>σ</sup>* allele, observed under conditions of expression (-*thi*) or repression (+*thi*) of *ap1<sup>σ</sup>*. Note that the absence of Ap1<sup>σ</sup> leads to a less orientated network, bearing vertical (arrows) and curved MTs (arrowheads), and, in some cases, the appearance of bright cortical spots (two to seven puncta/hypha, usually exhibiting perinuclear localization). (E) Subcellular localization of GFP-tagged versions of septins AspB, AspC, AspD, and AspE in a strain carrying a thiamine-repressible *thiA<sub>p</sub>-ap1<sup>σ</sup>* allele, observed under conditions of expression (-*thi*) or repression (+*thi*) of *ap1<sup>σ</sup>*. Note that when *ap1<sup>σ</sup>* is repressed, AspB, AspC, and AspD form less higher order structures (HOS) such as filaments or bars (*ap1<sup>+</sup>*: 1.58 HOS/hypha, *n* = 87, *ap1<sup>-</sup>*: 0.96 HOS/hypha,

*n* = 103) and instead label more cortical spots (see right panel for quantification), some of which appear as opposite pairs at both sides of the plasma membrane, resembling septum formation initiation areas. In contrast, AspE localization remains apparently unaffected under *ap1<sup>σ</sup>* repression conditions. Hyphal apex is at the right side of the image series. Unless otherwise stated, Bar, 5 μm.

(Steinberg 2011; Baumann *et al.* 2012; Egan *et al.* 2012; Salogiannis and Reck-Peterson 2017). Based on previous results showing that kinesin-1 KinA (Konzack *et al.* 2005;

Zekert and Fischer 2009) is the main motor responsible for anterograde traffic of RabE-labeled SVs, whereas kinesin-3 UncA has no significant role in SV secretion (Peñalva *et al.*

2017), we tested whether KinA and UncA are involved in powering the motility of AP-1 on MTs. The use of strains carrying deletions of KinA and UncA showed that the motility of AP-1 on MTs is principally powered by KinA, the absence of which leads to a redistribution and apparent “stalling” of Ap1 $\sigma$ -labeled foci at subapical regions, excluding localization at the hyphal tip area (Figure 6C). This picture is practically identical with the localization of apical cargoes, such as ChsB, in the absence of KinA (Takeshita *et al.* 2015). In the case of UncA, the Ap1 $\sigma$ -labeled foci appear to be largely unaffected; however, a more prominent localization at the level of Spk, and also rather lateral accumulation of relative foci is observed (55.2% of  $n = 25$  hyphae) (Figure 6C). These results suggest that UncA might have auxiliary roles in the anterograde traffic of Ap1-labeled SVs.

The functional association of AP-1 with the cytoskeleton was also investigated by following the appearance of MTs in a strain lacking AP-1. Figure 6D shows that repression of AP-1 expression led to prominent changes in the MT network, as monitored by mCherry-TubA fluorescence. These include more curved MTs toward the apex, distinct bright spots at the periphery of the hyphal head, and increased cross sections throughout the hypha, all together suggesting a possible continuous polymerization at the plus end and a problematic interaction with actin through cell-end markers (Takeshita *et al.* 2013, 2014; Zhou *et al.* 2018).

#### **AP-1 is critical for septin organization**

Given the role of AP-1 in MT organization, we also studied its role in septin localization. Septins are less well characterized GTP-binding proteins, which form hetero-polymers associating into higher order structures, and are thought to play a central role in the spatial regulation and coordination of the actin and MT networks in most eukaryotes (Mostowy and Cossart 2012; Spiliotis 2018). In *A. nidulans*, five septins have been under investigation, the four core septins AspA–D, which form hetero-polymers appearing in various shapes, including spots, rings, and filaments, and a fifth septin of currently unknown function, AspE, not involved in the hetero-polymer and appearing as dense cortical spots at the proximity of the plasma membrane (Hernández-Rodríguez and Momany 2012; Hernández-Rodríguez *et al.* 2014; Momany and Talbot 2017). Figure 6E shows that upon AP-1 repression, hetero-polymer forming core septins AspB, AspC, and AspD appear less in the form of filamentous structures, while distinct bright cortical spots tend to accumulate at the hyphal periphery, several of which possibly mark positions of new septa, in agreement with increased numbers of septa observed in the absence of AP-1. Interestingly, AspE, appears largely unaffected with the exception of the more frequent appearance of septa. All the above observations are in agreement with many other previously described phenotypes associating with AP-1 repression and suggest an implication of AP-1 in the processes regulating septin polymer formation. Noticeably, proper endosomal trafficking of septins at growth

poles is necessary for growth in *Ustilago maydis* (Baumann *et al.* 2014; Zander *et al.* 2016).

#### **AP-1 is involved in endosomal function**

The AP-1 complex has also been implicated in anterograde and retrograde traffic between endosomal compartments and the plasma membrane (Robinson 2004, 2015). However, the existence of a relative sorting or recycling endosome, originating from EEs, has not been shown formally in filamentous fungi (Steinberg *et al.* 2017), with the exception of a recently characterized endosome to TGN recycling route for chitin synthase ChsB (Hernández-González *et al.* 2018). Major determinants of EE identity are the Rab5 GTPases (Nielsen *et al.* 1999). The *A. nidulans* Rab5 paralogues RabA and RabB both localize to EEs moving on MT tracks, with RabB appearing also in relatively static late endosomes. Importantly, the RabA and RabB markers do not colocalize with RabE, which confirms that motile, anterograde-moving, SVs, and motile endosomes are distinct entities (Pantazopoulou *et al.* 2014). Here, we investigated whether AP-1 associates with Rab5 endosomes.

Figure 7A shows that AP-1 exhibits a degree of transient comigration with RabB (see also File S6). The coalescence of fluorescence is mostly observed in ring-like structures, which tend to accumulate and convert to more compact forms, suggesting an involvement of AP-1 in recycling, without excluding an additional involvement in vacuolar degradation. Importantly, knockdown of AP-1 led to increased numbers of both RabA and RabB-labeled endosomes (Figure 7B), the majority of which are immotile. In fact, the motile subpopulation of endosomes appears unaffected (Figure 7C). In the absence of AP-1, several distinct RabB foci were also stained by CMAC (Figure 7D), indicating that they are mini-vacuoles, resembling the phenotype of RabA/B in the absence of RabS<sup>Rab7</sup>, a mediator of vacuolar degradation (Abenza *et al.* 2012). Limited colocalization of RabA/B upon AP-1 depletion is also observed with DnfA (Figure 7E). The evidence presented above and the partial colocalization of the chitin synthase ChsB with CMAC shown (see Figure S1), strongly support that AP-1 is involved in endosome function, affecting direct recycling to the PM or retrograde sorting to the TGN or both.

#### **Discussion**

We have previously shown that the AP-2 complex of *A. nidulans* and probably other higher fungi have a clathrin-independent role in the endocytosis of cargoes necessary for apical recycling of plasma membrane and cell wall components, and thus for fungal polar growth maintenance. This was rather unexpected due to the generally accepted view that AP-2 functions uniquely as a cargo-clathrin adaptor, but also due to its compromised role in the growth of unicellular fungi. Thus, it seems that sorting and trafficking mechanisms are genetically and/or physiologically adaptable in order to meet the specific growth or homeostatic strategies different cells

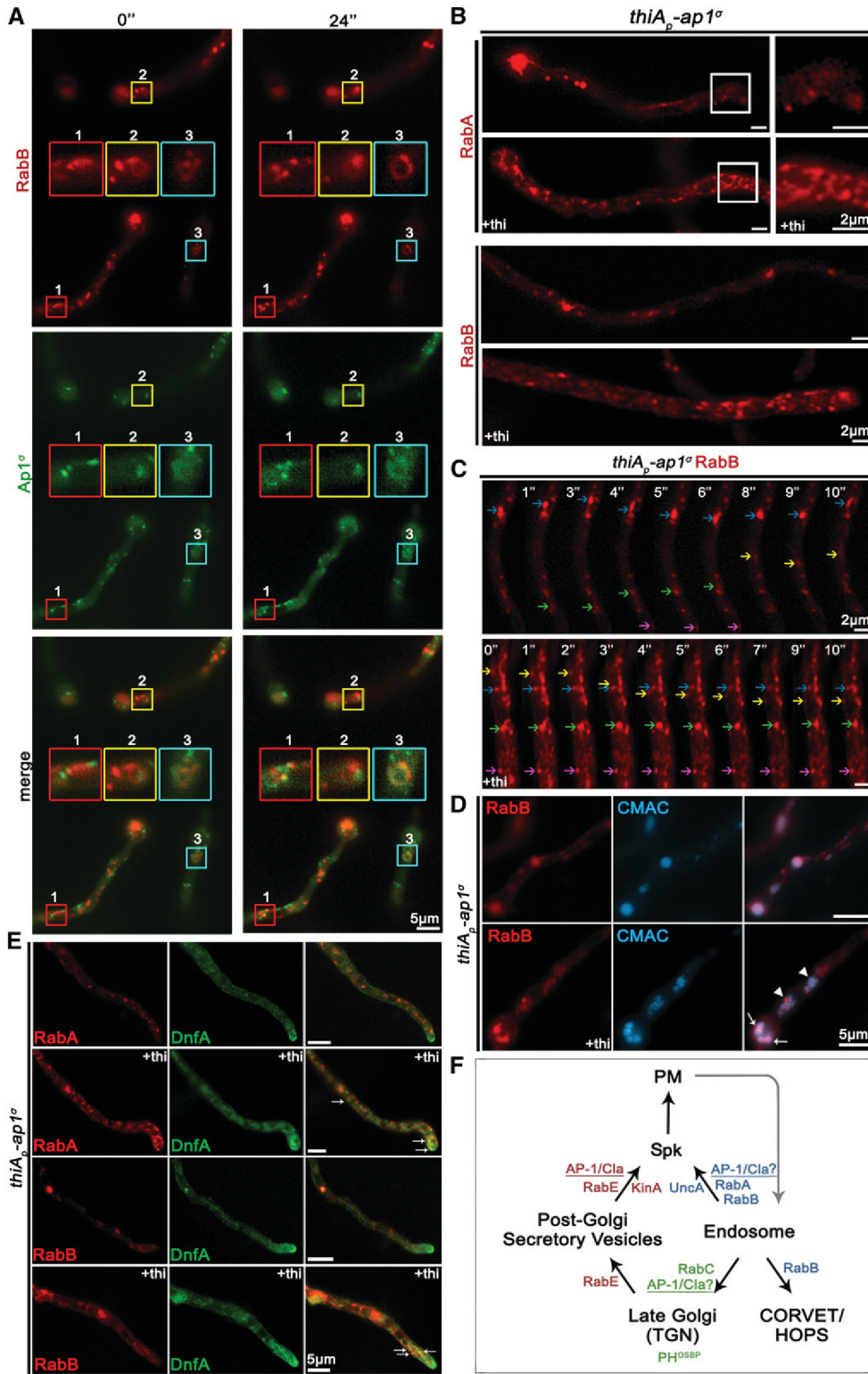


**Figure 7** AP-1 is involved in endosome recycling. (A) Images showing the relative localization of Ap1 $\sigma$  and the endosomal marker RabB (see also File S6). Selected areas in small color boxes are magnified, marked with the same border coloration and positioned at the center of the relevant subpanel. Notice the dynamic association of AP-1 with RabB (see also File S6). (B) Subcellular localization of RabA (upper panels) and RabB (lower panels) in a strain carrying a thi-repressible *thiA<sub>p</sub>-ap1 $\sigma$*  allele, observed under conditions of expression (-thi) or repression (+thi) of *ap1 $\sigma$* . Notice the increased numbers and clustering of both endosomal markers in rather immotile puncta when AP-1 expression is repressed. RabA endosomal subpopulation motility for  $n = 5$  hyphae is  $0.91 \pm 0.11$  static and  $2.8 \pm 0.49$  mobile endosomes per  $10 \mu\text{m}$  hyphal length in weight and  $3.03 \pm 0.10$  static and  $3.15 \pm 0.31$  motile endosomes per  $10 \mu\text{m}$  hyphal length in AP-1 depleted conditions. In the case of RabB and for  $n = 7$ , endosomal subpopulation motility data are  $1.41 \pm 0.36$  static and  $2.76 \pm 0.26$  mobile endosomes per  $10 \mu\text{m}$  hyphal length in weight and  $3.16 \pm 0.99$  static and  $2.72 \pm 0.63$  motile endosomes per  $10 \mu\text{m}$  hyphal length in AP-1 depleted conditions. The increase of immotile endosomes in AP-1 depleted conditions compared to wt is statistically significant ( $P < 0.001$  for RabA and  $P < 0.0001$  for RabB). The motile subpopulation appears to be unaffected and shows no statistically significant difference. Hyphal apex is at the right side of the image series. (C) Selected time-lapse images of RabB in a strain carrying a thi-repressible *thiA<sub>p</sub>-ap1 $\sigma$*  allele, showing that the immotile RabB foci increase in number when *ap1 $\sigma$*  is repressed (+thi). However, faster trafficking endosomes can still be observed, in both retrograde and anterograde direction. Colored arrows are used to point out specific endosomal dots at 1 sec intervals. Subapical hyphal regions are presented in the image series. (D) Expression of RabB in a strain carrying a thi-repressible *thiA<sub>p</sub>-ap1 $\sigma$*  allele, stained with CMAC. Note that when *ap1 $\sigma$*  expression is repressed

(+thi), most immotile RabB puncta are stained with CMAC. Note foci that colocalize with CMAC (arrow) and others that do not (arrowheads). Hyphal head is at the bottom left side of the image series. (E) Localization of endosomal markers RabA/B with the phospholipid flippase DnfA, in a strain carrying a thi-repressible *thiA<sub>p</sub>-ap1 $\sigma$*  allele, observed under conditions of expression (-thi) or repression (+thi) of *ap1 $\sigma$* . Colocalization in both cases occurs only in a few spots (arrows) dispersed mostly subapically, being, however, more prominent in the case of RabA. Hyphal apex is at the bottom right side of the image series. (F) Working model summarizing major findings on the role of the AP-1 complex. Unless otherwise stated, Bar,  $5 \mu\text{m}$ .

face. In the present work, we functionally analyzed the AP-1 complex of *A. nidulans*, as a prototypic example of a simple eukaryote that exhibits continuous polar growth, and showed that AP-1 is indeed essential for cell survival and growth, in a way similar to metazoan cells (Bonifacino 2014) and probably plants (Robinson and Pimpl 2014). To our knowledge, no previous study has addressed the role of the AP-1 in filamentous fungi.

In yeasts, which do not maintain polar growth and where the MT cytoskeleton is not critical for cargo traffic, AP-1 null mutants are viable, showing relatively moderate growth defects, which, in some cases, are associated with problematic traffic of specific cargoes, such as chitin synthase Chs3 (Valdivia *et al.* 2002; Ma *et al.* 2009; Yu *et al.* 2013; Arcones *et al.* 2016). Yeast AP-1 null mutants also have minor defects in lipid PtdIns(3,5)P<sub>2</sub>-dependent processes, and show reduced ability to traffic ubiquitylated cargoes to the vacuolar lumen (Phelan *et al.* 2006). In fact, in budding yeast, AP-1 seems to be involved in a bidirectional cycling route between the TGN and endosomes (Hirst *et al.* 2012; Robinson 2015). Notably, in *S. cerevisiae*, there are two forms of AP-1 that share the same large (Apl2 and Apl4) and small (Aps1) subunits, but distinct medium subunits (Apm1 or Apm2) that seem to confer differential cargo recognition and sorting (Valdivia *et al.* 2002; Renard *et al.* 2010; Whitfield *et al.* 2016). Additionally, in fission yeast, the AP-1 complex seems to co-operate with the exomer, a non-essential, fungal-specific heterotetrameric complex assembled at the *trans*-Golgi network, for the delivery of a distinct set of proteins to the plasma membrane (Hoya *et al.* 2017; Anton *et al.* 2018).

In contrast to yeasts, repression of AP-1 expression in *A. nidulans* leads to lack of growth, which is related to its inability to maintain apical sorting of all polar cargoes tested, including those necessary for plasma membrane and cell wall biosynthesis. Thus, not only the growth phenotype, but also several underlying cellular defects in AP-1 null mutants resemble those obtained previously with AP-2 loss-of-function mutants (Martzoukou *et al.* 2017). This is in perfect agreement with the notion that growth of filamentous fungi, unlike yeasts, requires polar apical exocytosis combined with sub-apical endocytosis and recycling to the apex of specific cargoes related to plasma membrane and cell wall modification (Taheri-Talesh *et al.* 2008; Peñalva 2010; Shaw *et al.* 2011). Overall, the results presented herein emphasize important differences in membrane trafficking mechanisms employed by yeasts and filamentous fungi, the latter proving a unique genetic and cellular system to dissect cargo sorting in cells characterized by membrane polarity.

Interestingly, despite the similarity in AP-2 and AP-1 phenotypic growth defects, AP-2 has been shown to act independently of clathrin at the PM, while AP-1 is shown here to associate and function with clathrin at several post-Golgi membrane trafficking steps. The similarity of effects caused by null mutations in AP-1 and clathrin chains, concerning RabE<sup>Rab11</sup>-labeled secretory vesicle anterograde traffic and

RabA/B<sup>Rab5</sup>-labeled endosome recycling, constitutes strong evidence that AP-1 function is clathrin-dependent. Interestingly, however, the  $\beta$  subunit of AP-1 of *A. nidulans* and all higher fungi lacks the C-terminal appendage domain that contributes to clathrin-binding (Martzoukou *et al.* 2017). Here, we identified specific short motifs in the C-terminal region of AP-1 <sup>$\beta$</sup>  that proved critical for proper clathrin subcellular localization and AP-1 function. These (LLNGF and LLDID) resemble motifs shown previously to bind clathrin in yeast (Yeung and Payne 2001). Thus, in contrast to the fact that clathrin is dispensable for the function of AP-2 in polar cargo endocytosis, it is essential for AP-1-driven polar exocytosis.

A novel point of this work concerns the interaction of AP-1 with RabE<sup>Rab11</sup>. To our knowledge, such an interaction has been described only in a single report in mammalian cells (Parmar and Duncan 2016). In this case, Rab11 and AP-1 colocalize with the reptilian reovirus p14 FAST protein at the TGN. In metazoa, Rab11 acts as a molecular switch essential for building the necessary molecular machinery for membrane cargo trafficking to the cell surface via its localization and action at the *trans*-Golgi network, post-Golgi vesicles and specialized recycling endosomes (Welz *et al.* 2014). In *A. nidulans*, the Rab11 homolog RabE has been previously shown to mark similar subcellular compartments (*e.g.*, late-Golgi and SVs) and to be involved in anterograde moving of cargoes to the Spk and eventually to the apical PM. Notably, however, RabE does not colocalize with RabA/B<sup>Rab5</sup>-labeled endosomes. The present work strongly suggests that AP-1 and clathrin are sequentially recruited on cargoes, after RabE-dependent maturation of late-Golgi membranes to pre-SVs, and that secreted cargoes travel embedded within AP-1/clathrin-coated vesicle carriers on MT (see later) to the Spk. At the Spk, AP-1/clathrin coat is most likely released, but RabE remains until the involvement of actin in the last step of fusion with the apical PM.

The impressive similarity of the *A. nidulans* trafficking mechanisms with those of higher organisms is also reflected in the absolute need for proper MT cytoskeleton organization and dynamics (Fischer *et al.* 2008; Takeshita *et al.* 2014). We showed that AP-1 is essential for MT organization and associates with MTs, mainly via KinA. Thus, a specific kinesin motor provides the molecular link between cargo/AP-1/clathrin complexes and cytoskeletal tracks. This is very similar to what has been found in mammalian epithelial cells, where the molecular motor kinesin KIF13A connects AP-1 coated SVs containing mannose-6-phosphate receptor to MT tracks, and thus mediates their transfer from the TGN to the plasma membrane (Nakagawa *et al.* 2000). Similarly, in HeLa cells another motor protein kinesin, KIF5, links TGN-derived endosomal vesicles via a direct interaction with Gadkin, a  $\gamma$ -BAR membrane accessory protein of the AP-1 complex, with the MT cytoskeleton (Schmidt *et al.* 2009). Thus, tripartite complexes, including transmembrane cargoes, coat adaptors, and motor kinesins, seem to constitute an

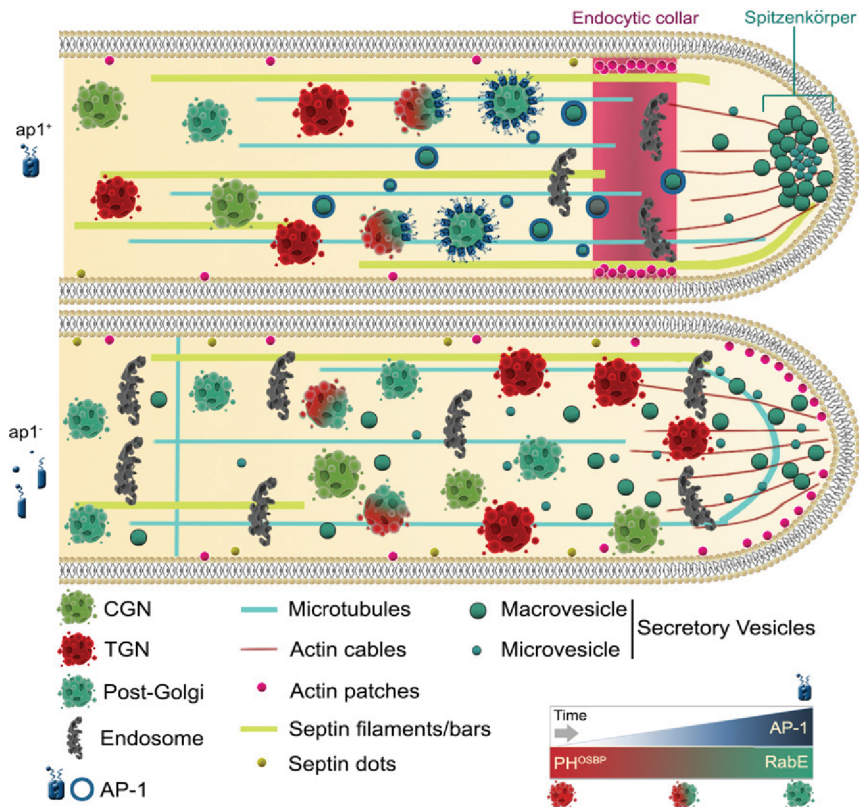


**Figure 8** Highly speculative scheme on the role of AP-1 in *A. nidulans* hyphal tip growth based on the herein described microscopic observation of fluorescent tagged protein markers. In an *ap1*<sup>+</sup> background the late-Golgi progressively turns into post-Golgi RabE-containing SVs coated by AP-1 (also depicted in the lower right panel). In the absence of a functional AP-1 complex (*ap1*<sup>-</sup>), apparent accumulation of Golgi toward the fungal apex, mislocalization of endocytic collar associated actin patches toward the tip, failure of accumulation of SVs at the level of Spk, septin, and MT disorganization, and an overall enrichment in “sorting” endosomal and/or vacuolar structures are observed.

evolutionary conserved molecular machinery for membrane protein subcellular transport in eukaryotes.

One simple explanation for the essentiality of AP-1 in proper MT organization would be that, in its absence, membrane-associated polarity markers, such as Rho GTPases TeaA or Tear, which are necessary for MT attachment to actin (Fischer *et al.* 2008; Takeshita and Fischer 2011; Takeshita *et al.* 2013; Takeshita 2018), are not sorted correctly in the apex of growing hyphae. Lack of such cell-end markers is known to result in curved or zigzagged organization of MTs and less straight hyphae, compatible with the picture we obtained in the AP-1 null mutant. Importantly, we further supported the essential role of AP-1 in MT organization and function by showing the dramatic effect of the absence of AP-1 on the subcellular organization of septins, proteins that play fundamental roles in the ability of diverse fungi to undergo shape changes and organize the cytoskeleton for polar growth (Momany and Talbot 2017; Zhang *et al.* 2017).

Another notable finding of this work concerns the association of AP-1 with endosomal routes that are distinct from those of RabE-labeled SVs. Thus, it seems that the combined action of genetically and cellularly distinct pathways serves the polar distribution of specific cargoes. In *A. nidulans*, EEs marked by the homologs of the Rab5 family (RabA and RabB) are generated via endocytosis and are easily distinguishable due to their high and long-distance bidirectional motility (Abenza *et al.* 2009; Steinberg 2014). A fraction of EEs matures to less motile late endosomes or multi-vesicular bodies (concurrent with increased replacing of RabA/B with RabS-

Rab7), which eventually fuse with vacuoles for cargo degradation (Abenza *et al.* 2010, 2012; Steinberg 2014). Another fraction of EEs, mostly the one localized at the subapical collar region of hyphae where very active endocytosis takes place, apparently recycles back to the Spk, and, from there, vesicular cargoes reach the PM (Steinberg 2014). Whether this takes place directly or via retrograde transport to the late-Golgi and anterograde transport in SVs, is not clear and might well depend on the nature of the cargoes studied. In a recent study in this context, it was shown that the chitin synthase ChsB segregates into “recycling” domains in sorting endosomes to be delivered to the TGN before being sorted back to the Spk via RabE<sup>Rab11</sup> SVs (Hernández-González *et al.* 2018). This leaves open the issue whether there is *bona fide* direct recycling endosome in fungi. Here, we showed that lack of AP-1 leads to a dramatic increase in nonmotile RabA or RabB endosomes, which might reflect either handicapped immotile endosomes and/or enhanced maturation to MVB/late endosomes. In any case, our results show that AP-1 has a critical role in the fueling endosomal cargoes to the PM, either directly or via the TGN. Similarly, lack of AP-1 function in mammalian cells leads to problematic maturation of EEs, associated with aberrant delivery of synaptic cargoes (Candiello *et al.* 2016). Establishing the essential role of AP-1 in polar secretion of specific cargoes in *A. nidulans* (for a schematic view of our findings see Figure 7F and Figure 8), which will probably hold true for other filamentous fungi, also opens a novel little-studied issue. How specific nonpolar cargoes are sorted to the plasma membrane? For example,

here and previously, we showed that AP-1 and AP-2 complexes are redundant for the proper subcellular expression of transporters that are homogeneously present in the PM of growing hyphae, and which do not show any indication of polar localization. A critical question to answer is which route(s) and mechanism(s) transporters, and possibly other nonpolar transmembrane cargoes (*i.e.*, channels and receptors), use for their sorting, endocytosis, or recycling. This question also concerns metazoan and plant cells, where nonpolar sorting remains largely understudied. Finally, under the light of previous results obtained in yeast, metazoa, or plants, our present work highlights the importance of using different model organisms to address common but evolutionary adaptable mechanisms for membrane cargo traffic in eukaryotes.

## Acknowledgments

We thank Reinhard Fischer for the tagged tubulin, chitin synthase and kinesins strains, Michele Momany for the tagged septins strains and Spyros Efthimiopoulos for the Anti-FLAG M2 antibody. The current research was supported by the *Fondation Santé*, to which we are grateful. O.M. is supported through the Action “Doctorate Scholarships Programs by the State Scholarships Foundation” by the Greek State Scholarships Foundation (IKY) and the European Social Fund (ESF), in the framework of the Operational Program “Education and Life Long Learning” within the NSRF 2014-2020 of the ESF.

Author contributions: O.M., Data curation, Software, Formal analysis, Investigation, Methodology, Conceptualization; G.D., Conceptualization, Resources, Formal analysis, Funding acquisition, Validation, Visualization, Manuscript Writing, Project administration; S.A., Data curation, Investigation, Methodology, Conceptualization; Manuscript Writing.

## Literature Cited

- Abenza, J. F., A. Pantazopoulou, J. M. Rodríguez, A. Galindo, and M. A. Peñalva, 2009 Long-distance movement of *Aspergillus nidulans* early endosomes on microtubule tracks. *Traffic* 10: 57–75. <https://doi.org/10.1111/j.1600-0854.2008.00848.x>
- Abenza, J. F., A. Galindo, A. Pantazopoulou, C. Gil, V. de los Ríos *et al.*, 2010 *Aspergillus* RabB Rab5 integrates acquisition of degradative identity with the long distance movement of early endosomes. *Mol. Biol. Cell* 21: 2756–2769. <https://doi.org/10.1091/mbc.e10-02-0119>
- Abenza, J. F., A. Galindo, M. Pinar, A. Pantazopoulou, V. de los Ríos *et al.*, 2012 Endosomal maturation by Rab conversion in *Aspergillus nidulans* is coupled to dynein-mediated basipetal movement. *Mol. Biol. Cell* 23: 1889–1901. <https://doi.org/10.1091/mbc.e11-11-0925>
- Anitei, M., and B. Hoflack, 2011 Exit from the trans-Golgi network: from molecules to mechanisms. *Curr. Opin. Cell Biol.* 23: 443–451. <https://doi.org/10.1016/j.ceb.2011.03.013>
- Anton, C., J. V. Taubas, and C. Roncero, 2018 The functional specialization of exomer as a cargo adaptor during the evolution of fungi. *Genetics* 208: 1483–1498. <https://doi.org/10.1534/genetics.118.300767>
- Apostolaki, A., L. Harispe, A. M. Calcagno-Pizarelli, I. Vangelatos, V. Sophianopoulou *et al.*, 2012 *Aspergillus nidulans* CkiA is an essential casein kinase I required for delivery of amino acid transporters to the plasma membrane. *Mol. Microbiol.* 84: 530–549. <https://doi.org/10.1111/j.1365-2958.2012.08042.x>
- Araujo-Bazán, L., M. A. Peñalva, and E. A. Espeso, 2008 Preferential localization of the endocytic internalization machinery to hyphal tips underlies polarization of the actin cytoskeleton in *Aspergillus nidulans*. *Mol. Microbiol.* 67: 891–905. <https://doi.org/10.1111/j.1365-2958.2007.06102.x>
- Arcones, I., C. Sacristán, and C. Roncero, 2016 Maintaining protein homeostasis: early and late endosomal dual recycling for the maintenance of intracellular pools of the plasma membrane protein Chs3. *Mol. Biol. Cell* 27: 4021–4032. <https://doi.org/10.1091/mbc.e16-04-0239>
- Bard, F., and V. Malhotra, 2006 The formation of TGN-to-plasma-membrane transport carriers. *Annu. Rev. Cell Dev. Biol.* 22: 439–455. <https://doi.org/10.1146/annurev.cellbio.21.012704.133126>
- Baumann, S., T. Pohlmann, M. Jungbluth, A. Brachmann, and M. Feldbrügge, 2012 Kinesin-3 and dynein mediate microtubule-dependent co-transport of mRNPs and endosomes. *J. Cell Sci.* 125: 2740–2752. <https://doi.org/10.1242/jcs.101212>
- Baumann, S., J. König, J. Koepke, and M. Feldbrügge, 2014 Endosomal transport of septin mRNA and protein indicates local translation on endosomes and is required for correct septin filamentation. *EMBO Rep.* 15: 94–102. <https://doi.org/10.1002/embr.201338037>
- Berepiki, A., A. Lichius, and N. D. Read, 2011 Actin organization and dynamics in filamentous fungi. *Nat. Rev. Microbiol.* 9: 876–887. <https://doi.org/10.1038/nrmicro2666>
- Bergs, A., Y. Ishitsuka, M. Evangelinos, G. U. Nienhaus, and N. Takeshita, 2016 Dynamics of actin cables in polarized growth of the filamentous fungus *Aspergillus nidulans*. *Front. Microbiol.* 7: 682. <https://doi.org/10.3389/fmicb.2016.00682>
- Bonifacino, J. S., 2004 The GGA proteins: adaptors on the move. *Nat. Rev. Mol. Cell Biol.* 5: 23–32. <https://doi.org/10.1038/nrm1279>
- Bonifacino, J. S., 2014 Adaptor proteins involved in polarized sorting. *J. Cell Biol.* 204: 7–17. <https://doi.org/10.1083/jcb.201310021>
- Cai, H., K. Reinisch, and S. Ferro-Novick, 2007 Coats, tethers, Rabs, and SNAREs work together to mediate the intracellular destination of a transport vesicle. *Dev. Cell* 12: 671–682. <https://doi.org/10.1016/j.devcel.2007.04.005>
- Candiello, E., M. Kratzke, D. Cassel, and P. Schu, 2016 AP-1/ $\sigma$ 1A and AP-1/ $\sigma$ 1 Badaptor-proteins differentially regulate neuronal early endosome maturation via the Rab5/Vps34-pathway. *Sci. Rep.* 6: 29950. <https://doi.org/10.1038/srep29950>
- Dell’Angelica, E. C., J. Klumperman, W. Stoorvogel, and J. S. Bonifacino, 1998 Association of the AP-3 adaptor complex with clathrin. *Science* 280: 431–434. <https://doi.org/10.1126/science.280.5362.431>
- Egan, M. J., K. Tan, and S. L. Reck-Peterson, 2012 Lis1 is an initiation factor for dynein-driven organelle transport. *J. Cell Biol.* 197: 971–982. <https://doi.org/10.1083/jcb.201112101>
- Evangelinos, M., O. Martzoukou, K. Choroziyan, S. Amillis, and G. Dhallinas, 2016 BsdA(Bsd2)-dependent vacuolar turnover of a misfolded version of the UapA transporter along the secretory pathway: prominent role of selective autophagy. *Mol. Microbiol.* 100: 893–911. <https://doi.org/10.1111/mmi.13358>
- Feyder, S., J. O. De Craene, S. Bär, D. L. Bertazzi, and S. Friant, 2015 Membrane trafficking in the yeast *Saccharomyces cerevisiae* model. *Int. J. Mol. Sci.* 16: 1509–1525. <https://doi.org/10.3390/ijms16011509>

- Fischer, R., N. Zekert, and N. Takeshita, 2008 Polarized growth in fungi—interplay between the cytoskeleton, positional markers and membrane domains. *Mol. Microbiol.* 68: 813–826. <https://doi.org/10.1111/j.1365-2958.2008.06193.x>
- Gallusser, A., and T. Kirchhausen, 1993 The beta 1 and beta 2 subunits of the AP complexes are the clathrin coat assembly components. *EMBO J.* 2: 5237–5244.
- Guo, Y., D. W. Sirkis, and R. Schekman, 2014 Protein sorting at the trans-Golgi network. *Annu. Rev. Cell Dev. Biol.* 30: 169–206. <https://doi.org/10.1146/annurev-cellbio-100913-013012>
- Harris, S. D., N. D. Read, R. W. Roberson, B. Shaw, S. Seiler *et al.*, 2005 Polarisome meets Spitzenkörper: microscopy, genetics, and genomics converge. *Eukaryot. Cell* 4: 225–229. <https://doi.org/10.1128/EC.4.2.225-229.2005>
- Hernández-González, M., I. Bravo-Plaza, M. Pinar, V. de Los Ríos, H. N. Arst, Jr. *et al.*, 2018 Endocytic recycling via the TGN underlies the polarized hyphal mode of life. *PLoS Genet.* 14: e1007291. <https://doi.org/10.1371/journal.pgen.1007291>
- Hernández-Rodríguez, Y., and M. Momany, 2012 Posttranslational modifications and assembly of septin heteropolymers and higher-order structures. *Curr. Opin. Microbiol.* 15: 660–668. <https://doi.org/10.1016/j.mib.2012.09.007>
- Hernández-Rodríguez, Y., S. Masuo, D. Johnson, R. Orlando, A. Smith *et al.*, 2014 Couto-Rodríguez M, Momany M. Distinct septin heteropolymers co-exist during multicellular development in the filamentous fungus *Aspergillus nidulans*. *PLoS One* 9: e92819. <https://doi.org/10.1371/journal.pone.0092819>
- Hervás-Aguilar, A., and M. A. Peñalva, 2010 Endocytic machinery protein SlaB is dispensable for polarity establishment but necessary for polarity maintenance in hyphal tip cells of *Aspergillus nidulans*. *Eukaryot. Cell* 9: 1504–1518. <https://doi.org/10.1128/EC.00119-10>
- Hirst, J., G. H. Borner, R. Antrobus, A. A. Peden, N. A. Hodson *et al.*, 2012 Distinct and overlapping roles for AP-1 and GGAs revealed by the “knocksways” system. *Curr. Biol.* 22: 1711–1716. <https://doi.org/10.1016/j.cub.2012.07.012>
- Hoya, M., F. Yanguas, S. Moro, C. Prescianotto-Baschong, C. Doncel *et al.*, 2017 Traffic through the trans-golgi network and the endosomal system requires collaboration between exomer and clathrin adaptors in fission yeast. *Genetics* 205: 673–690. <https://doi.org/10.1534/genetics.116.193458>
- Huang, K. M., K. D’Hondt, H. Riezman, and S. K. Lemmon, 1999 Clathrin functions in the absence of heterotetrameric adaptors and AP180-related proteins in yeast. *EMBO J.* 18: 3897–3908. <https://doi.org/10.1093/emboj/18.14.3897>
- Hunt, S. D., and D. J. Stephens, 2011 The role of motor proteins in endosomal sorting. *Biochem. Soc. Trans.* 39: 1179–1184. <https://doi.org/10.1042/BST0391179>
- Karachaliou, M., S. Amillis, M. Evangelinos, A. C. Kokotos, V. Yalilis *et al.*, 2013 The arrestin-like protein ArtA is essential for ubiquitination and endocytosis of the UapA transporter in response to both broad-range and specific signals. *Mol. Microbiol.* 88: 301–317. <https://doi.org/10.1111/mmi.12184>
- Konzack, S., P. E. Rischitor, C. Enke, and R. Fischer, 2005 The role of the kinesin motor KipA in microtubule organization and polarized growth of *Aspergillus nidulans*. *Mol. Biol. Cell* 16: 497–506. <https://doi.org/10.1091/mbc.e04-02-0083>
- Koukaki, M., E. Giannoutsou, A. Karagouni, and G. Diallinas, 2003 A novel improved method for *Aspergillus nidulans* transformation. *J. Microbiol. Methods* 55: 687–695. [https://doi.org/10.1016/S0167-7012\(03\)00208-2](https://doi.org/10.1016/S0167-7012(03)00208-2)
- Lee, M. C., E. A. Miller, J. Goldberg, L. Orci, and R. Schekman, 2004 Bi-directional protein transport between the ER and Golgi. *Annu. Rev. Cell Dev. Biol.* 20: 87–123. <https://doi.org/10.1146/annurev.cellbio.20.010403.105307>
- Ma, Y., M. Takeuchi, R. Sugiura, S. O. Sio, and T. Kuno, 2009 Deletion mutants of AP-1 adaptin subunits display distinct phenotypes in fission yeast. *Genes Cells* 14: 1015–1028. <https://doi.org/10.1111/j.1365-2443.2009.01327.x>
- Martzoukou, O., S. Amillis, A. Zervakou, S. Christoforidis, and G. Diallinas, 2017 The AP-2 complex has a specialized clathrin-independent role in apical endocytosis and polar growth in fungi. *eLife* 6: e20083. <https://doi.org/10.7554/eLife.20083>
- Meyer, C., D. Zizioli, S. Lausmann, E. L. Eskelinen, J. Hamann *et al.*, 2000 mu1A-adaptin-deficient mice: lethality, loss of AP-1 binding and rerouting of mannose 6-phosphate receptors. *EMBO J.* 19: 2193–2203. <https://doi.org/10.1093/emboj/19.10.2193>
- Momany, M., 2002 Polarity in filamentous fungi: establishment, maintenance and new axes. *Curr. Opin. Microbiol.* 5: 580–585. [https://doi.org/10.1016/S1369-5274\(02\)00368-5](https://doi.org/10.1016/S1369-5274(02)00368-5)
- Momany, M., and N. J. Talbot, 2017 Septins focus cellular growth for host infection by pathogenic fungi. *Front. Cell Dev. Biol.* 5: 33. <https://doi.org/10.3389/fcell.2017.00033>
- Mostowy, S., and P. Cossart, 2012 Septins: the fourth component of the cytoskeleton. *Nat. Rev. Mol. Cell Biol.* 13: 183–194. <https://doi.org/10.1038/nrm3284>
- Nakagawa, T., M. Setou, D. Seog, K. Ogasawara, N. Dohmae *et al.*, 2000 A novel motor, KIF13A, transports mannose-6-phosphate receptor to plasma membrane through direct interaction with AP-1 complex. *Cell* 103: 569–581. [https://doi.org/10.1016/S0092-8674\(00\)00161-6](https://doi.org/10.1016/S0092-8674(00)00161-6)
- Nakatsu, F., and H. Ohno, 2003 Adaptor protein complexes as the key regulators of protein sorting in the post-Golgi network. *Cell Struct. Funct.* 28: 419–429. <https://doi.org/10.1247/csf.28.419>
- Nakatsu, F., K. Hase, and H. Ohno, 2014 The role of the clathrin adaptor AP-1: polarized sorting and beyond. *Membranes (Basel)* 4: 747–763. <https://doi.org/10.3390/membranes4040747>
- Nayak, T., E. Szweczyk, C. E. Oakley, A. Osmani, L. Ukil *et al.*, 2006 A versatile and efficient gene-targeting system for *Aspergillus nidulans*. *Genetics* 172: 1557–1566. <https://doi.org/10.1534/genetics.105.052563>
- Nayak, T., H. Edgerton-Morgan, T. Horio, Y. Xiong, C. P. De Souza *et al.*, 2010 Gamma-tubulin regulates the anaphase-promoting complex/cyclosome during interphase. *J. Cell Biol.* 190: 317–330. <https://doi.org/10.1083/jcb.201002105>
- Nielsen, E., F. Severin, J. M. Backer, A. A. Hyman, and M. Zerial, 1999 Rab5 regulates motility of early endosomes on microtubules. *Nat. Cell Biol.* 1: 376–382. <https://doi.org/10.1038/14075>
- Pantazopoulou, A., 2016 The Golgi apparatus: insights from filamentous fungi. *Mycologia* 108: 603–622. <https://doi.org/10.3852/15-309>
- Pantazopoulou, A., and M. A. Peñalva, 2009 Organization and dynamics of the *Aspergillus nidulans* Golgi during apical extension and mitosis. *Mol. Biol. Cell* 20: 4335–4347. <https://doi.org/10.1091/mbc.e09-03-0254>
- Pantazopoulou, A., and M. A. Peñalva, 2011 Characterization of *Aspergillus nidulans* RabC/Rab6. *Traffic* 12: 386–406. <https://doi.org/10.1111/j.1600-0854.2011.01164.x>
- Pantazopoulou, A., M. Pinar, X. Xiang, and M. A. Peñalva, 2014 Maturation of late Golgi cisternae into RabE(RAB11) exocytic post-Golgi carriers visualized in vivo. *Mol. Biol. Cell* 25: 2428–2443. <https://doi.org/10.1091/mbc.e14-02-0710>
- Papadaki, G. F., S. Amillis, and G. Diallinas, 2017 Substrate specificity of the FurE transporter is determined by cytoplasmic terminal domain interactions. *Genetics* 207: 1387–1400. <https://doi.org/10.1534/genetics.117.300327>
- Parmar, H. B., and R. Duncan, 2016 A novel tribasic Golgi export signal directs cargo protein interaction with activated Rab11 and AP-1-dependent Golgi-plasma membrane trafficking. *Mol. Biol. Cell* 27: 1320–1331. <https://doi.org/10.1091/mbc.e15-12-0845>

- Peñalva, M. A., 2005 Tracing the endocytic pathway of *Aspergillus nidulans* with FM4-64. *Fungal Genet. Biol.* 42: 963–975. <https://doi.org/10.1016/j.fgb.2005.09.004>
- Peñalva, M. A., 2010 Endocytosis in filamentous fungi: cinderella gets her reward. *Curr. Opin. Microbiol.* 13: 684–692. <https://doi.org/10.1016/j.mib.2010.09.005>
- Peñalva, M. A., 2015 A lipid-managing program maintains a stout Spitzenkörper. *Mol. Microbiol.* 97: 1–6. <https://doi.org/10.1111/mmi.13044>
- Peñalva, M. A., J. Zhang, X. Xiang, and A. Pantazopoulou, 2017 Transport of fungal RAB11 secretory vesicles involves myosin-5, dynein/dynactin/p25, and kinesin-1 and is independent of kinesin-3. *Mol. Biol. Cell* 28: 947–961. <https://doi.org/10.1091/mbc.e16-08-0566>
- Phan, H. L., J. A. Finlay, D. S. Chu, P. K. Tan, T. Kirchhausen *et al.*, 1994 The *Saccharomyces cerevisiae* APS1 gene encodes a homolog of the small subunit of the mammalian clathrin AP-1 complex: evidence for functional interaction with clathrin at the Golgi complex. *EMBO J.* 13: 1706–1717.
- Phelan, J. P., S. H. Millson, P. J. Parker, P. W. Piper, and F. T. Cooke, 2006 Fab1p and AP-1 are required for trafficking of endogenously ubiquitylated cargoes to the vacuole lumen in *S. cerevisiae*. *J. Cell Sci.* 119: 4225–4234. <https://doi.org/10.1242/jcs.03188>
- Pinar, M., A. Pantazopoulou, H. N. Arst, Jr., and M. A. Peñalva, 2013 Acute inactivation of the *Aspergillus nidulans* Golgi membrane fusion machinery: correlation of apical extension arrest and tip swelling with cisternal disorganization. *Mol. Microbiol.* 89: 228–248. <https://doi.org/10.1111/mmi.12280>
- Pinar, M., H. N. Arst, Jr., A. Pantazopoulou, V. G. Tagua, V. de los Ríos *et al.*, 2015 TRAPP2 regulates exocytic Golgi exit by mediating nucleotide exchange on the Ypt31 ortholog RabERAB11. *Proc. Natl. Acad. Sci. USA* 112: 4346–4351. <https://doi.org/10.1073/pnas.1419168112>
- Renard, H. F., D. Demaegd, B. Guerriat, and P. Morsomme, 2010 Efficient ER exit and vacuole targeting of yeast Sna2p require two tyrosine-based sorting motifs. *Traffic* 11: 931–946. <https://doi.org/10.1111/j.1600-0854.2010.01070.x>
- Robinson, D. G., and P. Pimpl, 2014 Clathrin and post-Golgi trafficking: a very complicated issue. *Trends Plant Sci.* 19: 134–139. <https://doi.org/10.1016/j.tplants.2013.10.008>
- Robinson, M. S., 2004 Adaptable adaptors for coated vesicles. *Trends Cell Biol.* 14: 167–174. <https://doi.org/10.1016/j.tcb.2004.02.002>
- Robinson, M. S., 2015 Forty years of clathrin-coated vesicles. *Traffic* 16: 1210–1238. <https://doi.org/10.1111/tra.12335>
- Sambrook, J., E. F. Fritsch, and T. Maniatis, 1989 *Molecular Cloning: A Laboratory Manual*, Vol. 9, Ed. 2. Cold Spring Harbor Laboratory Press, Cold Spring Harbor, NY
- Salogiannis, J., and S. L. Reck-Peterson, 2017 Hitchhiking: a non-canonical mode of microtubule-based transport. *Trends Cell Biol.* 27: 141–150. <https://doi.org/10.1016/j.tcb.2016.09.005>
- Schmidt, M. R., T. Maritzen, V. Kukhtina, V. A. Higman, L. Doglio *et al.*, 2009 Regulation of endosomal membrane traffic by a Gadkin/AP-1/kinesin KIF5 complex. *Proc. Natl. Acad. Sci. USA* 106: 15344–15349. <https://doi.org/10.1073/pnas.0904268106>
- Schultzhaus, Z., and B. D. Shaw, 2015 Endocytosis and exocytosis in hyphal growth. *Fungal Biol. Rev.* 29: 43–53. <https://doi.org/10.1016/j.fbr.2015.04.002>
- Schultzhaus, Z., and B. D. Shaw, 2016 The flippase DnfB is cargo of fimbrin-associated endocytosis in *Aspergillus nidulans*, and likely recycles through the late Golgi. *Commun. Integr. Biol.* 9: e1141843. <https://doi.org/10.1080/19420889.2016.1141843>
- Schultzhaus, Z., H. Yan, and B. D. Shaw, 2015 *Aspergillus nidulans* flippase DnfA is cargo of the endocytic collar and plays complementary roles in growth and phosphatidylserine asymmetry with another flippase, DnfB. *Mol. Microbiol.* 97: 18–32. <https://doi.org/10.1111/mmi.13019>
- Schultzhaus, Z., T. B. Johnson, and B. D. Shaw, 2017 Clathrin localization and dynamics in *Aspergillus nidulans*. *Mol. Microbiol.* 103: 299–318. <https://doi.org/10.1111/mmi.13557>
- Shaw, B. D., D. W. Chung, C. L. Wang, L. A. Quintanilla, and S. Upadhyay, 2011 A role for endocytic recycling in hyphal growth. *Fungal Biol.* 115: 541–546. <https://doi.org/10.1016/j.funbio.2011.02.010>
- Spang, A., 2015 The road not taken: less traveled roads from the TGN to the plasma membrane. *Membranes (Basel)* 5: 84–98. <https://doi.org/10.3390/membranes5010084>
- Spiliotis, E. T., 2018 Spatial effects - site-specific regulation of actin and microtubule organization by septin GTPases. *J. Cell Sci.* 131: jcs207555. <https://doi.org/10.1242/jcs.207555>
- Steinberg, G., 2007 Hyphal growth: a tale of motors, lipids, and the Spitzenkörper. *Eukaryot. Cell* 6: 351–360. <https://doi.org/10.1128/EC.00381-06>
- Steinberg, G., 2014 Endocytosis and early endosome motility in filamentous fungi. *Curr. Opin. Microbiol.* 20: 10–18. <https://doi.org/10.1016/j.mib.2014.04.001>
- Steinberg, G., M. A. Peñalva, M. Riquelme, H. A. Wösten, and S. D. Harris, 2017 Cell Biology of Hyphal Growth. *Microbiol. Spectr.* 5: 231–265. <https://doi.org/10.1128/microbiolspec.FUNK-0034-2016>
- Taheri-Talesh, N. T., L. Horio, X. Araujo-Bazán, E. A. Dou, E. A. Espeso *et al.*, 2008 The tip growth apparatus of *Aspergillus nidulans*. *Mol. Biol. Cell* 19: 1439–1449. <https://doi.org/10.1091/mbc.e07-05-0464>
- Takeshita, N., 2018 Oscillatory fungal cell growth. *Fungal Genet. Biol.* 110: 10–14. <https://doi.org/10.1016/j.fgb.2017.12.002>
- Takeshita, N., and R. Fischer, 2011 On the role of microtubules, cell end markers, and septal microtubule organizing centres on site selection for polar growth in *Aspergillus nidulans*. *Fungal Biol.* 115: 506–517. <https://doi.org/10.1016/j.funbio.2011.02.009>
- Takeshita, N., D. Mania, S. Herrero, Y. Ishitsuka, G. U. Nienhaus *et al.*, 2013 The cell-end marker TeaA and the microtubule polymerase AlpA contribute to microtubule guidance at the hyphal tip cortex of *Aspergillus nidulans* to provide polarity maintenance. *J. Cell Sci.* 126: 5400–5411. <https://doi.org/10.1242/jcs.129841>
- Takeshita, N., R. Manck, N. Grün, S. H. de Vega, and R. Fischer, 2014 Interdependence of the actin and the microtubule cytoskeleton during fungal growth. *Curr. Opin. Microbiol.* 20: 34–41. <https://doi.org/10.1016/j.mib.2014.04.005>
- Takeshita, N., V. Wernet, M. Tsuizaki, N. Grün, H. O. Hoshi *et al.*, 2015 Transportation of *Aspergillus nidulans* class III and V chitin synthases to the Hyphal tips depends on conventional kinesin. *PLoS One* 10: e0125937. <https://doi.org/10.1371/journal.pone.0125937>
- Valdivia, R. H., D. Baggott, J. S. Chuang, and R. W. Schekman, 2002 The yeast clathrin adaptor protein complex 1 is required for the efficient retention of a subset of late Golgi membrane proteins. *Dev. Cell* 2: 283–294. [https://doi.org/10.1016/S1534-5807\(02\)00127-2](https://doi.org/10.1016/S1534-5807(02)00127-2)
- Viotti, C., 2016 ER to golgi-dependent protein secretion: the conventional pathway. *Methods Mol. Biol.* 1459: 3–29. [https://doi.org/10.1007/978-1-4939-3804-9\\_1](https://doi.org/10.1007/978-1-4939-3804-9_1)
- Vlanti, A., and G. Diallinas, 2008 The *Aspergillus nidulans* FcyB cytosine-purine scavenger is highly expressed during germination and in reproductive compartments and is downregulated by endocytosis. *Mol. Microbiol.* 68: 959–977. <https://doi.org/10.1111/j.1365-2958.2008.06198.x>
- Welz, T., J. Wellbourne-Wood, and E. Kerkhoff, 2014 Orchestration of cell surface proteins by Rab11. *Trends*



- Cell Biol. 24: 407–415. <https://doi.org/10.1016/j.tcb.2014.02.004>
- Whitfield, S. T., H. E. Burston, B. D. Bean, N. Raghuram, L. Maldonado-Báez *et al.*, 2016 The alternate AP-1 adaptor subunit Apm2 interacts with the Mill regulatory protein and confers differential cargo sorting. *Mol. Biol. Cell* 27: 588–598. <https://doi.org/10.1091/mbc.e15-09-0621>
- Yanai, K., N. Kojima, N. Takaya, H. Horiuchi, A. Ohta *et al.*, 1994 Isolation and characterization of two chitin synthase genes from *Aspergillus nidulans*. *Biosci. Biotechnol. Biochem.* 58: 1828–1835. <https://doi.org/10.1271/bbb.58.1828>
- Yeung, B. G., and G. S. Payne, 2001 Clathrin interactions with C-terminal regions of the yeast AP-1 beta and gamma subunits are important for AP-1 association with clathrin coats. *Traffic* 2: 565–576. <https://doi.org/10.1034/j.1600-0854.2001.20806.x>
- Yu, Y., C. Li, A. Kita, Y. Katayama, K. Kubouchi *et al.*, 2013 Sip1, an AP-1 accessory protein in fission yeast, is required for localization of Rho3 GTPase. *PLoS One* 8: e68488. <https://doi.org/10.1371/journal.pone.0068488>
- Zander, S., S. Baumann, S. Weidtkamp-Peters, and M. Feldbrügge, 2016 Endosomal assembly and transport of heteromeric septin complexes promote septin cytoskeleton formation. *J. Cell Sci.* 129: 2778–2792. <https://doi.org/10.1242/jcs.182824>
- Zanetti, G., K. B. Pahuja, S. Studer, S. Shim, and R. Schekman, 2011 COPII and the regulation of protein sorting in mammals. *Nat. Cell Biol.* 14: 20–28 (erratum: *Nat. Cell Biol.* 14: 221). <https://doi.org/10.1038/ncb2390>
- Zekert, N., and R. Fischer, 2009 The *Aspergillus nidulans* kinesin-3 UncA motor moves vesicles along a subpopulation of microtubules. *Mol. Biol. Cell* 20: 673–684. <https://doi.org/10.1091/mbc.e08-07-0685>
- Zhang, J., X. Yao, L. Fischer, J. F. Abenza, M. A. Peñalva *et al.*, 2011 The p25 subunit of the dynactin complex is required for dynein-early endosome interaction. *J. Cell Biol.* 193: 1245–1255. <https://doi.org/10.1083/jcb.201011022>
- Zhang, Y., T. Gao, W. Shao, Z. Zheng, M. Zhou *et al.*, 2017 The septins FaCdc3 and FaCdc12 are required for cytokinesis and affect asexual and sexual development, lipid metabolism and virulence in *Fusarium asiaticum*. *Mol. Plant Pathol.* 18: 1282–1294. <https://doi.org/10.1111/mpp.12492>
- Zhou, L., M. Evangelinos, V. Wernet, A. F. Eckert, Y. Ishitsuka *et al.*, 2018 Superresolution and pulse-chase imaging reveal the role of vesicle transport in polar growth of fungal cells. *Sci. Adv.* 4: e1701798. <https://doi.org/10.1126/sciadv.1701798>

Communicating editor: M. Rose